

IONIC LIQUIDS IN ANALYTICAL CHEMISTRY AND
CALIX[4]ARENE CHEMISTRY OF
NO_x GASES

by

ERANDA PATHIRANA WANIGASEKARA

Presented to the Faculty of the Graduate School of
The University of Texas at Arlington in Partial Fulfillment
of the Requirements
for the Degree of

DOCTOR OF PHILOSOPHY

THE UNIVERSITY OF TEXAS AT ARLINGTON

December 2010

Copyright © by Eranda Wanigasekara 2010

All Rights Reserved

This dissertation is dedicated to the memory of my father who loved me, raised me with good values and nudged me to study when my heart was to play all day alone and left me, my sister and my beloved mother all alone in this world on April 2nd 2001.

ACKNOWLEDGEMENTS

First, I would like to express my sincere gratitude to the first supervisor and mentor in my graduate career, the late Prof. Dmitry Rudkevich for his excellent guidance, valuable advice and mentoring throughout my stay in his research laboratory. I consider him to be one of the best professors I have had the opportunity to work with. I was lucky enough to learn about the fascinating science of supramolecular chemistry, calixarenes, and many other aspects of science and life. I wish I could meet him once again somewhere, someday in this endless cycle of life.

My sincere appreciation is extended to my current research supervisor, Prof. Daniel W. Armstrong for his excellent support, valuable advice, and guidance in the field of applied sciences throughout my research career at UTA. Without his valuable suggestions this work may not have been possible. I must express my special thanks to Prof. Armstrong for his kindness in accommodating me in his research group after the devastating loss of Dr. Dmitry Rudkevich in 2007.

Next, I am very thankful to my research committee: Prof. Carl Lovely and Prof. Kevin Schug for their valuable comments, suggestions and hard questioning sessions which guided me in research and helped make my academic and research work successful. I would like to acknowledge the help and suggestions from Prof. Lovely related to his expertise in synthesis and design strategies. I am also thankful to Prof. Schug for his suggestions and expertise in mass spectrometry and related techniques.

I am thankful to members of Dr. Rudkevich's group: Dr. Alexander Leontive, Dr. Valclav Stastny, Dr. Heng Xu, Dr. Voltaire Organo, Dr. Valentina Sgarlata, Dr.

Yanlong Kang, Hexiang Zhang, Zak Nixon, Luis Ryes, and Anas Saleh for sharing their knowledge and expertise with me and for the wonderful friendship throughout these years. I wish to thank former and present members of my current research group: Dr. Molly Warneke, Dr. Xinxin Han, Dr. Renee Sokupe-Hein, Dr. Jeff Crank, Dr. Ye Bao, Dr. Ping Sun, Dr. Chunlie Wang, Dr. Zach Breitbach, Dr. Ke Huang, Dr. Chunxia Jiang, Tharanga Payagala, Xioatong Zhang, Yasith Nanayakkara, Pritesh, Ying Zhang, Sirantha, Jonathan, Edra, Jason, Ross, Tran, Nilusha, Eva, Qing for their support and friendship.

I also wish to thank Dr. Brian Edwards and Mr. Chuck Savage for help with scientific instrumentation and techniques. I take this opportunity to thank all the faculty members of the Department of Chemistry, University of Peradeniya where I obtained my B.Sc. Special Degree in Chemistry which enabled me to pursue this PhD.

I like to express special thanks to my family; beloved mother, Swarna Wanigasekara, father, Amarapala Wanigasekara (1954-2001) and my sister Maheshika Wanigasekara who always encouraged me in everything I do and bestowed upon me the importance of the education throughout my life. Without my parents' love, kindness, and continuous support I would not have come this far. I wish to thank my wife's family for their love and support as well.

Finally, my sincere gratitude and utmost love is extended to my wife, Tharanga Payagala, who stood by me, supported me, encouraged and backed me up whenever I needed help in science or in the journey of life. You showed me strength when I most needed it and believed in me even when I was not sure myself. You made this possible. Thank you.

November 16, 2010

ABSTRACT

IONIC LIQUIDS IN ANALYTICAL CHEMISTRY AND CALIX[4]ARENE CHEMISTRY OF NO_x GASES

Eranda Wanigasekara, Ph.D.

The University of Texas at Arlington, 2010

Supervising Professor: Daniel W. Armstrong

Application of ionic liquids (ILs) in analytical chemistry can be numerous. The use of ILs in analytical techniques including gas chromatography (GC), electrospray ionization mass spectrometry (ESI-MS), capillary electrophoresis (CE), high performance liquid chromatography (HPLC), solid phase microextraction (SPME) and spectroscopy have attracted great attention of scientific community in the past few decades. Many advancements in this field are due to the development of multiply charged, multifunctional ionic liquids.

This dissertation mainly consists of two parts. The first part focuses on the use of new, structurally diverse, chemically robust ionic liquids for GC, SPME and ESI-MS applications. Within this section, highly thermally stable GC stationary phases with unique selectivities developed using ILs will be discussed. The design and synthesis of

new, flexible linear tricationic ILs will also be discussed. The use of these flexible tricationic ILs as ion pairing reagents in ultra-high sensitive detection of dianionic species in the positive mode of ESI-MS will be presented. Finally, development of a new IL-based silica-bonded polymeric material for SPME-GC headspace and direct immersion analysis will be discussed.

The second part of this dissertation focuses on the use of calix[4]arene-based supramolecular architectures for the complexation of NO_x gases. These calix[4]arene- NO^+ complexes which were prepared by reacting calix[4]arene derivatives with environmentally toxic nitrogen dioxide (NO_2) gas, were then simply reduced for cleaner generation of medically important nitric oxide (NO) gas.

TABLE OF CONTENTS

ACKNOWLEDGEMENTS	iv
ABSTRACT	v
LIST OF ILLUSTRATIONS.....	xiv
LIST OF SCHEMES.....	xviii
LIST OF TABLES.....	xix
Chapter	Page
PART ONE IONIC LIQUIDS IN ANALYTICAL CHEMISTRY	
1. INTRODUCTION.....	2
1.1 General Introduction to Ionic Liquids	2
1.2 Ionic Liquids in Separation Science.....	3
1.2.1 Ionic Liquids in Gas Chromatography	4
1.2.2 Characterization of IL-based GC Stationary Phases	8
1.3 Ionic liquids in Electrospray Ionization Mass Spectrometry	11
1.3.1 Electrospray Ionization Process.....	11
1.3.2 Anion Analysis by Electrospray Ionization Mass Spectrometry	14
1.4 Ionic liquids as Novel Coating Materials for Solid Phase Microextraction (SPME)	19
1.4.1 Sample Preparation in Chemical Analysis	19
1.4.2 Introduction to Solid Phase Microextraction	20

1.5 Organization of Dissertation	28
2. TRIGONAL TRICATIONIC IONIC LIQUIDS: A NEW GENERATION OF GAS STATIONARY PHASES	29
2.1 Abstract.....	29
2.2 Introduction	30
2.3 Experimental Procedures and Methods.....	34
2.3.1 Materials.....	34
2.3.2 Methods.....	34
2.4 Results and Discussion	40
2.4.1 Physical Properties of Trigonal Tricationic ILs.....	40
2.4.2 Ionic Liquid Solvation Parameters.....	44
2.4.3 The Grob Test Mixture.....	50
2.4.4 Alcohols and Alkane mixture.....	53
2.4.5 Flavor and Fragrance Mixture.....	58
2.4.6 Fame Isomer Separation	60
2.5 Conclusions	62
3. LINEAR TRICATIONIC IONIC LIQUIDS: SYNTHESIS, PHYSIOCHEMICAL PROPERTIES AND ELECTROWETTING PROPERTIES.....	64
3.1 Abstract.....	64
3.2 Introduction	64
3.3 Experimental Section	68
3.3.1 General Methods	69
3.3.2 Materials.....	72

3.4 Results and Discussion	78
3.4.1 Synthesis of Core Structures and Linear ILs	78
3.4.2 Physiocochemical Properties of Linear ILs	78
3.4.3 Electrowetting Properties	82
3.5 Conclusions	91
4. EVALUATION OF FLEXIBLE LINEAR TRICATIONIC SALTS AS GAS-PHASE ION-PAIRING REAGENTS FOR THE DETECTION OF DIVALENT ANIONS IN POSITIVE MODE ESI-MS	92
4.1 Abstract.....	92
4.2 Introduction	93
4.3 Experimental Section	96
4.3.1 Materials.....	96
4.3.2 ESI-MS Parameters.....	97
4.4 Results and Discussion	98
4.5 Conclusions	107
5. BONDED IONIC LIQUID MATERIAL FOR SOLID PHASE MICROEXTRACTION GC ANALYSIS.....	108
5.1 Abstract.....	108
5.2 Introduction	109
5.3 Experimental Section	111
5.3.1 Materials.....	111
5.3.2 Synthesis of the IL Derivatized Silica Gel.....	111
5.3.3 SPME Methods.....	115

5.4 Results and Discussion	119
5.4.1 Ethoxylated and Polymeric IL Derivatives	119
5.4.2 Headspace Analyses	120
5.4.3 Immersion Analyses	128
5.4.4 Durability of the IL Fibers	136
5.5 Conclusions	137
PART TWO CALIX[4]ARENE CHEMISTRY OF NO _x GASES	
6. CALIX[4]ARENE CHEMISTRY OF NO _x GASES.....	139
6.1 Introduction	139
6.2 Oxides of Nitrogen	141
6.3 Supramolecular Approaches for Molecular Recognition of Gases ..	143
6.4 Nitric Oxide Releasing Compounds.....	155
7. SUPRAMOLECULAR, CALIX[4]ARENE-BASED COMPLEXES THAT RELEASE NITRIC OXIDE GAS	160
7.1 Abstract.....	160
7.2 Nitric Oxide Generation by a Supramolecular Approach.....	160
7.3 Experimental Section	167
7.3.1 General Experimental Procedures and Methods.....	167
7.3.2 Synthesis of Calix[4]arene Derivatives.....	168
8. NITRIC OXIDE RELEASE MEDIATED BY CALIX[4]MONOHYDROQUINONE	173
8.1 Abstract.....	173
8.2 Introduction	173

8.3 NO Generation by Calix[4]monohydroquinone Systems.....	174
8.3.1 Headspace UV Analysis of Calix[4]monohydroquinone-NO ⁺ Complexes.....	178
8.3.2 Solution Phase UV Analysis of Calix[4]monohydroquinone-NO ⁺ Complexes.....	179
8.4 Experimental Section	182
8.4.1 General Methods and Procedures	182
8.4.2 Synthesis of Calix[4]monohydroquinone	182
9. GENERAL SUMMARY	186
APPENDIX	
1. ¹ H AND ¹³ C NMR OF 1-BROMODECYL-3-BROMODECYL IMIDAZOLIUM BROMIDE (1a)	188
2. ¹ H AND ¹³ C NMR OF 1-BROMOHEXYL-3-BROMHEXYL IMIDAZOLIUM BROMIDE (1b)	193
3. ¹ H AND ¹³ C NMR OF 1-BROMOPROPYL-3-BROMOPROPYL IMIDAZOLIUM BROMIDE (1c).....	198
4. ¹ H AND ¹³ C NMR OF 1-(1'-METHYL-3'-DECYLIMIDAZOLIUM)-3-(1''- METHYL-3''-DECYLIMIDAZOLIUM) IMIDAZOLIUM TRI [BIS(TRIFLUOROMETHANESULFONYL)IMIDE] (2a).....	203
5. ¹ H AND ¹³ C NMR OF 1-(1'-BUTYL-3'-DECYLIMIDAZOLIUM)-3- (1''-BUTYL-3''-DECYLIMIDAZOLIUM) IMIDAZOLIUM TRI [BIS (TRIFLUOROMETHANESULFONYL)IMIDE] (2b).....	210
6. ¹ H AND ¹³ C NMR OF 1-(1'-BENZYL-3'-DECYLIMIDAZOLIUM)-3-(1''- BENZYL-3''-DECYLIMIDAZOLIUM) IMIDAZOLIUM TRI [BIS(TRIFLUOROMETHANESULFONYL)IMIDE] (2c)	216
7. ¹ H, ¹³ C AND ³¹ P NMR OF 1-DECYLTRIPROPYLPHOSPHONIUM-3- DECYLTRIPROPYLPHOSPHONIUM IMIDAZOLIUM TRI [BIS(TRIFLUOROMETHANESULFONYL)IMIDE] (2d)	217
8. ¹ H AND ¹³ C NMR OF 1-(1'-METHYL-3'-HEXYLIMIDAZOLIUM)-3-(1''- METHYL-3''-HEXYLIMIDAZOLIUM) IMIDAZOLIUM TRI [BIS(TRIFLUOROMETHANESULFONYL)IMIDE] (3a).....	229

9. ^1H AND ^{13}C NMR OF 1-(1'-BUTYL-3'-HEXYLIMIDAZOLIUM)-3-(1''- BUTYL-3''-HEXYLIMIDAZOLIUM) IMIDAZOLIUM TRI [BIS(TRIFLUOROMETHANESULFONYL)IMIDE] (3b).....	230
10. ^1H AND ^{13}C NMR OF 1-(1'-BENZYL-3'-HEXYLIMIDAZOLIUM)-3-(1''- BENZYL-3''-HEXYLIMIDAZOLIUM) IMIDAZOLIUM TRI [BIS(TRIFLUOROMETHANESULFONYL)IMIDE] (3c)	231
11. ^1H , ^{13}C AND ^{31}P NMR OF 1-HEXYLTRIPROPYLPHOSPHONIUM-3-HEXYLTRIPROPYLPHOSPHONIUM IMIDAZOLIUM TRI [BIS(TRIFLUOROMETHANESULFONYL)IMIDE] (3d)	245
12. ^1H AND ^{13}C NMR OF 1-(1'-METHYL-3'-PROPYLIMIDAZOLIUM)-3-(1''- METHYL-3''-PROPYLIMIDAZOLIUM) IMIDAZOLIUM TRI [BIS(TRIFLUOROMETHANESULFONYL)IMIDE] (4a).....	252
13. ^1H AND ^{13}C NMR OF 1-(1'-BUTYL-3'-PROPYLIMIDAZOLIUM)-3-(1''- BUTYL-3''-PROPYLIMIDAZOLIUM) IMIDAZOLIUM TRI [BIS(TRIFLUOROMETHANESULFONYL)IMIDE] (4b).....	257
14. ^1H AND ^{13}C NMR OF 1-(1'-BUTYL-3'-BENZYLIMIDAZOLIUM)-3-(1''- BENZYL-3''-PROPYLIMIDAZOLIUM) IMIDAZOLIUM TRI [BIS(TRIFLUOROMETHANESULFONYL)IMIDE] (4c)	263
15. ^1H , ^{13}C AND ^{31}P NMR OF 1-PROPYLTRIPROPYLPHOSPHONIUM-3-PROPYLTRIPROPYLPHOSPHONIUM IMIDAZOLIUM TRI [BIS(TRIFLUOROMETHANESULFONYL)IMIDE] (4d)	268
16. ^1H NMR OF 1,1'-(1,6-HEXANEDIYL)BISIMIDAZOLE (8).....	275
17. ^1H NMR OF 1,1'-(1,6-HEXANEDIYL)BIS- <i>P</i> -VINYL BENZYLIMIDAZOLIUM CHLORIDE (9).....	278
18. ^1H NMR OF 25,27-HYDROXY-26,28-BIS(N-HEXYLOXY)- <i>P</i> - <i>TERT</i> -BUTYLCALIX[4]ARENE (17)	282
19. ^1H NMR OF 25,26,27,28-TETRAKIS(N-HEXYLOXY)- <i>P</i> - <i>TERT</i> -BUTYLCALIX[4]ARENE-1,3-ALTERNATE (10)	285
20. ^1H NMR OF 25,26,27,28-TETRAKIS(N-HEXYLOXY)- <i>P</i> - <i>TERT</i> -BUTYLCALIX[4]ARENE-1,3-ALTERNATE- NO^+ COMPLEX (11)	288

21. ¹ H NMR OF REDUCED 25,26,27,28-TETRAKIS (N-HEXYLOXY)-P-TERT-BUTYLCALIX[4]ARENE- 1,3-ALTERNATE-NO ⁺ (11)	291
22. ¹ H NMR OF CALIX[4]DIMERIC TUBE (12)	294
23. ¹ H NMR OF CALIX[4]DIMERIC TUBE- NO ⁺ COMPLEX (13)	297
24. ¹ H NMR OF REDUCED CALIX[4]DIMERIC TUBE- NO ⁺ COMPLEX (13)...	300
25. ¹ H NMR OF CALIX[4]ARENE TRIMERIC TUBE (14).....	303
26. ¹ H NMR OF CALIX[4]ARENE TRIMERIC TUBE-NO ⁺ COMPLEX (15).....	306
27. ¹ H NMR OF CALIX[4]ARENE REDUCED TRIMERIC TUBE-NO ⁺ COMPLEX (15).....	309
28. ¹ H AND ¹³ C NMR OF 25,26,28-TRIS(N-PROPYL)- <i>P-TERT</i> - BUTYLCALIX[4]MONOQUINONE (19)	312
29. ¹ H AND ¹³ C NMR OF 25,26,28-TRIS(N-PROPYLOXY)- <i>P-TERT</i> - BUTYLCALIX[4]MONOHYDROQUINONE (20)	315
30. ¹ H NMR OF <i>P-TERT</i> -BUTYLCALIX[4]MONOHYDROQUINONE- NITROSONIUM COMPLEX (21).....	320
31. ¹ H AND ¹³ C NMR OF 26,28-BIS(N-PROPYLOXY)-23-NITRO- <i>P-TERT</i> - BUTYLCALIX[4]MONOQUINONE (22)	324
32. FULL CITATIONS OF CHAPTERS 2-8.....	329
33. TGA CUREVES FOR LINEAR TRICATIONIC IONIC LIQUIDS	331
34. SEM IMAGES OF SILICA BONDED SPME COATINGS	335
35. REPRESENTATIVE GC-CHROMATOGRAMS OF SPME HEADSPACE AND IMMERSION ANALYSIS	339
36. RIGHTS AND PERMISSIONS	342
REFERENCES	364
BIOGRAPHICAL INFORMATION	386

LIST OF ILLUSTRATIONS

Figure	Page
1.1 Common cationic groups and anions of ionic liquids	3
1.2 Chromatograms comparing the retention and separation of eight compounds	6
1.3 Volatilization plots for various monocationic ILs	6
1.4 Thermal stability curves for geminal dicationic ILs	8
1.5 Schematic of the electrospray ionization process	13
1.6 Dicationic ion pair association with ClO_4^- ion to form the complex	15
1.7 Comparison of the chromatographic separation and sensitivity of five anions detected in the (A) positive and (B) negative SIM modes	16
1.8 Schematic representations of ion pairing of dianionic species (A) with trigonal tricationic IL-based reagents and (B) with flexible linear tricationic reagents.	18
1.9 Main steps in a chemical analysis (left) and sample preparation (right)	19
1.10 Classification of solvent-free sample preparation techniques	21
1.11 Three main equilibria exist in an SPME process.....	22
1.12 Common components present in a typical SPME device (a) and the configuration of the SMPE needle (b).....	24
1.13 Extraction and desorption procedure for a SPME-GC system	25
1.14 Scanning electron micrographs of a 100- μm inner diameter bare fused silica support (A) and various angles of the fused silica support coated with the poly(ViDDIm ⁺ NTf ₂ ⁻) polymeric IL (B–D)..	27

2.1 Structures of trigonal tricationic ionic liquids used in this analysis.....	35
2.2 Temperature profile for column bleeding in gas chromatography	39
2.3 Graphical representation illustrating the change of retention factor with the temperature treatment on D1, D2, D3 IL phases	43
2.4 X-ray crystallographic representation of C3(mim) ₂ 2Br ⁻ showing stacks along short a – axis and H-bonding	49
2.5 Separation of Grob test mixture in trigonal tricationic IL columns	52
2.6 Separation of homologous alkane and alcohol mixture.....	54
2.7 Comparison of separation of homologous alkane and alcohol mixture	56
2.8 Separation of flavor and fragrance mixture	59
2.9 Separation of a mixture of methyl oleate (5 mg mL ⁻¹) and methyl elaidate (10 mg mL ⁻¹)	61
3.1 Plot of contact angle vs voltage according to Young's and Lippmann's equation.....	67
3.2 Structures of linear tricationic ionic liquids	68
3.3 The electrowetting experimental setup	71
3.4 Structures of ILs 5a-6b	83
3.5 Electrowetting curves of linear tricationic ionic liquids with C6 linkage.....	85
3.6 Electrowetting curves of benzyl substituted linear and rigid type tricationic ionic liquids.....	86
3.7 Electrowetting curves of butyl substituted tricationic ionic liquids.....	88
3.8 Electrowetting curves of C10 core linear tricationic ionic liquids	89
3.9 Electrowetting curves of C3 core linear tricationic ionic liquids	90
4.1 Structures of linear tricationic ion-pairing reagents	95

4.2 Comparison of the detection of sulfate in the positive mode using tricationic ion-pairing reagents D3 (I) and E2 (II).....	103
4.3 Proposed fragmentation pattern for a typical SRM experiment using trication D3.....	104
5.1 Scanning electron microphotographs of fiber IL3.....	116
5.2 Profiles of the relative sorption expressed as [p.a. (t) over p.a. (15 min)] versus headspace exposure time for the polymeric IL 3 SPME fiber	121
5.3 Relative response ratios of analytes in headspace analyses with four ILs and two commercial fibers.....	126
5.4 Relative response ratios of analytes in immersion analyses at pH 2 with two ILs and two commercial fibers.	133
5.5 Relative response ratios of analytes in immersion analyses at pH 11 with two ILs and three commercial fibers (EtOAc reference)..	135
5.6 Relative response ratios of analytes in immersion analyses at pH 11 with two ILs and three commercial fibers (n-Propanol reference).....	136
6.1 Representation of the calix[4]arene and designation of the phases.....	140
6.2 Conformations of calix[4]arenes... ..	140
6.3 Major sources of nitrogen oxides (NO _x) emissions by sector	142
6.4 ORTEP diagram showing the tight binding with limited libration of the noncovalently bound nitric oxide in the complex (left) and the space-filling representation of the NO complex, showing the entrapped NO nestled within the cavity of cofacial phenylene.....	149
6.5 Reversible nature of calix[4]arene-NO ⁺ complex up on addition of water.....	151
6.6 Synthetic calixarene-based nanotubes for NO ₂ /N ₂ O ₄ fixation and high capacity nitrosonium ion (NO ⁺) storage	153
6.7 Partial ¹ H NMR spectra (500 MHz, (CDCl ₂) ₂ , 295 K) of calixtube-NO ⁺ complex.	154

6.8 Potential applications of nitric oxide releasing compounds	156
6.9 Commonly used synthetically produced NO releasing drugs	158
7.1 Calixarene-nitrosonium complex 11 obtained from reacting calixarene with 10 and NO ₂ /N ₂ O ₄ and the generation of NO gas.	161
7.2 NO release experiment using calix[4]arene-NO ⁺ complex	162
7.3 Selected portions of the ¹ H NMR spectra (300 MHz, CDCl ₃ , 295 K) in generation of NO using calix[4]arene-NO ⁺	163
7.4 The UV spectrum (gas phase, 295 K) of NO gas generated from calixarene-NO ⁺ complex 11 and hydroquinone	164
7.5 Filling of calixarene-based nanotubes with nitrosonium and generation of NO gas.	165
7.6 Selected portions of the ¹ H NMR spectra (300 MHz, (CDCl ₂) ₂ , 295 K) in generation of NO using calix ditube	166
8.1 ¹ H NMR spectra (300 MHz, CDCl ₃ , 295 K) illustrating NO ⁺ complexation and release in calix[4]monohydroquinone system	176
8.2 UV spectrum of the head space gas generated from the calix[4]monohydroquinone-NO ⁺ complex	179
8.3 Solution phase UV analysis of calix[4]monohydroquinone-NO ⁺ complex.....	180
8.4 UV UV-Vis spectrum of NO ⁺ complex prepared by <i>p-tert</i> -butylcalix[4]monohydroquinone 20 and <i>t</i> -BuONO in presence of TFA.....	184

LIST OF TABLES

Table	Page
2.1 Solute descriptor values for all the probe molecules used in this analysis	36
2.2 Physical properties of the trigonal tricationic ILs used as stationary phases	38
2.3 Variation of retention factors (k_{naph}) with thermal treatment of D core trigonal tricationic IL columns	43
2.4 Interaction parameters obtained for trigonal tricationic IL stationary phases	45
2.5 Comparison of the intraction parameters of monocationic and dicationic RTILs with trigonal tricationic ionic liquids	47
3.1 Physicochemical properties of linear tricationic ionic liquids	79
3.2 Electrowetting properties of linear tricationi ionic liquids	83
4.1 Limits of detection for divalent anions with linear tricationic reagents	99
4.2 Comparison of LODs in the SIM positive and SRM positive modes	105
5.1 Characteristics of the silica bonded ionic liquid adsorbents for SPME	116
5.2 Analytical figures of merit obtained for polar solutes extracted for 15 min at 50 °C in headspace SPME with different fibers	123
5.3 SPME results obtained with fiber IL4 in the ethanol analysis of real samples	127
5.4 SPME results obtained with different fibers by immersion in two different pH solutions	130

LIST OF SCHEMES

Scheme	Page
1.1 Synthesis of the polymeric ionic liquids evaluated as SPME coatings	27
3.1 Synthesis of LTIL with R-substituted methyl imidazole as the charge carrying moiety	68
5.1 Synthesis steps involved in the preparation of silica bonded IL material.....	113
6.1 Encapsulation of CO ₂ within the hemicarcerand developed by Cram et al	145
6.2 Molecular recognition of gases in nature	146
6.3 Encapsulation complexes of NO _x gases with calix[4]arenes and the X-ray crystal structure of the complex.....	148
6.4 Encapsulation complexes of NO _x gases with calix[4]arenes cone conformer (top) and the 1,3-alternate conformer (bottom)	150
6.5 Biosynthetic pathway of NO by L-arginine.....	157
7.1 Synthetic route for <i>o</i> -alkylated calix[4]arene <i>1,3 alternate</i>	168
8.1 Synthesis of tripropoxycalix[4]monohydroquinone.....	175
8.2 Generation of NO using calix[4]monohydroquinone	177
8.3 <i>ipso</i> nitrosation followed by oxidation of calix[4]monohydroquinone	180

PART ONE
IONIC LIQUIDS IN ANALYTICAL CHEMISTRY

CHAPTER 1

INTRODUCTION

1.1 General Introduction to Ionic Liquids

Ionic liquids (ILs) are a class of liquid compounds which are solely composed of ions.^{1,2,3} These ions often consist of a bulky organic cationic group and an inorganic or organic anionic group. Typical cations are based on imidazolium, pyridinium, phosphonium, pyrrolidinium or ammonium groups or their derivatives. Common anions include halides (X^-), nitrate (NO_3^-), cyanide (CN^-), tetrafluoroborate (BF_4^-), hexafluorophosphate (PF_6^-), trifluoromethanesulfonate (TfO^-) and bis[(trifluoromethyl)sulfonyl]amide (NTf_2^-) (see Figure 1.1). Although diverse chemistries can be used to form different types of ILs, their successful utilization remains a challenging task.

The term “room temperature ionic liquid” (RTIL) is used to classify ILs which exist in the liquid state at or below ambient temperatures. The first RTIL, ethylammonium nitrate (mp 12 °C), was reported by Paul Walden in 1914.⁴ However there are reports indicating that the first IL was discovered in 1888 by Gabriel and coworkers.⁵ It has been proposed and shown that these ILs can be used in place of volatile and non-eco friendly organic solvents which are used extensively in chemical manufacturing processes.⁶⁻⁸ During the past few years, ionic liquids have attracted much attention from academic and industrial community due to their remarkable physicochemical properties.^{6,9} As a result, there has been an exponential growth in the number of articles published related to ionic liquids.^{10,11}

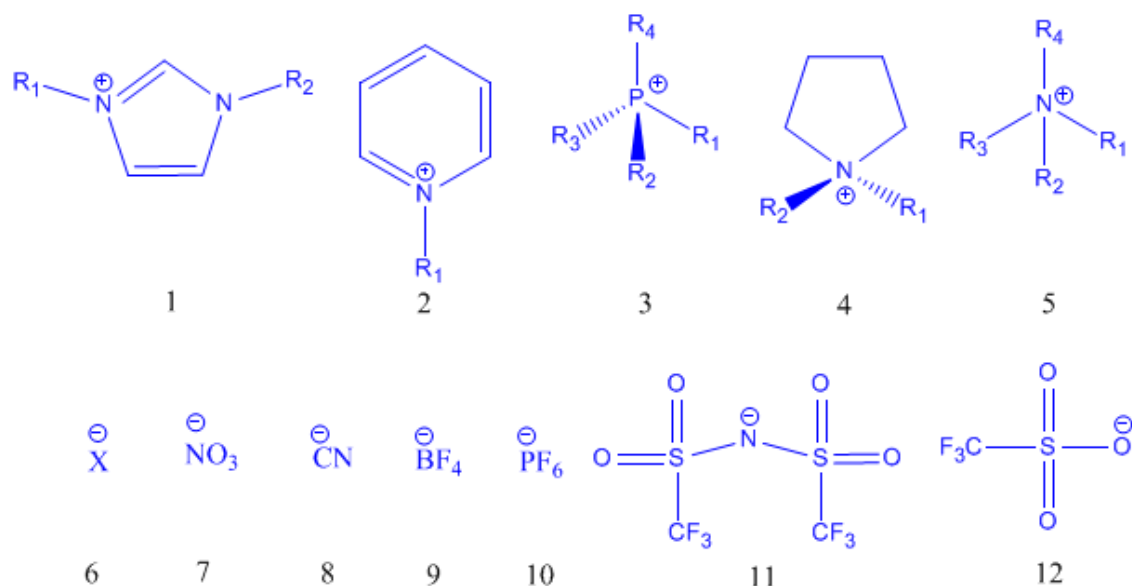


Figure 1.1 Common cationic groups and anions of ionic liquids.

Cations: 1, Imidazolium; 2, Pyridinium; 3, Phosphonium, 4, Pyrrolidinium, 5, Tetraalkyl ammonium; 6, Halides (Chloride, Bromide, Iodide); 7, Nitrate; 8, Cyanide, 9, Tetrafluoroborate; 10, Hexafluorophosphate; 11, bis(trifluoromethanesulfonyl)imide

Ionic liquids are often considered as “designer solvents.” This is because the unique properties of ILs (solvating power, miscibility with water and other solvents, viscosity, polarity, density, thermal stability, electrochemical window, conductivity, surface tension, flammability, etc) can be tuned by choosing an appropriate cation and anion combination.¹²⁻²¹ These unique physicochemical properties make ILs superior to conventional molecular liquids in that the tailoring of the properties of molecular solvents are limited or more often nonexistent.

1.2 Ionic liquids in Separation Science

ILs are widely considered as alternatives to classical organic solvents and have been applied in many fields of chemistry such as organic synthesis, electrochemistry, liquid-liquid extraction and catalysis for clean technology and polymer synthesis.²²⁻⁴²

Similarly the unique properties of ILs have made them favorable for few separation science applications as well. During the past decade, ILs have been used extensively as highly thermally stable gas chromatographic (GC) stationary phases, liquid chromatographic (LC) stationary phases and mobile phase additives in capillary electrophoresis (CE) and LC.⁴³⁻⁵⁰

1.2.1 Ionic Liquids in Gas Chromatography

1.2.1.1 Monocationic Ionic Liquids

In 1959, Barber *et al.* used stearates of divalent manganese, cobalt, nickel, copper, and zinc as liquid phases in gas chromatography. This was the first example of using salts as GC stationary phases in the literature.⁵¹ Here, separations of amines, alcohols and ketones were achieved with relatively low but acceptable efficiencies. Then in 1982, ethylammonium nitrate (mp 12 °C) and 1-ethylpyridinium bromide (mp 110 °C) were introduced as GC stationary phase by Pacholec and Poole.^{52,53} The operating ranges for ethylammonium nitrate and ethylpyridinium bromide phases were 40-120 °C and 110-170 °C respectively. These GC phases showed acceptable selectivities for polar and H-bonding analytes. However they suffered from poor column efficiencies and low thermal stabilities. In addition, these phases did not perform as well with non-polar analytes as they showed no significant retention for hydrocarbons.

In 1999 Armstrong *et al.* developed the first imidazolium-based monocationic ionic liquid stationary phase for GC.⁴⁶ Initial studies were carried out based on the 1-butyl-3-methylimidazolium [BuMIm] cation combined with chloride (Cl⁻), hexafluorophosphate (PF₆⁻) and tetrafluoroborate (BF₄⁻) anions. Retention and separation behaviors of these new [BuMIm] IL GC phases were compared with several commercial GC phases. It was found that these IL phases exhibit an unusual selectivity

with a “dual-nature.” That is they can separate polar compounds as if they were polar phases and non polar compounds as if they were non polar phases. This study suggested the potential of using imidazolium-based ILs as multi-modal separation media (see Figure 1.2). Four years later, in 2003 Anderson and Armstrong introduced benzylimidazolium-based ILs as GC stationary phases which were thermally stable, nearly up to 260°C.⁴⁴ Figure 1.3 shows the change in thermal stabilities depending on the counter anion of the IL system. Relative thermal stabilities of these ILs were affected by the type of anions and the order of stability is as follows: $\text{PF}_6^- > \text{NTf}_2^- \approx \text{BF}_4^- > \text{AsF}_6^- > \text{I}^-, \text{Br}^-, \text{Cl}^-$. 1-benzyl-3-methylimidazolium triflate (BeMIM-TfO) and 1-(4-methoxyphenyl)-3-methylimidazolium triflate (MPMIM-TfO) have shown the highest thermal stabilities out of the series investigated (see Figure 1.3).

These new ILs produced GC phases with efficiencies (determined by retention of naphthalene at 100 °C) of 1900-2800 plates per meter. The polarities and solvation parameters of these monocationic ILs were characterized by Rohrschneider–McReynolds constants and according to the Abraham solvation parameter model.^{54,55} The new benzylimidazolium-based IL phases gave symmetrical peak shapes and good peak efficiencies for both polar and non polar analytes in general. Also, two of these new phases (BeMIM and MPMIM) were shown to yield rapid separations with different selectivities and retention orders for complex mixtures (isomeric sulfoxides, poly chlorinated benzenes, etc) when compared to commercial GC phases such as DB-5 (5%-phenyl-methylpolysiloxane). In addition the “dual-nature” of the phases was also observed.

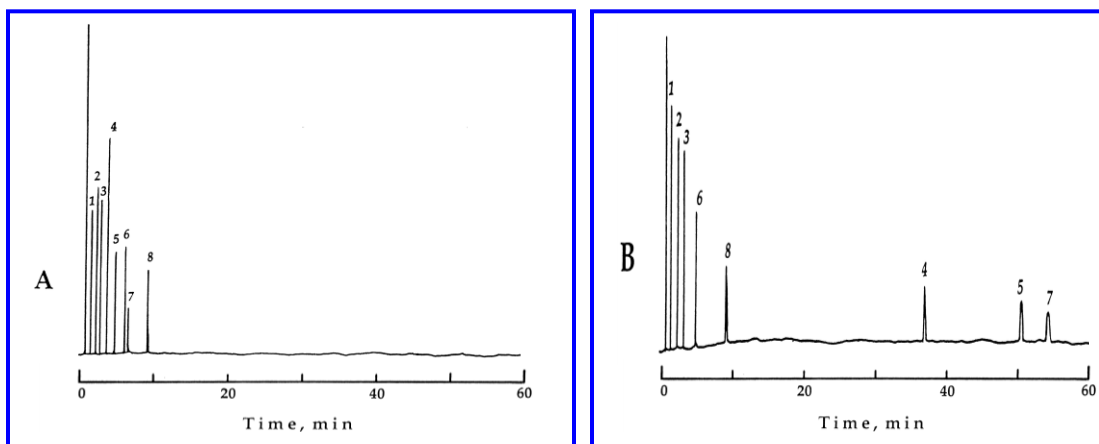


Figure 1.2 Chromatograms comparing the retention and separation of eight compounds.

Separated on the same size GC columns (15 m \times 0.25-mm i.d.) and under identical conditions (isothermal @ 100 °C). Column A (left) is a commercial DB-5 column, and Column B (right) utilizes the ionic liquid [BuMIm][PF₆] as the stationary phase. The test compounds are: 1, butyl acetate; 2, *n*-heptanol, 3, *p*-dichlorobenzene, 4, *o*-cresol, 5, 2,5-dimethylphenol, 6, *n*-dodecane, 7, 4-chloroaniline, and 8, *n*-tridecane. Reproduced with permission from reference 46.

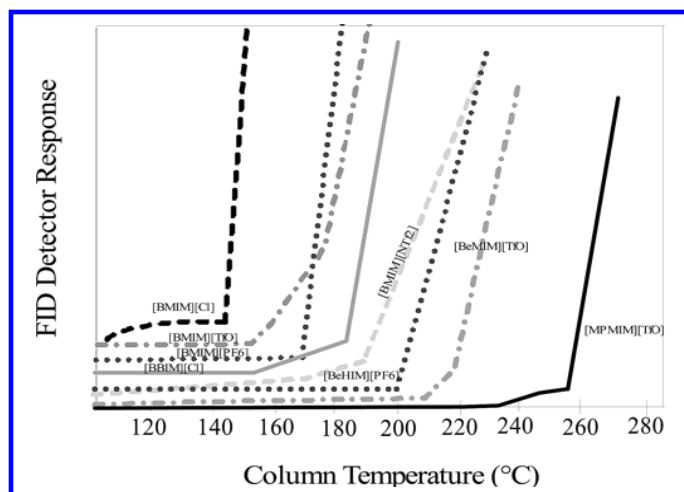


Figure 1.3 Thermal volatilization plots for various monocationic ILs.

Here RTILs include BMIM (1-Benzyl-3-methyl), BBIM (1,3-dibutyl), BeMIM (1-Benzyl-3-methyl), BeHIM (1-Benzyl-3-hexyl), MPMIM, BMIM-Cl (~145 °C), BMIM-TfO (~175 °C), BMIM-PF₆ (~170 °C), BBIM-Cl (~180 °C), BMIM-NTf₂ (~185 °C), BeHIM-PF₆ (~200 °C), BeMIM-TfO (~220 °C), and MPMIM-TfO (~250 °C). Reproduced with permission from reference 44.

1.2.1.2 Dicationic Ionic Liquids

Unlike monocationic ILs, geminal dicationic ionic liquids consist of two cationic groups (imidazolium, phosphonium, pyridinium, pyrrolidinium, etc) tethered together with a straight or branched chain alkane.^{56,45} Anderson *et al.* in 2005 reported the use of thirty nine dicationic ionic liquids as GC phases and characterized them by using the Abraham solvation parameter model. It has been shown that the thermal stabilities of these dicationic ILs are greater than those for many of the monocationic ILs. A comparison of the thermal stabilities of these dicationic ILs and monocationic ILs are shown in Figure 1.4.

The use of tricationic ILs, a third generation of ILs as GC stationary phases, their new separation capabilities, selectivities towards specific analyte types and stationary phase characterization using linear solvation energy relationship (LSER) will be discussed in subsequent chapters.

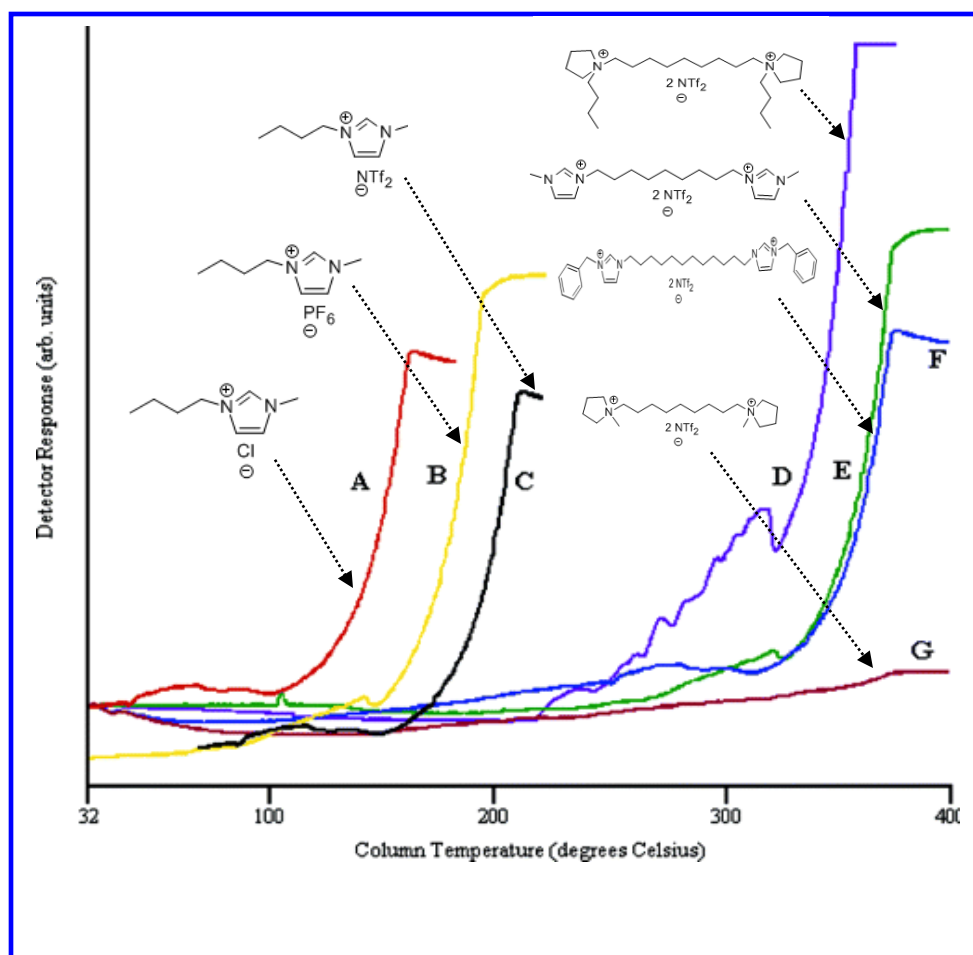


Figure 1.4 Thermal stability curves for geminal dicationic ILs.

The plot illustrates the fact that the geminal dicationic ionic liquids (D–G) have thermal stabilities much higher than those of conventional ionic liquids (A–C). (A) 1-Butyl-3-methylimidazolium chloride (BMIM-Cl); (B) BMIM- PF_6 ; (C) BMIM- NTf_2 ; (D) 1,9-Bis(butylpyrrolidinium-1-yl)nonane $\text{C}_9(\text{bpy})_2\text{-NTf}_2$; (E) 1,9-Bis(3-methylimidazolium-1-yl)nonane $\text{C}_9(\text{mim})_2\text{-NTf}_2$; (F) 1,12-Bis(3-benzylimidazolium-1-yl)dodecane $\text{C}_{12}(\text{benzim})_2\text{-NTf}_2$; (G) 1,9-Bis(methylpyrrolidinium-1-yl)nonane $\text{C}_9(\text{mpy})_2\text{-NTf}_2$.

Reproduced with the permission from reference 56.

1.2.2 Characterization of IL-based GC Stationary Phases

Recently, significant research efforts have been made towards the development of methods to determine polarities of solvents including ionic liquids. Solvent polarity

plays a major role in organic synthesis affecting product ratios, product yields, reaction rates, reaction pathways, and also in catalysis, extractions, and chromatographic separations.^{43,57-61} In 1979 Reichardt introduced an empirical solvent polarity parameter model based on solvatochromism.⁶² Here the shift of absorption maxima of solvatochromic dyes were measured for solvents with different polarities. Then, an empirical solvent polarity model was derived by correlating the absorption maxima of the solvatochromic dye which was used to evaluate the solvent of interest. Most commonly used solvatochromic probes include Reichardt's dye, Nile Red, dansylamide, pyrene, and 1-pyrenecarbaldehyde.^{66,67}

In 1999 Armstrong *et al.* successfully developed an inverse GC method which used the Rohrschneider-McReynolds polarity parameters to characterize ionic liquids.⁴⁶ In ionic liquid GC stationary phases, the thin liquid coating is considered the solvent and the analytes which are separated by this phase is known as solutes. In the Rohrschneider-McReynolds method that was used to characterize IL-based GC phases utilized a total number of five probe solutes.⁴⁶ These are: benzene, *n*-butanol, 2-pentanone, nitropropane and pyridine. Each probe molecule undergoes specific interactions with the liquid phase (solvent). For example, benzene which is a soft base in the gas phase can interact with the liquid stationary phase via π - π interactions and therefore act as an indicator for the solvent's π -bonding ability. Similarly *n*-butanol indicates the hydrogen bonding ability of the chromatographic phase. Use of 2-pentanone, which has an intermediate polar character, indicates the polarizability and dipolar character of the stationary phase. Nitropropane, a strongly polar aprotic molecule, represents retention behavior due to the electron donor, electron acceptor, and dipolar character of the phase. Pyridine, being a strong proton acceptor and a

polar molecule, indicates the acidic nature of the liquid stationary phase. Rohrschneider-McReynolds constants of ionic liquid GC phases were determined by using squalane as the reference stationary phase.⁶³ The empirical solvent polarity values were obtained by averaging the Rohrschneider-McReynolds constants of each probe molecule to get a single polarity parameter. For all ionic liquids this average value falls in the same constricted range.⁶⁴⁻⁶⁷ Thus two ionic liquids may have a similar “polarity parameter,” yet produce very different results when they are used in applications such as solvents for organic synthesis, in extractions or as GC stationary phases. The major drawback of using this method to characterize IL-based GC stationary phases is that it only uses five probe molecules which is not sufficient to fully elucidate the complex interaction capabilities of IL-based GC phases. Therefore this single parameter solvent polarity method was deemed not comprehensive for the characterization of ionic liquids.

1.2.2.1 Abraham’s Linear Solvation Energy Relationship (LSER)

Linear Solvation Energy Relationship (LSER) is a mathematical model based on linear regression analysis. This was developed by Abraham *et al.* and is now the most widely accepted method for the characterization of gas chromatographic phases or liquid chromatographic stationary phases.^{54,55,68-70} This method uses large pool of probe molecules (>25) which can interact with the ionic liquid stationary phase through various types of interactions. The LSER is given by eq 1:

$$\log k' = c + eE + sS + aA + bB + lL \dots\dots\dots (1)$$

Where,

E = excess molar refraction

S = dipolarity/ polarizability

A = hydrogen bond acidity

B = hydrogen bond basicity

L = gas-hexadecane partition coefficient

Solute descriptors

k' = retention factor of the analyte

c = system constant

e = π - and n-electron interaction

s = dipole type- interaction

a = hydrogen bond basicity

b = hydrogen bond acidity

I = dispersion force

Solvent descriptors

(Determined by Multiple
Linear Regression Analysis)

The solute descriptor values are evaluated and available in the literature.⁵⁴ The use of this LSER to characterize novel IL-based GC stationary phases will be discussed in later chapters.

1.3 Ionic liquids in Electrospray Ionization Mass Spectrometry

1.3.1 Electrospray Ionization Process

The concept of electrospray has been known about for over a hundred of years, but it was not until 1937 that its significance to science was understood.⁷¹ Later, in 1965 Dole *et.al* demonstrated the use of electrospray ionization (ESI) to ionize intact chemical species (a dilute polymer solution)⁷² and this is considered to be the first example of the use of ESI. Subsequently, 20 years later John Fenn demonstrated that the ESI technique can be used to ionize large biomolecules which could be analyzed

by mass spectrometry. This work lead John Fenn to win the Nobel Prize in 2002.⁷³ Nowadays, electrospray ionization mass spectrometry (ESI-MS) has become a versatile research tool which has shown great potential in all fields of chemistry including analytical chemistry.⁷³⁻⁷⁹ ESI-MS is considered as a soft ionization technique that will produce fewer fragments of the molecule during the electrospray process. ESI-MS has proven to be an effective tool in analyzing large biomolecules, peptides, proteins, biopolymers and inorganic ions. In the ESI-MS process, a high voltage (± 2 -5 kV) is applied to the spray needle which is kept in a coaxial flow of nitrogen which is the nebulizing gas. This creates a fine liquid aerosol consisting of very small droplets, each of which carries many excess charges at its surface. Once the solution containing analyte molecules is pumped through this spray needle with a low flow rate (0.1-100 μL), a high voltage causes analyte charging typically due to their acid/base properties. The electrospray voltage can be either positive or negative. In the positive mode, anionic species are attracted to the positively charged needle and the cationic species are repelled away from the needle tip. This process causes the formation of a "Taylor cone" which contains an excess of either positively or negatively-charged ions depending on the operating ion mode.⁸⁰ A schematic representation of the ESI process is shown in Figure 1.5.

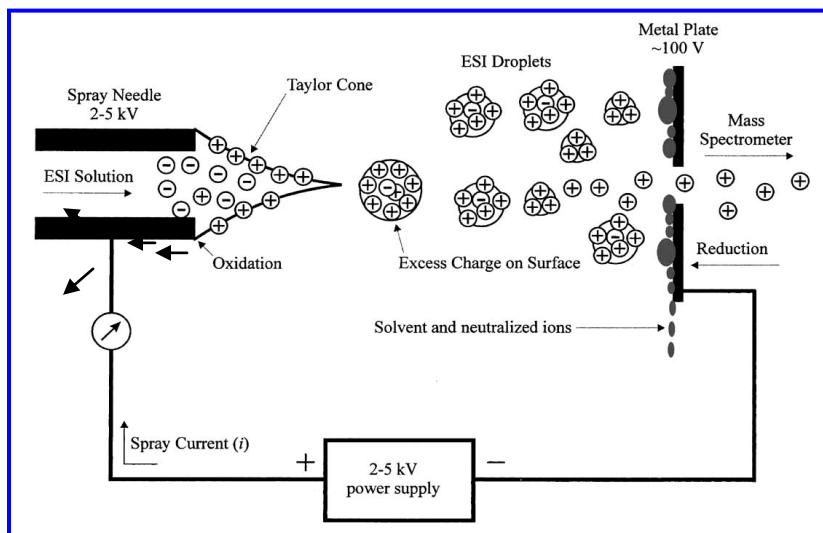


Figure 1.5 Schematic of the electrospray ionization process. Reproduced with permission from reference 80.

At a certain point, where the coulombic repulsion of the surface charge of the solution that comprises the Taylor cone is equal to the surface tension of the solvent, also referred to as the Rayleigh limit, droplets containing either excess positive or negative ions detach from the spray tip as a fine mist which is referred as the spray jet. After that, the detached charged droplets move from atmospheric pressure towards the high vacuum regions (1×10^{-5} Torr) through a high voltage gradient. During this migration naked ions are generated according to either of the two widely accepted mechanisms; the ion evaporation model^{81,82} and/or the charge residue model.^{72,83} According to the charge residue model, charge density of the droplet is increased due to the evaporation of the solvent which causes droplets to be disintegrated into smaller droplets which eventually consist of single ions. According to the ion evaporation model, increased charge density due to the solvent evaporation eventually causes coulombic repulsion to overcome the liquid's surface tension, resulting in a release of single ions from the droplet surface.

1.3.2 Anion Analysis by Electrospray Ionization Mass Spectrometry

High sensitive detection of anions is important in many areas of chemistry such as beverage and food industry,⁸⁴⁻⁸⁷ soil analysis,⁸⁸⁻⁹¹ environmental analysis,⁹²⁻¹⁰² water quality¹⁰³ and many others. A number of analytical techniques have been developed for anion analysis including ion chromatography,^{86,87,104-108} spectrophotometry,^{88,89,109-111} capillary electrophoresis,^{88,90,110,112-114} electrochemical methods (conductometry, amperometry, potentiometry),¹¹⁵⁻¹¹⁸ and flow injection analysis.^{109,119} These detection techniques may or may not include a separation method prior to the analysis.

Numerous research efforts have been put forward by scientists to use ESI-MS in the analysis of anions in a continuous effort to improve sensitivity.^{86,94,95,98,100,101,108,120-126} In general, anionic species are analyzed in the negative mode. However many inorganic anions have masses that fall below the low mass cutoff of the instrument and are unidentified in the negative ion mode. In addition, negative mode analysis has few inherent disadvantages such as poor spray stability and lower sensitivities.¹²⁷⁻¹²⁹ Typically charged solvent clusters and other interfering low mass ions give rise to higher background noise in lower mass regions. Negative ion mode is also more prone to corona discharge than the positive mode.⁸⁰ These corona discharges cause higher background noise which will lower the sensitivities. Reversed phase solvents such as water, methanol and acetonitrile are known to increase corona discharge in the negative mode thereby limiting the use of LC-MS for anion analysis. However use of halogenated solvents (CH_2Cl_2 , CHCl_3) and gases (SF_6) are known to act as electron scavenging media which can make the analyte signal more stable.¹³⁰

Recently, Martinelango et al. described a method of using dicationic IL-based ion pairing reagents to detect perchlorate ions (ClO_4^-) present in environmental samples.¹²⁰ This analysis was performed in the positive mode of ESI-MS. The dicationic ion pairing agent was allowed to complex in solution with perchlorate anions (see Figure 1.6). Then this complex mass was monitored using the SIM (Selected Ion Monitoring) mode. Instead of detecting ClO_4^- in the negative ion mode, it can now be detected at a higher mass range in the positive mode of ESI-MS where less noise is observed. Therefore this technique gives improved detection limits and higher sensitivities.¹²⁰

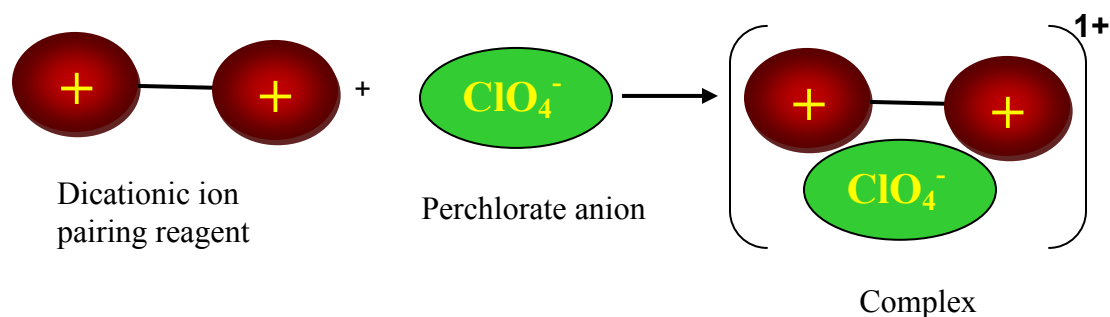


Figure 1.6 Dicationic ion pair association with ClO_4^- ion to form the complex

Later this technique was employed by Soukup *et al.* to detect a series of organic and inorganic anions with much higher sensitivities compared to the negative ion mode. For example, thiocyanate (SCN^-) could not be detected in the negative mode (injected 14.3 ng) but was detected in the positive mode after complexing it with a dicationic ion pairing reagent. This detection was achieved with a higher sensitivity even when the injected amounts were ten times less than that used for the negative mode analysis (see Figure 1.7).¹²⁷

Later in 2006, Armstrong and coworkers extended this technique to detect doubly-charged anions using IL-based trigonal tricationic ion pairing reagents.¹²⁸ Several synthesized tricationic IL-based salts were successfully evaluated as ion pairing reagents for detecting dianionic species in the positive mode of ESI-MS.

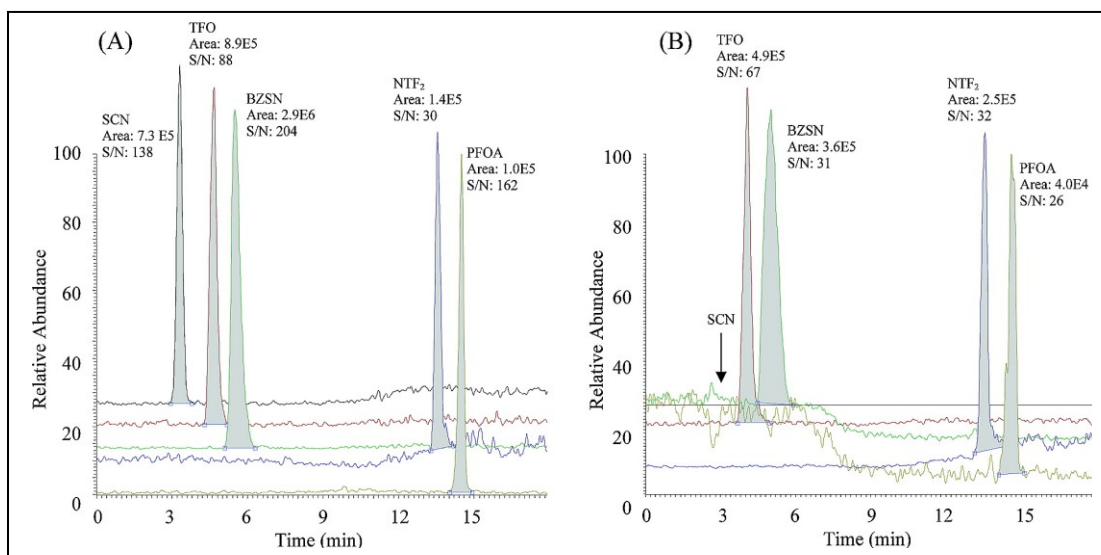


Figure 1.7 Comparison of the chromatographic separation and sensitivity of five anions detected in the (A) positive and (B) negative SIM modes.

The mass injected in B is 10× that of A for SCN, TfO, and BZSN; 5× for PFOA; and the same for NTf₂. The mass injected in A is 1.43 ng SCN, 9.92 ng TfO, 1.16 ng BZSN, 0.68 ng NTf₂, and 1.30 ng PFOA. The column (Cyclobond I) was equilibrated for 15 min with 100% water with a linear gradient to 100% MeOH beginning at 3 min and complete at 9 min. The flow rate was 300 µL/min. In A, the dicationic salt solution (40 µM in MeOH) was added post column at 100 µL/min whereas in B it is methanol only.

SCN, thiocyanate; TfO, triflate; BZSN, benzenesulfonate; PFOA, perfluorooctanoic acid; NTf₂, trifluoromethanesulfonimide. Reproduced with permission from the reference 127.

However, the tricationic ion pairing agents used in this study had rigid trigonal structures. In the previous dicationic ion pairing study it had been determined that flexibility was a desired structural feature of good ion pairing agents.¹²⁸ Thus, more flexible tricationic ion pairing reagents were synthesized and tested for their efficacy to

bind dianions in comparison to the rigid counterparts. It was expected that the structural flexibility would play a role in gas phase ion association. Unlike rigid trigonal structures, linear tricationic IL-based salts have more conformational freedom to pair with anionic species, in both solution and in gas phase. Synthesis and use of these linear tricationic IL-based salts as ion pairing reagents in anion analysis will be discussed further in the following chapters. Figure 1.8 illustrates rigid trigonal and linear tricationic ion association with dianionic species.

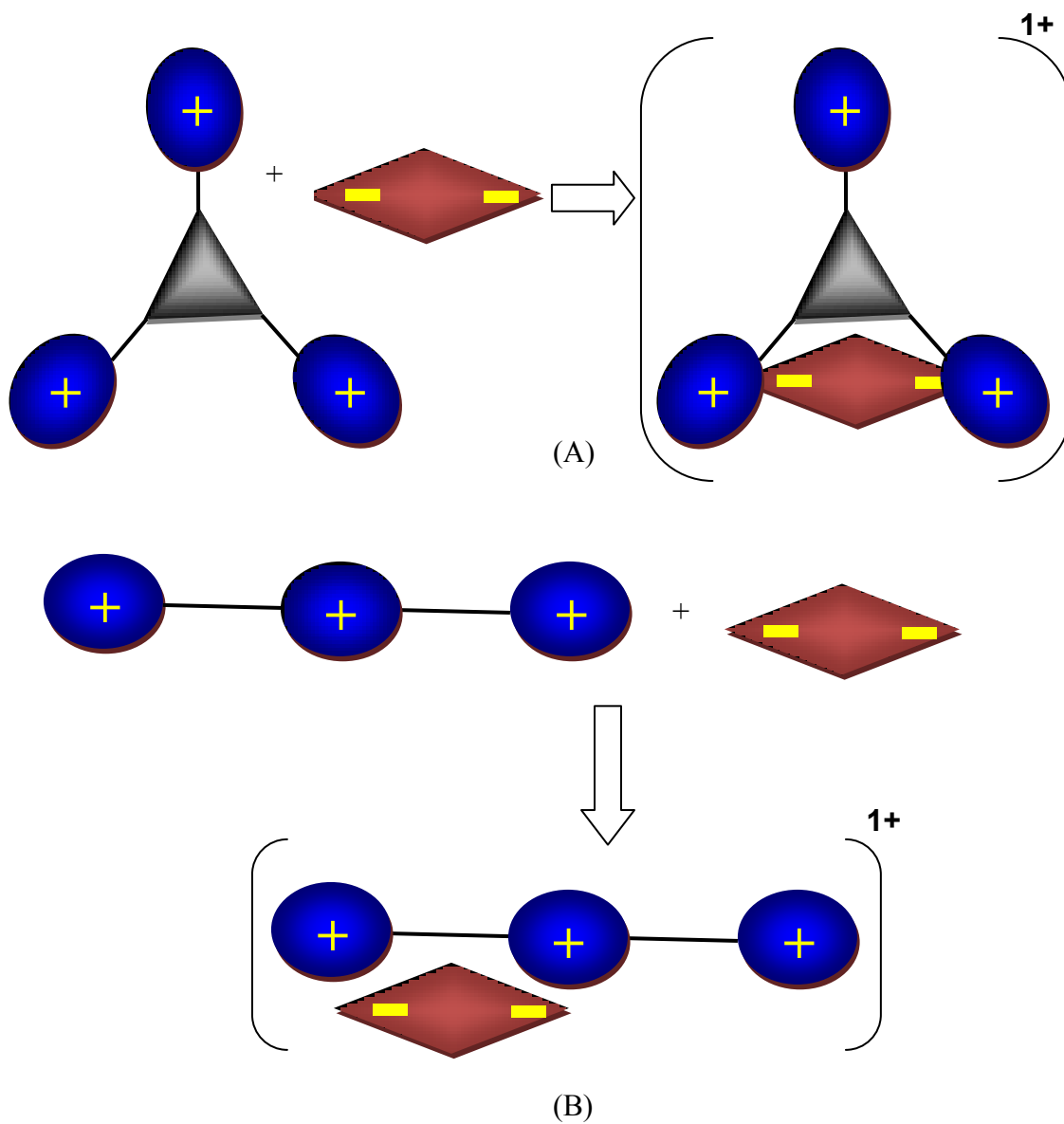


Figure 1.8 Schematic representations of ion pairing of dianionic species (A) with trigonal tricationic IL-based reagents and (B) with flexible linear tricationic reagents.

(Trications are represented in blue and dianion is represented in red.)

1.4 Ionic liquids as Novel Coating Materials for Solid Phase Microextraction (SPME)

1.4.1 Sample Preparation in Chemical Analysis

The main steps involved in a chemical analysis and sample preparation are shown in Figure 1.9. Sample preparation is a very important step and the first step is the sample collection from the appropriate source. The next step is sample preservation. Preservation prevents the degradation of analytes of interest present in the collected sample. Although complete preservation is practically impossible, a significant reduction of degradation or contaminations can be minimized by using standard sample preservation methods available in the literature.¹³¹⁻¹³³

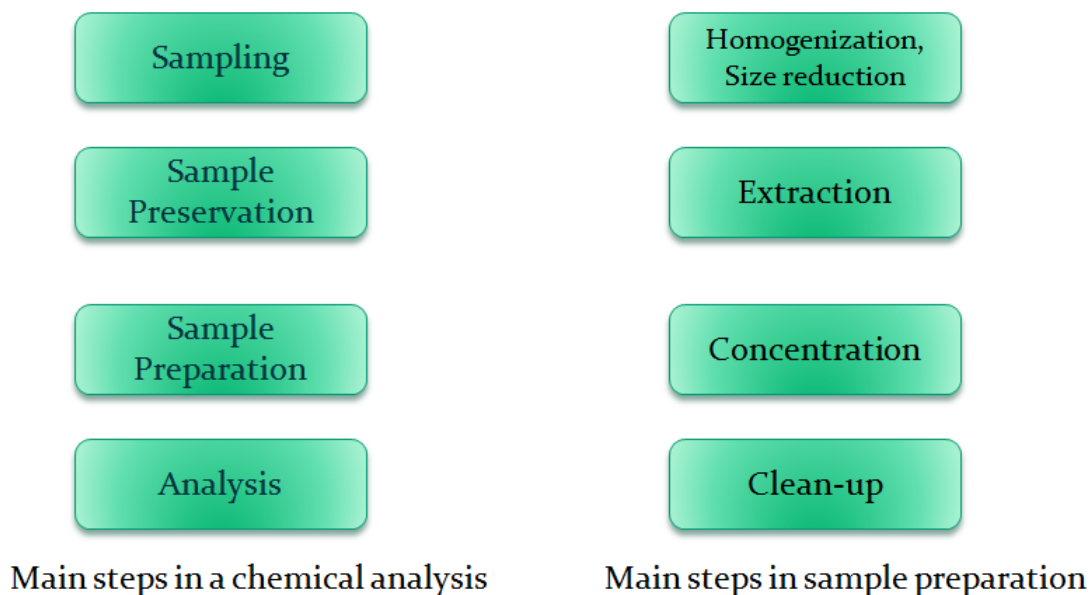


Figure 1.9 Main steps in a chemical analysis (left) and sample preparation (right).¹³⁴

After the sample collection and proper preservation, the next step is the sample preparation.¹³⁴ Most samples are not ready to be introduced into the analytical instrument directly after collection. Biological and environmental samples have to be properly prepared prior to the analysis.

For example, in pharmacokinetics and pharmacodynamics (PK/PD) of a blood plasma sample, direct injection is impossible because of the high background matrix signals. The pharmaceutically active ingredients first have to be extracted from the plasma and then subjected to further analysis.

Commonly used sample extraction techniques can be divided into two main categories, namely classical and modern techniques. Extraction techniques such as liquid-liquid, liquid-solid, membrane and protein precipitation are considered to be classical methods where as solid phase extraction (SPE), solid phase microextraction (SPME), accelerated fluid extraction (AFE), supercritical fluid extraction (SFE) and microwave assisted extraction (MAE) techniques are classified as modern extraction methods.

SPME is one of the fastest growing solvent-free sample preparation techniques. Figure 1.10 illustrates the classification of solvent-free sample preparation methods.

1.4.2 Introduction to Solid Phase Microextraction

Although multi-dimensional techniques such as gas chromatography-mass spectrometry (GC-MS) have improved separation and quantification, the sample preparation step is still the most time consuming step in a chemical analysis. Classical, liquid-liquid extraction type sample preparation techniques often use a significant volume of organic solvents. SPME simplifies the sample preparation step and is a solventless technique. SPME was invented in 1989 by Janusz Pawliszyn, a scientist from University of Waterloo, Canada.

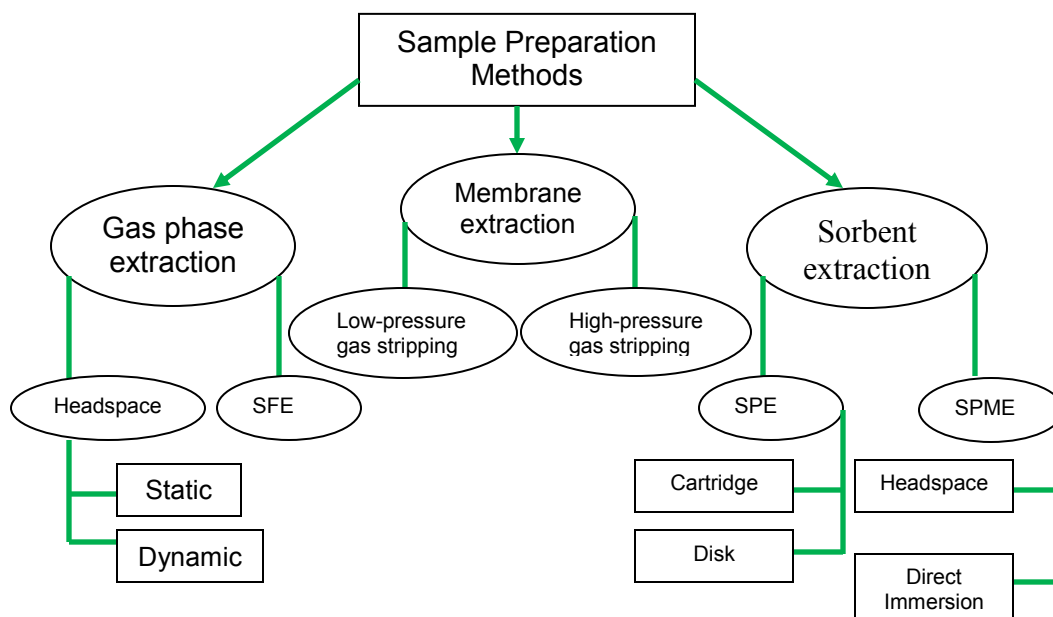


Figure 1.10 Classification of solvent-free sample preparation techniques.¹³⁵

In the SPME process, the amount of extraction solvent (extraction phase) is very small compared to the sample volume. As a result, exhaustive removal of analytes to the extracting phase does not occur, rather an equilibrium is established in between the sample matrix and the extracting phase.

1.4.2.1 Theory and overview of SPME

Solid phase extraction is driven by a non equilibrium process. However SPME process is a multiphase equilibrium process.¹³⁶⁻¹³⁸ Theory has been developed to understand the principle process of SPME by applying basic fundamentals of thermodynamics and mass transfer. Effective use of theory minimizes the number of experiments to be carried out during an analysis.¹³⁶ Both thermodynamic and kinetic parameters have been assessed when developing the theory for multiphase equilibria

that exist in the SPME process.¹³⁹ Development of theoretical models for the SPME process was reported by Pawliszyn and coworkers in 1992.¹⁴⁰

There are three main equilibria that exist in SPME process which are shown in Figure 1.11.

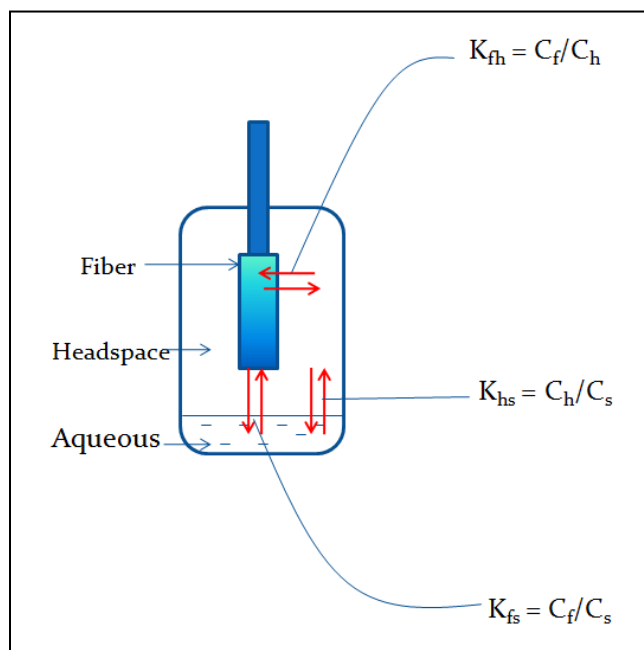


Figure 1.11 Three main equilibria exist in a typical SPME process.

Here K_{fs} = distribution constant between fiber and the sample, K_{hs} = distribution constant between headspace and the sample, K_{fh} = distribution constant between fiber and the head space, C_f , C_s and C_h represent the concentration of the analyte in fiber, sample and in headspace respectively.

Using the distribution constants it was shown that amount of an analyte adsorbed by the fiber coating n , can be written as:

$$n = \frac{K_{fs}K_{hs}C_0V_s}{K_{fs}V_f + K_{hs}V_h + V_s} \dots \dots \dots (2)$$

Where,

n = amount of analyte adsorbed by the coating

C_0 = initial concentration of analyte in the sample

K_{fs} = distribution constant of the analyte between coating and sample matrix

K_{hs} = distribution constant of the analyte between the headspace and sample matrix

V_f = volume of the coating

V_s = volume of the sample

By assuming that the vial containing the sample is fully filled with the aqueous phase and the headspace volume is negligible, then the $K_{hs}V_h$ term is zero. Therefore equation 2 can be written as:

$$n = \frac{K_{fs}V_fC_0V_s}{K_{fs}V_f + V_s} \dots \dots \dots (3)$$

If the volume of the aqueous sample V_s is much larger than the volume of the extracting stationary phase V_f , then the $V_s \gg K_{fs}V_f$. Therefore the equation 3 can be written as:

$$n = K_{fs}V_fC_0 \dots \dots \dots (4)$$

Therefore, when the sample volume is much higher than the volume of the extracting phase, the amount extracted does not depend on the volume of the sample.

1.4.2.2 SPME device and operation

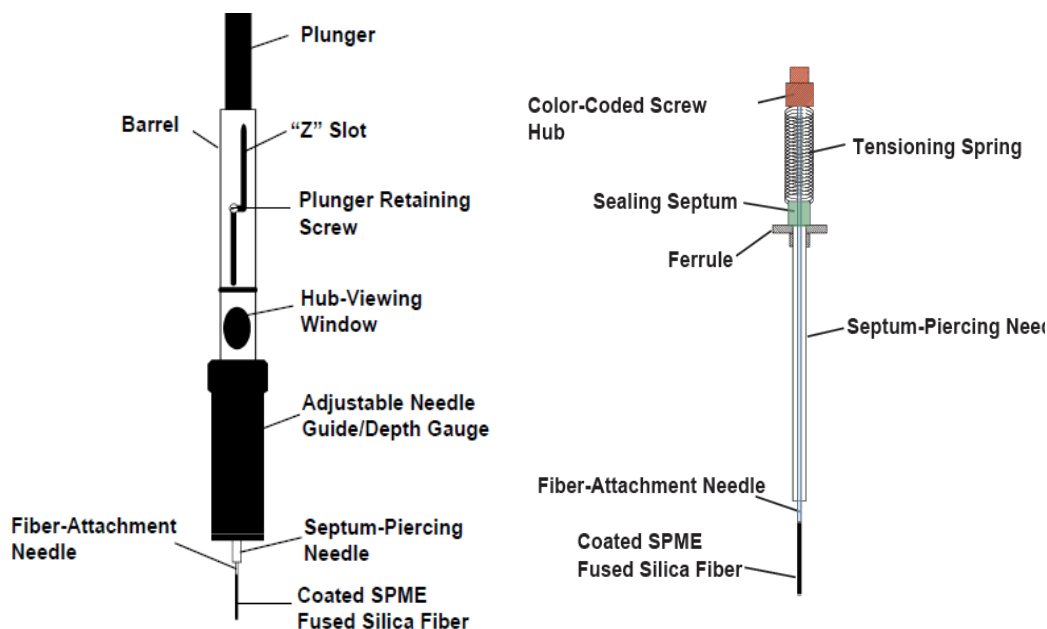


Figure 1.12 Common components present in a typical SPME device (a) and the configuration of the SPME needle (b).

(Source: <http://www.sigmaaldrich.com/etc/medialib/docs/promo/Bulletin/1/basic-spme-sept-09.Par.0001.File.tmp/basic-spme-sept-09.pdf>, Accessed: 08-08-2010)

Typical components present in a SPME device are shown in Figure 1.12. There are two main steps in an SPME process. The first step is the extraction of the analyte from the sample. The second step is the desorption process. Extraction can be performed on solid, liquid or gaseous sample matrices.¹⁴¹⁻¹⁴⁴ During the desorption process, the extracted analytes are released from the fiber coating into a separation device, typically a gas or liquid chromatograph. Figure 1.13 illustrates the extraction and desorption process for a SPME-GC system.

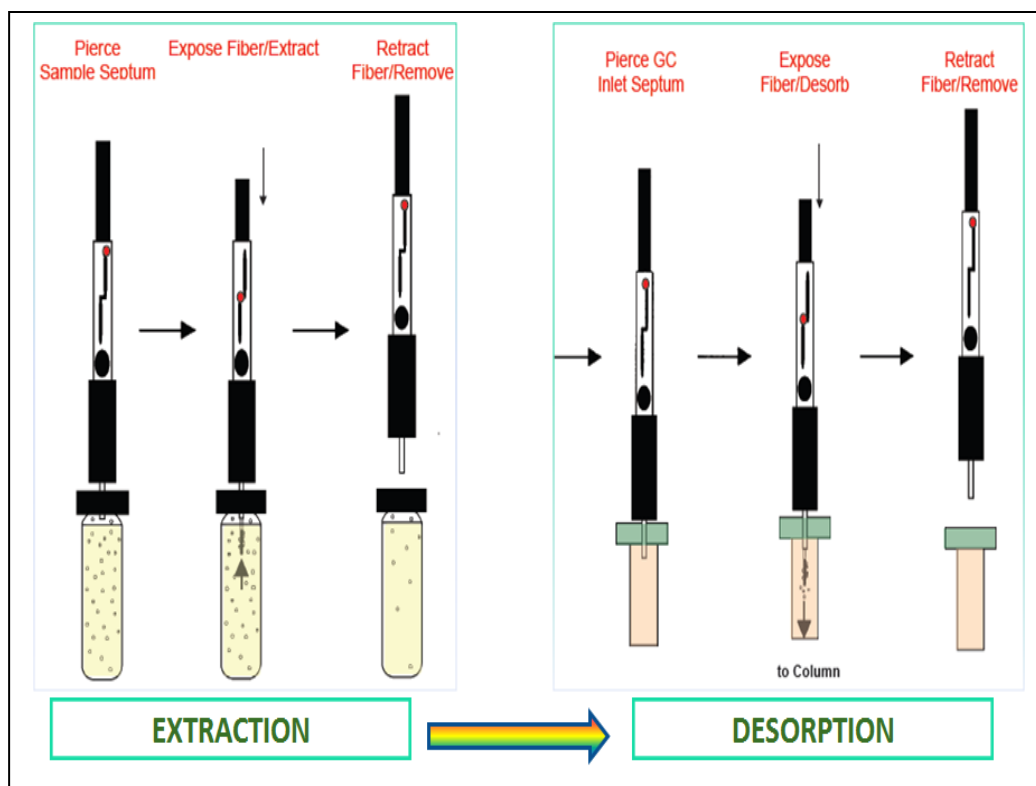


Figure 1.13 Extraction and desorption procedure for a SPME-GC system.

(Source: <http://www.sigmaaldrich.com/etc/medialib/docs/promo/Bulletin/1/basic-spme-sept-09.Par.0001.File.tmp/basic-spme-sept-09.pdf>, Accessed: 08-08-2010)

1.4.2.3 Commonly used coating materials in SPME

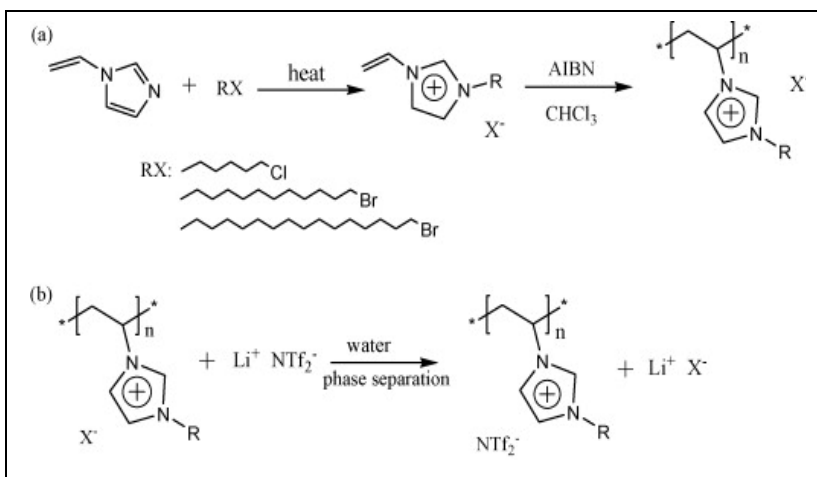
During the past decade quite a few coating materials have been introduced by various commercial and academic sources.¹⁴⁵⁻¹⁴⁷ The chemical nature of the analyte of interest determines the suitable coating material for an efficient analysis. These fibers are available in thicknesses ranging from 7-100 μm .¹⁴⁵ The most commonly used fiber in headspace SPME analysis is polydimethylsiloxane (PDMS).^{148,149} Fibers coated with polyacrylate are more suitable for analyzing polar compounds.^{148,150,151} Other available

fiber coatings composed of PDMS and divinylbenzene (DVB) mixtures and polyethylene glycol (PEG) and C-18 derivatized silica.¹⁵²

1.4.2.4 Ionic liquid-based coating materials for SPME

PDMS and PDMS/DVB type coating materials are thermally stable to 400 °C.¹⁵³ High thermal stabilities, high viscosities and ability to undergo multiple solvation interactions are some of the unique and interesting properties of ionic liquids. Due to these unique properties, ILs can be used as viable and useful coating materials for SPME. The first application of ILs as SPME coating materials was introduced in 2004 by Liu *et al.* Liu and coworkers used a 1-octyl-3-methyl imidazolium PF₆ monocationic ionic liquid as the coating material for the SPME fiber. This disposable IL coating was developed for the headspace extraction of benzene, toluene, ethylbenzene, and xylenes (BTEX) in paints. After that, Anderson and coworkers introduced dicationic polymeric IL-based coating materials¹⁵⁴ which were more thermally stable and durable when compared to monocationic type IL coatings. Scheme 1.1 and Figure 1.14 illustrate the synthesis and the morphology of the polymeric ionic liquid. This polymeric IL-based SPME phase has been used in the headspace extraction of esters.¹⁵⁴

Even though these coated polymeric IL materials were more stable than monocationic IL coatings, their use in direct immersion extractions were limited. This is because the polymeric ILs can be dissolved in immersing solvents and they give rise to higher levels of bleeding when exposed to high temperature GC inlet. We have developed a polymeric IL material that is covalently bonded to silica that can be used in both headspace and direct immersion experiments with minimal bleeding at inlet temperatures up to 250 °C. The development of silica bonded polymeric IL will be discussed in Chapter 4.



Scheme 1.1 Synthesis of the polymeric ionic liquids evaluated as SPME coatings.

(a) The vinyl-substituted IL monomer is prepared by the reaction of 1-vinylimidazole with the corresponding haloalkane followed by free radical polymerization to form the linear polymer. (b) Metathesis anion exchange is used to exchange the halide anion with the NTf_2^- anion. Reproduced with permission from reference 154.

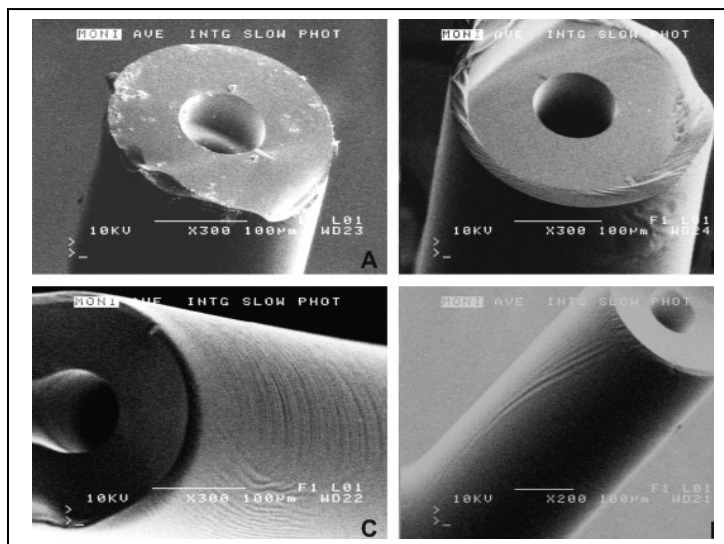


Figure 1.14 Scanning electron micrographs of a 100- μm inner diameter bare fused silica support (A) and various angles of the fused silica support coated with the poly(ViDDIm $^+$ NTf $_2^-$) polymeric IL (B–D).

The estimated film thickness is approximately 12–18 μm . Reproduced with permission from reference 154.

1.5 Organization of Dissertation

This dissertation consists of two parts. First part consists of studies towards synthesis of new ionic liquids, ionic liquid-based materials and their uses in analytical chemistry. The second part consists of studies of calix[4]arene-based supramolecular architectures that can entrap and release NO_x gases.

Chapter 2 examines the use of trigonal tricationic ILs as potential GC stationary phases. Since these ILs show very high thermal stabilities, they can be used as GC stationary phases over a wide range of temperatures. Chapter 3 describes the synthesis of new flexible linear tricationic ILs and their physiochemical properties. These newly synthesized linear tricationic ILs are used as new flexible ion pairing reagents in the detection of dianionic species in the positive mode of ESI-MS. Improved detection limits for dianion analysis was observed and the results are discussed in Chapter 4.

Chapter 5 examines a new ionic liquid-based bonded polymeric phase developed for solid phase microextraction (SPME). This polymeric coating material is the first example of a polymeric ionic liquid chemically attached to silica gel. Binding chemistry of the new SPME coating material and its applications are discussed in this chapter.

Chapters 6, 7, and 8 discuss calix[4]arene-based supramolecular approaches to entrap NO_x gases and cleaner generation of medically important nitric oxide (NO) using calix[4]arene-based nitrosonium complexes.

CHAPTER 2

TRIGONAL TRICATIONIC IONIC LIQUIDS: A NEW GENERATION OF GAS CHROMATOGRAPHIC STATIONARY PHASES

2.1 Abstract

Trigonal tricationic ionic liquids (ILs) are a new class of ILs that appear to be unique when used as gas chromatographic stationary phases. They consist of four core structures; 1. **A** = mesitylene core, 2. **B** = benzene core, 3. **C** = triethylamine core, and 4. **D** = tri(2-hexanamido)ethylamine core; to which three identical imidazolium or phosphonium cationic moieties were attached. These were coated on fused silica capillaries and their gas chromatographic properties were evaluated. They were characterized using a linear solvation parameter model and a number of test mixtures. Based on the literature, it is known that both monocationic and dicationic ionic liquids possess almost identical polarities, solvation characteristics, and chromatographic selectivities. However some of the trigonal tricationic ILs were quite different. The different solvation parameters and higher apparent polarities appear to generate from the more rigid trigonal geometry of these ILs as well as their ability to retain positive charges in relatively close proximity to one another in some cases. Their unique selectivities, retention behaviors and separation efficiencies were demonstrated using the Grob mixture, a flavor and fragrance test mixture, alcohols/alkanes test, and FAME isomer separations. Two ionic liquids **C1** (methylimidazolium substitution) and **C4** (2-hydroxyethylimidazolium substitution) had higher apparent polarities than any known ionic liquid (mono, di and tricationic ILs) or commercial stationary phases. The tri(2-

hexanamido)ethylamine core IL series proved to be very interesting in that it not only showed the highest separation efficiency for all test mixtures, but it also is the first IL stationary phase (containing NTf₂⁻ anions) that eliminates peak tailing for alcohols and other H-bonding analytes. The thermal stabilities were investigated using 3 methods: thermogravimetric analysis (TGA), temperature programmed gas chromatographic (TPGC) and isothermal gas chromatographic. The **D** core series had a high working temperature range, exceptional selectivities and higher separation efficiencies than comparable polarity commercial columns. It appears that this specific type of multifunctional ILs may have the most promising future as a new generation of gas chromatographic stationary phases.

2.2 Introduction

New types of stationary phases are explored constantly in order to come up with entities that have better physico-chemical properties in order to provide better stabilities, selectivities, resolutions and separation efficiencies for qualitative and quantitative determination of increasingly complex analyte systems. Ionic liquids have attracted much attention recently as stationary phases in gas-liquid chromatography (GLC) due to the unique properties these compounds seem to possess. These characteristics include negligible vapor pressure at room temperature, a wide liquid phase temperature range, good thermal stability, non-flammability, resistance to decomposition, ability to undergo multiple solvation interactions, ionic conductivity ($>10^{-4}$ S/cm), and large electrochemical windows (>2 V). These properties are highly desirable for many applications in areas of chemistry, physics, and engineering. Some of these applications include replacement for volatile organic solvents in organic synthesis,^{1,155-162} solvents for high temperature reactions,¹⁶³ solvents for enzyme

catalyzed reactions,¹⁶⁴⁻¹⁶⁷ electrochemical applications in photovoltaic cells and fuel cells,¹⁶⁸⁻¹⁷² high temperature lubricants,^{173,174} liquid – liquid extractions,¹⁷⁵⁻¹⁷⁹ and mass spectrometric applications.^{177,180-182} The thermal stability, ability to form multiple solvation interactions, and low volatility makes them ideal candidates for use in gas chromatography as stationary phases. In the recent past, ultra stable stationary phases based on ionic liquids were the focus of many important publications.^{43-46,52,56,183-188} Based on the literature it is evident that multifunctional ionic liquids can show greater thermal stability than most common monocationic ionic liquids in GC applications but have almost identical solvent properties.⁵⁶

However, when multiple cationic moieties are present the ionic liquid tends to be a solid at room temperature. For the best performance as a gas chromatographic stationary phase, it is necessary that the ionic liquid be a room temperature ionic liquid (RTIL). Literature indicates that the highest probability for a multi-functional ionic liquid to be a room temperature ionic liquid is by incorporating the bis(trifluoromethanesulfonyl)imide (NTf_2^-) anion.^{45,48,189-191} This anion not only gives low melting ionic liquids but also shows high thermal stability.^{48,191,192} These two characteristics make the NTf_2^- anion ideal for ILs in GC applications. However, there is a distinct disadvantage of using this anion. That is, NTf_2^- containing ILs produces peak tailing for alcohols and sometimes for other H-bonding analytes. Many different types of cation combinations have been tested in order to come up with a solution for this peak tailing and so far these attempts have failed. In this work we introduce another class of ionic liquids that not only solves this problem but also provides unique properties and selectivities not found in previously reported ILs. These are trigonal

tricationic ionic liquids and they are comprised of three positively-charged moieties linked to a central core.

Since trigonal tricationic ILs are a new class of ionic liquids, it is necessary to characterize them based on their solvation properties and relative polarity compared to general monocationic, dicationic ionic liquids and other common organic solvents. Many methods have been developed over the years for the characterization of ionic liquid solvation properties.^{193,194} Some of the earliest developments include an empirical solvent polarity scale derived either by a solvent-dependent reaction rate constant or by the shift in maxima of an absorption or emission band of a solvatochromic dye or a fluorescent probe dissolved in a particular solvent.¹⁹⁴⁻²⁰¹ However, these methods have failed to provide a comprehensive picture of the polarity of ionic liquids due to the fact that these are single parameter polarity scales and therefore specific solvent-solute interactions are not taken into account. Ionic liquids can undergo multiple solvation interactions simultaneously such as ionic, dispersive, dipole-dipole, dipole-induced dipole, H-bond donating, H-bond accepting, π - π interactions and π -nonbonding interactions. Furthermore, ionic liquids may have complex extended three-dimensional liquid structures and possibly a supramolecular structure depicted by hydrogen bonding.¹⁹⁶ Hence, single parameter polarity does not correlate with the actual chemical environment of the ionic liquid. The next major development in this field comes with the inverse GLC application of Rohrschneider-McReynolds process.⁴⁶ In this method, specific solute-solvent interactions are evaluated by utilizing 5 probe molecules which are assumed to undergo only specific types of interactions.^{46,194,201} However, due to the use of only one probe molecule per interaction, statistically the reliability of the values obtained is low.

The method used for the evaluation trigonal tricationic ILs is the Abraham solvation parameter model and it is the most comprehensive method available today.^{54,68-70,202,203} This is based on a linear free energy relationship. The principle is similar to Rohrschneider-McReynolds method in that different types of solvent-solute interactions are evaluated separately. However, instead of one probe molecule, several probe molecules are used to characterize one interaction parameter increasing the reliability of the parameter coefficients obtained. The linear solvation energy relationship is given by equation 1:

$$\log k = c + eE + sS + aA + bB + lL \text{-----Eq(1)}$$

Here, the upper case letters *E*, *S*, *A*, *B* and *L* are solute descriptors. *E* represents excess molar refraction of the solute at 20 °C, *S* is solute dipolarity and polarizability, *A* is Hydrogen bond acidity, *B* is Hydrogen bond basicity and *L* is gas-hexadecane partition coefficient at 25 °C. Solute descriptor values are evaluated and published in the literature for a number of solutes.⁵⁴ The lower case letters are assigned to characterize different types of interactions between the solutes and the solvent. In this case the solvent is the ionic liquid acting as the stationary phase. The value of these coefficients depicts the strength of the interaction. Here *e* is π and non-bonding electron interactions, *s* is the ability of the phase to interact with dipolar/polarizable solutes, *a* is H-bond donating (H-bond basicity) interactions, *b* is H-bond accepting (H-bond acidity) interactions, *l* coefficient is composed of dispersion forces (positive contribution) and cavity term (negative contribution) and *c* is the system constant. For all the solutes the retention factor *k* can be calculated chromatographically. These

values can then be subjected to multiple linear regression analysis (MLRA) to find the five coefficients and system constant.

2.3 Experimental Procedures and Methods

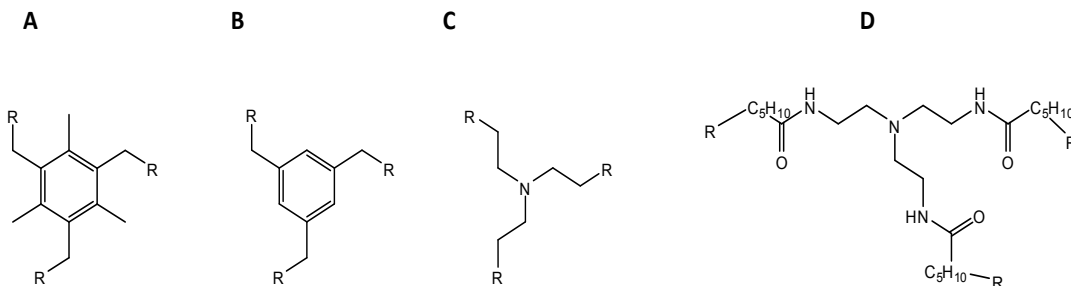
2.3.1 Materials

Figure 2.1 gives the structures of all the trigonal tricationic ionic liquids those have been synthesized previously. Detailed synthesis procedure is given elsewhere.¹⁹¹ All the probe molecules in Table 2.1 were purchased from Sigma Aldrich. Grob test mixture, flavor and fragrance mixture and alcohols and alkanes mixture were also purchased from Sigma Aldrich. The GC capillaries (250 μm internal diameter) were purchased from Supelco. The FAME isomer mixture and the commercial columns Equity-1701, SUPELCOWAX, and SP-2331 were graciously donated by Supelco.

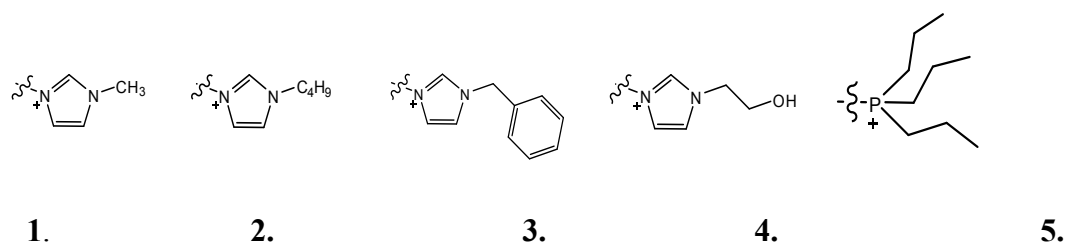
2.3.2 Methods

For the determination of solvation parameter the ionic liquids were coated using static coating technique on salt treated fused silica capillary (5m x .25mm). In this method, the IL was dissolved in dichloromethane to obtain 0.25% (w/v) coating solution and this was injected from one end of the capillary. The capillary tube was kept inside a water bath at 40 °C. After that, one end of the capillary was sealed while the solvent was evaporated from the other end under high vacuum conditions. Finally the coated columns were flushed with helium gas and conditioned overnight from 30 to 120 °C at 3 °C/min. Efficiencies of the 12 IL columns were determined by using naphthalene at 100 °C and were higher than 2000 plates m^{-1} .

Core Structures



Ligand (R) Structures



Accompanying anion: NTf₂⁻

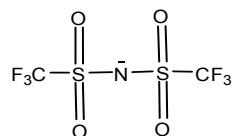


Figure 2.1 Structures of trigonal tricationic ionic liquids used in this analysis.

For the determination of solvation parameters, 30 probe molecules were used. The solute descriptors for the 30 probe molecules are listed in Table 2.1.

Table 2.1 Solute descriptor values for all the probe molecules used in this analysis.
(Reproduced with permission from reference 55)

Probe molecule	<i>E</i> (cm ³ /mol×10)	<i>S</i>	<i>A</i>	<i>B</i>	<i>L</i>
1,2-Dichlorobenzene	0.872	0.78	0.00	0.04	4.518
Phenol	0.805	0.89	0.60	0.31	3.766
Octylaldehyde	0.160	0.65	0.00	0.45	4.360
Valeraldehyde	0.163	0.65	0.00	0.45	2.851
o-Xylene	0.663	0.56	0.00	0.16	3.939
p-Xylene	0.613	0.52	0.00	0.16	3.839
m-Xylene	0.623	0.52	0.00	0.16	3.839
Cyclohexanol	0.460	0.54	0.32	0.57	3.758
Nitrobenzene	0.871	1.11	0.00	0.28	4.511
N,N-Dimethylformamide	0.367	1.31	0.00	0.74	3.173
2-Pentanone	0.143	0.68	0.00	0.51	2.755
1-Nitropropane	0.242	0.95	0.00	0.31	2.894
Toluene	0.601	0.52	0.00	0.14	3.325
Benzaldehyde	0.820	1.00	0.00	0.39	4.008
Pyridine	0.794	0.87	0.00	0.62	3.003
Aniline	0.955	0.96	0.26	0.53	3.993
Butanol	0.224	0.42	0.37	0.48	2.601
Acetic acid	0.265	0.65	0.61	0.44	1.750
1-Octanol	0.199	0.42	0.37	0.48	4.619
Acetophenone	0.818	1.01	0.00	0.49	4.501
2-Chloroaniline	1.033	0.92	0.25	0.31	4.674
Pyrrole	0.613	0.73	0.41	0.29	2.865
Benzonitrile	0.742	1.11	0.00	0.33	4.039
Propionitrile	0.162	0.90	0.02	0.36	2.082
1-Chlorohexane	0.201	0.40	0.00	0.10	3.777
p-Cresol	0.820	0.87	0.57	0.31	4.312
Ethylphenyl ether	0.681	0.70	0.00	0.32	4.242
Naphthalene	1.340	0.92	0.00	0.20	5.161
2-Propanol	0.212	0.36	0.30	0.14	2.786
Cyclohexanone	0.403	0.86	0.00	0.56	3.792

For the determination of each parameter, more than 4 probe molecules having significant range of solute descriptor values were used in order to meet the statistical requirement to obtain meaningful results for the parameters.²⁰³ The solvation

parameters were determined using inverse GC method at 2 different temperatures, 70 °C and 100 °C. Probe molecules were injected and retention times were measured in triplicate. Methane was used to measure the column hold-up time. For the trigonal tricationic IL columns the three retention factors calculated for each probe molecule were identical within the experimental error. The log of average retention factor from triplicate measurement ($\log k$) and solute descriptors (E , S , A , B , L) were then subjected to a multi parameter linear least squares fit on *Analyse-it*® for Microsoft Excel software to determine the coefficients. Helium carrier gas flow rate was set at 1 mL min⁻¹ for all the analysis with split ratio 100:1. Inlet and detector temperatures were kept at 250 °C. The values obtained for the solvation coefficients using inverse GC approach are listed in Table 2.4. The value n represents the maximum number of probe molecules that could be used for MLRA. The value is less than 30 because some compounds co-eluted with the solvent peak especially at the higher temperature. Also, some of the data points had to be removed in order to obtain higher correlation coefficients ($R^2 \geq 0.98$). It was noted that highly peak tailing analytes such as acetic acid and *N,N*-dimethylformamide were common among the analytes that were removed from the data set.

Separations of Grob test mixture, flavor and fragrance mixture, alcohols and alkanes mixture, and FAME isomers were carried out in Agilent 6890N Network GC System (Foster City, CA) equipped with Agilent 5975 inert Mass Selective Detector. Column dimensions: 30 m x .25 mm x 0.20 μ m. Separation conditions for Grob test mixture: 40 – 190 °C at 6 °C/min. Flavor and fragrance mixture: 40 °C for 3 min, 10 °C/min to 150 °C. Alcohols and alkanes mixture: 30 °C for 3 min, 10 °C/min to 160 °C. FAME isomers: 165 °C isothermal.

Thermal stability of ionic liquids was evaluated using three methods. The first method involves thermogravimetric analysis (TGA) of the pure ionic liquid at 10 °C/min heating rate.

Table 2.2 Physical properties of the trigonal tricationic ILs used as stationary phases.
(Adopted from Ref.190,191)

IL	M.W.	Melting Point (°C)	Density ^a (g/cm ³)	Refractive index	Viscosity ^b (cSt)	Thermal Stability ^c (°C)
A3	1474.3	60-62	1.59	-	-	365
B1	1203.9	-38*	1.56	1.467	1280	414
B2	1330.2	-24*	1.53	1.467	2320	401
B3	1432.2	-87*	1.55	1.588	20,000- 25,000	361
C1	1184.9	36-37	1.56	-	-	393
C2	1311.2	-47*	1.41	1.451	1580	363
C3	1413.2	-6*	1.51	1.493	25,000- 30,000	381
C4	1275	-38*	1.64	1.460	7980	392
D1	1524.4	-16*	1.59	1.465	7760	351
D2	1650.6	-54*	1.49	1.466	10,200	335
D3	1752.7	-15*	1.54	1.495	40,000- 45,000	337
D5	1758.8	-31*	1.48	1.466	35,000- 40,000	388
BMIM-Cl ^d	174.7	65	1.10	-	-	145 ^e
BMIM-TfO ^d	322.3	27	1.30	1.438	69.8	175 ^e
BMIM-NTf ₂ ^d	419.4	-4	1.43	1.427	36.4	185 ^e

* Phase transition temperature determined by using differential scanning calorimetry (DSC). ^a Measured using pycnometer. ^b Kinematic viscosity determined using capillary viscometer at 30 °C. ^c Temperature of 5% thermal degradation determined by thermogravimetric analysis (TGA). ^d Values taken from the references 44, 186. ^e Thermal stability determined by GC method.

The decomposition temperature of 5% weight loss of the sample is reported in Table 2.2. The second approach is a temperature programmed GC (TPGC) method where the ionic liquid is coated in a 5 m x .25mm capillary and a temperature ramp of 3 °C/min was applied from 100 °C until decomposition is observed (see Figure 2.2). The third method is carried out for **D** core ionic liquids only. In this method, the ionic liquid is coated on a NaCl treated fused silica capillary of 5m x .25mm x .15 µm film thickness and the retention factor of naphthalene was determined at 100 °C isothermally. It was then subjected to conditioning at higher temperatures for 12 hours (see Table 2.3) and the naphthalene retention factor was determined again at 100 °C after each conditioning step. This method yields the most relevant thermal decomposition temperature of the IL stationary phases.

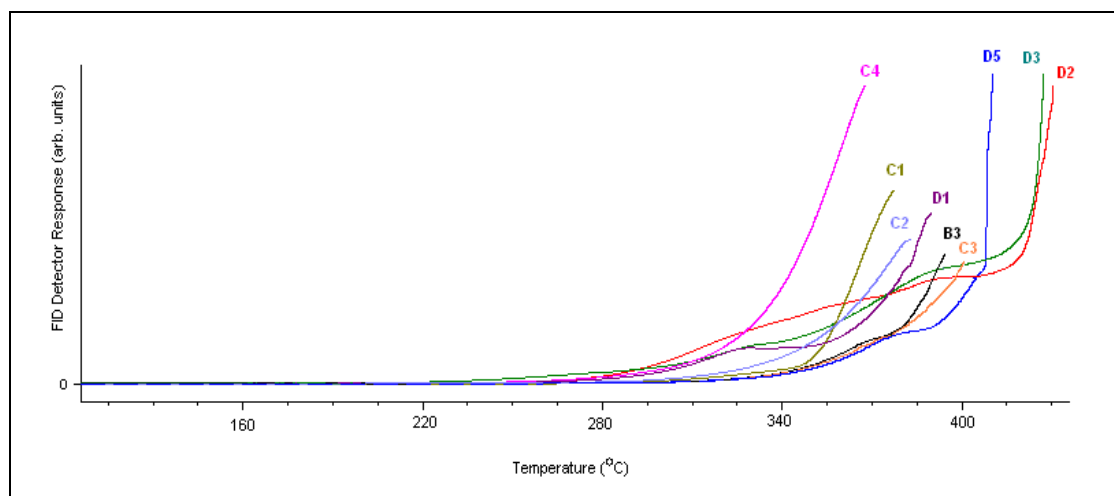


Figure 2.2 Temperature profile for column bleeding in gas chromatography.

Temperature profile for column bleeding in gas chromatography due to thermal decomposition or volatilization of trigonal tricationic ionic liquids **B3, C1, C2, C3, C4, D1, D2, D3, and D5**.

2.4 Results and Discussion

Four types of central cores were investigated in this study (see Figure 2.1) and in the order of increasing flexibility they are; **A** mesitylene core, **B** benzene core, **C** triethylamine core, and **D** tri(2-hexanamido)ethylamine core. These core structures also vary in their ability to form hydrogen bonds with the NTf_2^- anion and other solutes. The **A** and **B** cores do not have any intrinsic H-bonding capabilities. In the case of **C** core, the central nitrogen can be H-bond basic and in **D** core, the central nitrogen and amide oxygen both can be H-bond basic and the amide hydrogen can be H-bond acidic. It is important to note that to the best of our knowledge this is the first time an amide group is introduced in to the cationic fragment of an ionic liquid. Detailed information of synthesis and impurities present in these ionic liquids were discussed elsewhere.¹⁹¹

2.4.1 Physical Properties of Trigonal Tricationic Ionic Liquids

The physical properties of this series of multifunctional ILs are summarized in Table 2.2. Ionic liquid **A3** and **C1** were solids at room temperature with melting points 62 and 37 °C respectively. The remaining 10 ionic liquids were room temperature ILs with melting points below 20 °C. The RTILs were viscous liquids that did not show any air or moisture sensitivity that leads to decomposition at laboratory atmosphere. Densities of these tricationic ILs lie in the range observed for common monocationic and dicationic ILs⁴⁸ and are between 1.41 g/cm³ and 1.64 g/cm³. Refractive indices range from 1.451 to 1.588. However viscosities of trigonal tricationic ILs are at least one or two orders of magnitude higher than those observed for typical monocationic ILs and dicationic ILs. In fact these are the highest viscosities reported for any ionic liquids. Ionic liquids **D3** and **D5** have the highest viscosities which range between 40,000-

45,000 cSt and 35,000-40,000 cSt respectively. High viscosities are preferable for ILs that are to be used as stationary phases in GC.^{43,44} Furthermore when the benzyl imidazolium moiety is present the viscosities are markedly higher than other imidazolium cationic moieties. This trend was observed for symmetrical and unsymmetrical dicationic ILs as well.⁴⁸ This may be attributed to the added π - π stacking of the aromatic ring. Thermal stabilities of the trigonal tricationic ILs were measured using three methods (see Experimental Section) and a detailed discussion follows.

2.4.1.1 Thermal Stability

The thermal stability of ionic liquids is important as it defines the upper limit of the temperature range where the column can be used as a separation medium. Three methods were used to evaluate thermal stability: First two methods, TGA method and temperature programmed GC method were used to obtain a general idea of the thermal stability. Using the TGA method, the temperatures of 5% thermal degradation of the trigonal tricationic IL samples are reported as the decomposition temperature in Table 2.2. All ionic liquids were thermally stable to at least 335 °C in the TGA method. In the TPGC method, the baseline rise at the beginning of the decomposition event can be due to two reasons (see Figure 2.2). It can be due to the volatilization of the ionic liquid or it can be due to the actual decomposition. Either way, this region cannot be used for chromatographic separations due to the increasing baseline from column bleed. At the end of Table 2.2, the thermal stability of some common monocationic ionic liquids (determined by the TPGC method) is listed for comparison purposes.⁴⁴ It is important to note that the thermal stability values reported in Table 2.2 for monocationic ionic liquids can be directly compared to the values obtained for trigonal

tricationic ionic liquids by the TPGC method in Figure 2.2 as both experiments employed identical procedures. It is evident that the tricationic ionic liquids are much more thermally stable than the common monocationic ionic liquids. All 3 monocationic ILs start to decompose or volatilize before 185 °C while for the trigonal tricationic ILs, no appreciable bleed is observed before 280 °C. There is at least a 90 degree advantage of workable temperature range for tricationic ILs over the common monocationic IL stationary phases in gas chromatography. Within the tricationic series since all the ionic liquids have the same anion, the thermal stability variation are solely due to variations in the cationic fragment. IL **C4** with hydroxyethylimidazolium cationic moiety and nitrogen core seems to decompose at somewhat lower temperature whereas IL **D5** with propylphosphonium cationic moiety and amide linkage shows the highest onset temperature of decomposition. In fact it appears that for **D5** the base line does not start to rise appreciably until the temperature exceeds 315 °C. The above mentioned two methods were used to present general thermal stability comparison between the trigonal tricationic ILs and other ionic liquid-based stationary phases since these are the most common methods used in the literature. The third method, an isothermal GC method, is probably the most relevant method for the determination of actual upper limit of temperature for the use of ionic liquids as stationary phases. The retention factor of naphthalene after each thermal treatment is shown in Table 2.3 and Figure 2.3. For all the **D** core ILs listed, symmetrical sharp peaks were obtained up to 290 °C conditioning. At 300 °C thermal treatment the columns show reasonable retention for naphthalene.

Table 2.3 Variation of retention factors (k_{naph}) with thermal treatment of D core trigonal tricationic IL columns.^a

Thermal treatment ^b (°C)	k_{naph} in D1	k_{naph} in D3	k_{naph} in D5
100	3.2	8.1	7.2
130	3.1	6.9	7.0
150	3.0	6.5	6.8
200	2.9	5.2	6.5
230	2.9	4.6	6.4
250	2.8	4.3	6.3
270	2.5	3.2	6.2
290	2.1	2.3	6.0
300	3.0 ^c	2.3 ^c	6.7 ^c
310	d	d	d

^a Measured isothermally for naphthalene, column temperature 100 °C, He flow rate 1 ml/min. ^b Thermally treated for 12 hours under He 1 ml/min. ^c Peak tailing was observed. ^d No retention was observed for naphthalene.

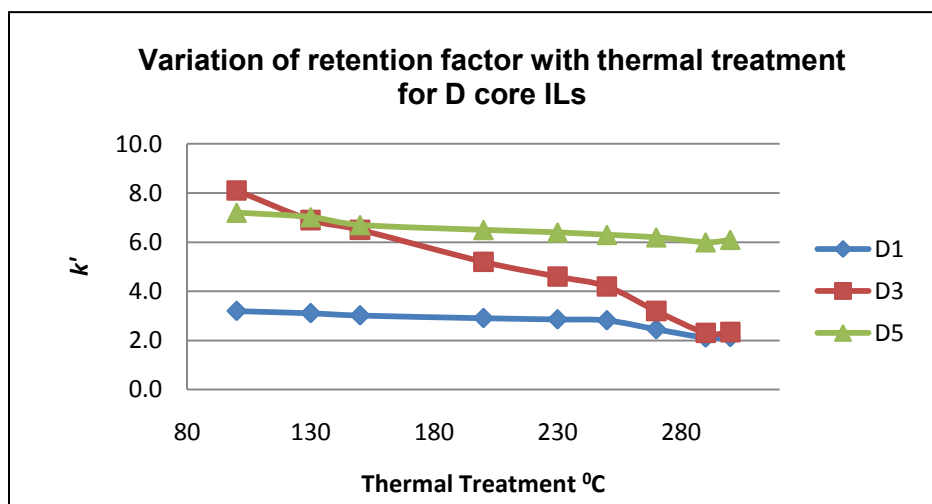


Figure 2.3 Graphical representation illustrating the change of retention factor with the temperature treatment on D1, D2, D3 IL phases.

However the peaks show some tailing. After 310 °C, there was no retention which indicates column bleed of the ionic liquid stationary phase. These results confirm that the **D** core IL series is thermally stable up to 300 °C as a GC stationary phase. In previous work it was shown that the phosphonium cationic moiety is more resistant to thermal degradation than most other N-based cations such as imidazolium and ammonium.²⁰³ This implies that from this set of tricationic ionic liquids, **D5** has the largest workable temperature range as a stationary phase in gas chromatography. It exists as a liquid for a range of 331 °C from – 31.4 °C to at least 300 °C. This in itself is quite impressive compared to the monocationic ionic liquids which generally have a liquid temperature range of about 200 °C or less. It is important to note that the commercial stationary phase SP-2331 which has similar polarity to **D5** ionic liquid has an upper temperature limit of 275 °C. Therefore, IL **D5** has at least 25 °C advantage over the comparable commercial stationary phase which in gas chromatographic terms leads to better separation efficiencies for heavy and highly polar compounds.

2.4.2. Ionic Liquid Solvation Parameters

The solvation parameters obtained for the trigonal tricationic ionic liquids are listed in Table 2.4. In Table 2.5 these values are compared with the same parameters found for common monocationic and dicationic ionic liquids.^{43,45,56} By comparison, nearly all interaction parameters obtained for monocationic and dicationic ILs are similar to each other whereas those obtained for some of the new tricationic ILs are quite unique.

Table 2.4 Interaction parameters obtained for trigonal tricationic IL stationary phases

Temperature (°C)	c	e	S	a	b	L	n	R ²
A3 (BzIM)Mst								
70 (std. err.)	-3.34 (.10)	0.07 (.08)	2.02 (.09)	1.86 (.08)	0.72 (.11)	0.47 (.02)	29	0.99
100 (std. err.)	-3.37 (.09)	0.10 (.07)	1.87 (.08)	1.61 (.07)	0.58 (.10)	0.39 (.02)	29	0.99
B1 (MIM)Ph								
70 (std. err.)	-2.94 (.12)	0.14 (.10)	1.67 (.11)	1.68 (.10)	0.05 (.14)	0.50 (.03)	29	0.98
100 (std. err.)	-3.00 (.11)	0.18 (.08)	1.51 (.09)	1.42 (.08)	0.02 (.12)	0.42 (.03)	29	0.99
B2 (BuIM)Ph								
70 (std. err.)	-3.18 (.08)	0.07 (.07)	1.72 (.08)	1.80 (.07)	0.23 (.10)	0.56 (.02)	29	0.99
100 (std. err.)	-3.26 (.08)	0.09 (.07)	1.56 (.08)	1.57 (.07)	0.15 (.10)	0.48 (.02)	29	0.99
B3 (BzIM)Ph								
70 (std. err.)	-3.49 (.10)	0.04 (.07)	2.11 (.08)	2.09 (.08)	0.46 (.10)	0.51 (.03)	28	0.99
100 (std. err.)	-3.55 (.09)	0.06 (.07)	1.97 (.07)	1.78 (.07)	0.39 (.10)	0.43 (.02)	28	0.99
C1 (MIM)N								
70 (std. err.)	-3.53 (.11)	0.05 (.08)	1.55 (.10)	1.81 (.08)	0.35 (.11)	0.53 (.03)	28	0.99
100 (std. err.)	-3.70 (.12)	0.04 (.08)	1.58 (.08)	1.51 (.08)	0.31 (.11)	0.45 (.03)	25	0.98
C2 (BuIM)N								
70 (std. err.)	-2.92 (.09)	0.05 (.07)	1.57 (.08)	1.55 (.07)	0.14 (.10)	0.55 (.02)	27	0.99
100 (std. err.)	-2.98 (.09)	0.06 (.07)	1.43 (.08)	1.29 (.06)	0.16 (.10)	0.46 (.02)	27	0.99

Table 2.4 Continued

C3 (BzIM)N	c	e	S	a	b	L	n	R²
70 (std. err.)	-3.23 (.09)	-0.03 (.07)	1.85 (.08)	1.62 (.07)	0.37 (.10)	0.54 (.02)	28	0.99
100 (std. err.)	-3.29 (.08)	-0.02 (.06)	1.10 (.07)	1.37 (.07)	0.30 (.09)	0.46 (.02)	28	0.99
C4 (HyIM)N								
70 (std. err.)	-3.18 (.10)	0.22 (.09)	0.66 (.10)	0.95 (.09)	0.09 (.12)	0.67 (.03)	29	0.99
100 (std. err.)	-3.05 (.09)	0.22 (.06)	0.45 (.07)	0.70 (.06)	0.03 (.08)	0.57 (.02)	25	0.99
D1 (MIM)NAmid								
70 (std. err.)	-3.42 (.12)	0.23 (.09)	2.15 (.11)	2.82 (.11)	0.31 (.14)	0.43 (.03)	28	0.99
100 (std. err.)	-3.58 (.12)	0.16 (.09)	2.10 (.10)	2.50 (.10)	0.17 (.14)	0.37 (.03)	26	0.99
D2 (BuIM)NAmid								
70 (std. err.)	-2.89 (.13)	0.11 (.11)	1.59 (.12)	2.23 (.10)	0.05 (.15)	0.52 (.03)	28	0.99
100 (std. err.)	-2.94 (.11)	0.10 (.09)	1.45 (.10)	1.84 (.09)	0.01 (.13)	0.45 (.03)	28	0.98
D3 (BzIM)NAmid								
70 (std. err.)	-3.10 (.12)	0.07 (.10)	1.85 (.11)	2.29 (.10)	0.15 (.14)	0.50 (.03)	29	0.99
100 (std. err.)	-3.16 (.10)	0.08 (.08)	1.69 (.09)	1.93 (.08)	0.10 (.11)	0.42 (.02)	29	0.99
D5 (PrP)NAmid								
70 (std. err.)	-3.30 (.10)	0.13 (.08)	1.91 (.09)	2.72 (.08)	0.03 (.11)	0.52 (.03)	29	0.99
100 (std. err.)	-3.34 (.10)	0.14 (.08)	1.72 (.09)	2.17 (.08)	0.07 (.11)	0.44 (.02)	29	0.99

Table 2.5 Comparison of the interaction parameters of monocationic and dicationic RTILs with trigonal tricationic ionic liquids.

Temperature (°C)	c	e	s	a	b	l	n	R ²
BMIM-NTf ₂ a								
70 (std. err.)	-3.03 (.09)	0 (.08)	1.67 (.09)	1.75 (.09)	0.38 (.11)	0.56 (.02)	35	0.99
100 (std. err.)	-3.13 (.12)	0 (.09)	1.60 (.10)	1.55 (.10)	0.24 (.12)	0.49 (.03)	32	0.98
C9(mim)2-NTf ₂ b								
70 (std. err.)	-2.95 (.14)	0.11 (.07)	1.76 (.08)	1.75 (.07)	0.20 (.10)	0.51 (.02)	33	0.99
100 (std. err.)	-3.06 (.08)	0.11 (.06)	1.64 (.07)	1.50 (.06)	0.15 (.09)	0.43 (.02)	32	0.99
D1 (MIM)NAmid								
70 (std. err.)	-3.42 (.12)	0.23 (.09)	2.15 (.11)	2.82 (.11)	0.31 (.14)	0.43 (.03)	28	0.99
100 (std. err.)	-3.58 (.12)	0.16 (.09)	2.10 (.10)	2.50 (.10)	0.17 (.14)	0.37 (.03)	26	0.99

These unique parameters give rise to different behaviors in terms of retention, selectivity and separation efficiency. Three of the five interaction parameter coefficients i.e., s = dipole–type interactions, a = H–bond donating interactions, and l = dispersion and cavity formation interactions have the greatest magnitude. This implies that solute retention is mainly due to these three types of interactions. Similar observations were made for monocationic and dicationic IL stationary phases.^{43-45,56} Ionic liquid **C4** (with hydroxyethylimidazole charge carrying moieties and a “N” core) had the lowest s and a terms ever reported for any ionic liquid stationary phases carrying NTf₂[−] anion. Hence the **C4** IL column exhibited the lowest retention for all the test mixtures investigated (Grob test, alcohols and alkanes, flavor and fragrance mixture, see Figures 2.4, 2.5 and 2.7.). The e term which corresponds to π - and nonbonding electron interactions is essentially negligible in this series of trigonal tricationic ionic liquids. It was observed

that the *s*, *a*, *b*, and *l* coefficients decrease with increasing temperature. The most substantial decrease in magnitude is observed for the *s* and *a* values (dipole–type interactions and H–bond basicity). This is mainly due to the fact that these interactions result from directional bonds and therefore depend largely on the orientation of the solute molecules and the interacting stationary phase molecules. As the temperature increases, translational and rotational energy of the molecules increase. This disrupts the intermolecular interactions between the solute and stationary phase and leads to lower retention and coefficients.²⁰³ When benzylimidazole is the ionic liquid's charge carrying moiety, the H–bond acidity term *b* is increased compared to the other cationic moieties (with the exception of the **D** core ionic liquids in which the methylimidazole cationic moiety shows a higher *b* value). This is observed in symmetrical dicationic ionic liquids as well.⁴⁵ This may be due to the increased H–bond acidity of the bridging methylene hydrogens of the benzyl group. This contention is supported by previously published results (illustrated in Figure 2.4 which is a packing diagram of a symmetrical dicationic ionic liquid, $C_3(\text{methylimidazolium})_2 2Br^-$). This crystal structure shows H–bonding between the acidic hydrogens and the bromide anion.⁴⁵ The hydrogens that are marked with a red arrow are from the methyl group substituted at the 3 position of the imidazole ring. If the methyl group is substituted by a benzyl group, these would be the bridging methylene hydrogens. In that case due to the presence of the benzene ring in the adjacent carbon these hydrogens would be even more acidic giving rise to a larger *b* term.

The **D** core series of tricationic ILs has the highest *a* values (i.e., hydrogen bond basicities). This is due to the three amide groups present in each ionic liquid. Both

amide nitrogen and carbonyl oxygen can participate in H-bonding. The central core nitrogen may be sterically hindered for effective hydrogen bonding.

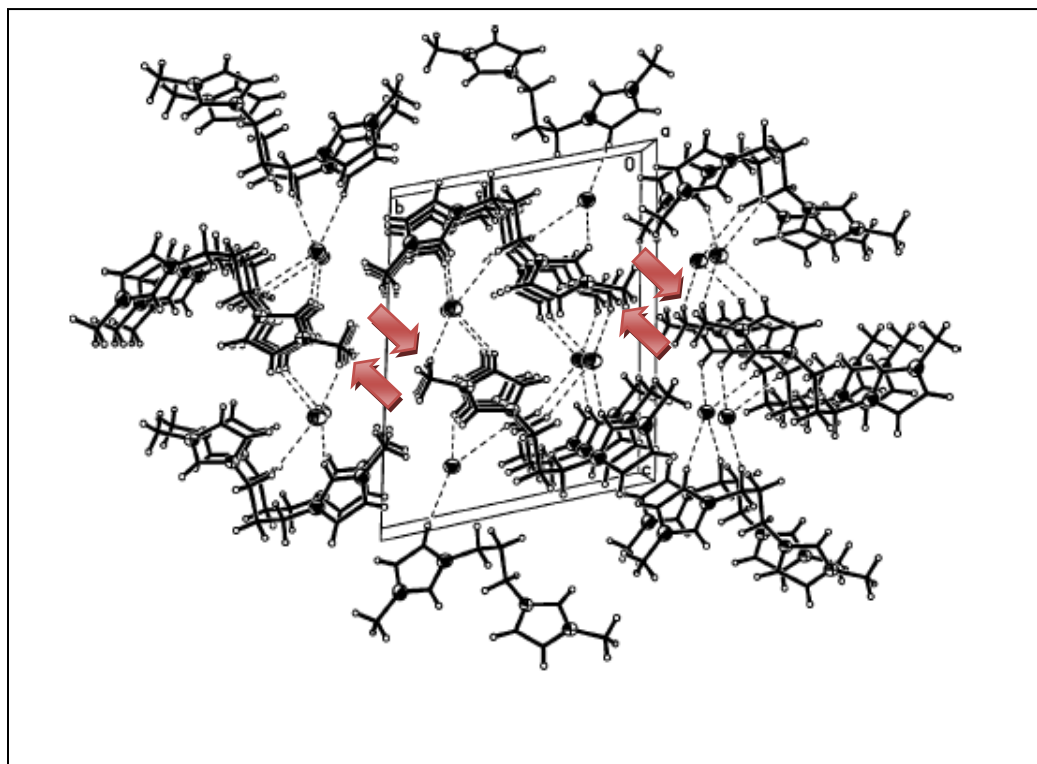


Figure 2.4 X-ray crystallographic representation of $C_3(\text{mim})_2 2\text{Br}^-$ showing stacks along short a – axis and H-bonding. Reproduced with the permission from reference 56.

The e term is probably the least significant coefficient for most of the tricationic ILs investigated. It implies that the interaction between solute and IL stationary phase through π - π and non-bonding electrons is minimal compared to other types of interactions. One would expect the benzylimidazole cationic moiety to introduce some π – bonding interactions but that is not what is observed. The only statistically significant e terms are observed for the **C4** ionic liquid, with the hydroxyethylimidazole charge carrying moiety; and for the **D1** ionic liquid with methylimidazole charge

carrying moiety. It is expected that **C**-core series has the lowest e term, as there are no core π – bonding electrons and only one relatively inaccessible non-bonding electron pair on the central nitrogen. However, **C4** with hydroxyethylimidazole as the cationic moiety shows the highest π - π and n - π interactions among the trigonal tricationic IL series. Furthermore this ionic liquid has a very low H-bond acidity (b coefficient). This implies that the hydroxyl group interacts with solutes through the non-bonding electrons of oxygen and not as much through H-bonding. Dispersion forces are one of the prominent type of interaction that contributes to analyte retention in these IL stationary phases. However, interaction of tricationic ILs through dispersion forces (l coefficient) seems to be similar since there is not much variation in the l value from one trigonal tricationic ionic liquid to another. The magnitude of l ranges from 0.43 to 0.67 and this falls within the range observed for symmetrical dicationic and monocationic ionic liquids.^{43-44,45,56}

2.4.3 The Grob Test Mixture

This is a single test mixture that is used to evaluate a capillary column chromatographically.^{193,204} This mixture can be used to evaluate separation efficiency, acid/base characteristics, adsorptive activity and relative polarity of the column. The mixture contains 12 components and each peak gives information about the column. 1. n-decane and 2. n-undecane represents 100% recovery marker. Symmetrical sharp peaks are expected for properly produced and installed columns. 3. 1-nonanal is used to identify adsorption unique to aldehydes independent of H-bonding. 4. 1-octanol and 5. 2,3-butanediol peak shapes indicate presence of H-bonding sites. Reduced peak heights and unsymmetrical peak shapes for 6. 2-ethylhexanoic acid and 7. 2,6-dimethylphenol indicate H-bonding or basic sites. 8. methyl decanoate, 9. methyl

undecanoate and 10. methyl dodecanoate are a homologous series of fatty acid methyl esters and is used to determine the separation efficiency of the column. 11. 2,6-dimethylaniline and 12. dicyclohexylamine peak shapes give information of the acidic nature of the column.

According to Figure 2.5, in trigonal tricationic ionic liquids with **B** and **C** core structures (see Figure 2.1), n-decane and n-undecane elute with or near the methylene chloride solvent peak and could not be separated with the given temperature program. Also, 2,3-butanediol, 2-ethylhexanoic acid, and dicyclohexylamine were either retained on the column or eluted with high peak tailing so that they were indistinguishable from the baseline. All of these 3 compounds are polar, have H-bonding capabilities and lack any aromatic substituents. Furthermore, 1-nonanal and 1-octanol showed peak tailing and reduced peak heights. These results imply that the **B** and **C** core structures can produce IL stationary phases that are highly polar with H-bond accepting capabilities. The **C4** IL shows the least retention for Grob test mixture compounds which is in accordance with the previously discussed solvation parameter coefficient results. The homologous series of fatty acid methyl esters were well separated with both **B** and **C** core IL stationary phases and showed good separation efficiencies. The acid 2,6-dimethylphenol and the base 2,6-dimethylaniline were the latest eluting detectable peaks. Despite the presence of H-bonding sites, these did not show much peak tailing.

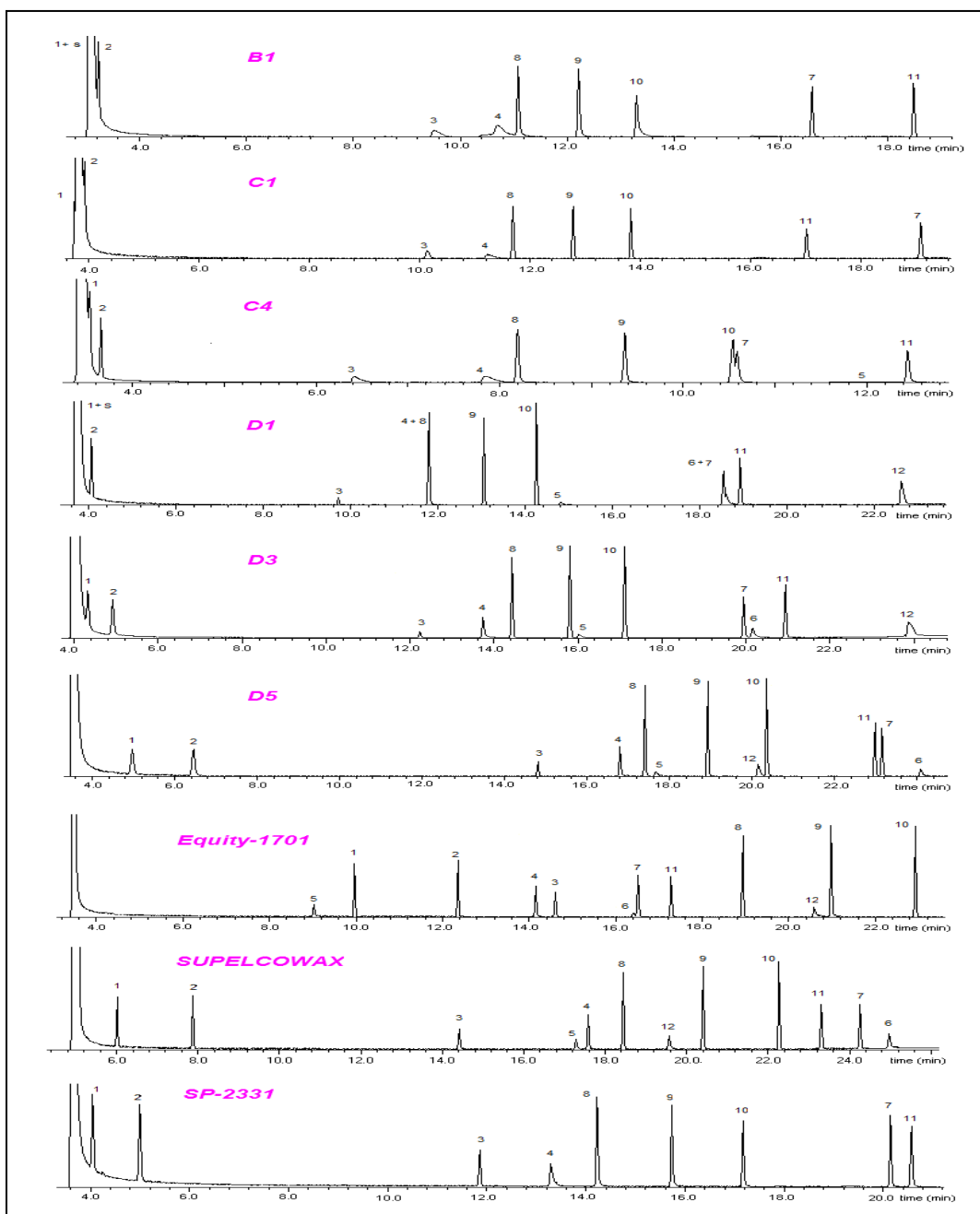


Figure 2.5 Separation of Grob test mixture in trigonal tricationic IL columns.

Separations were compared with commercial columns with varying degrees of polarity. Intermediate polar (Equity-1701), polar (SUPELCOWAX), and highly polar (SP-2331). 1 n-decan, 2 n-undecane, 3 1-nonanal, 4 1-octanol, 5 2,3-butanediol, 6 2-ethylhexanoic acid, 7 2,6-dimethylphenol, 8 methyl decanoate, 9 methyl undecanoate, 10 methyl dodecanoate, 11 2,6-dimethylaniline, 12 dicyclohexylamine, s dichloromethane; GC separation conditions: 40 °C to 190 °C at 6 °C min⁻¹; 1 mL min⁻¹ He; MS Detector. All chromatograms were obtained using 30 m x .25 mm x 0.20 µm d_f columns.

The elution orders on the **B1** and **C4** ILs were similar to highly polar commercial stationary phase SP-2331, whereas the elution order on the **C1** IL stationary phase was more comparable with the polar SUPELCOWAX column.

All 12 test compounds were eluted from stationary phases with **D** core ionic liquids. In **D3** and **D5** the alkanes are better separated from the solvent peak compared to the **B** and **C** core ILs. All **D**-type columns separated the homologous series of fatty acid methyl esters with exceptionally good separation efficiencies. In both **D1** and **D3**, the two bases elute after the acids which indicate that **D1** and **D3** are more acidic stationary phases than **D5**. This also is in agreement with the solvation parameter coefficients obtained. The H-bond acidity term (*b*) for **D5** is significantly smaller than that of **D1** and **D3**. In **D5**, the two acids elute last indicating a more basic, less acidic stationary phase. The **D** core IL stationary phases show elution orders similar to the highly polar SP-2331 column. This leads to the conclusion that the **D** series ionic liquids are highly polar and the polarity is comparable to that of SP-2331 (100% cyanopropyl polysiloxane) stationary phase.

2.4.4 Alcohol and Alkane Mixture

Figure 2.6 illustrates the separation of a mixture of alcohols and alkanes by the six trigonal tricationic ionic liquid columns and commercial columns of diverse polarity. Except for **C4**, the other IL columns show reasonable retention for both polar alcohols and nonpolar alkanes. This is due to the dual nature of ionic liquids¹⁸⁷ which suggests that ionic liquids act like a polar medium to retain polar compounds and like a nonpolar medium to retain nonpolar compounds simultaneously.

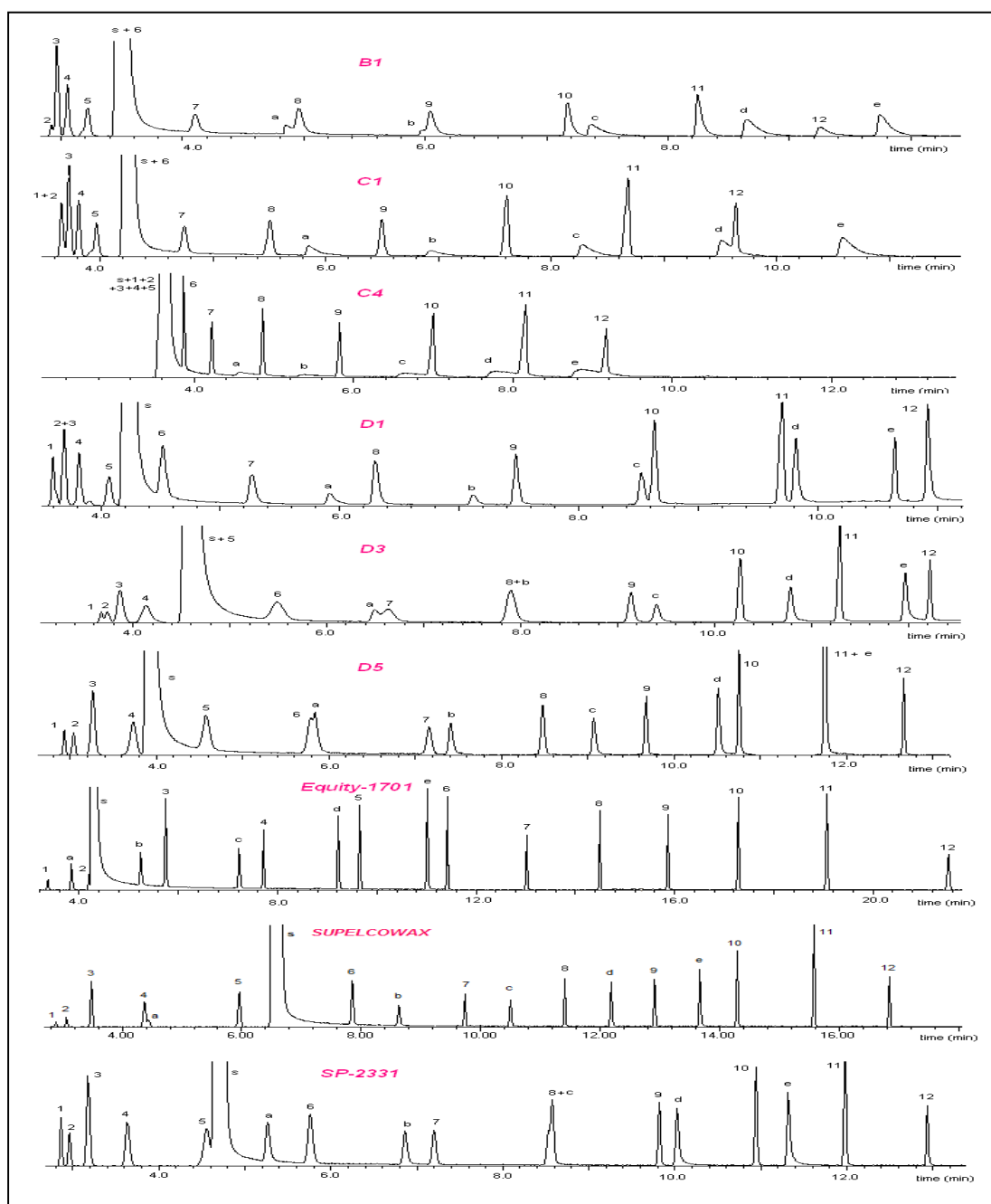


Figure 2.6 Separation of homologous alkane and alcohol mixture.

1 pentane, 2 hexane, 3 heptane, 4 octane, 5 nonane 6, decane, 7 undecane, 8 dodecane, 9 tridecane, 10 tetradecane, 11 pentadecane, 12 hexadecane, **a** ethanol, **b** 1-propanol, **c** 1-butanol, **d** 1-pentanol, **e** 1-hexanol, **s** dichloromethane. GC separation conditions: 30 °C for 3 min, 10 °C min⁻¹ to 160 °C; 1 mL min⁻¹ He; MS detector. All chromatograms were obtained using 30 m x .25 mm x 0.20 µm d_f columns.

One of the most interesting observations of this separation is the relative retention of alcohols and alkanes by these IL columns. In all of the six tricationic liquid stationary phases, the relative retention of alcohols compared to alkanes is much larger than that observed for common monocationic; (benzyl(methyl)imidazolium-TfO),⁴⁴ phosphonium monocationic; (trihexyl(tetradecyl)phosphonium-NTf₂),²⁰⁵ or polyethylene glycol linked dicationic; (MIM₂PEG₃-2NTf₂)¹⁹⁰ ionic liquid stationary phases (see Figure 2.7). For the **B1** and **C1** stationary phases, 1- hexanol elutes after hexadecane which is unusual. In fact, to the best of our knowledge, the **C1** ionic liquid has the distinction of having the largest relative retention for 1-hexanol with respect to hexadecane ever reported for any commercial stationary phase or any ionic liquid stationary phase. The lowest overall retention for all alcohol and alkane components was again observed for the **C4** column. All 18 compounds were eluted before 9.5 minutes. The shorter chain alkanes (pentane – nonane) seem to have almost no interaction with this stationary phase and come out with the solvent peak under these conditions. It appears that the **C1** and **C4** ILs may be the most polar GC stationary phases yet reported. This high polarity is unique to trigonal tricationic ionic liquids. All other monocationic, dicationic and linear tricationic ionic liquids show almost identical solvation characteristics and intermediate polarities. The higher apparent polarity and different solvation properties of trigonal tricationic ILs can be attributed to its more rigid trigonal geometry and the existence of three positive charges in close proximity compared to other forms of ILs.

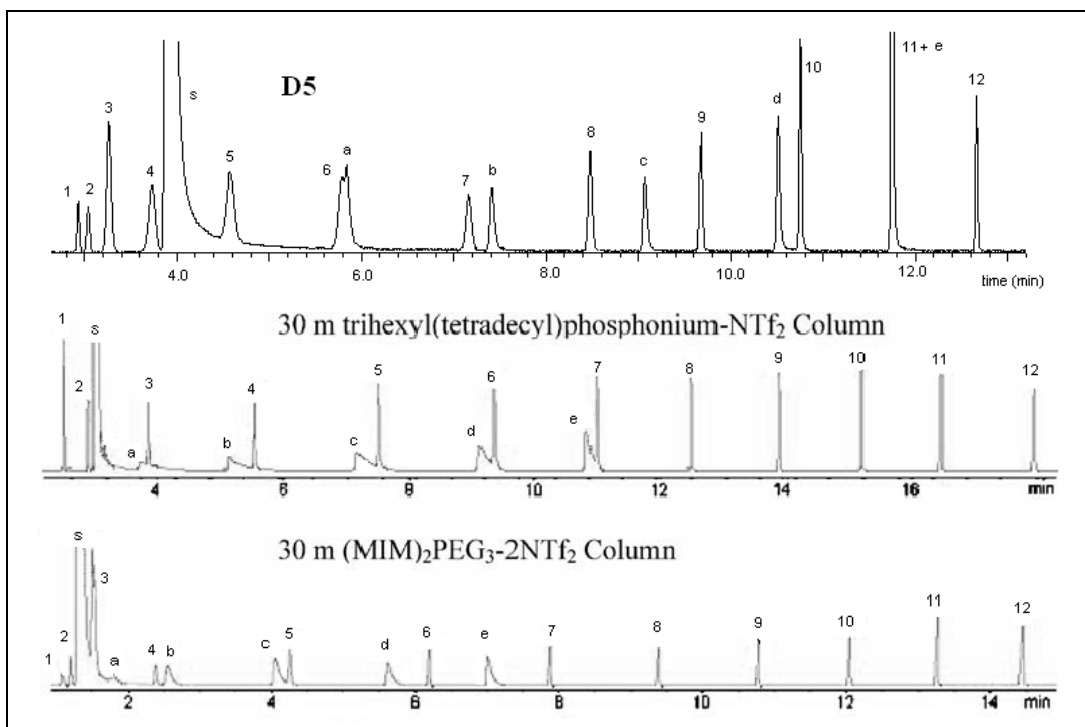


Figure 2.7. Comparison of separation of homologous alkane and alcohol mixture.

Comparison of separation of homologous alkane and alcohol mixture using trigonal tricationic IL **D5**, monocationic ionic liquid trihexyl(tetradecyl)phosphonium-NTf₂ and dicationic ionic liquid (MIM)₂PEG₃-NTf₂ columns under identical conditions.: 1 pentane, 2 hexane, 3 heptane, 4 octane, 5 nonane 6, decane, 7 undecane, 8 dodecane, 9 tridecane, 10 tetradecane, 11 pentadecane, 12 hexadecane, **a** ethanol, **b** 1-propanol, **c** 1-butanol, **d** 1-pentanol, **e** 1-hexanol, **s** dichloromethane,. GC separation conditions: 30 °C for 3 min, 10 °C min⁻¹ to 160 °C; 1 mL min⁻¹ He; MS detector for **D5**. FID for monocationic and dicationic columns. All chromatograms were obtained using 30 m x .25 mm x 0.20 μm d_f columns.

The **B** and **C** core ionic liquid stationary phases produce tailing peaks for the alcohols. This is a common phenomenon observed for ionic liquid stationary phases with the NTf₂⁻ (bis(trifluoromethane)sulfonimide) counter anion. Both monocationic and dicationic ionic liquids have shown peak tailing for alcohols and this has been one drawback of these types of ionic liquids as stationary phases. To overcome this problem NTf₂⁻ anion has been replaced by the triflate (TfO⁻) anion.¹⁹⁰ However, with

multifunctional ionic liquids the NTf_2^- anion is used more frequently in order to obtain lower melting point ILs.

One of the unique and probably the more important property of the trigonal tricationic ionic liquid stationary phases is that the **D** core ILs have reduced and in the some cases almost eliminated the peak tailing of alcohols even though the NTf_2^- anion is present. As discussed previously, the polarity of the **D5** IL stationary phase is comparable to the highly polar SP-2331 commercial phase. However, as shown in Figure 2.6, peak asymmetry for alcohols is less for the **D5** stationary phase than for the commercial SP-2331 phase at higher temperatures. Also nonane (5) and dichloromethane (s) were barely separated with SP-2331 phase whereas these compounds are much better separated with the **D5** IL stationary phase. Similarly dodecane (8) and 1-butanol (c) co-elute in SP-2331 while these two are completely separated with the **D5** IL column. Columns **D1** and **D5** seem to be complementary to one another in that one column always separates peaks that co-elute on the other (see Figure 2.5). For example hexane (2) and heptane (3) co-elute on **D1** and are baseline separated on **D5**. Decane (6) and ethanol (a) peaks overlap on **D5** and separate on **D1**. Pentadecane (11) and 1-hexanol (e) co-elute in **D5** but are well separated on **D1**. Furthermore, the **D**-core ILs shows the greatest retention for alkenes among the trigonal tricationic ILs evaluated. The retention times of alkanes in **D1**, **D3** and **D5** columns are directly proportional to the solvation parameter coefficient of interaction through dispersion forces (coefficient I). Within the **D** series, **D1** has the lowest I term, followed by **D3**, and **D5**. Accordingly, **D1** has the lowest retention for alkanes within the **D** series followed by **D3** and **D5** which shows the highest retention. The dual nature of ionic liquids is evident from these separations as both the alkane series and alcohol

series are easily separated. Finally it was observed that the retention of alkanes by the tricationic ionic liquids is generally lower than their retention on monocationic and dicationic ionic liquids.^{44,45} Therefore other than the high separation efficiency and low peak tailing for alcohols, the **D** series of ILs have the distinction of being stationary phases that produce good separations for variety of analytes, but with less retention times than conventional columns. This might render trigonal tricationic ILs as desirable stationary phases in two dimensional GC analysis.

2.4.5 Flavor and Fragrance Mixture

The flavor and fragrance mixture contains structurally related esters (including two homologous series) and has 24 compounds. The separation of this series provides another indication of the selectivity and separation efficiency of the trigonal tricationic ionic liquids compared to commercial columns. According to the Grob test mixture and the alcohol/alkane test results, the commercial column SP-2331 has comparable polarity to the trigonal tricationic ionic liquids, especially the **D** core series. The flavor and fragrance mixture is used to determine the separation efficiencies of columns with comparable polarities (see Figure 2.8). Column **C1** separated 21 compounds and co-eluted 3. The furfuryl homologous series elutes separately from the other esters. Only the last compound of the series furfuryl octanoate overlapped with benzyl butyrate. Again the **C4** column showed the least retention for the mixture and all the compounds were eluted before 14 minutes. Five compounds were not baseline separated with the **C4** column. However, with the **D** series columns the compounds are much better separated. Especially with the **D5** column, the retention and selectivity were comparable to a commercial (SP-2331) column, but the separation was much better. In

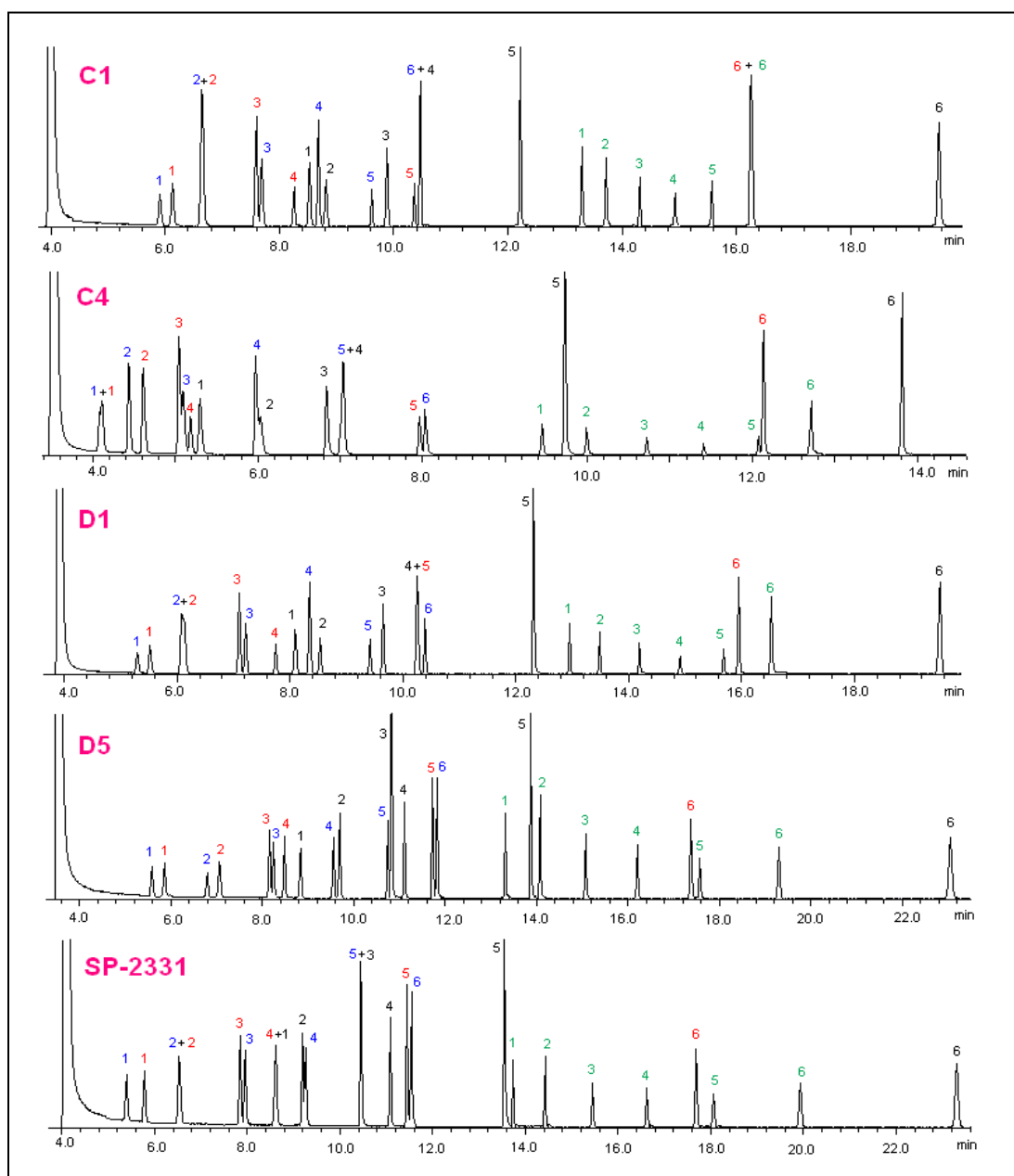


Figure 2.8 Separation of flavor and fragrance mixture.

1 ethyl propionate, 2 ethyl butyrate, 3 ethyl valerate, 4 ethyl hexanoate, 5 ethyl heptanoate, 6 ethyl octanoate, 1 methyl butyrate, 2 isopropyl butyrate, 3 propyl butyrate, 4 allyl butyrate, 5 hexyl butyrate, 6 benzyl butyrate, 1 methyl tiglate, 2 isopropyl tiglate, 3 propyl tiglate, 4 allyl tiglate, 5 hexyl tiglate, 6 benzyl triglate, 1 furfuryl propionate, 2 furfuryl butyrate, 3 furfuryl pentanoate, 4 furfuryl hexanoate, 5 furfuryl heptanoate, 6 furfuryl octanoate, 40 °C for 3 min, 10 °C min⁻¹ to 150 °C; 1 mL min⁻¹ He; MS detector. All chromatograms were obtained using 30 m x .25 mm x 0.20 μm d_f columns.

D5 column, all the 24 compounds are nearly base line separated whereas in the commercial column three esters co-elute and two are only partially separated (isopropyl tiglate and ethyl hexanoate). This confirms the fact that **D5** is a highly efficient and selective stationary phase for gas chromatography.

2.4.6 FAME Isomer Separation

Determination of fatty acid content in edible oils has been an area of high interest due to its importance in dietary, nutritional and therapeutic fields.²⁰⁶ Generally these isomeric unsaturated carboxylic acids are converted to their methyl esters and the fatty acid methyl esters (FAME) are separated using highly polar stationary phases.^{207,208} In this test, a mixture of methyl oleate (9*cis* 18:1) and methyl elaidate (9*trans* 18:1) were separated using the highly polar trigonal tricationic IL stationary phases **D1**, **D3**, **D5** and the commercial SP-2331 stationary phase (see Figure 2.9). The *trans*- isomer is twice the concentration (10 mg ml⁻¹) of the *cis*- isomer (5 mg ml⁻¹) for ease of identification. In the **D** core trigonal tricationic ionic liquid columns and the commercial SP-2331 column, the *trans* FAME elutes before the *cis* analogue. It is characteristic for cyanopropyl-based stationary phases to elute the *trans*- isomer first. With polyethylene glycol-based stationary phases, the *cis*- isomer elutes first. This indicates that the **D** core ionic liquids when used as stationary phases are more similar to the highly polar cyanopropyl stationary phase, but with greater thermal stability. Under similar separation conditions, **D5** shows the best separation for the *cis* and *trans* isomers by the **D** core series of ILs, followed by **D3** and **D1** respectively.

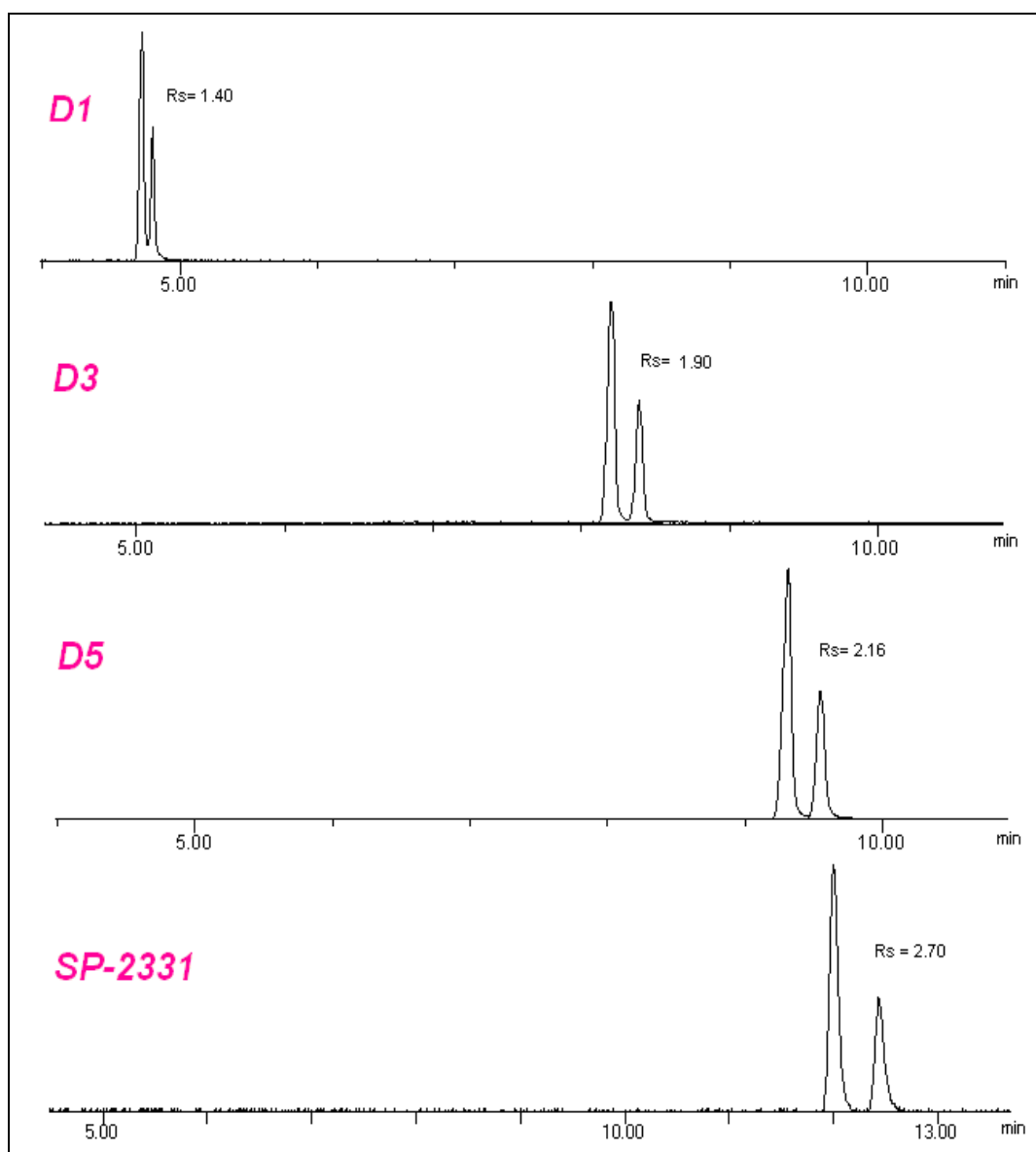


Figure 2.9 Separation of a mixture of methyl oleate (5 mg mL^{-1}) and methyl elaidate (10 mg mL^{-1}).

Column dimensions: $30\text{m} \times .25 \text{ mm} \times .20 \mu\text{m}$ d_f columns. GC separation conditions: isothermal at 165°C ; 1 mL min^{-1} He; MS detector.

2.5 Conclusions

Use of multifunctional ionic liquids as stationary phases for GC can be limited as the most common counter anion for many ionic liquids (i.e., bis(trifluoromethanesulfonyl)imide) results in peak tailing for alcohols and other H-bond forming analytes. Specific **D**-core trigonal tricationic ILs were shown to overcome this problem. According to the solvation parameter study, all monocationic, dicationic and long chain linear tricationic ionic liquids have almost identical apparent polarities and interaction parameters. However, those were quite different for the some trigonal tricationic ILs, namely the **C4**, and **D**-core series, and resulted in unique selectivities and retention behaviors. This uniqueness appears to be the result of two main factors. First is the rigid trigonal geometry which forces the three positive charges to reside in close proximity for ILs with short linkage chains. The second is the contribution from the Amide group. The prominent interaction types of trigonal tricationic ILs were dipole–type interactions, H–bonding interactions and dispersive interactions. Alcohol/alkane mixture and Grob test mixtures indicated that these ionic liquids are far more polar than either the monocationic or dicationic ionic liquids reported thus far. Nitrogen core ionic liquids **C1** and **C4** were the most polar stationary phases and displayed very low retention for alkanes. Grob test, FAME isomer separation, and elution order of C18:1 *cis-trans* FAME isomers indicated that **D** core ionic liquids, especially **D5** have polarities comparable to SP-2331, a 100% cyanopropylpolysiloxane commercial stationary phase. Ionic liquid **D5** stands out as it shows minimum peak tailing for alcohols and other H–bonding analytes. According to the flavor and fragrance test, **D1** and **D5** are complementary to each other and show higher selectivity and superior separation efficiencies than the commercial SP-2331 stationary phase which

has roughly comparable polarity. Furthermore, **D5** is more thermally stable than the SP-2331. It was observed that benzyliimidazolium cationic moiety introduces much higher viscosities to the ionic liquid systems. IL **D3** has the highest viscosity among ionic liquids ever to be reported. All these trigonal tricationic ILs were highly thermally stable and had a minimum liquid temperature range of about 300 °C. These values far exceed those observed for traditional monocationic ionic liquids. According to these results, trigonal tricationic ionic liquid **D5** is very promising as a highly polar stationary phase that has high thermal stability and yields symmetrical peaks for H-bonding analytes.

CHAPTER 3

LINEAR TRICATIONIC ROOM TEMPERATURE IONIC LIQUIDS:
SYNTHESIS, PHYSIOCHEMICAL PROPERTIES AND
ELECTROWETTING PROPERTIES

3.1 Abstract

Efficient and facile synthesis of novel linear tricationic room temperature ionic liquids was performed and their physiochemical properties were determined. Different physiochemical properties were observed according to the structural variations such as the cationic moiety and the counter anion of the ionic liquid. The electrowetting properties of these ionic liquids were also investigated and linear tricationic ionic liquids were shown to be advantageous as effective electrowetting materials due to their high structural flexibility.

3.2 Introduction

Room temperature ionic liquids (RTILs) are a class of salts that are liquids at or near room temperature.¹ Recently RTILs have attracted much attention in academic research and industry since they have shown profound advantages in the context of green chemistry and have great technological potential.^{10,209-211} Recently monocationic, dicationic and tricationic ionic liquids have been used extensively in the field of analytical chemistry as ion pairing reagents for the ultra trace detection of anions in the positive mode of electrospray ionization mass spectrometry (ESI-MS),^{127,128} high thermal stability gas chromatographic (GC) stationary phases,^{44,45,48,212} capillary electrophoresis (CE),²¹³ and electrowetting²¹⁴⁻²¹⁶ applications. Payagala *et al.* recently

reported the synthesis and physicochemical properties of a series of dicationic and tricationic ionic liquids.^{48,191} These reported ILs possessed good thermal stabilities and higher viscosities with compare to monocationic ILs. Moreover, it was shown by Payagala *et.al.* that physicochemical properties such as viscosity, density, thermal stability, melting point and solubility behaviors can be varied (tuned) to a greater extent in multi-cationic ILs than in the conventional ILs by changing the cation type, linkage chain length, etc.^{48,56,191} However, the tuning capability for trigonal tricationic ILs¹⁹¹ was lower than that of linear dicationic ILs.⁴⁸ This was because in most of the trigonal ILs synthesized, there were only two methylene moieties between the rigid trigonal core and the three pendant cationic moieties. The rigid trigonal geometry and the existence of three charge carrying moieties in the close proximity resulted in high apparent polarity and relatively high melting salts. Based on these observations, it was concluded that for multi-cationic ILs, the linear geometry would give the best tunability in terms of physicochemical properties and the highest probability of forming RTILs.

The interesting physicochemical properties of the ILs have led to their use in applications involving electrowetting on dielectric-based microfluidic devices.²¹⁴⁻²¹⁶ Electrowetting (EW) is the decrease in contact angle when an external voltage is applied across the solid/liquid interface. Simple EW which utilizes a metal base to hold the droplet is often associated with the drawback of droplet instability with change of the voltage whereas electrowetting on dielectric solid (e.g., Teflon) produces stable and reversible droplet shape with changes in the voltage.^{215,217,218} Since reversibility of the droplet shape with the change in voltage is an important factor in microfluidic devices, electrowetting on dielectric (EWOD) has shown greater success in applications such as fluid lens systems, electrowetting displays, optical filters, paint drying, micromotors,

electronic microreactors, and in controlling fluids in multichannel structures.²¹⁷⁻²²¹ Water or aqueous electrolytes are used in nearly all EWOD devices. Water-based systems were known to create complications due to their evaporation, low thermal stability and tendency to contribute to corrosion in integrated electronics.²¹⁷ The unique properties of RTILs including negligible vapor pressure, ultra high stability over a wide temperature range, and large electrochemical windows¹ make them ideal in EWOD applications over traditional aqueous or electrolyte solutions. Recently a detailed study was carried out to find electrowetting properties of traditional and multifunctional ILs.²¹⁶ These EWOD-based microreactors and microextraction devices have been used in various scientific areas. Dubois *et al.* demonstrated the use of IL droplets as electronic microreactors on an open digital microfluidic chips.²²² Also, Chatterjee *et al.* recently demonstrated that ILs can be used in digital microfluidic devices.²²³ Moon *et al.* used ILs in EWOD-based micro-heat transfer device and Kunchala *et al.* used an IL in a EWOD-based liquid-liquid extraction device.

The contact angle θ , between the dielectric surface and the ionic liquid droplet under an external voltage of V is derived from a combination of Young's and Lippmann's equations (eq 1).^{215,216}

$$\cos \theta = \cos \theta_0 + \frac{c}{2\gamma} V^2 = \cos \theta_0 + \frac{\epsilon \epsilon_0}{2\gamma t} V^2 \dots\dots\dots(3.1)$$

Here, c is the capacitance per unit area (specific capacitance), ϵ is the relative permittivity of the dielectric layer (dielectric constant), ϵ_0 is the permittivity of a vacuum, γ is the surface tension of the liquid, t is the thickness of the dielectric layer, θ is the

contact angle at the designated voltage across a dielectric layer, and θ_0 is the contact angle at zero voltage. As the voltage increases, the contact angle also increases according to eq 3.1. After a certain point, the contact angle starts to deviate from the regular behavior with increasing voltage. The voltage and corresponding contact angle where this occurs is referred to as the saturation voltage and saturation angle, respectively. According to eq 3.1, a plot of contact angle versus applied voltage should give a parabolic graph as shown in Figure 3.1.

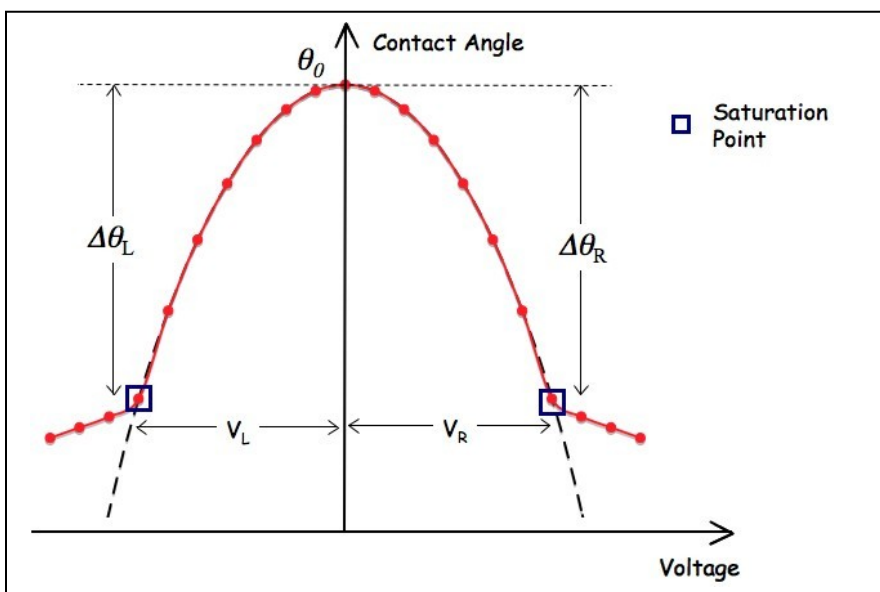


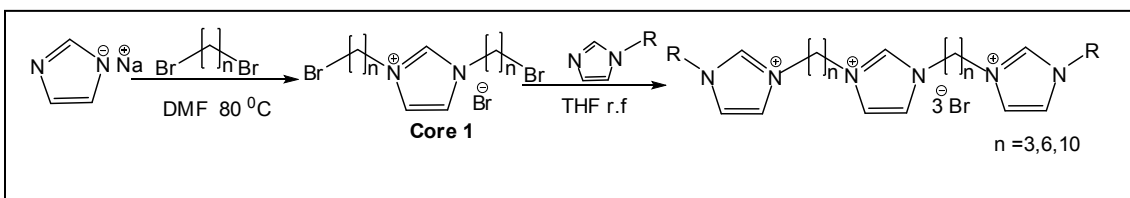
Figure 3.1 Plot of contact angle vs voltage according to Young's and Lippmann's equation.

Our previous studies have shown the use of a series of RTILs in EW experiments and a correlation between contact angle variation with the structure of the ionic liquid (IL). Monocationic, dicationic and tricationic ILs were used in those experiments. The trigonal tricationic ILs in our previous study were of trigonal geometry hence had relatively rigid structure.¹⁹¹

In this study, we report the synthesis and physiochemical properties and electrowetting properties of linear tricationic ionic liquids (LTILs) for the first time. Furthermore, we explore the electrowetting properties and their correlation with structural flexibility.

3.3 Experimental Section

Structures of the LTILs synthesized are illustrated in Figure 3.2 and scheme 1 illustrates the synthesis of the core structure.



Scheme 3.1 Synthesis of LTIL with R-substituted methyl imidazole as the charge carrying moiety.

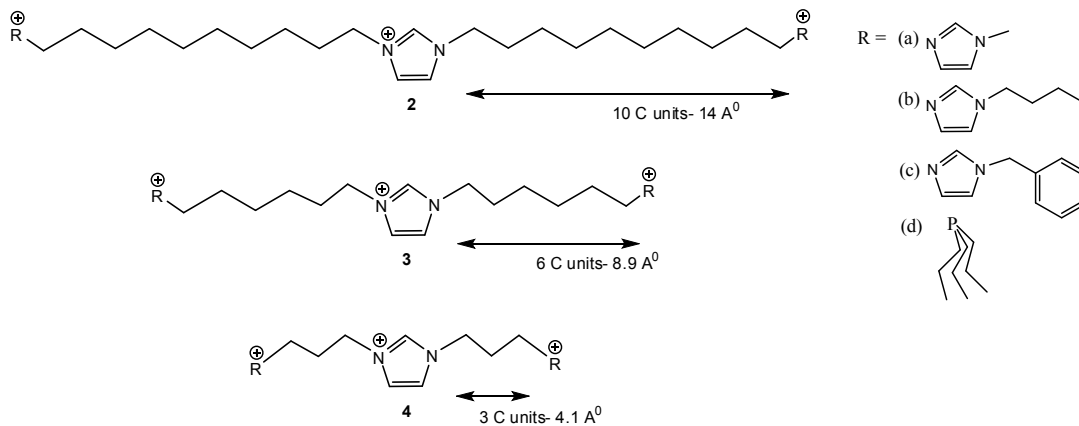


Figure 3.2 Structures of linear tricationic ionic liquids.

3.3.1 General Methods

All ^1H NMR, ^{13}C NMR (data reported are for bromide salts), and ^{31}P NMR spectra were recorded at 295 ± 1 K on JEOL Eclipse 300 MHz spectrometer. All NMR spectra were recorded in deuterated dimethylsulfoxide and the chemical shifts were measured relative to residual nondeuterated solvent resonances. Electrowetting experiments were conducted by using a slightly modified contact angle goniometer (www.ksvltd.com, Monroe, CT). Elemental analysis was performed on a Perkin-Elmer 2400 CHN analyzer. All experiments with moisture- and/or air-sensitive compounds were run under a dried nitrogen or argon atmosphere.

Caution 1: Tripropylphosphine is a pyrophoric substance and should be handled carefully under a stream of nitrogen or argon.

Caution 2: Toxicity data for the synthesized ionic liquids are unavailable hence should be handled carefully.

3.3.1.1 Glass transition temperature / melting point

The thermal measurements were performed with a differential scanning calorimeter (DSC, PerkinElmer Diamond DSC, 710 Bridgeport Av, Shelton, CT, USA). Diamond DSC was calibrated using an indium primary standard, with solid-solid transitions for cyclohexane and ethylbenzene as supplementary low temperature standards. IL samples (5-10 mg) were sealed in aluminium pans and an empty aluminium pan was used as reference. The measurements were carried out in the temperature range -120 °C to a predetermined temperature. The samples were sealed in aluminium pans, and then heated and cooled at scan rate of 10 °C min^{-1} under a flow of nitrogen. For solid compounds, the melting points were verified using a capillary melting point apparatus (MEL-TEMP, 68 Cambridge, MA, USA).

3.3.1.2 Density

The densities of the ionic liquids were determined at 23 ± 1 °C with Kimble Glass Specific Gravity Pycnometer (Vineland, NJ).

3.3.1.3 Refractive Index

Refractive index measurements were conducted at 23 ± 1 °C using a Bausch & Lomb Abbe-3L refractometer.

3.3.1.4 Viscosity

Kinematic viscosities were determined at 30 ± 1 °C using Cannon-Manning Semi-Micro capillary viscometer (State College, PA).

3.3.1.5 Thermal stability analysis

Thermogravimetric analysis (TGA) was done using a TGA 2050 (TA Instruments Inc., Thermal Analysis & Rheology, New Castle, DE, USA). Samples (ca. 20 mg) were placed on the platinum pans, and heated at 10 °C min^{-1} from room temperature to 600 °C in a dynamic nitrogen atmosphere. The decomposition temperatures were reported as the temperatures of 1%, 5% and 50 % weight loss of the sample.

3.3.1.6 Electrowetting experiments

Electrowetting experiments were conducted by using a slightly modified contact angle goniometer (www.ksvltd.com, Monroe, CT). Figure 3.3 shows the arrangement for the electrowetting experiment. Indium-tin-oxide (ITO, 30 nm thickness) pre-coated unpolished float glass slides (www.delta-technologies.com, Stillwater, MN) were used as purchased. They were dip-coated in a 4% (w/v) of Teflon AF1600 (www2.dupont.com, Wilmington, DE) in Fluoroinert FC75 solvent (www.fishersci.com Barrington, IL) solution. The dipping speed was approximately 0.78 ± 0.03 mm/s in a

custom made dipcoater. Only 3/4 of the slide was dipped in the solution, then it was stopped for 5 seconds and after that the slide was raised at the same speed. The coated slides were kept in an oven at 112 °C for 6 min, at 165 °C 5 min and at 328 °C for 15 min. Once Teflon coated glass slides were taken out from the oven, they were allowed to cool to room temperature. Then they were washed thoroughly with acetone and deionized water followed by air-drying.

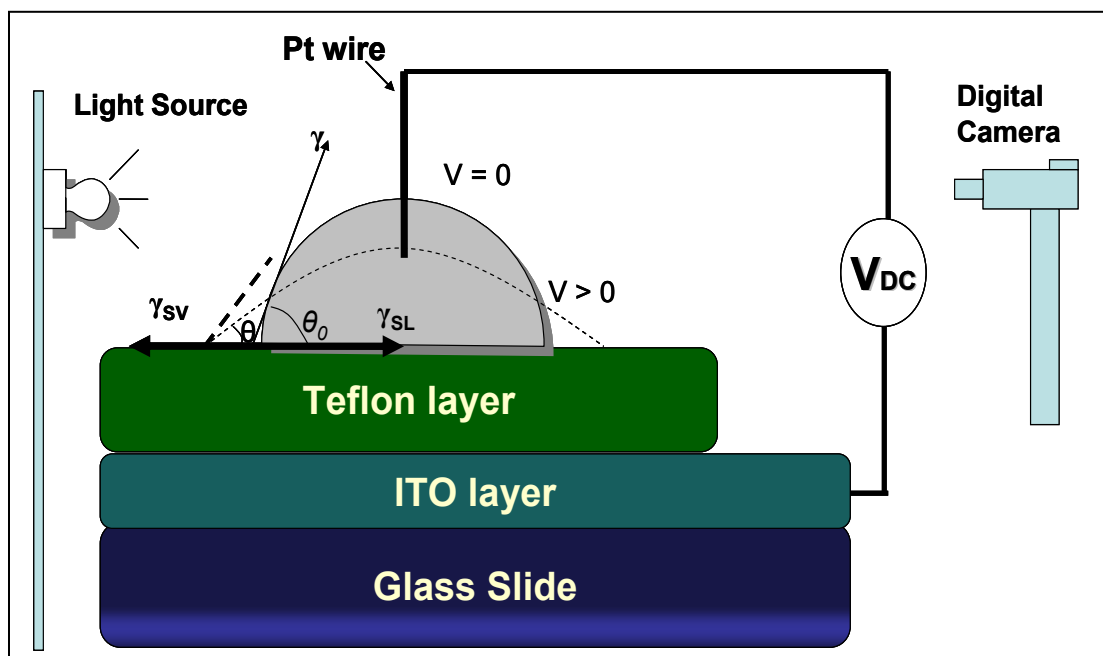


Figure 3.3 The electrowetting experimental setup.

Here, γ , γ_{SV} , and γ_{SL} are the interfacial tensions associated with the liquid/vapor, solid/vapor, and solid/liquid interfaces.

A capillary tube was used to place a drop of IL on top of the Teflon layer. CAM 200 software (www.ksvltd.com, Monroe, CT) was used to calculate drop volume, it was between $5 \pm 2 \mu\text{L}$ for all experiments. Keithley 2400 SourceMeter (www.keithley.com, Cleveland, OH) was used to apply voltage in 5 V increments starting from 0 to + 70 V. The positive probe was connected to the Pt wire and negative probe was connected to

the ITO layer (see Figure 3.3). Afterwards, the above procedure was repeated for 0 to – 70 V for a fresh drop of IL placing at a different position on the surface. At each voltage increment a picture was taken and then CAM 200 software was used to measure corresponding contact angles. Finally, the contact angle versus voltage curves were plotted.

3.3.2 Materials

The reagents required for synthesis included anhydrous dimethylformamide, anhydrous acetonitrile, anhydrous tetrahydrofuran, sodium imidazole, 1,3-dibromopropane, 1,6-dibromohexane, 1,10-dibromodecane, methylimidazole, butylimidazole, benzylimidazole, benzyl imidazole and tripropylphosphine which were purchased from Sigma-Aldrich (Milwaukee, WI, USA). All chemicals were of reagent grade and were used without further purification. For column chromatography, Silica Gel 60 Å (Sorbent Technologies, Inc.; 200-425 mesh) was used.

Procedure for the synthesis of the core structure **(1-bromodecyl-3-bromodecyl imidazolium bromide salt (1a))**: Sodium imidazole (1.0 g, 12.1 mmol) in anhydrous 20 ml of DMF was added slowly in to a solution of dibromodecane (18.2 g 60.5 mmol) in 100 ml of anhydrous DMF by using a syringe pump over a period of 3 hr at room temperature. After completion of the addition, the reaction mixture was heated up to 70 °C for 12 hr. Then DMF was evaporated under vacuum and the resulting crude material was washed with hexane (5 × 100 ml) to remove excess dibromoalkane. Then the crude product was subjected to column chromatography using CH₃OH:CH₂Cl₂ 1:9 as the eluent system. The purified product was then dried under vacuum overnight to yield the desired product in 55% (3.8 g). ¹H NMR: δ 9.21 (s, 1H), 7.80 (d, *J* = 1.7 Hz, 2H), 4.15

(t, J = 7.0 Hz, 4H), 3.51 (t, J = 7.0 Hz, 4H), 1.77 (m, 8H), 1.33 (m, 4H), 1.24 (br s, 20H); ^{13}C NMR: δ 136.4, 123.0, 49.4, 35.8, 32.7, 29.7, 29.2, 28.8, 28.6, 28.0, 25.9. Anal Calcd for $\text{C}_{23}\text{H}_{43}\text{N}_2$: C, 47.04; H, 7.38; Br, 40.82; N, 4.77; Found: C, 47.1; H, 7.9; N, 4.8. ESI-MS (m/z): 507.4 (M^+), found 507.2.

Procedure for the synthesis of the core structure **(1-bromohexyl-3-bromohexyl imidazolium bromide salt (1b))**: This compound was prepared by a similar procedure as described above for **1a**. Sodium imidazole (1.0 g, 12.1 mmol) in 20 ml anhydrous DMF was added slowly in to a solution of dibromodecane (14.8 g, 60.5 mmol) 100 ml of anhydrous DMF by using a syringe pump over a period of 3 hr at room temperature. After completion of the addition, the solution was stirred for additional 12 hr. Then DMF was evaporated under vacuum and the resulting crude material was washed with hexane (5 \times 100ml) to remove excess dibromoalkane. Then the resulting crude product was subjected to column chromatography using $\text{CH}_3\text{OH}:\text{CH}_2\text{Cl}_2$ 1:9 as the eluent system. The purified product was then dried under vacuum overnight to yield the desired product in 62 % (2.9 g). ^1H NMR: δ 9.38 (s, 1H), 7.84 (s, 2H), 4.18-4.13 (t, J = 7.2, 4H), 3.50-3.46 (t, J = 6.5, 4H), 1.81-1.70 (m, 8H), 1.41-1.31 (m, 4H), 1.25-1.15 (m, 4H); ^{13}C NMR: δ 136.5, 122.9, 60.9, 49.2, 32.6, 29.8, 25.8, 25.3; Anal Calcd for $\text{C}_{15}\text{H}_{27}\text{N}_2$: C, 37.92; H, 5.73; N, 5.90; Found: C, 37.9; H, 5.8; N, 5.9. ESI-MS (m/z): 475.10 (M^+), found 475.1.

Procedure for the synthesis of the core structure **(1-bromopropyl-3-bromopropyl imidazolium bromide salt (1c))**: This compound was prepared in a similar procedure to **1b** (Yield 70 %, 3.3 g). ^1H NMR: δ 9.27 (s, 1H), 7.83 (d, J = 1.4 Hz, 2H), 4.28 (t, J = 7.0 Hz, 4H), 3.54 (t, J = 7.0 Hz, 4H), 2.37 (m, 4H); ^{13}C NMR: δ 136.4, 122.9, 49.3, 29.9,

29.2, 28.9, 20.4, 19.8, 15.9, 15.2. Anal Calcd for $C_9H_{15}N_2$: C, 27.65; H, 3.87; Br, 61.32; N, 7.17; Found: C, 27.6; H, 3.9; N, 7.2. ESI-MS (m/z): 311.0 (M^+), found 311.0.

Procedure for the synthesis of LTILs (**2a-d**, **3a-d**, **4a-d**): All the reactions were carried out in tetrahydrofuran (THF) except for **4a-d** in which acetonitrile (ACN) was used as the reaction solvent. Linear core structures **1a**, **b** or **c** 1eq in THF (or ACN) were reacted with 2.5 eq of methyl imidazole, butyl imidazole, benzyl imidazole or tripropyl phosphine under reflux over 36-48 hrs. (Phosphonium ILs need to be reacted for 48 hrs). Then the solvent was removed in vacuo and resulting thick liquid or solid was dissolved in 5-10 ml of deionized water. The aqueous layer was then washed with ethyl acetate (6 × 100 ml) and water was removed in vacuo. The final product as the bromide salt was then dried in high vacuum (75-85 % yield).

Final products were synthesized through a metathesis reaction of the bromide salts with lithium trifluoromethanesulfonimide ($LiNTf_2$), sodium tetrafluoroborate ($NaBF_4$) and lithium trifluoromethanesulfonate ($LiTfO$) according to the previously published procedure.⁴⁸

1-(1'-methyl-3'-decylimidazolium)-3-(1''-methyl-3''-decylimidazolium) imidazolium tri [bis(trifluoromethanesulfonyl)imide] (2a). 1H NMR (300 MHz, $DMSO-d_6$): δ 9.15 (s, 1H), 9.08 (s, 2H), 7.78 (d, $J = 1.4$ Hz, 2H), 7.75 (t, $J = 1.4$ Hz, 2H), 7.69 (t, $J = 1.4$ Hz, 2H), 4.14 (t, $J = 7.2$ Hz, 8H), 3.84 (s, 6H), 1.65-1.80 (m, 8H), 1.24 (br s, 26H); ^{13}C NMR: δ 137.2, 136.4, 124.1, 122.9, 122.8, 49.3, 49.2, 36.3, 29.9, 29.3, 28.9, 26.1; ^{19}F NMR: δ -78.6. Anal. Calcd for $C_{37}H_{55}N_9$: C, 32.86; H, 4.10; N, 9.32; Found: C, 32.8; H, 4.3; N, 9.3. ESI-MS (m/z): 170.4 (M^{3+}), found 170.5.

1-(1'-butyl-3'-decylimidazolium)-3-(1''-butyl-3''-decylimidazolium)imidazolium tri [bis(trifluoromethanesulfonyl)imide] (2b). 1H NMR: δ 9.17 (s, 1H), 9.15 (s, 2H),

7.80-7.77 (m, 6H), 4.18 (q, $J = 6.8$ Hz, 12H), 1.81-1.74 (m, 12H), 1.30-1.18 (br s, 28H), 0.89 (t, $J = 7.5$ Hz, 6H); ^{13}C NMR: δ 136.5, 122.9, 122.8, 49.3, 49.0, 31.8, 29.8, 29.2, 28.8, 26.0, 19.3, 13.8; ^{19}F NMR: -78.6. Anal. Calcd for $\text{C}_{43}\text{H}_{67}\text{N}_9$: C, 35.95; H, 4.70; N, 8.78; Found: C, 35.5; H, 4.8; N, 8.8. ESI-MS (m/z): 198.51 (M^{3+}), found 198.5.

1-(1'-benzyl-3'-decylimidazolium)-3-(1''-benzyl-3''-decylimidazolium)imidazolium tri [bis(trifluoromethanesulfonyl)imide] (2c) ^1H NMR: δ 9.25 (s, 2H), 9.12 (s, 1H), 7.79-7.75 (m, 6H), 7.38 (m, 10H) 5.38 (s, 2H), 4.14 (q, $J = 7.0$ Hz, 8H), 1.79-1.72 (m, 8H), 1.20 (br s, 24H); ^{13}C NMR: δ 136.6, 136.4, 135.4, 129.5, 129.3, 128.7, 123.3, 123.1, 122.9, 52.4, 49.5, 29.8, 29.3 28.8, 26.1; ^{19}F NMR: -78.6. Anal. Calcd for $\text{C}_{49}\text{H}_{63}\text{N}_9$: C, 39.12; H, 4.22; N, 8.38; Found: C, 39.2; H, 4.3; N, 8.4. ESI-MS (m/z): 221.1 (M^{3+}), found 221.2.

1-decyltripropylphosphonium-3-decyltripropylphosphonium imidazolium tri [bis(trifluoromethanesulfonyl)imide] (2d). ^1H NMR (300 MHz, $\text{DMSO}-d_6$): δ 9.33 (s, 1 H), 7.83 (d, $J = 1.4$, 2H), 4.18 (t, $J = 7.2$, 4H), 2.17-2.10 (m, 18H), 1.77-1.73 (m, 18 H), 1.37-1.22 (m, 20H), 0.98 (t, $J = 7.0$, 18H); ^{13}C NMR: δ 136.4, 122.9, 49.3, 29.9, 29.3, 28.8, 26.1, 21.24, 20.4, 19.8, 18.5, 17.9, 15.9, 15.2; ^{19}F NMR: -78.6. Anal. Calcd for $\text{C}_{47}\text{H}_{85}\text{N}_5$: C, 37.42; H, 5.68; N, 4.64; Found: C, 37.7; H, 5.7; N, 4.6. ESI-MS (m/z): 222.5 (M^{3+}), found 222.5.

1-(1'-methyl-3'-hexylimidazolium)-3-(1''-methyl-3''-hexylimidazolium)imidazolium tri [bis(trifluoromethanesulfonyl)imide] (3a). ^1H NMR: δ 9.50 (s, 1H), 9.35 (s, 2H), 7.86 (s, 2H), 7.84 (s, 2H), 7.73 (s, 2H), 4.17 (m, 8H), 3.84 (s, 6 H), 1.77 (m, 8H), 1.24 (m, 8H); ^{13}C NMR: δ 137.1, 136.5, 124.1, 122.9, 122.8, 49.1, 49.1, 36.3, 29.6, 29.5, 25.3; ^{19}F NMR: -78.6. Anal. Calcd for $\text{C}_{29}\text{H}_{39}\text{N}_9$: C, 28.09; H, 3.17; N, 10.17; Found: C, 28.1; H, 3.2; N, 10.2. ESI-MS (m/z): 133.1 (M^{3+}), found 133.1.

1-(1'-butyl-3'-hexylimidazolium)-3-(1''-butyl-3''-hexylimidazolium)imidazolium tri [bis(trifluoromethanesulfonyl)imide] (3b). ¹H NMR: δ 9.47 (s, 1H), 9.43 (s, 2H), 7.86 (s, 4H), 7.84 (s, 2H), 4.17 (t, J = 7.2 Hz, 12H), 1.79-1.72 (m, 12H), 1.24-1.17 (m, 12H), 0.85 (t, J = 7.2 Hz, 6H); ¹³C NMR: δ 136.5, 122.9, 49.1, 49.0, 31.8, 29.5, 25.3, 19.3, 13.8; ¹⁹F NMR: -78.6. Anal. Calcd for C₃₅H₅₁N₉: C, 31.75; H, 3.88; N, 9.52; Found: C, 31.7; H, 3.9; N, 9.5. ESI-MS (m/z): 161.1 (M³⁺), found 161.1.

1-(1'-benzyl-3'-hexylimidazolium)-3-(1''-methyl-3''-hexylimidazolium)imidazolium tri [bis(trifluoromethanesulfonyl)imide] (3c). ¹H NMR: δ 9.52 (s, 1H), 9.44 (s, 2H), 7.85 (s, 6H), 7.44-7.34 (M, 10H), 5.45 (s, 4H), 4.19-4.15 (m, 8 H), 1.77 (s, 8H), 1.24 (m, 8H); ¹³C NMR (75 MHz, DMSO-*d*₆): δ 136.6, 135.4, 129.5, 129.4, 128.8, 123.3, 123.0, 122.9, 52.3, 49.3, 49.1, 29.6, 29.5, 25.3; ¹⁹F NMR: -78.6. Anal. Calcd for C₄₁H₄₇N₉: C, 35.37; H, 3.40; N, 9.05; Found: C, 35.3; H, 3.4; N, 9.1. ESI-MS (m/z): 183.7 (M³⁺), found 183.8.

1-(hexyltripropylphosphonium)-3-(hexyltripropylphosphonium)imidazolium tri [bis(trifluoromethanesulfonyl)imide] (3d). ¹H NMR: δ 9.55 (s, 1H), 7.87 (s, 2H), 4.21 (t, J = 6.9 Hz, 4H), 2.24-2.12 (m, 16H), 1.85-1.75 (m, 4H), 1.56-1.26 (m, 24H) 1.00-0.95 (t, J = 6.8 Hz, 18H); ¹³C NMR: δ 136.6, 122.9, 49.2, 29.5, 25.3, 21.0, 20.5, 19.9, 15.9, 15.7, 15.3; ¹⁹F NMR: -78.6. Anal. Calcd for C₃₉H₆₉N₅: C, 33.55; H, 4.98; N, 5.02; Found: C, 33.6; H, 5.0; N, 5.0. ESI-MS (m/z): 185.1 (M³⁺), found 185.2.

(1'-methyl-3'-propylimidazolium)-3-(1''-methyl-3''-propylimidazolium)imidazolium tri [bis(trifluoromethanesulfonyl)imide] (4a). ¹H NMR: δ 9.50 (s, 1H), 9.32 (s, 2H), 4.31-4.25(m, 8H), 3.87 (s, 6H), 2.46-2.42 (m, 4H); ¹³C NMR: δ 137.1, 123.0, 49.6, 26.0, 22.1, 20.4, 19.8, 15.9, 15.7, 15.3, ¹⁹F NMR: -78.6. Anal. Calcd for C₂₃H₂₇N₉: C, 23.90;

H, 2.3; N, 10.9; Found: C, 23.9; H, 2.40; N, 10.97. ESI-MS (m/z): 105.0 (M^{3+}), found 105.1.

1-(1'-butyl-3'-propylimidazolium)-3-(1''-butyl-3''-propylimidazolium)imidazolium tri [bis(trifluoromethanesulfonyl)imide] (4b). ^1H NMR: δ 9.50 (s, 1H), 9.43 (s, 2H), 7.90-7.84 (m, 6H), 4.32-4.29 (m, 8H), 4.19 (t, $J = 7.2$ Hz, 4H), 2.48-2.43 (m, 4H), 1.81-1.76 (m, 4H), 1.31-1.23 (m, 4H), 0.90 (t, $J = 7.2$, 6H); ^{13}C NMR: δ 137.1, 136.8, 49.2, 46.4, 31.7, 29.9, 19.3, 13.8; ^{19}F NMR: -78.6. Anal. Calcd for $\text{C}_{29}\text{H}_{39}\text{N}_9$: C, 28.09; H, 3.17; F, 27.58; N, 10.17; Found: C, 28.0; H, 3.2; N, 10.2. ESI-MS (m/z): 133.1 (M^{3+}), found 133.1.

1-(1'-benzyl-3'-propylimidazolium)-3-(1''-benzyl-3''-propylimidazolium)imidazolium tri [bis(trifluoromethanesulfonyl)imide] (4c). ^1H NMR: δ 9.52 (s, 2H), 9.48 (s, 1H), 7.48-7.38 (m, 10H), 5.47 (s, 4H), 4.29 (q, $J = 5.8$ Hz, 8H), 2.45 (m, 4H); ^{13}C NMR: δ 137.2, 123.0, 62.5, 49.4, 26.0, 22.1, 20.5, 19.9, 16.1, 15.9, 15.3; ^{19}F NMR: δ -78.6. Anal. Calcd for $\text{C}_{35}\text{H}_{35}\text{N}_9$: C, 32.14; H, 2.70; N, 9.64; Found: C, 32.1; H, 2.7; N, 9.6. ESI-MS (m/z): 155.7 (M^{3+}), found 155.7.

1-propyltripropylphosphonium-3-propyltripropylphosphonium imidazolium tri[bis(trifluoromethanesulfonyl)imide] (4d). ^1H NMR: δ 9.12 (s, 1H), 7.84 (s, 2H), 4.24 (t, $J = 6.8$, 4H), 2.23-2.21 (m, 20H), 1.57-1.47 (m, 12H), 1.04-1.00 (m, 12H), 1.04 (t, $J = 7.2$ Hz, 18H); ^{13}C NMR: δ 137.9, 123.0, 62.5, 49.6, 26.0, 22.1, 20.4, 19.8, 15.9, 15.3, ^{19}F NMR (282 MHz): -78.6. Anal. Calcd for $\text{C}_{33}\text{H}_{57}\text{N}_5$: C, 30.21; H, 4.38; N, 5.34; Found: C, 30.2; H, 4.4; N, 5.3. ESI-MS (m/z): 157.1 (M^{3+}), found 157.1.

3.4 Results and Discussion

3.4.1 Synthesis of Core Structures and Linear ILs

The synthetic strategy involved in these linear tricationic ILs was different from previously reported ionic liquids for the following reasons: 1. **Core 1** (Scheme 1) was designed and synthesized in-house. It was separated and isolated from the dicationic and polycationic impurities that were formed during the reaction, by running through flash chromatographic column (SiO₂ 60 Å, CH₂Cl₂:CH₃OH 1:9). 2. Reaction solvent. In previous dicationic and trigonal tricationic IL syntheses, isopropyl alcohol was used as the reaction solvent in most cases.^{48,191} However, when alcohols are used, the basic imidazole tends to deprotonate the alcohol enabling unwanted nucleophilic substitution reactions.²²⁴ This complicated the separation of the pure LTILs from the reaction mixture. Therefore the solvent used in the synthesis of **Core 1** was dimethylformamide (DMF). This was because DMF dissolved sodium imidazole (NaIM) and it minimized the side reactions that take place with protic solvents. Other reaction solvents for the synthesis of ILs involving imidazolium moieties were found to be acetonitrile (ACN) and tetrahydrofuran (THF). However isopropyl alcohol can be used as the solvent in reactions involving tripropyl phosphonium which has a weak basic character compared to imidazole.

3.4.2 Physicochemical Properties of Linear Tricationic Ionic Liquids

In this study, 14 linear tricationic ionic liquids were synthesized and their physicochemical properties were investigated. The results are listed in Table 1.

Table 3.1 Physicochemical properties of linear tricationic ionic liquids

Ionic Liquid	MW g/mol	melting	Density[b] gcm-3	Refractive index	Viscosity[c] (cSt)	Thermal stability [d]			Miscibility [e]	
		point [a] (°C)				99 %w	95%w	50%w	Heptane	Water
2a-NTf2	1352.25	-53	1.65	1.45	1800	334	400	444	I	I
2b-NTf2	1435.29	-53	1.54	1.44	2400	350	390	430	I	I
2c-NTf2	1504.44	-36	1.36	1.48	4200	320	390	450	I	I
2d-NTf2	1507.37	-41	1.46	1.45	2100	360	410	440	I	I
2b-BF4	856.55	-18	1.33	-	-	191	308	369	I	M
2b-TfO	1043.18	-42	1.28	-	-	290	376	430	I	M
3a-NTf2	1240.03	-57	1.57	1.44	372	320	380	480	I	I
3b-NTf2	1324.19	-51	1.41	1.49	429	330	380	470	I	I
3c-NTf2	1391.14	-36	1.43	1.47	840	340	370	470	I	I
3d-NTf2	1396.3	-45	1.38	1.45	770	355	400	440	I	I
4a-NTf2	1155.88	-24	1.54	1.46	1200	290	360	410	I	I
4b-NTf2	1240.04	-44	1.48	1.49	600	310	370	470	I	I
4c-NTf2	1308.07	-27	1.41	1.48	4080	300	350	470	I	I
4d-NTf2	1312.14	71-72	1.59	-	-	320	390	480	I	I

[a] Determined by using Differential Scanning Calorimeter upon heating cycle and melting points are reported as the onset temperature of melting endotherm. [b] Determined by using a pycnometer, [c], Measured using capillary viscometer at 30 °C, [d] Decomposition temperature was determined by using TGA, 99% w = at 1% mass decrease of sample, 95% w = temperature at 5% mass decrease of the sample, 50% w = temperature at 50% mass decrease of sample [e] I = immiscible, M = miscible, [f] amorphous solid.

3.4.2.1 Phase transitions

Phase transition temperatures, including glass transition temperatures (T_g), were determined using differential scanning calorimetry (DSC). LTILs show significantly lower glass transition temperatures (except for **4d**) compared to many other types of ILs in the literature, such as symmetrical dicationic ILs.⁴⁸ It has been shown for most dicationic ILs that when the chain length is smaller than 3 methylene units, the IL becomes solid regardless of other structural changes.⁵⁶ However we found that LTILs with C-3 linkage chains (**4a**, **4b**, **4c**) (see Figure 3.1) do exist as RTILs when

the counter anion is bis(trifluoromethylsulfonyl)imide (NTf_2^-). This can be explained by the relative flexibility of the LTILs. Unlike trigonal tricationic ILs, the LTILs have greater conformational degrees of freedom which help to minimize charge repulsion interactions.²²⁵ The T_g values are mainly governed by the size and charge distribution of the anion and or cation.²²⁶ According to the literature, most ILs containing NTf_2^- are observed to be liquids at room temperature.^{45,48,56,191,227,228} When the negative charge carrying moiety is a halide, X^- ($\text{X}^- = \text{F}^-, \text{Cl}^-, \text{Br}^-, \text{I}^-$), BF_4^- , TfO^- (trifluoromethanesulfonate) or PF_6^- the ILs tend to have higher melting points.^{48,191}

The LTILs with methylimidazolium charge carrying moieties **2a**, **3a** and **4a** showed the lowest melting temperatures of the series. According to the melting point data in Table 1, the butylimidazole cationic moiety produces ILs with higher melting points compared to the methylimidazole moiety. This is probably because of the butyl group's greater van der Waals interactions. Relatively higher melting temperatures were observed when the IL incorporated the benzyl imidazole moiety, mainly because of the additional π - π stacking introduced by the phenyl groups.

3.4.2.2 Viscosities

The kinematic viscosities of these LTILs range from 372 to 4200 cSt at 303 K. LTILs with the C6 linkage chain generally showed lower viscosities ranging from 60-840 cSt. Typically monocationic ILs have lower kinematic viscosities.²²⁹ The viscosities are markedly higher in ILs with benzyl groups (see Table 3.1). The same phenomenon was observed in dicationic and trigonal tricationic ILs.^{48,191} It is interesting to note that ILs with a C3 linkage chain have higher viscosities compared to ILs with C6 linkage chain and lower viscosities when compared to those with C10 linkage chains. According to these results, ILs having C3 linkage chains seem to possess greater ionic

nature owing to closeness of the charged groups. When the distance between charged groups is increased to six methylene units ($\sim 8.9 \text{ \AA}$) as in ILs with C6 linkage chain, the ionic nature is reduced resulting a lower viscosity. However when the linkage chain is further increased up to ten methylene units ($\sim 14 \text{ \AA}$), higher viscosities are observed again due to the increase of intermolecular vander Waals interactions over ionic interactions.²²⁶

3.4.2.3 Densities

The densities of LTILs accompanying NTf_2^- anion range from 1.36 to 1.65 g cm^{-3} . The lowest density was observed for **2c** which has benzyl imidazolium cation and C10 linkage chains. The higher density values are obtained for LTILs with methylimidazolium groups. Moreover, when the chain length of the substituent at the 3-position of the imidazole increases from methyl imidazolium to butylimidazolium, the density decreases (**2a-2b**, **3a-3b**, and **4a-4b**). Similar observations have been reported for monocationic and dicationic ILs as well.⁴⁸

3.4.2.4 Refractive indices and solubilities

The refractive indices of the LTILs range from 1.44 to 1.49 and lies in between the general range observed for monocationic ILs.^{227,228}

The solubility of these LTILs parallels that of monocationic ILs^{227,228,230} in which all Br^- , BF_4^- , and TfO^- (trifluoromethane sulfonate) salts synthesized were soluble in water while all NTf_2^- salts were insoluble in water. All of the LTILs synthesized were insoluble in n-heptane.

3.4.2.5 Thermal Stability

For RTILs to be used in applications such as high temperature organic reactions^{231,232} and as GC stationary phases; they should possess a good thermal stability. Generally, phosphonium cation-based ILs show higher thermal stabilities compared to nitrogen cation-based ILs such as imidazolium and pyrrolidinium ILs.^{48,191,230} This trend was clearly seen in this study as well. LTIL **2d** which accompanies two tripropyl phosphonium cations has the highest thermal stability with only 5% thermal degradation at 410 °C.

3.4.3 Electrowetting Properties

Electrowetting properties of ILs are listed in Table 3.2. Figure 3.5 shows the electrowetting curves of linear tricationic ionic liquids with C6 linkage chain and Figure 3.7 shows the electrowetting curves of benzylimidazolium substituted tricationic ionic liquids with different linkage chain lengths and core structures.

Table 3.2 Electrowetting properties of linear tricationic ionic liquids.

Ionic Liquid	θ_o	$\Delta\theta_L$	$\Delta\theta_R$	V_L	V_R
2a	83	16	18	-40	50
2b	80	14	15	-35	30
2c	83	17	18	-50	40
2d	80	16	16	-60	40
3a	85	13	18	-40	40
3b	81	15	14	-30	35
3c	84	12	16	-35	40
3d	78	11	11	-30	35
4a	82	21	16	-35	40
4b	88	19	14	-40	50
4c	86	23	16	-60	55
4d	-	-	-	-	-
5a*	77	>25	>20	<-70	>70
5b*	88	18	18	-65	60
6a*	77	20	25	-55	60
6b*	82	>15	>14	<-70	>70

θ_o -Contact angle at zero voltage, $\Delta\theta_L$ - Change in contact angle at negative voltages, $\Delta\theta_R$ - Analogous contact angle change at positive voltages, V_L - Saturation voltage in the negative voltage realm, V_R -Analogous saturation voltage in the positive voltage realm. Structures of 5a-6b are shown in Figure 3.5. * Data taken from ref 216.

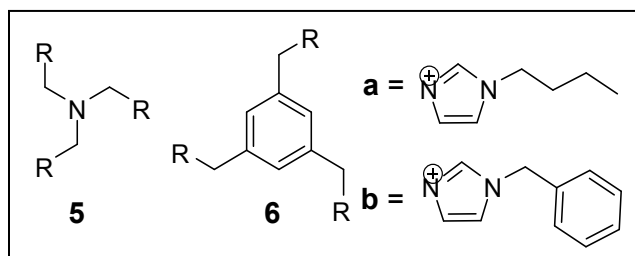


Figure 3.4 Structures of ILs 5a-6b.

3.4.3.1 θ_0 values

Since there is no external voltage at θ_0 , only the three interfacial tensions [solid/liquid, liquid/air and air/solid] govern the θ_0 value. However solid (Teflon) is common in all experiments, therefore only the surface tension of the IL governs the θ_0 value.²¹⁶ The higher the surface tension value of the IL, the higher the θ_0 value obtained.²¹⁶ Therefore from the observed θ_0 values the relative surface tension of these ILs can be deduced. This is a good indirect method to evaluate the relative surface tensions of this new class of ILs. According to Figure 3.5 and Table 2, ionic liquids **3a**, **3b**, **3c** and **3d** which have the same anion i.e. NTf_2^- and the same linkage chain length i.e. C6, the θ_0 values decrease in the order of **3a**>**3c**>**3b**>**3d**. This decrease is solely due to the end cationic moieties. The θ_0 value directly correlates with the surface tension. Therefore the surface tension of these ILs decrease based on the cation in the order; methyl imidazolium> benzyl imidazolium> butyl imidazolium> tripropyl phosphonium.

According to Figure 3.6 and Table 2, by considering θ_0 , surface tension values of benzyl substituted ILs are decreasing in the order of IL **14** >**4c**>**3c**>**2c**>**6b**. Surface tension values of liquids tend to increase with increasing of hydrophilicity.²³³ IL **5b** with a nitrogen core (see Figure 3.6) has more hydrophilic character compared to **6b** with a mesitylene core. Therefore IL **5b** has higher surface tension than IL **6b** which is reflected by the θ_0 value. Similarly when the alkyl chain length of the LTILs increases from C3 to C10 as in **4c** to **2c**, the hydrophobic character increases and therefore surface tension decreases.²¹⁴

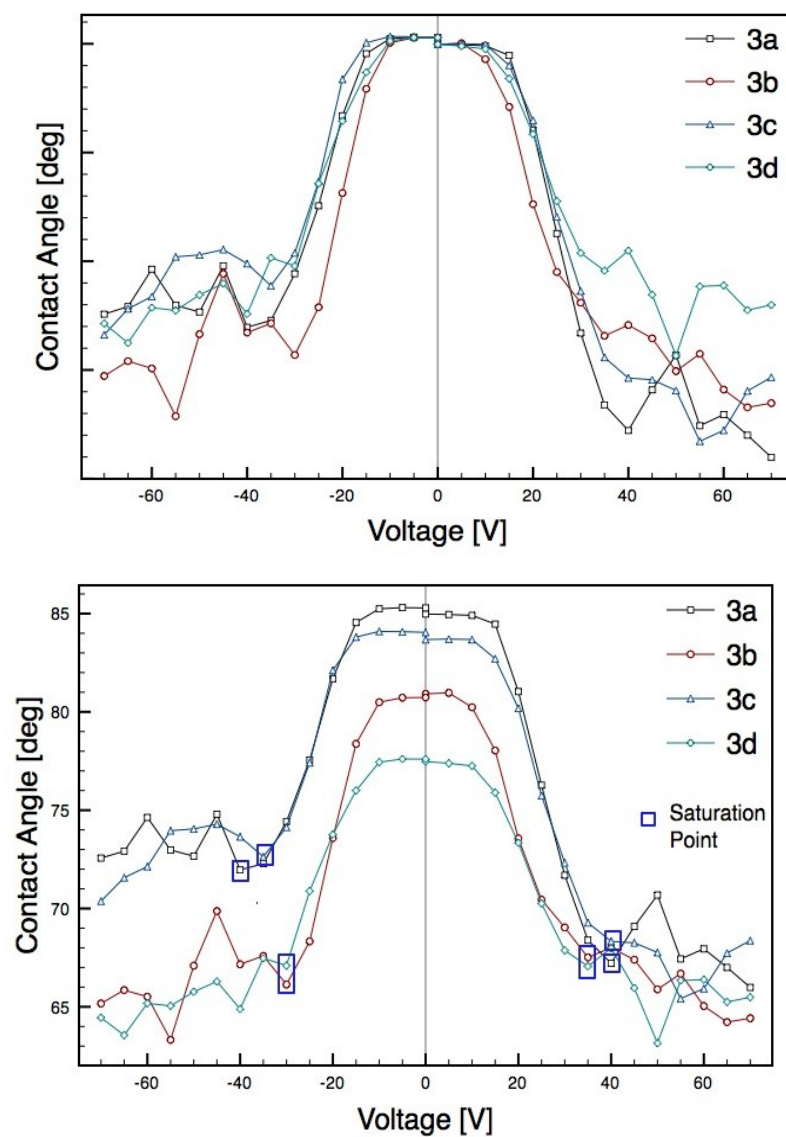


Figure 3.5 Electrowetting curves of linear tricationic ionic liquids with C6 linkage chains.

Electrowetting curves of linear tricationic ionic liquids with C6 linkage chains (a) were overlaid normal to the maximum θ_0 value (b).

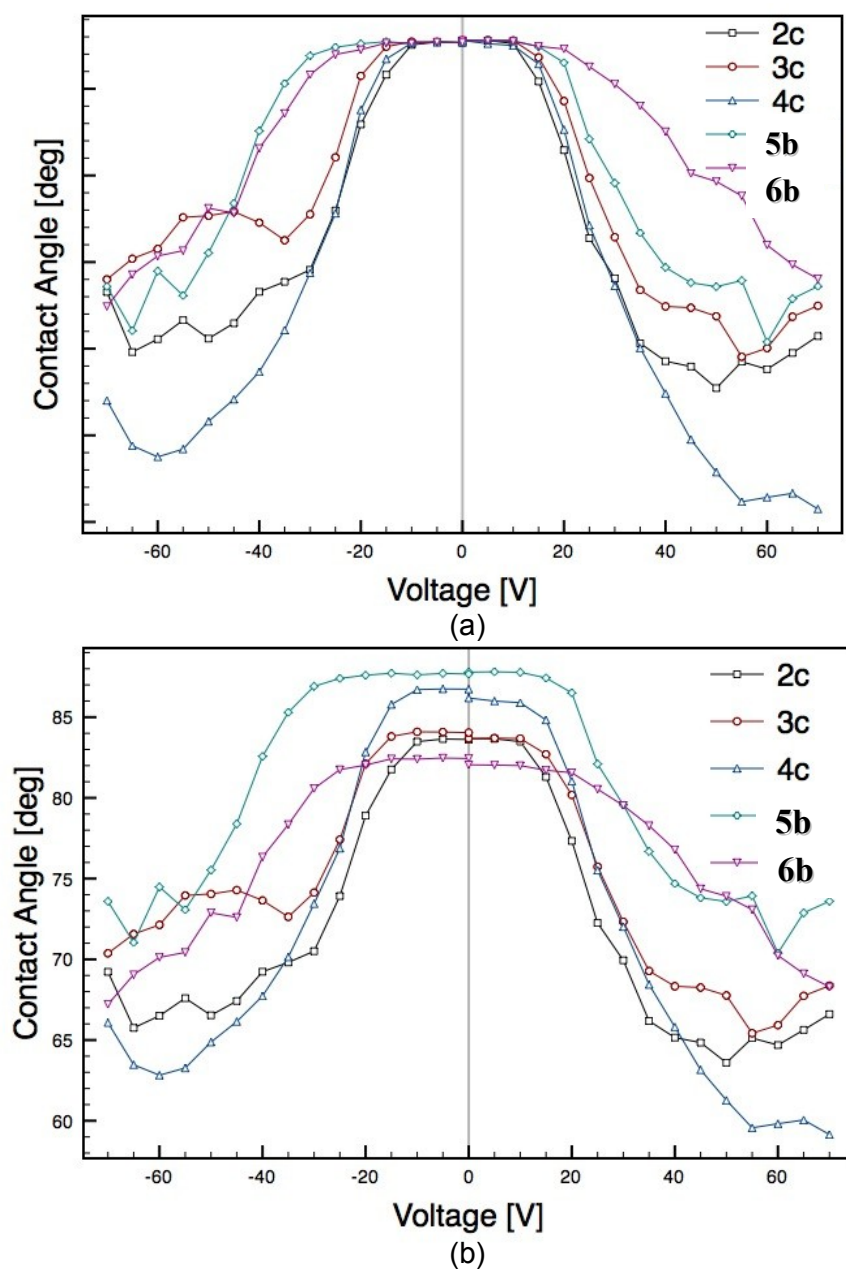


Figure 3.6 Electrowetting curves of benzyl substituted linear and rigid type tricationic ionic liquids.

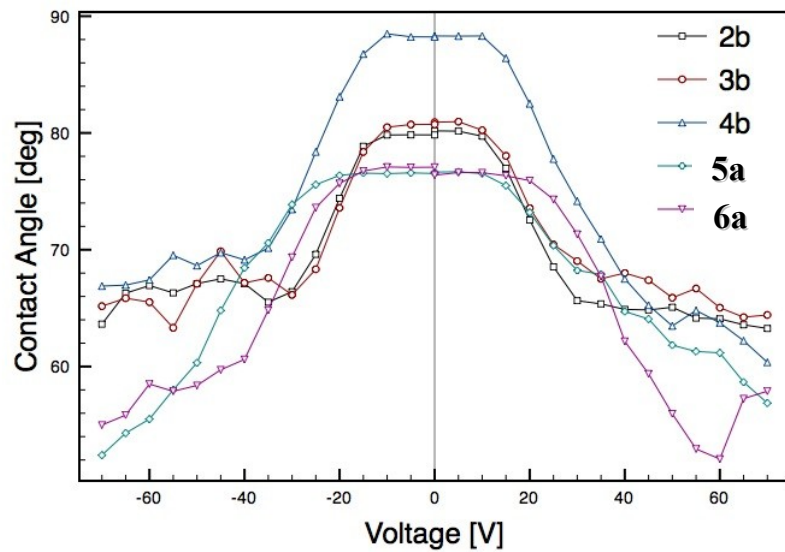
Electrowetting curves of benzyl substituted linear and rigid type tricationic ionic liquids (a) were overlaid normal to the maximum θ_0 value (b).

3.4.3.2 Rigid Core Structure vs. Flexible Core Structure

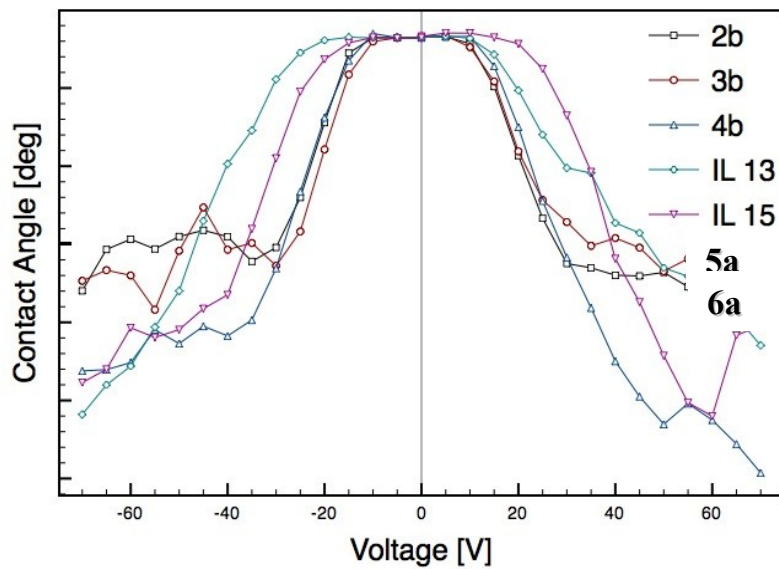
Figure 3.6(a) shows the electrowetting curves of benzylimidazole substituted ILs, both rigid core (**5b**, **6b**) and flexible core (**2c**, **3c**, **4c**) ILs. In Figure 3.6 (b) curves are overlaid normal to maximum θ_0 value. According to Figure 6(b) and Table 2, it can be clearly observed that rigid core ILs (**5a** and **5b**) have wider V_L and V_R values than those of flexible core ILs (**2c**, **3c**, **4c**). However, flexible core ILs produced much smoother curves than rigid core ILs. This means their electrowetting properties are much closer to the ideal behavior expected according to Young's and Lippmann's equations. Similar observations can be seen in butylimidazolium substituted rigid ILs (**5a**, **6a**) and flexible ILs (**2b**, **3b**, **4b**) as well (see Figure 3.7).

3.4.3.3 Effect of end groups

Electrowetting curves of linear tricationic ILs with C6 linkage chain each with four different end substituted groups were plotted in Figure 3.5(a). In Figure 3.5(b) they were overlaid normal to maximum θ_0 value. There are no significant differences in electrowetting properties by changing the end substituted groups, except θ_0 values. θ_0 values are different from one IL to the other due to their surface tension differences which was explained previously. It is interesting to note that the electrowetting properties of these ILs are fairly similar regardless of their different physicochemical properties. This unique situation enables one to choose an ionic liquid with the desired physical property from a large library of ionic liquids that have the same electrowetting properties. For example, if fast changes in contact angles are required in an electrowetting application, ILs with lower viscosities can be used. LTIL **3a** has significantly lower viscosity than **3c**, but their electrowetting properties are approximately the same (Table 3.2).



(a)

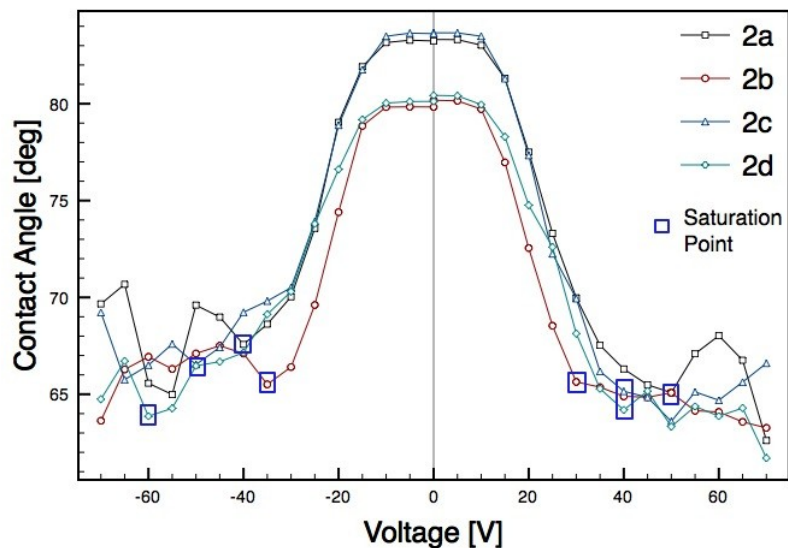


(b)

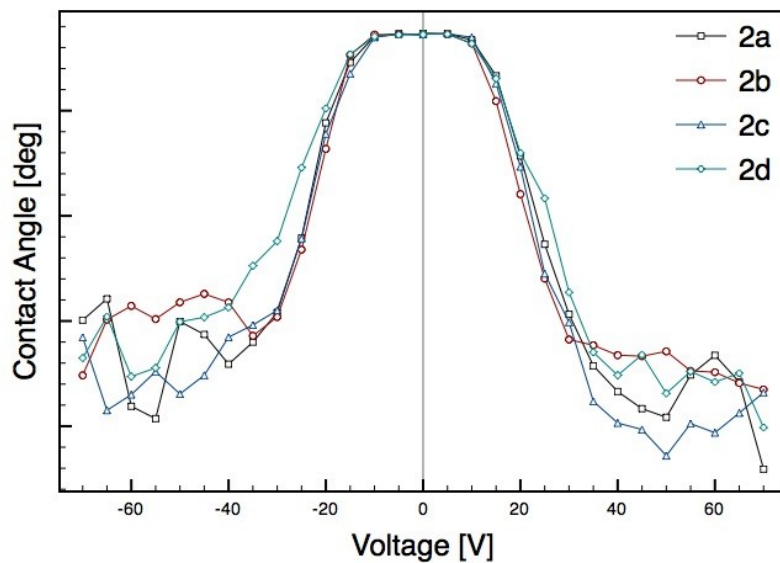
Figure 3.7 Electrowetting curves of butyl substituted tricationic ionic liquids

Electrowetting curves of butyl substituted tricationic ionic liquids (a) were overlaid normal to the maximum θ_0 value (b).

These observations are valid for the other C3 linkage chain and C10 linkage chain ILs as well (see Figures 3.8 and 3.9).



(a)



(b)

Figure 3.8 Electrowetting curves of C10 core linear tricationic ionic liquids

Electrowetting curves of C10 core linear tricationic ionic liquids (a) were overlaid normal to the maximum θ_0 value (b).

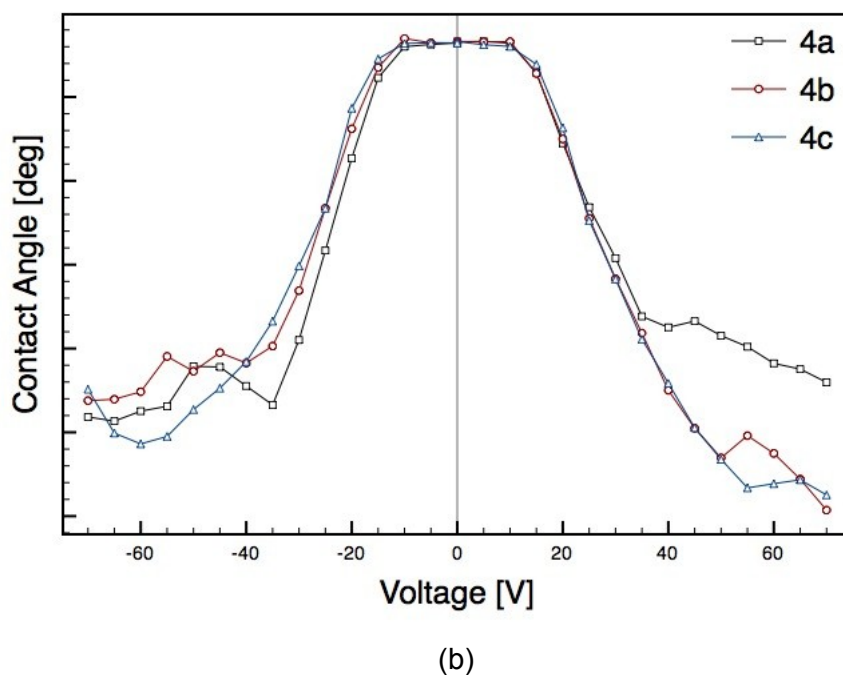
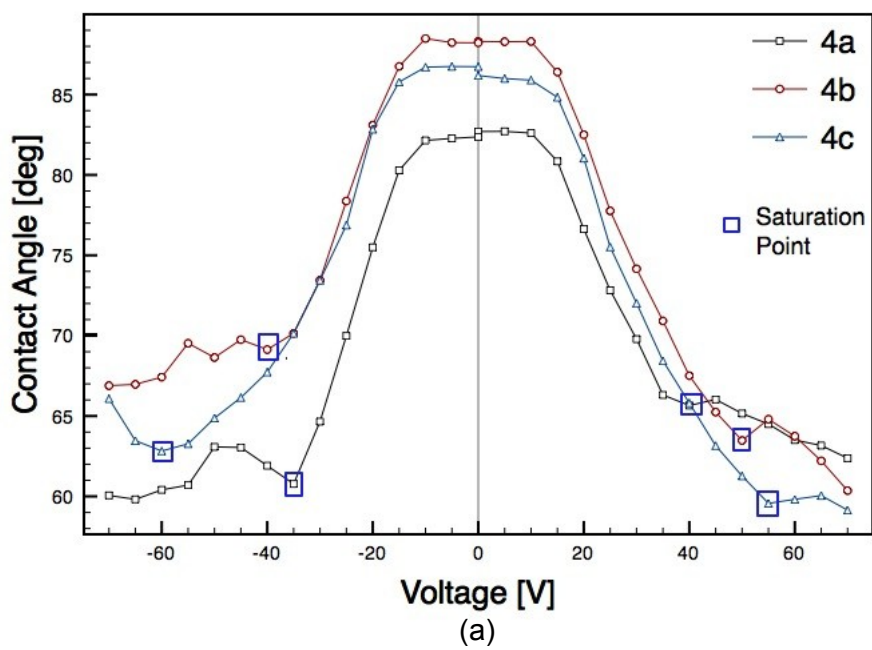


Figure 3.9 Electrowetting curves of C3 core linear tricationic ionic liquids

Electrowetting curves of C3 core linear tricationic ionic liquids (a) were overlaid normal to the maximum θ_0 value (b).

Examining electrowetting properties and physical properties of the relevant ILs listed here, one can find a suitable replacement for aqueous electrowetting in traditional EWOD-based devices.

3.5 Conclusion

Synthesis and physiochemical properties of 14 linear tricationic ionic liquids were reported and these have been explored as potential electrowetting liquids. These LTILs have shown high thermal stabilities and considerably high viscosities compared to traditional monocationic and dicationic ionic liquids. Most of the LTILs synthesized were room temperature ILs due to their higher structural flexibilities. This structural flexibility was advantageous in electrowetting applications as LTILs were observed to be much closer to the ideal behavior described in Young's and Lippmann's equation than any other ionic liquids reported in the literature.

CHAPTER 4

EVALUATION OF FLEXIBLE LINEAR TRICATIONIC SALTS AS GAS-PHASE ION-PAIRING REAGENTS FOR THE DETECTION OF DIVALENT ANIONS IN POSITIVE MODE ESI-MS

4.1 Abstract

Anion analysis is of great importance to many scientific areas of interest. Problems with the negative mode ESI-MS prevent researchers from achieving sensitive detection for anions. Recently, we have shown that cationic reagents can be paired with anions, such that detection can be done in the positive mode, allowing for low limits of detections for anions using ESI-MS. In this analysis, we present the use of 16 newly synthesized flexible linear tricationic ion-pairing reagents for the detection of 11 divalent anions. These reagents greatly differ in structure from previously reported trigonal tricationic ion-pairing agents, such that they are far more flexible. Here we present the structural features of these linear trications that make for good ion-pairing agents, as well as, show the advantage of using these more flexible ion-pairing reagents. In fact, the limit of detection for sulfate using the best linear trication was found to be 25 times lower than when the best rigid trication was used. Also, MS/MS experiments were performed on the trication/di-anion complex to significantly reduce the detection limit for many di-anions. Limits of detection in this analysis were as low as 50 fg.

4.2 Introduction

Anion analysis is of great importance to environmental researchers, biochemists, food and drug researchers, and the pharmaceutical industry; all of which are continually in need of facile, sensitive analytical techniques that can be used to both detect and quantitate trace anions.²³⁴⁻²⁵² Often, the anions of interest exist in complex matrices such as blood, water, and urine.^{235,239,241,244,246-249} For this reason, separation techniques are routinely coupled with anion detection. Currently, some of these techniques utilize flow injection analysis or ion chromatography,²⁵²⁻²⁵⁸ with detection frequently obtained through the use of ion selective electrodes, conductivity, or spectroscopic techniques.²⁵⁹⁻²⁶³ Yet, these detection methodologies lack either universality or specificity.²⁶³

For many analytes, ESI-MS has provided broad specificity and lower detection limits. Given the anion's inherent charge, it is not surprising that negative ion electrospray ionization mass spectrometry (ESI-MS) has come to the forefront as a general analytical approach that can be directly coupled with liquid chromatography (LC) if desired. Unfortunately, for most types of analytes, the negative ion mode often results in poorer limits of detection (LOD) than the preferred positive ion mode.^{264,265} Due to high negative voltages, the negative ion mode is more prone to corona discharge than the positive mode.²⁶⁶ This causes the negative mode to have an increased chance for arcing events and ultimately more noise resulting in unsatisfactory LODs.²⁶⁴ Corona discharge in the negative mode can be controlled by using halogenated solvents and substituting more alkylated alcohols (i.e., butanol or IPA) for methanol.^{266,267} Ideally, LC-ESI-MS methodologies would use more common

solvents, such as, methanol, water, and acetonitrile. Furthermore, it would be more practical to do all ion detection in the more stable and sensitive positive ion mode.

Recently, we have developed a method for the detection of singly-charged anions in positive mode ESI-MS using only water/methanol solvents.¹²⁷ This technique involves the addition of a low concentration of a dicationic ion pairing reagent to the mobile phase. The dication pairs with the singly-charged anion, resulting in a complex possessing an overall plus one charge, which can be detected in the positive ion mode. Benefits of this technique include: (a) the use more practical solvents, (b) substantial increases in the sensitivity, (c) ease of use, (d) the ability to detect anions that fall below a trapping mass spectrometer's low mass cutoff region, and (e) detection of the complex at a much higher mass-to-charge region where there is far less chemical noise. To fully take advantage of factor (e) alone, it is best to choose a relatively high molecular weight pairing agent that will result in a complex of a single positive charge.

Subsequently, the dicationic ion-pairing agent was used to determine the LODs for over 30 singly-charged anions.¹²⁷ Also in this work, it was shown for the first time that MS/MS can often be used to further lower the LODs of these anions. Overall, this analysis showed the true ultra-sensitivity of ion-pairing by producing the lowest reported LODs for several anions by any know technique.¹²⁷ The effectiveness of over 20 dicationic ion-pairing agents was evaluated in order to determine the structural properties that allow for low LODs.¹²⁹ A major finding in this study was that flexibility of the dication seemed essential for good sensitivity. Therefore, the best dicationic ion-pairing reagents cited were those which possessed a flexible alkyl chain that linked the two cationic moieties. Recently, the ion-paring technique was extended to the use of tri-cationic reagents for the detection of divalent anions.¹²⁸ The essential tricationic

reagents were found to bind divalent anions, and monitoring the complex in the positive ion mode was a more sensitive detection method than monitoring the naked doubly-charged anions in the negative mode.

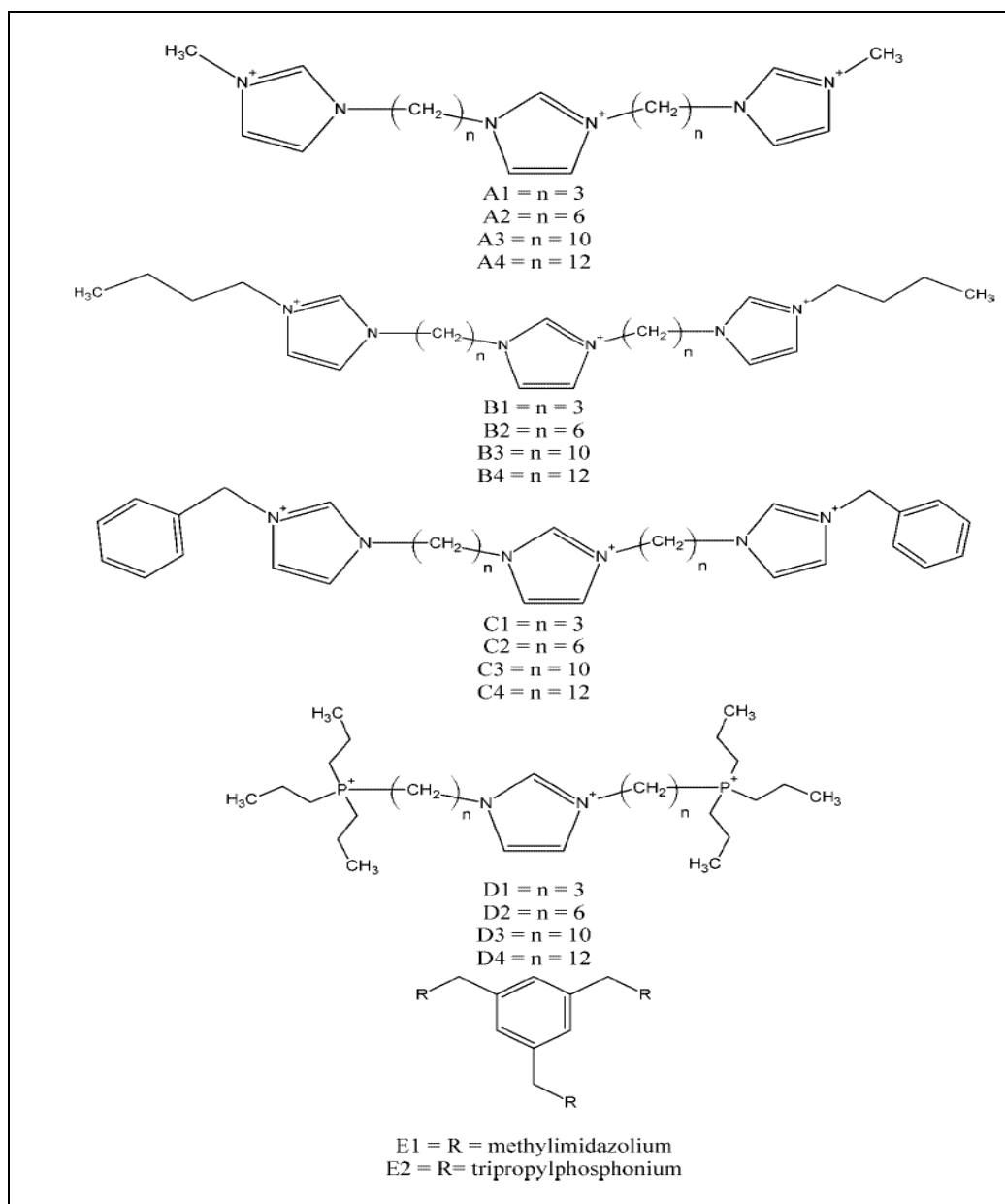


Figure 4.1 Structures of linear tricationic ion-pairing reagents.

However, the tricationic reagents used had a somewhat rigid trigonal structure (for a representative structure see the bottom of Figure 4.1), which may be an undesirable feature of an ion-pairing agent from a sensitivity standpoint.

Recently, we devised a synthetic method to produce more flexible linear trications (see Chapter 3). In this work, we present the use of 16 newly synthesized linear tricationic ion-pairing reagents to determine the LOD for 11 divalent anions. Herein, we describe the differences and advantages of using the more flexible linear trications versus the more rigid trigonal trications. Also, we show that MS/MS experiments can be performed on the linear trication/di-anion complex, and that by monitoring a fragment of the complex, the LOD often can be dramatically lowered. This is the first ever report of using this type of an MS/MS experiment to detect doubly-charged anions in the positive ion mode with any tricationic ion-pairing agent.

4.3 Experimental Section

4.3.1 Materials

Figure 4.1 gives the structures of all the linear tricationic ion-pairing reagents used in this study. Detailed synthesis of these ILs were discussed in Chapter 3. The anions that were tested for LOD (listed in Table 4.1) were ordered as the lithium, sodium, or potassium salt or as the disassociative free acid. They were also obtained from Sigma-Aldrich and were used as the reagent grade without further purification. HPLC grade water and methanol were purchased from Burdick and Jackson (Honeywell Burdick and Jackson, Morristown, NJ, USA).

4.3.2 ESI-MS Parameters

The ESI-MS conditions used here were the same as those previously used and optimized for the detection of perchlorate with a dicationic reagent, and were as follows: spray voltage, 3kV; sheath gas flow, 37 arbitrary units (AU); auxiliary gas flow rate, 6 AU; capillary voltage, 11 V; capillary temperature, 350°C; tube lens voltage, 105 V. When detecting the trication/dianion complex in the positive SIM mode, the SIM width was 5. When performing the SRM experiments, the isolation widths were between 1 and 5, the normalized collision energy was 30, and the activation time was 30 ms. All data analysis was performed using the Xcalibur and Tune Plus software.

Throughout this study, a Finnigan LXQ (Thermo Fisher Scientific, San Jose, CA, USA) ESI-MS was used for all of the analyses. The MS was equipped with a six port injector (5 μ L loop) and was coupled with a Finnigan Surveyor MS Pump. Between the injector and the ionization source, a Y-type mixing tee allowed for the addition of flow from a Shimadzu LC-6A pump. It was from this pump that the tricationic ion-pairing agent was introduced to the solvent flow. Overall, the total flow to the ESI was 400 μ L/min. The MS pump accounted for 300 μ L/min (67% MeOH: 33% H₂O), while the LC pump applied the 40 μ M trication solution in water at a rate of 100 μ L/min. All the anions were dissolved HPLC grade water, such that their initial concentration was 1 mg/mL. Serial dilutions were made from the stock solutions and the anions were directly injected using the six port injector. New stock solutions were prepared weekly and the injector was expected to be the largest cause for possible experimental error (\pm 5%). The limits of detection were determined to be when an injection at a given concentration resulted in peaks giving a signal-to-noise ratio of three.

4.4 Results and Discussion

In previous reports, we have shown that dicationic ion-pairing reagents can be used to pair with singly-charged anions, such that, the positively-charged complex can be monitored in the positive mode, resulting in extremely low LODs.^{128,129} More recently, we demonstrated that tricationic reagents could also be used to complex doubly-charged anions, leading to much lower LODs for those divalent anions when detecting the complex in the positive mode.¹²⁸ Since the trications used previously had relatively rigid structures, a series of flexible ion-pairing agents were synthesized and tested to see if they offer greater sensitivity for the detection of anions in positive mode ESI. In addition, MS/MS of the paired ions was examined in hopes of further lowering the LOD in many cases.

Figure 4.1 shows the structures of the 16 linear trications used in this analysis (A1-4, B1-4, C1-4, and D1-4). All of the 16 linear trications have the same imidazolium core. They differ in the length of the alkyl chain (C_3 , C_6 , C_{10} , and C_{12}) that tethers the terminal charged moieties to the central imidazolium, as well as, in the nature of the terminal charged moieties (methylimidazolium, butylimidazolium, benzylimidazolium, and tripropylphosphonium). By examining this series of linear trications, we were able to observe possible advantages of varying the chain length (i.e., flexibility), as well as, determining which cationic moieties produce the lowest LOD for the sample anions. Also shown in Figure 4.1, are the structures of two previously reported rigid trications.¹²⁸ Of these, the E1 trication was shown to be a moderately successful pairing agent, while trication E2 was found to be the best known trigonal tricationic ion-pairing agent.¹²⁸

Table 4.1 Limits of detection for divalent anions with linear tricationic reagents*

Sulfate		Thiosulfate		Oxalate		Fluorophosphate	
Trication	LOD (pg)	Trication	LOD (pg)	Trication	LOD (pg)	Trication	LOD (pg)
D3	$(2.00 \pm 0.01) \times 10^1$	D3	$(6.25 \pm 0.31) \times 10^1$	C2	$(1.20 \pm 0.06) \times 10^1$	D4	$(2.50 \pm 0.13) \times 10^1$
D4	$(7.50 \pm 0.38) \times 10^1$	C2	$(6.25 \pm 0.31) \times 10^1$	D2	$(3.50 \pm 0.18) \times 10^1$	D3	$(2.63 \pm 0.13) \times 10^1$
D2	$(1.25 \pm 0.06) \times 10^2$	B3	$(6.25 \pm 0.31) \times 10^1$	A2	$(8.10 \pm 0.41) \times 10^1$	E2	$(3.75 \pm 0.19) \times 10^1$
B3	$(2.00 \pm 0.01) \times 10^2$	B2	$(6.25 \pm 0.31) \times 10^1$	D4	$(1.25 \pm 0.06) \times 10^2$	D2	$(4.25 \pm 0.21) \times 10^1$
B4	$(2.60 \pm 0.13) \times 10^2$	D2	$(7.50 \pm 0.38) \times 10^1$	B4	$(1.25 \pm 0.06) \times 10^2$	B3	$(9.00 \pm 0.45) \times 10^1$
C1	$(3.00 \pm 0.15) \times 10^2$	B4	$(7.50 \pm 0.38) \times 10^1$	D3	$(2.50 \pm 0.13) \times 10^2$	C3	$(1.50 \pm 0.08) \times 10^2$
B2	$(3.25 \pm 0.16) \times 10^2$	C1	$(8.75 \pm 0.43) \times 10^1$	E2	$(2.50 \pm 0.13) \times 10^2$	A3	$(2.00 \pm 0.10) \times 10^2$
C4	$(3.50 \pm 0.18) \times 10^2$	D4	$(9.00 \pm 0.45) \times 10^1$	A3	$(3.00 \pm 0.15) \times 10^2$	A2	$(2.00 \pm 0.10) \times 10^2$
C3	$(3.75 \pm 0.19) \times 10^2$	D1	$(1.00 \pm 0.05) \times 10^2$	B1	$(3.00 \pm 0.15) \times 10^2$	D1	$(2.00 \pm 0.10) \times 10^2$
C2	$(4.50 \pm 0.22) \times 10^2$	C4	$(1.00 \pm 0.05) \times 10^2$	B2	$(3.25 \pm 0.16) \times 10^2$	C4	$(2.10 \pm 0.11) \times 10^2$
B1	$(5.00 \pm 0.25) \times 10^2$	A3	$(1.00 \pm 0.05) \times 10^2$	C4	$(4.00 \pm 0.20) \times 10^2$	C2	$(2.25 \pm 0.11) \times 10^2$
E2	$(5.00 \pm 0.25) \times 10^2$	A4	$(1.00 \pm 0.05) \times 10^2$	C3	$(4.40 \pm 0.22) \times 10^2$	B2	$(2.75 \pm 0.14) \times 10^2$
A2	$(5.50 \pm 0.28) \times 10^2$	A2	$(1.25 \pm 0.06) \times 10^2$	C1	$(5.00 \pm 0.25) \times 10^2$	A4	$(4.50 \pm 0.23) \times 10^2$
A4	$(5.75 \pm 0.29) \times 10^2$	B1	$(1.25 \pm 0.06) \times 10^2$	E1	$(5.00 \pm 0.25) \times 10^2$	B4	$(5.00 \pm 0.25) \times 10^2$
A3	$(6.00 \pm 0.30) \times 10^2$	E2	$(1.25 \pm 0.06) \times 10^2$	A4	$(5.50 \pm 0.28) \times 10^2$	B1	$(8.75 \pm 0.44) \times 10^2$
D1	$(6.25 \pm 0.31) \times 10^2$	C3	$(1.75 \pm 0.09) \times 10^2$	A1	$(6.50 \pm 0.33) \times 10^2$	C1	$(1.50 \pm 0.08) \times 10^3$
E1	$(6.25 \pm 0.31) \times 10^2$	A1	$(5.00 \pm 0.25) \times 10^2$	D1	$(8.25 \pm 0.41) \times 10^2$	A1	$(4.50 \pm 0.23) \times 10^3$
A1	$(1.75 \pm 0.09) \times 10^3$	E1	$(7.50 \pm 0.38) \times 10^2$	B3	$(2.08 \pm 0.10) \times 10^3$	E1	$(5.00 \pm 0.25) \times 10^4$
Dibromosuccinate		Hexachloroplatinate		Nitroprusside		Dichromate	
Trication	LOD (pg)	Trication	LOD (pg)	Trication	LOD (pg)	Trication	LOD (pg)
D3	$(1.25 \pm 0.06) \times 10^2$	D2	$(3.50 \pm 0.18) \times 10^1$	C2	7.00 ± 0.35	C4	$(3.50 \pm 0.18) \times 10^3$
E2	$(1.79 \pm 0.09) \times 10^2$	B2	$(3.50 \pm 0.18) \times 10^1$	D1	7.50 ± 0.38	B4	$(3.75 \pm 0.19) \times 10^3$
D1	$(2.00 \pm 0.10) \times 10^2$	D1	$(3.75 \pm 0.19) \times 10^1$	E2	7.50 ± 0.38	C3	$(3.88 \pm 0.19) \times 10^3$
C1	$(2.75 \pm 0.14) \times 10^2$	D3	$(4.00 \pm 0.20) \times 10^1$	C1	$(1.00 \pm 0.05) \times 10^1$	B3	$(4.25 \pm 0.21) \times 10^3$
B4	$(3.25 \pm 0.16) \times 10^2$	C2	$(5.00 \pm 0.25) \times 10^1$	D2	$(1.25 \pm 0.06) \times 10^1$	A3	$(5.00 \pm 0.25) \times 10^3$
B1	$(3.50 \pm 0.18) \times 10^2$	B1	$(7.00 \pm 0.35) \times 10^1$	B1	$(1.25 \pm 0.06) \times 10^1$	D4	$(5.50 \pm 0.28) \times 10^3$
B3	$(3.75 \pm 0.19) \times 10^2$	B3	$(7.50 \pm 0.38) \times 10^1$	D3	$(2.00 \pm 0.10) \times 10^1$	D3	$(6.25 \pm 0.31) \times 10^3$
A3	$(4.50 \pm 0.23) \times 10^2$	B4	$(7.50 \pm 0.38) \times 10^1$	B2	$(2.00 \pm 0.10) \times 10^1$	A4	$(6.25 \pm 0.31) \times 10^3$
C3	$(5.00 \pm 0.25) \times 10^2$	C1	$(7.50 \pm 0.38) \times 10^1$	C3	$(2.25 \pm 0.11) \times 10^1$	B1	$(6.25 \pm 0.31) \times 10^3$
D4	$(5.00 \pm 0.25) \times 10^2$	A2	$(7.50 \pm 0.38) \times 10^1$	B3	$(2.50 \pm 0.13) \times 10^1$	C2	$(6.38 \pm 0.32) \times 10^3$
A4	$(5.00 \pm 0.25) \times 10^2$	E2	$(7.50 \pm 0.38) \times 10^1$	A2	$(2.50 \pm 0.13) \times 10^1$	C1	$(6.50 \pm 0.33) \times 10^3$
D2	$(6.25 \pm 0.31) \times 10^2$	C4	$(8.50 \pm 0.43) \times 10^1$	A3	$(3.00 \pm 0.15) \times 10^1$	D2	$(7.50 \pm 0.38) \times 10^3$
C2	$(7.50 \pm 0.38) \times 10^2$	D4	$(1.00 \pm 0.05) \times 10^2$	B4	$(3.25 \pm 0.16) \times 10^1$	B2	$(7.50 \pm 0.38) \times 10^3$
B2	$(7.50 \pm 0.38) \times 10^2$	C3	$(1.25 \pm 0.06) \times 10^2$	D4	$(3.75 \pm 0.19) \times 10^1$	A2	$(7.50 \pm 0.38) \times 10^3$
A2	$(2.50 \pm 0.13) \times 10^3$	A3	$(1.25 \pm 0.06) \times 10^2$	C4	$(3.75 \pm 0.19) \times 10^1$	D1	$(8.75 \pm 0.44) \times 10^3$
A1	$(3.00 \pm 0.15) \times 10^3$	A4	$(1.75 \pm 0.09) \times 10^2$	A1	$(3.75 \pm 0.19) \times 10^1$	E2	$(1.00 \pm 0.05) \times 10^4$
E1	$(5.00 \pm 0.25) \times 10^3$	A1	$(5.00 \pm 0.25) \times 10^2$	E1	$(4.86 \pm 0.24) \times 10^1$	E1	$(1.25 \pm 0.06) \times 10^4$
C4	$(5.00 \pm 0.25) \times 10^4$	E1	$(1.58 \pm 0.08) \times 10^3$	A4	$(5.00 \pm 0.25) \times 10^1$	A1	$(1.50 \pm 0.08) \times 10^4$

Table 4.1 continued

Selenate		o-Benzenedisulfonate		Bromosuccinate	
Trication	LOD (pg)	Trication	LOD (pg)	Trication	LOD (pg)
E2	$(7.50 \pm 0.38) \times 10^1$	E2	$(1.50 \pm 0.08) \times 10^1$	E2	$(7.50 \pm 0.38) \times 10^1$
B3	$(2.50 \pm 0.13) \times 10^2$	D1	$(1.63 \pm 0.08) \times 10^1$	C4	$(6.25 \pm 0.31) \times 10^2$
C4	$(2.75 \pm 0.14) \times 10^2$	C1	$(1.75 \pm 0.09) \times 10^1$	D3	$(7.50 \pm 0.38) \times 10^2$
D3	$(3.75 \pm 0.19) \times 10^2$	B1	$(2.00 \pm 0.10) \times 10^1$	D1	$(7.50 \pm 0.38) \times 10^2$
B1	$(4.00 \pm 0.20) \times 10^2$	C2	$(3.20 \pm 0.16) \times 10^1$	A4	$(8.00 \pm 0.40) \times 10^2$
C2	$(4.25 \pm 0.21) \times 10^2$	B4	$(4.00 \pm 0.20) \times 10^1$	C2	$(1.00 \pm 0.05) \times 10^3$
C3	$(4.40 \pm 0.22) \times 10^2$	B2	$(4.00 \pm 0.02) \times 10^1$	B4	$(1.00 \pm 0.05) \times 10^3$
D4	$(5.00 \pm 0.25) \times 10^2$	D2	$(4.75 \pm 0.24) \times 10^1$	C3	$(1.50 \pm 0.08) \times 10^3$
D2	$(5.00 \pm 0.25) \times 10^2$	D3	$(6.50 \pm 0.33) \times 10^1$	D4	$(2.00 \pm 0.10) \times 10^3$
C1	$(5.00 \pm 0.25) \times 10^2$	A4	$(6.50 \pm 0.33) \times 10^1$	D2	$(2.25 \pm 0.11) \times 10^3$
B2	$(5.00 \pm 0.25) \times 10^2$	C3	$(7.50 \pm 0.38) \times 10^1$	A3	$(3.75 \pm 0.19) \times 10^3$
B4	$(5.25 \pm 0.26) \times 10^2$	E1	$(7.50 \pm 0.38) \times 10^1$	B3	$(4.00 \pm 0.20) \times 10^3$
A4	$(5.50 \pm 0.28) \times 10^2$	D4	$(1.00 \pm 0.05) \times 10^2$	E1	$(5.00 \pm 0.25) \times 10^3$
A3	$(7.00 \pm 0.35) \times 10^2$	B3	$(1.00 \pm 0.05) \times 10^2$	C1	$(5.00 \pm 0.25) \times 10^3$
D1	$(7.50 \pm 0.38) \times 10^2$	A3	$(1.00 \pm 0.05) \times 10^2$	A2	$(5.00 \pm 0.25) \times 10^3$
A2	$(7.50 \pm 0.38) \times 10^2$	A2	$(1.25 \pm 0.06) \times 10^2$	B2	$(5.50 \pm 0.28) \times 10^3$
E1	$(1.13 \pm 0.06) \times 10^3$	A1	$(3.75 \pm 0.19) \times 10^2$	B1	$(7.50 \pm 0.38) \times 10^3$
A1	$(3.38 \pm 0.17) \times 10^3$	C4	$(8.75 \pm 0.44) \times 10^3$	A1	$(1.25 \pm 0.06) \times 10^4$

*The limit of detection was determined to be the amount of analyte that resulted in S/N = 3. Also, the data for E1 and E2 was extracted from reference 128.

The results of these two rigid trications allows for a definitive comparison to the new flexible trications developed for this study.

Table 4.1 lists the LODs for the 11 doubly-charged anions, when paired with the 16 linear trications and monitored in the positive mode. Overall, the LODs for the divalent anions ranged from the nanogram (ng) to the picogram (pg) level. In order to evaluate the effect of the chain length in the linear tricationic ion-pairing reagent, one can compare the trications of the same letter. For example, trications D1-4 differ only in the length of the hydrocarbon chain connecting the charged moieties (see Figure. 4.1). In general, it appears that the common trend is that linear trications with hexyl or decyl linkage chains gave the lowest LODs, whereas, trications with propyl or dodecyl

linkages resulted in higher LODs. This trend can be easily seen by comparing the LOD for thiosulfate when using the “D” series of linear trications. In this comparison, the order from best to worst ion-pairing agent was found to be D3, D2, D4, and D1. A likely explanation for this observation is that when the alkyl linkage chain is too short, the linear trication is less flexible and not as likely to “bend” around the anion. This finding supports our hypothesis that flexibility is a key feature in a good tricationic ion-pairing reagent. In contrast, when the alkyl chain gets too long, the cationic moieties are too far from each other and could not work as a single unit when binding the anion. However, the effect of the linkage chain being too short is far more unfavorable than it being too long. An example of this can be seen in Table 4.1, where trication A1 with the shortest linkage chain was found to be one of the three worst ion-pairing agents for all anions. Clearly, the results (Table 4.1 and Figure 4.1) suggest that when using linear tricationic ion-pairing reagents, the alkyl linkage chain should be between six and ten carbons in length.

By evaluating the data for a series of trications that all have the same linkage chain, but different cationic moieties, the best terminal charged groups can be determined. Typically, the linear trications possessing the benzylimidazolium (the “C” moiety) and the tripropylphosphonium (the “D” moiety) terminal charged groups resulted in lower LODs than the methylimidazolium (the “A” moiety) or butylimidazolium (the “B” moiety) cationic groups. This observation is shown by the LODs for oxalate when paired with the linear tricationic “2” series. The order from best to worst ion-pairing agents was found to be C2, D2, A2, and B2. Another example of this can be seen in the LODs for both nitroprusside and dichromate, where (from best to worst) the order was C2, D2, B2, and A2. These results, along with the previously noted optimum

linkage chain lengths, allow for the determination that trications C2 and D3 were the overall best tricationic ion-pairing agents. Trication C2 has hexyl linkage chains and benzyliimidazolium terminal charged groups, and trication D3 has decyl linkage chains and tripropylphosphonium cationic moieties. Interestingly, in the three comprehensive studies we have done on ion-pairing agent structures, the tripropylphosphonium cationic moiety is the only one that has always resulted in a recommended ion-pairing agent.^{128,129}

The other important comparison to be made with the data in Table 4.1 is the LODs resulting from using the flexible linear trication versus the more rigid trigonal trications (E1 and E2). As can be seen, the best linear trications, C2 and D3, rank very near the top for most of the anions tested. However, the best trigonal trication, E2, also ranks very near the top for many of the tested anions. From this observation, it was determined that the best linear trications and the best trigonal trications both work well when monitoring the same divalent anions. Interestingly, the linear and trigonal ion-pairing reagents seem to be complimentary to one another. Overall, the best linear trication was not found to be a greatly superior ion-pairing agent when compared to the best trigonal trication. Yet, some very useful and somewhat complimentary tricationic ion-pairing reagents were added to our repertoire. However, if you compare trigonal trication E1 (the moderately successful trigonal trication) to the flexible linear trications, it can be seen that trication E1 ranks near the bottom for all the anions tested. It was determined that in general, the more flexible trications are better ion-pairing agents than the rigid trications. Obviously, there are other factors that play a part in finding the optimum ion-pairing agent, which allow trication E2 to work as well as the linear

trications. Perhaps the most important factor is that it contains the highly favorable tripropylphosphonium moiety.

Figure 4.2 illustrates the benefits of using a linear trication versus a trigonal trication for the detection of sulfate in the positive mode. In both detection scenarios, the same concentration of sulfate was injected (500 pg). In the upper panel (I), the ion-pairing agent was the best linear trication D3, and in the lower panel (II) the best trigonal trication E2 was used.

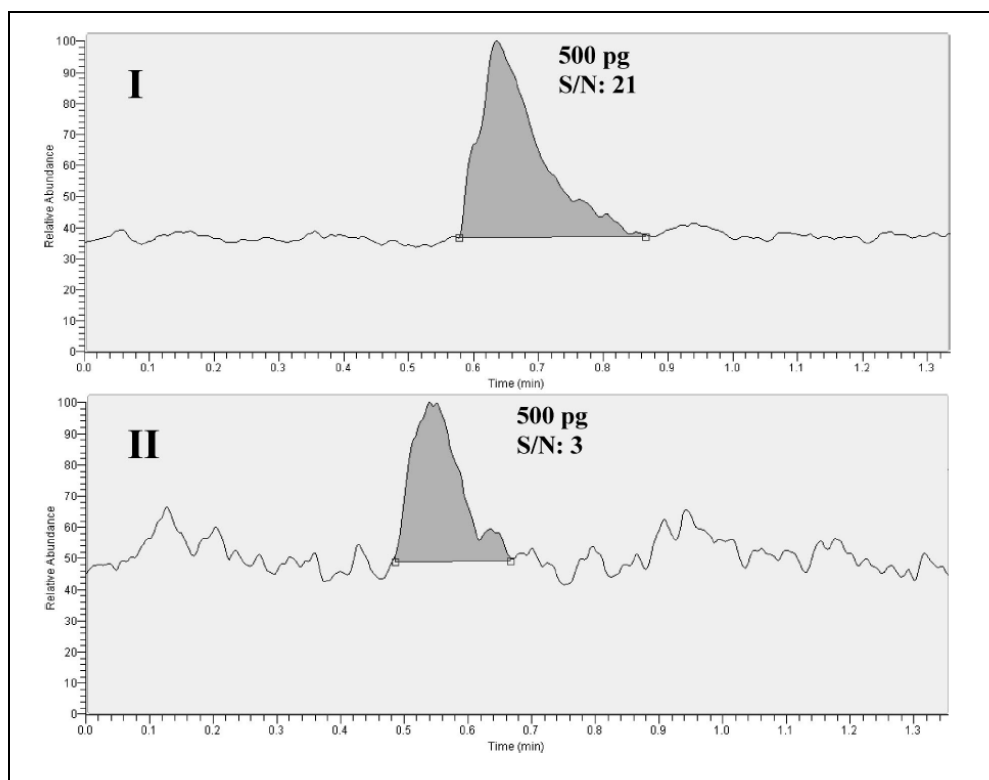


Figure 4.2 Comparison of the detection of sulfate in the positive mode using tricationic ion-pairing reagents D3 (I) and E2 (II).

It is apparent that the linear trication resulted in superior detection of sulfate, with a signal-to-noise seven times greater than that for the trigonal trication. It should be noted

Table 4.2 lists the results for the SRM experiments that were performed in this analysis. Trications D3 and C2 were paired with 11 divalent anions and tested for their LOD using the SRM method. For comparison, the SIM results are listed next to the SRM results. As can be seen, the SRM mode often resulted in lower LODs than the SIM mode. There were two analytes (D3/bromosuccinate and C2/oxalate) that showed no improvement, but in general there was nearly an order of magnitude improvement when using the SRM mode. In three cases, the SRM mode resulted in a two order of magnitude decrease in the LOD. One of these cases was the detection of nitroprusside using trication C2 as the ion-pairing agent and employing the SRM mode. For this system, the LOD for nitroprusside was determined to be 50 femtograms (fg), which is the lowest LOD for any mono- or divalent anion that has tested to date. Clearly this is a very facile and sensitive method.

Table 4.2 Comparison of LODs in the SIM positive and SRM positive modes.

	Trication D3			Trication C2		
	SIM LOD (pg)	SRM LOD (pg)	SRM Mass	SIM LOD (pg)	SRM LOD (pg)	SRM Mass
Sulfate	$(2.00 \pm 0.10) \times 10^1$	$(1.50 \pm 0.08) \times 10^1$	367.4	$(4.50 \pm 0.23) \times 10^2$	$(3.00 \pm 0.15) \times 10^2$	309.2
Thiosulfate	$(6.25 \pm 0.10) \times 10^1$	$(5.00 \pm 0.20) \times 10^1$	367.4	$(6.25 \pm 0.31) \times 10^1$	$(3.50 \pm 0.18) \times 10^1$	309.2
Oxalate	$(2.50 \pm 0.13) \times 10^2$	$(1.00 \pm 0.05) \times 10^2$	367.4	$(1.20 \pm 0.06) \times 10^1$	$(7.50 \pm 0.38) \times 10^1$	549.2
Fluorophosphate	$(2.63 \pm 0.13) \times 10^1$	$(2.05 \pm 0.10) \times 10^1$	367.4	$(2.25 \pm 0.11) \times 10^2$	$(1.00 \pm 0.05) \times 10^2$	309.2
Dibromosuccinate	$(1.25 \pm 0.06) \times 10^2$	$(1.25 \pm 0.06) \times 10^1$	745.4	$(7.50 \pm 0.38) \times 10^2$	$(2.00 \pm 0.10) \times 10^1$	629.4
Hexachloroplatinate	$(4.00 \pm 0.20) \times 10^1$	4.50 ± 0.23	1003.5	$(5.00 \pm 0.25) \times 10^1$	$(2.00 \pm 0.10) \times 10^1$	889.4
Nitroprusside	$(2.00 \pm 0.10) \times 10^1$	3.50 ± 0.18	853.5	7.00 ± 0.35	$(5.00 \pm 0.25) \times 10^{-2}$	737.4
Dichromate	$(6.25 \pm 0.31) \times 10^3$	$(5.75 \pm 0.29) \times 10^2$	367.4	$(6.38 \pm 0.32) \times 10^3$	$(3.00 \pm 0.15) \times 10^3$	643.4
Selenate	$(3.75 \pm 0.19) \times 10^2$	2.00 ± 0.10	367.4	$(4.25 \pm 0.21) \times 10^2$	$(6.00 \pm 0.30) \times 10^1$	309.2
o-Benzenedisulfonate	$(6.50 \pm 0.33) \times 10^1$	$(1.00 \pm 0.05) \times 10^1$	367.4	$(3.20 \pm 0.16) \times 10^1$	$(3.75 \pm 0.19) \times 10^1$	309.2
Bromosuccinate	$(7.50 \pm 0.38) \times 10^2$	$(1.00 \pm 0.05) \times 10^3$	745.4	$(1.00 \pm 0.05) \times 10^3$	$(1.00 \pm 0.05) \times 10^3$	629.4

Also, listed in Table 4.2 are the SRM fragment masses that were monitored. As noted previously, many complexes produce the same fragment; 367.4 for trication D3 and 309.2 for trication C2. However, it was observed that there are some trication/di-

anions that follow different disassociation pathways. For example, the trication D3/hexachloroplatinate complex produced a fragment with a mass-to-charge ratio of 1003.5. This fragment corresponds to the loss of one chlorine atom from the hexachloroplatinate, while the overall cation-anion complex remained intact. A similar effect was seen with the SRM detection for nitroprusside. Here, nitroprusside loses a nitro group and still stays complexed with the trication. For these cases, it is interesting to see that the non-covalent trication/di-anion complex remains intact, while covalent bonds have been broken. One more example of this type of fragmentation was for bromine containing anions. Here the central imidazolium loses its acidic proton (in the 2 position of the imidazolium ring) and becomes a dication. This dication then complexes with a bromide anion that was lost from the di-anion. This means that for any bromine containing di-anions, the same fragment could be monitored (m/z : 745/747 for D3 and m/z : 629/631 for C2).

It should be noted that although the LODs for the 11 divalent anions in SIM and SRM are already quite low, they could be lowered further by completely optimizing the conditions for a particular complex. In this analysis, one general set of conditions were used for the entire study. Previously, it has been shown that the LODs can be further decreased by a factor of three to ten with individual optimization.^{127,128,129} Finally, the use of some other types of MS systems (triple quad, etc.) with this technique can further reduce detection limits.

4.5 Conclusions

Sixteen newly synthesized linear tricationic ion-pairing agents were evaluated for their ability to detect doubly-charged anions in positive mode ESI-MS. It was found that for linear trications, the optimum alkyl chain lengths coupling the cationic moieties should be between six and ten carbons in length. It was determined that the best cationic moieties were tripropylphosphonium and benzylimidazolium. In comparison to previously reported rigid tricationic ion-pairing agents, the flexible linear trications presented here generally make better MS ion-pairing agents. It was shown that when the same amount of sulfate was injected, the signal-to-noise ratio when using the best linear trication was seven times greater than when using the best trigonal trication. However, it was found that trigonal trication E2 remained useful as it was often complimentary to the linear trications. Lastly, one to three orders of magnitude decreases in the LODs were found when using SRM.

CHAPTER 5
BONDED IONIC LIQUID POLYMERIC MATERIAL FOR SOLID PHASE MICRO
EXTRACTION GC ANALYSIS

5.1 Abstract

Four new ionic liquid-based materials were bonded onto 5 μm silica particles for use as adsorbent in solid phase micro extraction (SPME). Two ILs contained styrene units that allowed for polymerization and higher carbon content of the bonded silica particles. Two polymeric ILs differing by the anion were used to prepare two SPME fibers that were used in both headspace and immersion extractions and compared to commercial fibers. In both sets of experiments, ethyl acetate was used as an internal standard to take into account adsorbent volume differences between the fibers. The polymeric IL fibers are very efficient in headspace SPME for short chain alcohols. Immersion SPME can also be used with the IL fibers for short chain alcohols but also for polar and basic amines that can be extracted at pH 11 without damage to the fiber contained silica particles. The sensitivities of the two IL fibers differing by the anion were similar. Their efficacy compares favorably to that of commercial fibers for polar analytes. The mechanical strength and durability of the polymeric IL fibers were excellent.

5.2 Introduction

Solid phase microextraction (SPME) was developed by Pawliszyn in the early 1990s as a simple and "green" technique for sample preparation without the use of any solvent.²⁶⁸⁻²⁷⁰ SPME is simply performed by exposing a silica fiber covered by an absorbing agent to the headspace (HS) volume of a vial or directly immersing into the matrix of the liquid sample. A rapid preconcentration of analytes into the fiber surface is observed if the coating absorbing agent is appropriate. The extracted agents are analyzed by simply placing the fiber into the injection port of a gas chromatograph (GC). The injector is heated at an elevated temperature that will cause the vaporisation of the absorbed analytes into the GC insert and a classical GC chromatogram can be developed for full identification and quantitation of all extracted compounds.

The chemistry of the sorptive SPME coating layer plays a significant role in enhancing the extraction of specific classes of compounds and discriminating against others.^{271,272} The SPME extractant must primarily be thermally stable so as not to decompose during the GC injection process. It must also be mechanically strong to support agitation and manipulation. Finally, it must be able to withstand harsh chemical media when immersed in the sample solution including extreme pHs, high ionic strengths, and organic solvent concentrations. Bare silica gel, polydimethylsiloxane (PDMS), divinylbenzene (PDMS-DVB), polyacrylate (PA), high density polyoxyethylene (Carbowax) are used in commercially available SPME fiber.²⁷³ Since higher selectivity as well as higher sensitivity are needed as the technique gains wide-spread popularity, the quest for new coating adsorbents is the goal of numerous research teams.

Ionic liquids are a new class of non molecular solvents with unique properties such as a very low volatility, often good thermal stability, electrical conductivity, good

solvating properties associated to adjustable polarity, and water or solvent solubility.^{274,275} Ionic liquids are actually salts with a melting point close to or below room temperature. Their low volatility and peculiar solvating properties were soon considered as attractive properties that would make them very useful for use in separation techniques²⁷⁶ and especially, possible candidates for new adsorbents for SPME fibers.

Considerable insights into solute-IL interactions and affinities were obtained during the development and evaluation of GC stationary phases made with ILs.^{44,45,46,56,277} This experience was first used to develop microextractions on a single ionic liquid drop, i.e. without fiber support.^{278,279} Next ionic liquid coated fibers were prepared for a single determination of trace amount of polyaromatic hydrocarbons in water samples.²⁸⁰ The contamination of the GC injection liner precluded the widespread use of this method. Polymerized ionic liquids were used to coat on the silica fiber and obtain thermally stable and reusable SPME fibers for esters¹⁵⁴ and amphetamine metabolite²⁸¹ determination.

So far, the works reported with ionic liquid SPME fibers were successful with mixtures containing mainly hydrophobic and semi-polar compounds. It was found in GC analyses on ionic liquid stationary phase^{44,45,46,56} and in ionic liquid-water liquid-liquid extractions¹⁷⁷ that alcohols had an unusually high affinity for ILs. In this work, attention will be given to hydrophilic and polar compounds such as short chain alcohols and amines. For this purpose, completely new and different ionic liquids were prepared and tested as new adsorbents for SPME. To reduce contamination and/or loss of adsorbent, the different ionic liquid derivatives were bonded to silica microparticles that were used to prepare a porous and mechanically strong fiber coating. Both headspace

and immersion techniques were tested to evaluate the capabilities of the newly developed bonded ionic liquid sorbents with a large variety of polar solutes.

5.3 Experimental Section

5.3.1 Materials

The reagents sodium imidazolate, 1-methylimidazole, 1-hydroxyethyl imidazole, triethylene glycol, phosphorous tribromide, ethyl acetate, toluene, 4-chloromethyl styrene, tetrahydrofuran (THF), *n*-butanol, methylene chloride, chloroform, dioxane, butyric acid, phenol, dimethylamine, trimethylamine, pyridine and aniline were purchased from Sigma-Aldrich, Milwaukee, WI, USA. The common HPLC solvents: acetonitrile (ACN), isopropyl alcohol (IPA), ethanol and methanol were OmniSolv™ solvents obtained from EMD Merck, Darmstadt, Germany. Kromasil spherical azobis-isobutyronitrile-derivatized silica gel with 5 µm particle diameter, 10 nm pore size and 310 m² surface area was obtained from Supelco, Sigma-Aldrich. The beverages tested were obtained from different local grocery stores. The standard reference material used for calibration was SRM 1828b from the National Institute of Standards and Technology (Gaithersburg, MD, USA).

5.3.2 Synthesis of the Ionic Liquid Derivatized Silica

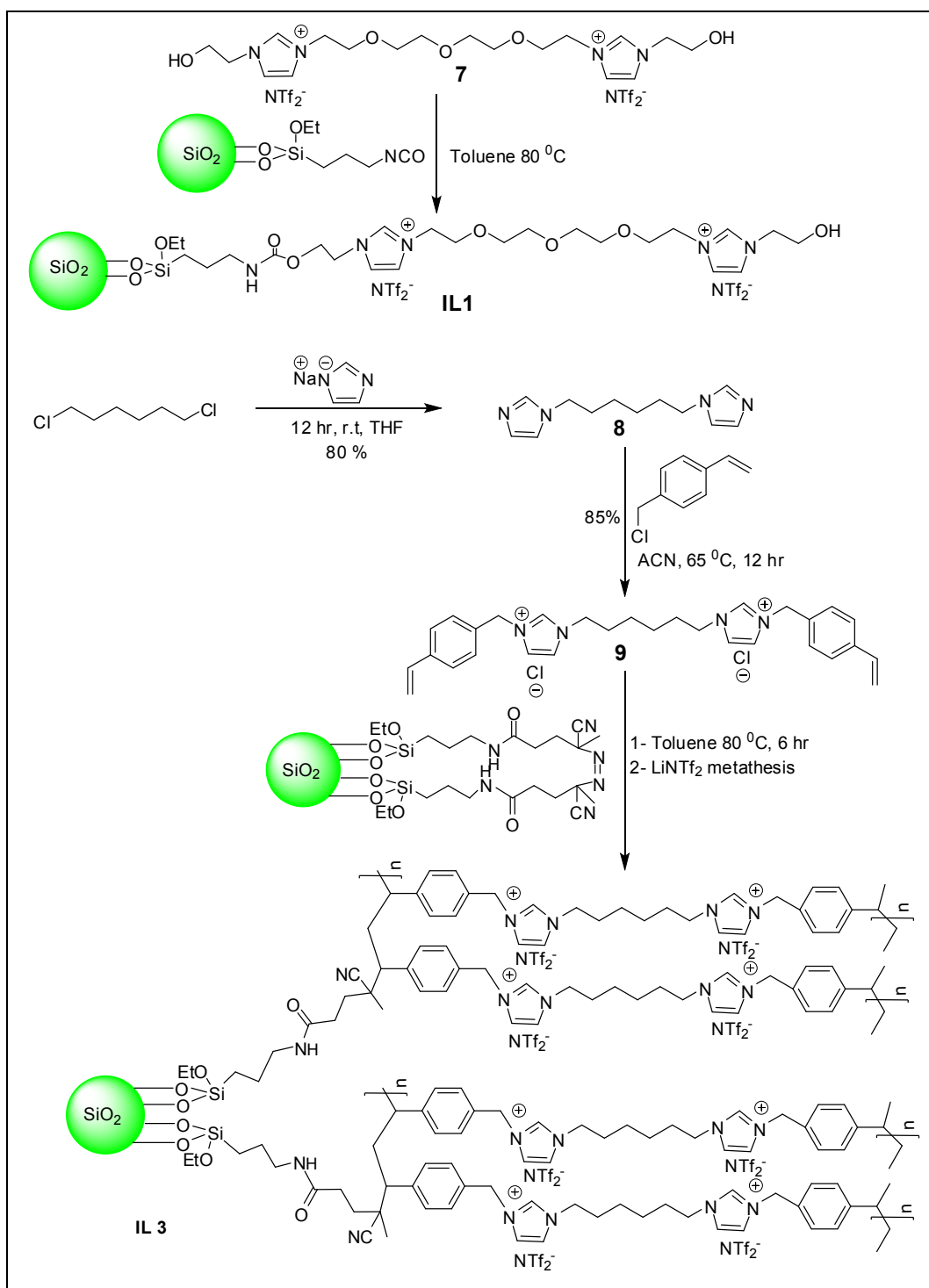
Bis-hydroxyethyl imidazolium trioxyethylene derivative

Bis-hydroxyethyl imidazolium trioxyethylene bis-(trifluoromethylsulfonyl) imide, noted (HeIM)₂PEG₃, 2 NTf₂⁻ (**7**) was synthesized following a method previously reported.¹⁹⁰ Equimolar mixture of trioxyethylene dibromide and hydroxyethyl imidazole was refluxed in tetrahydrofuran (THF) overnight. The bromide ionic liquid obtained was converted to NTf₂ anionic form by stirring a 1.0 g of the above dibromide salt with 4.0 g of LiNTf₂ in water for 5 hr. Then the NTf₂ ionic liquid was extracted with methylene chloride,

washed with water and ether and dried in a vacuum oven with P₂O₅. After that (H₂IM)₂PEG₃, 2NTf₂⁻ (1.0 g) was stirred in a slurry of (3-Isocyanatopropyl)triethoxysilane derivatized silica gel (2.0 g, C% 3.2) in toluene at 110 °C to obtain the silica bonded monomeric IL1 (see Figure 5.1, top). Obtained silica gel was filtered through a sintered glass funnel and washed with 60 ml portions of acetone, dimethyl formamide, methanol, chloroform and acetone to remove remaining unbound ionic liquids and other impurities. Derivatized silica gel was dried under vacuum over P₂O₅. The elemental analyses and coverage are listed in Table 5.1. The second ionic liquid polar derivative was done following the same protocol as for **IL1** but the bromide ions were exchanged for trifluoromethyl sulfate or triflate ions (TfO⁻) instead of NTf₂⁻ ions giving **IL2** bonded particles (Table 5.1).

1,1'-(1,6-hexanediyl)bisimidazole (8).²⁸²

A 250-ml round-bottom flask was charged with 100 mL anhydrous dimethylformamide (DMF) and 2.0 g sodium imidazole (22.2 mmol). Next, 3.8 mL of 1,6-dichlorohexane (3.8 mmol) were slowly added into the DMF solution and stirred overnight at room temperature. After filtering off remaining solids, the filtrate was concentrated under reduced pressure and the resulting crude product was purified by column chromatography (SiO₂ 20 µm, 60 Å; CH₂Cl₂/methanol 9:1) to give the desired product 1,1'-(1,6-hexanediyl)bisimidazole in 80 % yield (see Figure 5.1, bottom). ¹H NMR (300 MHz, DMSO-*d*₆): δ, 7.56 (s, 1H), 7.12 (s, 2H), 6.84 (s, 2H), 3.89 (t, *J* = 7.2 Hz, 4H), 1.64 (m, 4H), 1.21 (m, 4H). Calculated analytical mass: C₁₂H₁₈N₄: C, 66.02; H, 8.31; N, 25.67; found: C, 66.2; H, 8.4; N, 25.7.



Scheme 5.1 Synthesis steps involved in the preparation of silica bonded IL material.

1,1'-(1,6-hexanediyl)bis-*p*-vinylbenzylimidazolium chloride (9).²⁸² 1.0 g of 1,1'-(1,6-hexanediyl)bisimidazole (4.6 mmol) was dissolved in 20 mL CH₃CN in a 100-mL round-bottom flask. 4-chloromethylstyrene (1.5 g; 10.1 mmol) was added with a syringe and the reaction was heated at 65 °C overnight. The reaction was then allowed to cool to room temperature and was poured into 100 mL diethyl ether. A precipitate formed immediately, and the crude product was cooled to -10 °C in the freezer. Et₂O was decanted and the product dissolved in 20 mL deionized water. The aqueous phase was washed with ethyl acetate (3×50 mL) and water was removed by reduced pressure to obtain the dicationic imidazolium monomer in the chloride form (Figure 5.1, bottom). ¹H NMR (300 MHz, DMSO-*d*₆): δ 9.58 (s, 2H), 7.83 (s, 4H), 7.50 (dd, *J* = 8.2 Hz, 8H), 6.71 (dd, *J* = 11.0 Hz, 2H), 5.86 (d, *J* = 17.5 Hz, 2H), 5.41 (s, 4H), 5.41 (s, 4H), 5.28 (d, *J* = 12.0 Hz, 2H), 4.15 (t, *J* = 7.2 Hz, 4H); 1.22 (m, 4H). Calculated analytical mass: C₃₀H₃₆N₄; C, 68.82; H, 6.93; N, 13.54; found: C, 68.9; H, 7.0; N, 10.9.

Synthesis of the silica-bonded polymer (IL3 & IL4)

To a suspension of 2.0 g of azobis-isobutyronitrile-derivatized silica (Obtained from Supelco) in Toluene was added 1.0 g of the dicationic monomer (**9**) and the mixture was heated to 80 °C for 6 h. Then it was allowed to cool to room temperature with continued stirring overnight. Next, the content was filtered through fine-pore-sintered glass filter funnel. The collected silica-bonded polymeric product was successively washed with 80 mL portions of toluene, chloroform, ethanol, DMF, methanol, and acetone. The final product was dried under vacuum at 50 °C.

Metathesis reaction

The bonded silica is in the chloride form. One gram of silica-bonded ionic liquid polymer in chloride form was mixed with 3.0 g of sodium triflate (NaTfO) and stirred overnight. After filtration, it was washed with deionized water until no white precipitate was seen testing the filtrate with dilute silver nitrate. This silica gel was then further washed with 80 mL portions of toluene, chloroform, ethanol, DMF, methanol, and acetone. The resulting silica-bonded polymer was vacuum dried overnight to obtain the bonded silica in the triflate form. Similar metathesis was carried out to obtain the silica-bonded ionic liquid polymer in its bis-trifluoromethanesulfonimide (NTf₂⁻) form.

5.3.3 SPME Methods

5.3.3.1 Solid Phase Microextraction

For all headspace extractions, a Supelco SPME fiber assembly and holder Model 57330 was used with a 57357-U sampling stand, a 57358-U heater block holding eight 15-mm vials of 4.0 mL and a Corning PC420-D heat/stir plate, all provided by Supelco (Sigma-Aldrich). Immersion extractions were done using the Supelco fiber assembly and a Varian CX 8200 autosampler (Varian Inc. Palo Alto, CA, USA) using 2 mL mini-vials. The ionic-liquid-derivative-bonded silica particles were sent to Supelco Bellefonte to be glued as a 50-μm layer onto SPME flexible core wire fitting the holder (Supelco® proprietary protocol). Figure 5.2 shows scanning electron microphotographs of fiber **IL3**. A very porous 50 μm layer is coated on the solid core. At high magnification (Figure 5.2, bottom), it is possible to see the polymeric IL bonded onto each silica particle. All SEM images were obtained on Zeiss Supra 55 VP with Genesis 4000 EDAX (Located at UTA Nanofab facility).

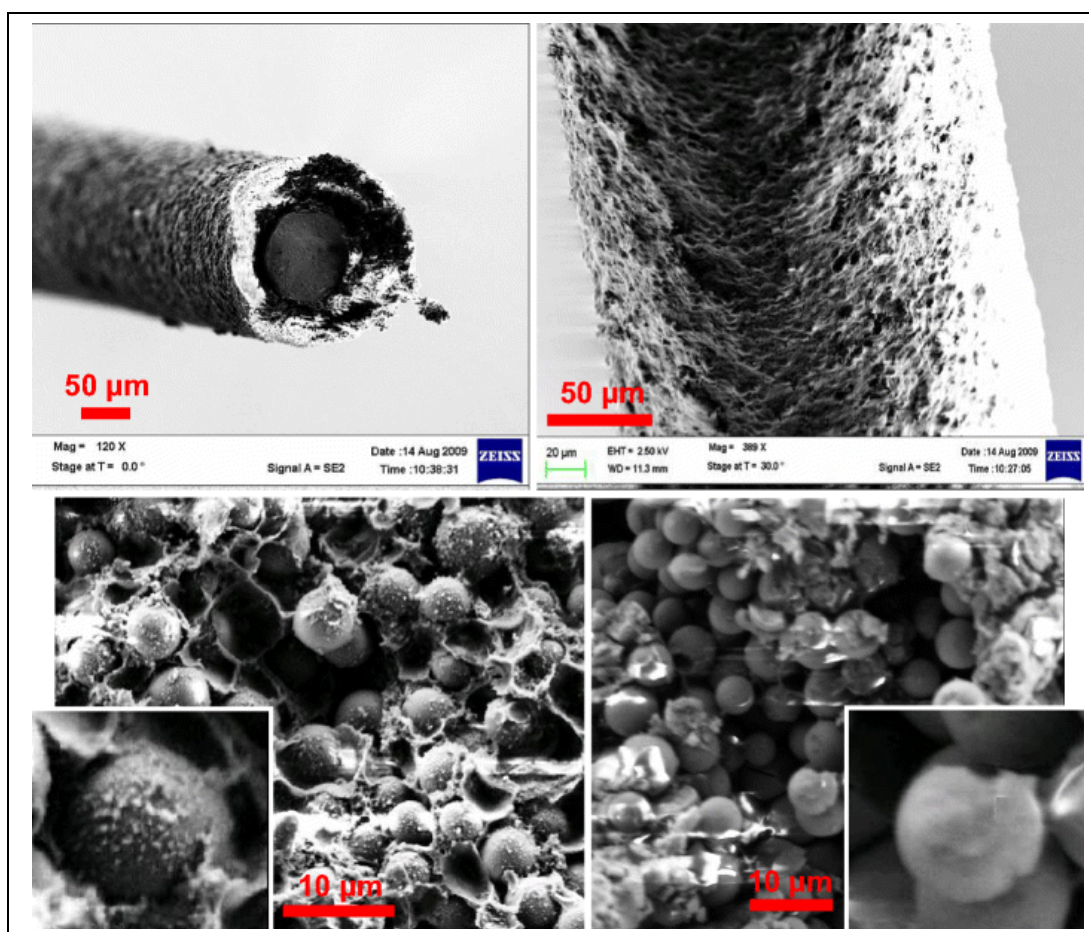


Figure 5.1 Scanning electron microphotographs of fiber IL3.

Granular structure of the coating due to the silica particles. *Bottom right* Enlargement of the coated layer showing the porous structure of the Stableflex® layer holding the bonded silica particles. The *left inset* is an enlargement of a single silica particle showing the IL polymeric coating as white spots covering the particles. *bottom right* For comparison, the same procedure was followed with bare silica particles.

Table 5.1 Characteristics of the silica bonded ionic liquid adsorbents for SPME.

fiber #	bonded moiety	C%	coverage $\mu\text{mol}/\text{m}^2$
IL1	$(\text{HeIM})_2\text{PEG}_3, 2 \text{ NTf}_2^-$	9.2	1.5
IL2	$(\text{HeIM})_2\text{PEG}_3, 2 \text{ TfO}^-$	8.5	1.2
IL3	$[(\text{StyrlIM})_2\text{C}_6, 2 \text{ NTf}_2^-]_n$	21.1	Polymeric
IL4	$[(\text{StyrlIM})_2\text{C}_6, 2 \text{ TfO}^-]_n$	23.4	Polymeric

For comparison, commercial fibers were used in the same conditions as the newly developed fibers. They were a 65- μm polydimethylsiloxane / divinylbenzene fiber (PDMS/DVB) Stableflex 57326-U, a 60- μm polyoxyethylene glycol (PEG) 57354-U, a 100- μm PDMS 57300-U and an 85- μm polyacrylate fiber (PA) fused silica 57304 (Supelco). Before use, all the fibers were conditioned at 220 °C in the GC injection port under a flow of helium for 15 min.

5.3.3.2 Gas Chromatography

An Agilent GC 6850 was used with a split injector and FID detector both set at 300 °C. A Chemstation software (Agilent, Palo Alto, CA, USA) was used to drive the chromatograph and process the chromatograms. The column for polar compounds and headspace analysis was a 30 m, 250 μm i.d., 0.25 μm film thickness Supelcowax™ 10 capillary column (Supelco). The stationary phase is a polyethylene glycol polymer of about 20 million molecular weight (Carbowax® 20 M). The column for polar and amine compounds analyzed by immersion was a 30 m, 320 μm i.d., 4 μm film thickness SPB-1 Sulfur PDMS capillary column (Supelco). Both columns were operated with helium as the carrier gas.

5.3.3.3 SPME Protocol-Headspace Analysis

A known amount of the polar test compounds: ACN, methanol, ethanol, *n*-propanol, IPA, *n*-butanol, acetone, and ethyl acetate, were added to 2.5 mL distilled water in a Teflon®-capped 4 mL vial. Seven hundred fifty milligrams of sodium chloride and a magnetic stir bar were added to the solution. The fiber holder needle was then inserted in the vial headspace. The fiber was exposed for 15 min to the headspace vapors obtained at 50 °C under fast 1,000 rpm stirring. After 15 min, the fiber was retracted inside the needle and the fiber holder was withdrawn from the vial. The

needle containing the fiber was next inserted into the GC split injector set with a low split ratio of 5 to 1. The fiber was immediately exposed for thermal desorption of the adsorbed compounds at 200 °C for 2 min. After 2 min, the fiber was retracted inside the needle, the latter being simultaneously withdrawn from the injector. The sample was analyzed with the 30-m capillary column maintained at 50 °C for 4 min followed by a temperature gradient of 15 °C/min for 6 min and 40 s up to 150 °C, with 1 min at 150 °C. The helium carrier gas linear velocity was 35 cm/s (hold-up time 1.45 min) with an average flow rate of 1.0 mL/min. The FID solute peak areas were used for quantitation rather than the peak heights.

5.3.3.4 SPME Protocol-Immersion Analysis

Stock solutions of the volatile analytes were prepared at concentration in the g/L range in water. A volume of 1.2 mL of buffer at different pH and containing 30% w/v NaCl was introduced in a 2-mL vial. Spiking additions using the stock solutions were made to prepare the mixture with known concentrations of the desired analytes at the selected pH. A total of five to six extractions by fully immersing the fiber in the liquid mixture for 10 min with strong agitation (50 Hz vibration) at room temperature were made with each sample. In all cases, the first extraction was excluded because results from the first extraction were usually not consistent with the remaining extractions. After 10 min, the vibration-agitation is stopped; the fiber is retracted inside the needle and withdrawn from the vial for immediate GC analysis. The needle is inserted into the GC injector at 220 °C or 250 °C and the fiber is exposed in splitless condition for 45 s then the split is opened at a ratio of 20 to 1 (total helium flow is ~30 mL/min) for 1 min 15 s before being retracted into the needle and withdrawn from the injector. The chromatogram was developed with the capillary column maintained at 45 °C for

1.5 min followed by a temperature gradient of 8 °C/min for 4 min and 22 s up to 80 °C, followed by a faster gradient of 20 °C per min for 8 min and 30 s up to 250 °C with a 5-min hold at 250 °C. The helium carrier gas linear velocity was 30 cm/s (hold-up time 1.67 min) with an average flow rate of 1.5 mL/min. The FID detector was set at 290 °C. The solute peak areas were used for quantitation rather than the peak heights.

5.4 Results and discussion

5.4.1 Ethoxylated and Polymeric IL Derivatives

Polar analytes are hydrophilic. As such, they are more difficult to extract by the SPME protocol even maximizing the salting-out effect of adding sodium chloride close to the saturation concentration (359 g/L or 28% w/v at 25 °C).²⁶⁹ SPME was used to identify the fuel used in arson cases and was very effective with gas or petroleum derivatives but was much less so when alcohols were used as fuel source igniters.²⁸³ Thus, enhancing the capabilities of SPME with new adsorbents that have a high affinity for polar compounds is of considerable interest. The specific affinity of ionic liquids for alcohols and polar compounds may be used for this purpose. Considering the problems due to ionic-liquid-coated fibers (liner contamination in the GC injector and irreproducibility),²⁸⁰ bonded IL silica materials were tailored for the task. Oxyethylene adducts were also selected to enhance to polarity of the ionic liquid derivative.

The **IL1** (NTf₂) and **IL2** (TfO) derivatives were bonded as oxyethylene adduct monomers onto the silica particle surface (Scheme 5.1). The carbon loading and moiety molecular weight (Table 5.1) allows for an estimate of the bonding density as 1.2–1.5 µmol/m². Such bonding density would be somewhat low for bonded silica particles used as the sorbent in stationary phase HPLC. The 8.5% to 9.2% carbon loading makes it acceptable for SPME extraction. Derivatives **IL3** and **IL4** were

designed to increase substantially the carbon load by polymerizing a styrene bonded di-imidazolium monomer (**9**). The significantly higher carbon loads between 21 and 23% cannot be related to a coverage density since the additional carbon is strictly the result of the chain lengthening polymerization reaction up to the point that spots can be seen on the silica particle surface (Figure 5.1, bottom).

The specific role of the anion in selectivity was pointed out previously.^{43,190,276,284} Specifically, linear solvation energy relationship (LSER) studies found that the triflate anion had less proton acceptor ability than the bis-(trifluoromethylsulfonyl)imide anion (lower *b* coefficient in the Abraham LSER regression equation).^{43,190,284} This is not surprising since triflic acid is one of the strongest acids known. TfO⁻ also had a significantly higher *a* parameter (basicity) than NTf₂⁻.^{43,190,270} It is then interesting to compare the effect of the anion in our ionic liquid sorbent derivatives.

5.4.2 Headspace Analyses

5.4.2.1 Effect of the fiber exposure time

The same trend was observed for all studied new SPME fiber coated sorbents used in headspace extractions. The adsorbed amount of all analytes increases up to a plateau value reached after about 15 min of headspace exposure at 50 °C. A small decrease may be observed for some compounds exposed for times greater than 20 min. Figure 5.2 shows the results obtained with the polymeric sorbent **IL3** using the relative response value: {peak area (p.a.) at time *t*} over {p.a. at time 15 min}. The trend is the same for all compounds in this study. The absolute response in concentration depended on the nature of the solute as shown by the inset of Figure 5.2. Similar sorption-time profiles were obtained for polymeric IL-coated fibers (30 min

plateau time at 25 °C)¹⁵⁴ or IL-coated fibers for amphetamine detection (20 min plateau time at 50 °C).²⁸¹

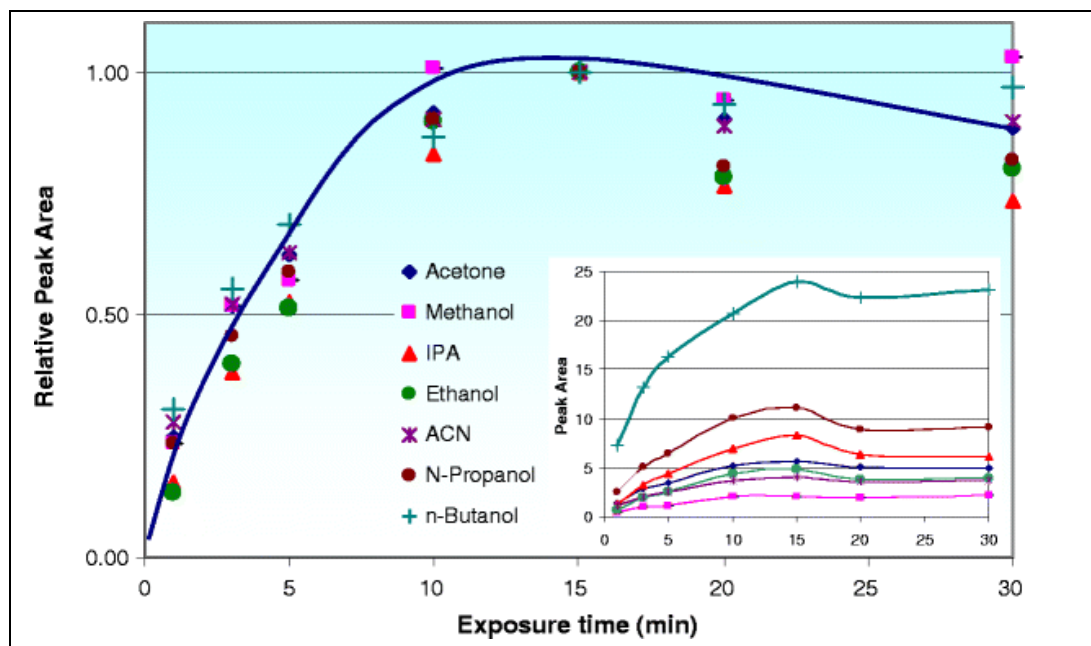


Figure 5.2 Profiles of the relative sorption expressed as [p.a. (t) over p.a. (15 min)] versus headspace exposure time for the polymeric IL 3 SPME fiber.

All solute concentrations were 5 µg/ml (ppm). Exposure temperature 50 °C, 3.0 g NaCl added to 10 mL as salting-out agent

5.4.2.2 Extraction parameter optimization

Salting-out agent: Sodium chloride is added to the solution as a salting-out agent. Previous work showed that the maximum amount of added NaCl produced the highest partial pressure of volatile analytes in the headspace volume and, consequently, the highest amount of analytes extracted by the fiber.^{154,268-270,278-281,285}

This result was confirmed with our fibers. A saturated NaCl solution at 20 °C contains 316 g/L and has a density of 1.20 g/mL. To avoid any precipitation and/or solubility

problems, the amount of NaCl added to all solutions was 30% w/v (750 mg NaCl in 2.5 mL water) just below the saturation concentration.

Extraction temperature: Temperature is another parameter increasing the partial vapor pressure of the analytes in the headspace volume. However, it also increases the vapor pressure of water making the pressure of the headspace volume higher than atmospheric pressure. If leaks occur, the concentration of the extracted analytes may be biased. The working extraction temperature for all headspace experiments was set at 50 °C.

The sensitivities obtained with the two monomeric IL fibers (**IL1** and **IL2**, Tables 5.2) are clearly lower than the corresponding sensitivities obtained with the polymeric IL fibers **IL3** and **IL4**. The two polymeric-bonded IL fibers have a better absolute sensitivity than the commercial PA and PDMS–DVB fibers for the three lightest polar analytes: acetonitrile, methanol, and ethanol. The commercial fibers PA and especially PDMS–DVB have better sensitivities than the new IL-based fibers for all other tested polar compounds. Fiber **IL4** (bonded polymeric $[(\text{StyrlM})_2\text{C}_6, 2 \text{ TfO}^-]_n$, Table 5.1) showed higher absolute sensitivities than its NTf_2^- fiber **IL3** counterpart for all analytes (Table 5.2).

Table 5.2 Analytical figures of merit obtained for polar solutes extracted for 15 min at 50°C by headspace SPME with different fibers.

Solute	fiber	Sensitivity p.a. per ($\mu\text{g/mL}$)	LOD $\mu\text{g/L}$ or ppb	Correlation coefficient	Calibration range $\mu\text{g/mL}$ or ppm
<i>acetonitrile</i>					
	IL1	0.47	$(4.0 \pm 0.3) \times 10^1$	0.992	0.5-50
	IL2	0.40	$(4.0 \pm 0.3) \times 10^1$	0.991	0.5-50
	IL3	1.05	$(1.0 \pm 0.1) \times 10^1$	0.991	0.5-50
	IL4	1.54	$(1.0 \pm 0.1) \times 10^1$	0.994	0.5-50
	PA	0.99	$(2.0 \pm 0.1) \times 10^1$	0.993	1-50
	PDMS/DVB	1.56	$(1.00 \pm 1) \times 10^1$	0.998	1-50
<i>methanol</i>					
	IL1	0.64	$(3.5 \pm 0.2) \times 10^1$	0.995	0.5-50
	IL2	0.70	$(3.0 \pm 0.2) \times 10^1$	0.997	0.5-50
	IL3	0.62	$(3.0 \pm 0.2) \times 10^1$	0.994	0.5-50
	IL4	1.31	$(1.0 \pm 0.1) \times 10^1$	0.993	0.5-50
	PA	0.71	$(3.0 \pm 0.2) \times 10^1$	0.998	1-50
	PDMS/DVB	0.70	$(3.0 \pm 0.2) \times 10^1$	0.996	1-50
<i>ethanol</i>					
	IL1	0.92	$(2.0 \pm 0.2) \times 10^1$	0.993	0.5-50
	IL2	0.91	$(2.0 \pm 0.2) \times 10^1$	0.991	0.5-50
	IL3	0.95	$(2.0 \pm 0.2) \times 10^1$	0.993	0.5-50
	IL4	1.76	$(1.0 \pm 0.1) \times 10^1$	0.995	0.5-50
	PA	1.33	$(1.5 \pm 0.1) \times 10^1$	0.996	1-50
	PDMS/DVB	1.17	$(2.0 \pm 0.2) \times 10^1$	0.993	1-50
<i>n-propanol</i>					
	IL1	1.77	$(1.0 \pm 0.1) \times 10^1$	0.997	1-100
	IL2	1.62	$(1.0 \pm 0.1) \times 10^1$	0.992	1-100
	IL3	2.12	$(1.0 \pm 0.1) \times 10^1$	0.996	1-100
	IL4	3.23	5.0 ± 0.4	0.998	1-100
	PA	2.98	5.0 ± 0.4	0.996	1-100
	PDMS/DVB	3.05	7.0 ± 0.5	0.997	1-100
<i>i-propanol</i>					
	IL1	1.29	$(1.5 \pm 0.1) \times 10^1$	0.993	1-100
	IL2	1.31	$(1.5 \pm 0.1) \times 10^1$	0.991	1-100
	IL3	1.56	$(1.5 \pm 0.1) \times 10^1$	0.998	1-100
	IL4	2.66	8.0 ± 0.6	0.991	1-100
	PA	2.02	$(1.0 \pm 0.1) \times 10^1$	0.995	1-100
	PDMS/DVB	2.34	9.0 ± 0.6	0.999	1-100

Table 5.2 Continued

<i>n</i>-butanol					
	IL1	4.50	$(4.0 \pm 0.3) \times 10^1$	0.993	1-100
	IL2	4.21	5.0 ± 0.4	0.992	1-100
	IL3	5.40	3.0 ± 0.2	0.992	1-100
	IL4	6.52	2.0 ± 0.2	0.994	1-100
	PA	8.16	1.0 ± 0.1	0.991	1-100
	PDMS/DVB	11.5	0.50 ± 0.04	0.992	1-100
<i>acetone</i>					
	IL1	0.99	$(2.0 \pm 0.2) \times 10^1$	0.996	1-100
	IL2	0.82	$(2.5 \pm 0.2) \times 10^1$	0.993	1-100
	IL3	1.36	$(1.5 \pm 0.1) \times 10^1$	0.997	1-100
	IL4	1.95	$(1.0 \pm 0.1) \times 10^1$	0.996	1-100
	PA	1.25	$(1.5 \pm 0.1) \times 10^1$	0.995	1-100
	PDMS/DVB	2.60	5.0 ± 0.4	0.999	1-100
<i>ethyl acetate</i>					
	IL1	3.12	$(1.0 \pm 0.1) \times 10^1$	0.992	1-100
	IL2	3.04	$(1.0 \pm 0.1) \times 10^1$	0.992	1-100
	IL3	3.20	$(1.0 \pm 0.1) \times 10^1$	0.994	1-100
	IL4	4.88	5.0 ± 0.4	0.995	1-100
	PA	6.59	4.0 ± 0.4	0.995	1-100
	PDMS/DVB	8.70	3.0 ± 0.2	0.996	1-100

Fibers **IL 1** to **4**: see full structures in Table 1; PA: polyacrylate fiber 85 μm coating thickness; PDMS/DVB: polydimethylsiloxane/divinylbenzene fiber 65 μm coating thickness; p.a.: peak area; LOD: limit of detection; ppm: part per million or mg/L; ppb: part per billion or $\mu\text{g/L}$.

It should be noted that with the IL-coated fibers, both the binder and silica used to prepare the adsorbing layer take a significant percentage of the coating volume having limited extraction capabilities. Furthermore, the coating volume of the IL-based fibers with a coating thickness of around 50 μm (see Figure 5.2) is itself lower than the coating volume of the commercial PA fiber (85 μm) and the PDMS–DVB fiber (65 μm). To take into account these composition and volume differences, we used ethyl acetate as an internal standard to normalize the results.

Figure 5.3 represents the Table 5.2 absolute results as relative results, i.e., plotting for each analyte the ratios of the analyte absolute response over the same fiber ethyl acetate response. This representation shows that the IL fibers have a better relative response for all selected analytes. For the polymeric-bonded IL fibers **IL3** and **IL4**, the short-chain alcohols' relative response can be twice higher than that of the commercial fibers. For *n*-butanol that shows the highest absolute response for all fibers, the polymeric **IL3** (NTf₂⁻ anion) relative response is about 20% higher than the other fiber response (Figure 5.3).

However, the relative representation of the results in Fig 5.4 shows that, except for *n*-butanol, there is no significant difference between the NTf₂⁻ and TfO⁻ IL fiber response. The higher absolute values obtained for fiber **IL4** (Table 5.2) compared to fiber **IL3** may be due to the accumulation of excess silica particles during the coating procedure. The relative response in headspace analysis for the two polymeric IL fibers is very similar being somewhat better than the two monomeric IL fibers. The enhanced affinity of ILs for short-chain alcohols observed with IL gas chromatography stationary phases^{44,46} was confirmed in headspace analysis with IL-based adsorbents.

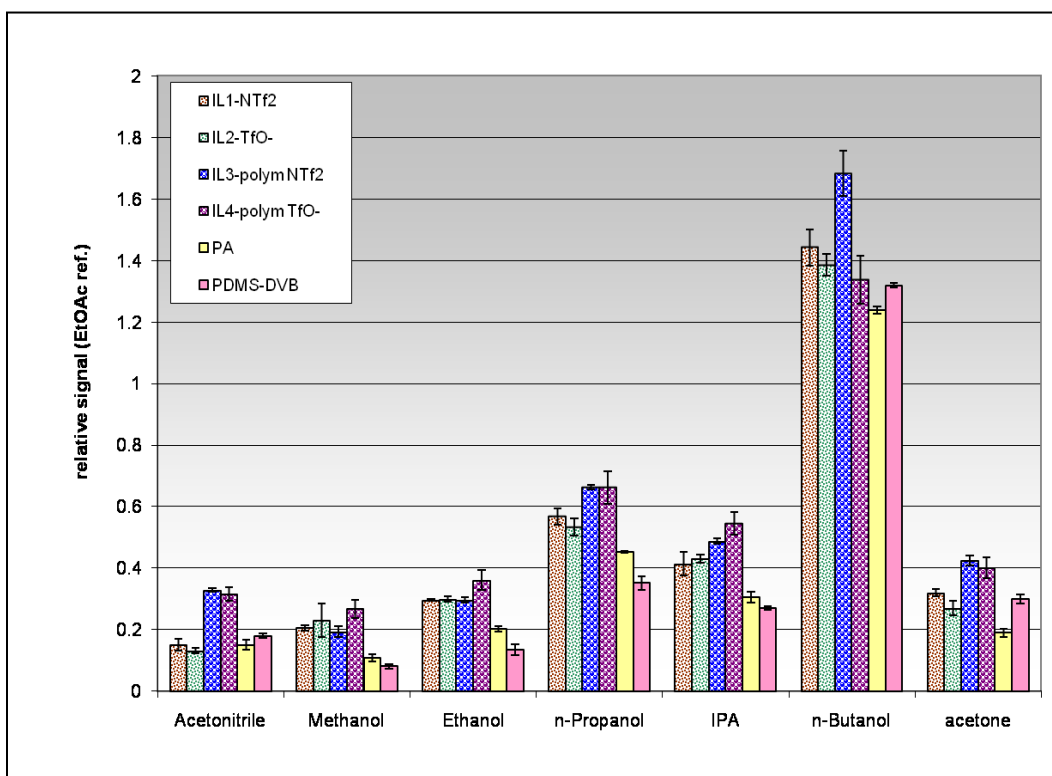


Figure 5.3 Relative response ratios of analytes in headspace analyses with four ILs and two commercial fibers.

5.4.2.3 Use of the polymeric IL fiber for ethanol determination in beverages

The headspace analysis process was validated using the reference material NIST SRM (National Institute of Standards and Technology-Standard Reference Material) 1828b and it was used with fiber IL4 to assess the ethanol content of several alcoholic beverages. A calibration curve was prepared between 5.0 and 100.0 ppm in volume (microliters of ethanol per liter of water). The NIST reference material was calibrated in the units of % mass. The beverage items were all labeled in ethanol % v/v. Considering the low concentrations involved, the water density was taken as 1.0 g mL^{-1} and the ethanol density (0.789 g mL^{-1}) was used to establish the correspondence: 1,000 ppm in mass=0.1% w/w=0.1267% v/v. Table 5.3 lists the

results obtained comparing them with the beverage labels. The relative standard deviation (RSD) on four experiments were between 6% and 12%. These RSDs may appear high for an analytical technique; they are the usual RSD values obtained in quantitative SPME experiments.^{153,269,270,286} The average values obtained for the SPME ethanol extraction of the two reference materials with certified 0.02% and 0.1% w/w values, were respectively $0.024 \pm 0.002\%$ v/v and $0.12 \pm 0.01\%$ v/v validating the method with an 8% RSD.

Table 5.3 SPME results obtained with fiber IL4 in the ethanol analysis of real samples.

Sample ^a	label indication	SPME value ^b % v/v	RSD ^c	deviation ^d
NIST SRM 1828b	0.02%w/w or 0.0253%v/v	0.024 ± 0.002	7.1%	-5.1%
NIST SRM 1828b	0.1%w/w or 0.1267%v/v	0.12 ± 0.01	8.2%	-3.1%
Miller Lite beer	3%v/v	2.9 ± 0.3	11.7%	-3.3%
Coors original	5%v/v	4.8 ± 0.4	9.4%	-4.0%
Shiner beer	4.4%v/v	4.3 ± 0.4	8.6%	-2.3%
Dos Equis XX	4.2%v/v	4.0 ± 0.3	7.6%	-5.0%
Steel Reserve 211	8.1%v/v	8.6 ± 0.5	6.4%	+6.2%
Crown Royal Whisky	40%v/v	38 ± 3	8.1%	-5.0%
Antique Whiskey	30%v/v	29 ± 3	11.9%	-1.7%

- a) SRM = standard reference material, the other samples were obtained from local groceries stores (Arlington, Texas).
- b) Average values of 4 measurements, headspace protocol.
- c) Relative standard deviation on 4 measurements.
- d) Relative difference with the label indication and SPME result.

Five different beers and two liquors were analyzed for their ethanol content. The samples were diluted using the label indication in percent v/v so that the ethanol content for SPME analysis was around 50 ppm in volume, a value in the middle of the calibration curve. With ethanol being rapidly eluted in gas chromatography, no

interferences were encountered in the sample analyses. Except for the beer sample containing the highest ethanol percentage, all SPME results, including the two certified samples, were found slightly below the label values (see Table 5.3). SPME headspace extraction could be used to estimate the ethanol content of blood samples in a non-destructive way.

5.4.3 Immersion Analyses

This study is done in collaboration with Supelco R&D laboratories Bellefonte, PA. The protocol for immersion extractions is necessarily different from the headspace protocol (see Experimental section). Only the two polymeric fibers **IL3** and **IL4** were evaluated. Six extractions were performed successively for each sample at room temperature. The very first extraction of a new sample always gave results that differed significantly from the five following extractions, it was discarded. Ion-exchange could be responsible for this phenomenon. Since the cationic part of the IL is chemically attached to the fiber and the anion is bound by electrical interaction only, the fiber can behave as an anion-exchanger. Ion-exchange can occur between the high ionic strength solution and the fiber anions. The fiber can exchange its triflate or bis-triflylimide anions for chloride and/or phosphate anions in the sample.

5.4.3.1 Extractions at pH 2

Since bonded silica is known to be sensitive to pH, extractions at pH 2 and pH 11 were done with different analytes. Table 5.4 lists the results obtained for nine selected typical solutes with the two polymeric IL fibers **IL3** and **IL4**, two commercial fibers: a 60- μm thick PEG fiber and a 100- μm thick PDMS fiber, and the same compounds that were used in headspace analyses plus a variety of other less volatile compounds. A more complete table listing 19 compounds can be found in the Appendix.

The listed values are the average of five successive experiments. The low percent RSD for most of the extracted analytes indicate that the fibers are quite stable. The relatively higher RSD for methanol was associated to a slowly declining response with repeated extractions. This may be due to an experimental artifact (slow evaporation during sampling). The same trend was observed with phenol and butyric acid.

The IL fibers were compared to a polar 60- μm PEG-coated fiber and to a non-polar 100- μm PDMS coated fiber. Table 5.4 lists the sensitivity obtained for each fiber expressed as GC peak area per parts per million (micrograms per milliliter) of analyte concentration. As observed in the headspace extraction study, the amount of extracting material has a great influence on the experimentally observed fiber sensitivity. Therefore, in the immersion extraction study also, ethyl acetate was used as an internal standard. Figure 5.4 presents the relative response ratios for each analyte and each fiber expressed as the absolute value for analyte on a given fiber (from Table 5.4) divided by the corresponding ethyl acetate value.

Table 5.4 SPME results obtained with different fibers by immersion in two different pH solutions.

Solute	fiber^a	Sensitivity pH 2 p.a. per (µg/mL)	RSD^b %	Sensitivity pH 11 p.a. per (µg/mL)	RSD^b %
acetonitrile	IL3	47.2	0.5%	43.5	0.8%
	IL4	27.4	0.5%	24.3	1.2%
	PEG	67.9	2.1%	-	-
	PDMS	15.8	1.6%	-	-
methanol	IL3	11.1	13.0%	25.1	1.5%
	IL4	12.6	13.6%	25.4	2.8%
	PEG	54.0	49%	-	-
	PDMS	6.8	17%	-	-
ethanol	IL3	23.2	0.9%	34.8	1.7%
	IL4	18.5	1.2%	27.8	3.7%
	PEG	62.4	2.4%	-	-
	PDMS	12.2	1.5%	-	-
n-propanol	IL3	176.0	0.6%	91.8	1.0%
	IL4	97.0	2.1%	49.3	1.2%
	PEG	381.0	2.2%	185.0	1.9%
	PDMS	123	0.8%	55	1.1%
isopropanol	IL3	49.4	1.3%	49.1	1.5%
	IL4	27.2	2.8%	26.6	1.3%
	PEG	104	2.2%	96.1	1.8%
	PDMS	41.4	0.6%	60.1	1.4%
n-butanol	IL3	331	1.0%	69.9	0.9%
	IL4	131	2.6%	27.0	2.8%
	PEG	611	1.7%	-	-
	PDMS	327	1.2%	-	-
acetone	IL3	78.0	0.5%	75.7	1.2%
	IL4	32.9	1.0%	30.9	1.4%
	PEG	65.7	2.3%	-	-
	PDMS	58.6	0.8%	-	-
ethyl acetate	IL3	90.3	1.1%	93.1 ^c	2.1%
	IL4	44.8	0.9%	75.1 ^c	1.0%
	PEG	129	2.1%	290 ^c	2.3%
	PDMS	178	1.5%	1036 ^c	4.4%
methyl-tert-butyl ether	IL3	235	1.2%	-	-
	IL4	89.8	2.8%	-	-
	PEG	245	2.5%	-	-
	PDMS	4580	1.2%	-	-

Table 5.4 Continued

dioxane	IL3	33.7	0.9%	28.6	1.2%
	IL4	12.1	2.6%	10.9	2.4%
	PEG	41.3	2.7%	-	-
	PDMS	67.2	1.1%	-	-
butyric acid	IL3	323	6.7%	ion.	-
	IL4	143	24%	ion.	-
	PEG	585	7.8%	ion.	-
	PDMS	48.7	6.0%	ion.	-
phenol	IL3	2200	12%	-	-
	IL4	1220	12%	-	-
	PEG	11600	2.6%	-	-
	PDMS	477	7.4%	-	-
methylamine	IL3	ion.	-	105	0.8%
	IL4	ion.	-	34.7	5.6%
	PEG	ion.	-	191	2.2%
	PDMS	ion.	-	137	2.3%
	PDMS/DVB	ion.	-	288	4.2%
dimethylamine	IL3	ion.	-	135	1.7%
	IL4	ion.	-	81	1.4%
	PEG	ion.	-	229	2.2%
	PDMS	ion.	-	319	1.8%
	PDMS/DVB	ion.	-	684	4.1%
trimethylamine	IL3	ion.	-	115	1.1%
	IL4	ion.	-	200	1.1%
	PEG	ion.	-	213	1.4%
	PDMS	ion.	-	2082	4.2%
	PDMS/DVB	ion.	-	699	3.5%
isopropylamine	IL3	ion.	-	134	1.7%
	IL4	ion.	-	161	0.7%
	PEG	ion.	-	470	1.1%
	PDMS	ion.	-	492	1.2%
	PDMS/DVB	ion.	-	1594	3.2%
diethylamine	IL3	ion.	-	216	1.8%
	IL4	ion.	-	161	0.7%
	PEG	ion.	-	602	1.5%
	PDMS	ion.	-	1220	3.1%
	PDMS/DVB	ion.	-	3390	3.4%

Table 5.4 Continued

butylamine	IL3	ion.	-	556	1.2%
	IL4	ion.	-	353	1.8%
	PEG	ion.	-	1560	2.5%
	PDMS	ion.	-	2334	3.8%
	PDMS/DVB	ion.	-	9228	5.1%
triethylamine	IL3	ion.	-	365	1.4%
	IL4	ion.	-	815	1.9%
	PEG	ion.	-	960	2.1%
	PDMS	ion.	-	-	-
	PDMS/DVB	ion.	-	-	-

a) Fiber #3 is polymeric $[(\text{StirIM})_2\text{C}_6, 2 \text{NTf}_2^-]_n$; Fiber IL4 is the triflate version of IL3 (Table 5.1); PEG: polyethylene glycol, fiber 60 μm coating thickness; PDMS: polydimethylsiloxane, fiber 100 μm coating thickness; PDMS/DVB: polydimethylsiloxane divinylbenzene, fiber 65 μm coating thickness.

b) RSD: relative standard deviation on six successive extractions of the same sample.

c) Ethyl acetate decomposes in ethanol and sodium acetate at pH 11. The measurements were especially done at pH 7. p.a.: peak area; ion.: the compound ionizes at the measurement pH.

“-“ Fibers were not evaluated under these conditions.

In absolute terms, fiber **IL3** (polymeric IL with NTf_2^- anion) gave higher sensitivity factors for all studied analytes compared to its counterpart Fiber **IL4** with the triflate anion (Table 5.4). The sensitivity factors for the PEG fiber were also higher than these obtained with the two IL fibers for all analytes. The picture is completely different when considering the relative fiber responses. Figure 5.4 shows that the two ILs fibers gave similar results in this relative representation. The IL fibers results compare well with the polar PEG fiber. Both results are clearly superior to the PDMS results except for MTBE (see Figure 5.4). The relative results obtained in headspace extraction (Figure. 5.4) and immersion extractions (Figure 5.4) were quite coherent. Compared to the two IL fibers, the PEG fiber seems to be slightly more efficient in immersion extractions than in headspace extractions in acidic media.

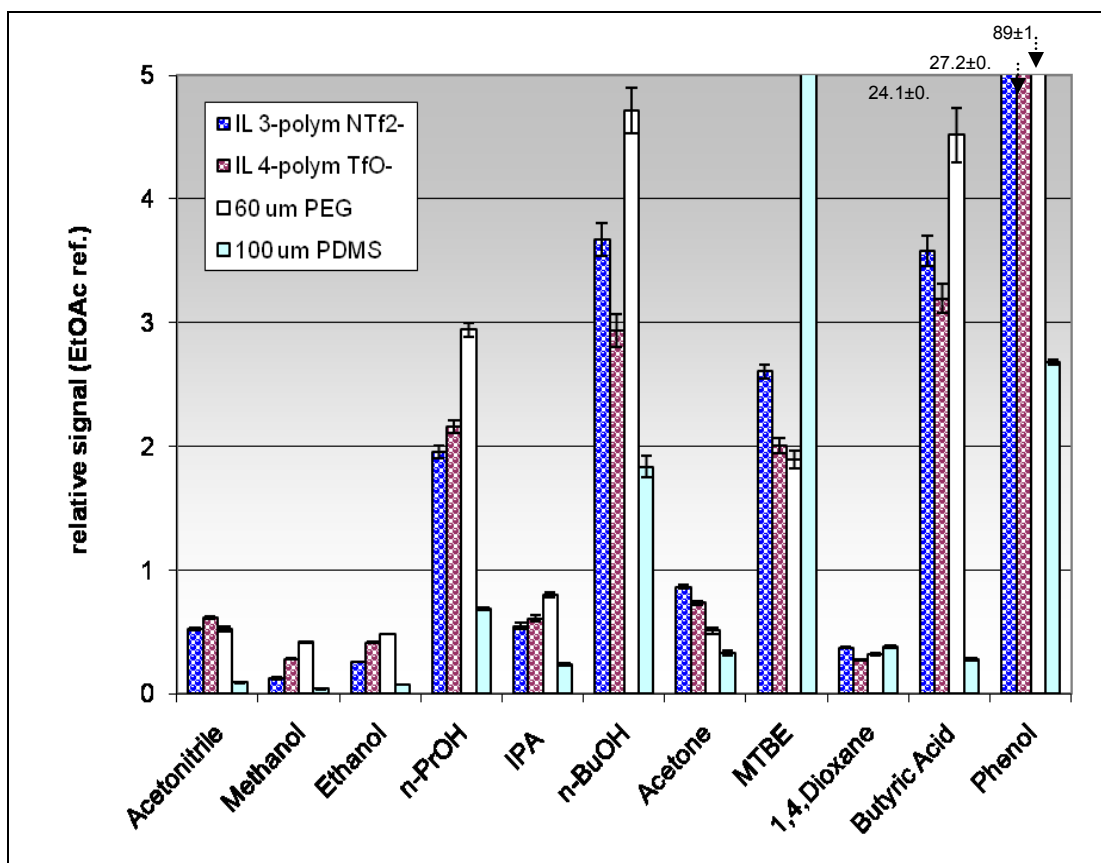


Figure 5.4 Relative response ratios of analytes in immersion analyses at pH 2 with two ILs and two commercial fibers.

5.4.3.2 Extractions at pH 11

Phosphate buffer was used to obtain a matrix of pH 11 allowing an evaluation of fiber stability. Since the polymeric ionic liquids are bonded to silica particles, alkaline solutions could damage the particle and/or deteriorate the bonding. Many of the pH 2 neutral analytes and seven basic analytes were used as test solutes. Table 5.4 lists all the results in the two rightmost columns.

The first observation is that there is ample stability and good reproducibility of the results at pH 11. The RSDs of the experiments were similar to those obtained at

pH 2. Experiments at different pHs were repeated with the same fibers over several months to study different mixtures. The reproducibility of the silica-based fibers was comparable to that of the polymer-based commercial fibers.

Table 5.4 also lists the sensitivity factors obtained for seven small amines at pH 11. The two polymeric IL fibers were able to extract all of the tested amines with sensitivity factors equal or higher to those obtained for short-chain alcohols at both pHs (Table 5.4). The amine sensitivity factors are however significantly lower than the corresponding factors obtained with the three commercial fibers. It must be pointed out that the 65- μ m PDMS/DVB commercial fiber was specially designed to extract basic compounds. It did produce sensitivity factors for amines higher than those of all other fibers except for trimethylamine.

When considering these extractions in relative terms, the picture is different. Figure 5.5 shows the relative response ratios (ethyl acetate reference compound) of the amines extracted by immersion at pH 11. The IL fiber sensitivities for the amine compounds seem significantly better than the commercial fibers sensitivities. This figure will not be commented on any further because it was not obtained with a true internal standard. The internal standard, ethyl acetate, used to prepare Figures 5.4 and 5.5 is not stable at pH 11 as it slowly decomposes to ethanol and sodium acetate. So its sensitivity factor was specially measured at pH 7 meaning that the standard was not present with the amine compounds as a true internal standard should be. This could induce a bias in Figure 5.6. Figure 5.6 shows the same Table 4 data using *n*-propanol as an internal standard. *n*-Propanol is not the same standard as the one used in Figures 5.4 and 5.5 but it was present with the amine compounds since it is stable at pH 11. Figure 5.5 and Figure 5.6 show very similar results for the two IL fibers

compared to one another and also compared to the commercial PEG fiber. The PDMS and PDMS/DVB commercial fiber relative responses look very different and much higher than those of the two IL fibers when the true internal standard *n*-propanol is the reference compound. Polar *n*-propanol is not as good as the less polar ethyl acetate as an internal standard. Since *n*-propanol adsorbs more on the polymeric IL fibers and PEG fiber than on the less polar PDMS/DVB fiber (Figure 5.4), used as the internal standard, it tends to produce underestimated relative sensitivity factors for the IL fibers and/or overestimated values for the PDMS-based fibers.

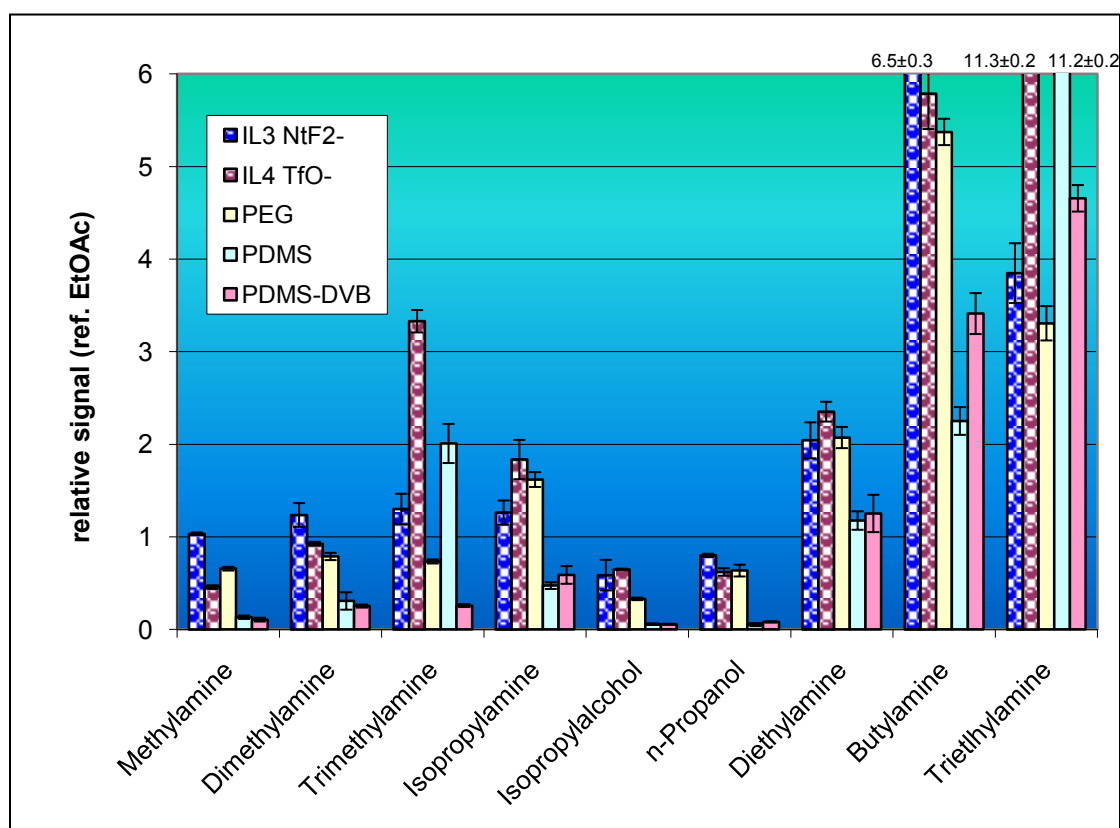


Figure 5.5 Relative response ratios of analytes in immersion analyses at pH 11 with two ILs and three commercial fibers (EtOAc reference).

There is no definitive conclusion comparing the new polymeric IL fibers to the commercial PDMS and PDMS/DVB fibers; however, there is no doubt that the IL fibers are able to extract short amines effectively.

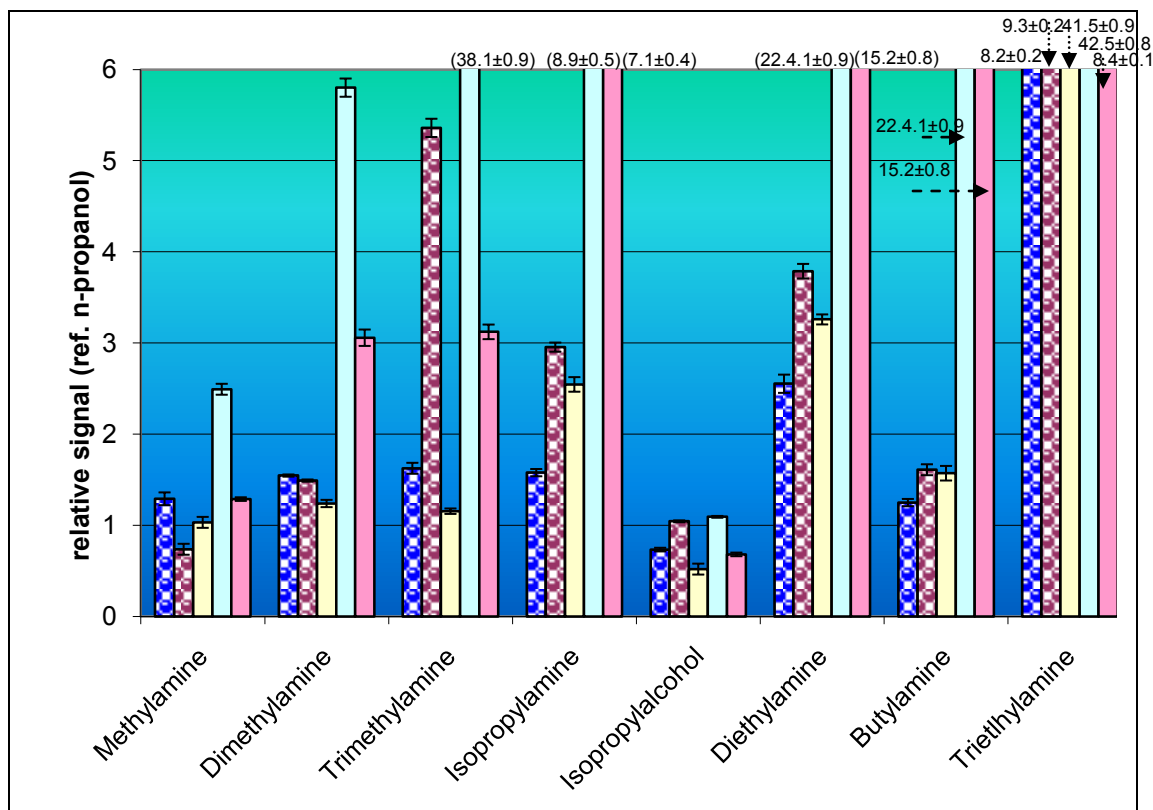


Figure 5.6 Relative response ratios of analytes in immersion analyses at pH 11 with two ILs and three commercial fibers (n-Propanol reference).

5.4.4 Durability of the IL Fibers

The headspace procedure is a very gentle process for the fibers and did not pose any durability problems. The immersion procedure put much more mechanical strain on the fiber itself since the Varian 8200 auto sampler uses a strong vibrator similar to that used in an electrical razor. It is extremely harsh on the fiber coating vibrating it at about 50 Hz. However, a single triflate fiber **IL4** was used to do all the

more than 50 immersion experiments done in this study. The fibers were very durable. The thickness of the fiber coating remained the same. The fiber coloration did change after the initial 220 °C conditioning but remained stable and consistent after all immersions and GC analyses done for the study. No indications of visual fiber coating deterioration were noted throughout the study.

Peak tailings were observed on the GC peaks of amines. A 30 °C desorption temperature increase was tried to improve the peak shape increasing the amine desorption rate. The GC injector temperature was raised to 250 °C. No significant changes were observed in either the analyte sensitivities or the GC peak shapes. However, the IL fibers withstood this temperature increase without damage further showing their durability.

5.5 Conclusions

Upon polymerization and bonding to silica particles, the liquid state of ILs is lost but the other unique properties, such as low volatility and polarity associating apolar and charge–charge interactions, are maintained. It was demonstrated that the polymerized IL-bonded silica particles could be coated on SPME fibers to be used for the extraction of small and polar molecules. The headspace, as well as the immersion SPME protocols, was used to quantitate short-chain alcohols down to the 10 ppb level. The efficacy of the method was tested by checking the ethanol content of a variety of beverages and a NIST standard material. Small amines were extracted using the immersion procedure at pH 11 demonstrating the stability of the polymerized IL-coated silica particles. The nature of the anion, triflate or bis-triflyl amide, could influence the overall polarity of the IL. However, no clear differences were found between the two fibers made respectively with these two anions.

PART TWO
CALIX[4]ARENE CHEMISTRY OF NO_x GASES

CHAPTER 6

CALIX[4]ARENE CHEMISTRY OF NO_x GASES

6.1 Introduction to Calix[4]arenes

Calixarenes are a class of macrocyclic polyphenols that have been widely employed for the construction of sophisticated supramolecular architectures with numerous applications. In 1975, Gutsche coined the term “calix” deriving from the resemblance of the simplest calixarene which is calix[4]arene, to that of the classical Greek vase, the calyx crater.²⁸⁷ Calixarene can be represented by Calix[n]arenes where n represents the number of phenolic units present in the molecule. Calix[4]arenes have 4 phenolic units linked together in the macrocyclic ring system. Calixarenes are used in sensing,²⁸⁸ biomimicing,^{289,290} fluorescent probes,²⁹¹ catalysis,²⁹² electrochemistry,²⁹³ and liquid chromatographic^{294,295} applications.

Calix[4]arenes are by far the most widely known derivative in host-guest chemistries compared with other Calix[n]arenes (n= 5,6,7,8). This is mainly due to ease of synthesis and functionalizations. Calix[4]arene molecule can be subdivided into three sections called the upper rim, annulus and lower rim (see Figure 6.1).

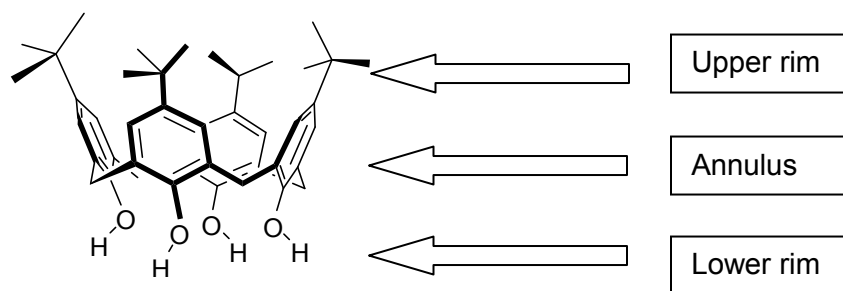


Figure 6.1 Representation of calix[4]arene and designation of the sections.

Calix[4]arenes can exist in four major conformations termed *cone*, *partial cone*, *1,2-alternate* and *1,3-alternate* (see Figure 6.2). These names were given based on the projection of the aryl groups upwards (“u”) or downwards (“d”) relative to an average plane, typically the annulus. Therefore, “u,u,u,u” represents cone “u,u,u,d” represents *partial cone*; “u,u,d,d” represents *1,2 alternate* and “u,d,u,d” represents *1,3-alternate* conformations. As the number of aryl groups increases (i.e. “n” increases) the number of possible conformations increase.

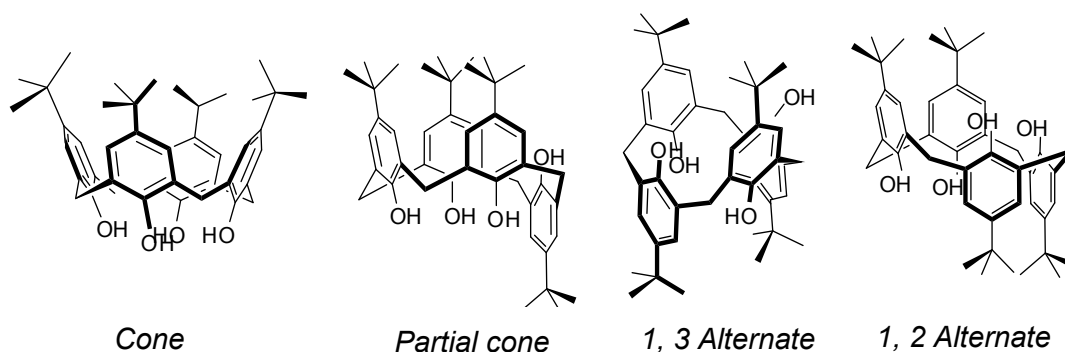


Figure 6.2 Conformations of calix[4]arenes.

Out of the four major conformations of calix[4]arene the *1,3-alternate* conformation has proven to be particularly useful. With symmetrical substitutions in the upper and lower rims, it is the only isomer with a zero net dipole moment.²⁹⁶ Apart from *1,3-alternate* conformation, the *cone* conformation is also widely used in variety of host guest complexation studies. Functionalization can be generally carried out at the upper or lower rim of the molecule. Typical functionalizations include alkylation, acylation, nitration, amination and sulfonation.

Replacement of all four –OH groups present in calix[4]arene with alkyl, acyl, or aroyl groups can increase the conformational stability.^{297,298} These types of derivatizations results in conformational immobilization, therefore non-interconverting *cone*, *partial cone*, *1,2-alternate* and *1,3-alternate* conformations can be synthesized.²⁹⁹

The interior of the calix[4]arene is a perfect binding site for many types of guest molecules. This cavity can accompany guests such as metal ions,³⁰⁰⁻³⁰² anions³⁰³⁻³⁰⁶ and neutral molecules.^{307,308}

6.2 Oxides of Nitrogen

Oxides of nitrogen are commonly known as NO_x gases. In the ambient air, NO_x primarily consists of nitrogen dioxide (NO₂) and nitric oxide (NO) and nitrous oxide (N₂O). Nitric oxide is readily converted to NO₂ which is considered to be much more harmful to the environment.³⁰⁹ These NO_x pollutants can cause serious health hazards to humans and animals.³¹⁰ Figure 6.3 shows the main sources of NO_x gases by human actions (anthropogenic sources).

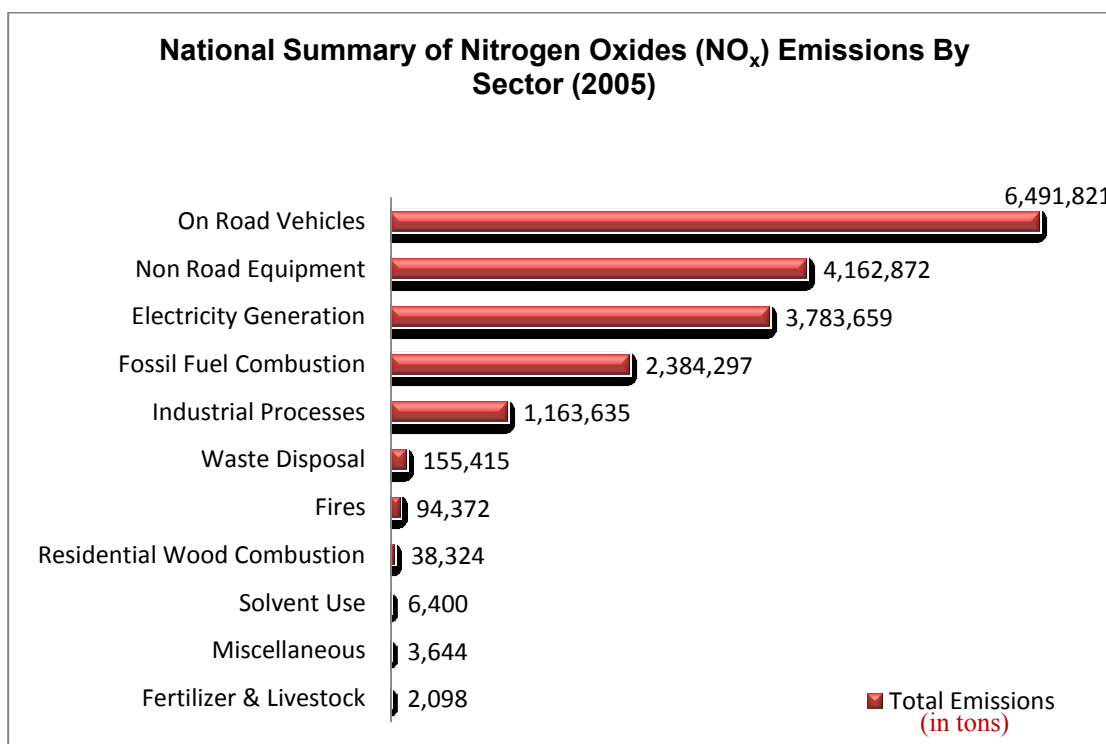


Figure 6.3 Major sources of nitrogen oxides (NO_x) emissions by sector.
(source: <http://www.epa.gov/air/emissions/NOx.htm>, accessed 08/16/2010).

According to Environmental Protection Agency (EPA) records, worldwide annual NO_x emissions are estimated to be 50 million metric tons. The United States generates about 20 million metric tons of NO_x per year. About 90% of these anthropogenic emissions come from fossil fuel burning used in electricity, heat generating power plants and by motor vehicles. Natural sources of NO_x include lightning, forest fires, grass fires, trees, bushes, grasses, and yeasts.³¹⁰ Emissions of NO_x gases from combustion primarily exist in the form of NO while the rest consists of NO₂/N₂O₄. Biogenic sources contribute about 10% of the total NO emissions.

NO₂ present in the atmosphere is a cause for acid rains. This is due to the production of HNO₃ and HNO₂ by NO₂ reacting with water. During the lightning

process, after absorbing high energetic photons, NO_2 and O_2 reacts to give NO and O_3 . Since NO produced in this pathway can easily be reconverted back to NO_2 , some scientists think NO_x gases are mainly composed of NO_2 .

Nitrous oxide (N_2O) is also one of the major oxides of nitrogen that contribute to the total NO_x content. N_2O is also known as laughing gas. This is used as a local anesthesia in medicine. N_2O not only has anesthetic properties but also analgesic properties which will make the patient comfortable by masking the pain. However, N_2O itself is not capable of acting as an anesthetic. It has to be mixed with oxygen to obtain the desired anesthetic and analgesic effects. N_2O is also used in food industry, as propellants, and in combustion engines. N_2O is an ozone depleting substance which reacts with ozone present in both the troposphere and the stratosphere. N_2O also has a long half-life of approximately 150 years.

Emission control, sensing, fixating and storage/release of these NO_x gases are of very high importance due to the environmental implications. The development of chemical and non chemical methods for the control of these processes has attracted much attention in industry and academia.

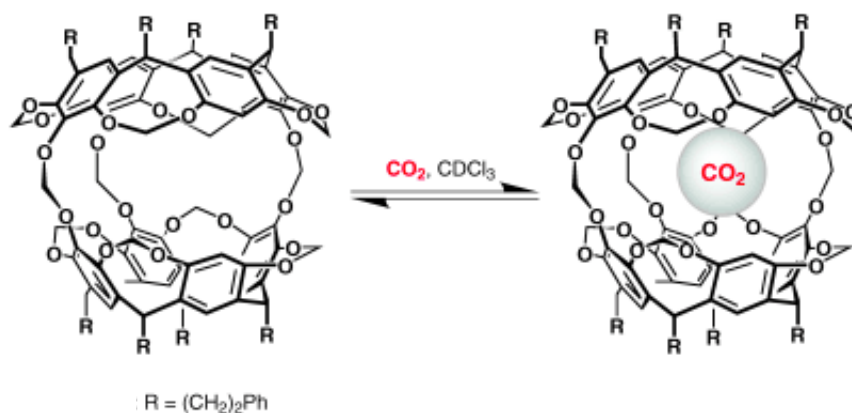
6.3 Supramolecular Approaches for Molecular Recognition of Gases

Molecular recognition of gases is an emerging area of chemistry.³¹¹ Molecular chemistry is based on covalent bonds. However noncovalent forces play a major role in supramolecular chemistry.^{312,313} Its interdisciplinary nature has brought a wide range of collaborations between crystallographers, inorganic chemists, biochemists and synthetic organic chemists. Supramolecular chemistry of gases helps to understand how gaseous molecules interact with biological systems and offers an understanding of the mechanisms of their physiological activity. Humans live in the troposphere and are

in constant contact with gases. Along with industrial development in the world, gas emission levels have increased, thus breaking the natural environmental equilibrium. Oxygen (O_2) gas is extensively utilized in the steel manufacturing industry and nitrogen (N_2) is used to produce ammonia (NH_3). All fossil fuel burning results in gases such as carbon dioxide (CO_2), carbon monoxide (CO) and NO_x gases. If the utilization of these gases is slower than their emissions to the atmosphere, then the environment has to face critical pollution conditions.

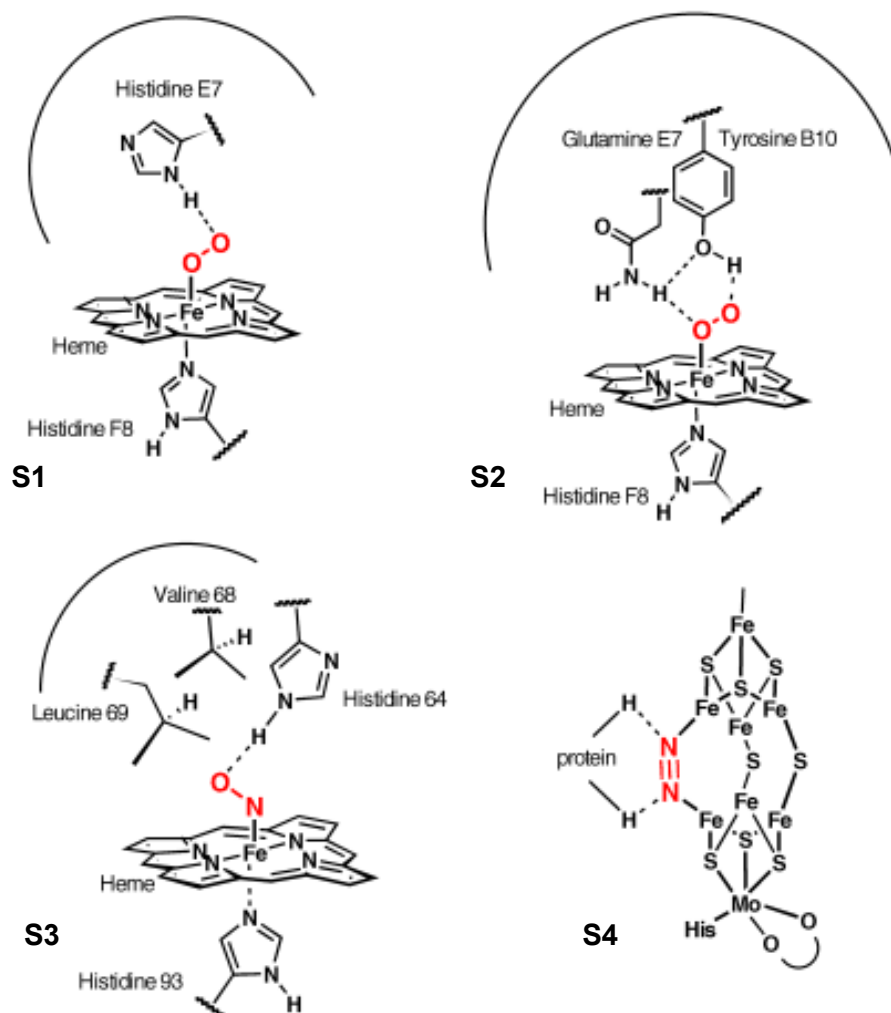
Recently, significant efforts have been made to build and develop new supramolecular architectures for the purpose of molecular recognition, sensing and storage/release of gases. Figure 6.4 illustrates a calix[4]resorcarene-based molecular receptor (developed by Cram et al.) encapsulated O_2 , N_2 , CO_2 , and Xe.³¹⁴ The host-guest exchange between the free and occupied hemicarcerand was slow on the NMR time-scale. Association constants (K_{ass}) of 180 M^{-1} (N_2), 44 M^{-1} (O_2), and 200 M^{-1} (Xe) were obtained in $CDCl_3$ at 22°C , assuming the binding between host and guest is 1:1.^{311,314}

The volume of the inner cavity of the hemicarcerand is approximately about 120 \AA^3 and the volume of the guest gas molecule is approximately 40 \AA^3 . It is predicted that this hemicarcerand (Scheme 6.1) can likely encapsulate more than one gas molecule.³¹¹ However this was not investigated by the initial developers.



Scheme 6.1 Encapsulation of CO_2 within the hemicarcerand developed by Cram et al.
Reproduced with the permission from reference 311.

Nature employs molecular recognition methods for effective discriminating of gases dissolved in blood. Differentiation of O_2 and CO by a heme molecule is one of the most extraordinary examples.³¹⁵ Here, in addition to the iron–gas interaction, the histidine residue on the distal porphyrin face of hemoglobin and myoglobin is involved in hydrogen bonding with O_2 (see **S1**, Scheme 6.2), as evident from EPR (Electron Paramagnetic Resonance), X-ray, and neutron-diffraction studies. Such hydrogen-bonding interactions not only affect oxygen affinity, but may also stabilize the oxy form and prevent auto oxidation. The properties of the distal cavity are also important in molecular recognition, particularly the polarity of the walls, the functional composition, and the 3D arrangement.



Scheme 6.2 Molecular recognition of gases in nature.
Reproduced with permission from reference 311.

In oxygen-avid *Ascaris* hemoglobin, glutamine and tyrosine residues participate in hydrogen bonding with O_2 (see **S2**, Scheme 6.2).³¹⁶ The crystal structure of complex **S2** shows the tyrosine hydroxyl group to be perfectly aligned to make a strong hydrogen bond with the distal atom of the complexed O_2 , and the glutamine forms a relatively weaker hydrogen bond to the oxygen atom coordinated to the iron center.

There is also another hydrogen bond between the tyrosine and glutamine moieties. Such a hydrogen-bonding network is believed to be responsible for the K_d values for O_2 being four orders of magnitude greater than that of human hemoglobin.

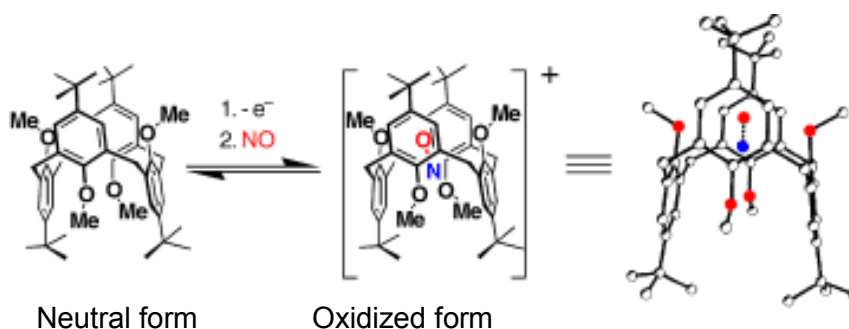
The crystal structures of complexes of heme protein with NO also suggest that the distal cavity is important in gas binding. Such cavities are rather hydrophobic and possibly help to exclude the noncoordinated H_2O molecule prior to the complexation of NO. The X-ray structure of the iron(II)–nitric oxide complex of native sperm whale myoglobin **S3** (see **S3**, Scheme 6.2) shows a Fe–NO interaction as well as the formation of a hydrogen bond between the gas molecule and the histidine 64 residue on the distal porphyrin face of the myoglobin.³¹⁷ Here, the NO binding event takes place in a tight cavity formed by the lipophilic leucine 69 and valine 68 moieties as well as histidine 64.

Reports have indicated that N_2 fixation in the atmosphere involves enzymes such as Fe Mo nitrogenase. It has been shown that the NH nitrogen-metal intermediate **S4** (see **S4**, Scheme 6.2) participate in H-bonding with the amino acid residues of the enzymes.³¹¹

6.3.1 Calix[4]arene-based Supramolecular Approaches in NO_x Gas Complexation

As mentioned in the beginning of this chapter, NO_x gases are a crucial group of gases contribute to environmental pollution and global warming.³¹⁰ NO_x mainly consists of nitrogen dioxide (NO_2), dinitrogen tetroxide (N_2O_4), dinitrogen pentoxide (N_2O_5) and nitric oxide (NO). Only NO has multiple biological roles in human organisms.^{318,319} All the other NO_x gases are toxic pollutants derived from fossil fuel burning, power plants, and large scale industrial processes. NO_x gases cause ground level ozone, toxic particulate matter, acid rain and global warming.

Recently, Kochi and co-workers demonstrated the encapsulation of NO by 1,3-*alternate* calix[4]arene (Scheme 6.3). Initially, the calix[4]arene was oxidized to its radical cation by reacting calix[4]arene with Na(Hg), which then complexed NO gas with the formation of the calix[4]arene–nitrosonium (NO⁺) complex (see scheme 6.3).



Scheme 6.3 Encapsulation complexes of NO_x gases with calix[4]arenes and the X-ray crystal structure of the complex.
 Reproduced with permission from reference 311.

Strong charge-transfer interactions between NO⁺ and the π electron rich interior of the calixarene placed the gas molecule at a distance of ~2.4 Å from the cofacial aromatic rings, which is much shorter than the typical van der Waals contact (3.2 Å). The association constant estimated for this complex was estimated to be 5×10⁸ M⁻¹. However, NO⁺ was easily released from the cavity upon the addition of Cl⁻ ions, as a result of the formation of nitrosyl chloride (NOCl). Variations in the redox chemistry and temperatures can control the complexation of NO⁺. This charge-transfer complex has a deep purple color and thus can be used in colorimetric NO sensing applications.³²⁰

Prior to finding of this calixarene-based NO⁺ complexes, a non calixarene host based on a stilbenoid was developed by Kochi and coworkers, and used for

entrapment studies of NO in the form of NO^+ .³²¹ Figure 6.4 shows the ORTEP diagram and the space filling model of the nitrosonium complex.

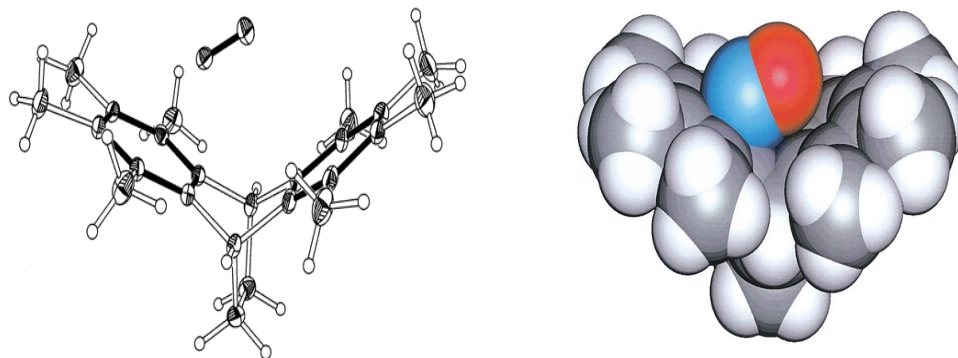
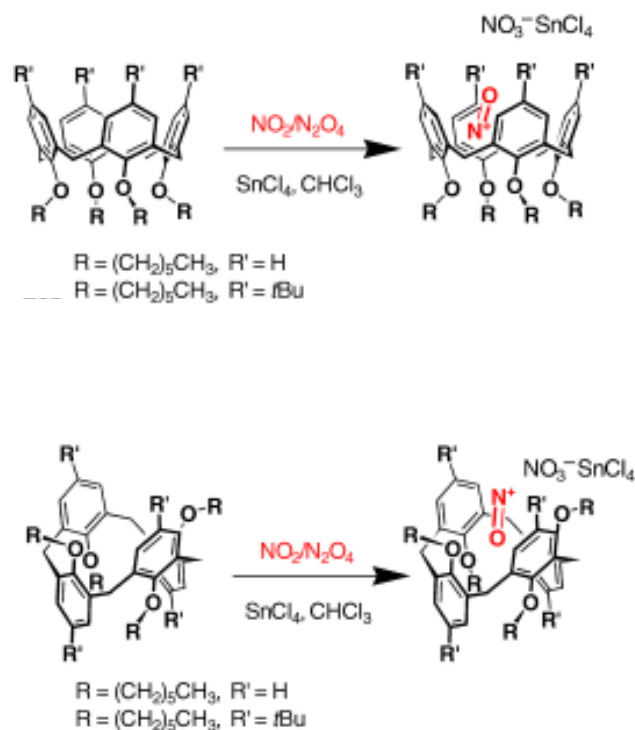


Figure 6.4 ORTEP diagram showing the tight binding with limited liberation of the noncovalently bound nitric oxide in the complex (left) and the space-filling representation of the NO complex, showing the entrapped NO nestled within the cavity of cofacial phenylene donor. Reproduced with permission from reference 321.

More recently, in 2002 Zyryanov and coworkers, employed calix[4]arenes to visually detect and chemically transform $\text{NO}_2/\text{N}_2\text{O}_4$ gases.³²² The tetrakis-*O*-alkylated calix[4]arenes (see scheme 6.4) reversibly interacted with $\text{NO}_2/\text{N}_2\text{O}_4$ and entrapped the highly reactive NO^+ ion within their cavities. NO^+ is generated from N_2O_4 , which is known to disproportionate to NO^+NO_3^- upon exposure to aromatic compounds.³²³ Stable nitrosonium complexes of these calix[4]arene derivatives were quantitatively isolated upon addition of a stabilizer such as Lewis acidic SnCl_4 or CF_3COOH . Only one NO^+ ion was found per cavity. This observation is also in agreement with the previously reported nitrosonium complexes prepared by Kochi and coworkers.³²⁴ These interactions between calix[4]arene and NO^+ were determined to be reversible.



Scheme 6.4 Encapsulation complexes of NO_x gases with calix[4]arenes cone conformer (top) and the 1,3-alternate conformer (bottom).
 Reproduced with permission from reference 311.

The addition of H_2O or alcohols to a solution of calix[4]arene- NO^+ complexes resulted in the dissociation of the complexes and the recovery of original calix[4]arene host molecule (see Figure 6.5). The complex prepared with the 1,3-alternate conformation of calix[4]arene, ($\text{R}'=\text{H}$) dissociated instantly. However the complex prepared by the use of calix[4]arene bearing *cone* conformer takes several minutes to dissociate. Bulky *tert*-butyl groups at the upper rim of the cone conformer protect the encapsulated NO^+ ion.

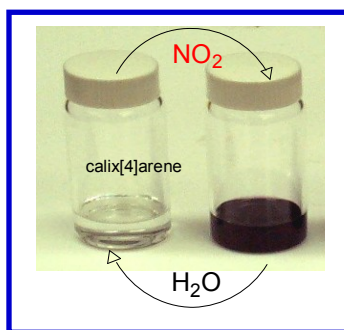


Figure 6.5 Reversible nature of Calix[4]arene-NO⁺ complex up on addition of water.

The dramatic color change results from the charge transfer between the nitrosonium cation and π electron rich calix[4]arene moiety. The selective detection of NO₂ in the presence of gases such as H₂O, O₂, HCl, HBr, SO₂, NH₃, and neat generation of NO can be fully expected, since none of these vapors/gases undergoes reactions with calixarenes. All this may be of interest for sensing and cleaner NO generation technology.

In contrast to the entrapment of a single NO⁺ guest inside the cavity of O-alkylated calix[4]arenes, calix[4]arene nanotubes that can accommodate more than one nitrosonium cation have been developed by Zyryanov and Organo *et.al.*³²⁵⁻³²⁷ In the design of nanotubes, several calix[4]arenes were rigidly connected from both sides of their rims, with at least two symmetrical bridging units. This is achieved by using the *1,3-alternate* conformation which is known as the “smart conformation” of calix[4]arene.³²⁸ Calix[4]arenes in a 1,3-alternate conformation are much more rigid than other conformers and possess a cylindrical inner tunnel defined by two cofacial pairs of aromatic rings oriented orthogonally along the cavity axis. According to a number of X-ray studies, this tunnel is approximately 5–6 Å in diameter.³²⁸ Two pairs of

phenolic oxygens are oriented in opposite directions providing a simple route to enhance the tube length modularly. Findings have shown that these developed calix[4]arene-based nanotubes also reversibly interact with $\text{NO}_2/\text{N}_2\text{O}_4$ and entrap highly reactive nitrosonium (NO^+) cation within their π -electron-rich interiors.³²⁵ Stable nitrosonium complexes of these new hosts were quantitatively isolated upon addition of a Lewis acid such as SnCl_4 . These complexes can be used as an alternative to alkyl nitrites, nitrosamines/amides, and nitrosothiols that are used in biomedicine as NO-releasing drugs.³²⁹

Structures and X-ray crystal structures of calix[4]arene-based nanotubes are shown in Figure 6.6. Figure 6.7 shows NMR spectra of empty and filled high capacity calix[4]arene nanotubes used to prepare NO^+ complexes using NO_x gases.

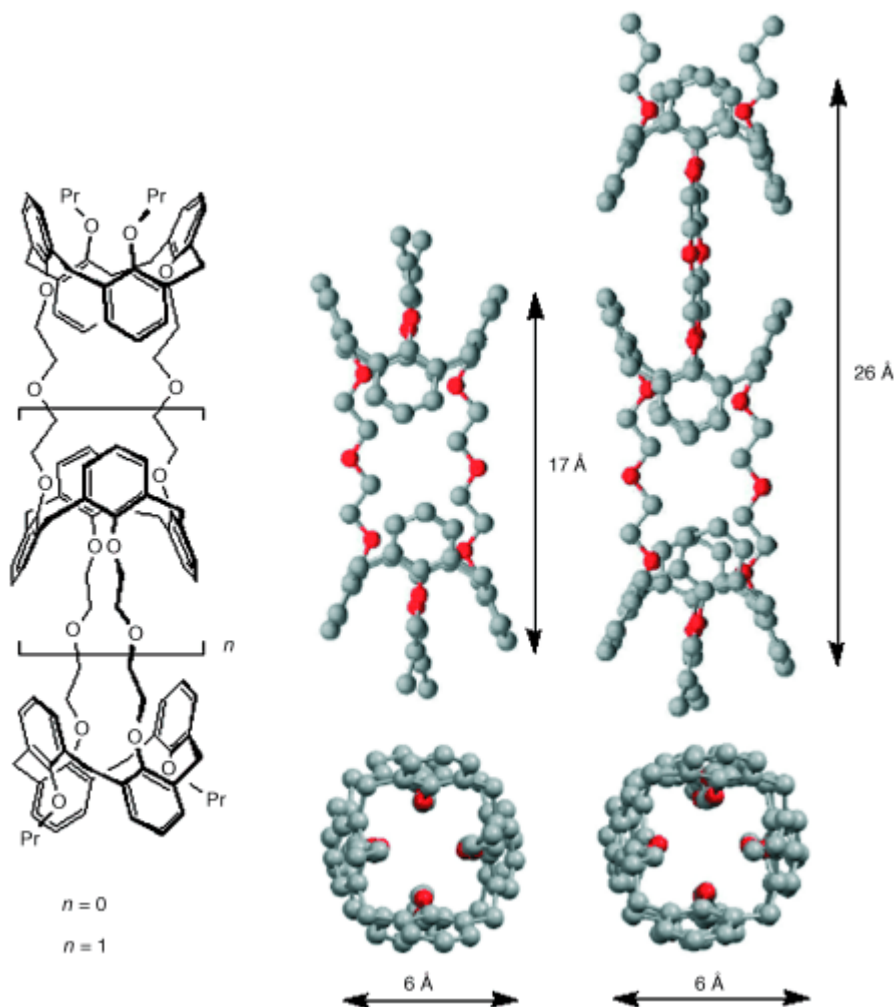


Figure 6.6 Synthetic calixarene-based nanotubes for $\text{NO}_2/\text{N}_2\text{O}_4$ fixation and high capacity nitrosonium ion (NO^+) storage.

X-ray crystal structures of synthetic nanotubes (from $\text{CHCl}_3/\text{MeOH}$; side and top views; O red, C gray). Hydrogen atoms are omitted for clarity (right).
Reproduced with permission from reference 326.

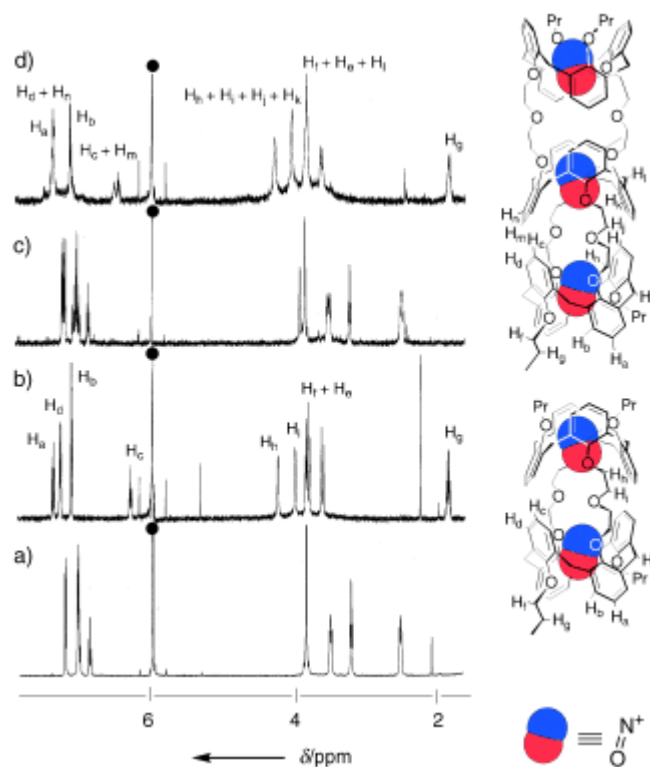


Figure 6.7 Partial ^1H NMR spectra (500 MHz, $(\text{CDCl}_2)_2$, 295 K) of calixtube- NO^+ complex.

a) empty calixarene-based di-tube b) filled ditube with NO^+ , c) empty tri-tube and d) filled tri-tube . The residual solvent signals are marked with filled circles (•).
Reproduced with permission from reference 326.

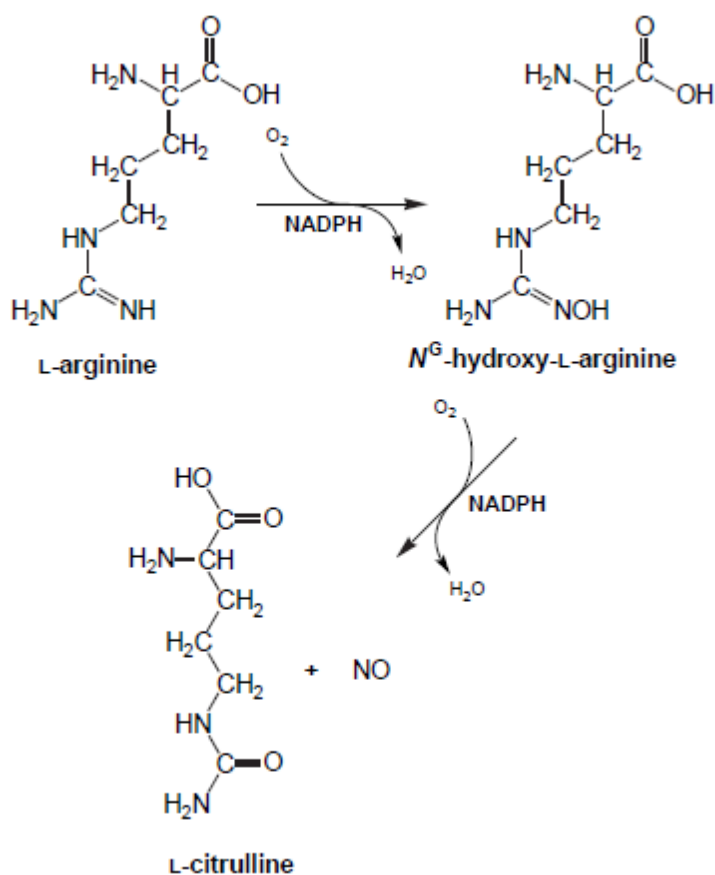
6.4 Nitric Oxide Releasing Compounds

Nitric oxide is known to chemists for more than two centuries since its discovery by John Priestley in 1772. As recently as 1987 this diatomic free radical was widely considered to be just a toxic gas, one of the constituents of toxic NO_x gases causing acid rain, smog, and tobacco smoke as well as a precursor of other harmful oxides of nitrogen responsible for nitrosamine formation.^{330,310} However in 1992, an issue of *Science magazine* introduced NO as the molecule of the year.³³¹ This is mainly because of contributions from three US scientists, Furchgott,³³²⁻³³⁷ Ignarro³³⁸⁻³⁴⁵ and Murad³⁴⁶⁻³⁴⁹ who received the honor of Nobel Prize in 1998 because their contribution to the research on nitric oxide. After the discovery of NO's signaling role in the cardiovascular and nervous systems as the main biological messenger in brain, many myths about toxicity due to NO evanescend. After these major discoveries related to biological roles of NO, pharmaceutical industry all around the world started developing NO releasing drugs for medicinal use. Figure 7.8 shows some potential applications of NO in biology and medicine.^{331,350-355}



Figure 6.8 Potential applications of nitric oxide releasing compounds

The NO synthases (NOS) generally handles all the NO production needs in the human body to ensure our well-being as long as a proper balance is maintained. Scheme 6.5 shows biosynthetic pathway of NO generation from L-arginine.



Scheme 6.5 Biosynthetic pathway of NO by L-arginine.
Reproduced with permission from reference 356.

However, excessive NO formation can invasively lower blood pressure and may contribute to tissue damage in chronic diseases like rheumatoid arthritis. NO reacts with superoxide ($O_2^{\cdot-}$), a by-product of mitochondrial respiration, giving reactive nitrogen species that can effectively damage proteins and DNA.³⁵⁶

To contravene the consequences of physiological overproduction of NO inside the body, numerous drug development efforts in NO synthase inhibitors have been reported in the literature^{319,355} On the other hand, when the essential amount of NO is

insufficient to make through biosynthetic pathways serious health problems such as respiratory distress, impotence, blood clot formation, and collapsed blood vessels can arise as well. Therefore, synthetically developed NO releasing drugs are of great interest to prevent these diseases. Some of the commonly used NO releasing drugs are shown in Figure 6.9.

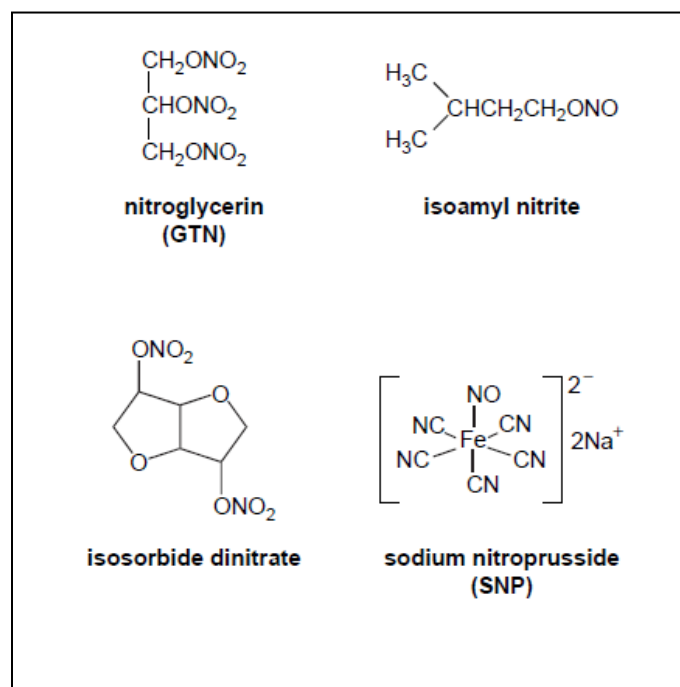


Figure 6.9 Commonly used synthetically produced NO releasing drugs. Reproduced with permission from reference 356.

We have developed calix[4]arene-based supramolecular systems to encapsulate toxic NO_2 to form stable calix[4]arene- NO^+ complexes for the cleaner generation of nitric oxide after a simple reduction using hydroquinone. This cleaner NO generation was then further developed to design a calix[4]arene system with a hydroquinone moiety is embedded into the calix ring system.

This prevents external addition of hydroquinone and the NO generation can be achieved successfully upon an addition of an alkyl nitrite in the presence of a lewis acid such as SnCl_4 or trifluoroacetic acid.

CHAPTER 7

SUPRAMOLECULAR, CALIXARENE-BASED COMPLEXES THAT RELEASE NO GAS

7.1 Abstract

Calix[4]arenes and nanotubes based on them convert $\text{NO}_2/\text{N}_2\text{O}_4$ gases into nonvolatile NO^+ species and encapsulate them. In a one-electron reduction scheme with hydroquinone, the complexed NO^+ transforms into NO gas. While NO is released, calixarenes are regenerated and can be loaded again. Supramolecular materials for generation, storage and release of NO can be potentially created, with high-capacity calixarene nanotubes holding a special promise.

7.2 Nitric Oxide Generation by a Supramolecular Approach

The well-documented biological importance of nitric oxide (NO) includes protective, regulatory, and deleterious functions.^{356,357} To control the gas release, compounds have been developed that deliver NO via their thermochemical or photochemical decomposition.^{358,359,360} At the same time, there are only very few examples of supramolecular systems that have the capability to reversibly trap, store and release NO.³⁶¹⁻³⁶³ We recently described synthetic, molecular containers for $\text{NO}_2/\text{N}_2\text{O}_4$ gases, which are based on calix[4]arenes.^{325,364} These reversibly react with $\text{NO}_2/\text{N}_2\text{O}_4$ with the quantitative formation of stable calixarene-nitrosonium (NO^+) complexes. NO^+ is generated from N_2O_4 upon its disproportionation to NO^+NO_3^- . In this work, we further extend the supramolecular chemistry between calixarenes and NO_x

gases and demonstrate their use for the effective generation of NO, in a simple and reliable protocol.

While there are several available agents, capable of clean, one-electron reduction of NO^+ ,³⁶⁵⁻³⁶⁷ we identified commercially available hydroquinone as the most suitable. Hydroquinone quantitatively reduces NO^+ with the formation of NO and benzoquinone.³⁶⁵ We found, that when mixed with hydroquinone in apolar, chlorinated solution, calixarene- NO^+ complexes smoothly react and release NO.

Preliminary experiments started with simple calixarene **10** (see Figure 7.1).

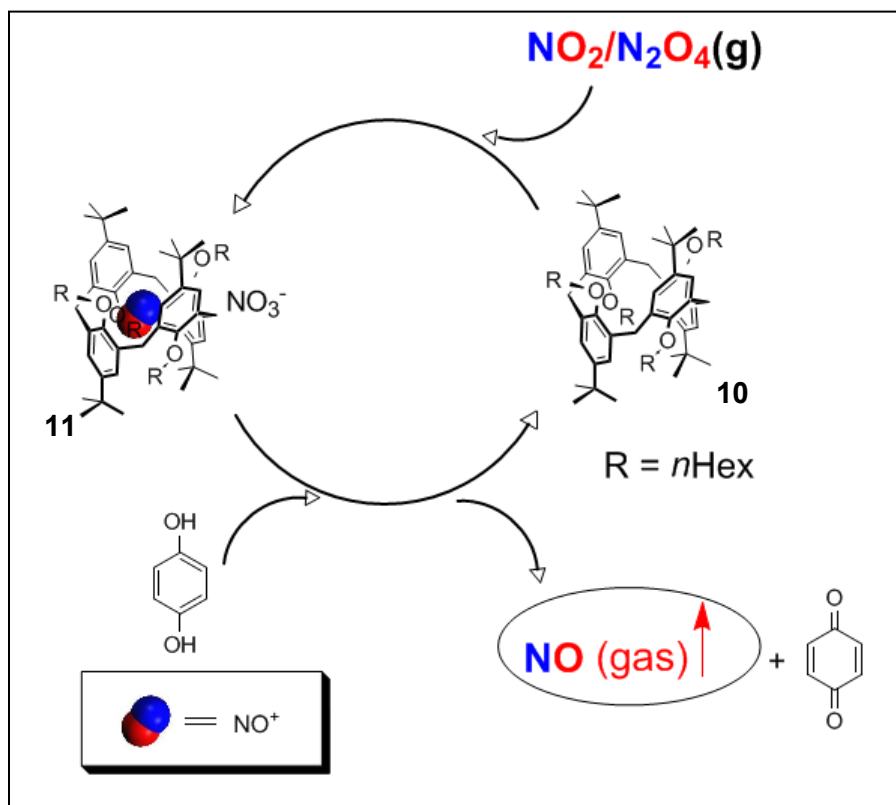


Figure 7.1 Calixarene-nitronium complex **11** obtained from reacting calixarene **10** with $\text{NO}_2/\text{N}_2\text{O}_4$ and the generation of NO gas.

Bubbling $\text{NO}_2/\text{N}_2\text{O}_4$ gas through the CDCl_3 solution of tetrakis(*O*-*n*-hexyloxy)calix[4]arene **10** led to the rapid, quantitative formation of calixarene- NO^+ complex **11** (Figure 7.1).

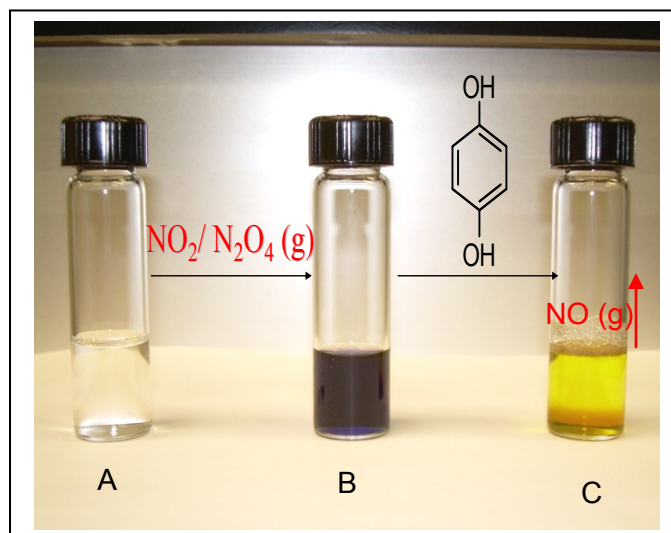


Figure 7.2 NO release experiment using calix[4]arene- NO^+ complex.

Calixarene dissolved in chloroform (A), dark purple colour calixarene-nitrosonium complex when A is treated with $\text{NO}_2(\text{g})$ (B), disappearance of dark purpled colour calixarene-nitrosonium complex and (C) the appearance of pale yellow solution containing empty calixarene with oxidized hydroquinone formed after releasing of $\text{NO}(\text{g})$.

In complex **11**, NO^+ is tightly encapsulated inside a π -electron rich calix[4]arene tunnel with a remarkably high $K_{\text{assoc}} \gg 10^6 \text{ M}^{-1}$.³²⁴ Calixarene- NO^+ complexes were originally prepared from calix[4]arenes and nitrosonium salts,^{325,364,368} calix[4]arenes and $\text{NO}_2/\text{N}_2\text{O}_4$ ³²⁵ or calix[4]arene cation radicals and free NO ³⁶⁸. In the ^1H NMR spectrum of **10** in CDCl_3 the aromatic protons were recorded as a singlet at $\delta = 6.95$ (Figure 7.3). In nitrosonium complex **11**, it was transformed into a singlet at $\delta =$

7.02. The methylene bridge CH₂ protons of **11** were seen as a singlet at δ = 3.74. In complex **10**, this was observed at δ = 3.60. The OCH₂ protons in **10** were recorded at δ = 3.39, and they characteristically moved to δ = 3.77 in complex **11**.

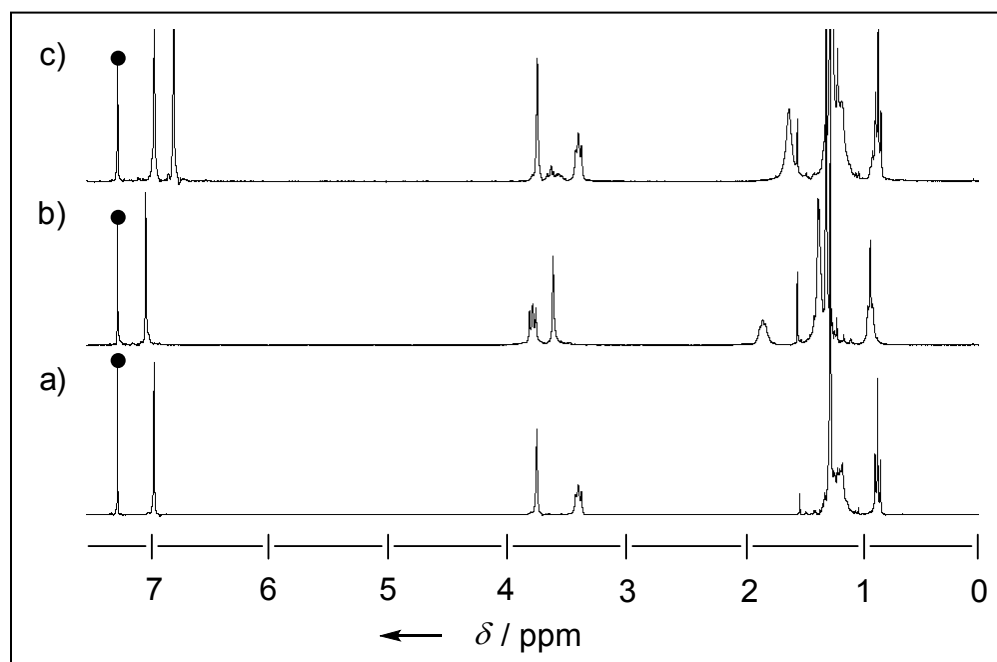


Figure 7.3 Selected portions of the ¹H NMR spectra (300 MHz, CDCl₃, 295 K) in generation of NO using calix[4]arene-NO⁺.

Here a) calixarene **10**. b) calixarene-NO⁺ complex **11** prepared from calixarene **10** and NO₂/N₂O₄. c) same as b) after mixing with hydroquinone; the benzoquinone singlet is situated at δ = 6.78. The residual solvent signals are marked “•”.

In a typical NO generating experiment, a ~20-fold excess of hydroquinone was added to a CHCl₃ (or CDCl₃) solution of complex **11** and shaken vigorously. At this point, the NO gas release could be detected with a naked eye, and the solution color changed from deep-purple to yellow (Figure 7.2). The former color belongs to charge-transfer complex **11**, while the latter reflects the formation of 1,4-benzoquinone. The

released NO gas was identified by UV spectrophotometry, showing the fine vibrational structure of three sharp absorption peaks at $\lambda_{\text{max}} = 204, 214$ and 226 (Figure 8.4). This is in agreement with the previously published absorption data for the identification of NO.^{365, 369} In addition, the ^1H NMR spectrum clearly showed the quantitative regeneration of free calixarene **10** (Figure 7.3). Noteworthy, NO itself has no affinity to calix[4]arenes.³⁶⁸

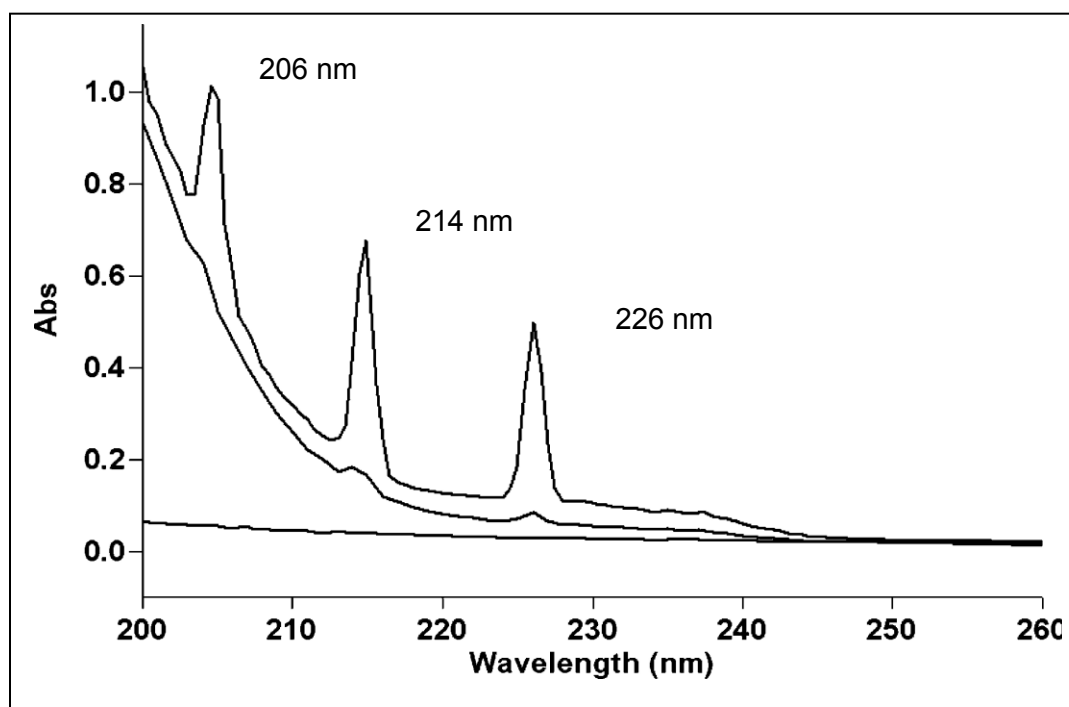


Figure 7.4 The UV spectrum (gas phase, 295 K) of NO gas generated from calixarene- NO^+ complex **11** and hydroquinone.

The calix[4]arene cavity is too narrow for hydroquinone, and the electron-transfer reaction, most probably, occurs outside, in the bulk solution. The encapsulated NO^+ must be released first. While the equilibrium between calixarene **10** and its complex **11** provides only small ($<1\%$) quantities of free NO^+ for the outside reaction, hydroquinone may facilitate the NO^+ release. Electron rich aromatic molecules are

known to form strong complexes with NO^+ .³⁶⁶ In a model experiment, 1,4-O,O-dimethylated hydroquinone was mixed with complex **11**. Indeed, the NO^+ release was observed and free calixarene **10** was also regenerated.

To explore our findings, we tested recently prepared calixarene-based synthetic nanotubes (see Figure 7.5).³²⁶

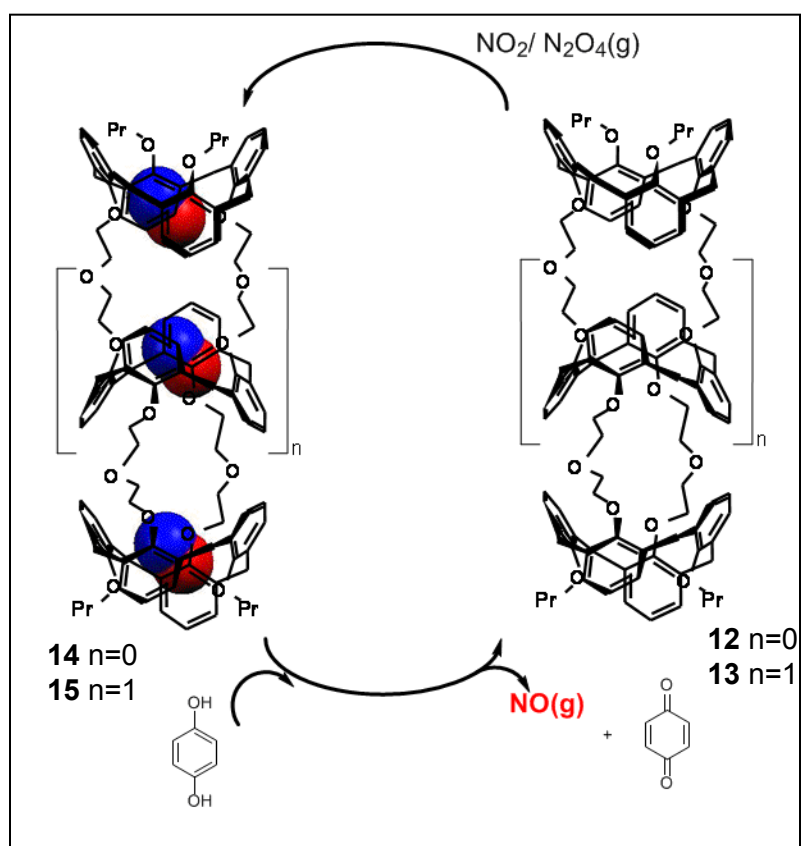


Figure 7.5 Filling of calixarene-based nanotubes with nitrosonium and generation of NO gas.

These nanotubes are several nanometers long and can reversibly interact with $\text{NO}_2/\text{N}_2\text{O}_4$ with the formation of complexes with multiple NO^+ . Accordingly, nanotubes **12** and **13** were filled with NO^+ species by simply bubbling $\text{NO}_2/\text{N}_2\text{O}_4$ gases through their $(\text{CDCl}_3)_2$ solutions (Figure 7.5). Deep-purple complexes **14** and **15** quantitatively

formed, which entrap two and three NO^+ cations, respectively. They were identified by ^1H NMR and absorption spectroscopy (Figure 7.6).³²⁶ For example, the propyl Ar-O- CH_2 protons in **14** and **15** were both seen at $\delta \sim 3.85$, which is significantly downfield comparing to empty tubes **12** and **13** ($\delta \sim 3.26$). Similarly, downfield shifts ($\Delta\delta > 1$) of the Ar-O- CH_2 and $\text{CH}_2\text{-O-CH}_2$ protons in filled tubes **14** and **15** were observed.

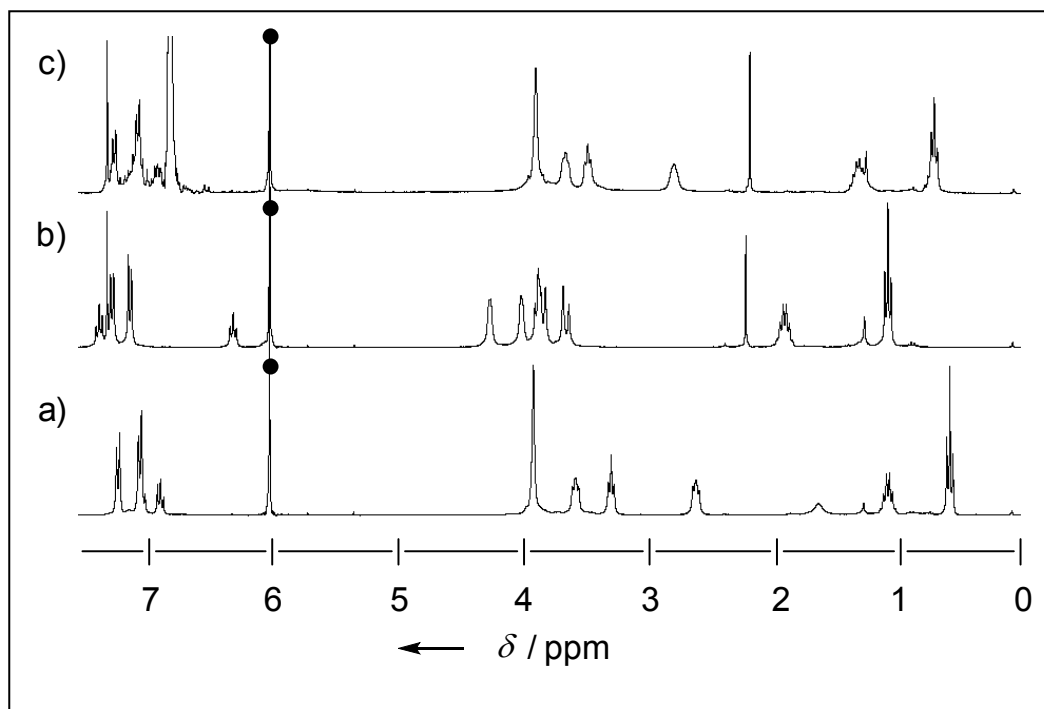


Figure 7.6 Selected portions of the ^1H NMR spectra (300 MHz, $(\text{CDCl}_2)_2$, 295 K) in generation of NO using calix ditube.

Here a) calixarene-based tube **14**. b) nitrosonium complex **12**, prepared from **14** and $\text{NO}_2/\text{N}_2\text{O}_4$. c) same as b) after mixing with hydroquinone; the benzoquinone singlet is situated at $\delta = 6.78$. The residual solvent signals are marked “•”.

When a ~ 20 -fold excess of hydroquinone was added to the $(\text{CDCl}_2)_2$ solutions of **14** and **15**, the color changed from deep-purple to yellow. The ^1H NMR spectrum clearly showed the quantitative regeneration of free nanotubes **12** and **13** (Figure 7.6). The NO release could be visually detected and identified by UV spectrophotometry.

The use of calixarene nanotubes, capable of storing multiple NO^+ species, could potentially lead to interesting NO releasing materials with the high gas capacity.

In conclusion, novel supramolecular systems are now available for the generation of NO gas, which are based on calix[4]arenes. The gas is safely stored in the form of NO^+ , which is not volatile and strongly bound within the calixarene cage. The NO^+ is produced from higher NO_x , namely $\text{NO}_2/\text{N}_2\text{O}_4$. In a one-electron reduction scheme involving calixarene- NO^+ complexes and simple hydroquinone, NO is smoothly released and free calixarenes are quantitatively regenerated, which can be reloaded using $\text{NO}_2/\text{N}_2\text{O}_4$. The reversibility can also be achieved through spontaneous, atmospheric oxidation of the newly generated NO to $\text{NO}_2/\text{N}_2\text{O}_4$. There is the possibility to modify the cage structure through conventional calixarene syntheses.

7.3 Experimental Section

7.3.1 General Experimental Procedures and Methods

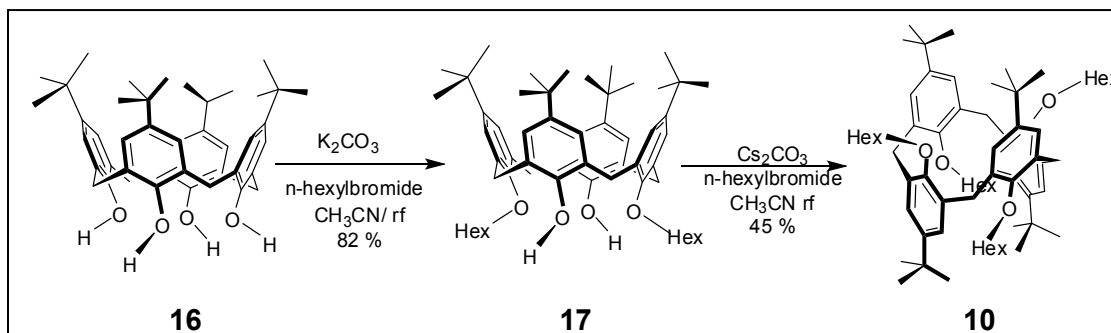
^1H NMR spectra were recorded in CDCl_3 and $\text{C}_2\text{D}_2\text{Cl}_4$ at 295 ± 1 K unless stated otherwise, on JEOL Eclipse 300/500 MHz spectrometer. The chemical shifts were measured relative to the nondeuterated solvent resonance. UV – Visible spectra were measured on a VARIAN Cary 50 UV spectrophotometer. All the solvents were distilled and purified according to standard procedures. All chemicals were purchased from Sigma Aldrich and used as received. $\text{NO}_2/\text{N}_2\text{O}_4$ gas was generated by reacting Cu with concentrated Nitric acid and the gas was passed through a packed CaCl_2 tube to remove traces of moisture.

All experiments with moisture and /or air sensitive compounds were run under dried nitrogen atmosphere.

Caution: NO_2 gas is a prominent air pollutant and very toxic when inhaled.

7.3.2 Synthesis of Calix[4]arene Derivatives

Scheme 7.1 summarizes the synthetic pathway for 25,26,27,28-Tetrakis(*n*-hexyloxy)-*p*-*tert*-butylcalix[4]arene-1,3-*alternate*.³⁶⁴



Scheme 7.1 Synthetic route for *o*-alkylated calix[4]arene 1,3 *alternate*

25,27-Hydroxy-26,28-bis(*n*-hexyloxy)-*p*-*tert*-butylcalix[4]arene (17). *n*-Hexylbromide (4.3 ml, 30.0mmol) was added to a suspension of 25,27,26,28-tetrahydroxycalix[4]arene (4.8 g, 10.0 mmol) and K₂CO₃ (4.2 g, 30.0 mol) in MeCN (200 mL), and the reaction mixture was refluxed under nitrogen for 48 h. The precipitate was filtered off, and the solution was evaporated to dryness. The residue was redissolved in CH₂Cl₂ (200 mL), and the solution was washed with water (3 × 150 mL) and dried over MgSO₄. After evaporation, the solid residue was treated with MeOH (200 mL) to yield the corresponding 25,27-Hydroxy-26,28-bis(*n*-hexyloxy)-*p*-*tert*-butylcalix[4]arene as a white solid (80 %). ¹HNMR (CDCl₃, 298 K): δ 7.82 (s, 2 H), 7.03 (s, 4H), 6.84 (s, 4H), 4.32 (d, *J* = 13.5 Hz, 4H), 3.96 (t, *J* = 6.0 Hz, 4H), 3.32 (d, *J* = 13.5 Hz, 4H), 2.04 (m, 4H), 1.41 (m, 4H), 1.32 (m, 8H), 1.26 (s, 18H), 1.00 (s, 18H), 0.93 (t, *J* = 7.5 Hz, 6H).

25,26,27,28-Tetrakis(*n*-hexyloxy)-*p*-*tert*-butylcalix[4]arene-1,3-*alternate* (10).

n-Hexylbromide (5.7ml, 40.0mmol) was added to a suspension of corresponding 25,27-Hydroxy-26,28-bis(*n*-hexyloxy)-*p*-*tert*-butylcalix[4]arene (10.0 mmol) and Cs₂CO₃ (50 g, 150.0 mmol) in MeCN (300 mL), and the reaction mixture was refluxed under nitrogen for 48 h. After cooling, the precipitate was filtered off and treated with a mixture of water (100 mL) and CH₂Cl₂ (100 mL). The organic layer was separated, washed with water (2 × 100 mL), dried over MgSO₄, and evaporated. After evaporation, the solid residue was recrystallized from 10:1 MeOH-CHCl₃ to give desired 1,3-*alternate* O-alkylated calix[4]arene (40%). mp 231-233 °C; ¹H NMR (CDCl₃, 298 K): δ 6.95 (s, 8H), 3.73 (s, 8H), 3.38 (t, *J* = 7.5 Hz, 8H), 1.28 (s, 36H), 1.25-1.1 (m, 32H), 0.86 (t, *J* = 7.5 Hz, 12H).

25,26,27,28-Tetrakis(*n*-hexyloxy)-*p*-*tert*-butylcalix[4]arene-1,3-*alternate*-NO⁺ complex (11).

25,26,27,28-Tetra(*n*-hexyloxy)calix[4]arene 5 mg (0.005 mmol) was dissolved in 0.5 ml of CDCl₃ in an NMR tube. Dry NO₂ gas was then bubbled through the solution for 2~3 seconds followed by bubbling Nitrogen gas for 3 minutes to remove excess dissolved NO₂ gas. ¹H NMR (CDCl₃, 298 K): δ 7.02 (s, 8H), 3.77 (t, *J* = 8.0 Hz, 8H), 3.6 (s, 8H), 1.8 (m, 8H) 1.30 (m, 24H), 0.93 (t, *J* = 7.0 Hz, 12H), UV-Vis (CDCl₃): λ_{max} 525.0 nm.

Reduction of 25,26,27,28-Tetrakis(*n*-hexyloxy)-*p*-*tert*-butylcalix[4]arene-1,3-*alternate*-NO⁺ (11).

Excess hydroquinone 5 mg (0.05 mmol) was added in to the 25,26,27,28-Tetrakis(*n*-hexyloxy)-*p*-*tert*-butylcalix[4]arene-1,3-*alternate*-NO⁺(11) (0.003 mmol) complex formed above and shook well. After the gas ceased, the ¹H NMR spectrum was recorded of

the resulting pale yellow color solution. ^1H NMR (CDCl_3 , 298 K): δ 6.94 (s, 8H), 6.78 (s), 3.73 (s, 8H), 3.39 (t, J = 7.0 Hz, 8H), 1.27 (s, 36H) 1.19 (m, 16H) 0.87 (t, J = 7.0 Hz, 12H). This resembles the original chemical shifts for free, 25,26,27,28-Tetrakis(*n*-hexyloxy)-*p*-*tert*-butylcalix[4]arene-1,3-*alternate* (**10**).

Calix[4]arene Dimeric tube (12)

^1H NMR(300 MHz $\text{C}_2\text{D}_2\text{Cl}_4$): δ 7.20 (d, J = 7.5 Hz, 8H), 7.03 (m 12H), 6.87 (t, J = 8.0 Hz 4H), 3.88 (s, 18H), 3.57 (t, J = 7.0 Hz, 8H), 3.28 (t, J = 7.0 Hz, 8H), 2.60 (t, J = 8.0 Hz, 8H), 1.06 (m, 8H), 0.58 (t, J = 7.0 Hz, 12H). These spectral data are in agreement with previously published data.^{326,370}

Calix[4]arene Dimeric tube- NO^+ complex (13)

Calix[4]arene dimeric tube (**12**) 5 mg (0.004 mmol) was dissolved in 0.5 mL of $\text{C}_2\text{D}_2\text{Cl}_4$ in NMR an tube and bubbled dry NO_2 gas through the solution for 3~4 seconds. Nitrogen was purged through the solution to remove excess dissolved NO_2 . ^1H NMR(300 MHz $\text{C}_2\text{D}_2\text{Cl}_4$): δ 7.34 (t, J = 8.0 Hz, 4H), 7.26 (d, J = 7.0 Hz, 8H), 7.10 (d, J = 8.0 Hz, 8H), 6.29 (t, J = 7.5 Hz, 4H), 4.25 (m, 8H), 4.02 (m, 8H), 3.86 (t, J = 7.0 Hz, 8H), 3.83, 3.84 (2 x d, J = 16.0 Hz, 2H), 1.91-1.87 (m, 8H), 1.07 (t, J = 8.0 Hz, 12H). These spectral data are in agreement with previously published complex (**13**) which was obtained from $\text{NO}_2/\text{N}_2\text{O}_4$.^{326,370}

Reduction of Calix[4]arene dimeric tube- NO^+ complex (13)

The Calix[4]arene dimeric tube- NO^+ (0.004 mmol) (**13**) complex formed above was treated with excess solid hydroquinone (5 mg) to reduce NO^+ inside the calix[4]arene dimeric tube. Presence of free Calix[4]arene dimeric tube was confirmed by ^1H NMR after the Nitric Oxide gas was ceased. ^1H NMR(300 MHz $\text{C}_2\text{D}_2\text{Cl}_4$): δ 7.20 (d, J = 7.5 Hz, 8H), 7.03 (m 12H), 6.87 (t, J = 8.0 Hz, 4H), 3.88 (s, 18H), 3.57 (t, J = 7.0 Hz, 8H),

3.28 (t, $J = 7.0$ Hz, 8H), 2.60 (t, $J = 8.0$ Hz, 8H), 1.06 (m, 8H), 0.58 (t, $J = 7.0$ Hz, 12H). Along with the empty calix[4]arene ditube, benzoquinone peak was observed at 6.78 ppm.

Calix[4]arene trimeric tube (14)

Calix[4]arene trimeric tube was synthesized according to previously reported method.³²⁶ ^1H NMR (300 MHz $\text{C}_2\text{D}_2\text{Cl}_4$): δ 7.22, 7.19 (2 x d, $J = 8.0$ Hz, 16 H), 7.05 (t, $J = 8.0$ Hz, 4H), 7.03 (d, $J = 8.0$ Hz, 8H), 6.98, 6.85 (2 x t, $J = 7.2$ Hz, 8H), 3.94 (s, 8 H), 3.88 (AB q, 16H), 3.55 (m, 16H), 3.27 (t, $J = 6.5$ Hz, 8H), 2.55 (m, 16H), 1.06 (m, 8H), 0.56 (t, $J = 7.2$ Hz, 12H). The spectral data are in agreement with previously published data.³²⁶

Calix[4]arene trimeric tube- NO^+ complex (15)

Calix[4]arene trimeric tube (**14**) 5.0 mg (0.003 mmol) was dissolved in 0.5 ml of $\text{C}_2\text{D}_2\text{Cl}_4$ gently warmed the solution to dissolve all solids in the NMR tube and bubbled dry NO_2 gas through the solution for 3~4 seconds. Nitrogen was purged through the solution to remove excess dissolved NO_2 . ^1H NMR (300 MHz $\text{C}_2\text{D}_2\text{Cl}_4$): δ 7.35 (m, 20 H), 7.11 (d, $J = 7.3$ Hz, 8H), 6.50 (t, $J = 7.0$ Hz, 4H), 6.47 (t, $J = 7.0$ Hz, 4H), 4.3 (m, 16 H), 3.9 (m, 24H), 3.66 (d, $J = 14.0$ Hz, 8H), 1.85 (m, 8H), 1.08 (t, $J = 7.3$ Hz, 12H). This spectral data is in agreement with previously published Calix[4]arene trimeric tube- NO^+ complex which was obtained after the reaction of free empty tube with $\text{NO}_2/\text{N}_2\text{O}_4$.³²⁶

Reduction of Calix[4]arene trimeric tube- NO^+ complex (15)

The Calix[4]arene trimeric tube- NO^+ complex (**15**) (0.003 mmol) formed above was treated with excess solid hydroquinone (10 mg) to reduce NO^+ inside Calix[4]arene trimeric tube. Presence of free Calix[4]arene trimeric tube was confirmed by ^1H NMR after the nitric Oxide gas was ceased. ^1H NMR (300 MHz $\text{C}_2\text{D}_2\text{Cl}_4$): δ 7.22, 7.19 (2 x d,

$J = 8.0$ Hz, 16 H), 7.05 (t, $J = 8.0$ Hz, 4H), 7.03 (d, $J = 8.0$ Hz, 8H), 6.98, 6.85 (2 x t, $J = 7.2$ Hz, 8H), 3.94 (s, 8 H), 3.88 (AB q, 16H), 3.55 (m, 16H), 3.27 (t, $J = 6.5$ Hz, 8H), 2.55 (m, 16H), 1.06 (m, 8H), 0.56 (t, $J = 7.2$ Hz, 12H).

CHAPTER 8

NITRIC OXIDE RELEASE MEDIATED BY CALIX[4]MONOHYDROQUINONES

8.1 Abstract

Calix[4]monohydroquinone has been used as supramolecular system for the generation of NO gas. In a one-electron reduction scheme involving calix[4]monohydroquinone-NO⁺ complex, NO is released without the presence of an external reducing agent. Free calix[4]monoquinone, thus obtained, can be reused for a new NO-releasing cycle after NaBH₄-reduction to calix[4]monohydroquinone.

8.2 Introduction

Nitric oxide (NO) is a colorless odorless gas, which plays important roles in several biological functions.^{371,372} In particular, in the human body nitric oxide is involved in the regulation of cardiovascular, respiratory, and nervous systems. The development of therapeutic agents designed to release NO is an intensively active area of research, since NO gas has shown beneficial effects against several types of disease states. Thus, NO-releasing organic nitrates, as glyceryltrinitrate, are used as antianginal drugs³⁷³ by the utilization of vasodilation properties of NO gas, while the antiinflammatory properties of NO gas have been used in NO-NSAIDS³⁷⁴ a class of nonsteroidal anti-inflammatory drugs able to release NO. In addition, NO gas has shown antibacterial³⁷⁵ and antitumoral³⁷⁶⁻³⁷⁸ activity, and consequently there is a strong interest in the search of synthetic compounds that chemically store and release NO in a controlled fashion.³⁷⁹⁻³⁸¹

Thus, Schoenfish and coworkers have reported the synthesis and characterization of NO-releasing systems based on diazeniumdiolate³⁸² NO-donors.^{383,384} The diazenium-diolate groups, covalently bound to dendrimer or silica nanoparticles, were able to dissociate spontaneously under physiological condition to give NO gas. At the same time, there has been a growing interest in supramolecular systems that have the capability to reversibly trap, store, and release NO.³⁸⁵⁻³⁸⁷ Among them, increasing attention has been devoted to the development of calixarene-based^{311,326,388} materials able to store NO in the form of entrapped nitrosonium (NO⁺) ion.^{364,370,389} Thus, Rathore and Rudkevich have described stable complexes between calixarene derivatives and NO⁺ ion,^{370,389} with this ion strongly bound within the calixarene aromatic cavity by means of cation- π interactions.³⁹⁰ This work was also extended to the storage of NO⁺ ion into the cavity of synthetic calixarene-based nanotubes.^{326,391}

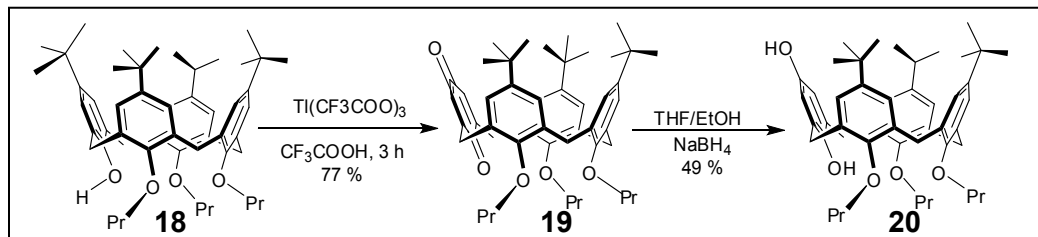
We have shown that nitric oxide (NO) can be smoothly released from the calixarene cavity after a one-electron reduction scheme involving calixarene-NO⁺ complexes and an external reducing agent such as hydroquinone molecule.³⁹² After releasing NO, the starting calixarene was regenerated in quantitative yield and can be reused for a new NO-releasing cycle.

8.3 NO Generation by Calix[4]monohydroquinone Systems

In this work, we developed a new calixarene-based supramolecular system endowed with an internal hydroquinone reducing moiety and therefore able to release NO without the addition of external reducing agents.

The designed compound, *p*-*tert*-butylcalix[4]monohydroquinone **20**, was obtained by NaBH₄ reduction of the corresponding tripropoxycalix[4]monoquinone

19,³⁹³ which in turn was prepared by $\text{Ti}(\text{CF}_3\text{COO})_3$ mediated oxidation³⁹⁴ of tripropoxy-*p*-*tert*-butylcalix[4]arene **18** (Scheme 8.1).³⁹⁵



Scheme 8.1 Synthesis of tripropoxycalix[4]monohydroquinone

Examination of its ^1H and ^{13}C NMR spectra (see experimental section) indicated that calix[4]monohydroquinone **20** adopts a cone conformation.³⁹⁶ In fact, two AX systems relative to ArCH_2Ar groups [4.32/3.17 ppm ($J = 12.5$ Hz), 4.36/3.16 ppm ($J = 13.2$ Hz)] were present in the ^1H NMR spectrum (Figure 8.1a), whereas the ^{13}C NMR spectrum displayed two ArCH_2Ar resonances at 31.2 and 31.4 ppm.³⁹⁷⁻³⁹⁹ Tripropoxycalix[4]monoquinone **19** shows the presence of a broad singlet (or a very tight AB system) at 3.51 ppm relative to ArCH_2Quin protons adjacent to quinone ring and an AX system [4.14/3.10 ppm $J = 12.5$ Hz, 4H] relative to ArCH_2Ar protons (see for comparison its spectrum in the presence of TFA reported in Figure 8.1d). This is indicative of a fixed *syn* orientation of ArOPr rings associated to a fast *through-the-annulus* rotation of the quinone ring. This behavior was confirmed by the presence of two resonances at 35.5 and 31.0 ppm relative to ArCH_2Quin and ArCH_2Ar carbon, respectively, in the ^{13}C NMR spectrum of **19**.^{397,399}

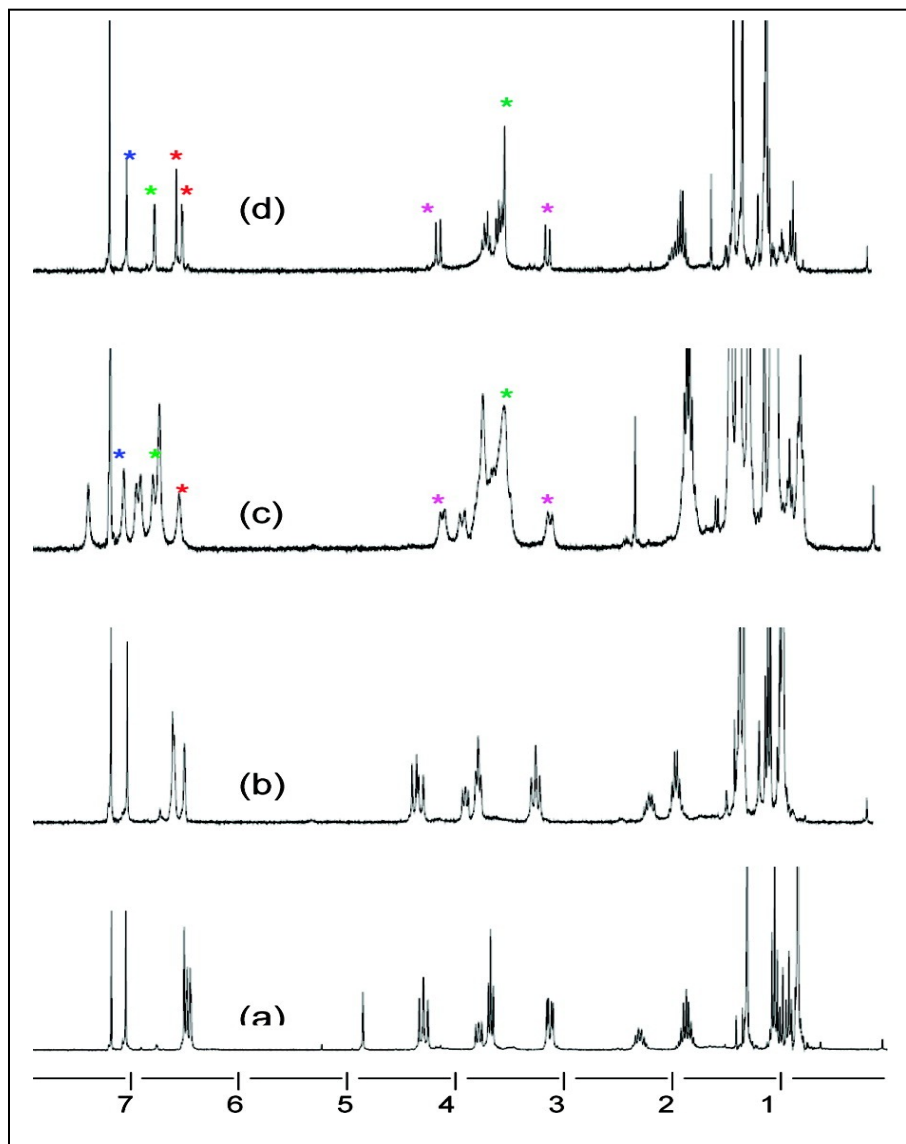
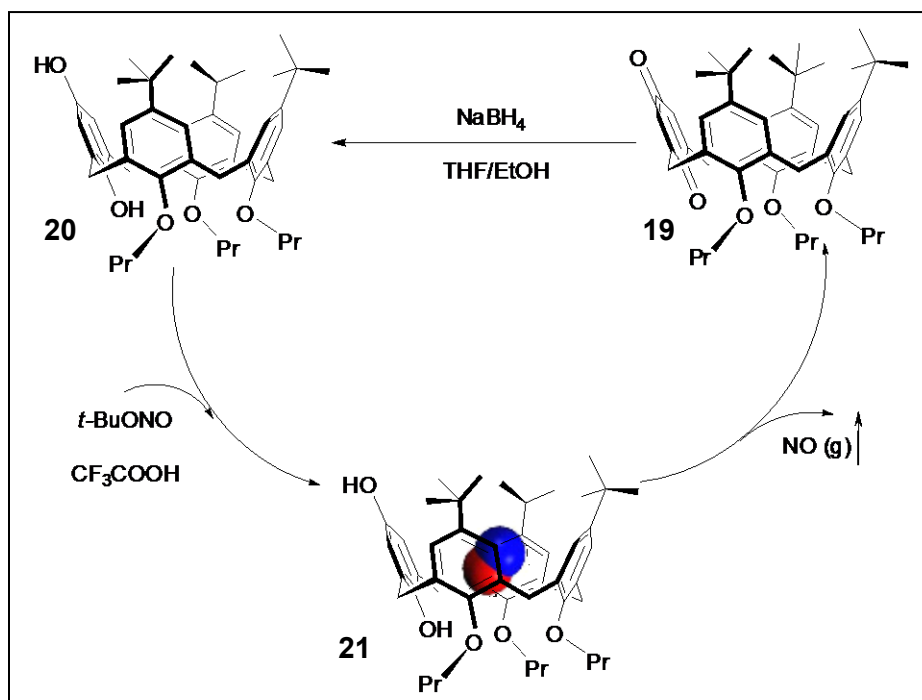


Figure 8.1 ^1H NMR spectra (300 MHz, CDCl_3 , 295 K) illustrating NO^+ complexation and release in calix[4]monohydroquinone system.

Here (a) *p*-*tert*-butylcalix[4]monohydroquinone **20**; (b) monohydroquinone **20** in the presence of TFA; (c) formation of NO^+ -**20** complex (**16**) upon addition of *t*-BuONO to solution "b"; (d) Solution "c" after 5 min from the addition of *t*-BuONO, corresponding to monoquinone **19** in the presence of TFA. Relevant signals of monoquinone **19** are marked with asterisks in "c" and "d".

When *tert*-butylnitrite (2 equiv) was added to a mixture of calix[4]monohydroquinone **20** and TFA in CDCl₃, a deep-purple color initially appeared (see experimental section). Subsequently, NO gas was released out from the system, and within 5 min, the solution turned to a transparent pale-yellow color (Scheme 8.2).



Scheme 8.2 Generation of NO using calix[4]monohydroquinone

These results are consistent with an initially formed NO⁺ ion encapsulated into the calixarene cavity and then quickly reduced to NO by means of a one-electron reduction scheme by the hydroquinone moiety of calix[4]monohydroquinone **20**, which was oxidized to calix[4]monoquinone **19**. Clearly, there are two possibilities for the reduction of NO⁺ ion to NO: the first is an encapsulated π -complex, with NO⁺ situated inside the calix[4]monohydroquinone cavity, whereas the second postulates an external π -complex, with NO⁺ situated outside the calixarene cavity. Energetically, the encapsulated π -complex seems much more favorable; in fact, it is well known that NO⁺ is easily encapsulated into the π -electron rich calix cavity and generally shows K_{assoc}

106 M⁻¹.³⁷⁰ The deep-purple color initially developed is an additional proof of the formation of calix[4]monohydroquinone-NO⁺ complex. In fact, as shown in previous works,^{364,370,389,392} this deep-purple color is caused by the strong charge transfer interaction between NO⁺ and the electron rich π -surface of aromatic rings present in **20**. This was corroborated by a broad charge-transfer band at λ_{max} 545 nm in CHCl₃, typical for these systems.^{370,400} ¹H NMR analysis confirmed the above conclusions. In fact, the ¹H NMR spectrum of the mixture of *p-tert* butylcalix[4]monohydroquinone **20** and TFA (Figure 8.1b) changed substantially after the addition of *tert*-butylnitrite. In particular, a new set of resonances relative to NO⁺**20** complex (Figure 8.1c) appeared, whose aromatic protons were shifted downfield with respect to calix[4]monohydroquinone **20**, in accordance with our previous results.^{326,392} In addition, the ¹H NMR spectrum (Figure 8.1c) displayed also the resonances relative to tripropoxycalix[4]monoquinone **19** (see marked signals). After that the reduction had taken place completely and neutral NO molecule was released, calix[4]monoquinone **19** was obtained in quantitative yield, as confirmed by NMR analysis (Figure 8.1d) and by the transparent pale-yellow color of solution. Calix[4]monoquinone **19** thus obtained was sufficiently pure (Figure 8.1d) and, after NaBH₄-reduction to **20**, can be reused for a new NO-releasing cycle (Scheme 8.2).

8.3.1 Headspace UV Analysis of Calix[4]monohydroquinone-NO⁺ Complexes

The headspace NO gas generated by the reaction between **20** and *tert*-butylnitrite in TFA was analyzed using UV spectrophotometry, and three characteristic peaks were obtained at λ_{max} 206, 214, and 226 nm (Figure 8.2). These UV data are in agreement with previously published UV absorption data for identification of NO.^{365,401}

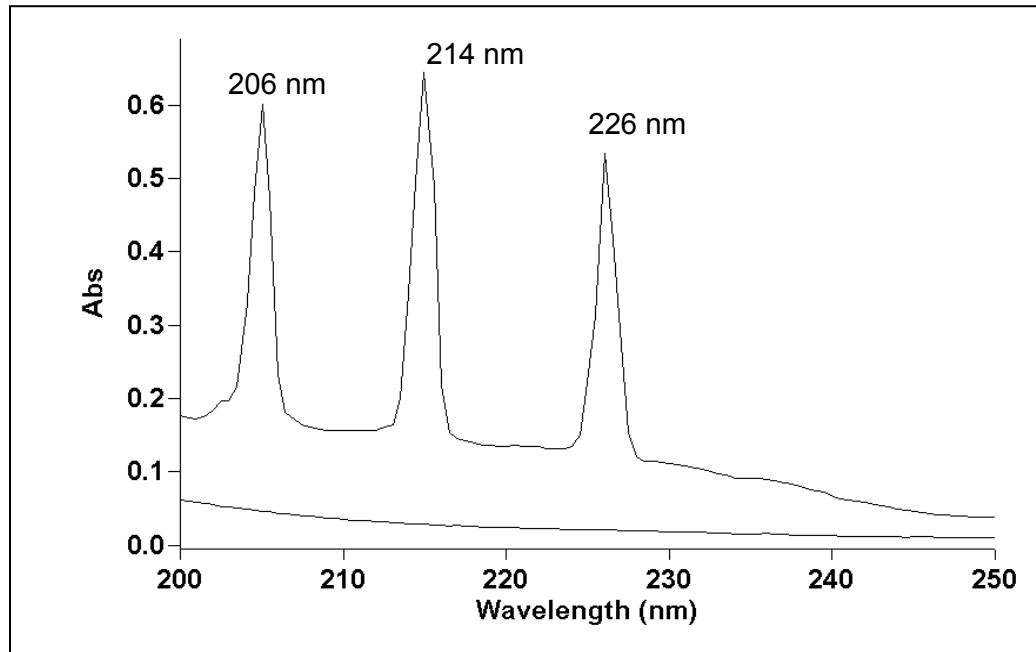


Figure 8.2 UV spectrum of the headspace gas generated from the calix[4]monohydroquinone-NO⁺ complex.

8.3.2 Solution Phase UV Analysis of Calix[4]monohydroquinone-NO⁺ Complexes

The solution phase complex between calix[4]monohydroquinone and *tert*-butylnitrite in the presence of TFA was monitored by UV spectrometry. UV traces were recorded immediately after mixing and then monitored until disappearance of the complex with time. The complex was disappeared within approximately after 5-6 minutes (see Figure 8.3).

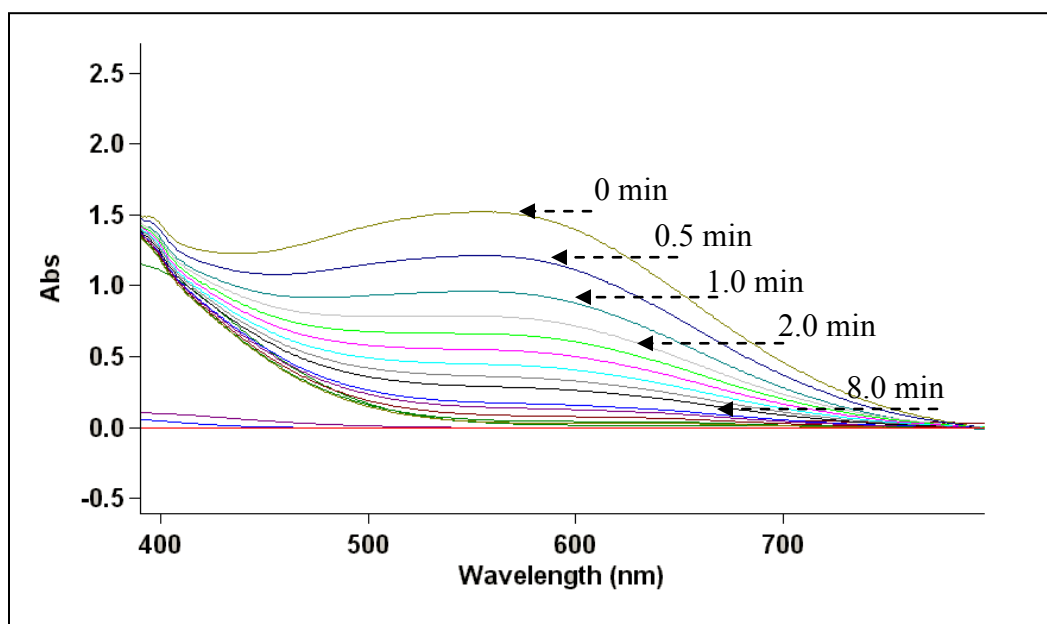
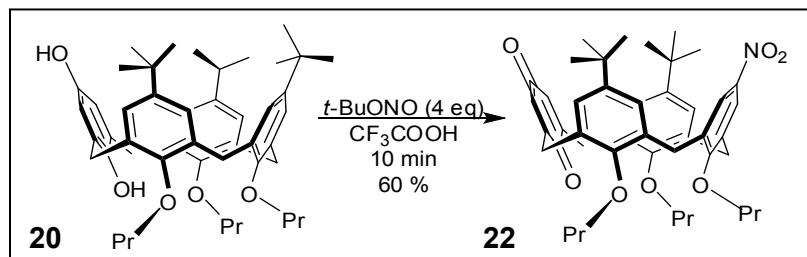


Figure 8.3 Solution-phase UV analysis of calix[4]monohydroquinone-NO⁺ complex

In contrast to the NO-releasing experiment reported in Scheme 8.2, if 4 equiv of *tert*-butylnitrite was added to a mixture of **20** and TFA (10 equiv) in dry chloroform, the excess nitrosonium ion reacted further with calix[4]quinone **19** and allowed the selective *ipso*-nitration of **19** at the distal aromatic ring with respect to the quinine moiety, yielding **22** in 60% yield (Scheme 8.3). The reaction outcome is likely to be the result of an initial *ipso*-nitrosation of **19**, followed by an oxidation of the nitroso intermediate to nitroderivative **22** by oxygen.⁴⁰²



Scheme 8.3 *ipso* nitration followed by oxidation of calix[4]monohydroquinone

The structure of **22** was assigned by spectral analysis. In particular, the presence of a pseudomolecular ion peak at m/z 723 in the ESI(+) mass spectrum confirmed the molecular formula. The molecular structure of **22** was confirmed by the pertinent signals in the ^1H NMR spectrum. In fact, a singlet was present at 8.07 ppm relative to protons in *ortho* to nitro group, whereas an AB system relative to the remaining aromatic protons was present at 6.54 and 6.89 ppm ($J = 2.1$ Hz, 4 H). In addition, a resonance was present at 6.74 ppm (2H) relative to the protons of the quinone moiety. Also in this case, the presence of a broad singlet at 3.56 ppm and of an AX system at 4.22/3.27 ppm ($J = 13.0$ Hz) relative to ArCH_2Quin and ArCH_2Ar protons, respectively, were indicative of a fast *through the-annulus* rotation of the quinone ring of **22**, which was confirmed by the pertinent ^{13}C NMR signals. The regiochemical outcome of the nitrosation can be explained by considering that very likely the excess NO^+ ion is complexed by quinone **19**, as indicated by the deep purple color of the solution. In this complex, the nitrosonium cation should be sandwiched between the two distal Ar-OPr rings, which would be parallel to one another. In this way, the NO^+ ion is perfectly oriented to give the *ipso* nitrosation onto the central Ar-OPr ring opposite to quinone system, with high regioselectivity.^{364,370} This reaction can be considered as an interesting example of supramolecular control of a reaction outcome,^{403,404} which could be probably exploited in a larger context.

In conclusion, we have shown that *p-tert*-butylcalix[4]-monohydroquinone **20** can be used for the generation of NO gas. In a one-electron reduction scheme involving NO^+ -**20** complex (**21**), NO is released without the presence of an external reducing agent. Free tripropoxycalix[4]monoquinone **19**, thus obtained, can be reused for a new NO-releasing cycle after NaBH_4 -reduction to **20**.

8.4 Experimental Section

8.4.1 General Methods and Procedures

ESI-MS measurements were performed on a Micromass Bio-Q triple quadrupole mass spectrometer equipped with electrospray ion source, using a mixture of H₂O/CH₃CN (1:1) and 5% HCOOH as solvent, or a Perkin-Elmer 2400 CHN Analyzer. Flash chromatography was performed on Merck silica gel (60 Å, 40-63 µm). All experiments with moisture- and/or air-sensitive compounds were run in freshly distilled over P₂O₅ chloroform, under a dried nitrogen atmosphere. Head space UV analysis of the nitric oxide releasing experiment was carried out under inert and dry nitrogen environment. All the other chemicals were purchased from Sigma Aldrich and used as received. Reaction temperatures were measured externally; reactions were monitored by TLC on Merck silica gel plates (0.25 mm) and visualized by UV light and spraying with H₂SO₄-Ce(SO₄)₂. Compound **18** was prepared according to a literature procedure.⁴⁰⁵ All 1D NMR spectra were recorded on a Bruker Avance-400 spectrometer or a JEOL Eclipse 300 MHz spectrometer; chemical shifts are reported relative to the residual solvent peak (CHCl₃: δ 7.26, CDCl₃: δ 77.23). UV-Visible spectra were measured on a VARIAN Cary 50 UV spectrophotometer.

8.4.2 Synthesis of Calix[4]monohydroquinone

25,26,28-tris(*n*-propyl)-*p*-tert-butylcalix[4]monoquinone (19).

A solution of **18** (2.65 g, 3.42 mmol) and Ti(CF₃COO)₃ (5.57 g, 10.20 mmol) in trifluoroacetic acid (14.0 ml) was stirred for 3 h in the dark at room temperature. The mixture was dried under vacuum and the residue was dissolved in CH₂Cl₂ (50 mL), and washed with cold 1N HCl (4 × 50 mL) and brine (2 × 10 mL). The organic phase was dried over Na₂SO₄. The crude product, obtained after solvent evaporation under

vacuum, was subjected to flash chromatography on silica gel (petroleum ether/dichloromethane, 6/4 v/v), to give **14** (1.93 g, 77%). Compound **19**: ESI(+) MS: $m/z = 733$ (MH^+); 1H NMR ($CDCl_3$, 400 MHz, 298 K): δ 0.78 (t, $OCH_2CH_2CH_3$, $J = 7.6$ Hz, 3H), 1.02 (t, $OCH_2CH_2CH_3$, $J = 7.9$ Hz, 6H), 1.03 [s, $C(CH_3)_3$, 18H], 1.34 [s, $C(CH_3)_3$, 9H], 1.83 (m, $OCH_2CH_2CH_3$, 4H), 1.91 (m, $OCH_2CH_2CH_3$, 4H), 3.10 and 4.14 (AX, $ArCH_2Ar$, $J = 12.8$ Hz, 4H), 3.51 (br s, $ArCH_2Quin$, 4H), 3.55 (m, $OCH_2CH_2CH_3$, 4H), 3.69 (m, $OCH_2CH_2CH_3$, 2H), 6.57 and 6.84 (AB, ArH , $J = 2.4$ Hz, 4H), 6.60 (s, $Quin-H$, 2H), 7.10 (s, ArH , 2H); ^{13}C NMR ($CDCl_3$, 100 MHz, 298 K): δ 9.4, 11.0, 22.3, 23.9, 31.0, 31.6, 31.9, 34.0, 34.3, 35.5, 75.8, 76.6, 125.8, 126.4, 126.5, 127.6 (s), 132.9, 133.7, 135.9, 145.1, 147.1, 154.3, 154.4, 186.5 and 189.5 (C=O). Anal. Calcd for $C_{49}H_{64}O_5$: C, 80.29; H, 8.80. Found: C, 80.20; H, 8.90.

25,26,28-tris(*n*-propyloxy)-*p*-tert-butylcalix[4]monohydroquinone (20). To a solution of **19** (0.61 g, 8.32 mmol) in a mixture of THF/EtOH (20 mL, 1:1 v/v) was added $NaBH_4$ (0.16 g, 42.8 mmol) and the mixture was stirred for 2 h at r.t. The solvent was removed by evaporation in vacuo and the residue was partitioned between $CHCl_3$ (20 mL) and H_2O (20 mL). The organic phase was taken to dryness, and the residue was subjected to flash chromatography on silica gel (petroleum ether/dichloromethane, 3/7 v/v), to give **20** (0.30 g, 49%). Compound **20**: ESI(+) MS: $m/z = 735$ (MH^+); 1H NMR ($CDCl_3$, 400 MHz, 298 K): δ 0.85 [s, $C(CH_3)_3$, 18H], 0.93 (t, $OCH_2CH_2CH_3$, $J = 7.5$ Hz, 3H), 1.07 (t, $OCH_2CH_2CH_3$, $J = 7.4$ Hz, 6H), 1.32 [s, $C(CH_3)_3$, 9H], 1.90 (m, $OCH_2CH_2CH_3$, 4H), 2.33 (m, $OCH_2CH_2CH_3$, 2H), 3.16 and 4.36 (AX, $ArCH_2Ar$, $J = 13.2$ Hz, 4H), 3.17 and 4.32 (AX, $ArCH_2Ar$, $J = 12.6$ Hz, 4H), 3.71 (t, $OCH_2CH_2CH_3$, $J = 7.0$ Hz, 4H), 3.82 (t, $OCH_2CH_2CH_3$, $J = 7.4$ Hz, 2H), 4.18 (s, $ArOH$, 1H), 4.91 (s, $ArOH$, 1H), 6.51 and 6.54 (AB, ArH , $J = 1.8$ Hz, 4H), 6.57 (s, ArH , 2H), 7.12 (s, ArH , 2H); ^{13}C NMR ($CDCl_3$, 100 MHz, 298 K): δ 9.8, 11.0, 22.6, 23.6, 31.3, 31.4, 31.9, 33.9, 34.3,

76.4, 78.0, 114.9, 124.7, 125.2, 125.9, 131.6, 132.1, 132.6, 136.2, 145.4, 146.5, 147.2, 148.1, 152.2, 154.0. Anal. Calcd for $C_{49}H_{66}O_5$: C, 80.07; H, 9.05. Found: C, 80.16; H, 8.96.

Preparation of *p*-*tert*-butylcalix[4]monohydroquinone-nitrosonium complex (21).

Trifluoroacetic acid 25 μ L (10 eq) and *tert*-butylnitrite 4 μ L (1 eq) was added to a solution of **20** (0.025 g, 0.034 mmol) in 1 ml of dry $CDCl_3$. UV-Vis ($CHCl_3$) λ_{max} = 545 nm (Figure 8.4).

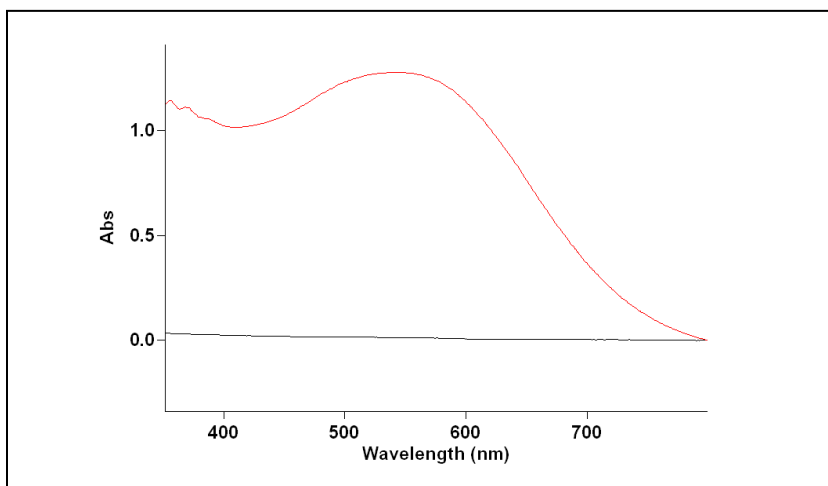


Figure 8.4 UV-Vis spectrum of NO^+ complex prepared by *p*-*tert*-butylcalix[4]monohydroquinone **20** and *t*-BuONO in presence of TFA.

26,28-bis(*n*-propyloxy)-23-nitro-*p*-*tert*-butylcalix[4]monoquinone (22).

Trifluoroacetic acid (25 μ L, 0.34 mmol) and *tert*-butylnitrite (16 μ L, 0.136 mmol) was added to a solution of **20** (0.025 g, 0.034 mmol) in 1 mL of dry chloroform and the mixture was stirred for 10 min at r.t. Evaporation of the solvent gave the crude product which was purified by the preparative TLC (silica gel, ethyl acetate/hexane, 1/4, v/v), to give **4** in 60% yield. ESI(+) MS: m/z = 723 (MH^+); 1H NMR ($CDCl_3$): δ 8.04 (s, ArH, 2H), 6.89 and 6.54 (AB, ArH, J = 2.1 Hz, 4H), 6.75 (s, ArH, 2H), 4.21 and 3.26 (AX, $ArCH_2Ar$, J = 13.0 Hz, 4H), 3.70-3.55 (overlapping, $OCH_2CH_2CH_3$, 6H), 3.59 (br s,

ArCH₂Quin, 4H), 1.97-1.79 (overlapping, OCH₂CH₂CH₃, 6H), 1.02 [s, C(CH₃)₃, 18H], 1.01 (t, OCH₂CH₂CH₃, *J* = 7.5 Hz, 6H), 0.79 (t, OCH₂CH₂CH₃, *J* = 7.5 Hz, 3H). ¹³C NMR (CDCl₃, 100 MHz, 298 K): δ 9.1, 10.7, 21.9, 23.7, 30.8, 31.4, 33.9, 76.7, 77.2, 124.1, 126.1, 127.1, 131.2, 133.5, 138.2, 142.9, 145.8, 147.1, 154.1, 162.9, 186.5, 189.9. Anal. Calcd for C₄₅H₅₅NO₇: C, 74.87; H, 7.68; N, 1.94. Found: C, 74.97; H, 7.60; N, 2.02. ESI-TOF MS, *m/z*: 722.33, Calcd for C₄₅H₅₅NO₇.

CHAPTER 9

GENERAL SUMMARY

First five chapters of this dissertation focus on the design and synthesis of new ionic liquids and their potential applications in analytical chemistry. In Chapter 2, new class of trigonal tricationic ionic liquids were used as gas chromatographic (GC) stationary phases and these new GC phases were characterized based on Abraham's linear solvation energy relationships. Use of multifunctional IL stationary phases for GC can be limited as the most common counter anion for many ILs (i.e., bis(trifluoromethanesulfonyl)imide) results in peak tailing for alcohols and other H-bond forming analytes. Specific amide core containing trigonal tricationic ILs were shown to overcome this problem. In addition they were also shown to give efficient, symmetric peak shapes for most of the analytes used in this study. Amide core containing trigonal tricationic IL-based GC phases were shown to have comparable polarities to the commercial SP-2331 phase.

In Chapter 3, the design and synthesis of new linear tricationic ILs were discussed. Previously synthesized ILs had rigid trigonal structures. Thus the design and synthesis of more flexible tricationic ionic liquids offered the opportunity for enhanced results. These ILs were the first example found in the literature with a tricationic charge that still existed as liquids at room temperature. Physicochemical properties of these linear ILs were discussed and their ability to be used in electrowetting applications has also been examined. These new linear tricationic ILs which were more flexible compared to trigonal rigid core structures, were used as ion

pairing reagent in detection of dianionic species using the positive mode of ESI-MS. These results were described in Chapter 4. The results of this study revealed that the complexation or ion pairing ability decreased when the imidazole or phosphonium charged moieties were separated by 3 methylene units. In general, use of these flexible tricationic ILs in detecting anions in the positive mode of ESI-MS produced higher sensitivities compared to what was observed in the negative mode.

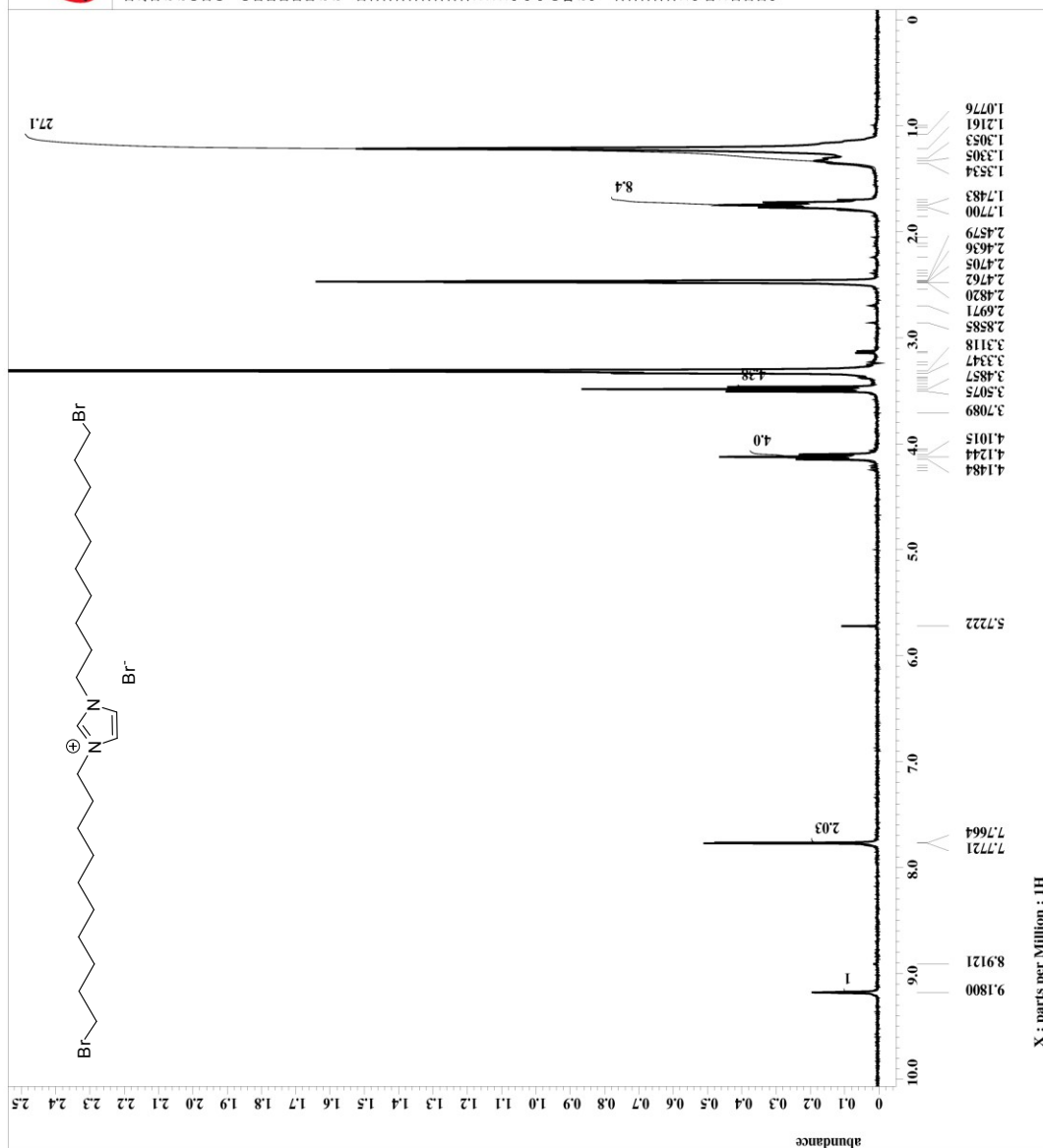
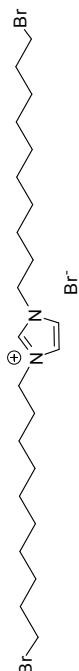
Chapter 5 described development of a polymeric IL type sorbent material designed for solid phase microextraction (SPME). Most of the commercially available adsorbent materials used in SPME applications are physically coated siloxane and polyacrylate-based sorbents. This newly developed IL-based polymeric coating material was covalently bonded to silica surface and therefore could be used in direct immersion applications without any loss of the material. These silica bonded new polymeric IL sorbent materials also show less bleeding at higher GC inlet temperatures compared to commercial fibers with PMDS (poly dimethyl siloxane) and PDMS/DVB (poly dimethyl siloxane-divinyl benzene) type coatings. In this study, these new IL-based polymeric coatings were used in both headspace and direct immersion experiments and their extraction capabilities were found to be comparable to commercial coatings.

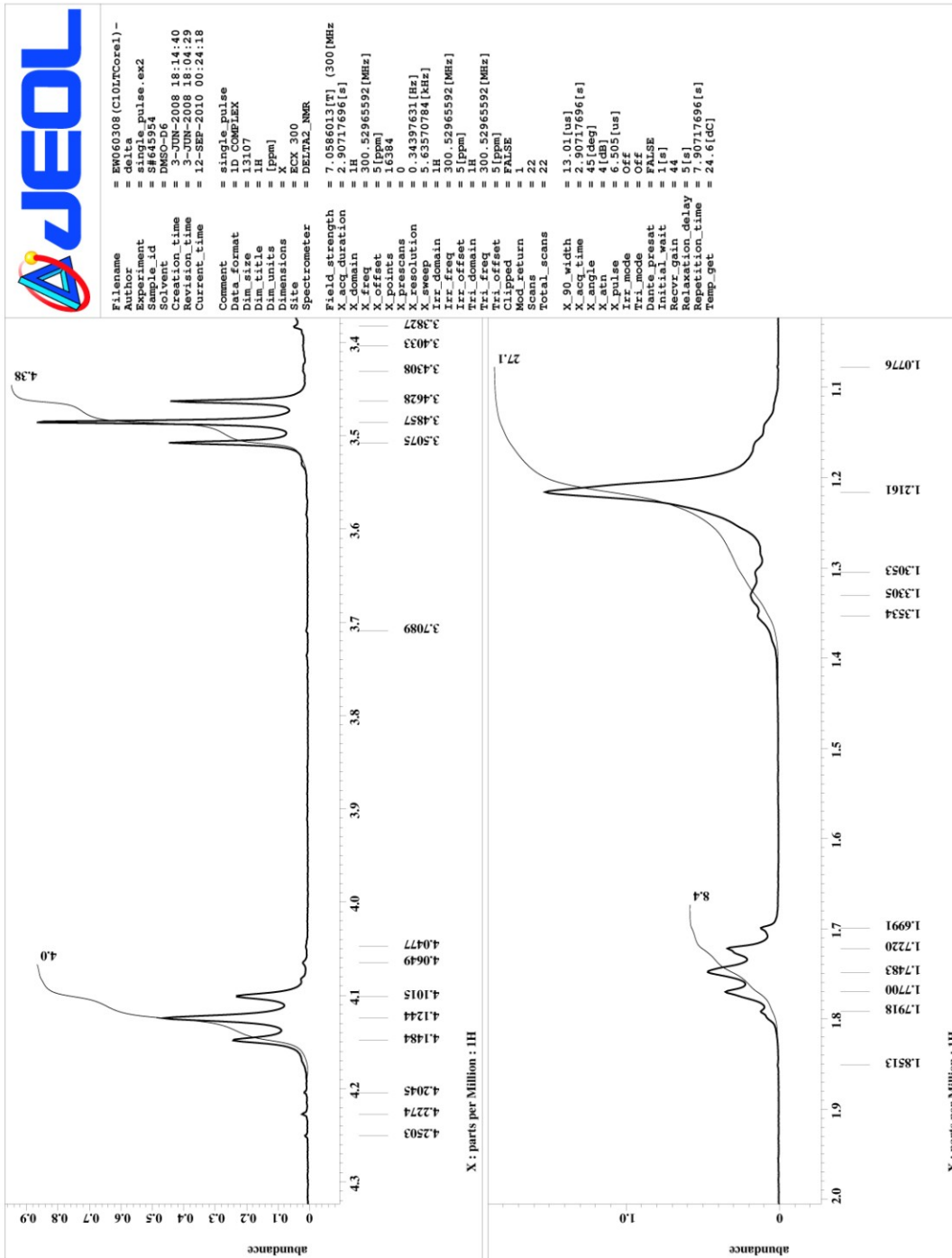
Chapter 6 through 8 discussed calix[4]arene-based supramolecular chemistry of NO_x gases. General introduction to supramolecular chemistry and NO_x gases were given in Chapter 6. In Chapter 7, cleaner generation of medically important nitric oxide gas (NO) using calix[4]arene-NO⁺ after a simple reduction by hydroquinone was discussed. As described in Chapter 8, NO generation without any external addition of hydroquinone was shown by using calix[4]monohydroquinone.

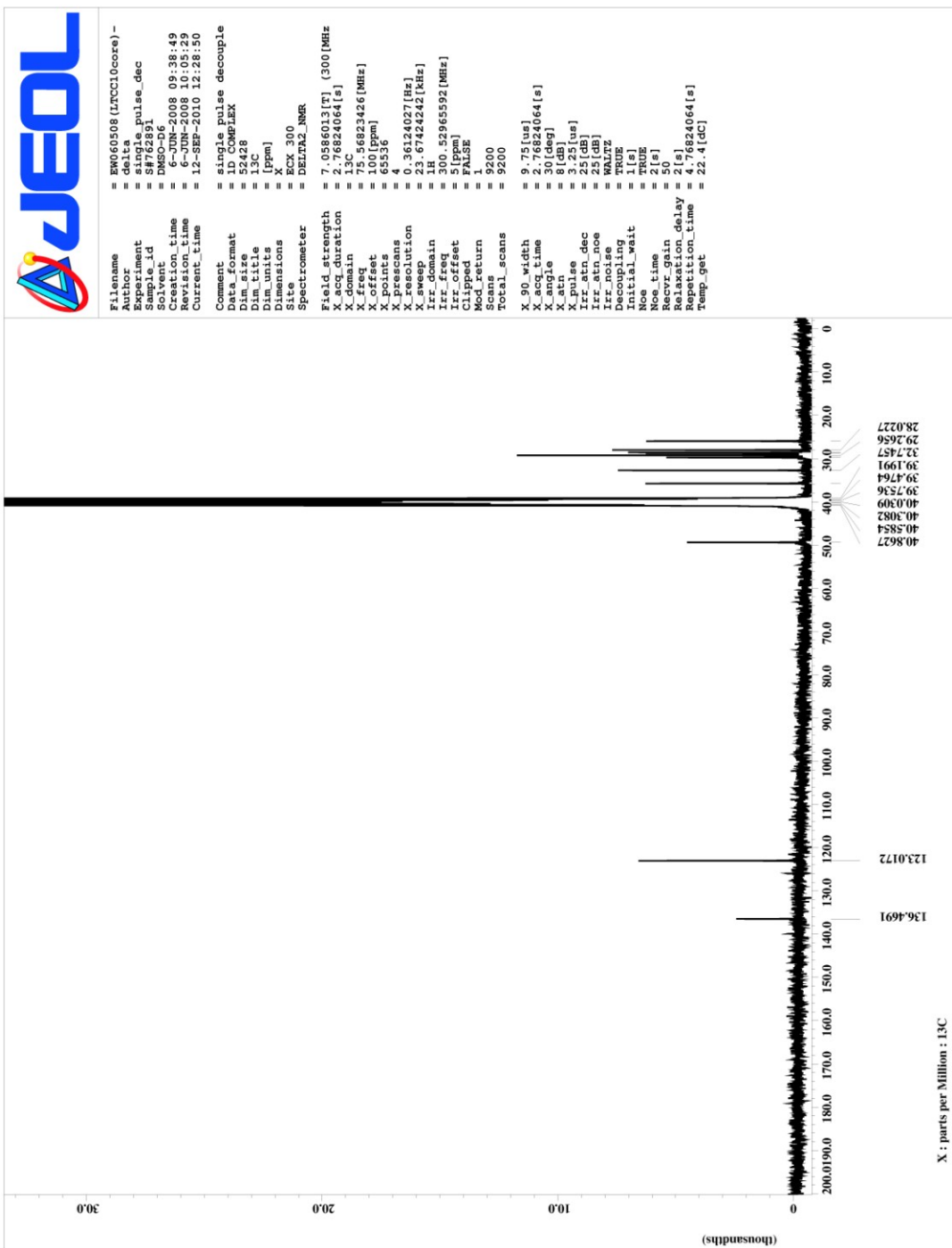
APPENDIX 1

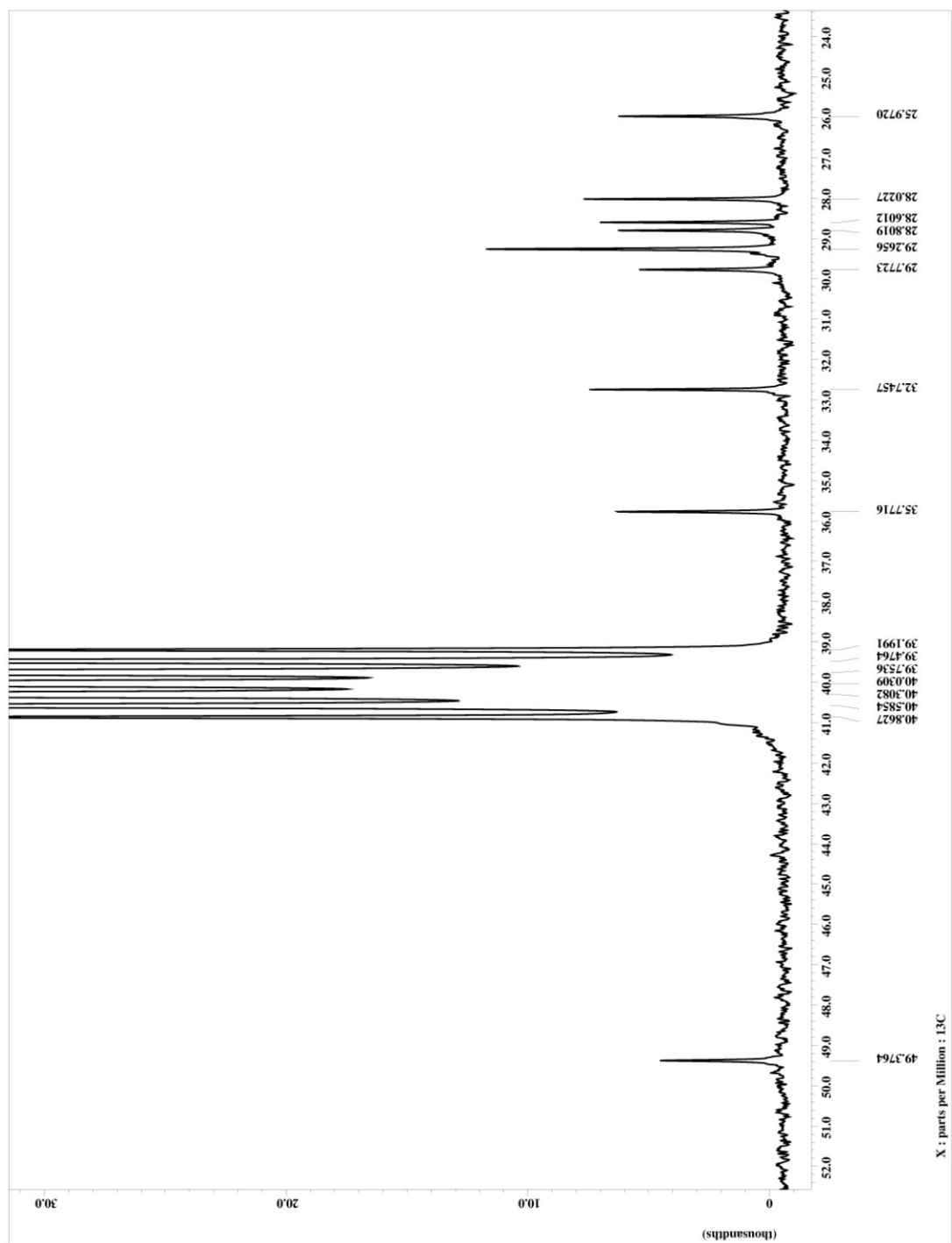
^1H AND ^{13}C NMR SPECTRA OF

1-BROMODECYL-3-BROMODECYL IMIDAZOLIUM BROMIDE SALT (1a)





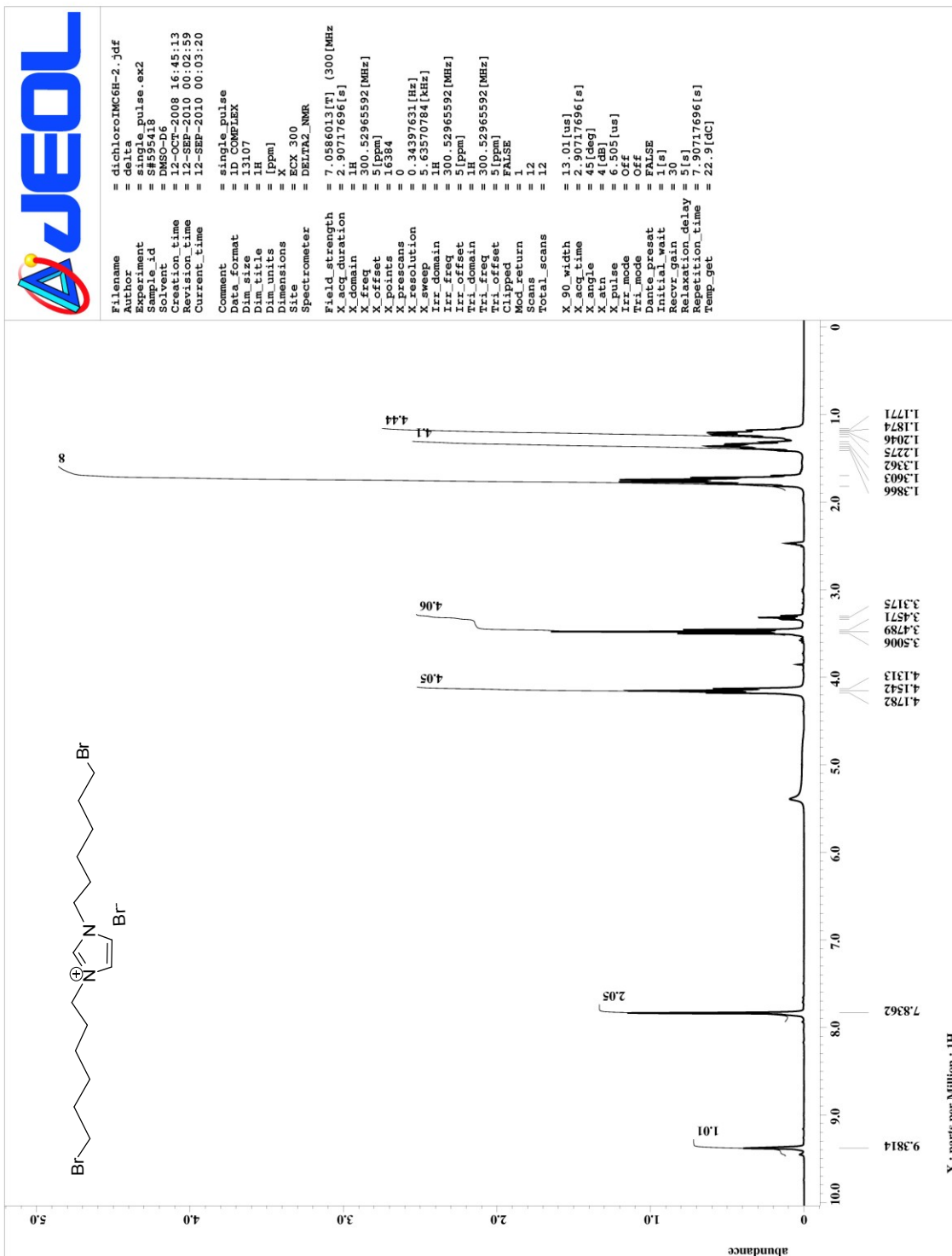


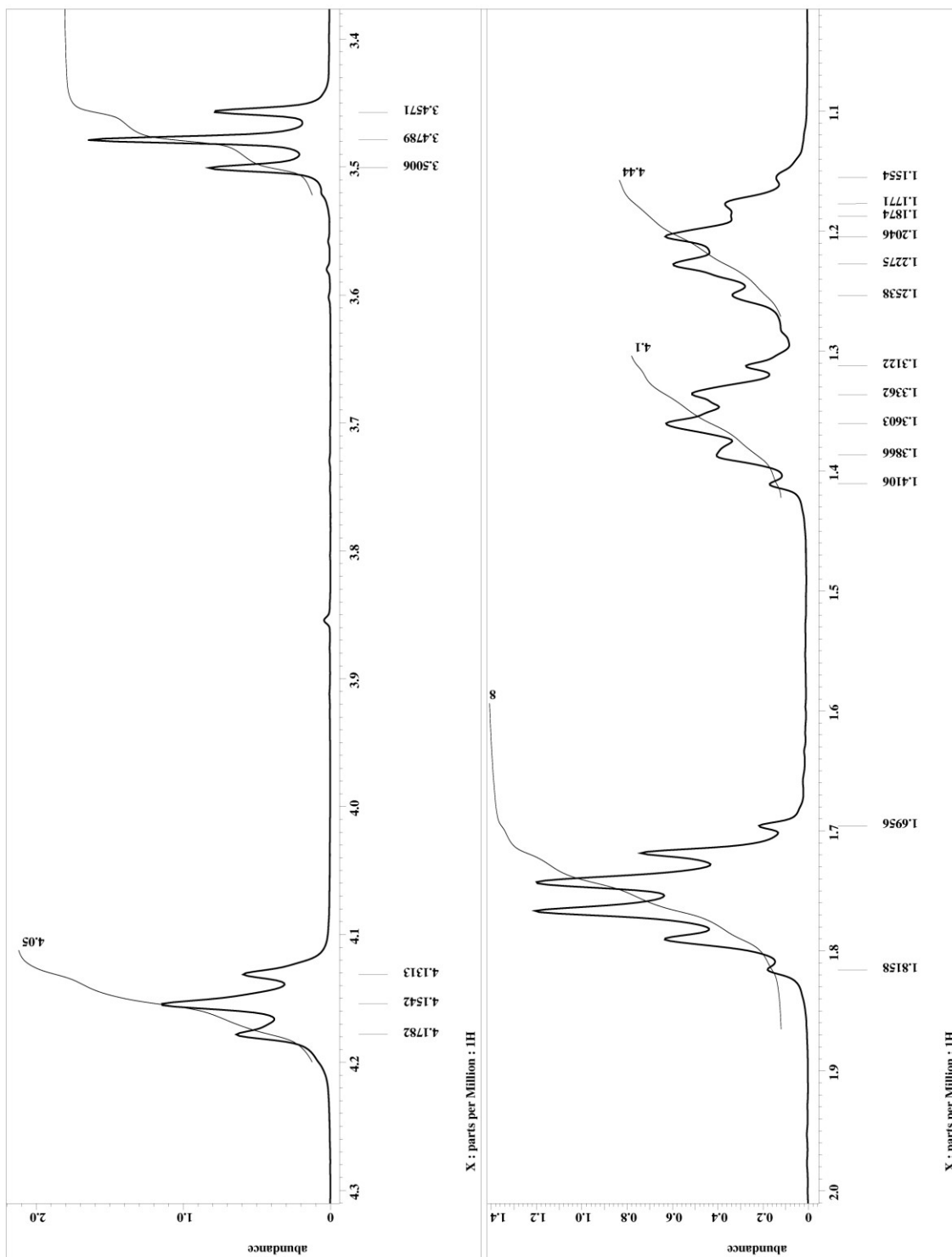


APPENDIX 2

¹H NMR SPECTRA OF

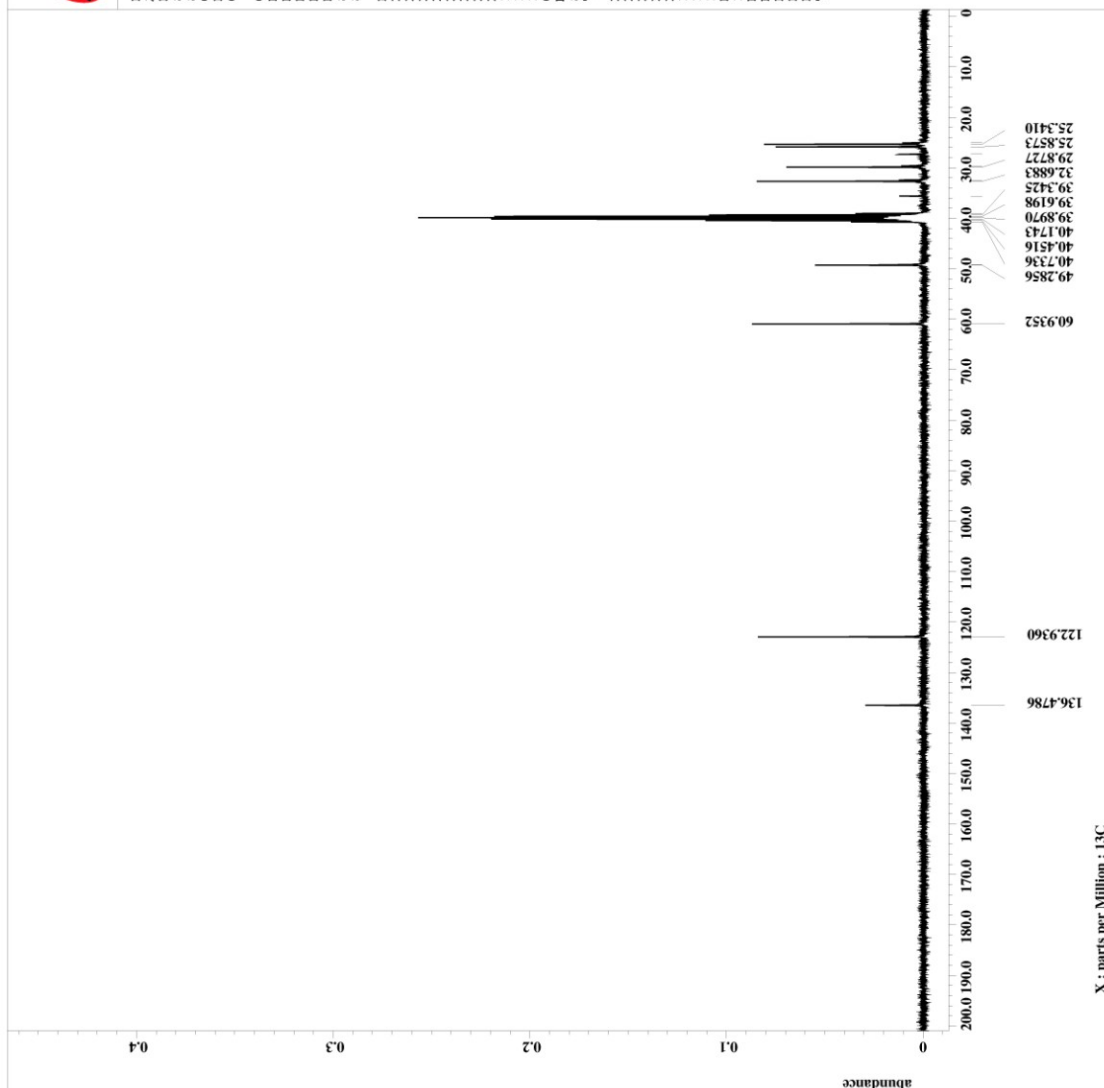
1-BROMOHEXYL-3-BROMOHEXYL IMIDAZOLIUM BROMIDE SALT (1b)







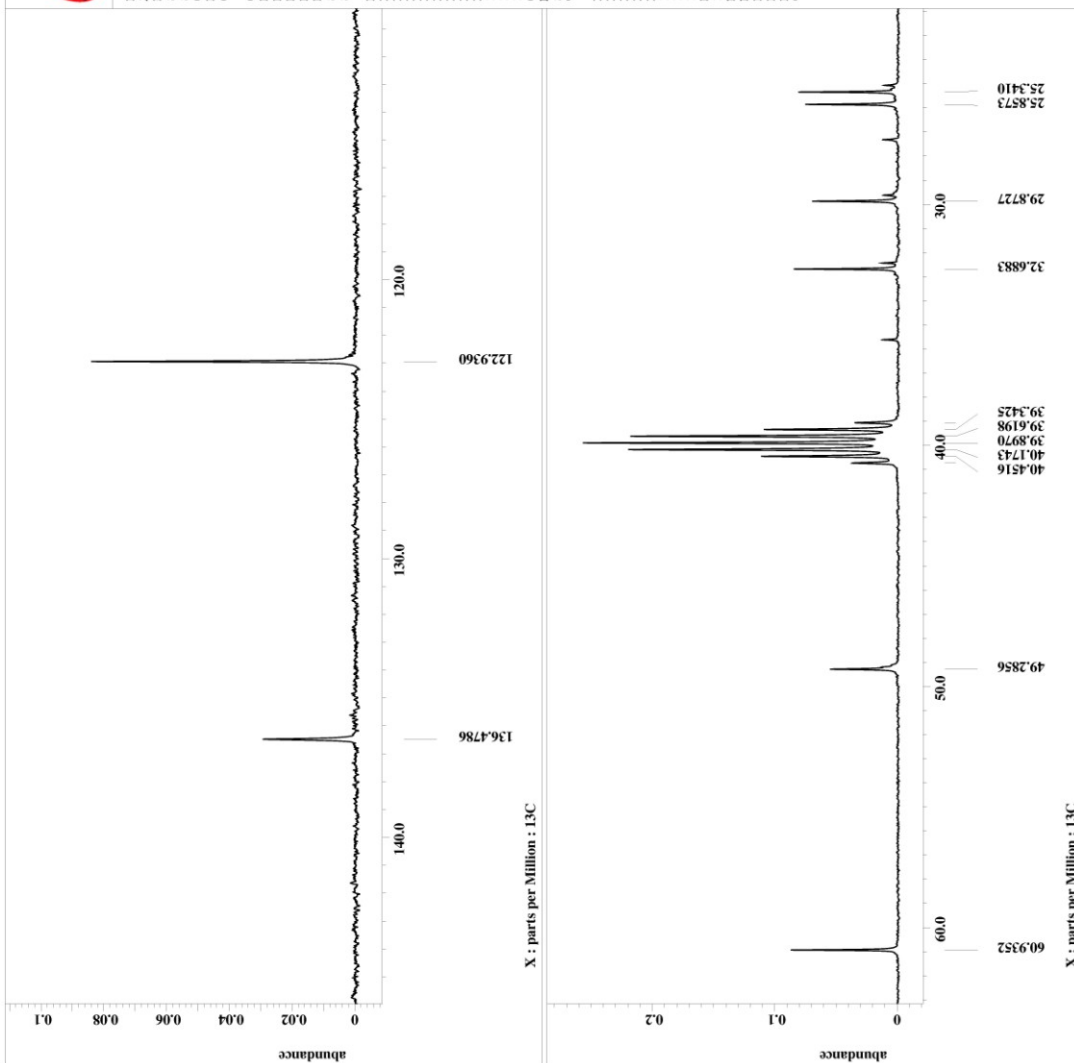
Filename = 20081125-2.jdf
Author = delta
Experiment = single_pulse_dec
Sample_id = MW5-06
Solvent = DMSO-d6
Creation_time = 25-NOV-2008 23:20:02
Revision_time = 21-SEP-2010 22:06:45
Current_time = 21-SEP-2010 22:09:36
Comment = single pulse decouple
Data format = 1D GMPLEX
Dimensions = 52428
Dim_1 = 13C
Dim_units = [ppm]
Dimensions = X
Site = ECX 300
Spectrometer = DELTA2_NMR
Field_strength = 7.0586013[T] (300[MHz]
X_acq_duration = 2.76824064[s]
X_domain = 13C
X_freq = 75.56823426[MHz]
X_offset = 100[ppm]
X_points = 65536
X_resolution = 0.36124027[Hz]
X_sweep = 23.67424242[kHz]
Irr_domain = 1H
Irr_freq = 300.52965592[MHz]
Irr_offset = 5[ppm]
Clipped = FALSE
Acq_return = 0
Scans = 800
Total_scans = 800
X_90_width = 9.75[us]
X_acq_time = 2.76824064[s]
X_angle = 30[deg]
X_tau = 1.25[us]
X_pulse = 3.25[us]
Irr_atn_dec = 25[db]
Irr_atn_noe = 25[db]
Irr_noise = WALTZ
Decoupling = TRUE
Initial_wait = 1[s]
Nuc1 = 13C
Nuc2 = 1H
Noe_time = 2[s]
Recvr_gain = 50
Relaxation_delay = 2[s]
Repetition_time = 4.76824064[s]
Temp_get = 23.2[dc]



X : parts per Million : 13C



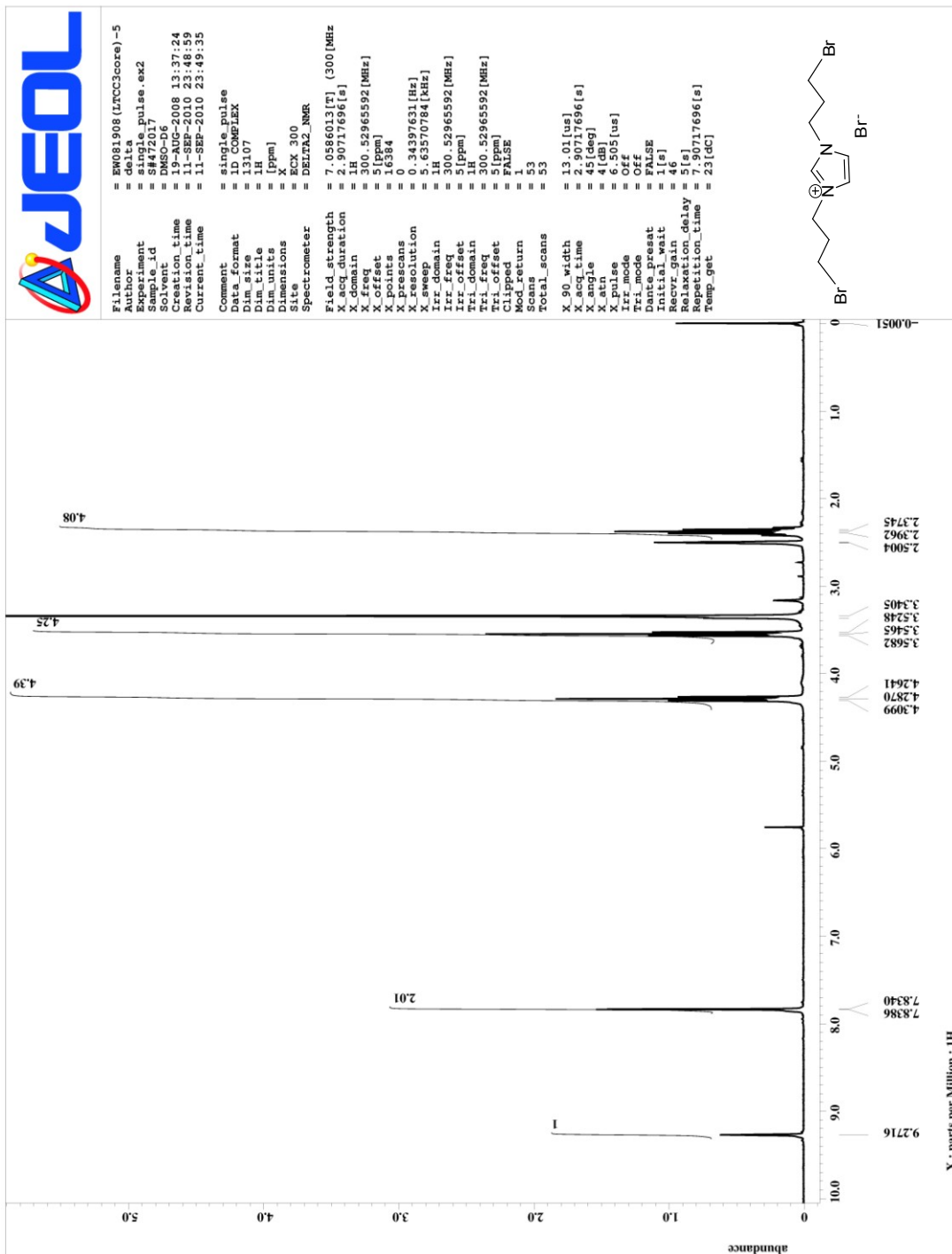
Filename = 20081125-3.jdf
Author = delta
Experiment = pulse_dec
Sample_id = S8733488
Solvent = DMSO-d6
Creation_time = 25-NOV-2008 23:20:02
Revision_time = 21-SEP-2010 22:10:07
Current_time = 21-SEP-2010 22:10:29
Comment = single pulse decouple
Data_format = 1D COMPLEX
Dim_size = 52428
Dim_title = 13C
Dim_units = [ppm]
Dimensions = 1
Site = ECK 300
Spectrometer = DELTA2 NMR
Field_strength = 7.0586013[T] (300[MHz]
X_acq_duration = 1.76824064[s]
X_freq = 75.56823426[MHz]
X_offset = 100[ppm]
X_points = 65536
X_prescans = 4
X_resolution = 35124027[Hz]
X_resolution_ppm = 23.67424242[MHz]
X_domain = 1H
X_freq = 300.52965592[MHz]
Irr_freq = 5[ppm]
Irr_offset = FALSE
Mod_return = 10
Saves = 800
Total_scans = 800
X_90_width = 9.75[us]
X_acq_time = 2.76824064[s]
X_angle = 0[deg]
X_delay = 8[us]
X_pulse = 3.25[us]
Irr_atn_dec = 25[db]
Irr_atn_noe = 25[db]
Irr_noise = WALZ
Decoupling = TRUE
Pulprog_wait = 1[s]
Noe_time = 2[s]
Recvr_gain = 50
Relaxation_delay = 2[s]
Repetition_time = 4.76824064[s]
Temp_get = 23.2[deg]

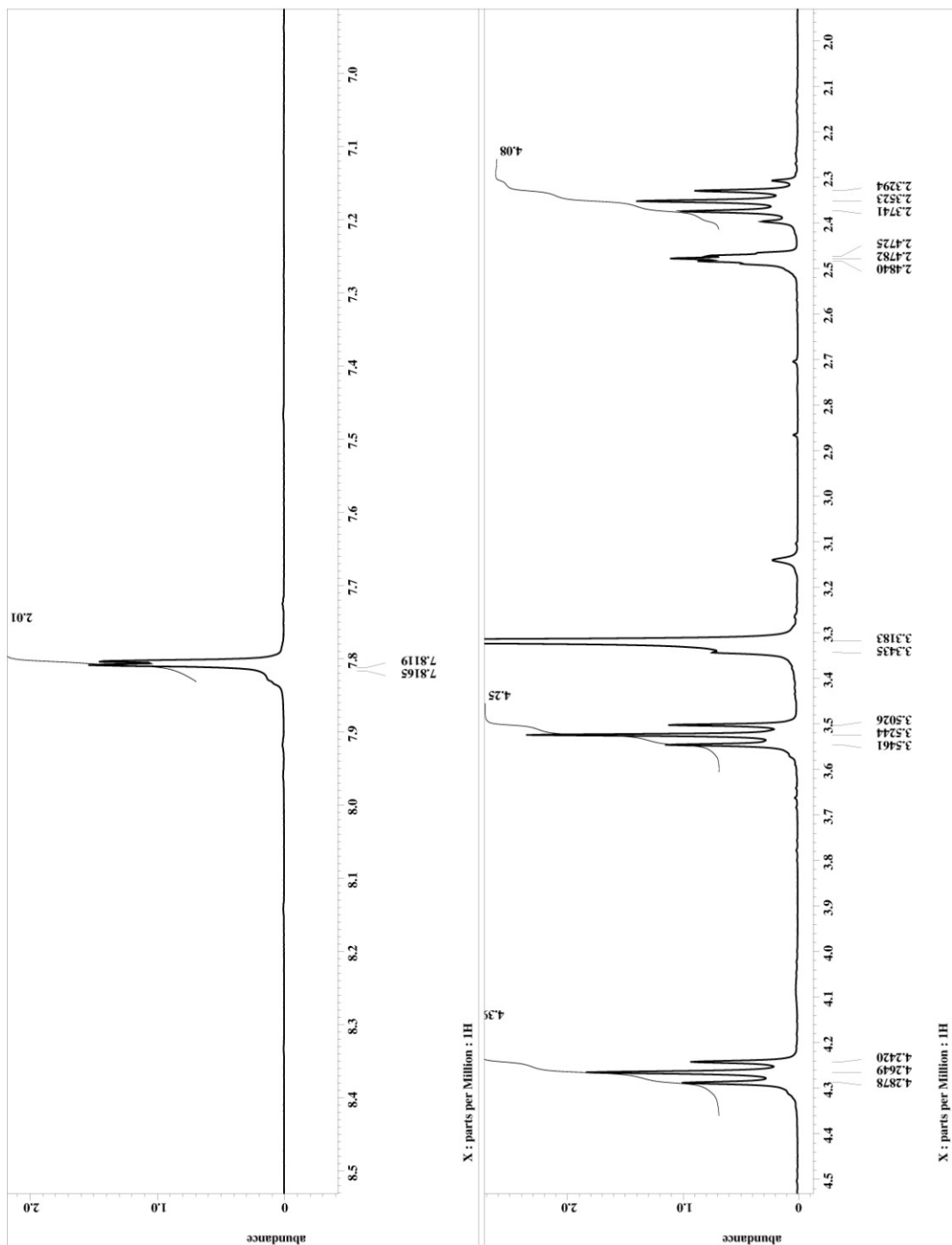


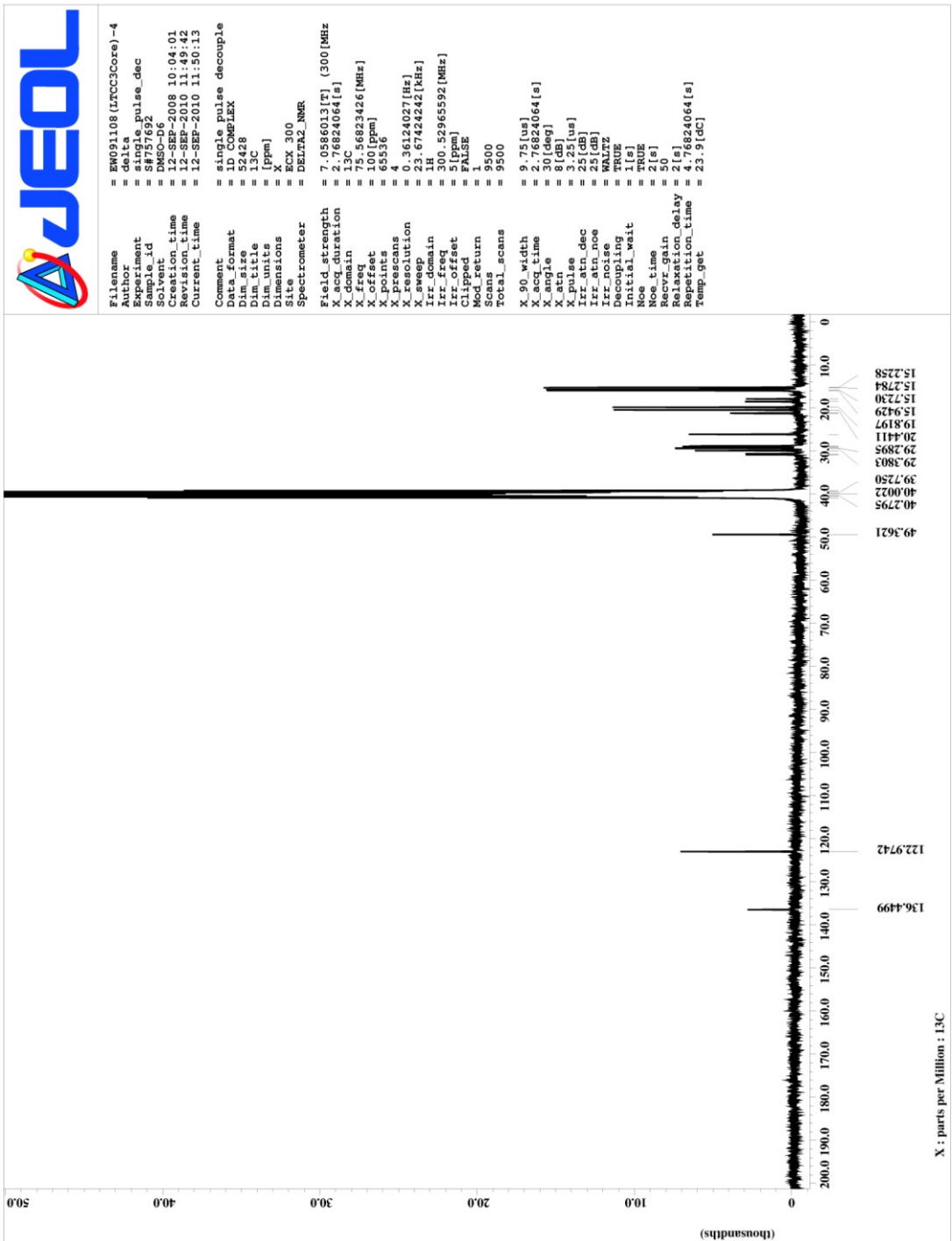
APPENDIX 3

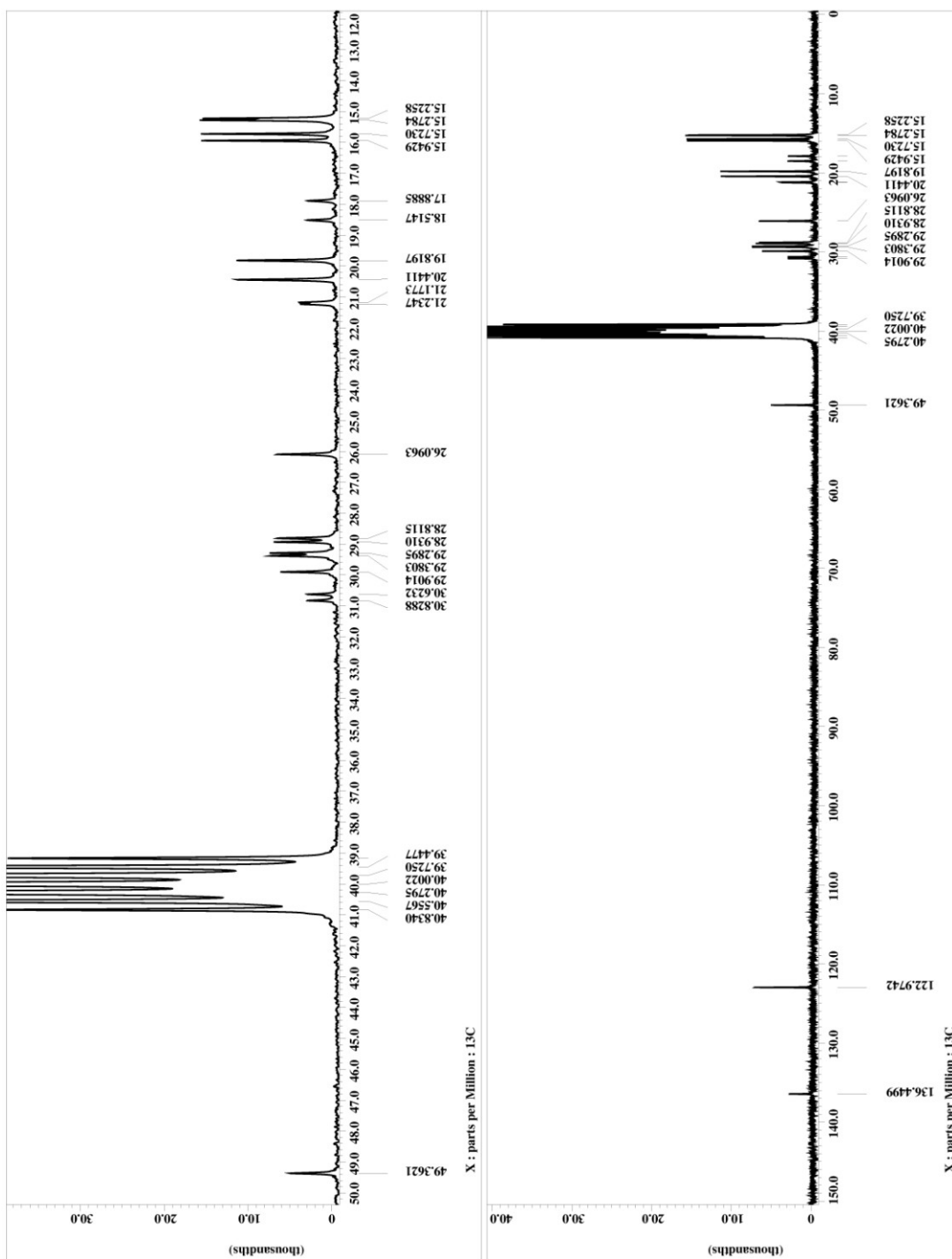
^1H AND ^{13}C NMR SPECTRA OF

1-BROMOPROPYL-3-BROMOPROPYL IMIDAZOLIUM BROMIDE SALT (1c)







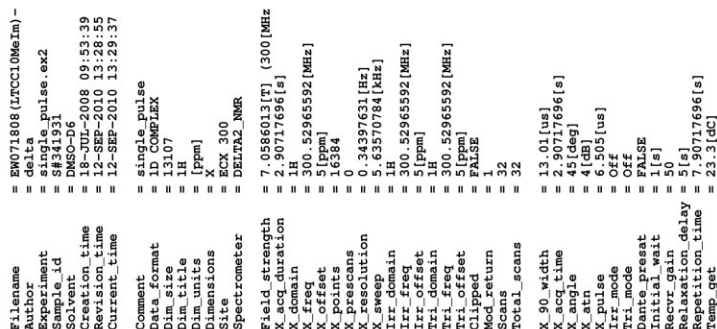


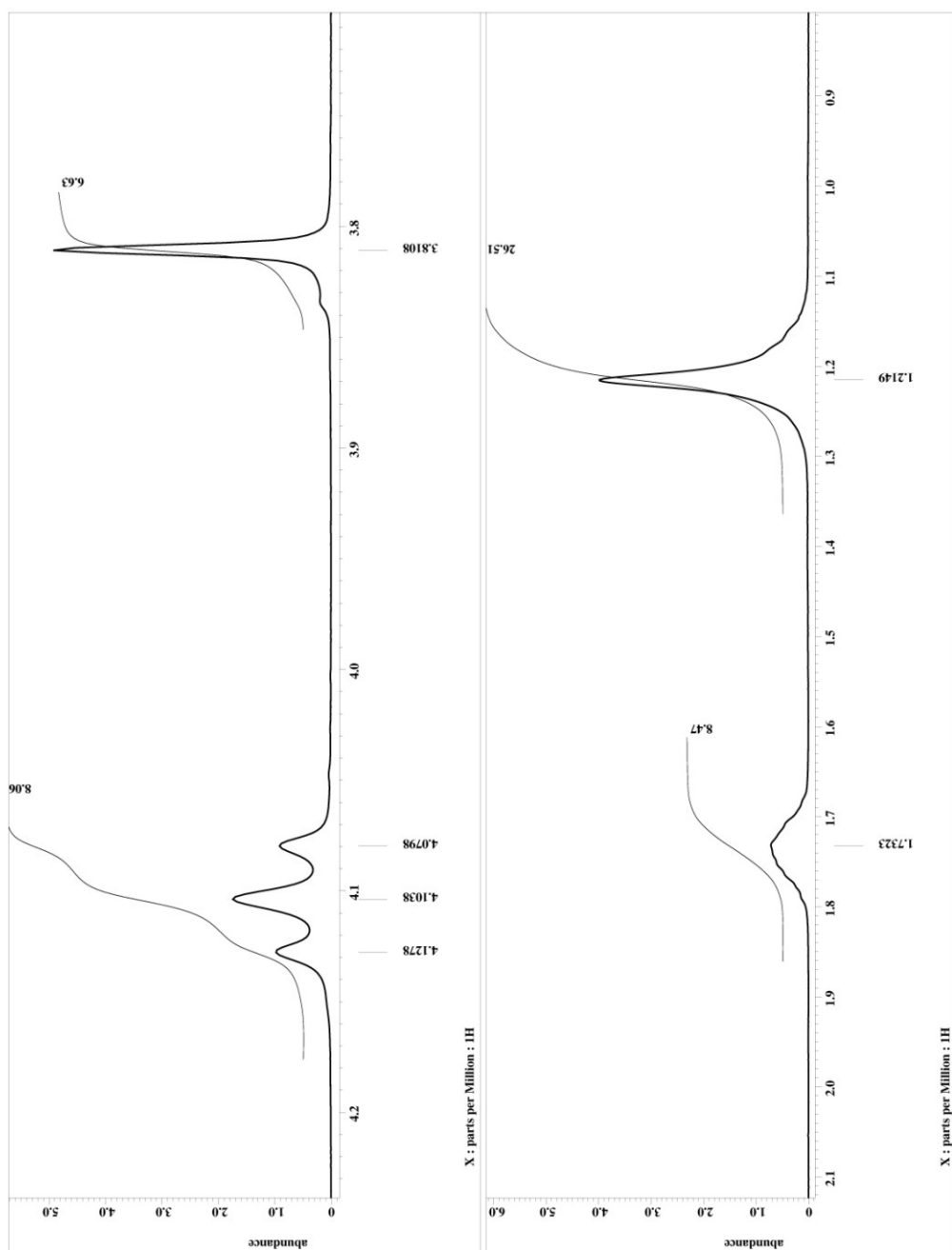
APPENDIX 4

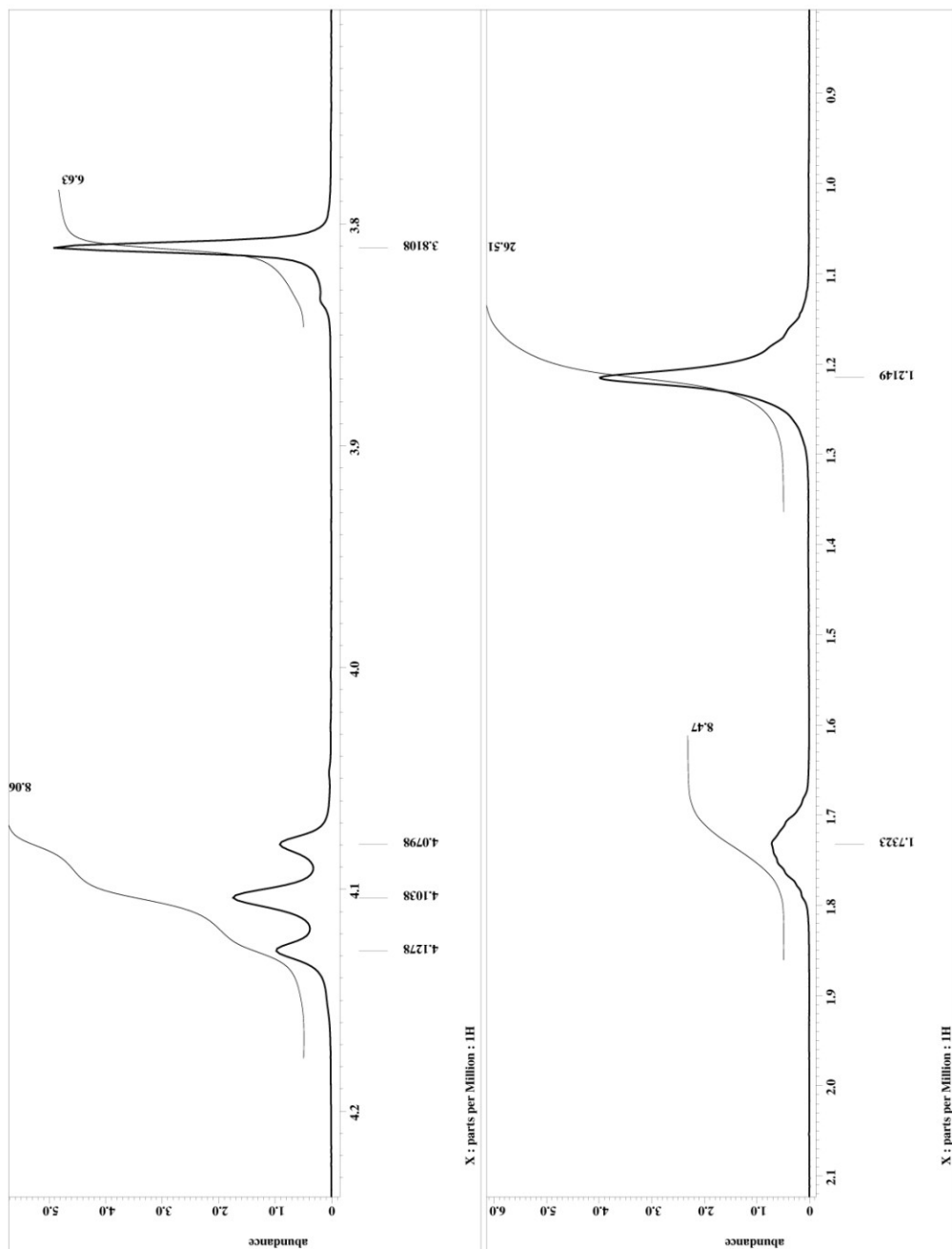
¹H AND ¹³C NMR SPECTRA OF

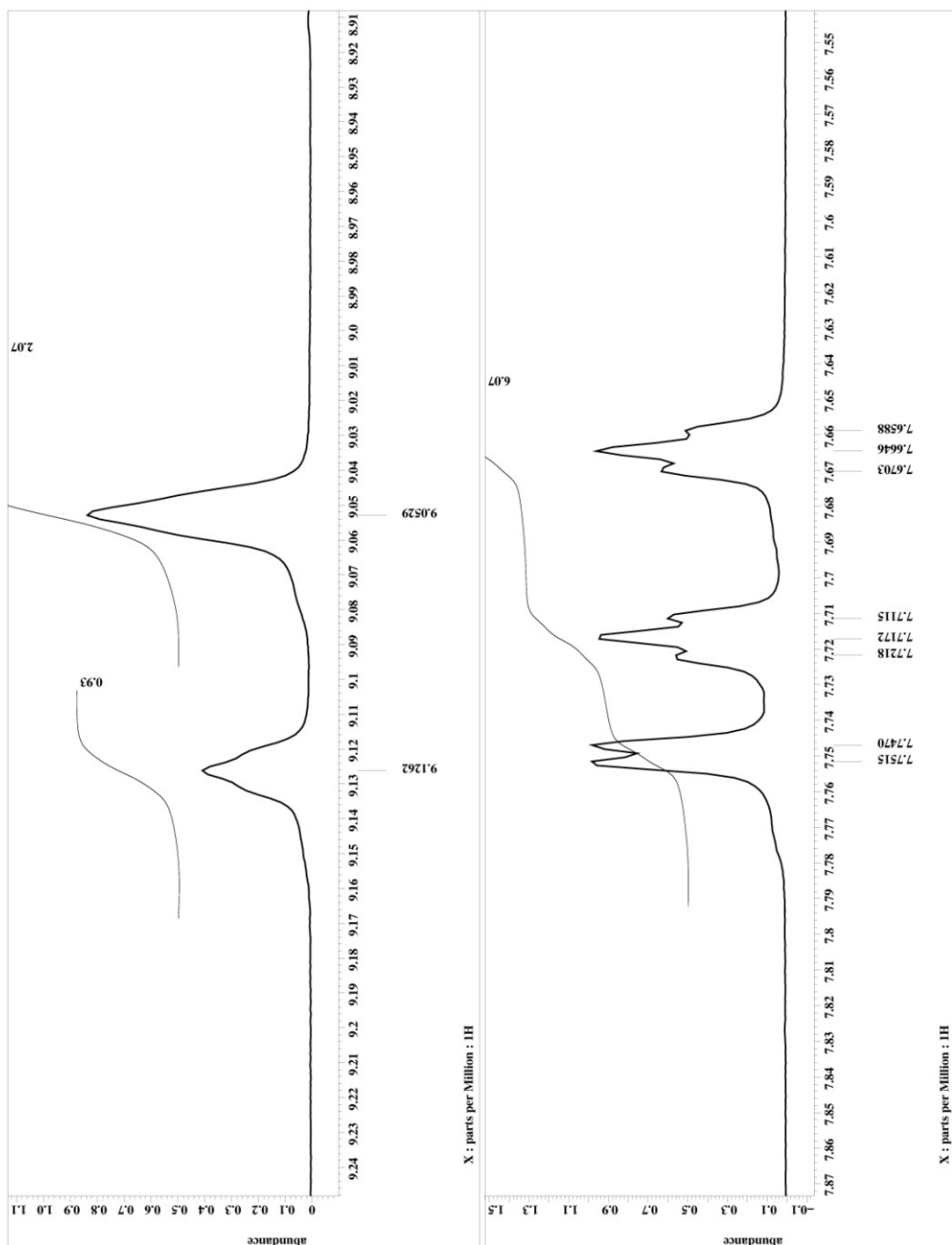
1-(1'-METHYL-3'-DECYLIMIDAZOLIUM)-3-(1''-METHYL-3''-DECYLIMIDAZOLIUM)

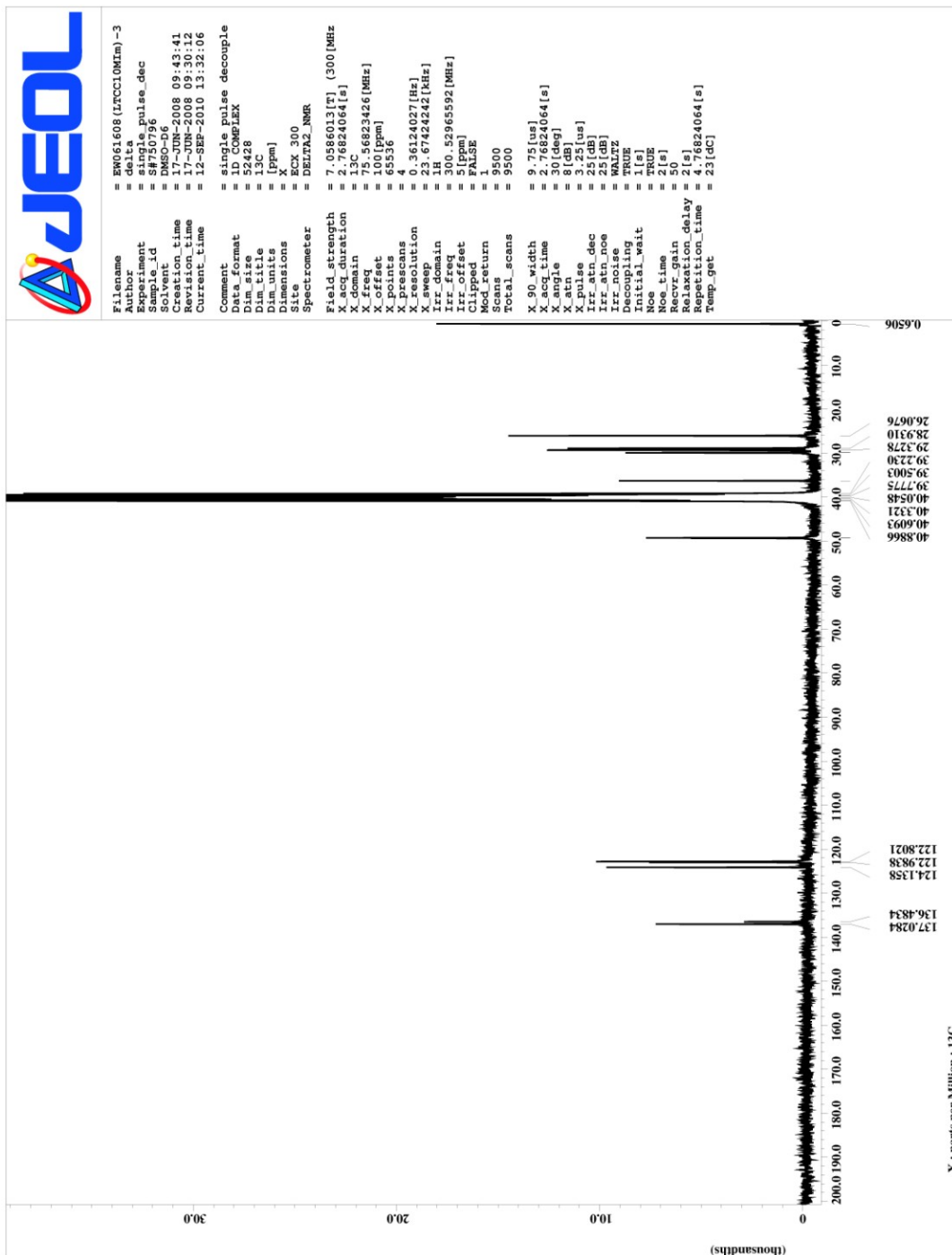
IMIDAZOLIUM TRI [BIS(TRIFLUOROMETHANESULFONYL)IMIDE] (2a)

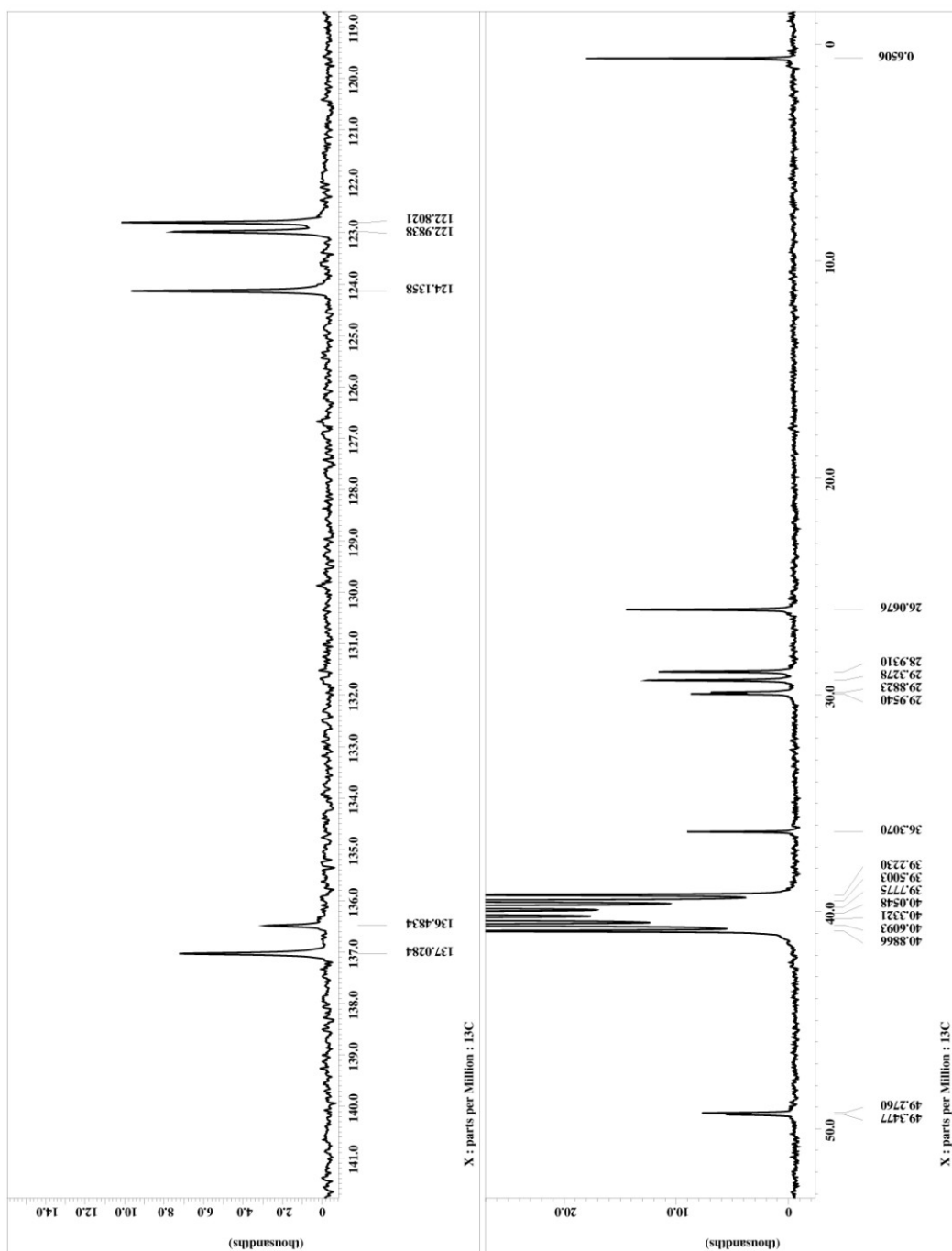








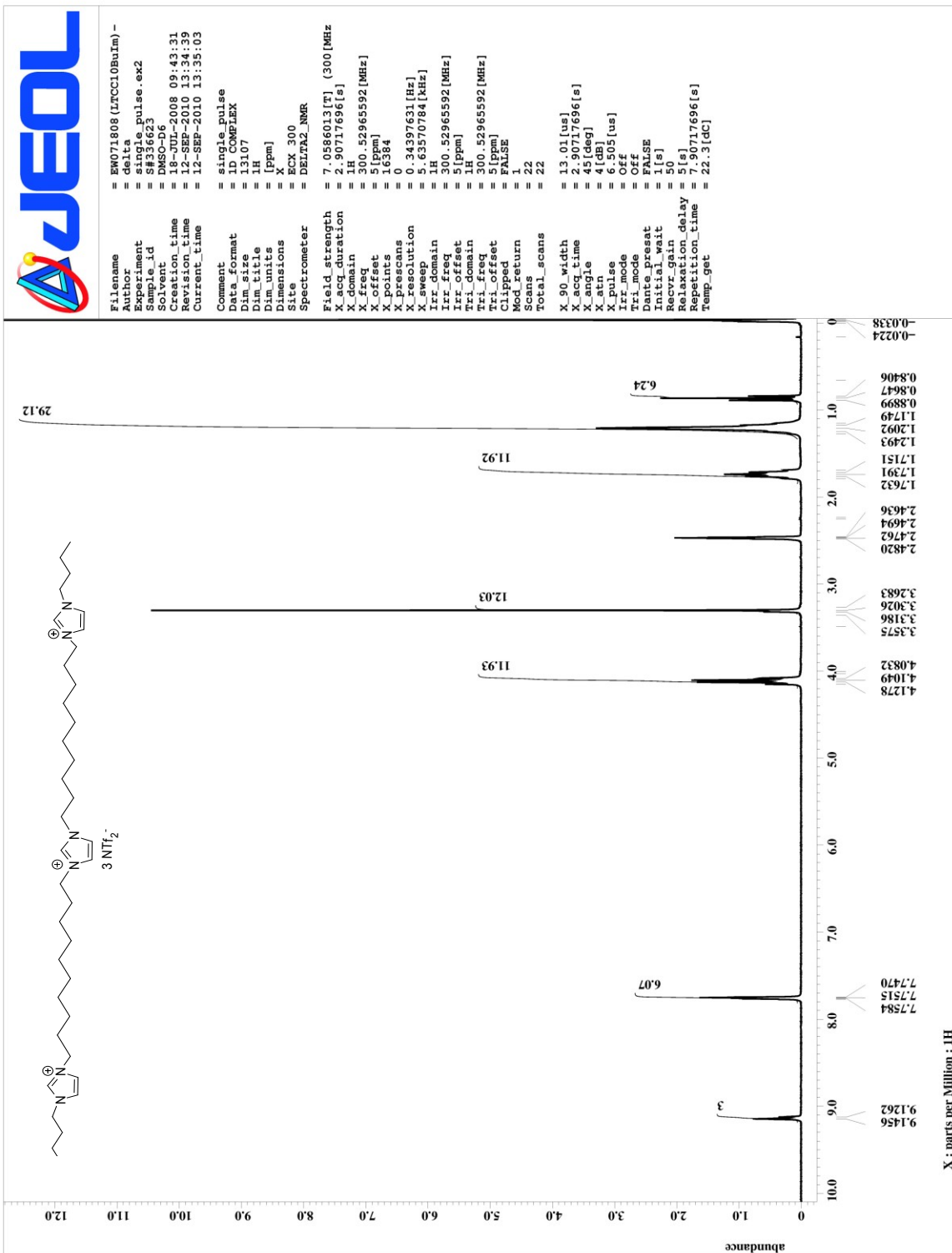


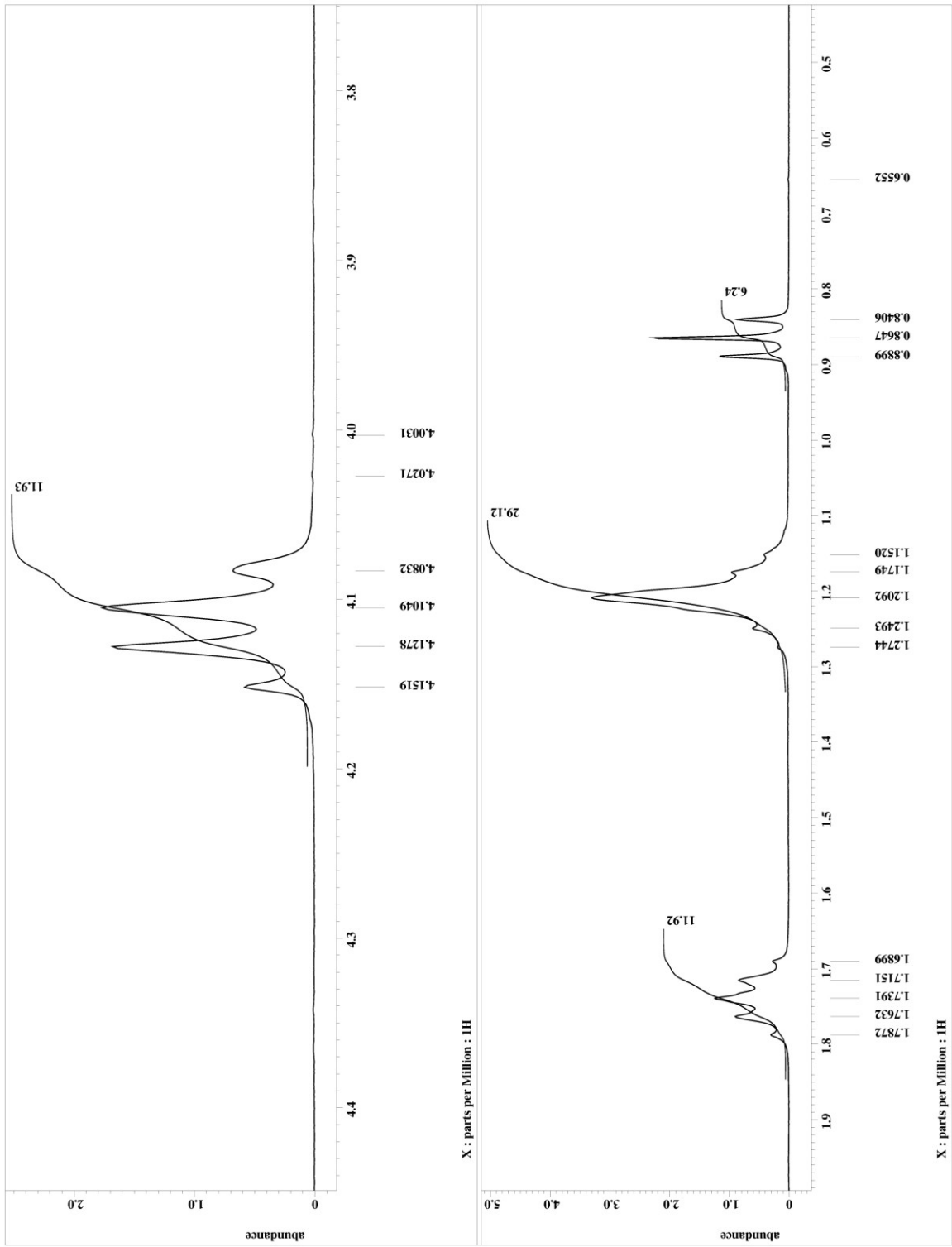


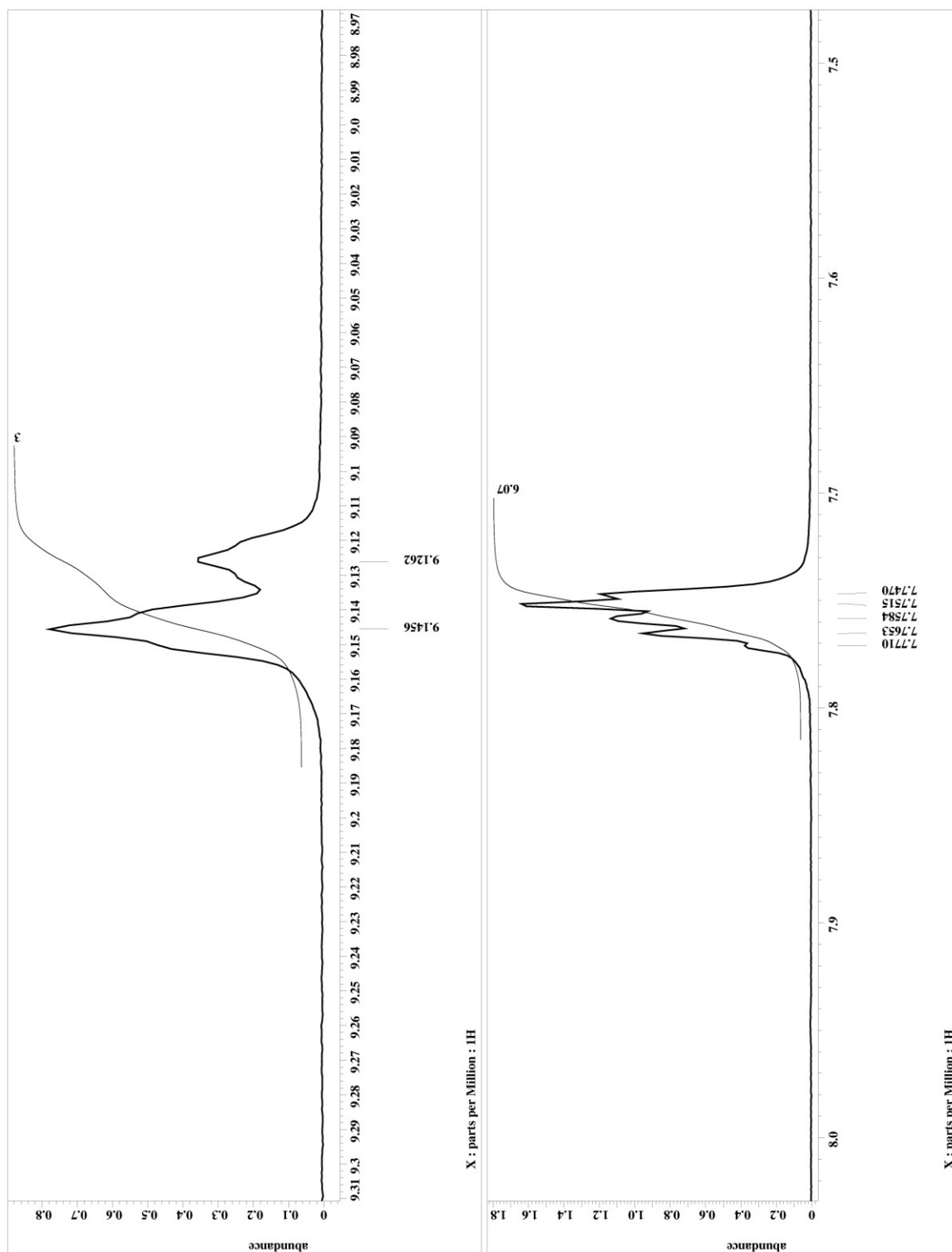
APPENDIX 5

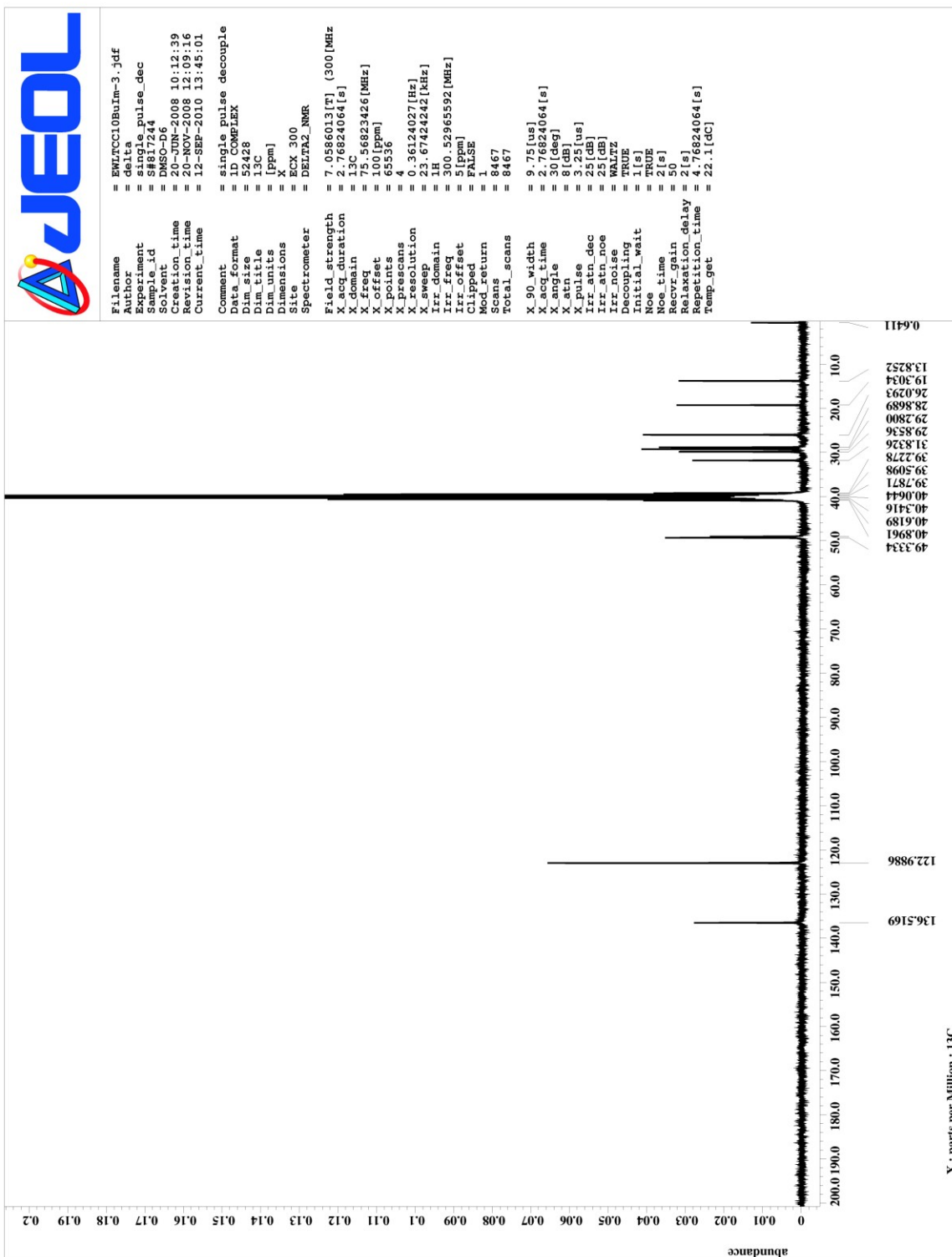
¹H AND ¹³C NMR SPECTRA OF

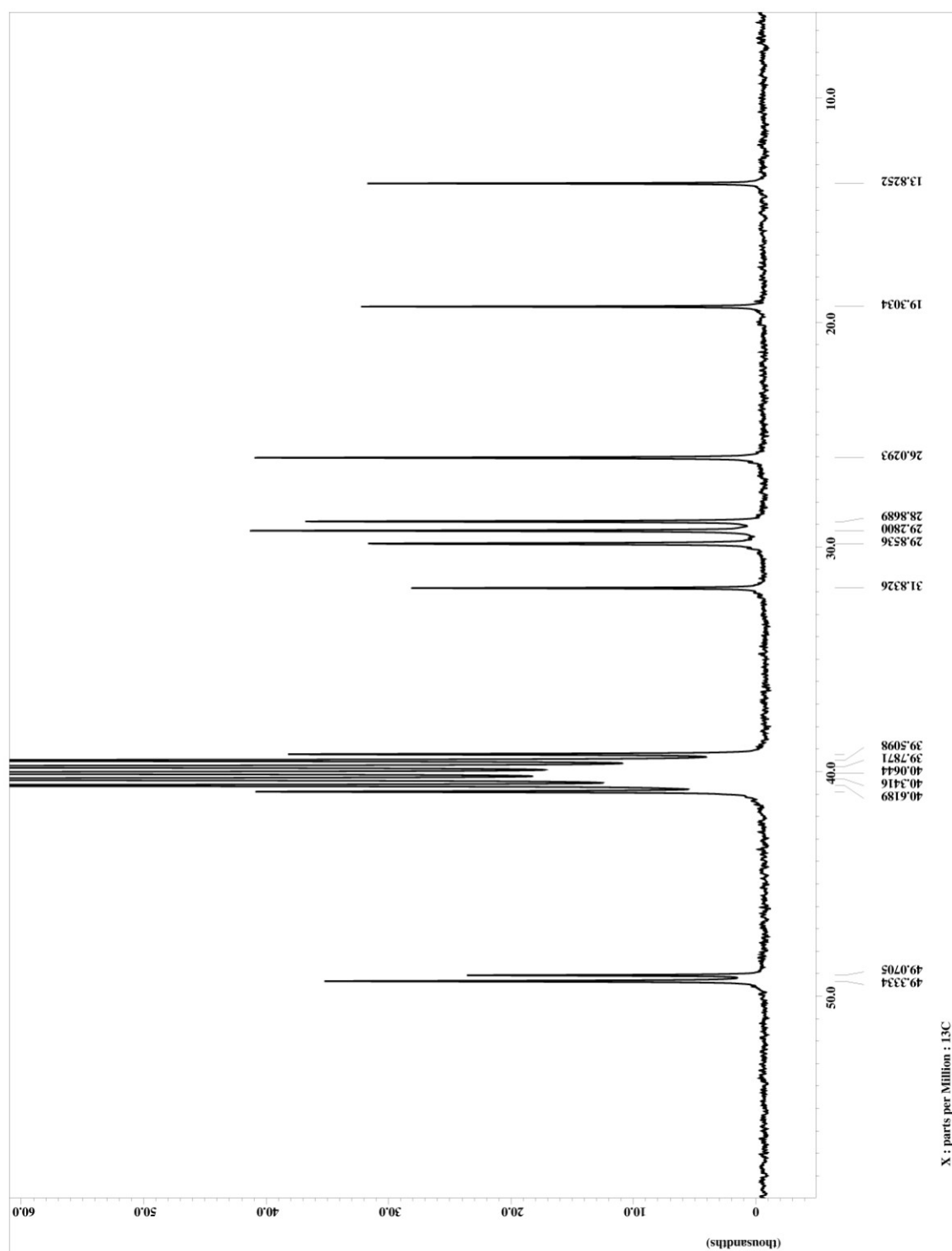
1-(1'-BUTYL-3'-DECYLIMIDAZOLIUM)-3-(1"-BUTYL-3"-
DECYLIMIDAZOLIUM)IMIDAZOLIUM TRI
[BIS(TRIFLUOROMETHANESULFONYL)IMIDE] (2b)







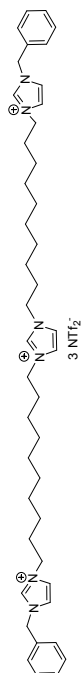
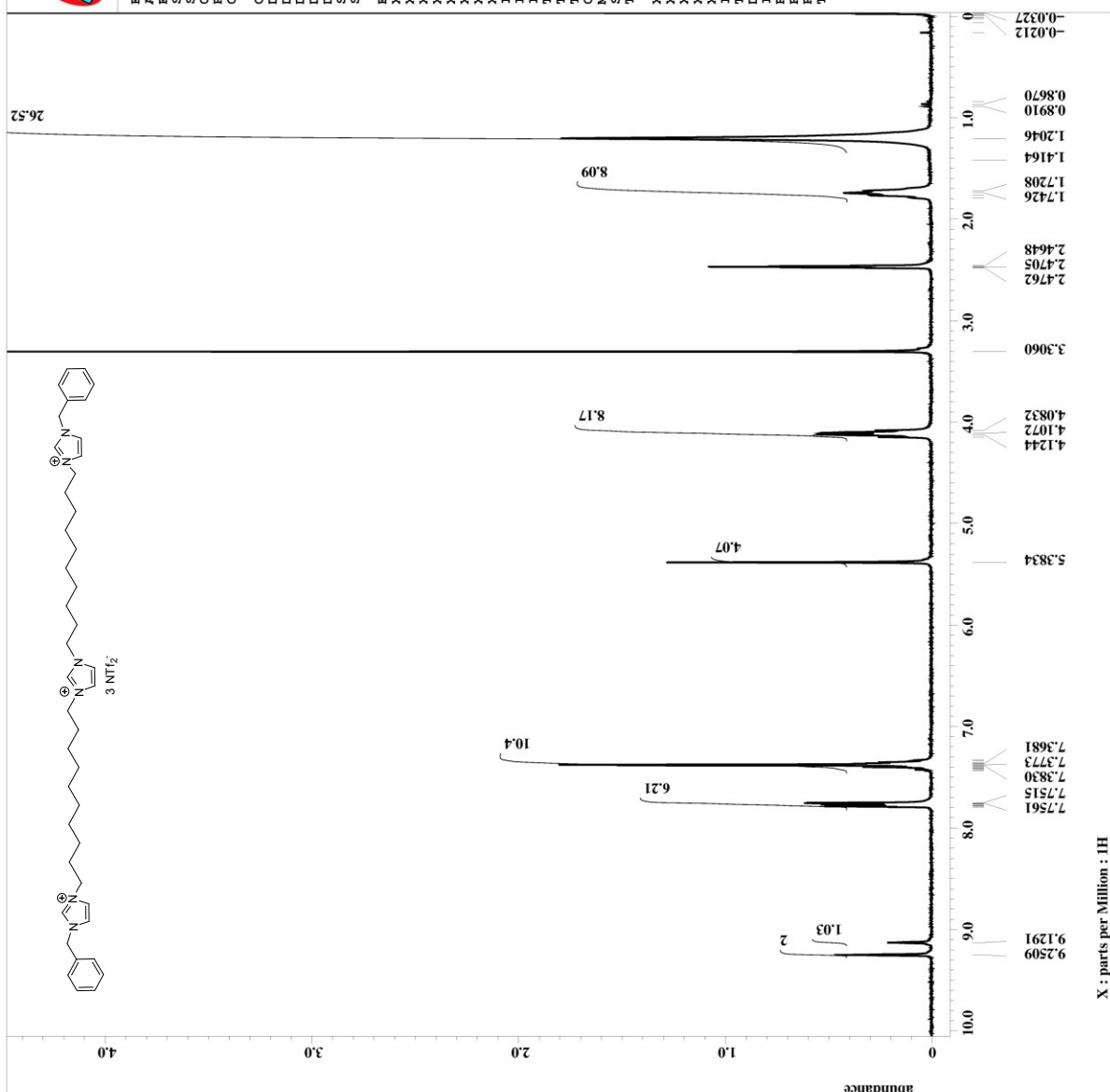




APPENDIX 6

¹H AND ¹³C NMR SPECTRA OF

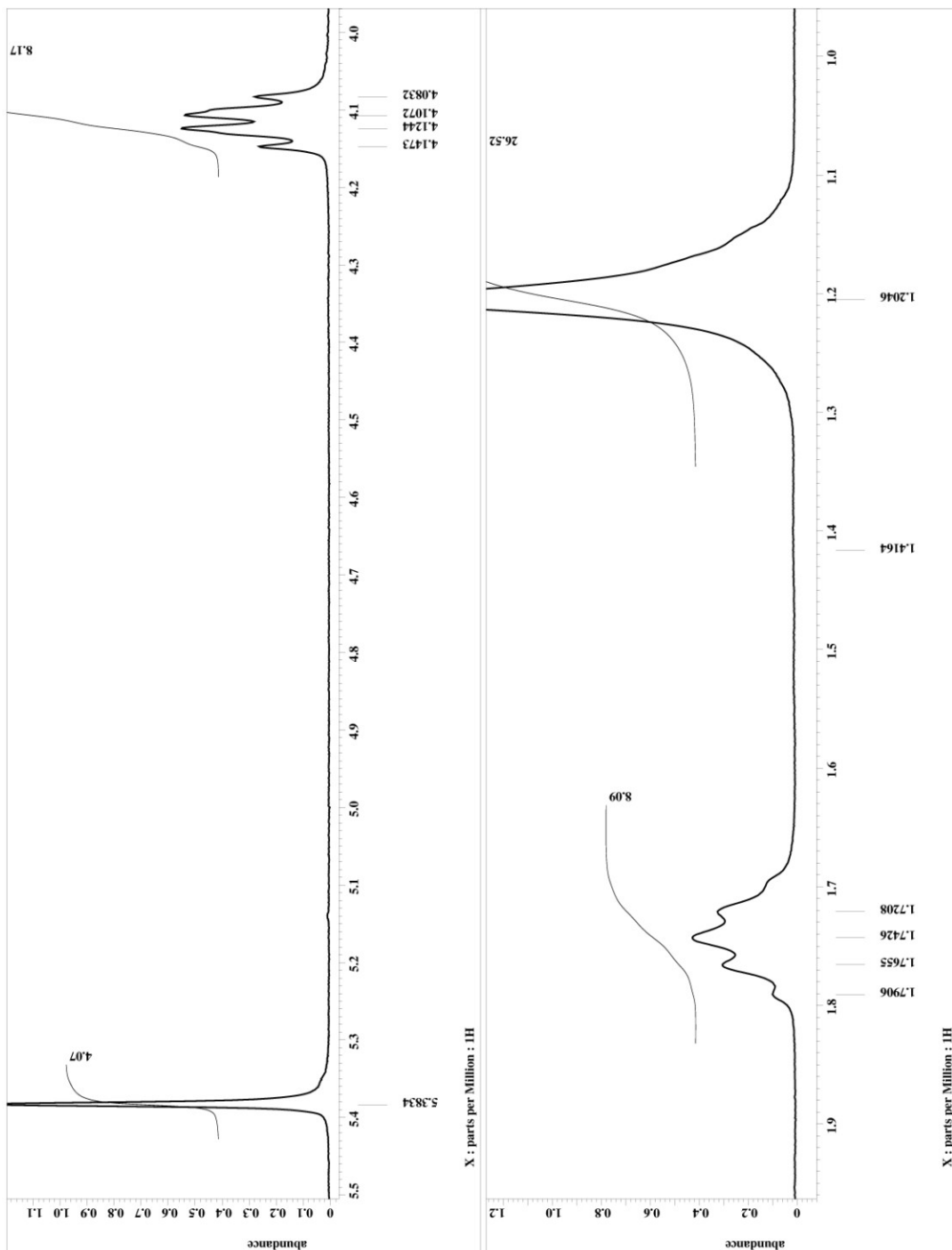
1-(1'-BENZYL-3'-DECYLIMIDAZOLIUM)-3-(1"-BENZYL-3"-
DECYLIMIDAZOLIUM)IMIDAZOLIUM TRI
[BIS(TRIFLUOROMETHANESULFONYL)IMIDE] (2c)

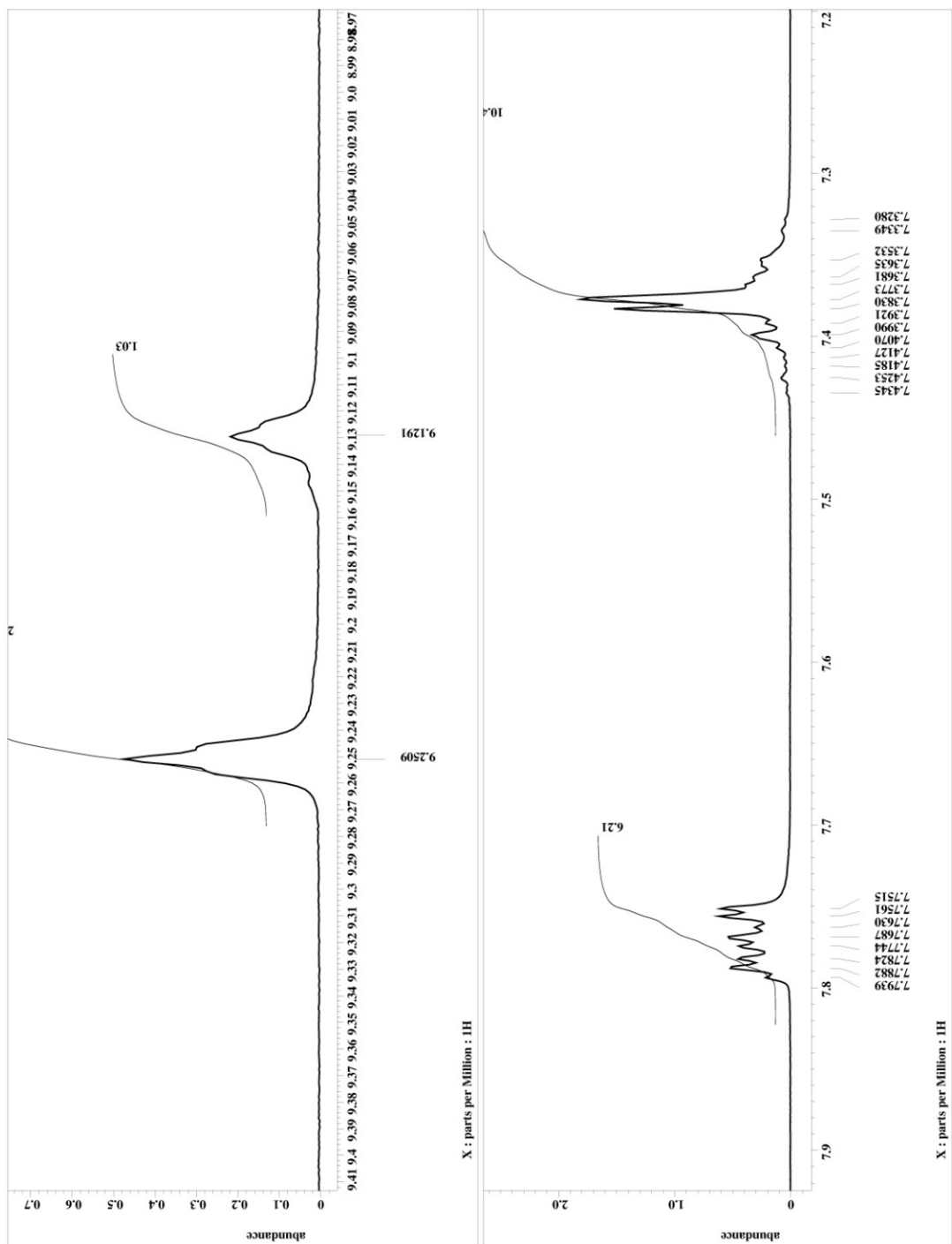
 3 NTf_2^- 

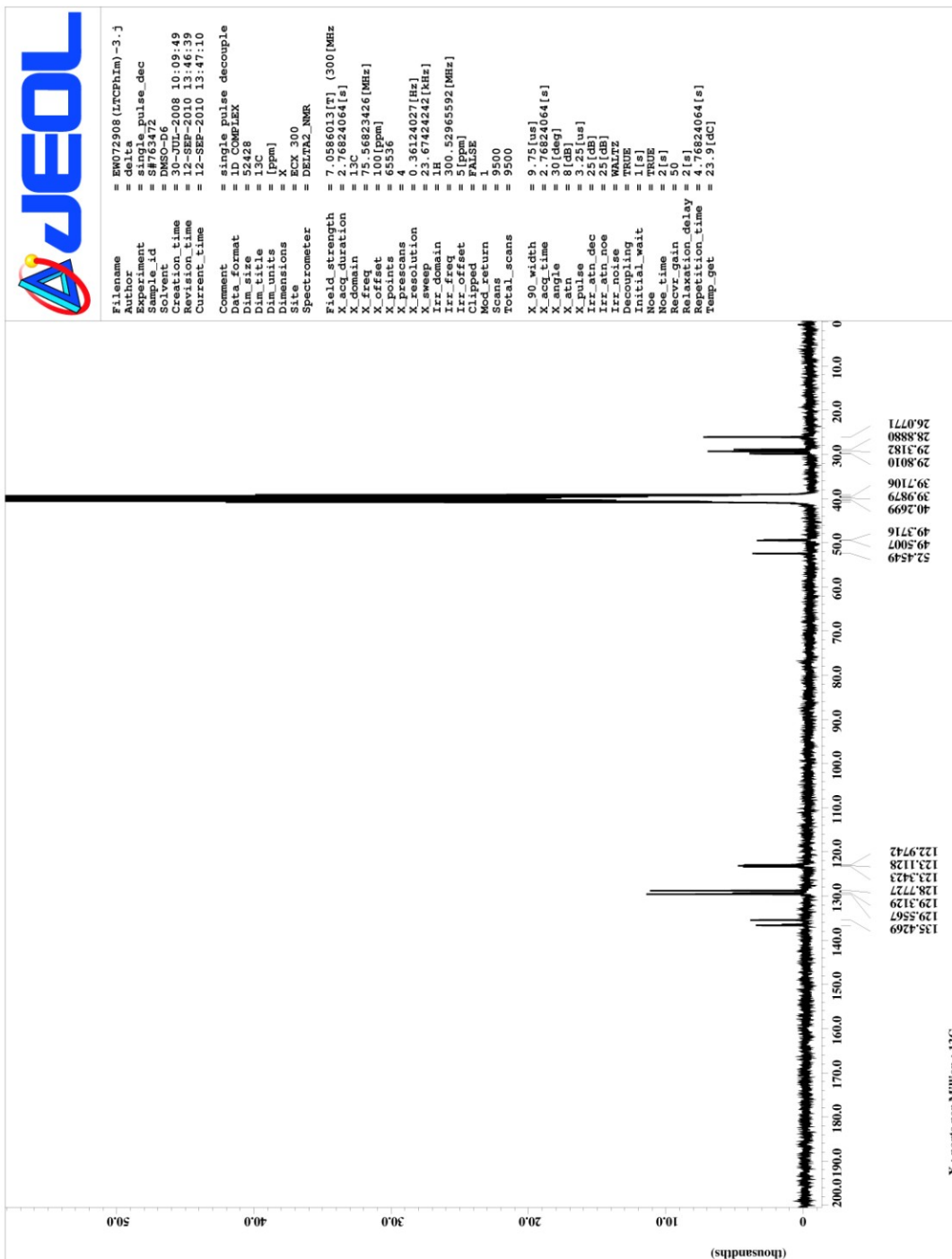
X : parts per Million : 1H

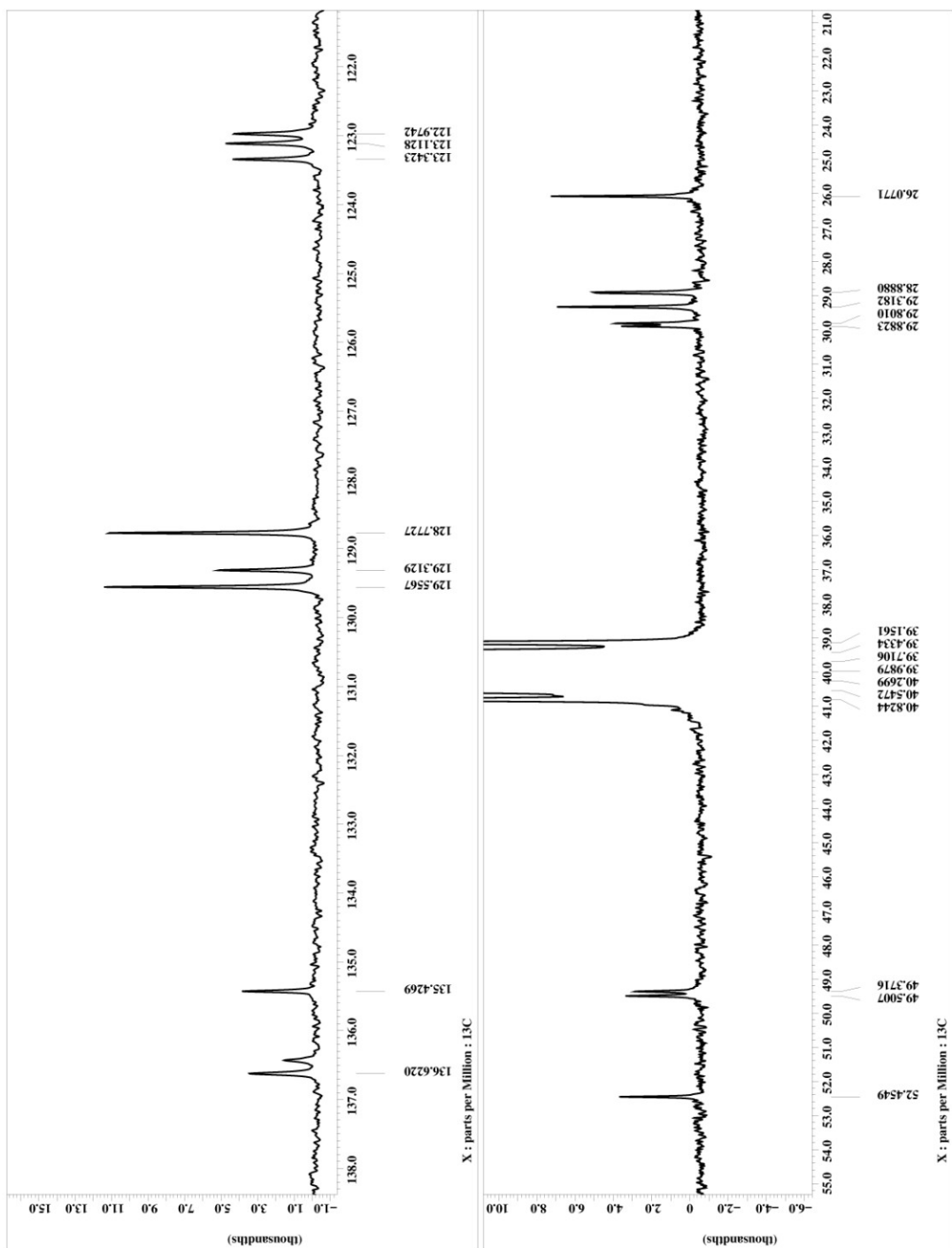


Filename	=	EW072808.LTCC10P1m
Sample name	=	single_pulse
Experiment	=	single_pulse.ex2
Sample id	=	SF688126
Solvent	=	DMSO-d6
Creation time	=	28-JUL-2008 19:29:24
Revision time	=	12-SEP-2010 13:38:24
Current time	=	12-SEP-2010 13:38:44
Comment	=	single-pulse
Data format	=	1D COMPLEX
Dim size	=	13107
Dim title	=	1H
Dim units	=	[ppm]
Dimensions	=	CX3 300
Site	=	CX3 300
Spectrometer	=	DELTA2_NMR
Field strength	=	7.0586013[T] 300 [MHz]
X acq duration	=	2.90717696[s]
X domain	=	1H
X freq	=	300.52965592 [MHz]
X offset	=	5 [ppm]
X points	=	16384
X prescans	=	0
X resolution	=	0.34397631 [Hz]
X sweep	=	1H
Y1 domain	=	5.63570784 [kHz]
Y1 freq	=	300.52965592 [MHz]
Y1 offset	=	5 [ppm]
Y1 points	=	16384
Y1 prescans	=	0
Y1 resolution	=	0.34397631 [Hz]
Y1 sweep	=	1H
Y2 domain	=	5.63570784 [kHz]
Y2 freq	=	300.52965592 [MHz]
Y2 offset	=	5 [ppm]
Y2 points	=	16384
Y2 prescans	=	0
Y2 resolution	=	0.34397631 [Hz]
Y2 sweep	=	1H
Y3 domain	=	5.63570784 [kHz]
Y3 freq	=	300.52965592 [MHz]
Y3 offset	=	5 [ppm]
Y3 points	=	16384
Y3 prescans	=	0
Y3 resolution	=	0.34397631 [Hz]
Y3 sweep	=	1H
Y4 domain	=	5.63570784 [kHz]
Y4 freq	=	300.52965592 [MHz]
Y4 offset	=	5 [ppm]
Y4 points	=	16384
Y4 prescans	=	0
Y4 resolution	=	0.34397631 [Hz]
Y4 sweep	=	1H
Y5 domain	=	5.63570784 [kHz]
Y5 freq	=	300.52965592 [MHz]
Y5 offset	=	5 [ppm]
Y5 points	=	16384
Y5 prescans	=	0
Y5 resolution	=	0.34397631 [Hz]
Y5 sweep	=	1H
Y6 domain	=	5.63570784 [kHz]
Y6 freq	=	300.52965592 [MHz]
Y6 offset	=	5 [ppm]
Y6 points	=	16384
Y6 prescans	=	0
Y6 resolution	=	0.34397631 [Hz]
Y6 sweep	=	1H
Y7 domain	=	5.63570784 [kHz]
Y7 freq	=	300.52965592 [MHz]
Y7 offset	=	5 [ppm]
Y7 points	=	16384
Y7 prescans	=	0
Y7 resolution	=	0.34397631 [Hz]
Y7 sweep	=	1H
Y8 domain	=	5.63570784 [kHz]
Y8 freq	=	300.52965592 [MHz]
Y8 offset	=	5 [ppm]
Y8 points	=	16384
Y8 prescans	=	0
Y8 resolution	=	0.34397631 [Hz]
Y8 sweep	=	1H
Y9 domain	=	5.63570784 [kHz]
Y9 freq	=	300.52965592 [MHz]
Y9 offset	=	5 [ppm]
Y9 points	=	16384
Y9 prescans	=	0
Y9 resolution	=	0.34397631 [Hz]
Y9 sweep	=	1H
Y10 domain	=	5.63570784 [kHz]
Y10 freq	=	300.52965592 [MHz]
Y10 offset	=	5 [ppm]
Y10 points	=	16384
Y10 prescans	=	0
Y10 resolution	=	0.34397631 [Hz]
Y10 sweep	=	1H
Y11 domain	=	5.63570784 [kHz]
Y11 freq	=	300.52965592 [MHz]
Y11 offset	=	5 [ppm]
Y11 points	=	16384
Y11 prescans	=	0
Y11 resolution	=	0.34397631 [Hz]
Y11 sweep	=	1H
Y12 domain	=	5.63570784 [kHz]
Y12 freq	=	300.52965592 [MHz]
Y12 offset	=	5 [ppm]
Y12 points	=	16384
Y12 prescans	=	0
Y12 resolution	=	0.34397631 [Hz]
Y12 sweep	=	1H
Y13 domain	=	5.63570784 [kHz]
Y13 freq	=	300.52965592 [MHz]
Y13 offset	=	5 [ppm]
Y13 points	=	16384
Y13 prescans	=	0
Y13 resolution	=	0.34397631 [Hz]
Y13 sweep	=	1H
Y14 domain	=	5.63570784 [kHz]
Y14 freq	=	300.52965592 [MHz]
Y14 offset	=	5 [ppm]
Y14 points	=	16384
Y14 prescans	=	0
Y14 resolution	=	0.34397631 [Hz]
Y14 sweep	=	1H
Y15 domain	=	5.63570784 [kHz]
Y15 freq	=	300.52965592 [MHz]
Y15 offset	=	5 [ppm]
Y15 points	=	16384
Y15 prescans	=	0
Y15 resolution	=	0.34397631 [Hz]
Y15 sweep	=	1H
Y16 domain	=	5.63570784 [kHz]
Y16 freq	=	300.52965592 [MHz]
Y16 offset	=	5 [ppm]
Y16 points	=	16384</





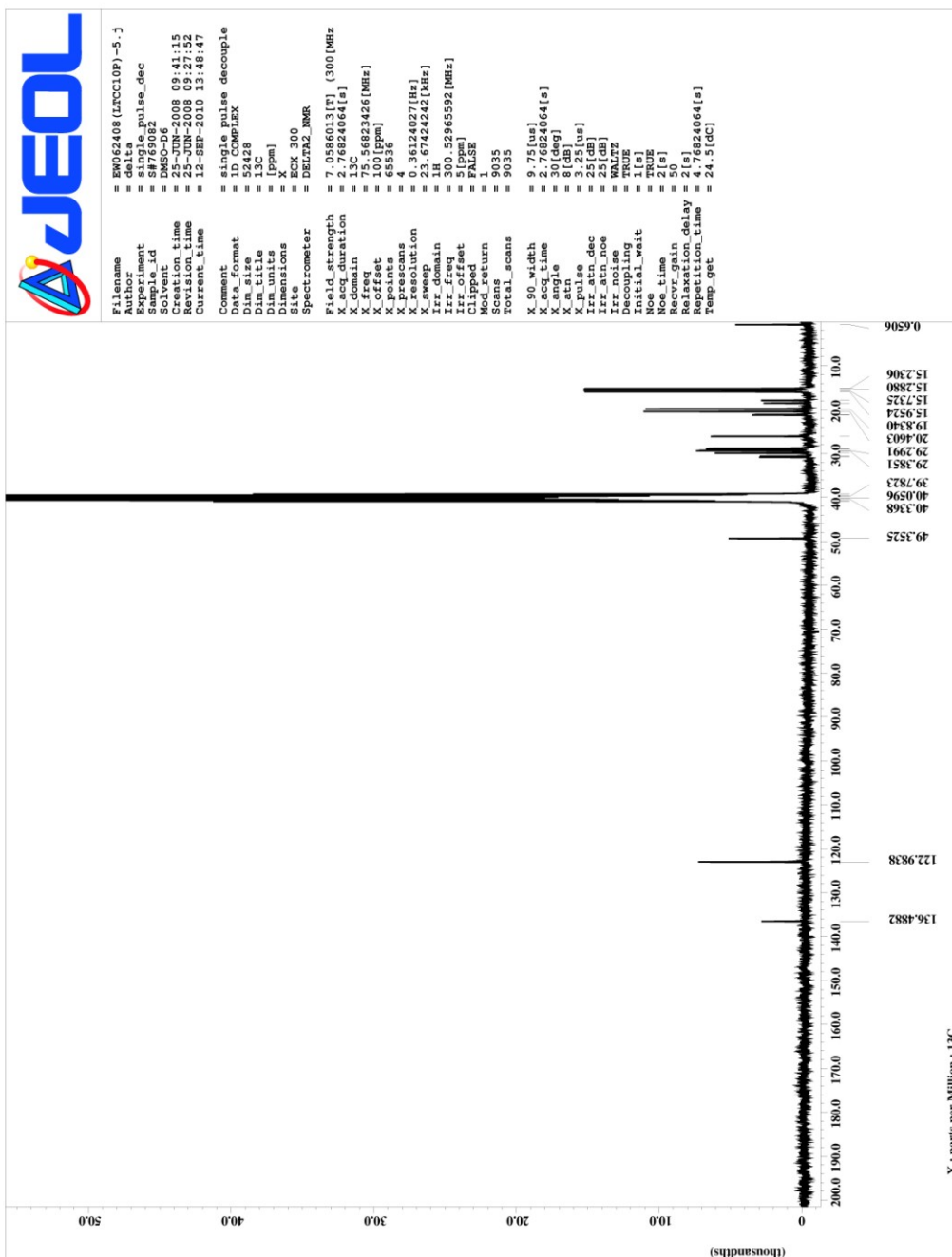


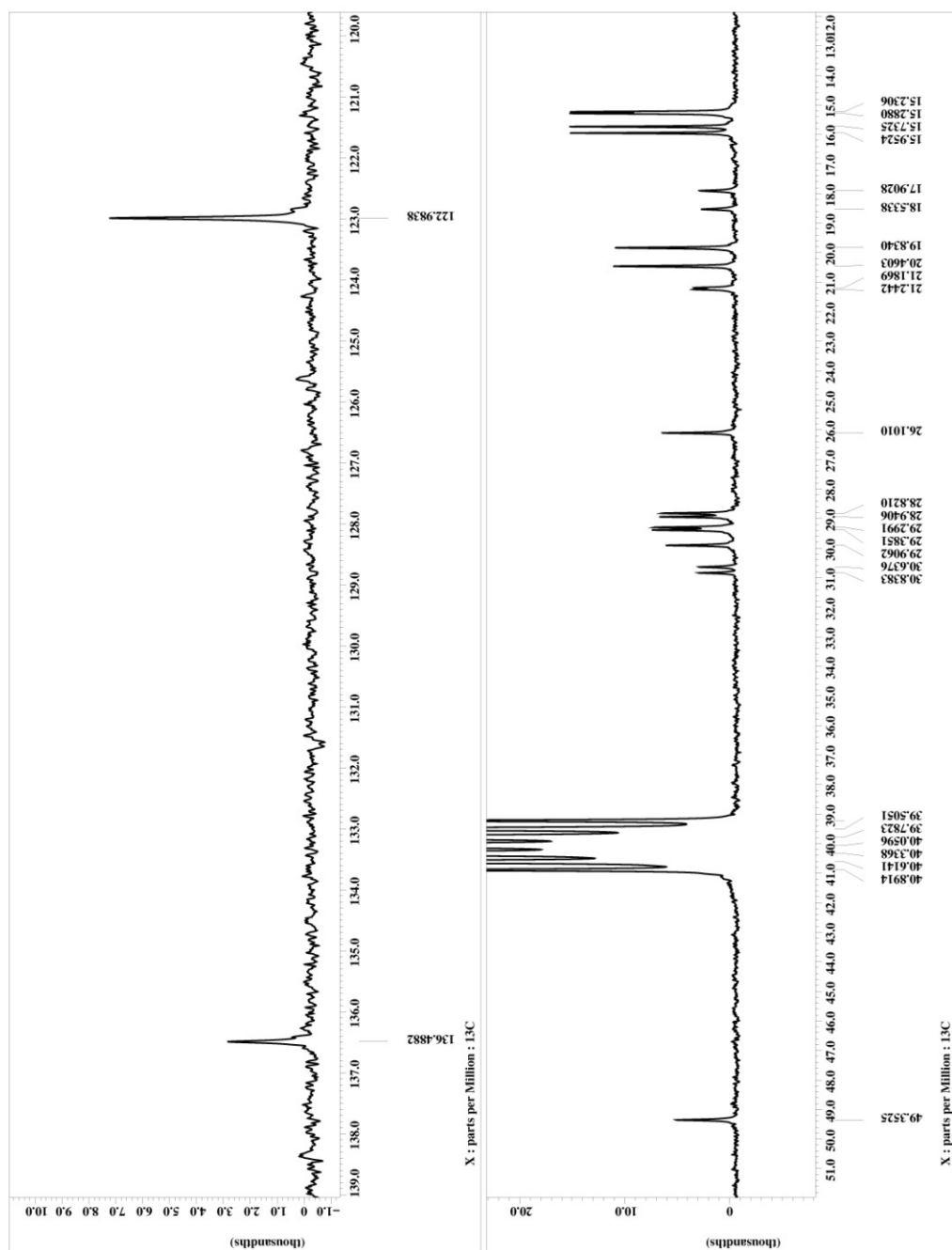


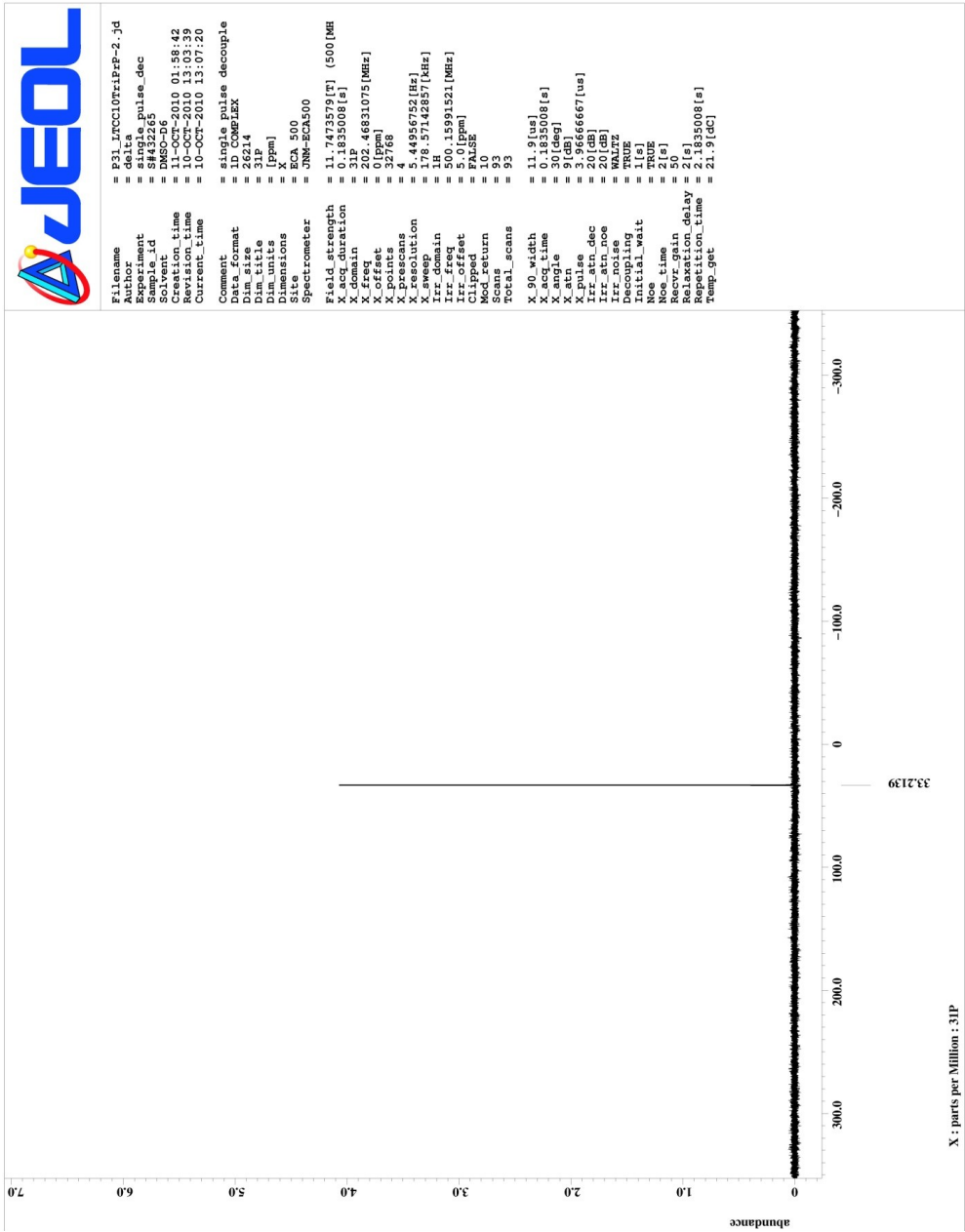
APPENDIX 7

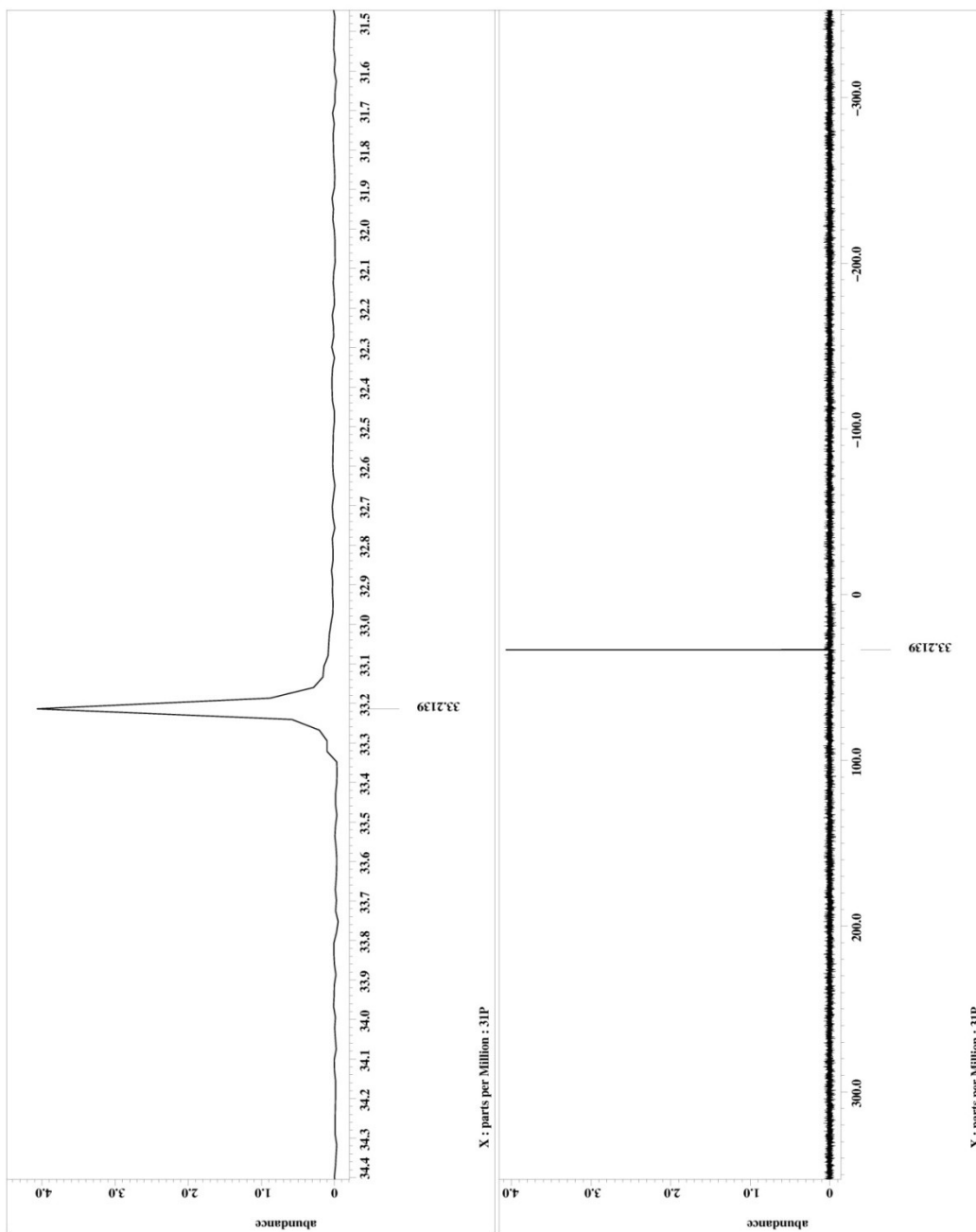
^1H , ^{13}C AND ^{31}P NMR SPECTRA OF

1-DECYLTRIPROPYLPHOSPHONIUM-3-DECYLTRIPROPYLPHOSPHONIUM
IMIDAZOLIUM TRI [BIS(TRIFLUOROMETHANESULFONYL)IMIDE] (2d).





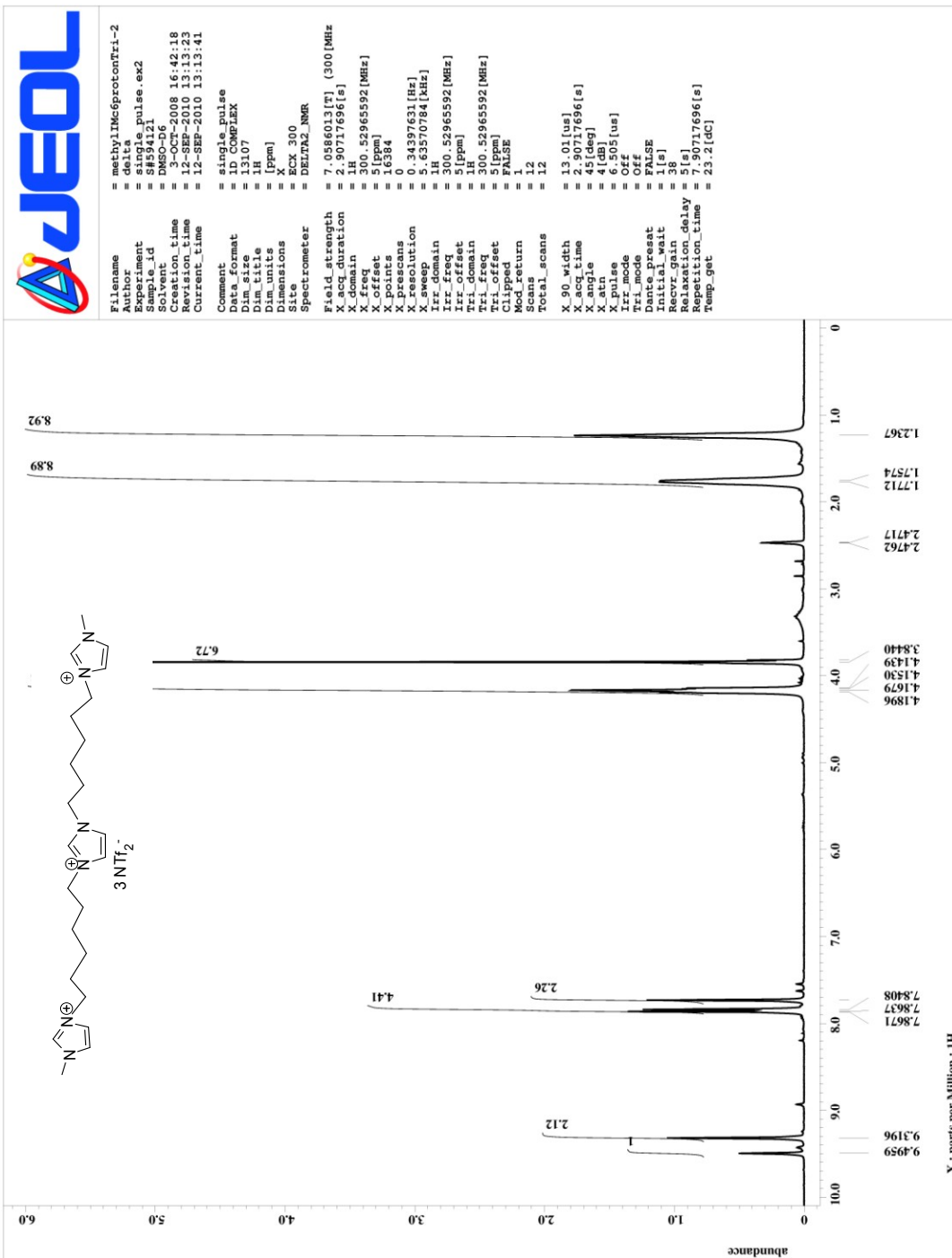


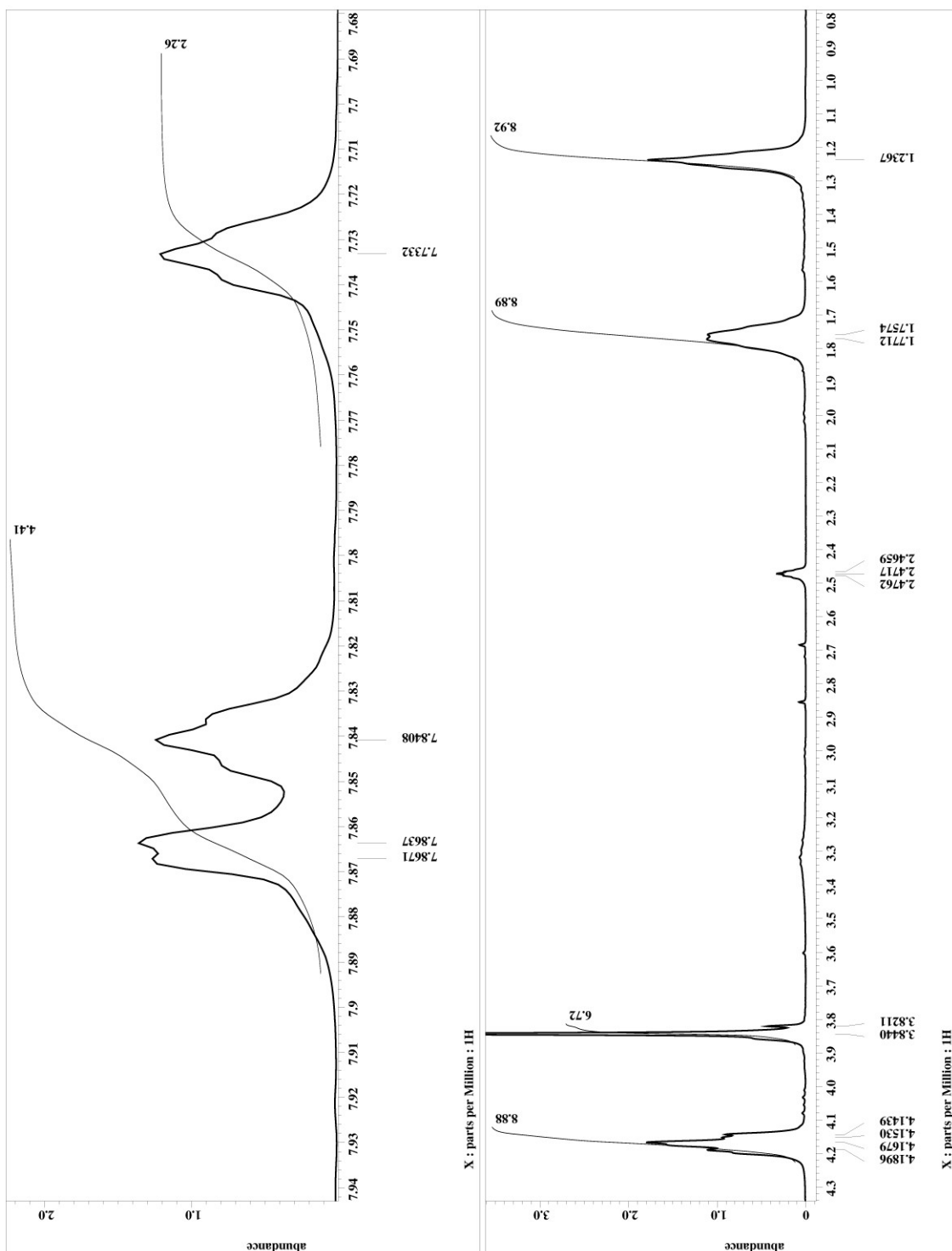


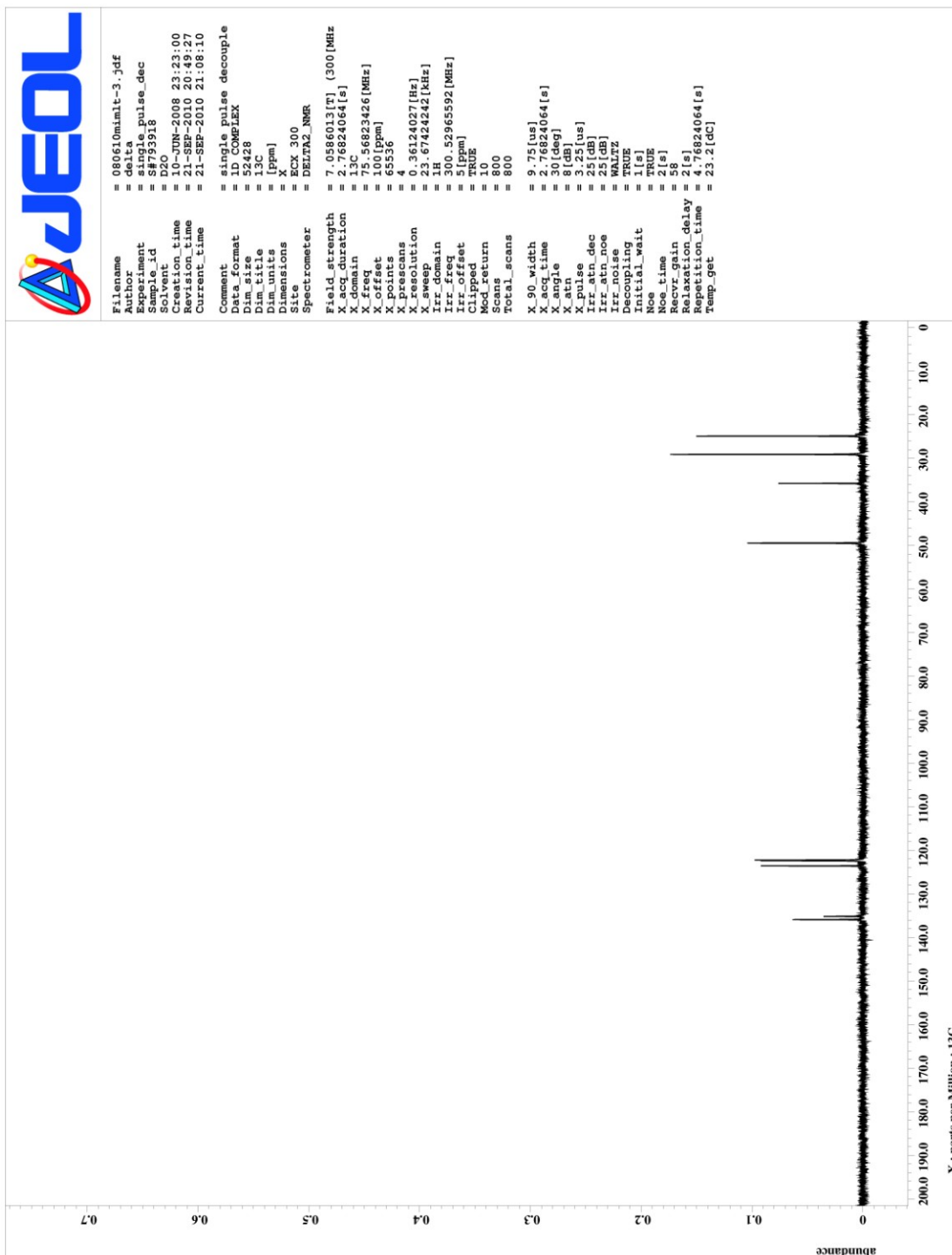
APPENDIX 8

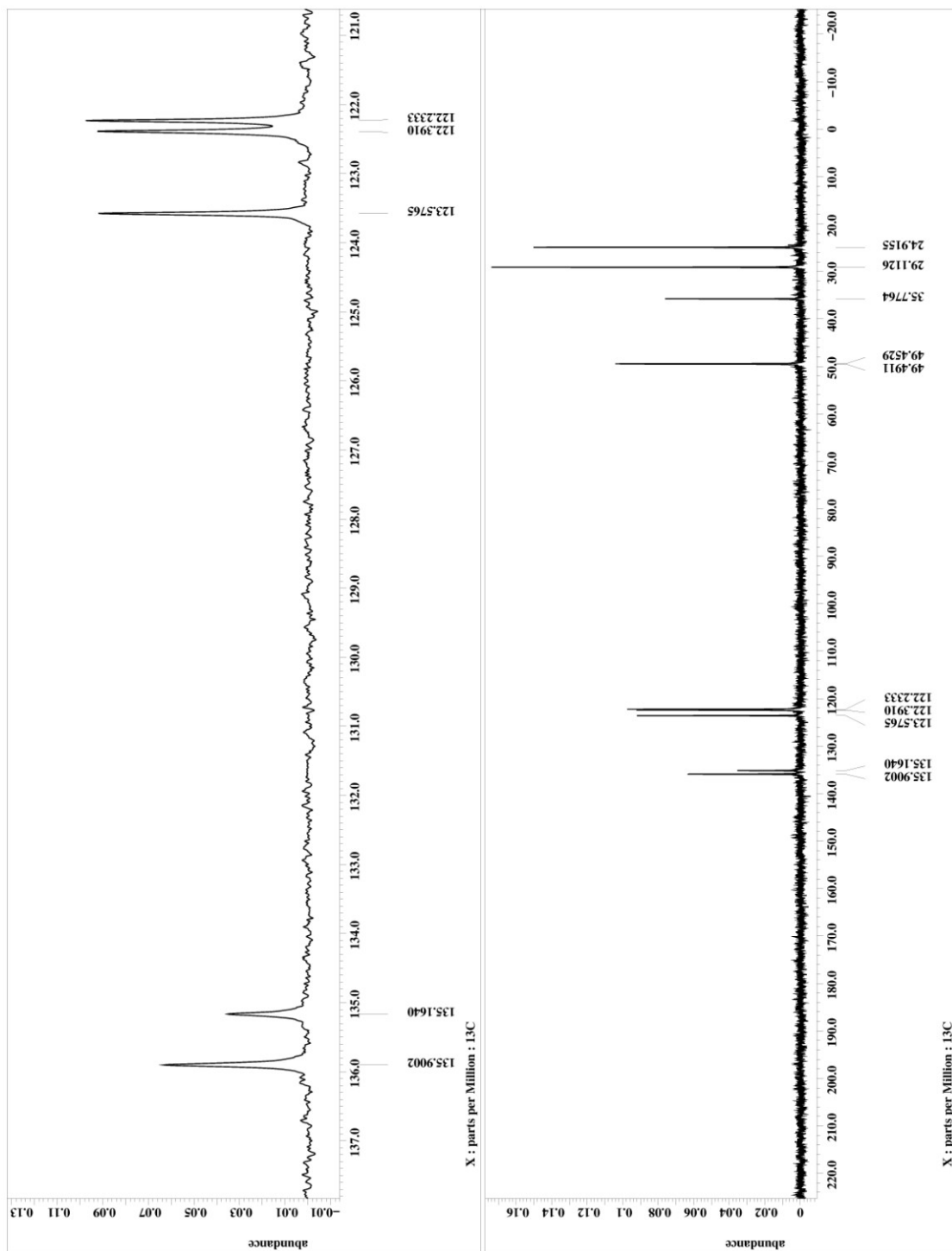
¹H AND ¹³C NMR SPECTRUM OF

1-(1'-METHYL-3'-HEXYLIMIDAZOLIUM)-3-(1''-METHYL-3''-
HEXYLIMIDAZOLIUM)IMIDAZOLIUM TRI
[BIS(TRIFLUOROMETHANESULFONYL)IMIDE] (3a).





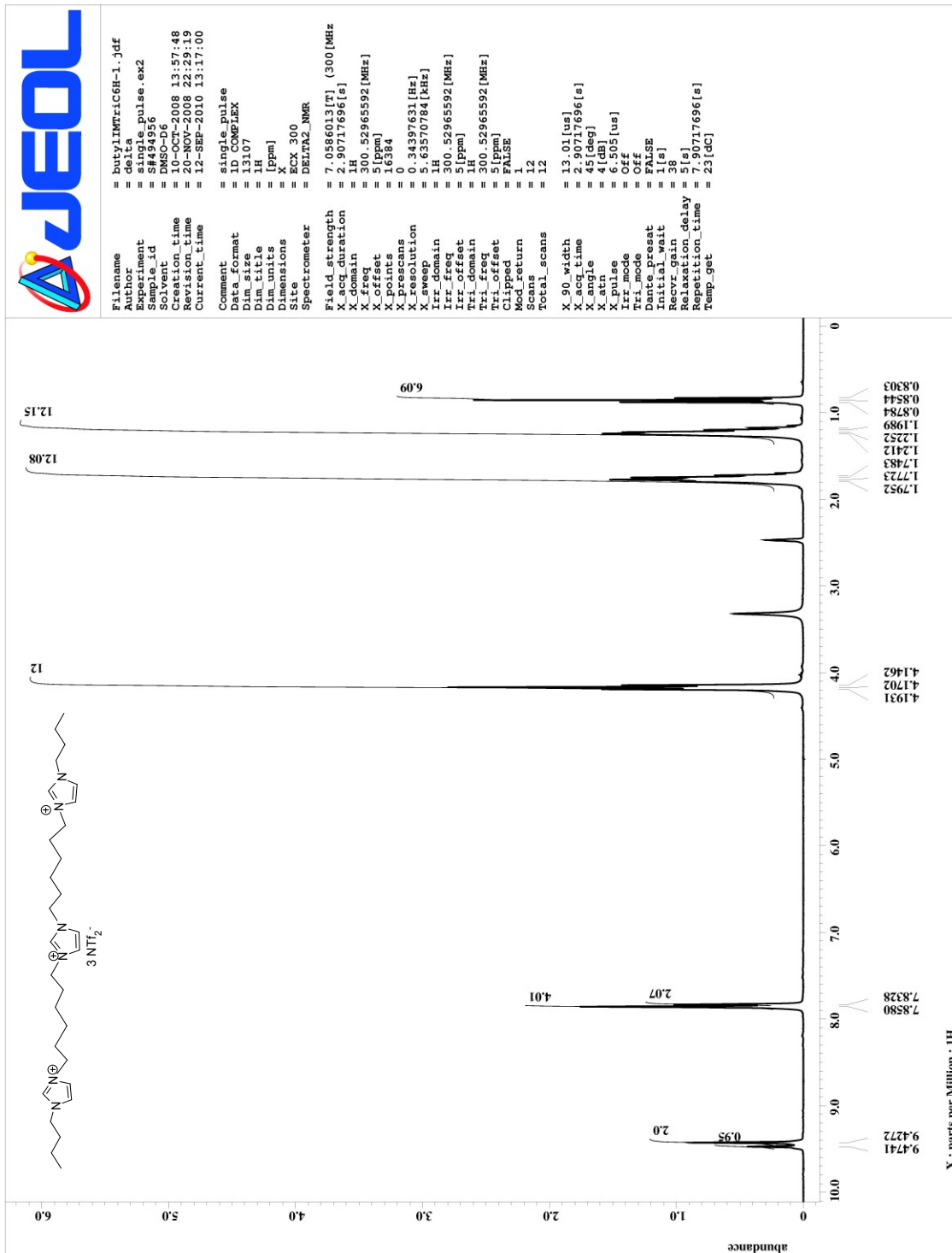


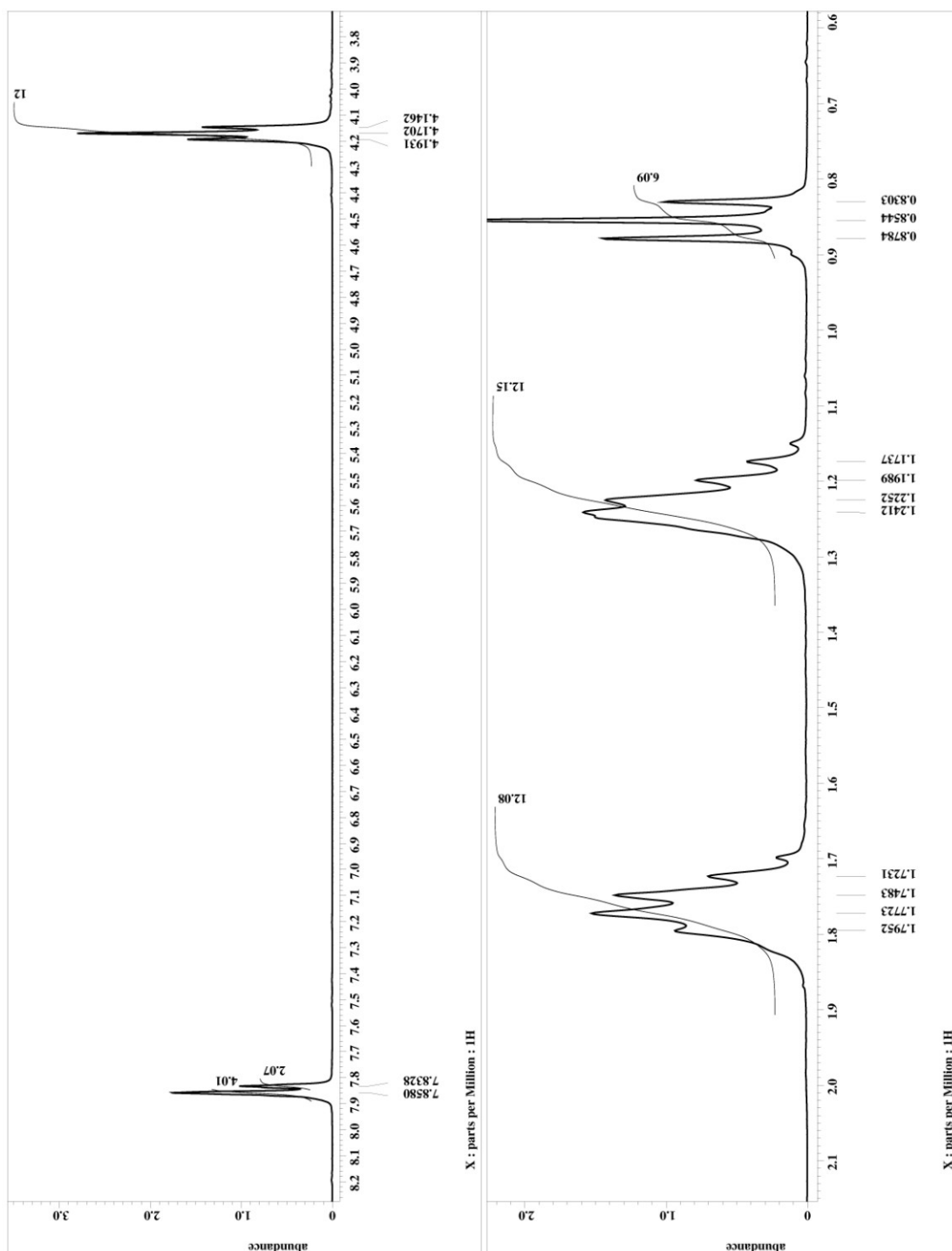


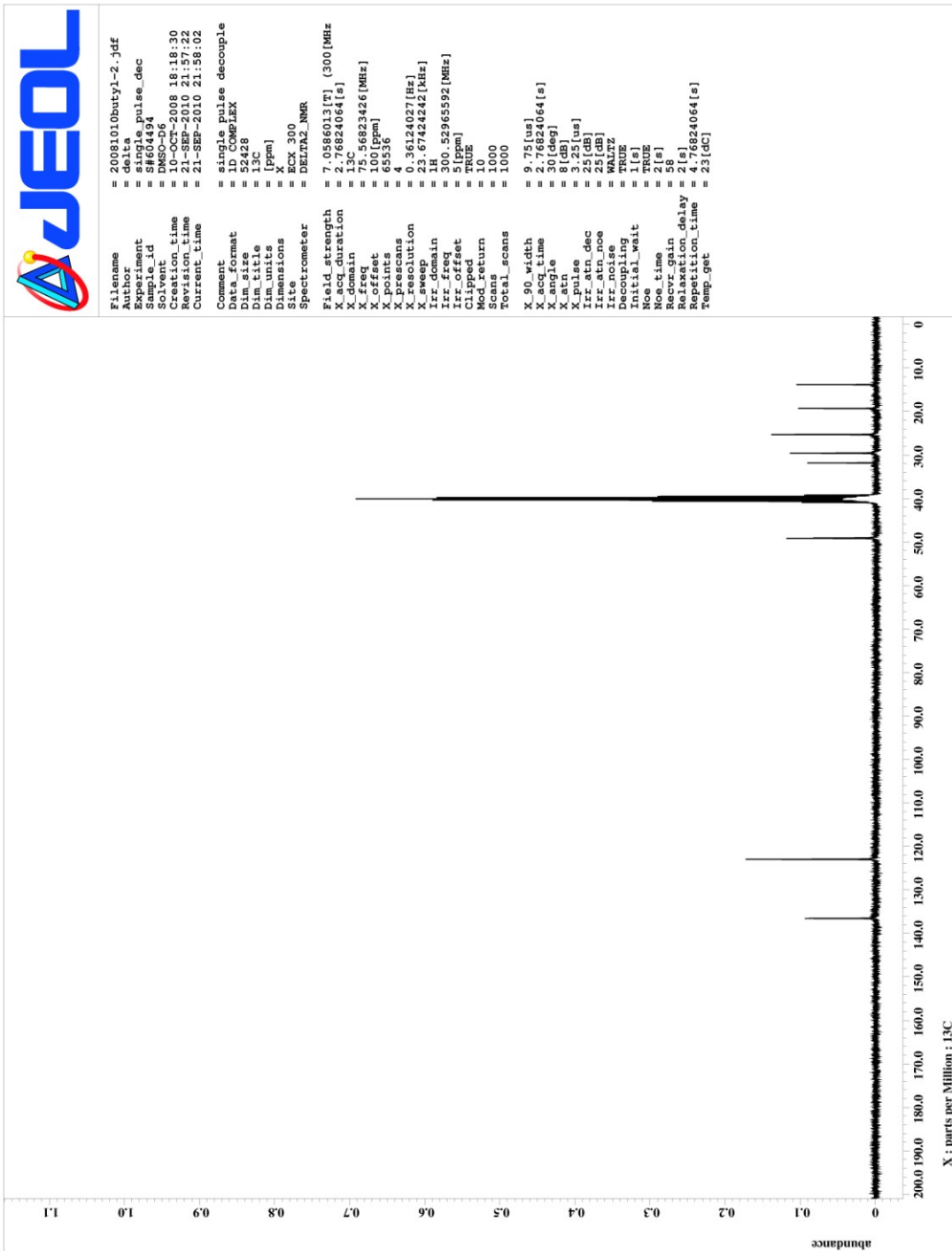
APPENDIX 9

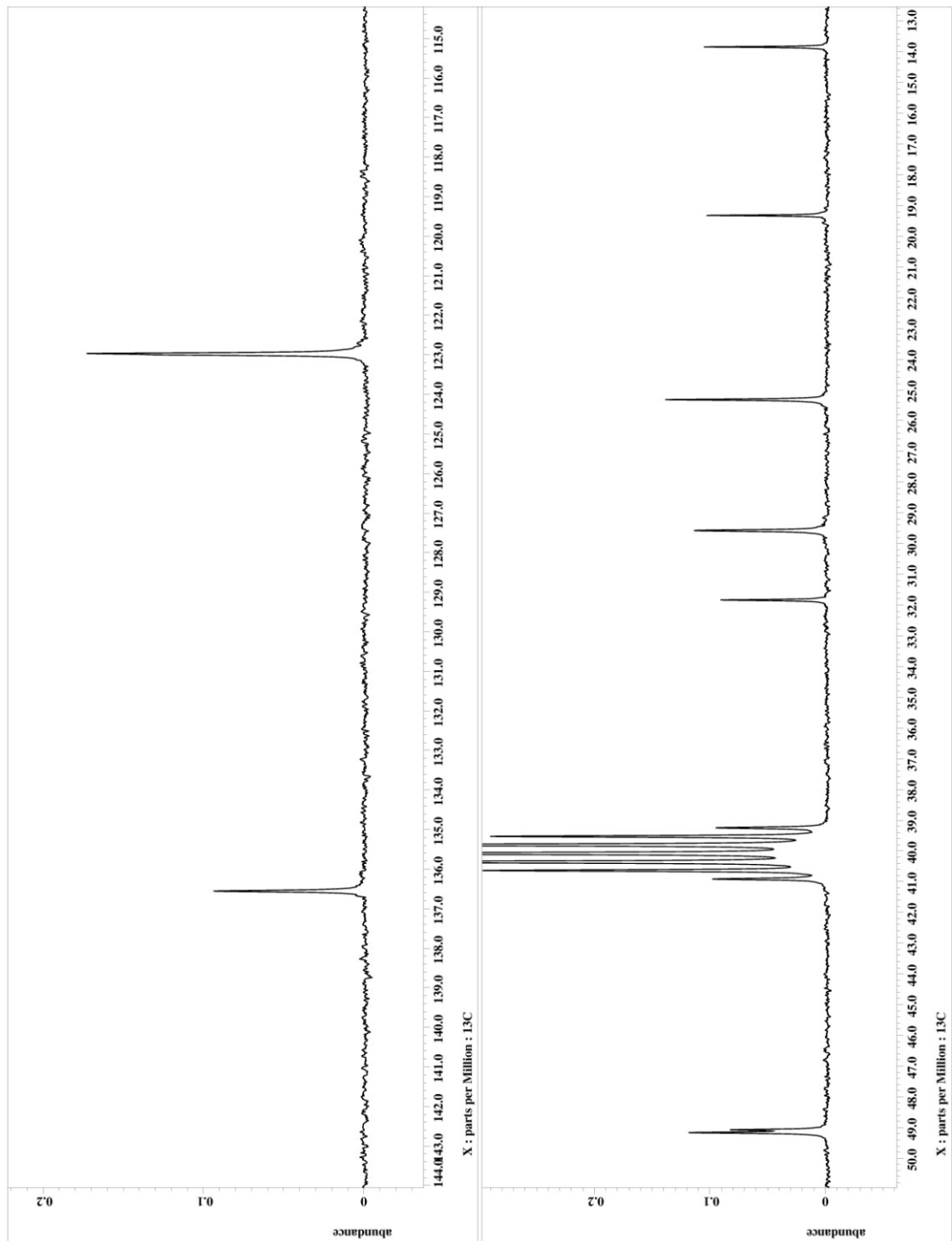
¹H NMR SPECTRUM OF

1-(1'-BUTYL-3'-HEXYLIMIDAZOLIUM)-3-(1''-BUTYL-3''-
HEXYLIMIDAZOLIUM)IMIDAZOLIUM TRI
[BIS(TRIFLUOROMETHANESULFONYL)IMIDE] (3b).



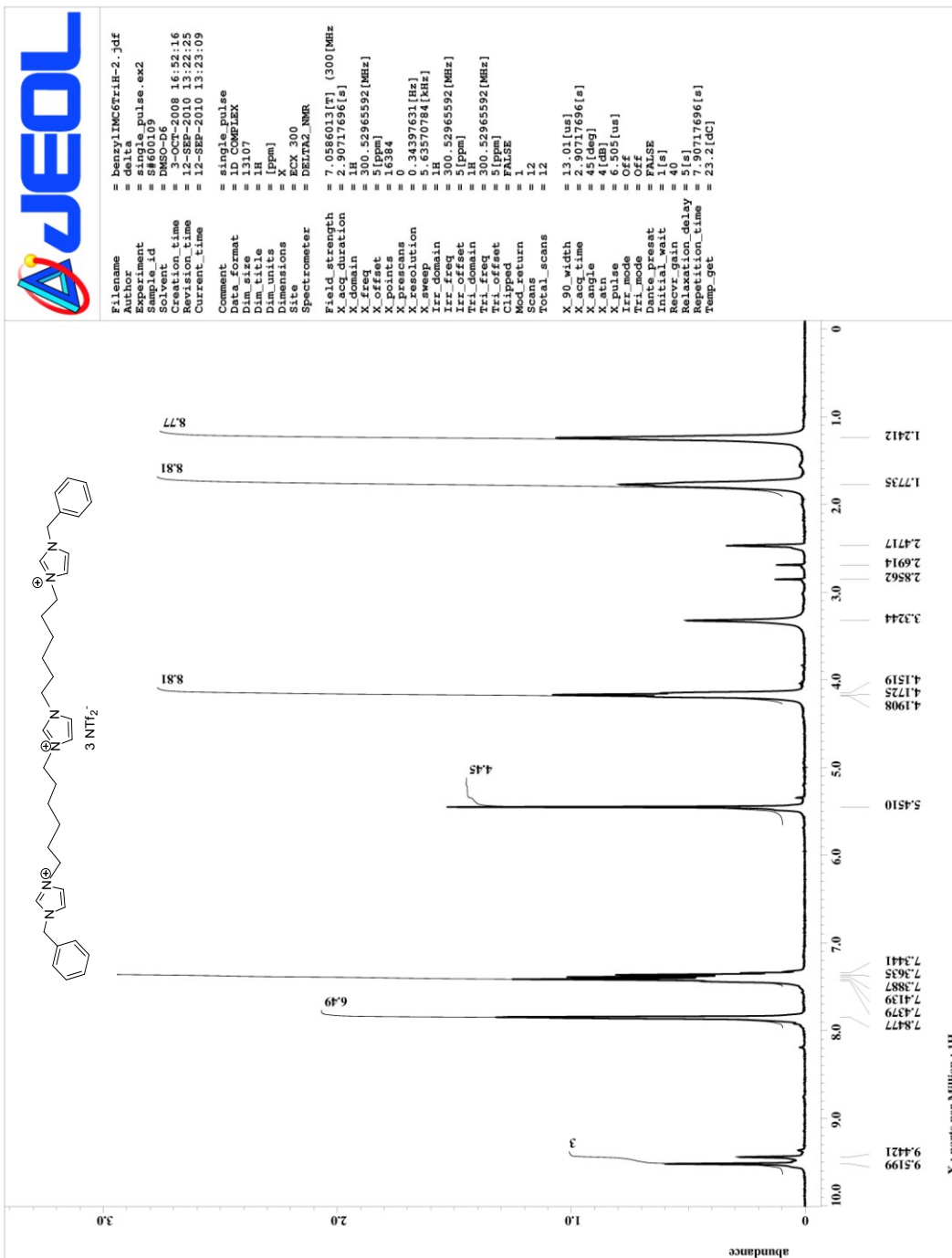


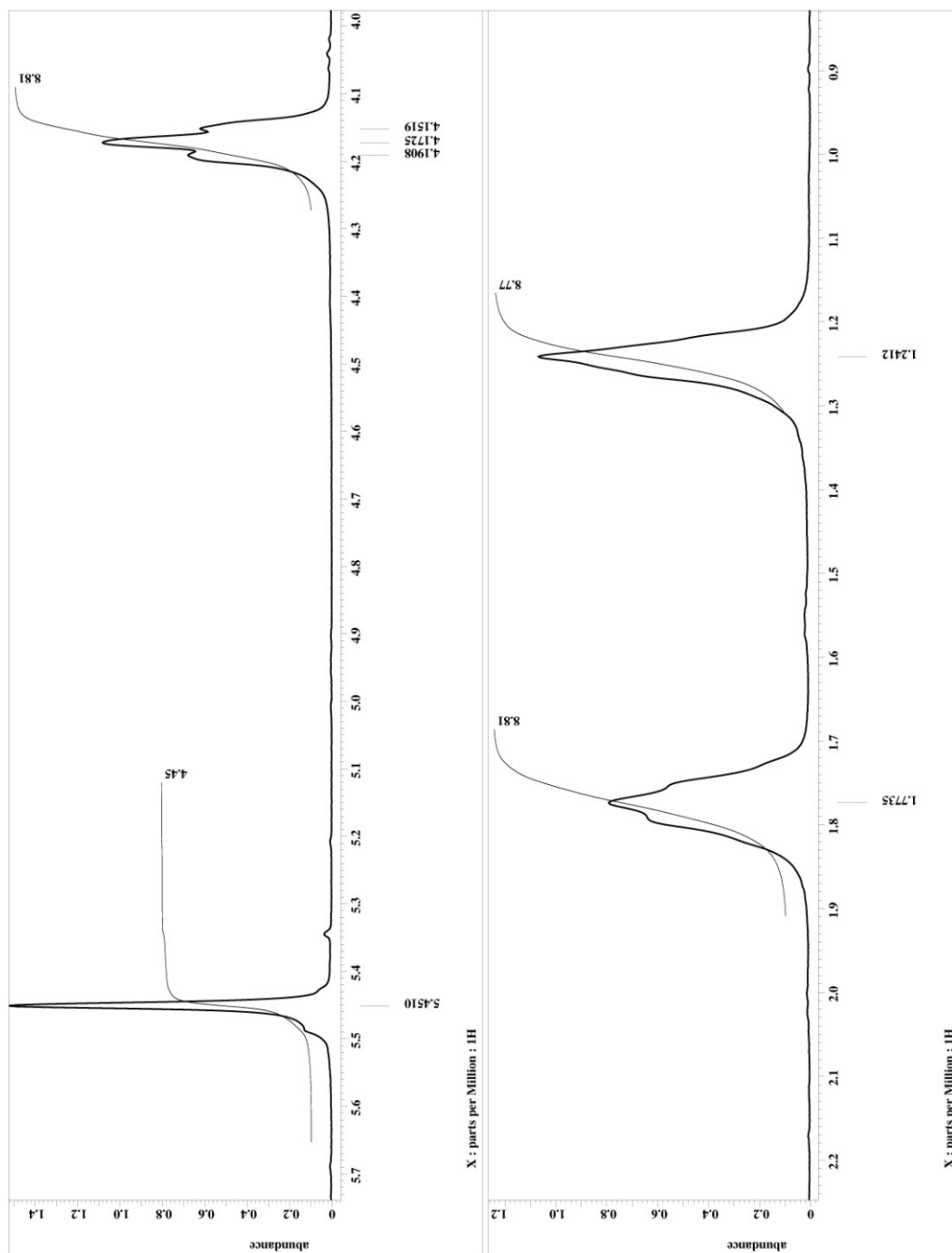


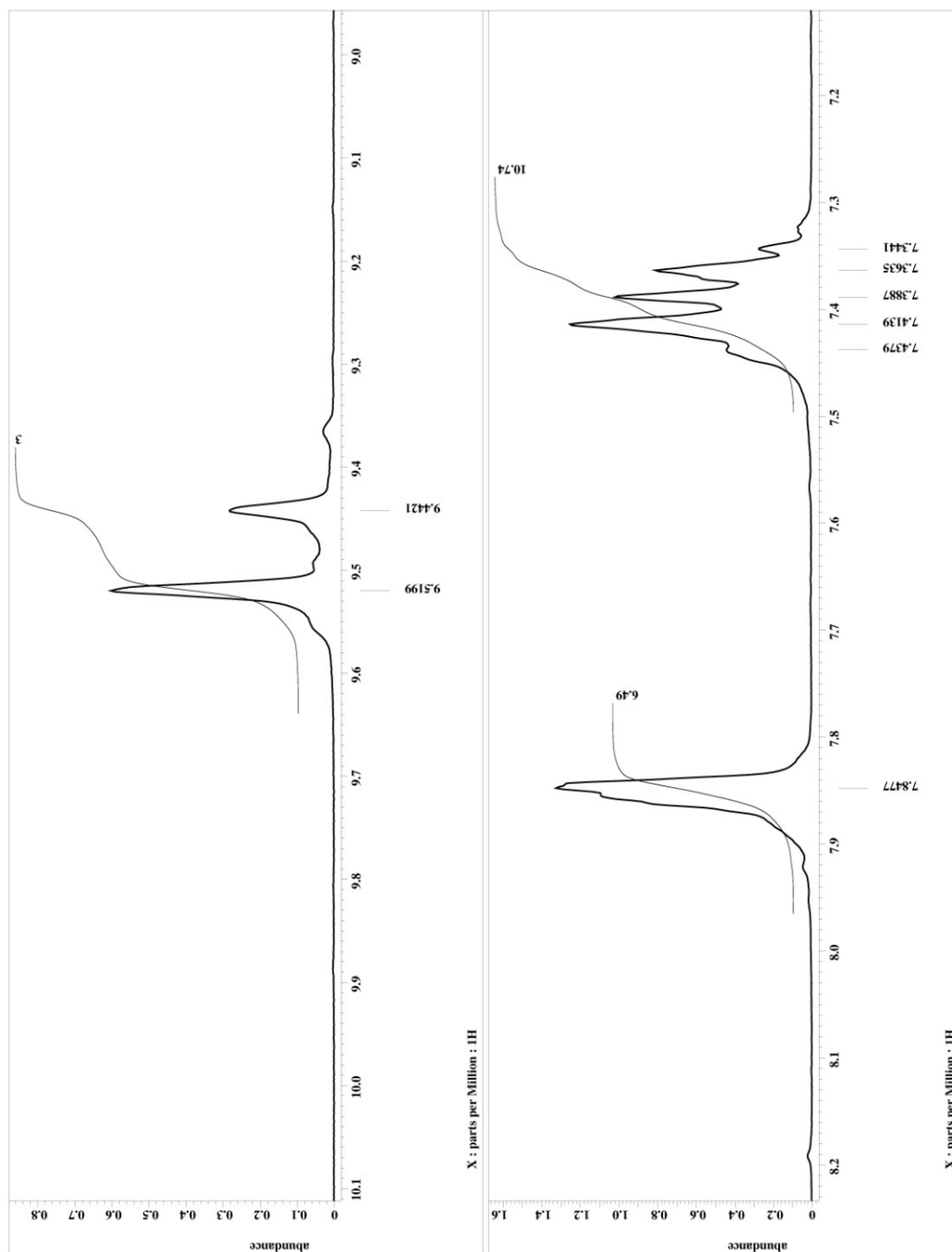


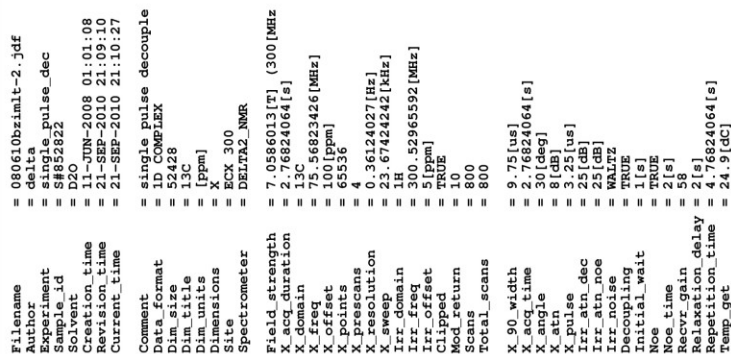
APPENDIX 10

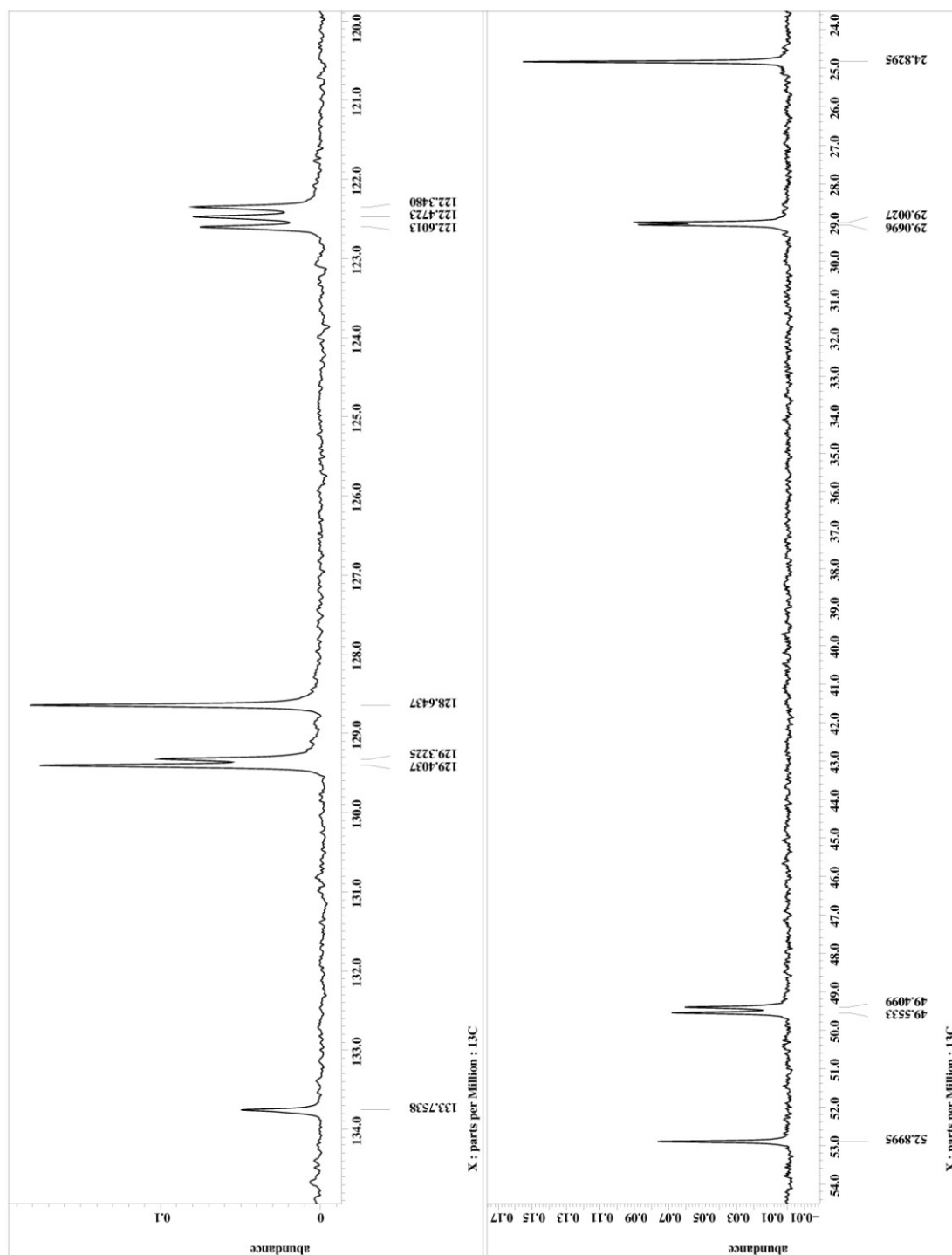
¹H AND ¹³C NMR SPECTRUM OF
1-(1'-BENZYL-3'-HEXYLIMIDAZOLIUM)-3-(1''-BENZYL-3''-
HEXYLIMIDAZOLIUM)IMIDAZOLIUM TRI
[BIS(TRIFLUOROMETHANESULFONYL)IMIDE] (3b).











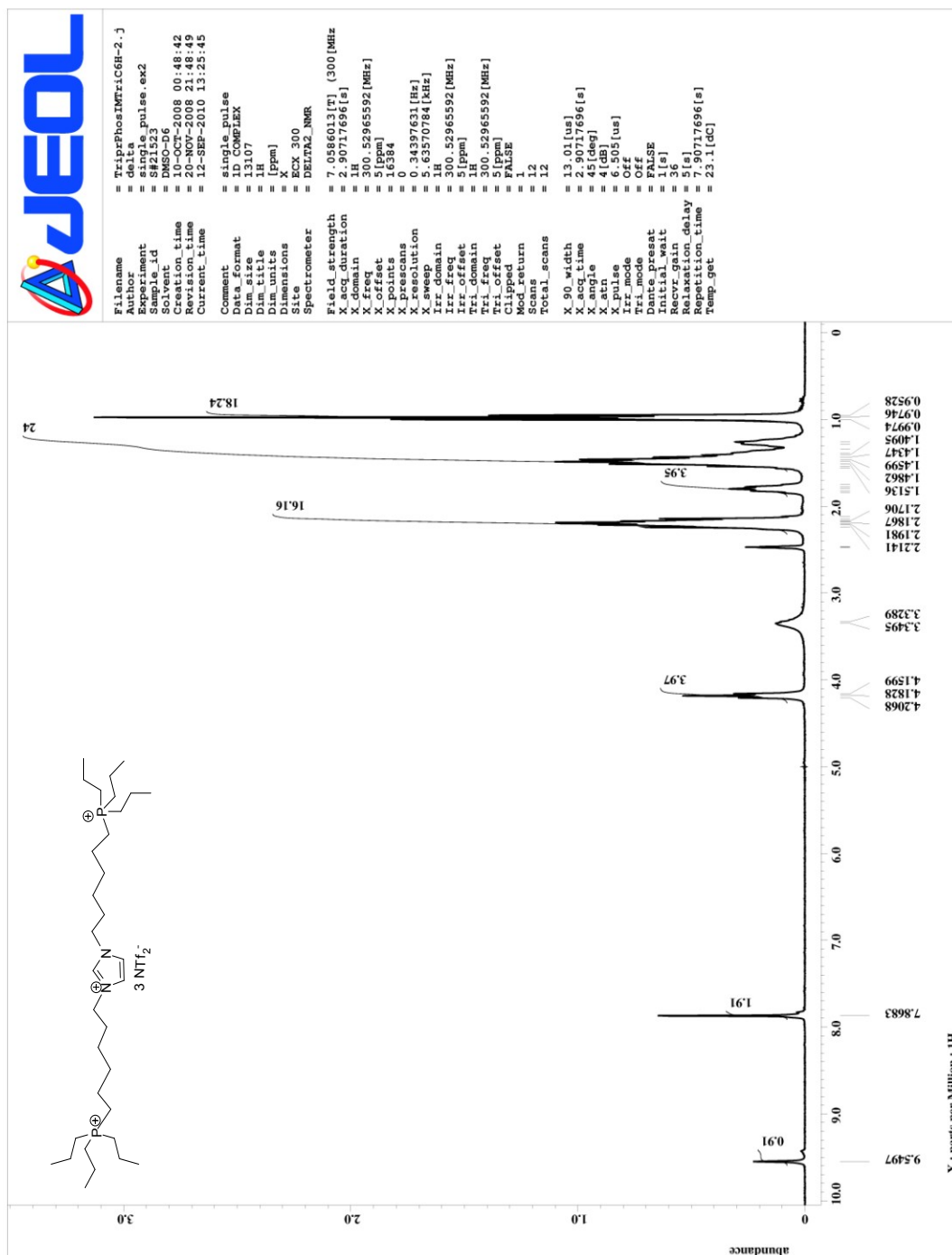
APPENDIX 11

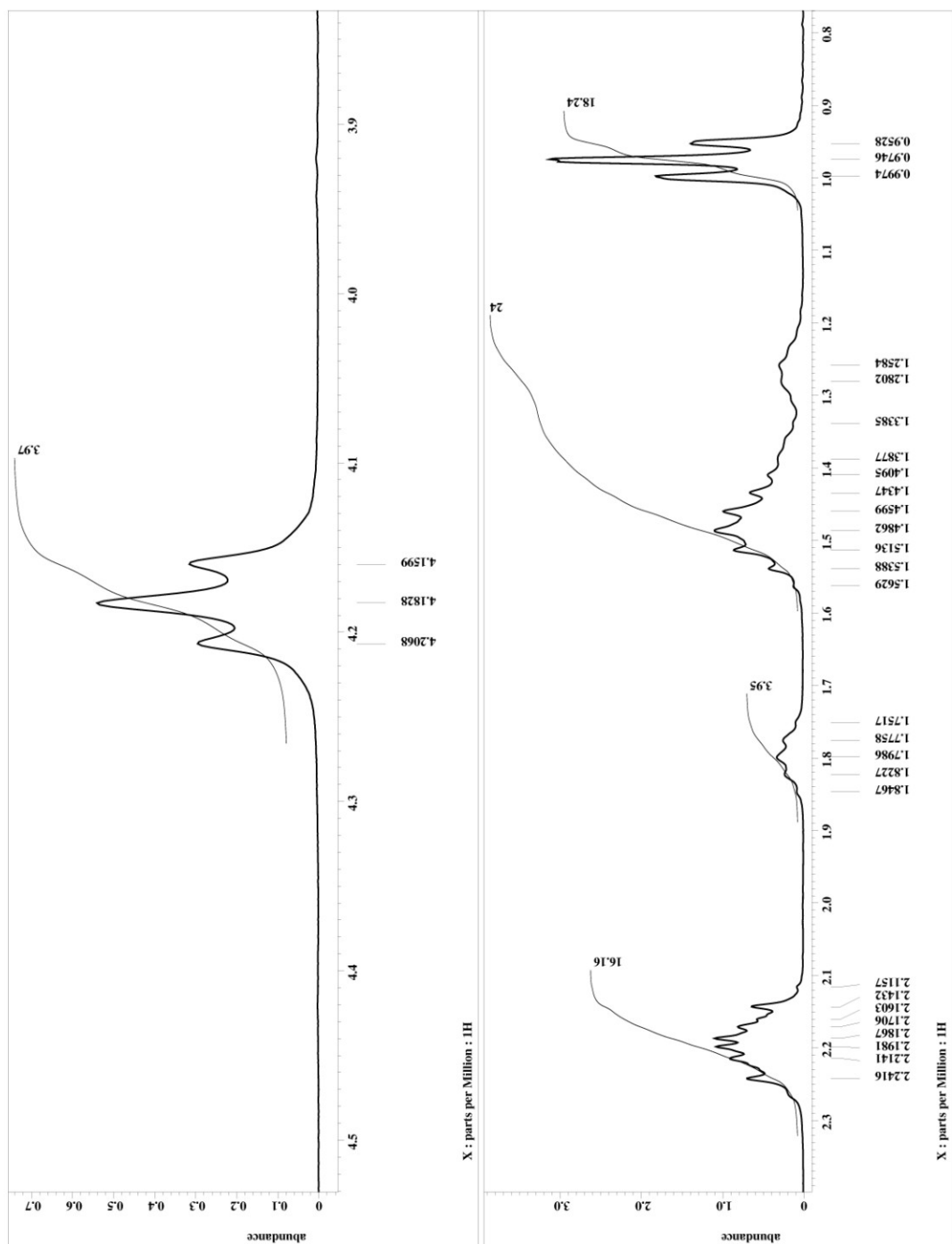
^1H , ^{13}C AND ^{31}P NMR SPECTRA OF

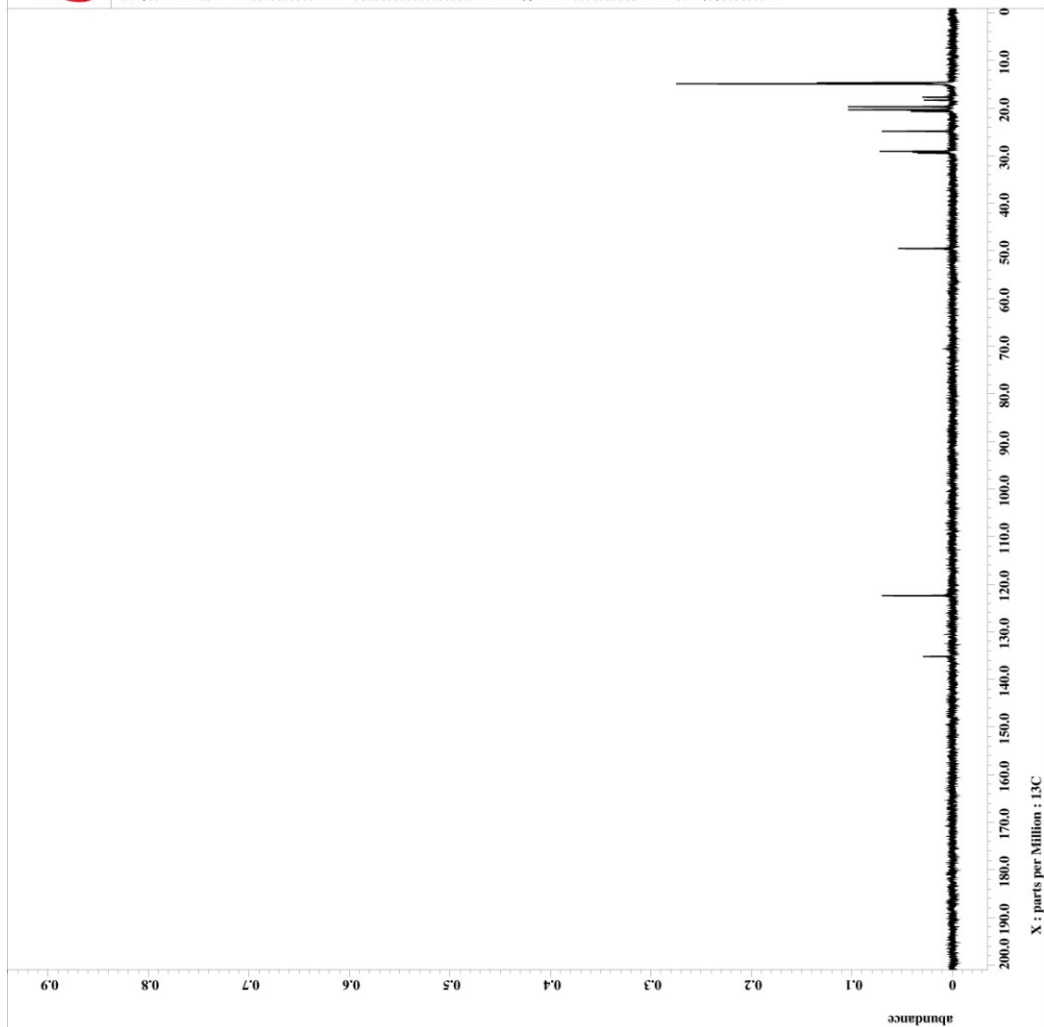
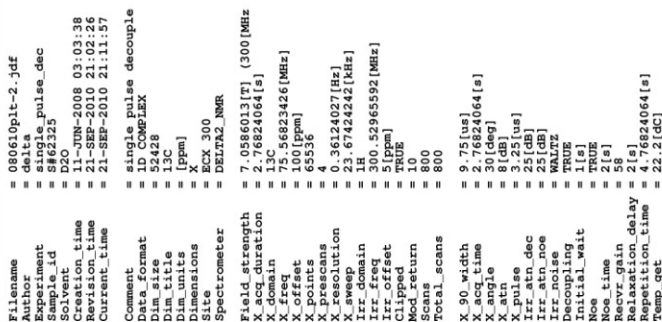
1-(HEXYLTRIPROPYLPHOSPHONIUM)-3-

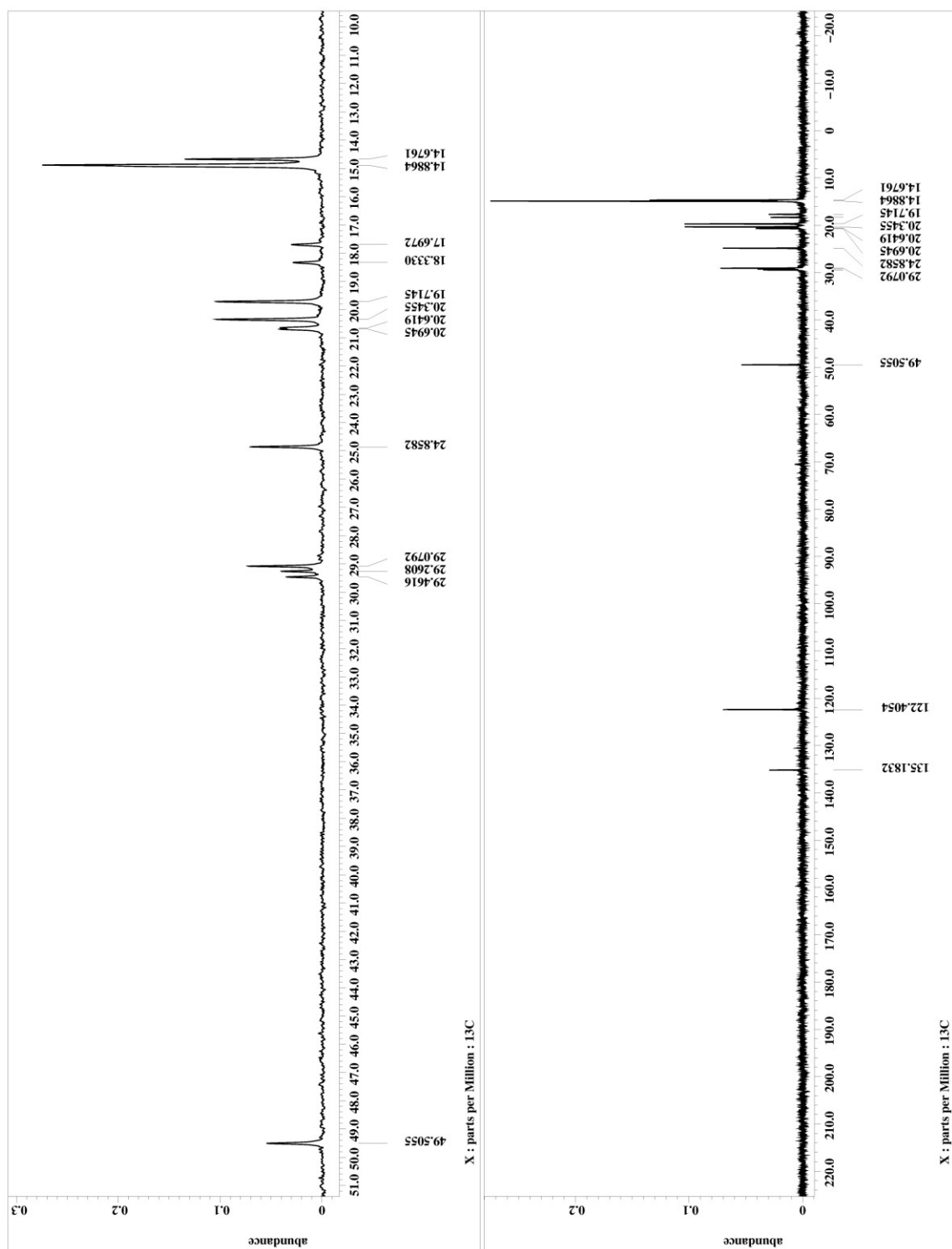
(HEXYLTRIPROPYLPHOSPHONIUM)IMIDAZOLIUM TRI

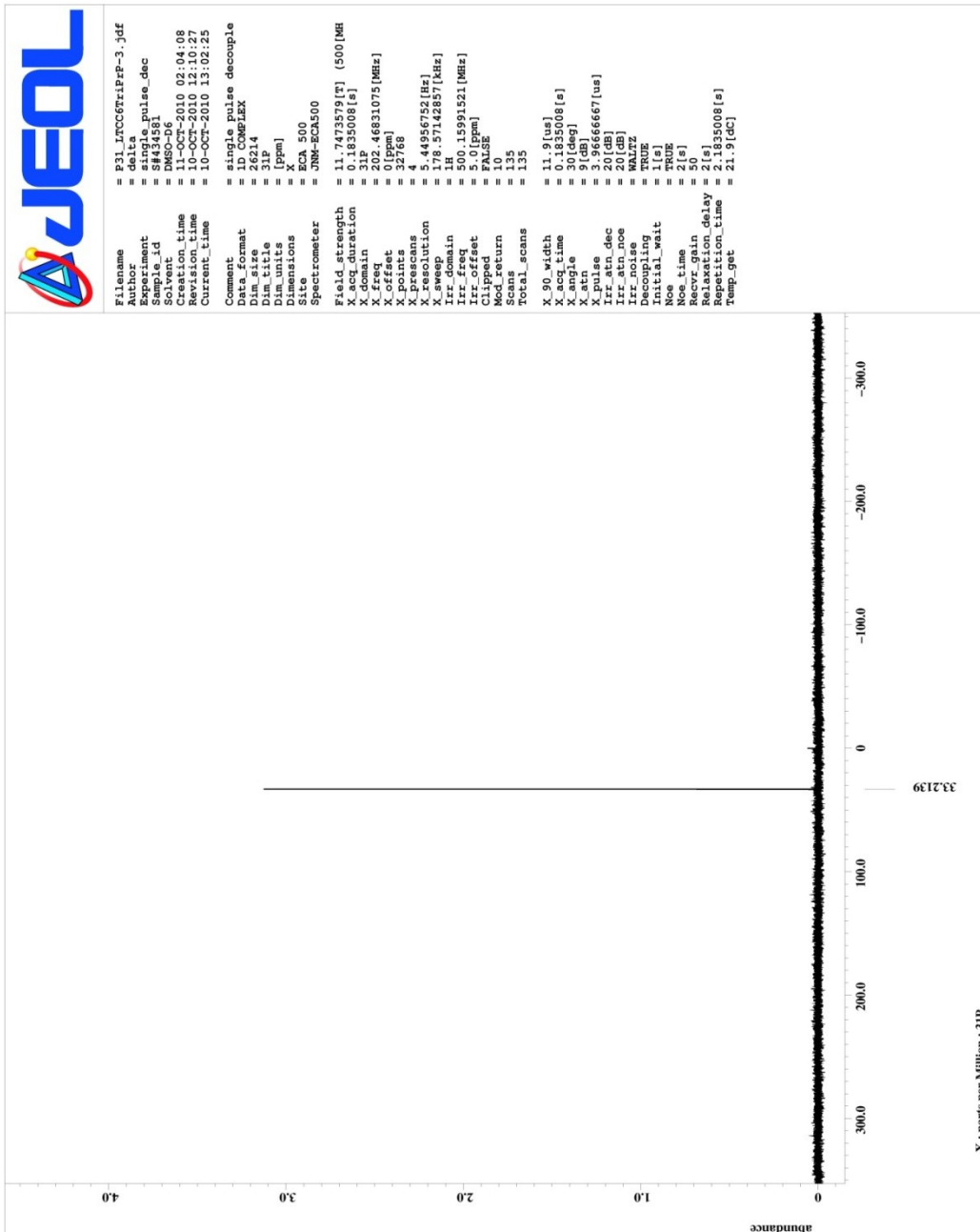
[BIS(TRIFLUOROMETHANESULFONYL)IMIDE] (3d).

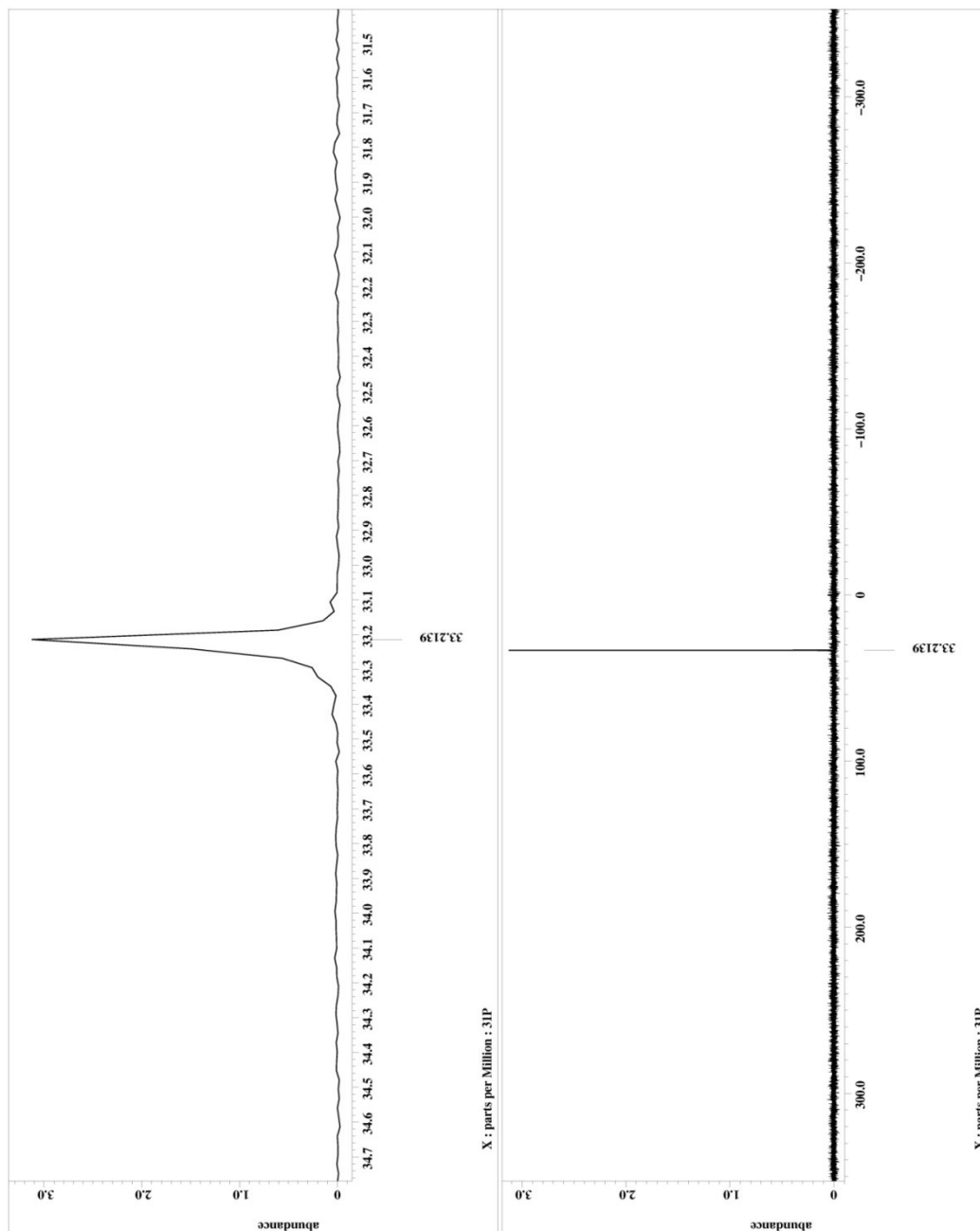








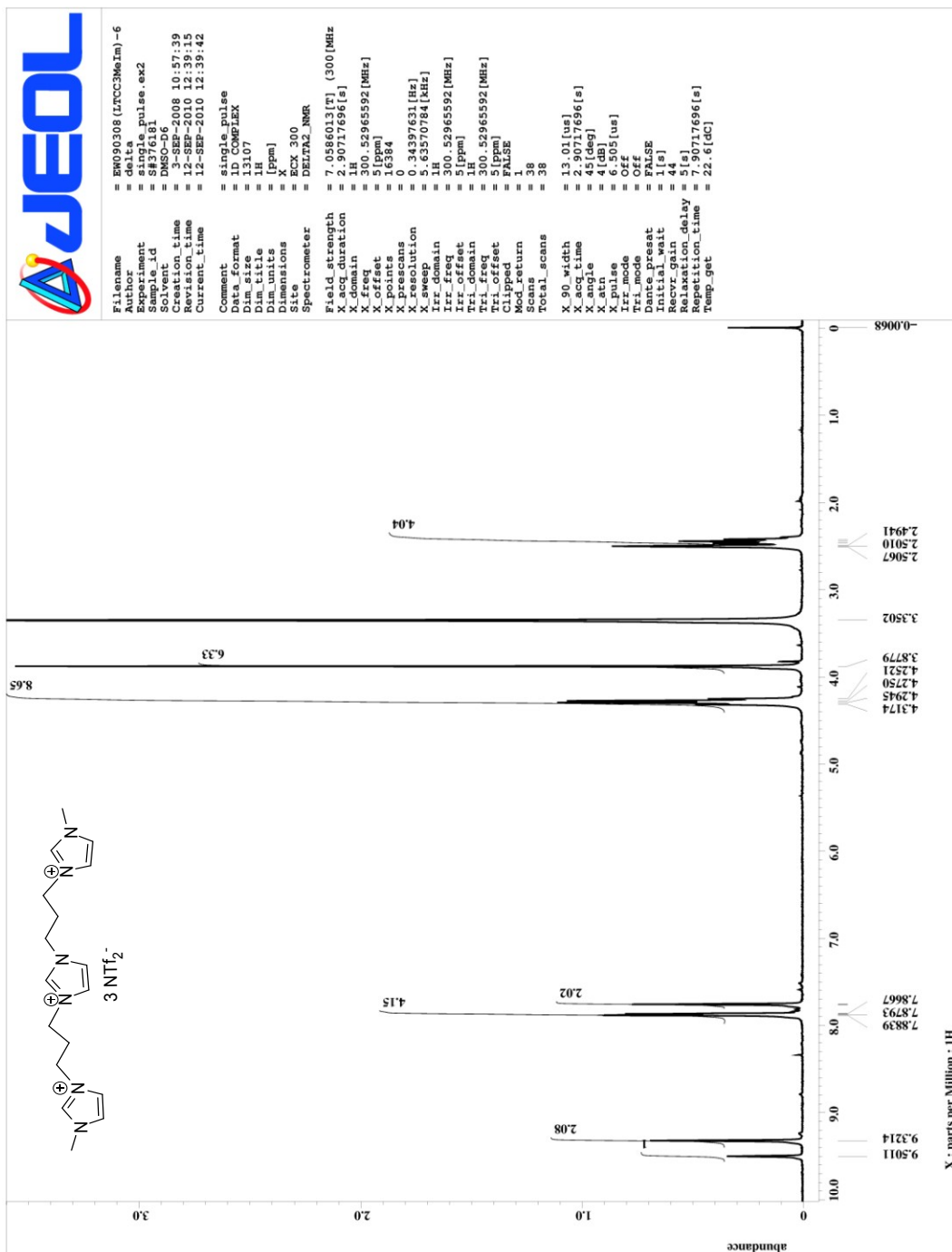


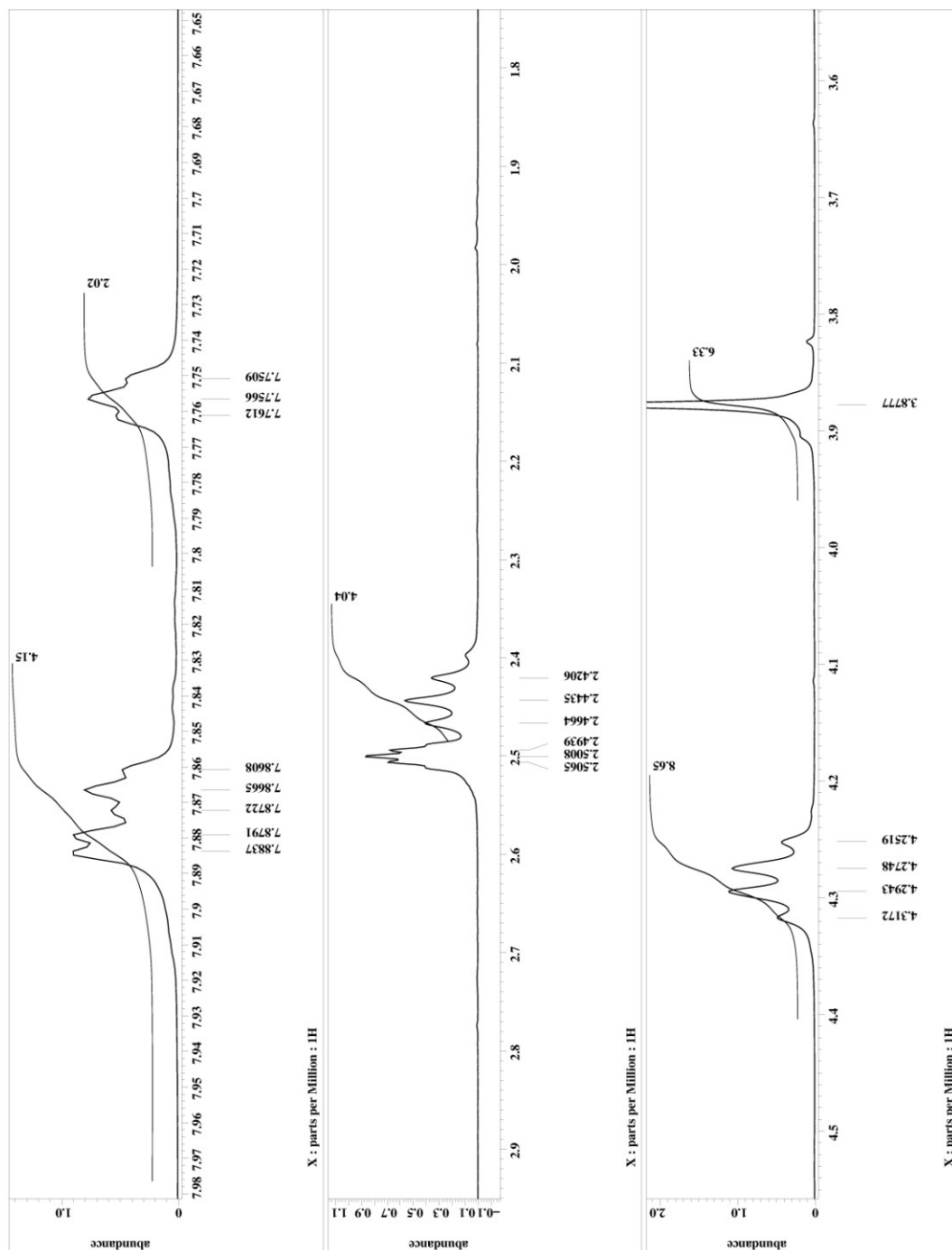


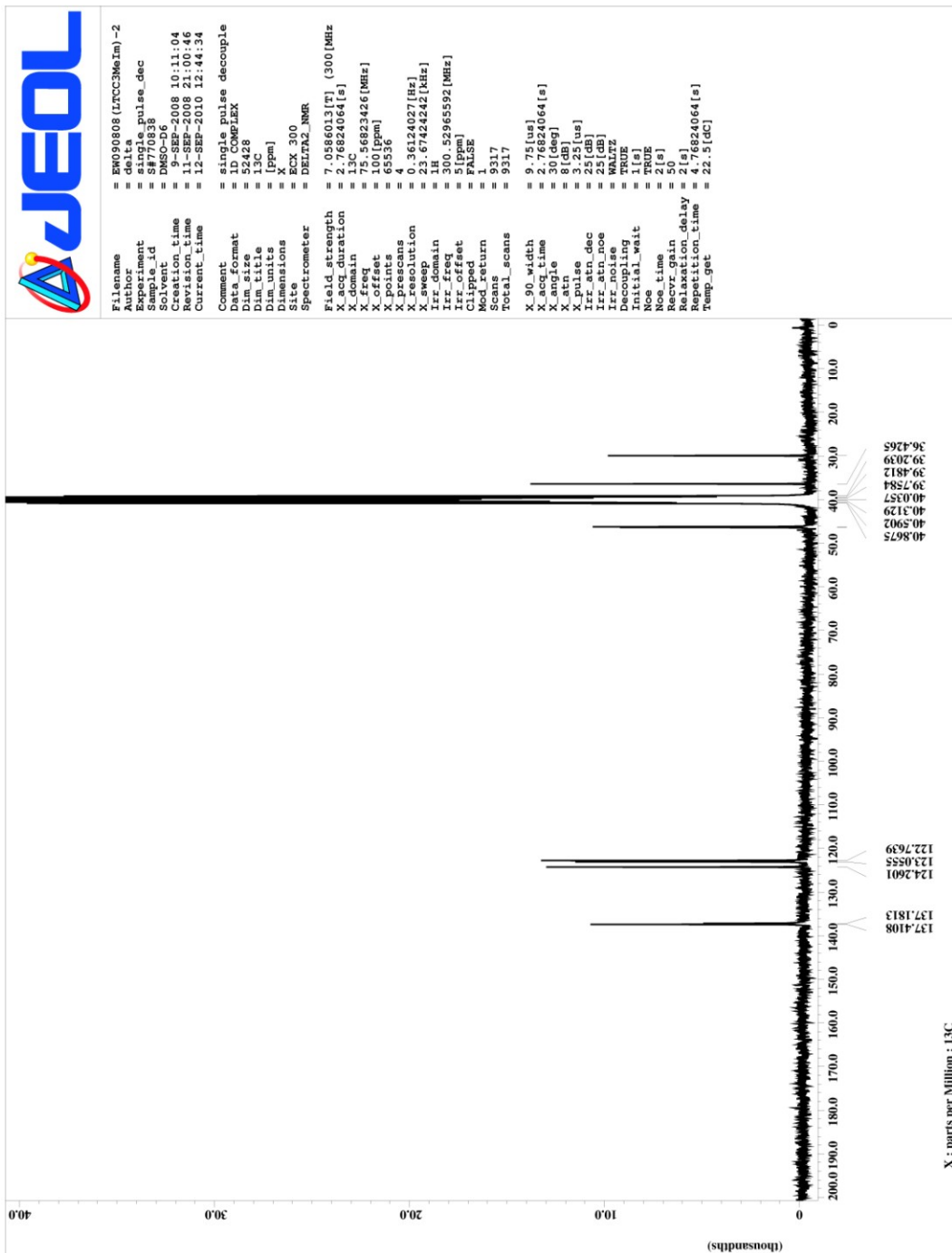
APPENDIX 12

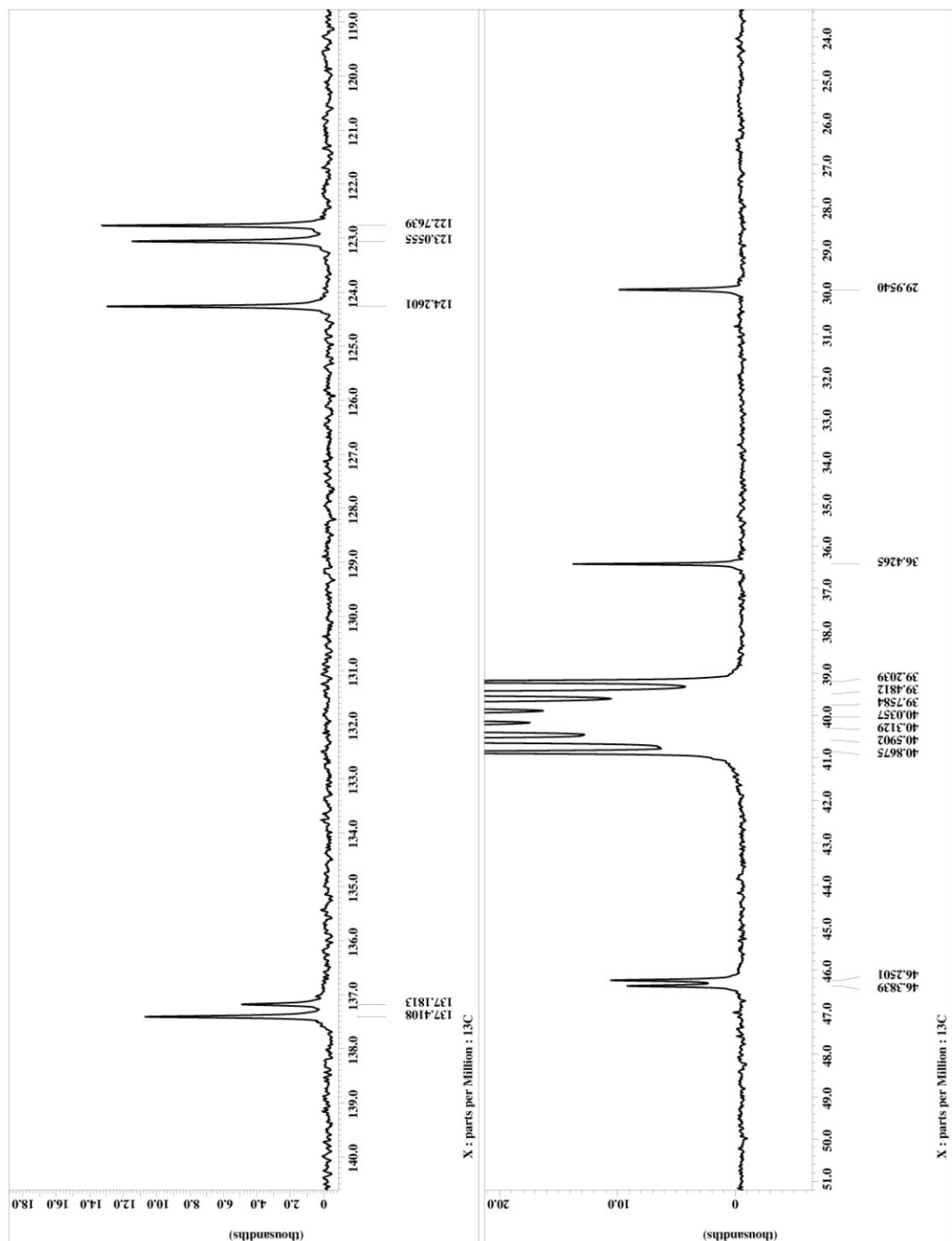
¹H AND ¹³C NMR SPECTRA OF

(1'-METHYL-3'-PROPYLMIDAZOLIUM)-3-(1''-METHYL-3''-
PROPYLMIDAZOLIUM)IMIDAZOLIUM TRI
[BIS(TRIFLUOROMETHANESULFONYL)IMIDE] (4a).









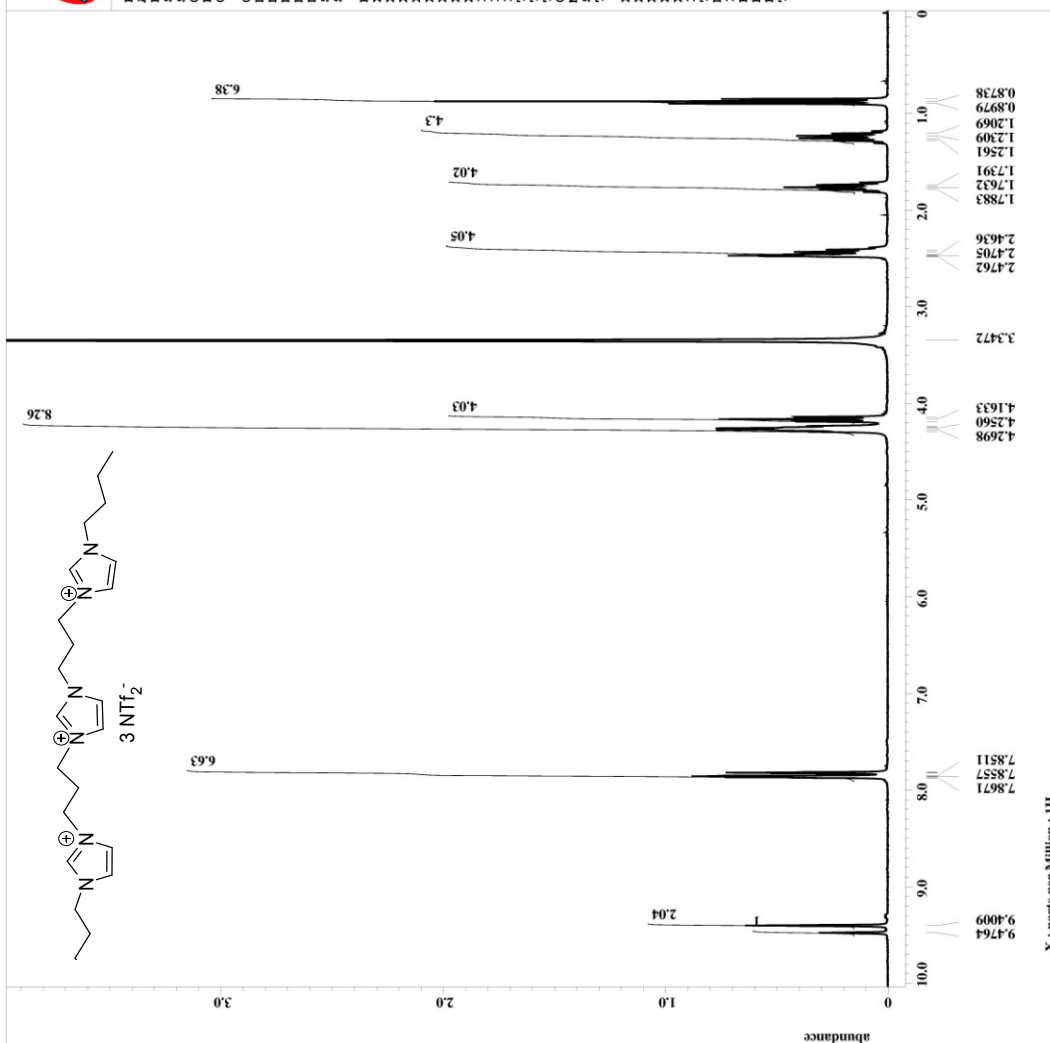
APPENDIX 13

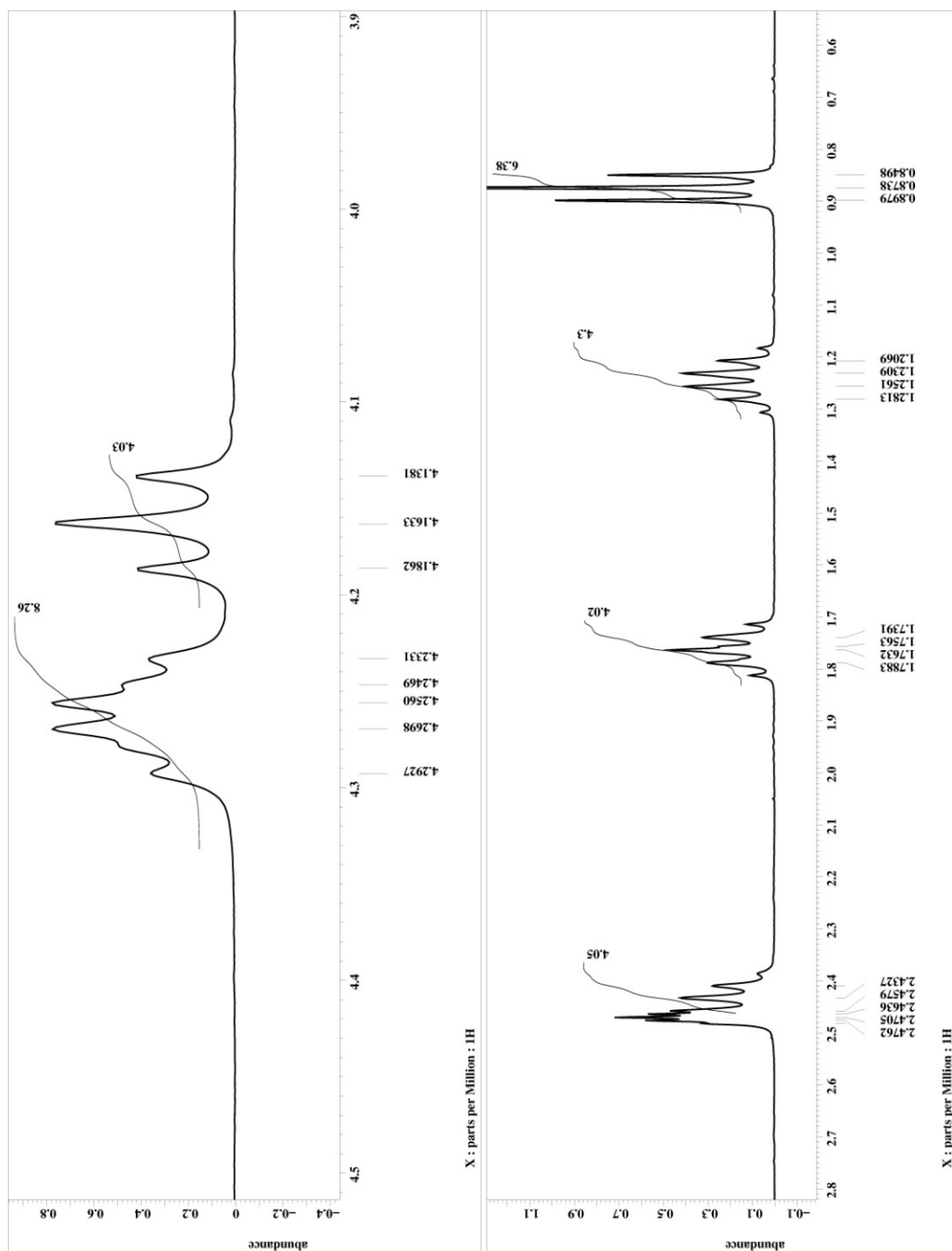
¹H AND ¹³C NMR SPECTRA OF

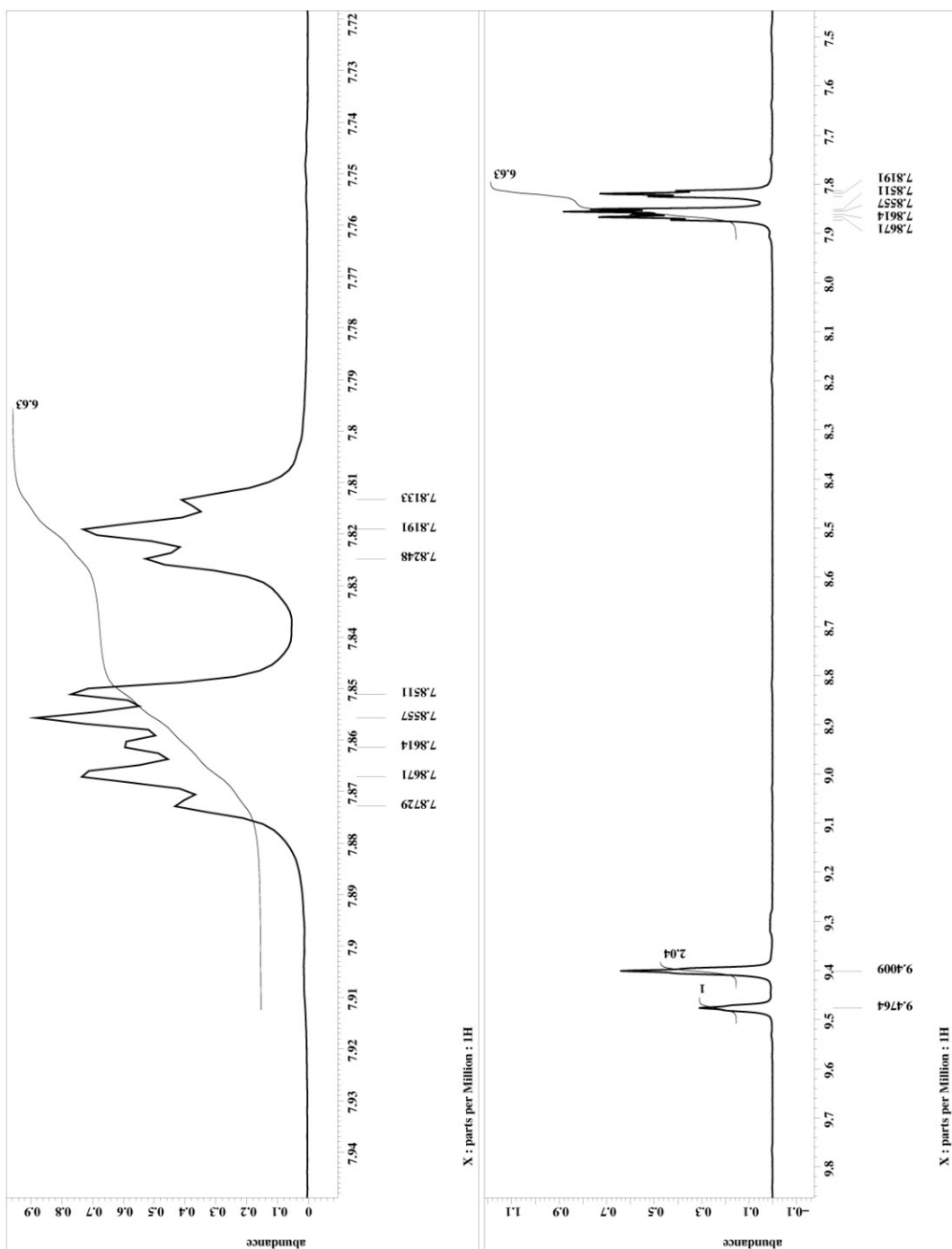
(1'-BUTYL-3'-PROPYLMIDAZOLIUM)-3-(1''-BUTYL-3''-
PROPYLMIDAZOLIUM)IMIDAZOLIUM TRI
[BIS(TRIFLUOROMETHANESULFONYL)IMIDE] (4b).

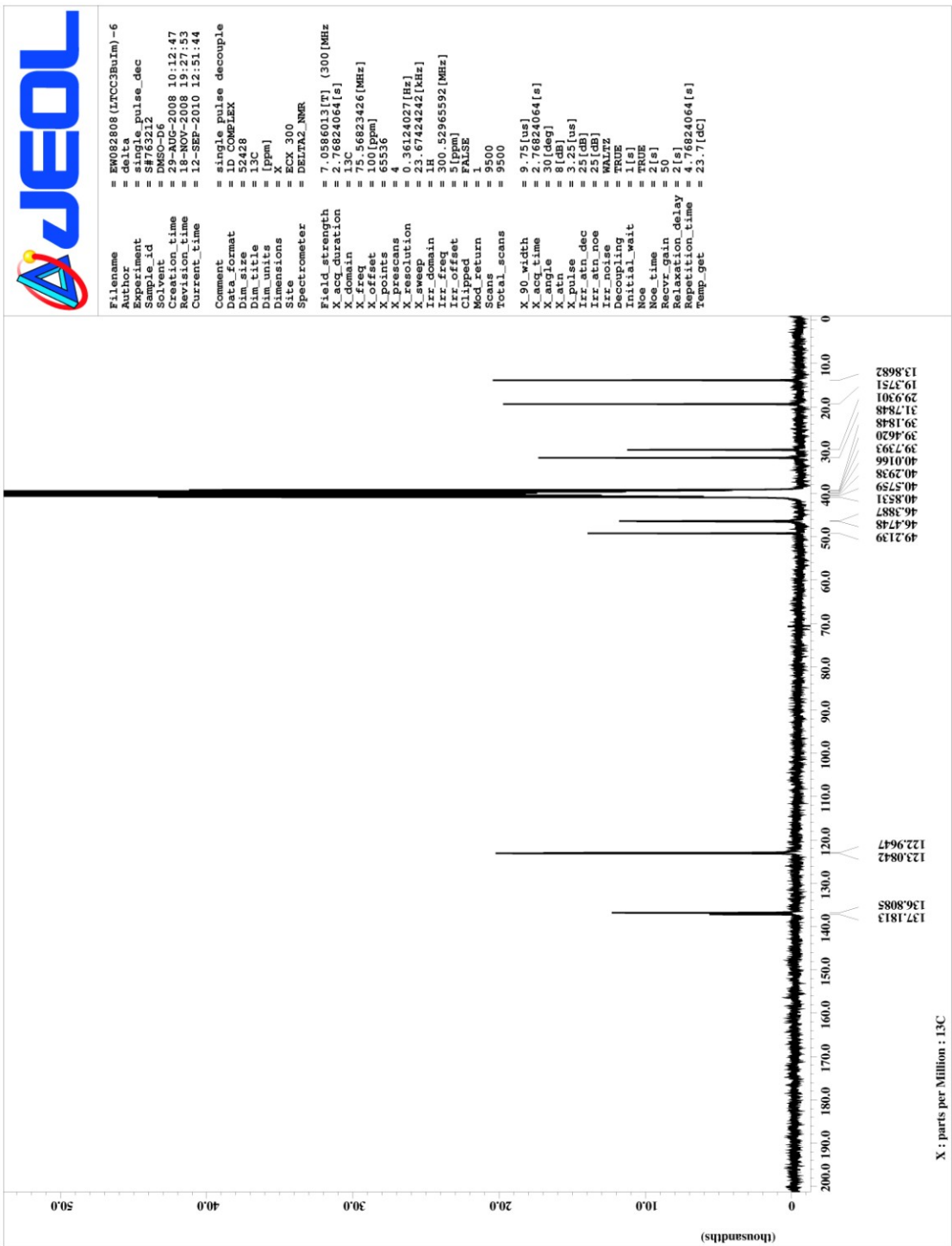


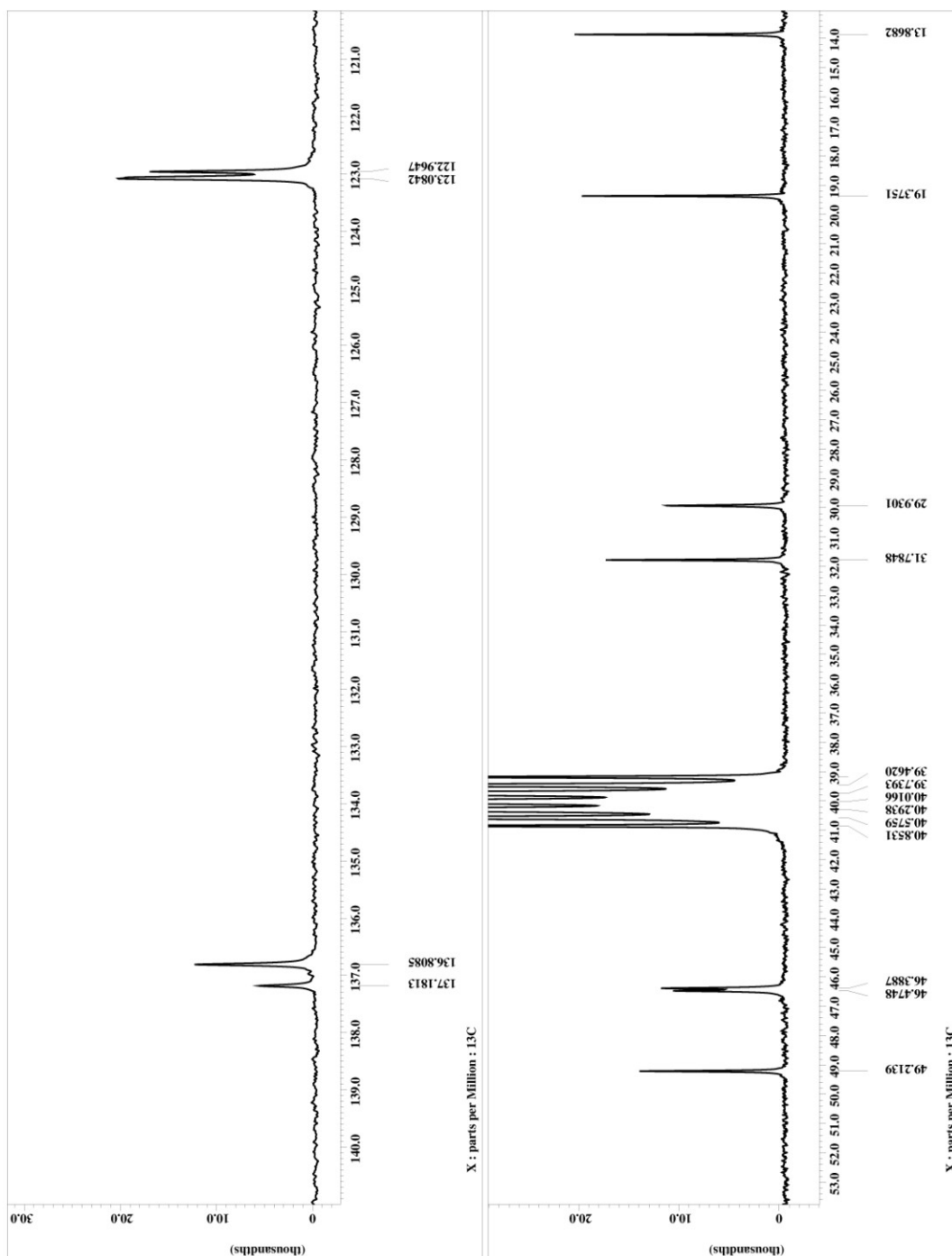
Filename = EW02808 (LTCBuIM)-4.j
Author = det12
Experiment = single_pulse.ex2
Sample_id = S8758962
Solvent = DMSO-D6
Creation_time = 28-AUG-2008 21:32:49
Experiment_time = 28-AUG-2008 21:32:41
Current_time = 12-SEP-2010 12:48:55
Comment = single_pulse
Data_format = ID COMPLEX
Dir_name = IN 107
Dim_title = [ppm]
Dim_units = X
Dimensions = ECX 300
Site = DELTA2_NMR
Spectrometer = DELTA2_NMR
Field_strength = 7.0586013[T] (300 [MHz]
X_acq_duration = 2.90717696[s]
X_domain = 1H
X_freq = 300.52965592[MHz]
X_offset = 145884
X_points = 65884
X_prescans = 0
X_resolution = 0.34397631[Hz]
X_sweep = 5.63570784[kHz]
Irr_domain = 1H
Irr_freq = 300.52965592[MHz]
Irr_offset = 5[ppm]
Tri_domain = 1H
Tri_freq = 300.52965592[MHz]
Tri_offset = 5[ppm]
C1p1 = 145884
Mod_return = FALSE
Scans = 22
Total_scans = 22
X_90_width = 13.01[us]
X_acq_time = 2.90717696[s]
X_angle = 45[deg]
X_atn = 4[db]
X_pulse = 6.503[us]
Irr_mode = Off
Irr_presat = FALSE
Dante_presat = FALSE
Initial_wait = 1[s]
Recvr_gain = 40
Relaxation_delay = 5[s]
Repetition_time = 2.90717696[s]
Temp_get = 22.6[deg]







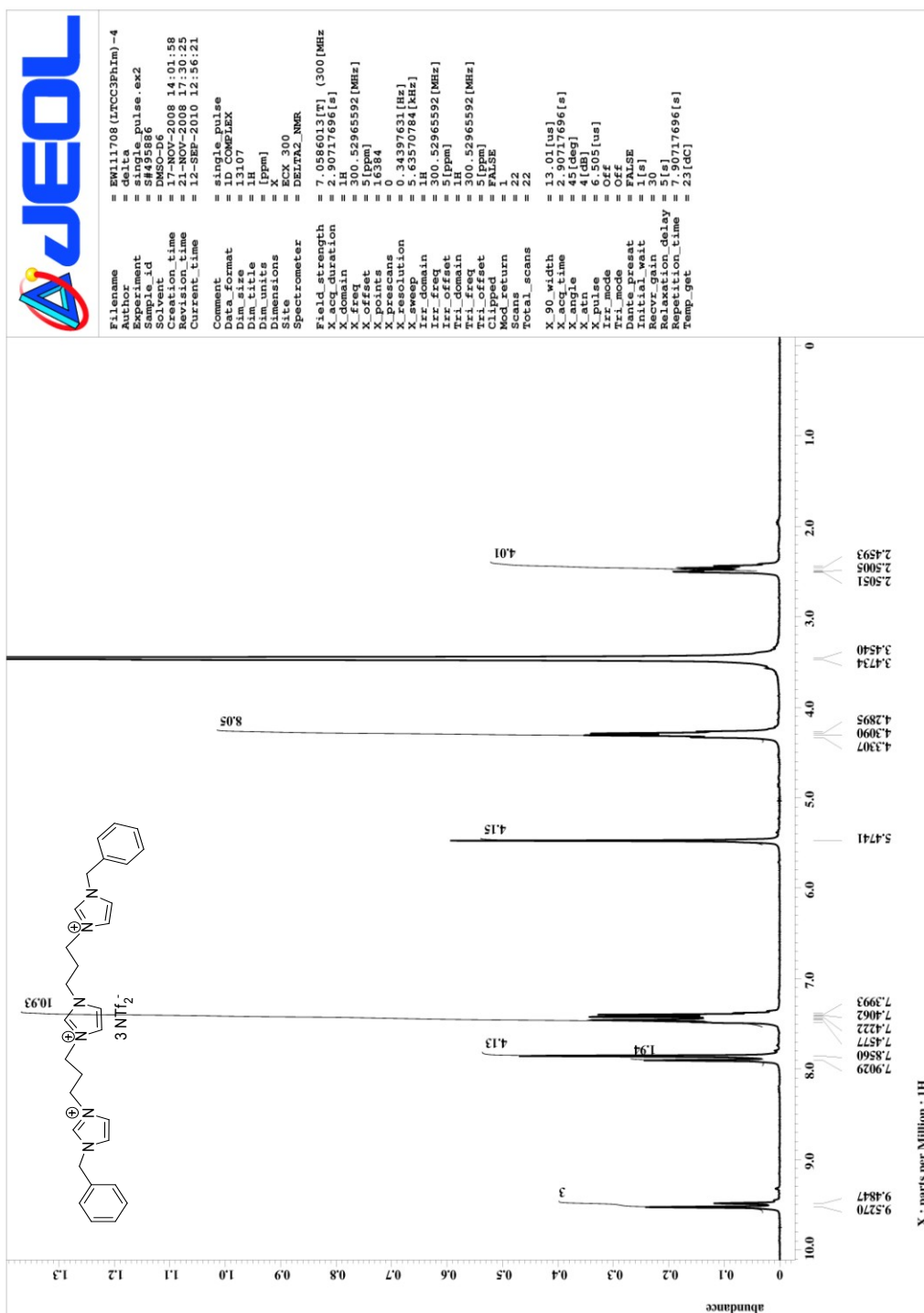


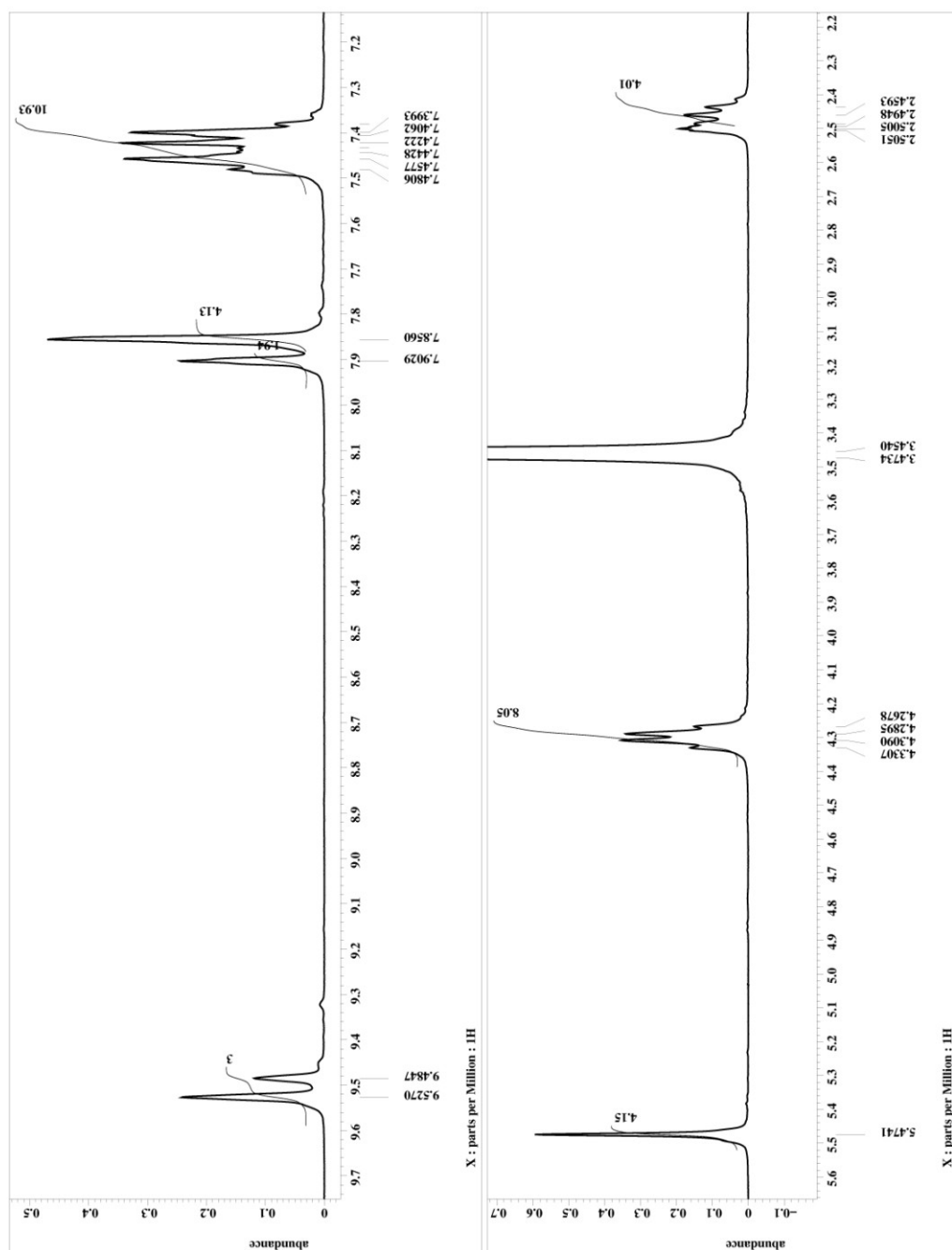


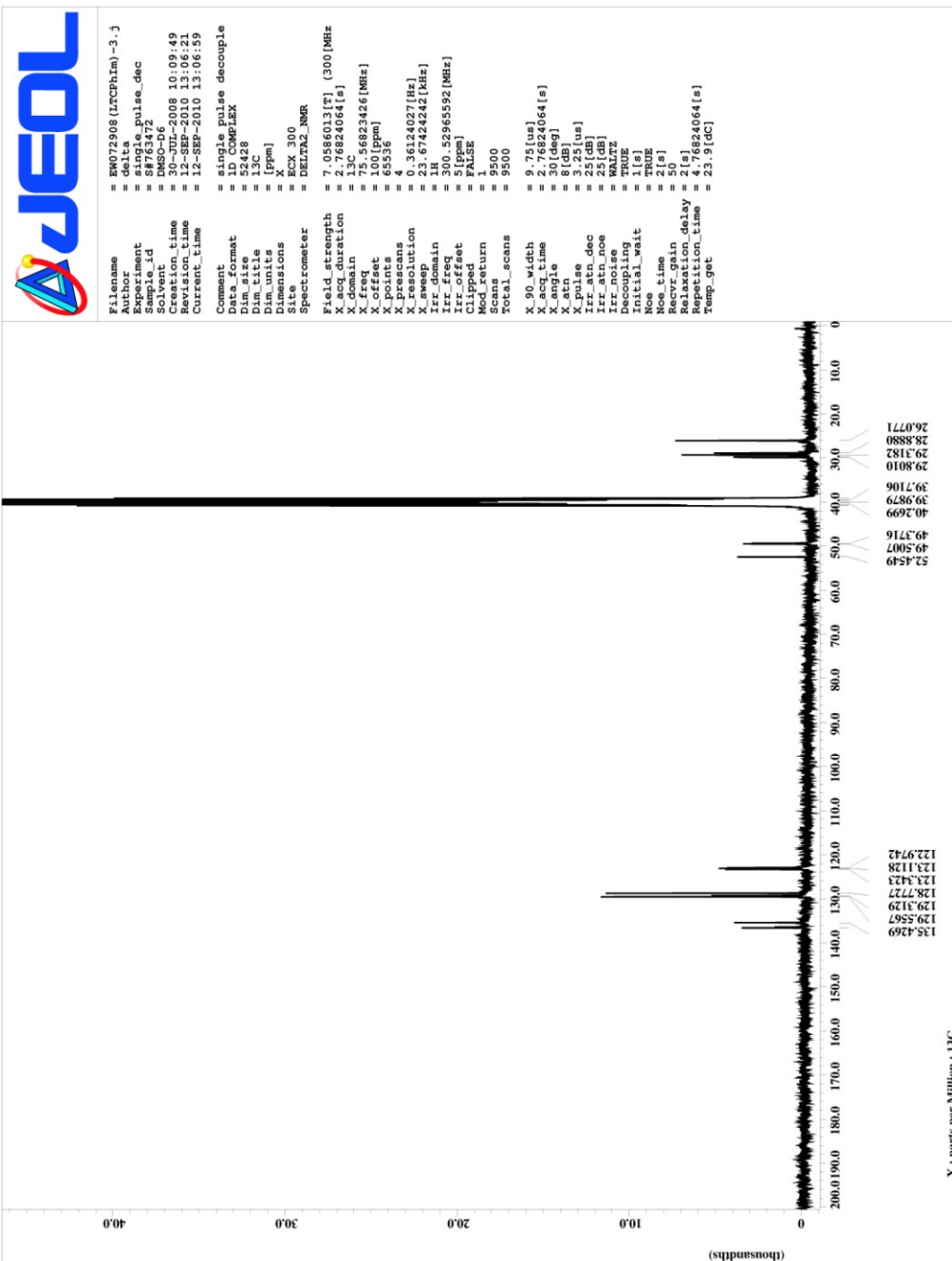
APPENDIX 14

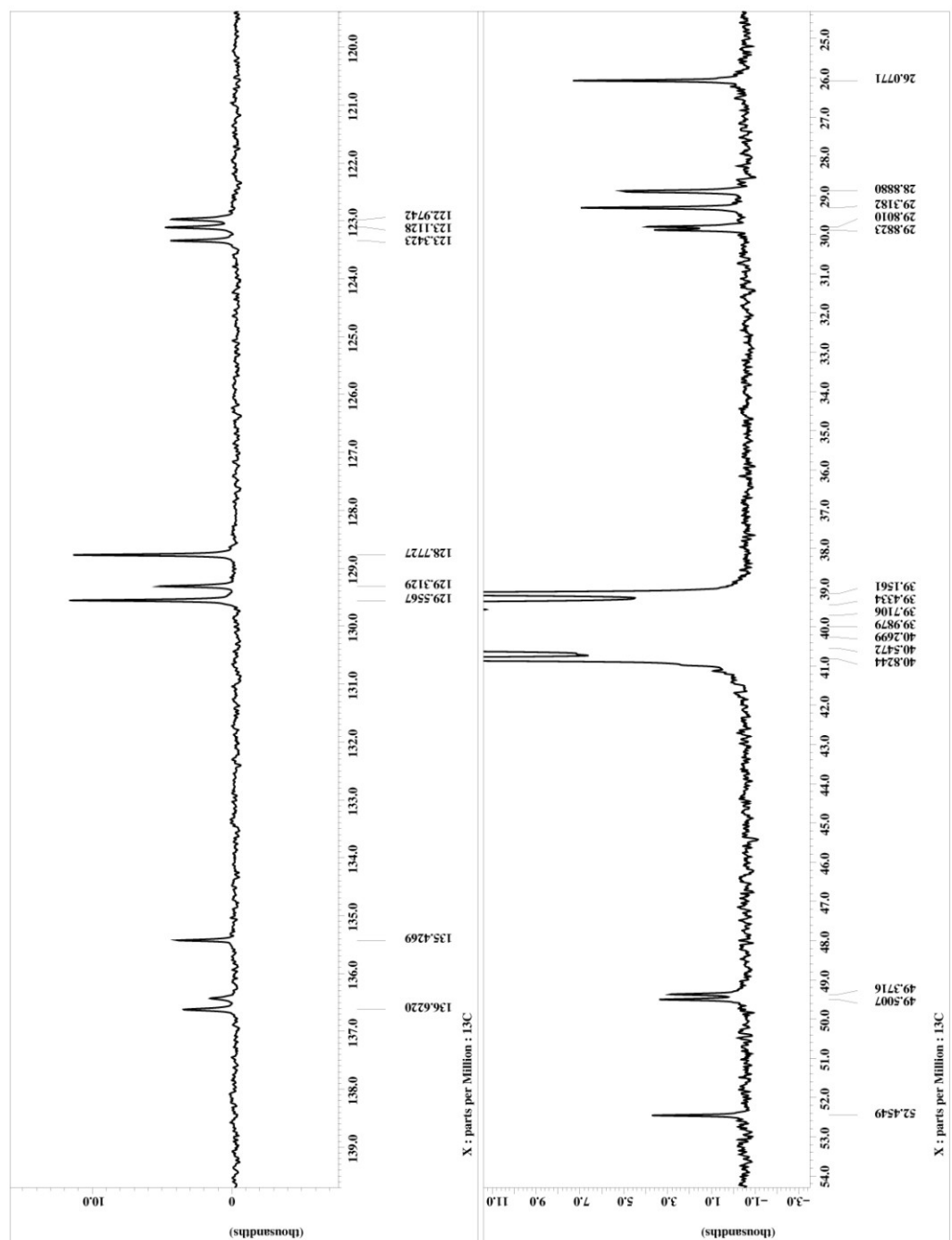
¹H AND ¹³C NMR SPECTRA OF

(1'-BENZYL-3'-PROPYLMIDAZOLIUM)-3-(1''-BENZYL-3''-
PROPYLMIDAZOLIUM)IMIDAZOLIUM TRI
[BIS(TRIFLUOROMETHANESULFONYL)IMIDE] (4c).







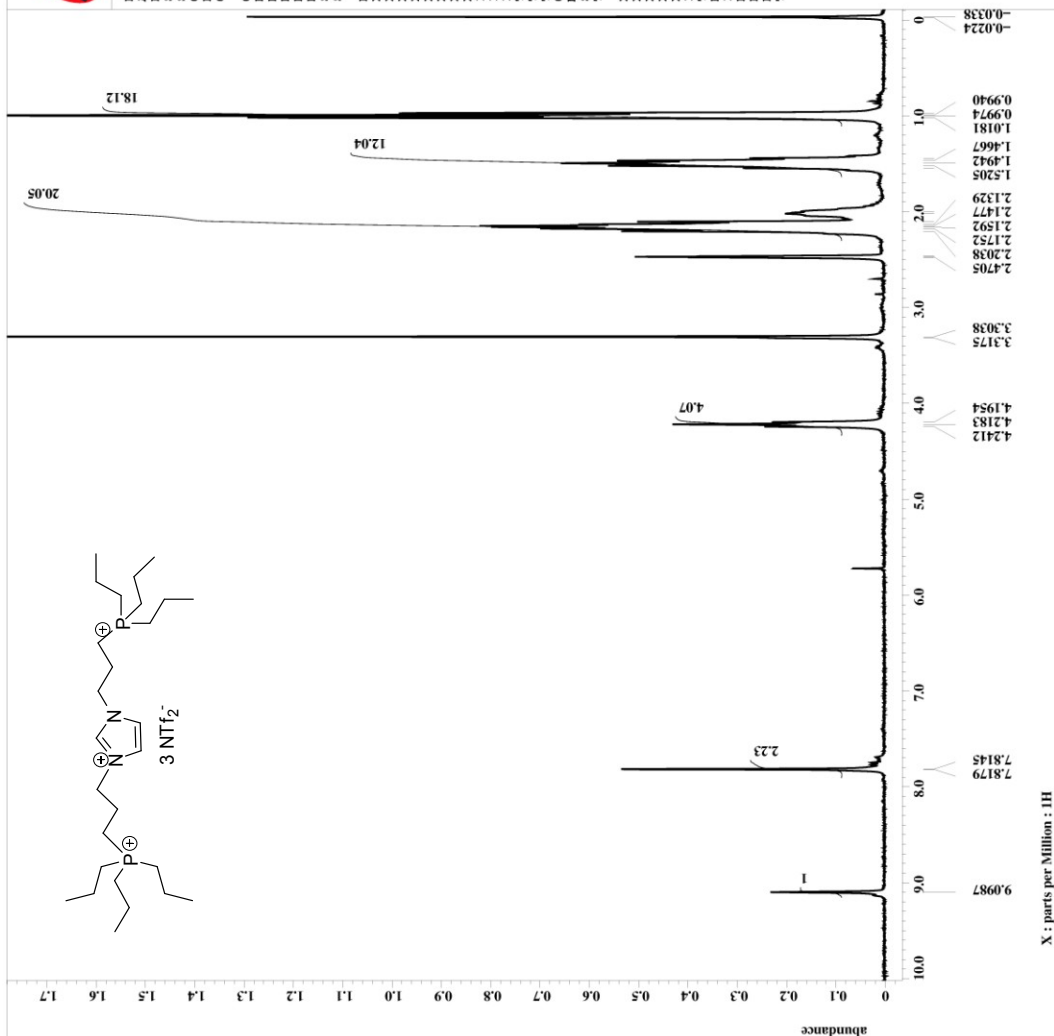


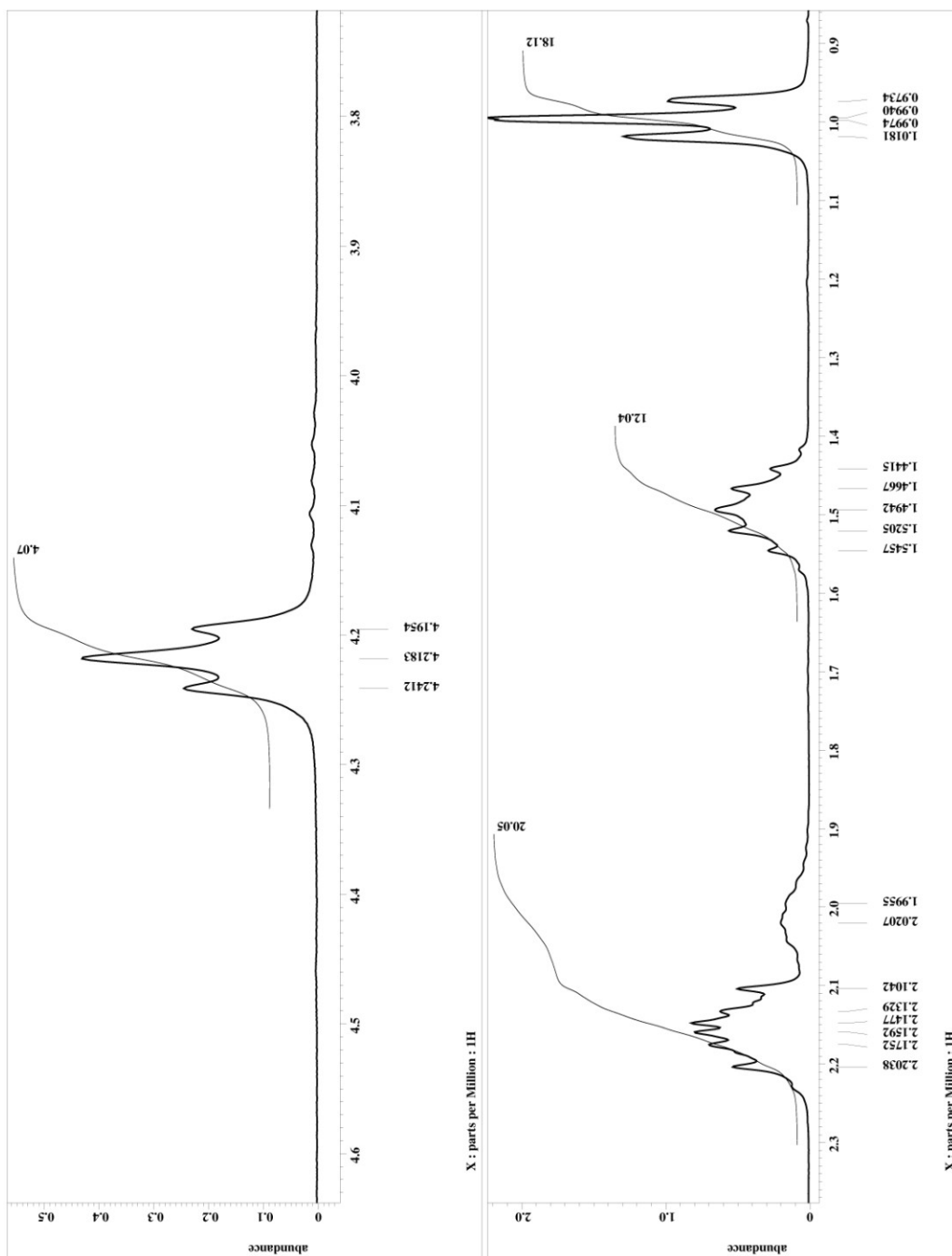
APPENDIX 15

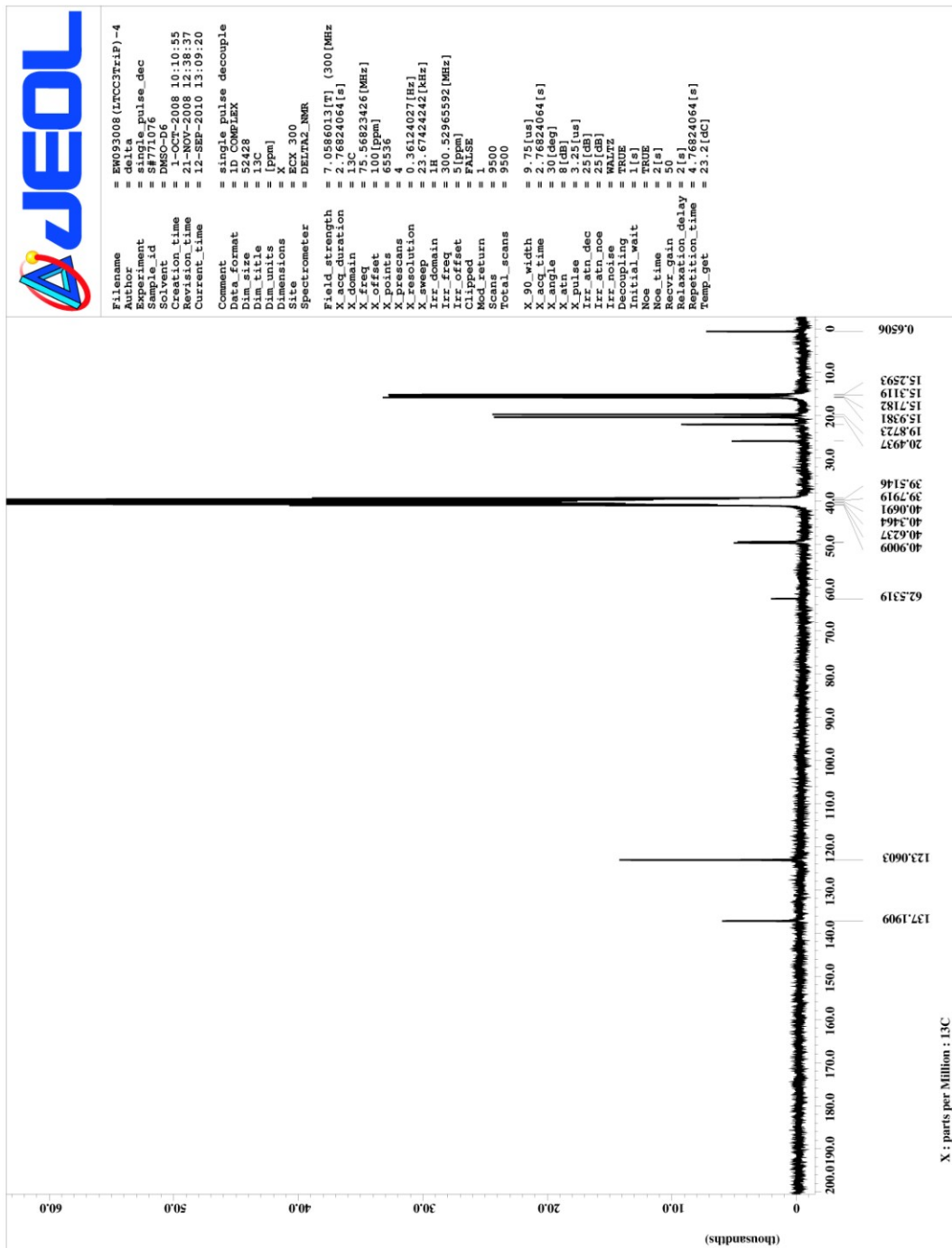
^1H , ^{13}C AND ^{31}P NMR SPECTRA OF

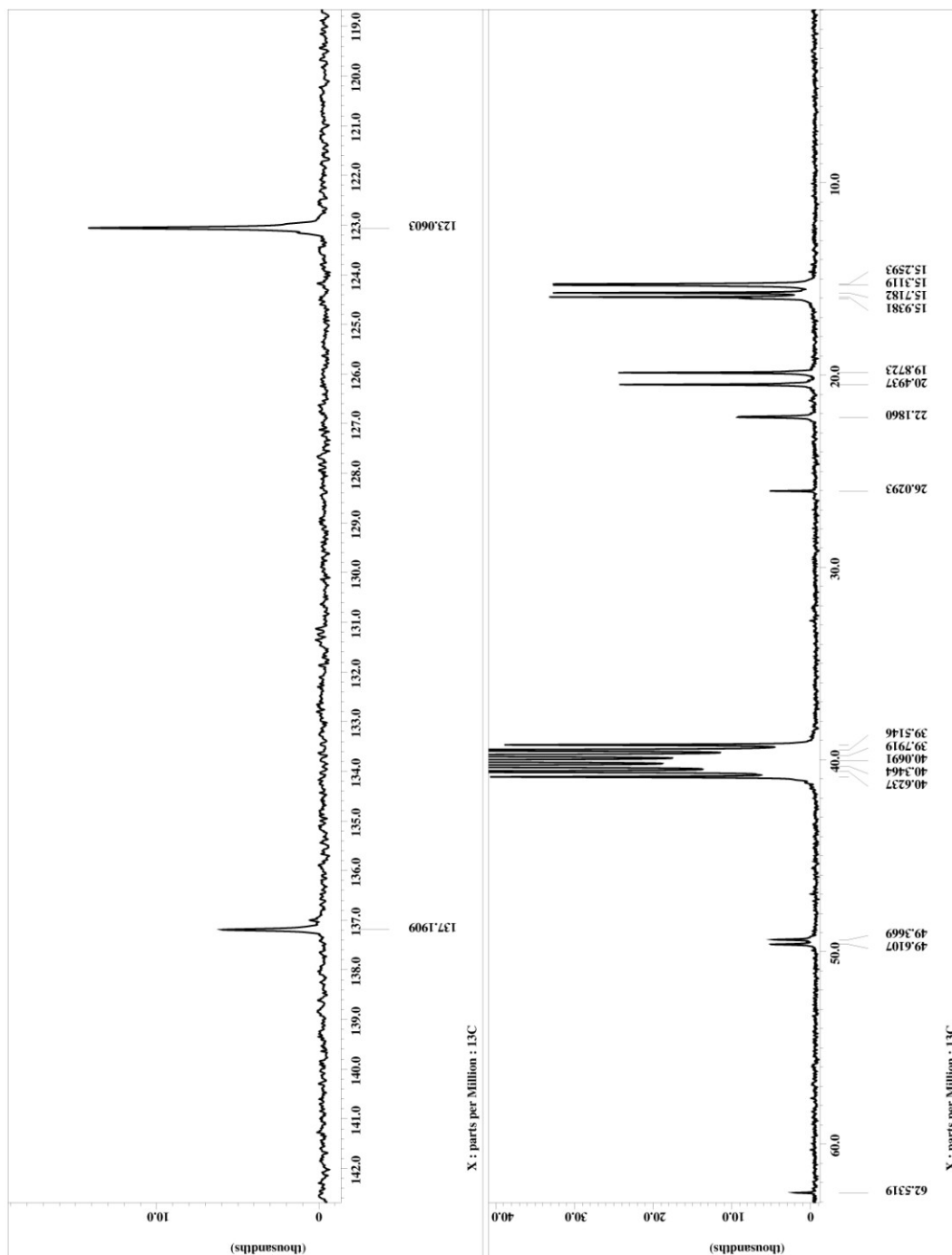
1-PROPYLTRIPROPYLPHOSPHONIUM-3-PROPYLTRIPROPYLPHOSPHONIUM

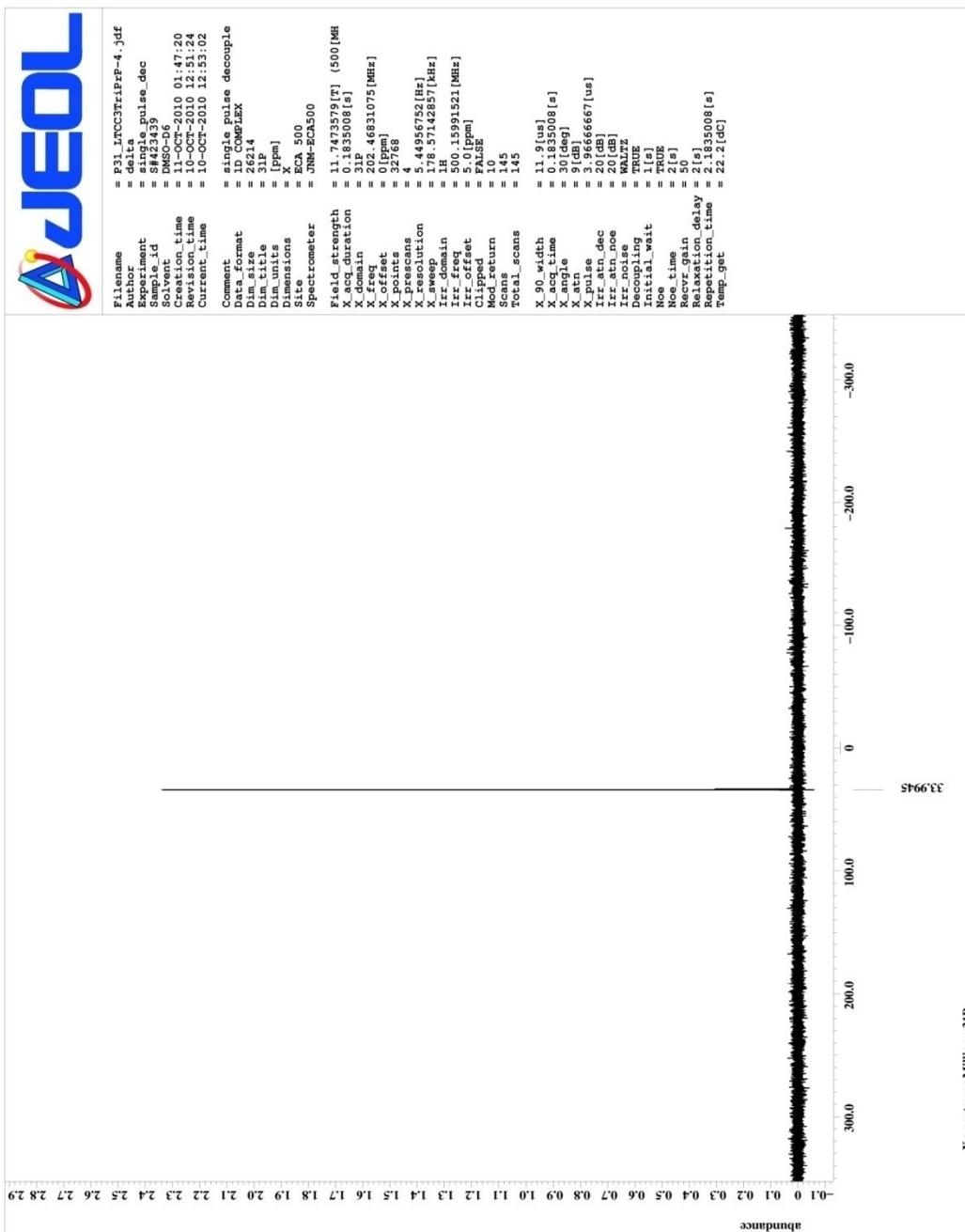
IMIDAZOLIUM TRI[BIS(TRIFLUOROMETHANESULFONYL)IMIDE] (4d)

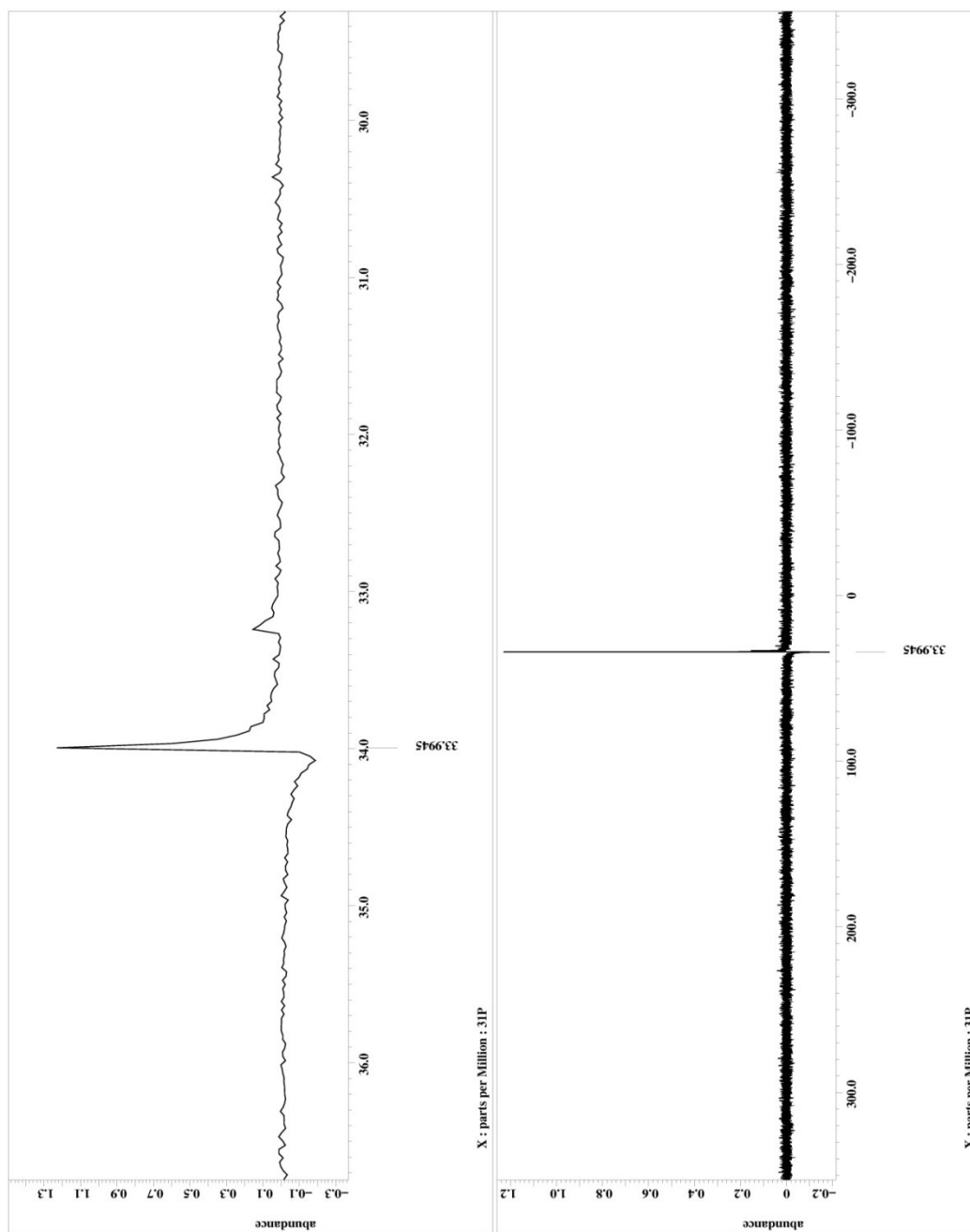








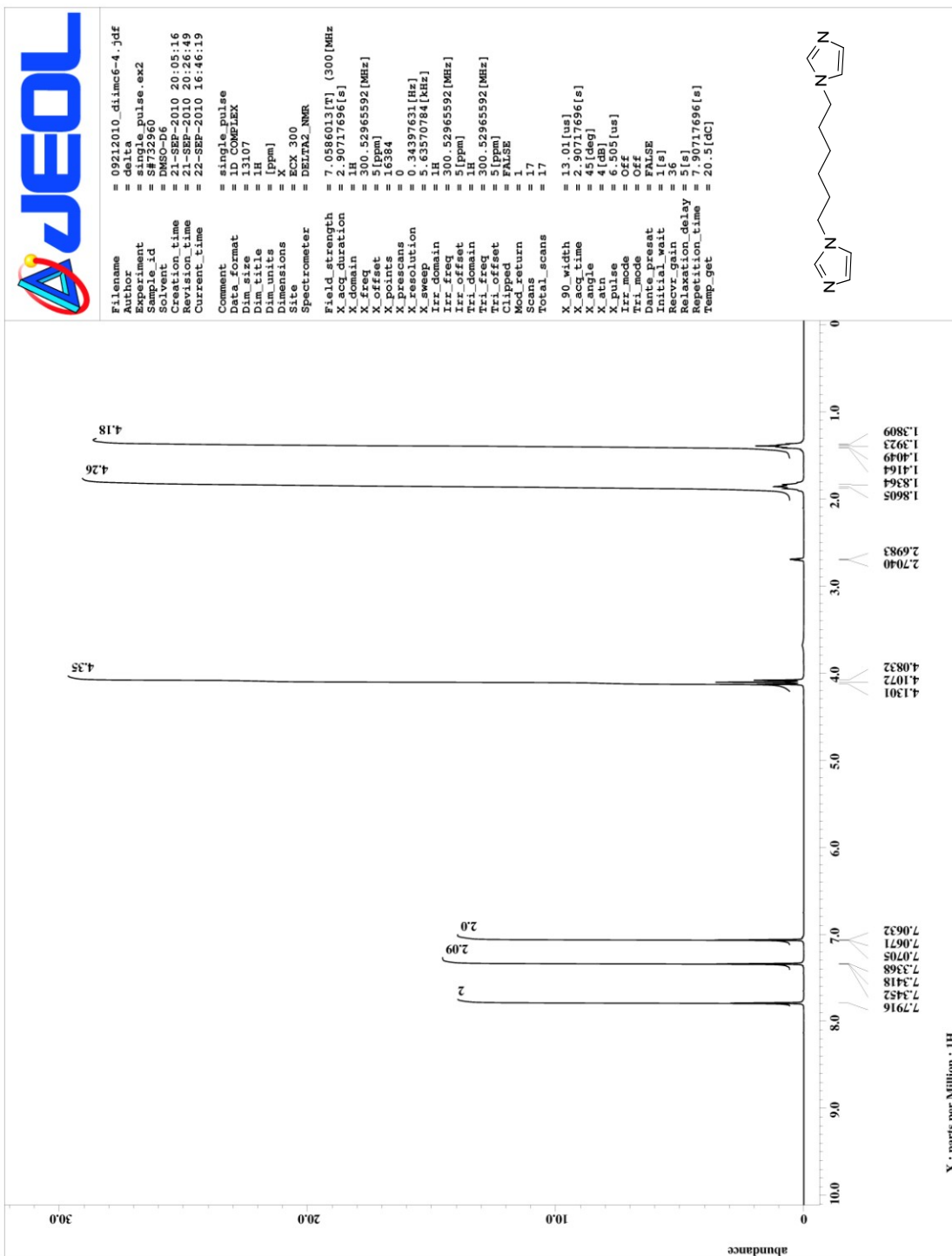


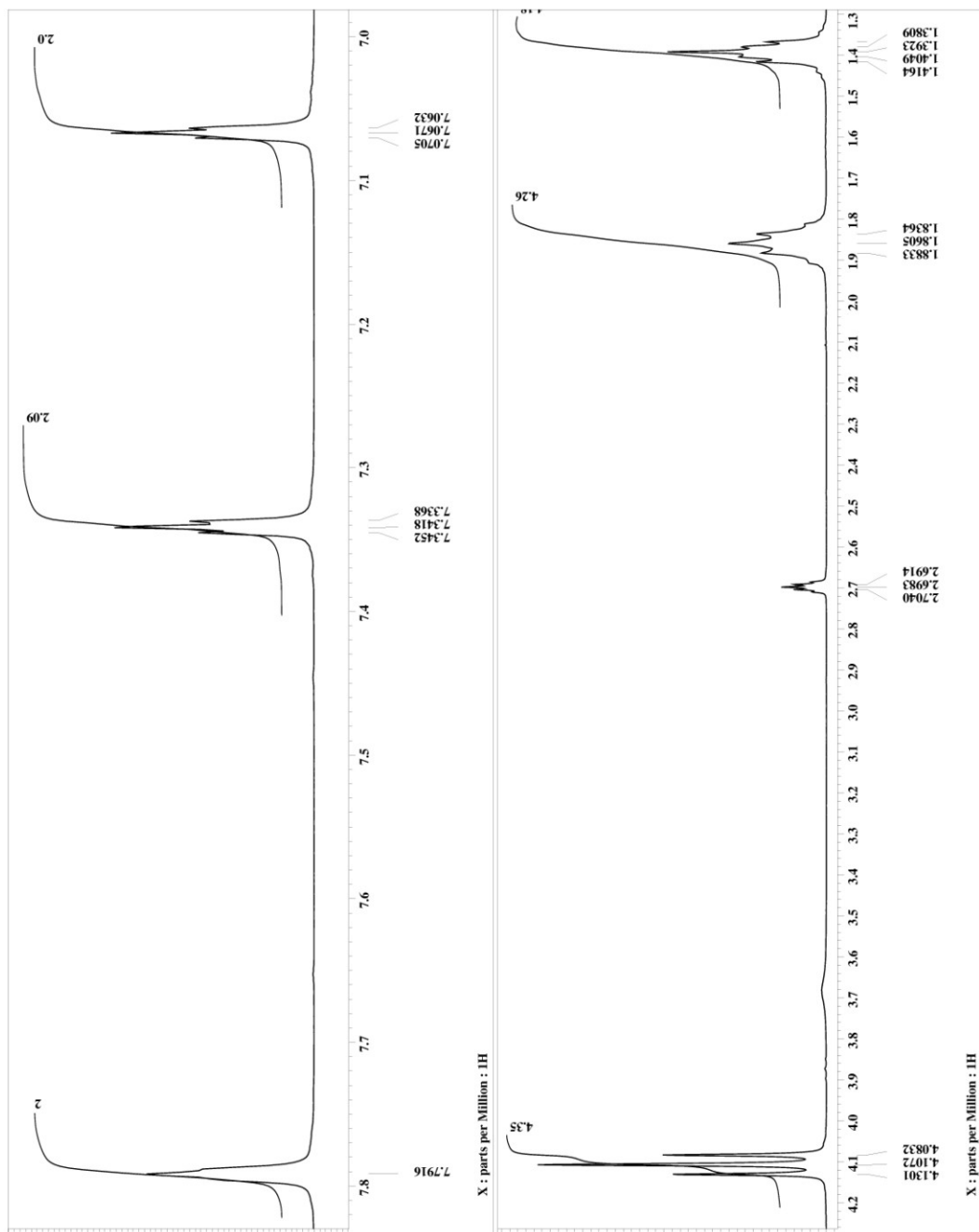


APPENDIX 16

¹H NMR SPECTRA OF

1,1'-(1,6-HEXANEDIYL)BISIMIDAZOLE (8)

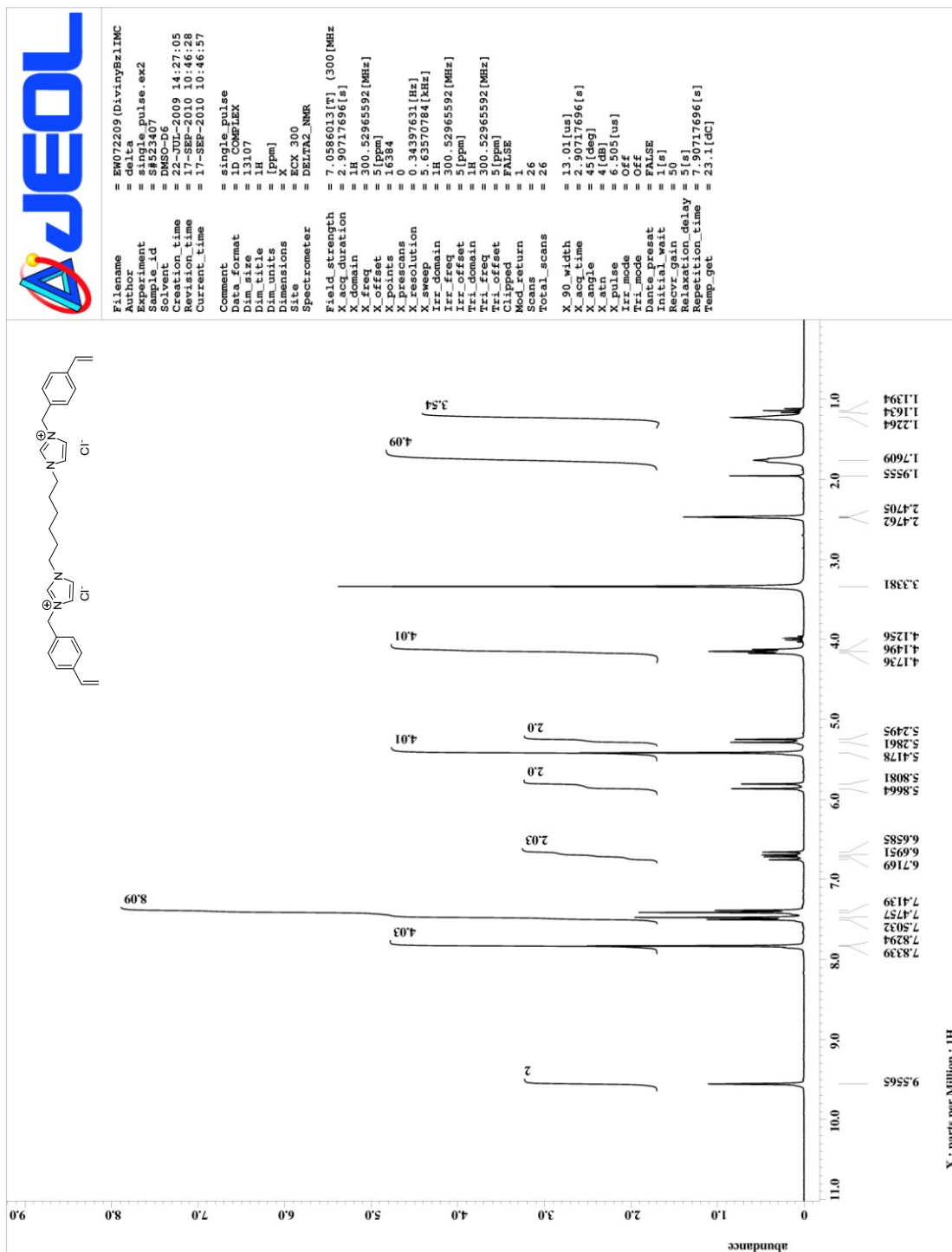


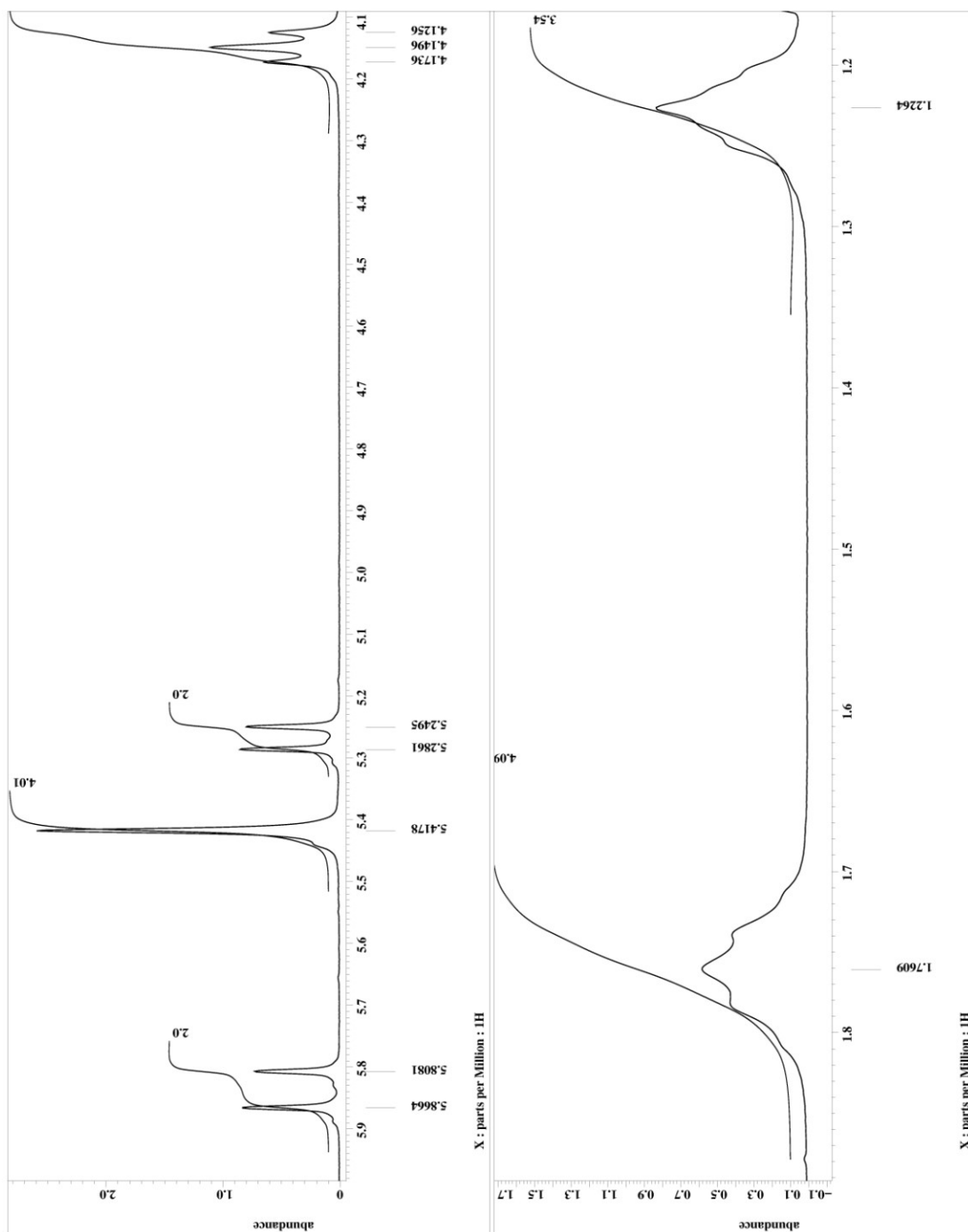


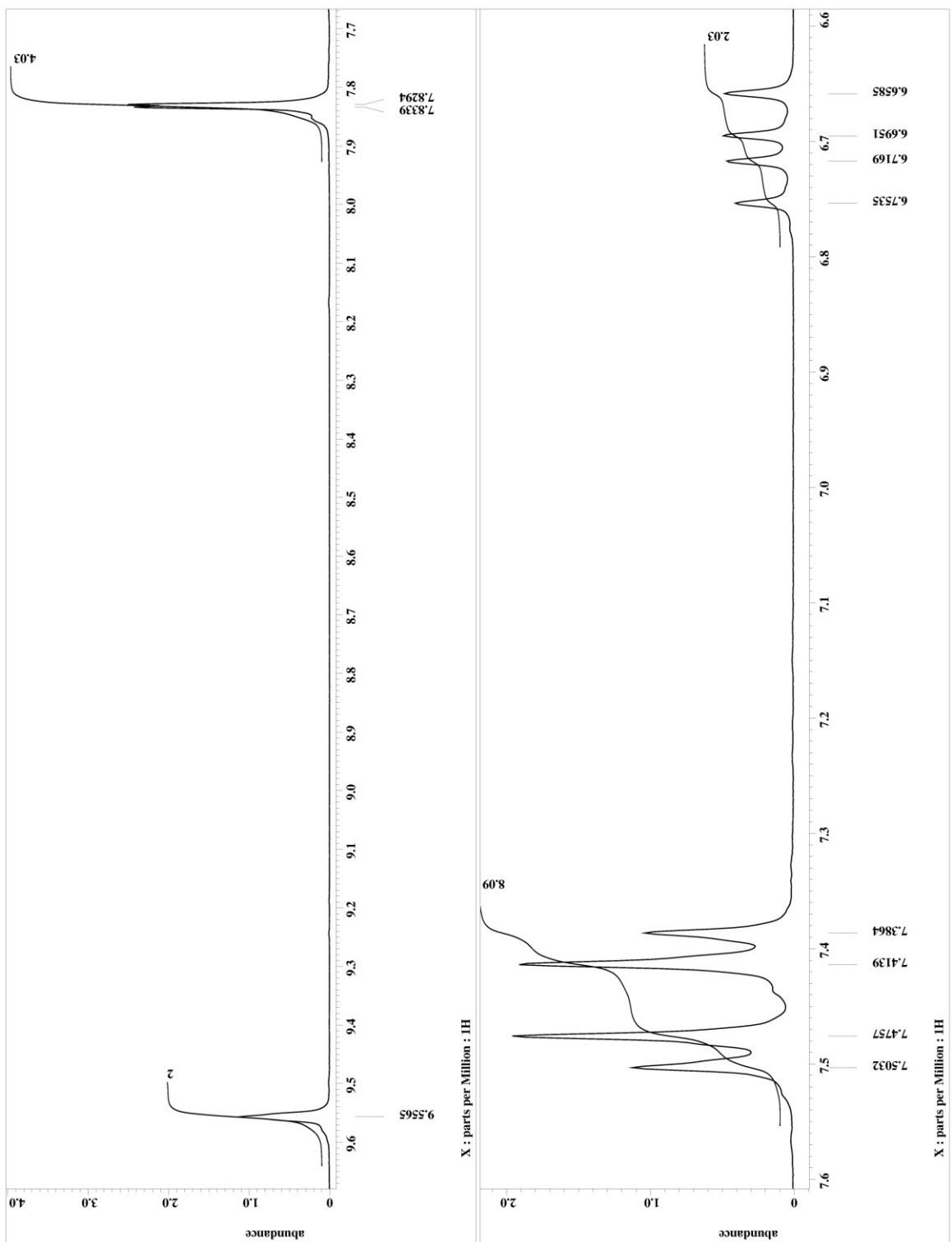
APPENDIX 17

¹H NMR SPECTRA OF

1,1'-(1,6-HEXANEDIYL)BIS-*P*-VINYLBENZYLIMIDAZOLIUM CHLORIDE (9)



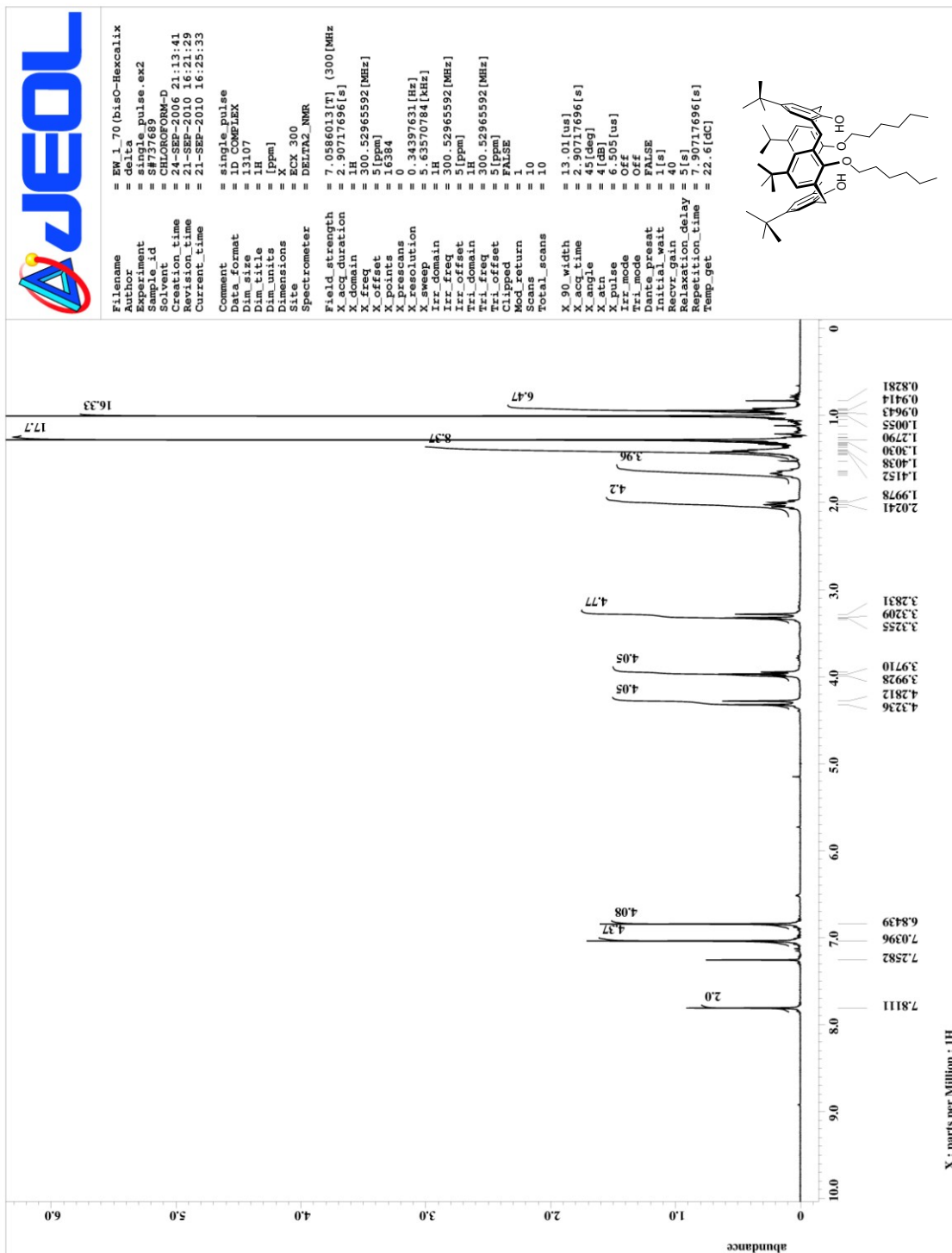


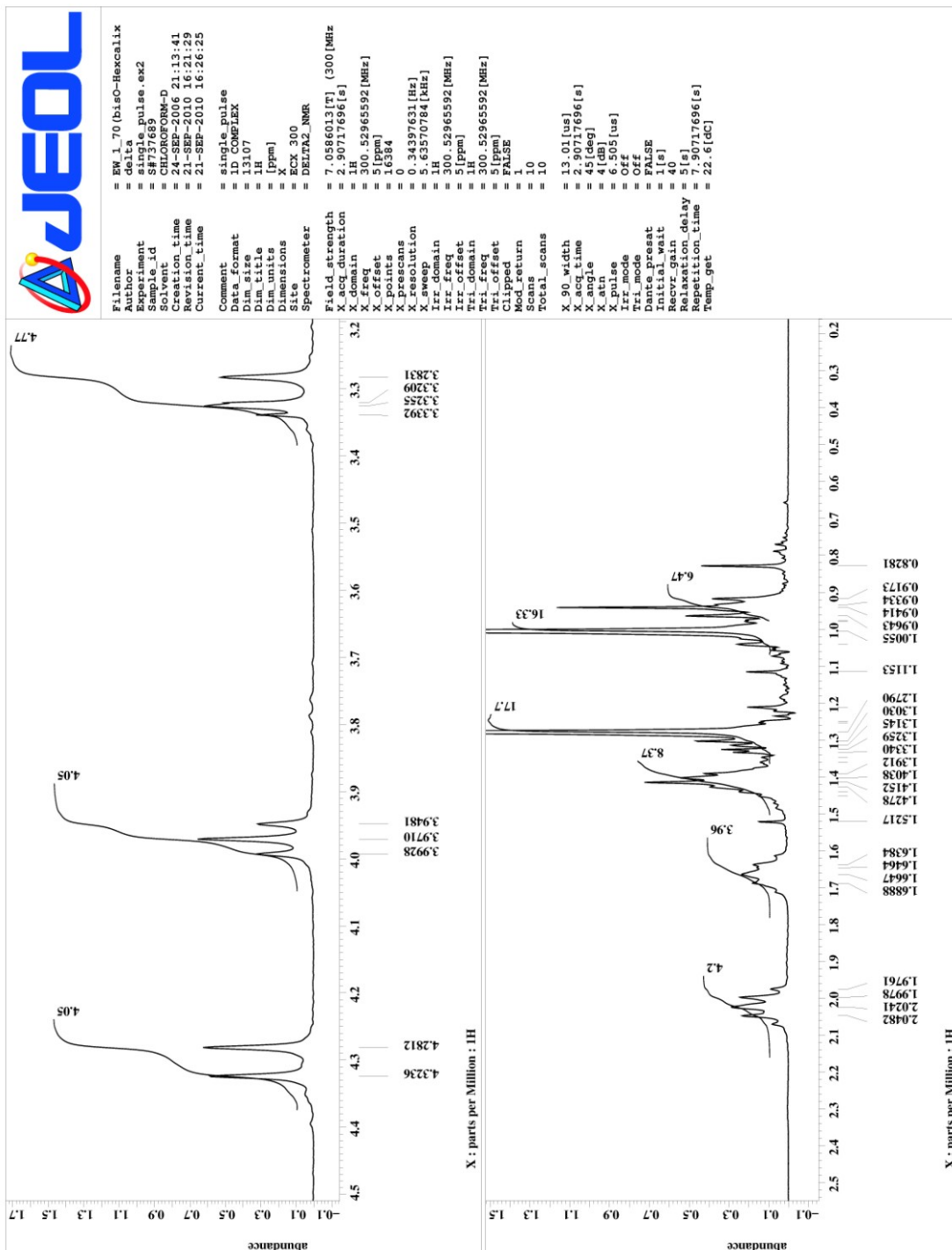


APPENDIX 18

¹H NMR SPECTRA OF

25,27-HYDROXY-26,28-BIS(*N*-HEXYLOXY)-*P*-*TERT*-BUTYLCALIX[4]ARENE (17)

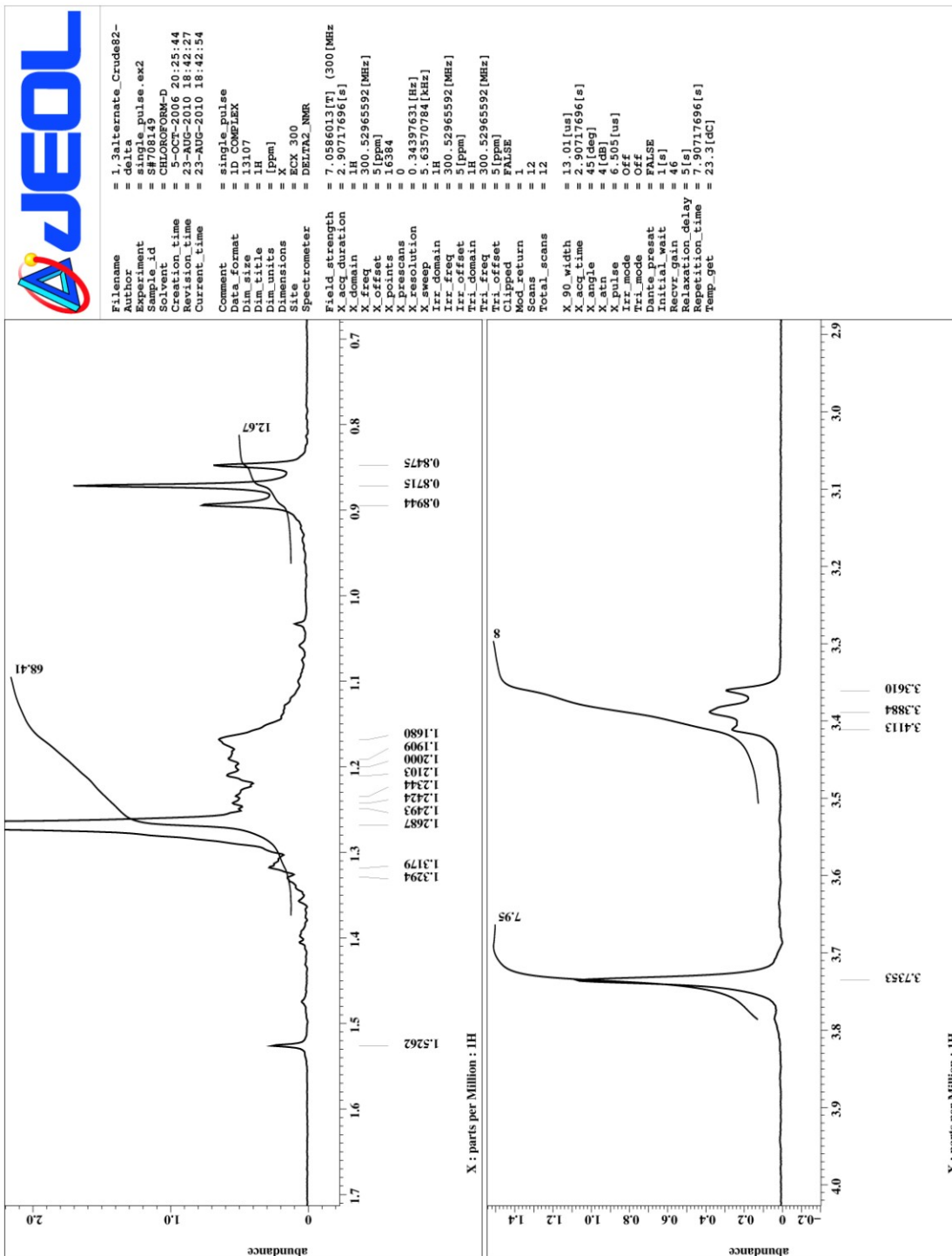




APPENDIX 19

¹H NMR SPECTRA OF

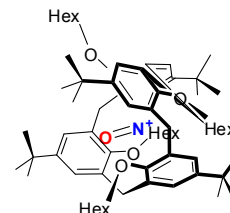
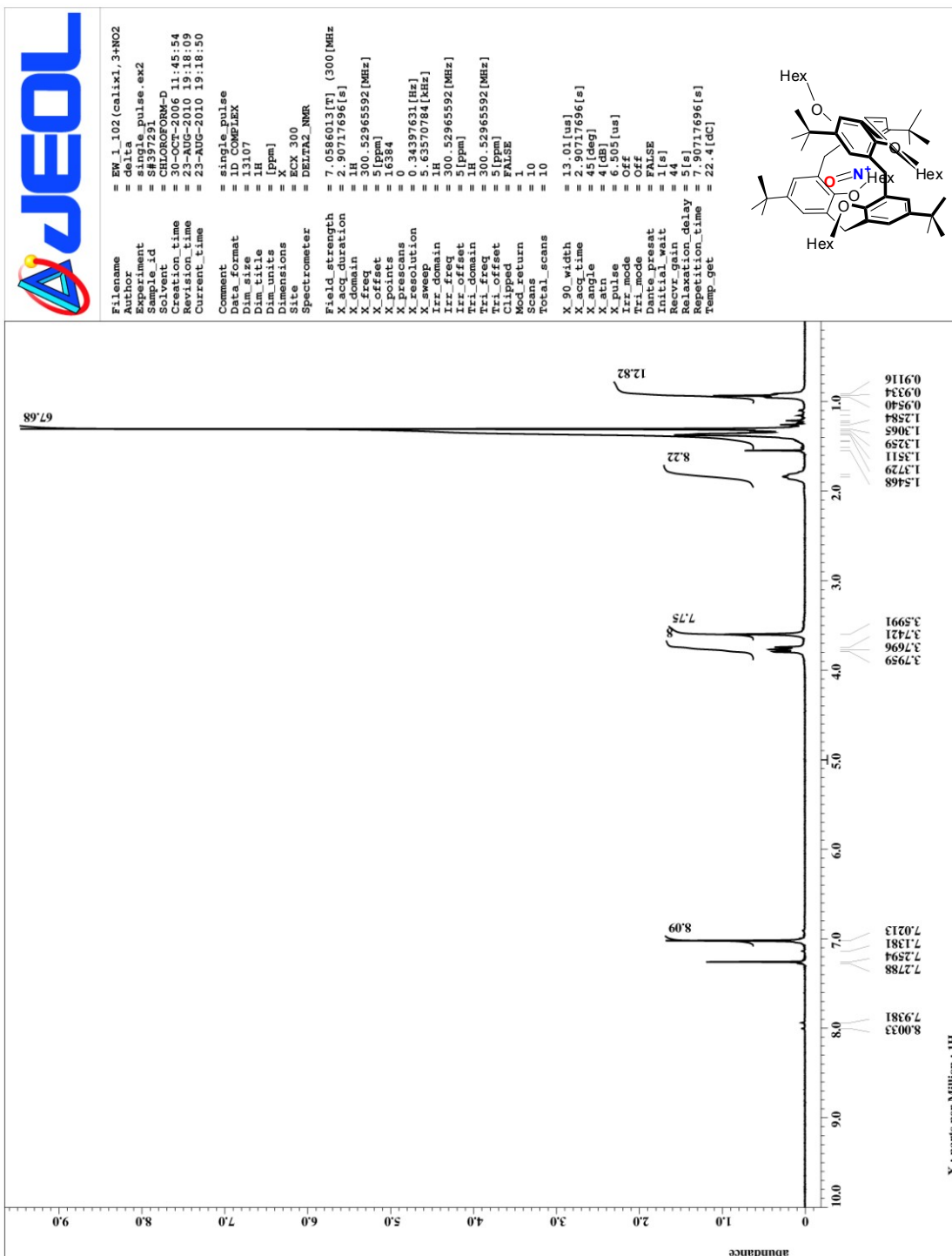
25,26,27,28-TETRAKIS(*N*-HEXYLOXY)-*P*-*TERT*-BUTYLCALIX[4]ARENE-1,3-
ALTERNATE (10)

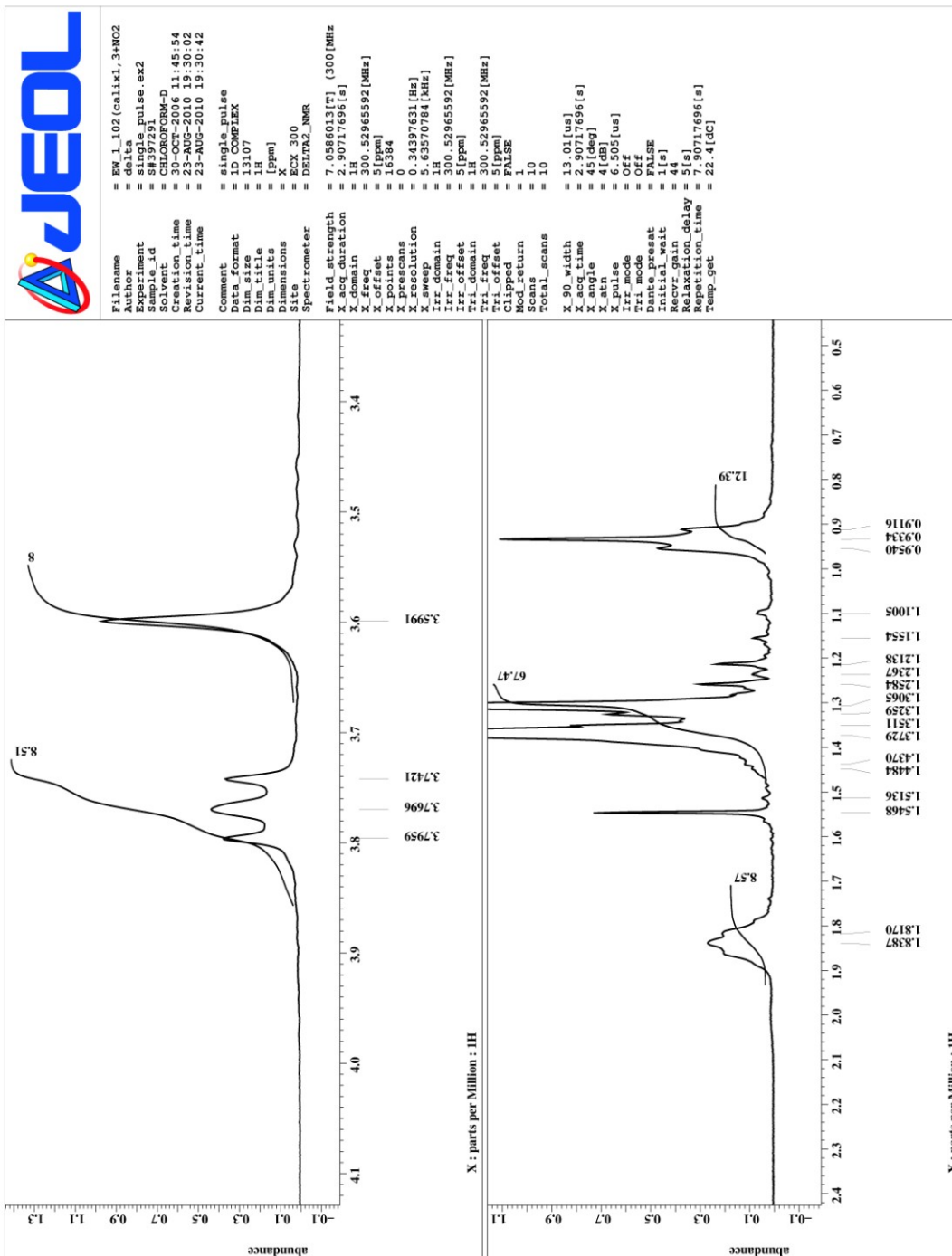


APPENDIX 20

¹H NMR SPECTRA OF

25,26,27,28-TETRAKIS(*N*-HEXYLOXY)-*P*-*TERT*-BUTYLCALIX[4]ARENE-1,3-
ALTERNATE-NO⁺ COMPLEX (11)



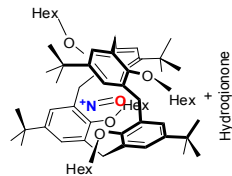


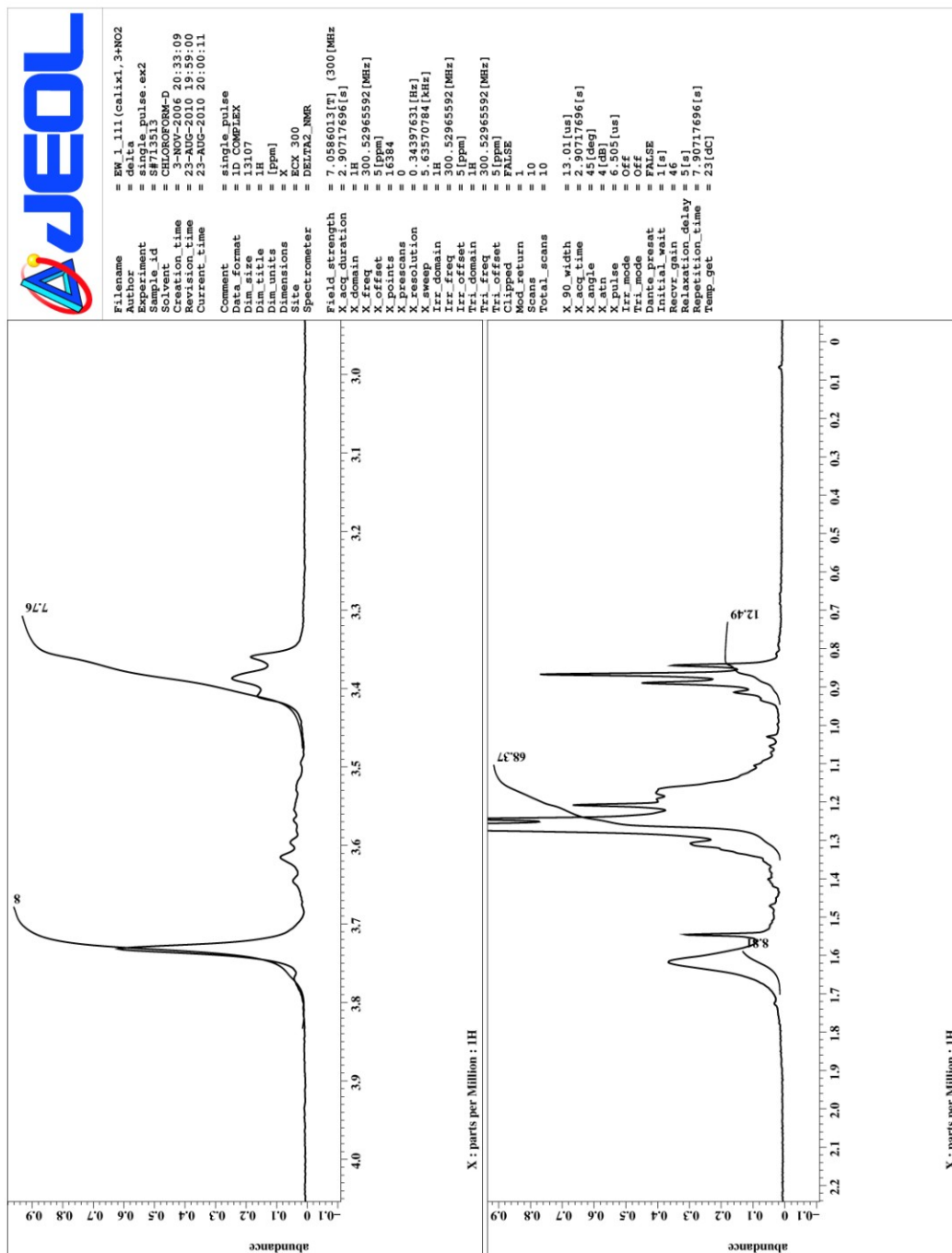
APPENDIX 21

¹H NMR SPECTRA OF

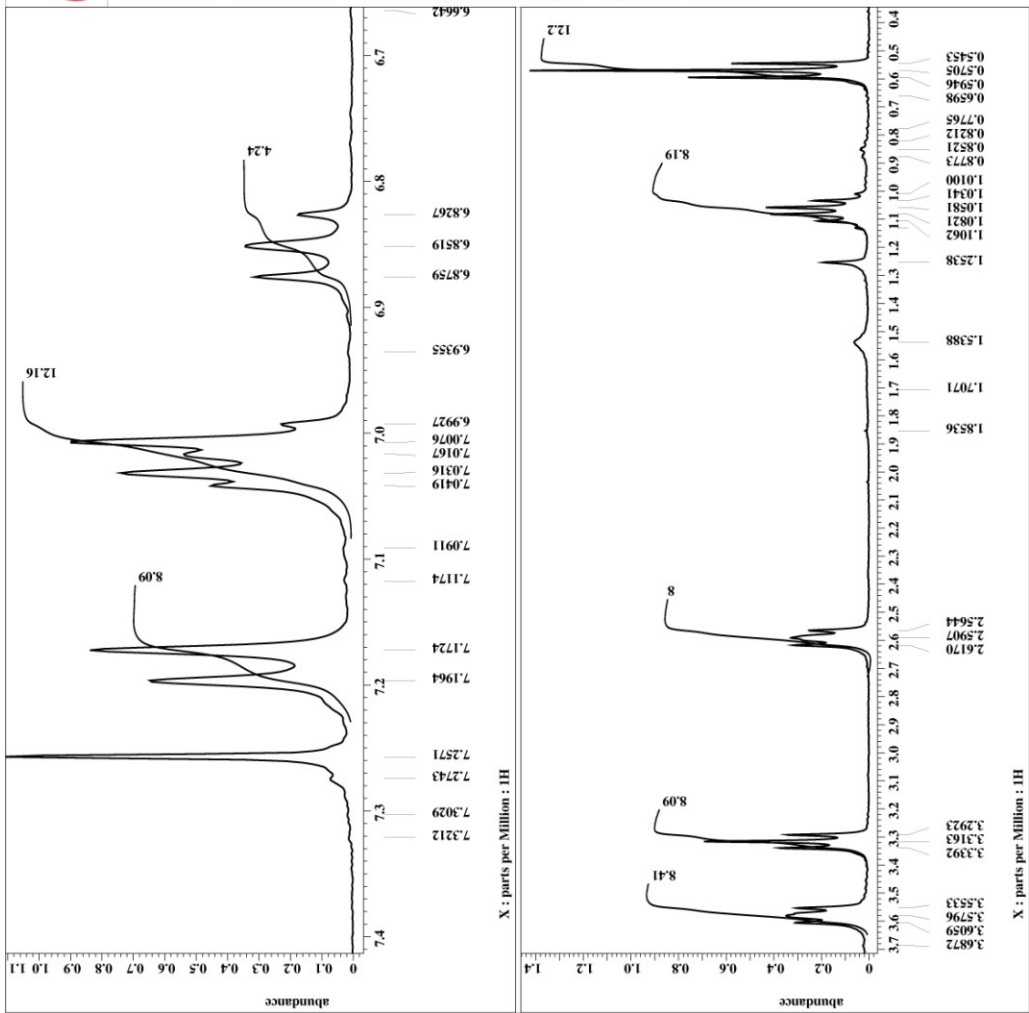
REDUCED 25,26,27,28-TETRAKIS(*N*-HEXYLOXY)-*P*-*TERT*-

BUTYLCALIX[4]ARENE-1,3-*ALTERNATE-NO*⁺ (11)





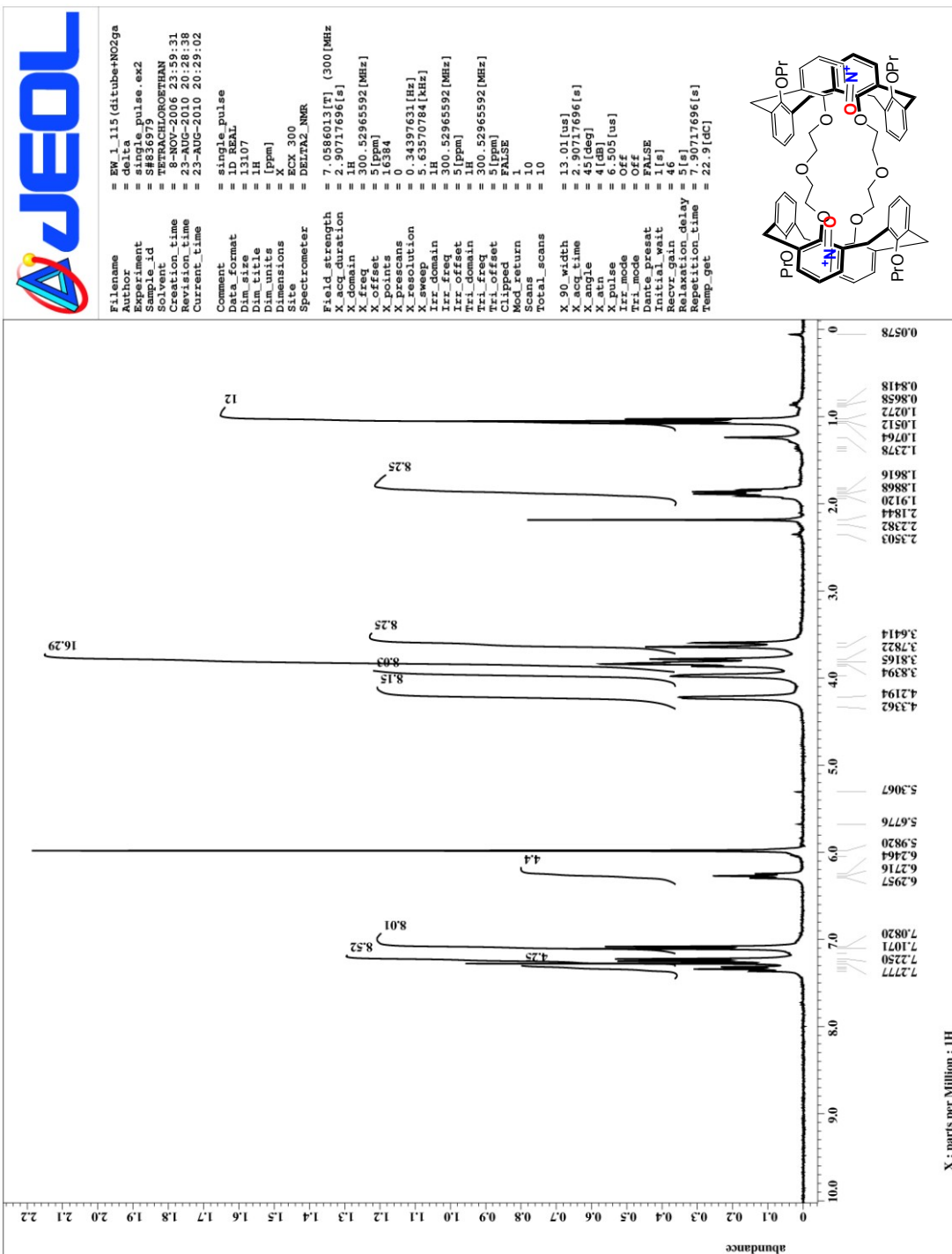
APPENDIX 22
¹H NMR SPECTRA OF
CALIX[4]DIMERIC TUBE

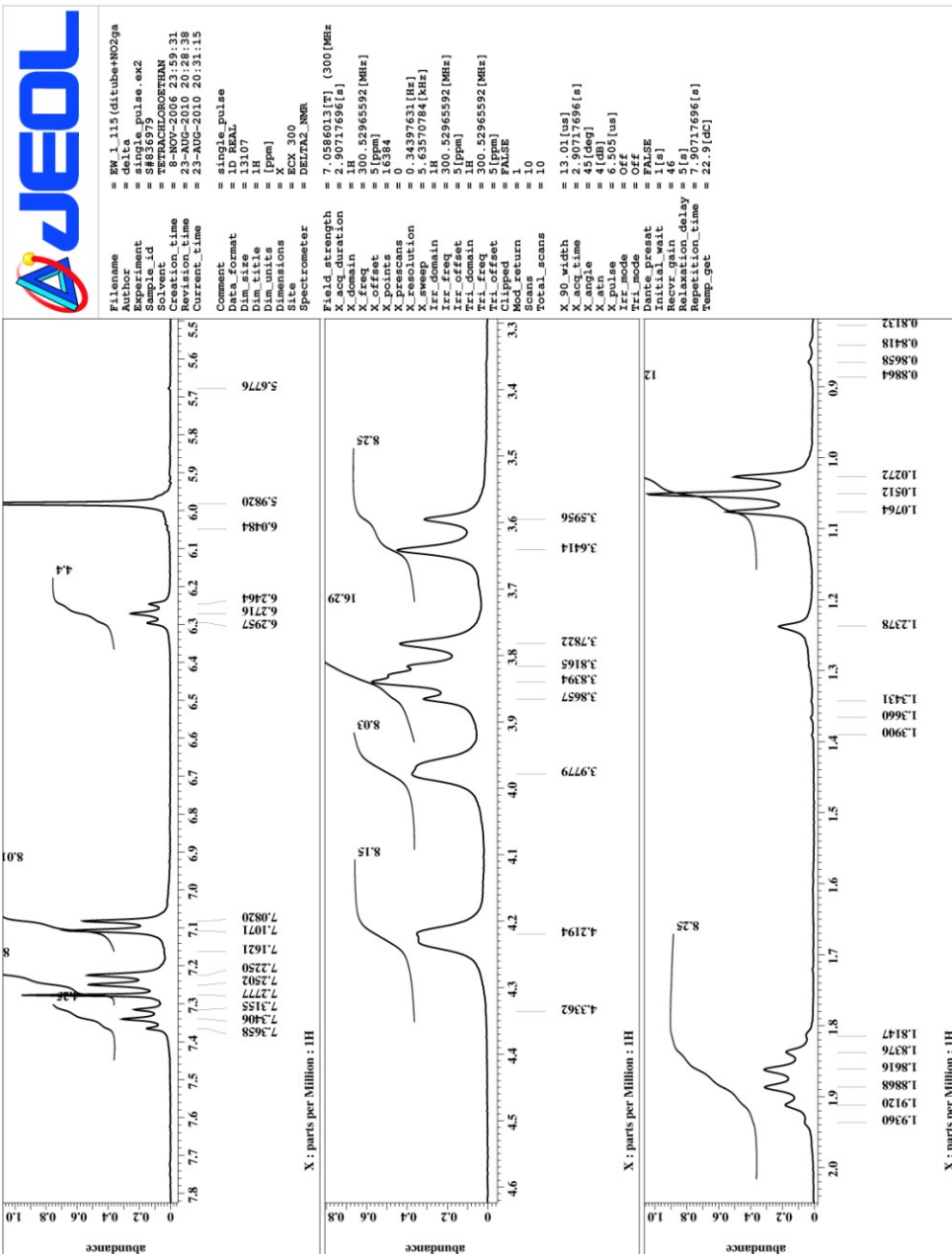


APPENDIX 23

¹H NMR SPECTRA OF

CALIX[4]DIMERIC TUBE_NO⁺ COMPLEX

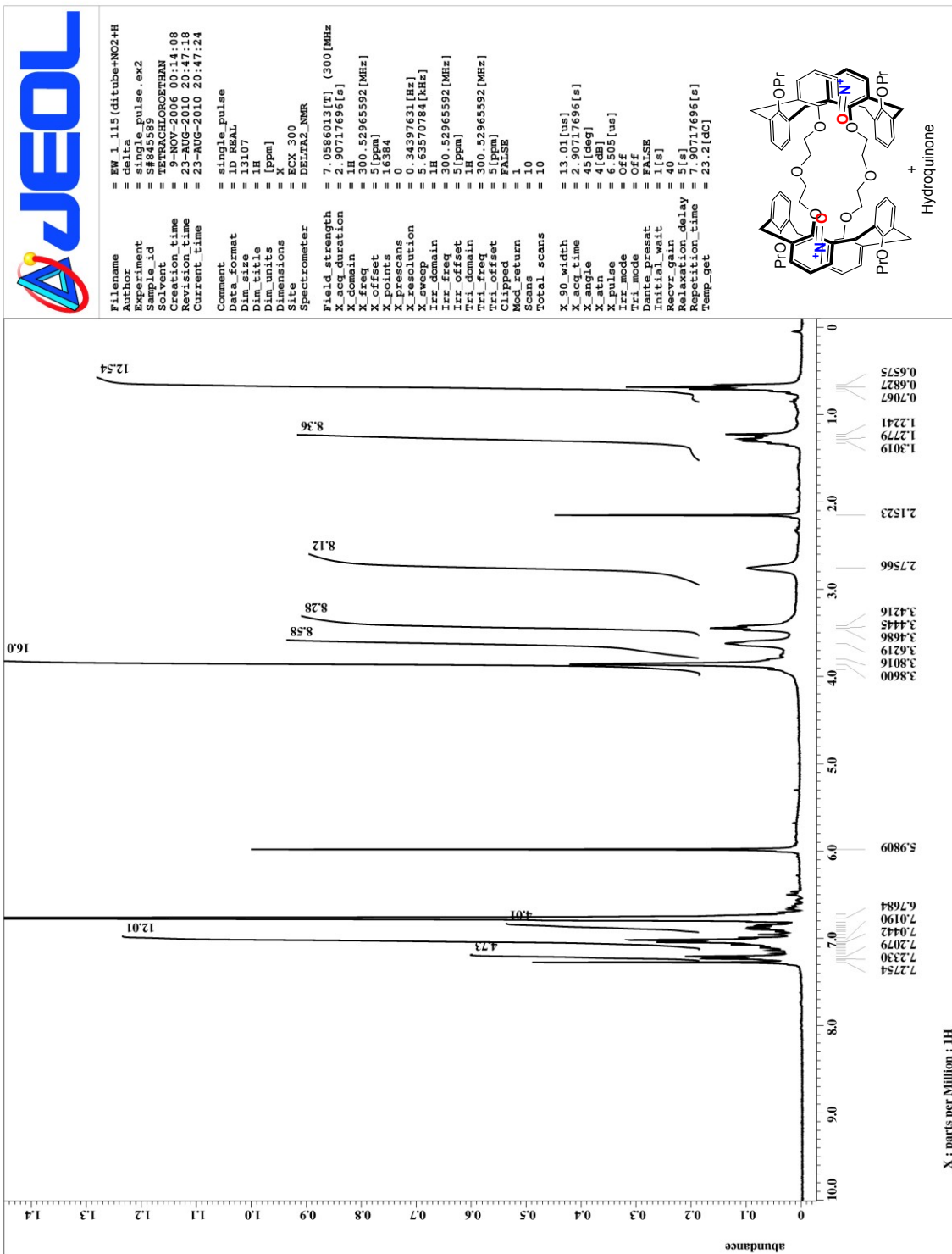




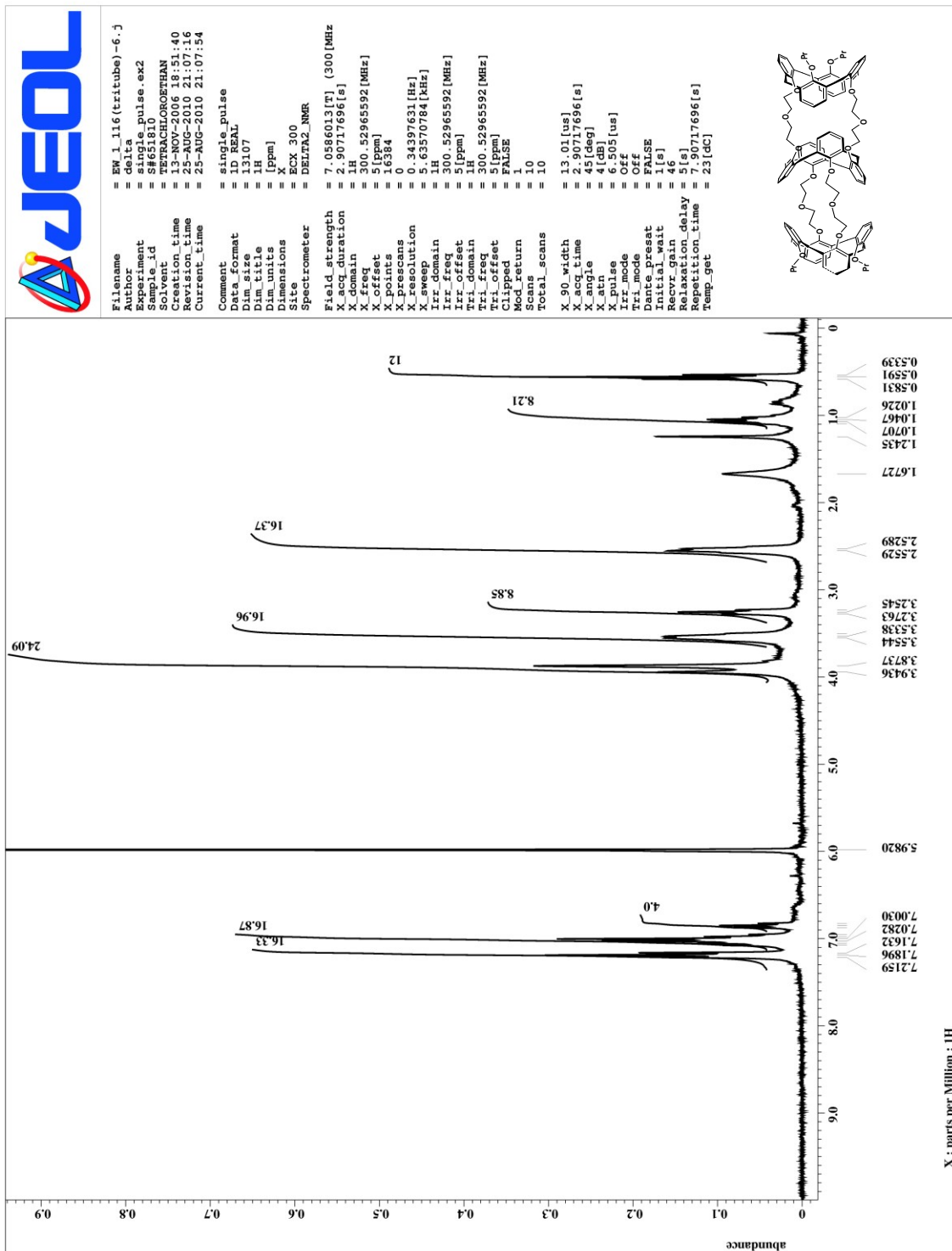
APPENDIX 24

¹H NMR SPECTRA OF

REDUCED CALIX[4]ARENE DIMERIC TUBE-NO⁺ COMPLEX (13)



APPENDIX 25
¹H NMR SPECTRA OF
CALIX[4]ARENE TRIMERIC TUBE (14)



APPENDIX 26

¹H NMR SPECTRA OF

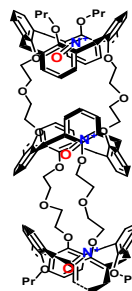
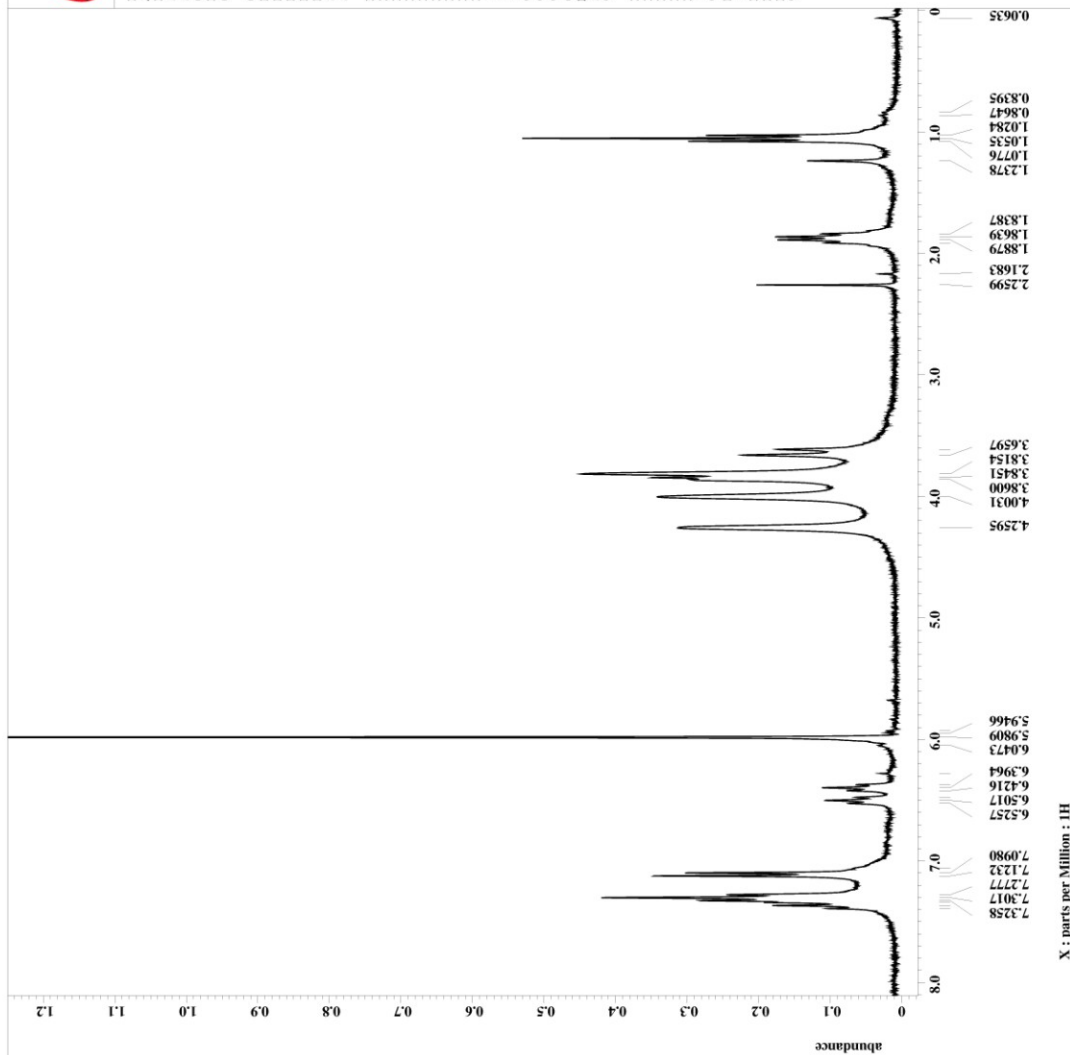
CALIX[4]ARENE TRIMERIC TUBE-NO⁺ COMPLEX (15)



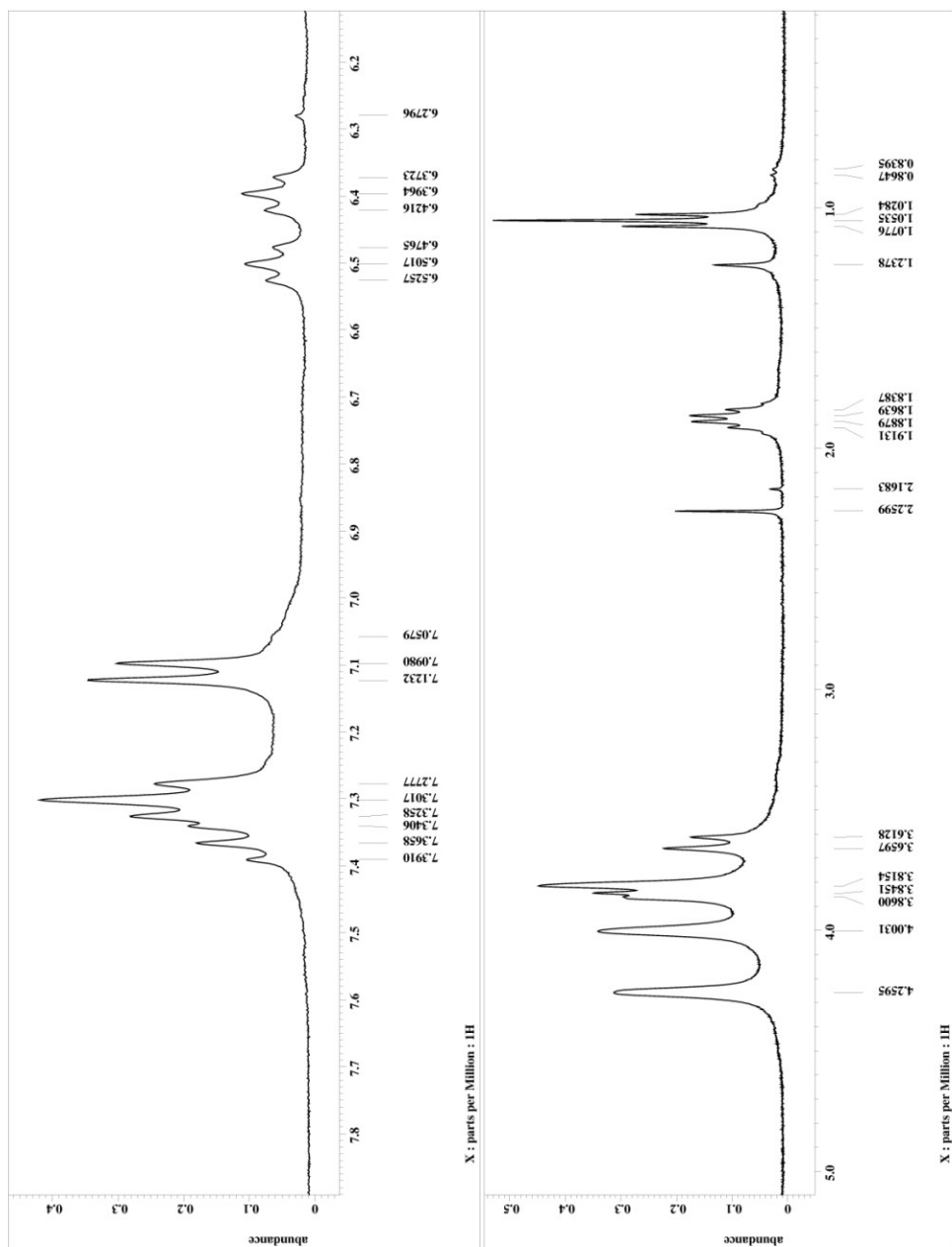
```

=====
Filename      = EW_1_116(tritube+NO2+)
Author       =
Experiment   = single_pulse.ex2
Sample_id    = tritube+NO2
Solvent      = TETRACHLOROETHAN
Creation_time = 14-NOV-2006 10:37:38
Experiment_time = 14-NOV-2006 10:38:14
Current_time  = 21-SEP-2010 23:15:42
=====
Comment      = single_pulse
Data_format   = ID COMPLEX
Dim_size     = 13107
F2_offset    = [Hz]
F2_resolution = [ppm]
Dim_units    = X
Dimensions   = X
Site         = ECX 300
Spectrometer = DELTA2_NMR
=====
Field_strength = 7.0586013[T] (300[MHz]
X_acq_duration = 2.90717696[s]
X_domain       = 1H
X_freq         = 300.52965592[MHz]
X_offset       = 5[ppm]
X_resolution   = 6.384
X_sweep        = 0.34397631[Hz]
X_resolution   = 5.63570784[kHz]
Irr_domain     = 1H
Irr_freq       = 300.52965592[MHz]
Irr_offset     = 5[ppm]
Tri_domain     = 1H
Tri_freq       = 300.52965592[MHz]
Tri_offset     = 5[ppm]
Clipped        = FALSE
Mod_return     = 1
Scan           = 12
Total_scans    = 12
=====
X_90_width    = 13.01[us]
X_acq_time     = 2.90717696[s]
X_angle       = 45[deg]
X_offset      = 6.384[ppm]
X_pulse       = 6.505[us]
Irr_mode      = Off
Tri_mode      = Off
Dante_preset  = FALSE
Initial_wait  = 1[s]
Relaxation_delay = 5[s]
Repetition_time = 7.90717696[s]
Temp_get      = 22.8[dc]
=====

```



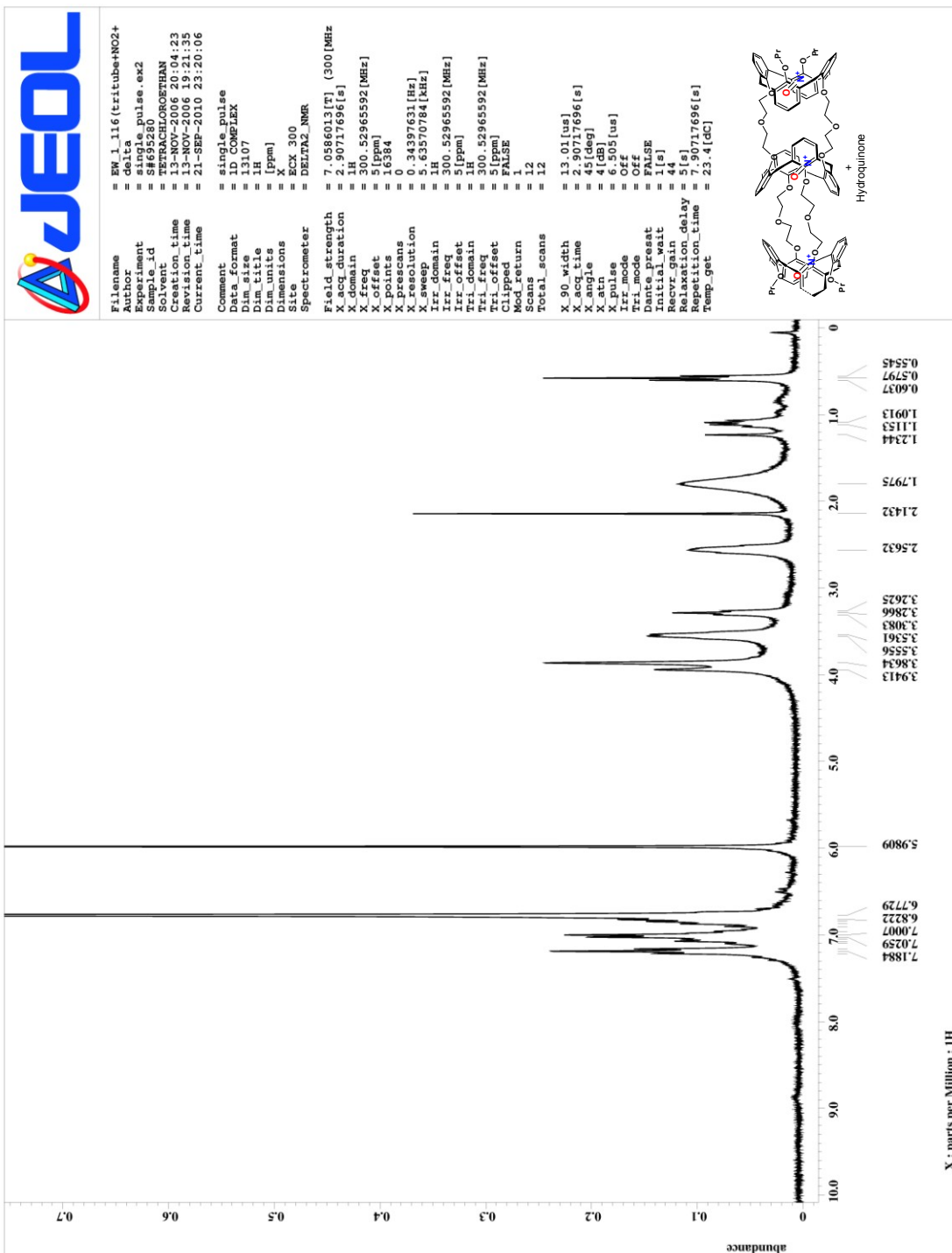
X : parts per Million : 1H

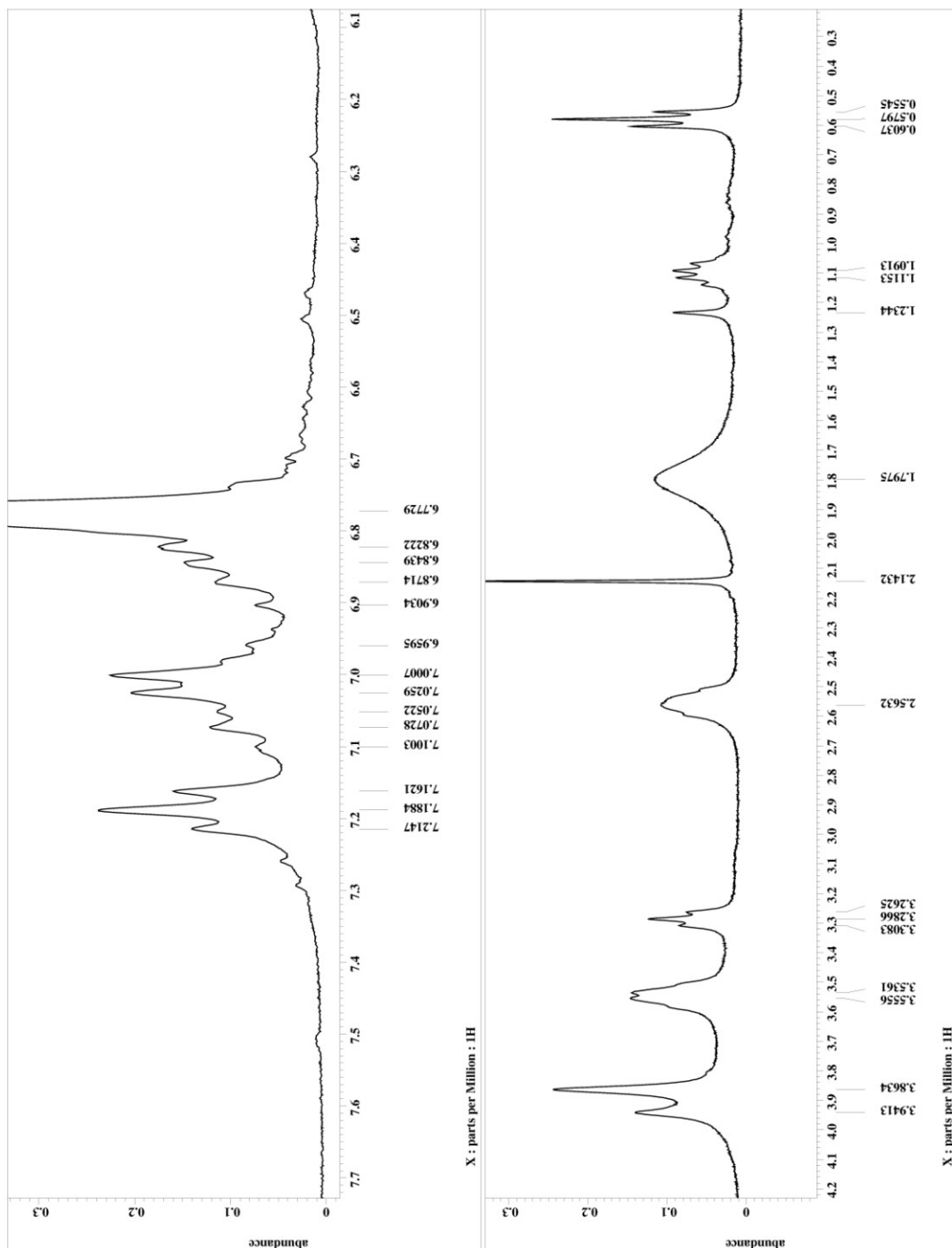


APPENDIX 27

¹H NMR SPECTRA OF

REDUCED CALIX[4]ARENE TRIMERIC TUBE-NO⁺ COMPLEX (15)

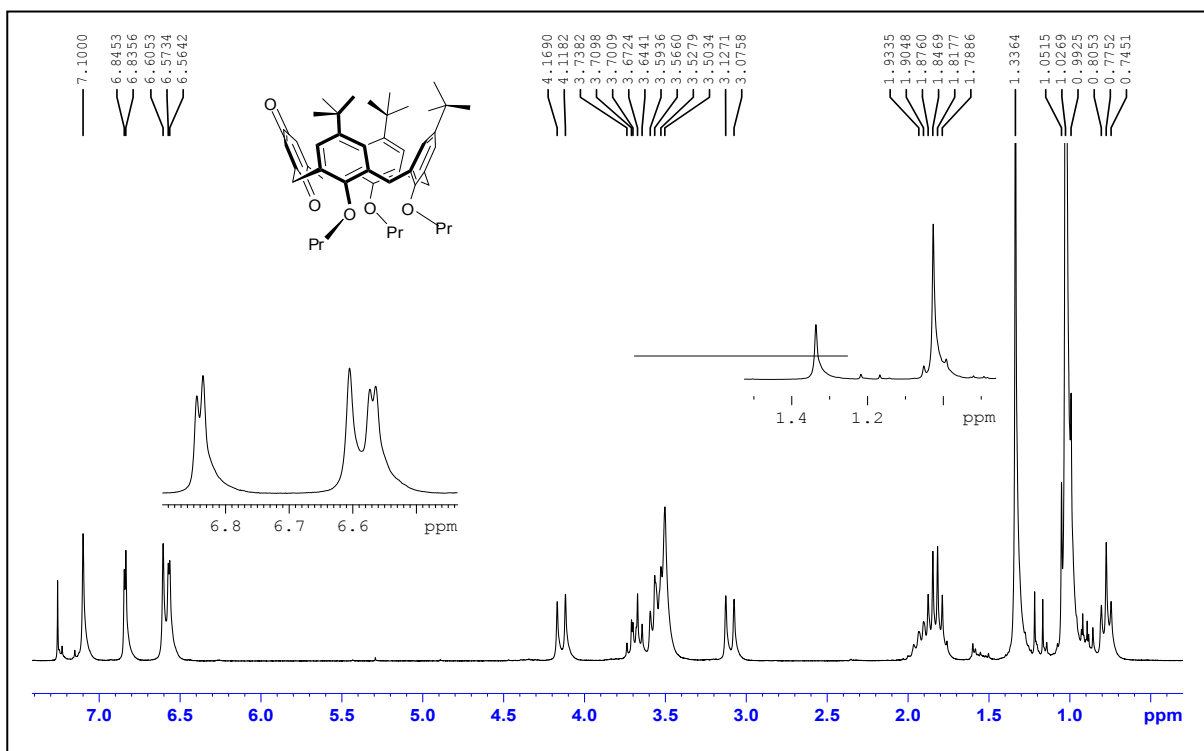




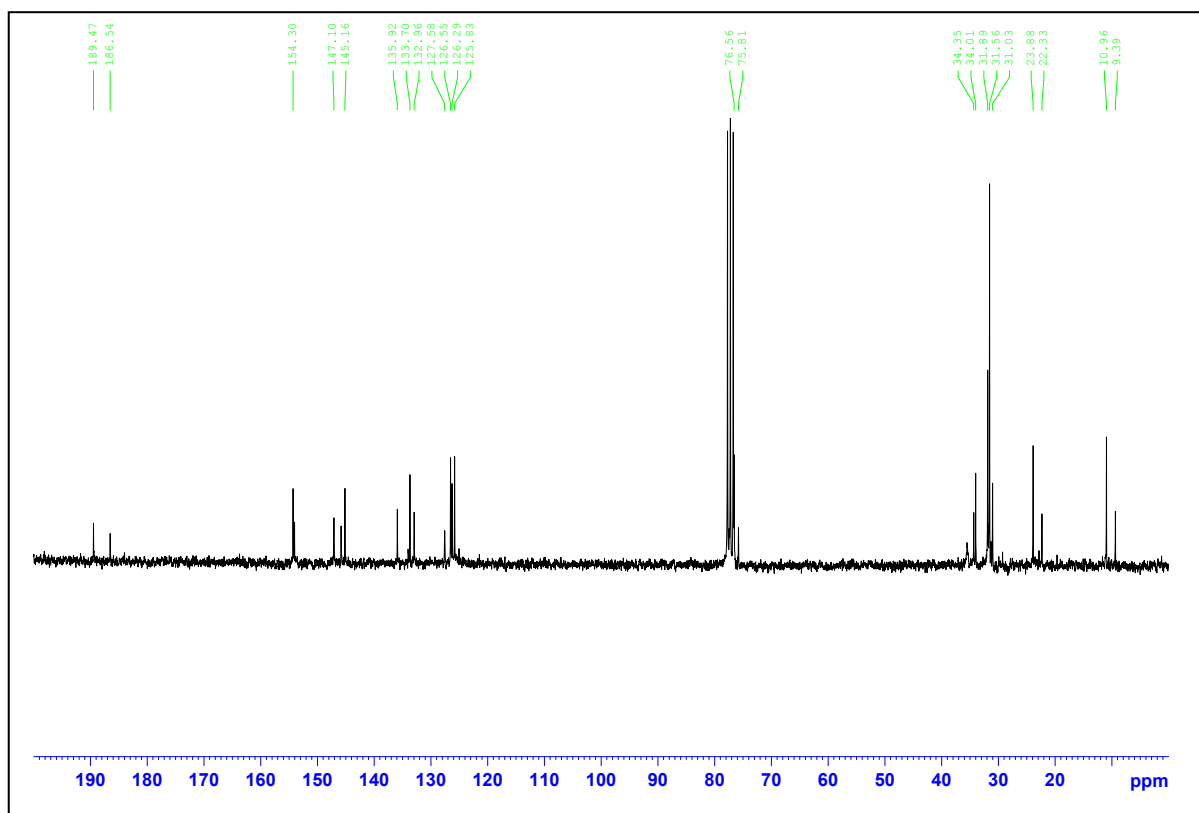
APPENDIX 28

¹H AND ¹³C NMR SPECTRA OF

25,26,28-TRIS(*N*-PROPYL)-*P*-*TERT*-BUTYLCALIX[4]MONOQUINONE (19)



¹H NMR was recorded on Bruker Avance-400 MHz spectrometer.



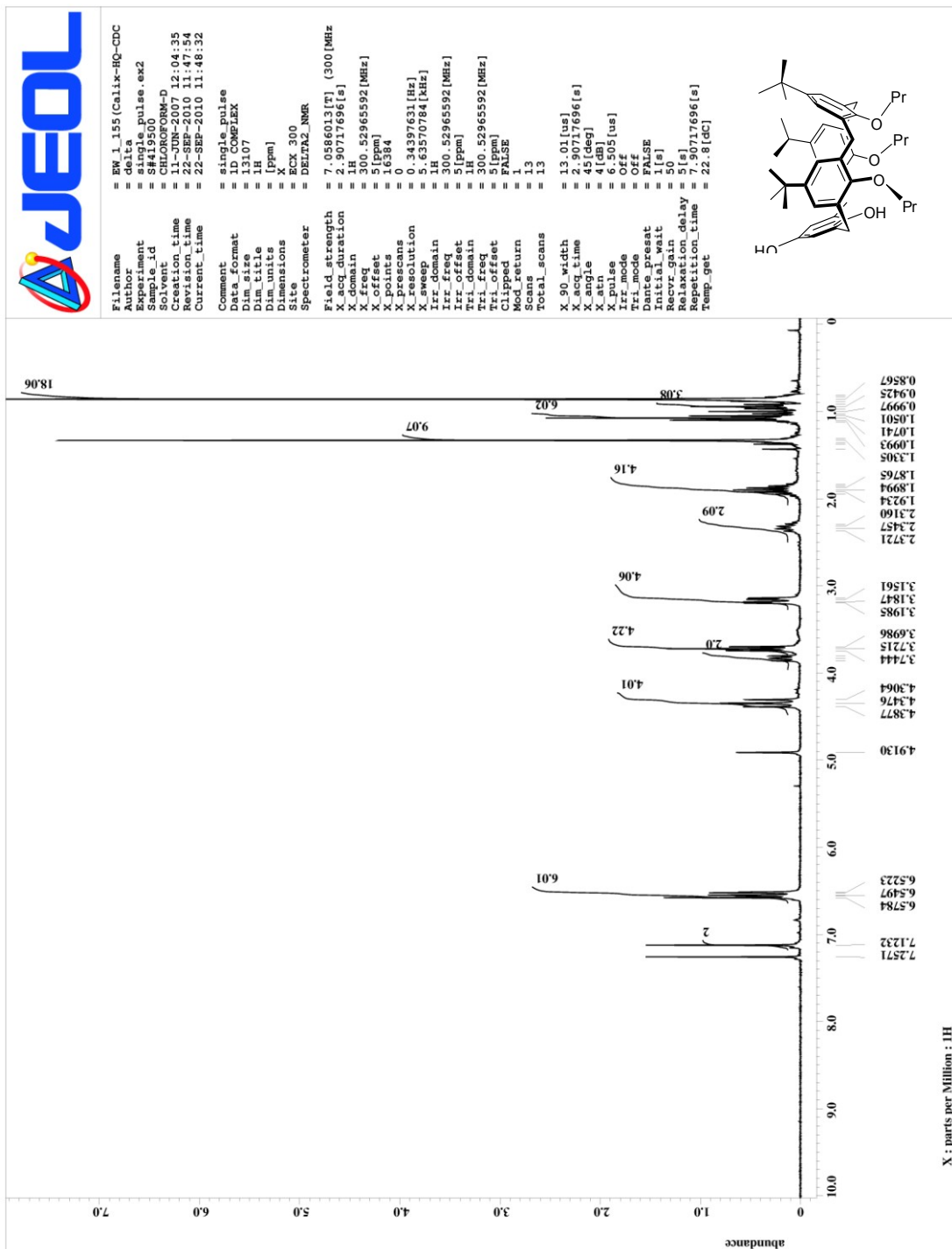
¹³C NMR was recorded on Bruker Avance-400 MHz spectrometer.

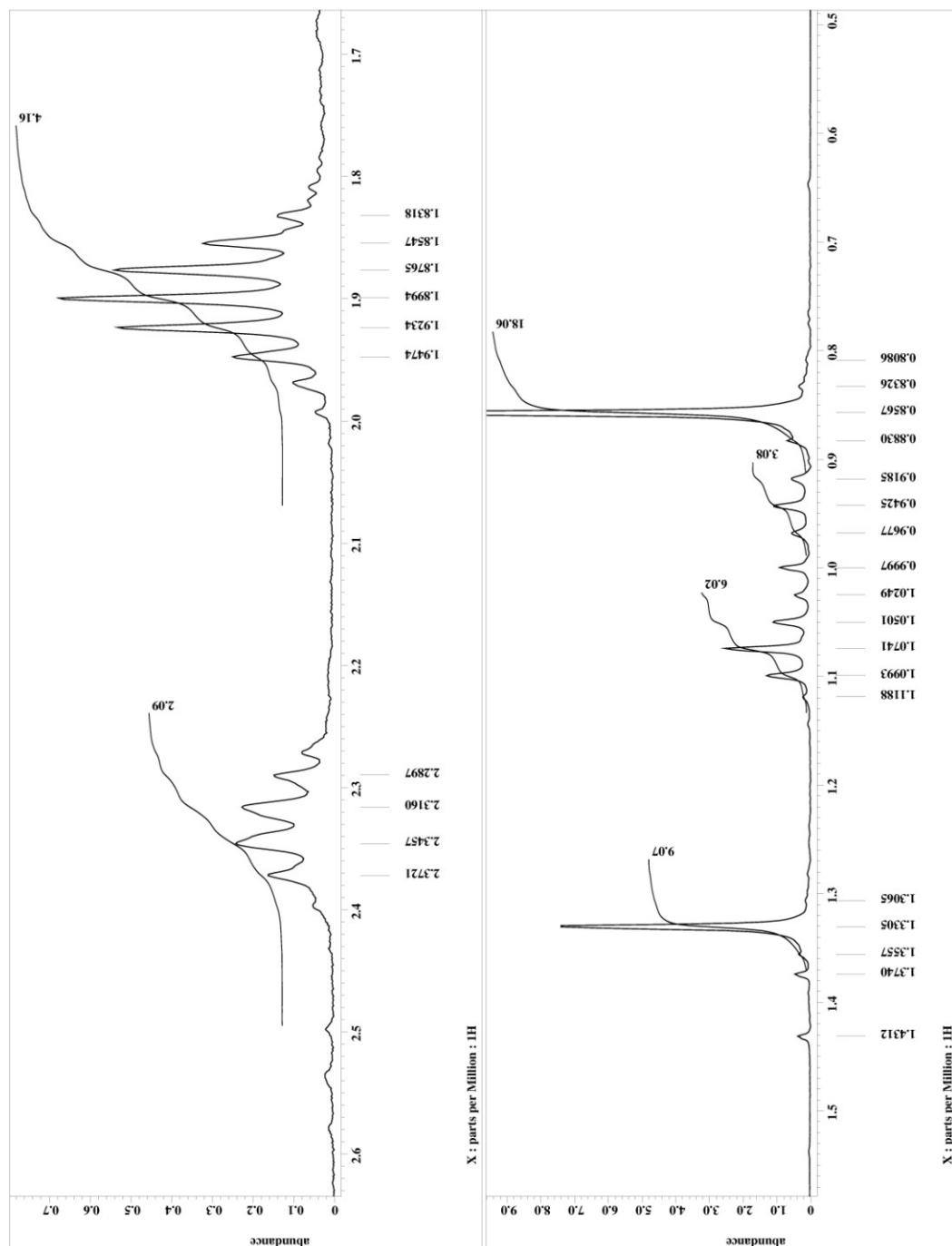
APPENDIX 29

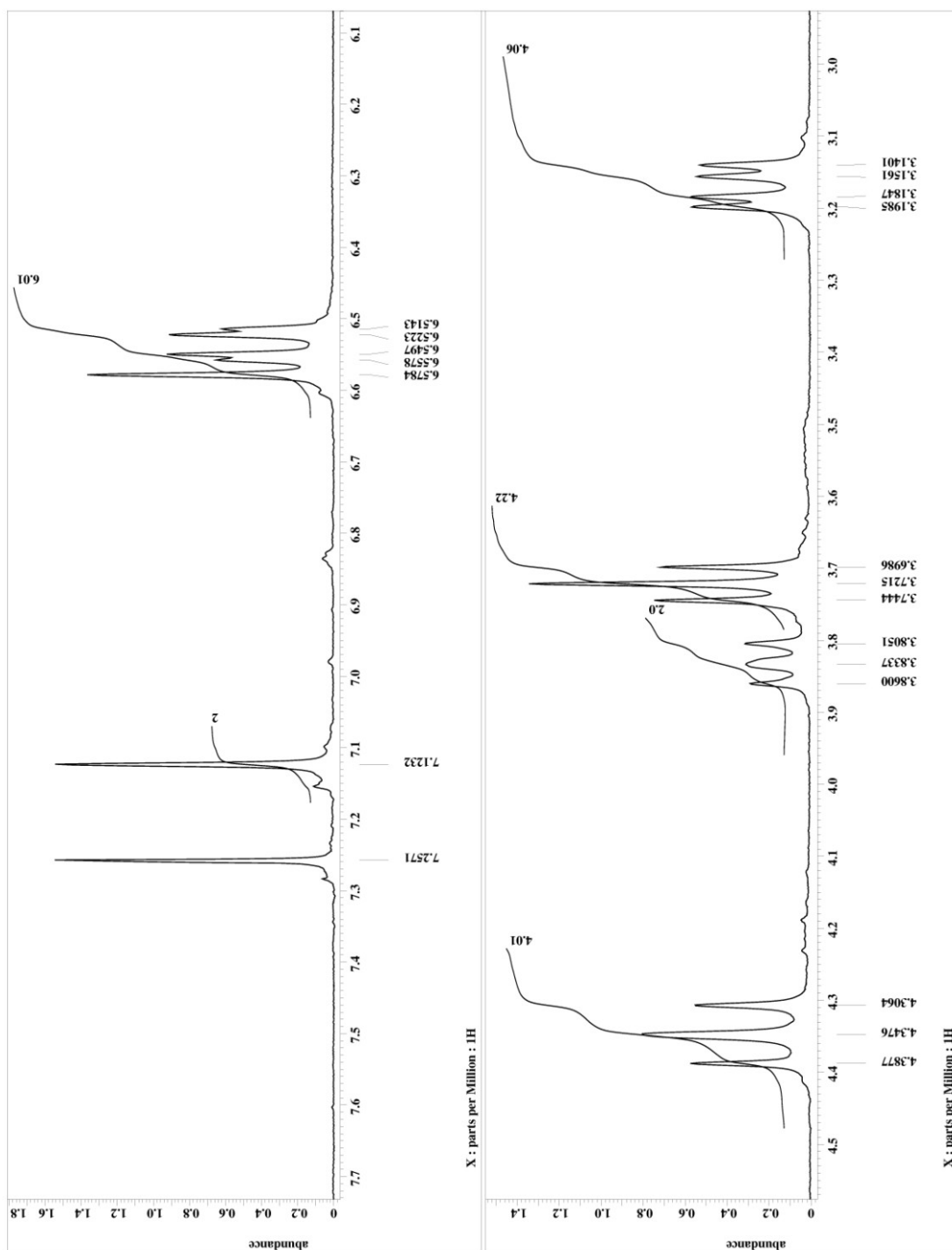
^1H AND ^{13}C NMR SPECTRA OF

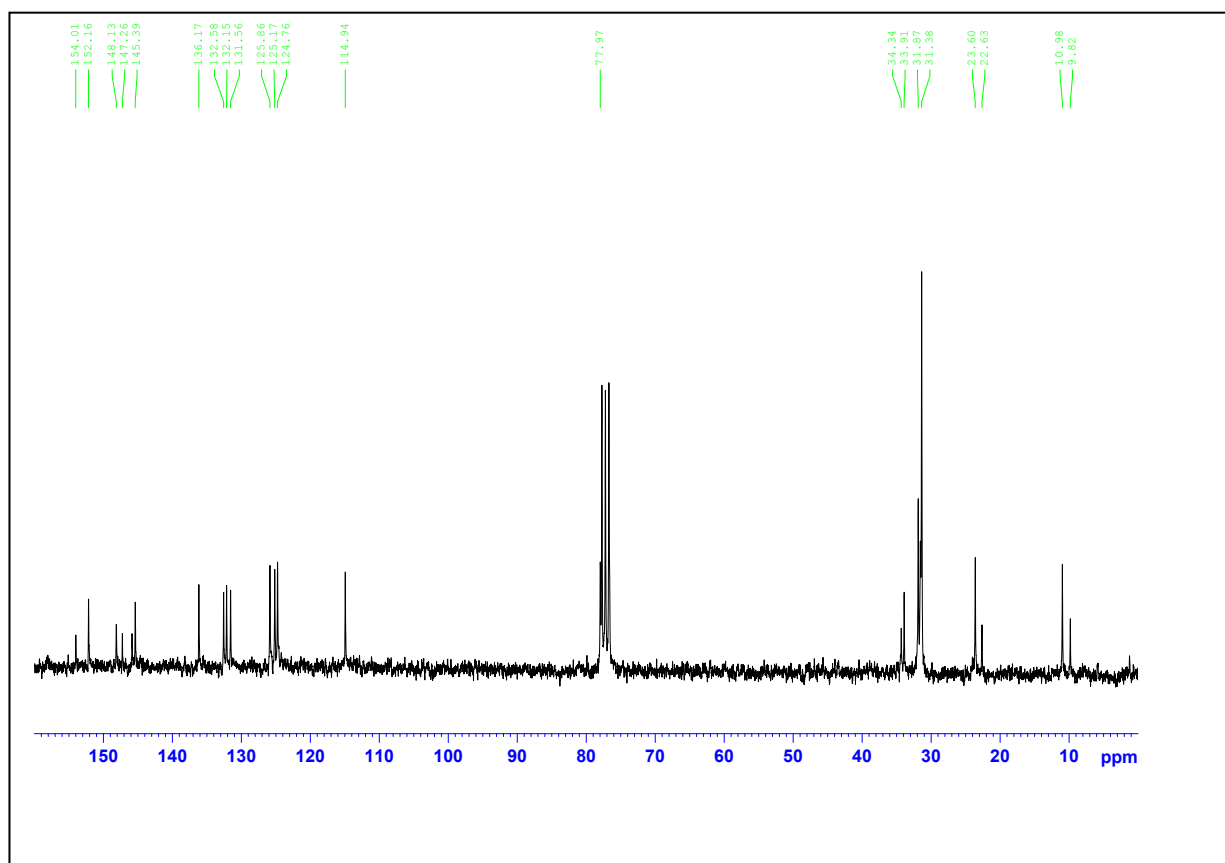
25,26,28-TRIS(*N*-PROPYLOXY)-*P*-*TERT*-BUTYLCALIX[4]MONOHYDROQUINONE

(20)







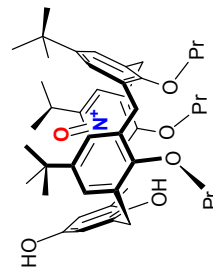
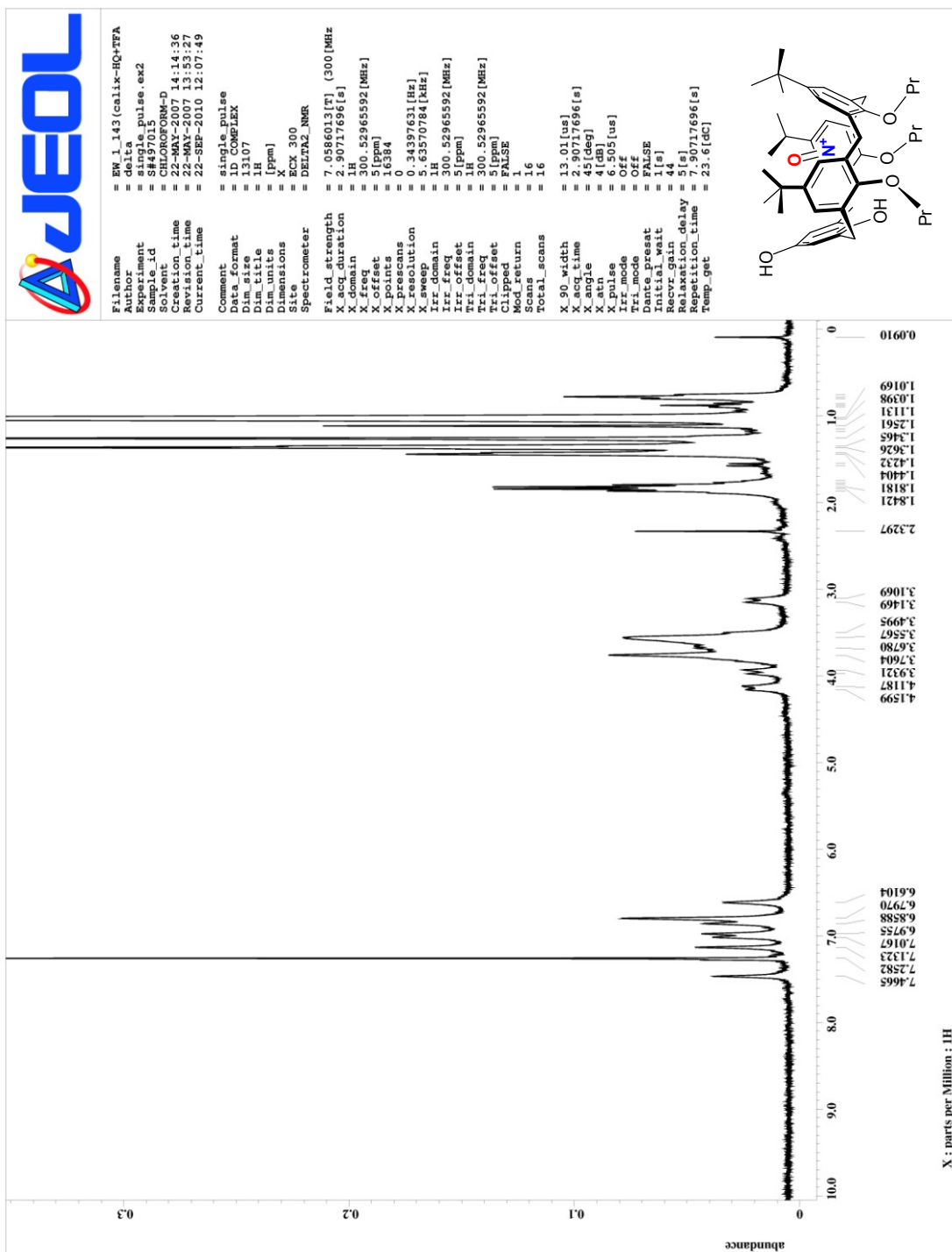


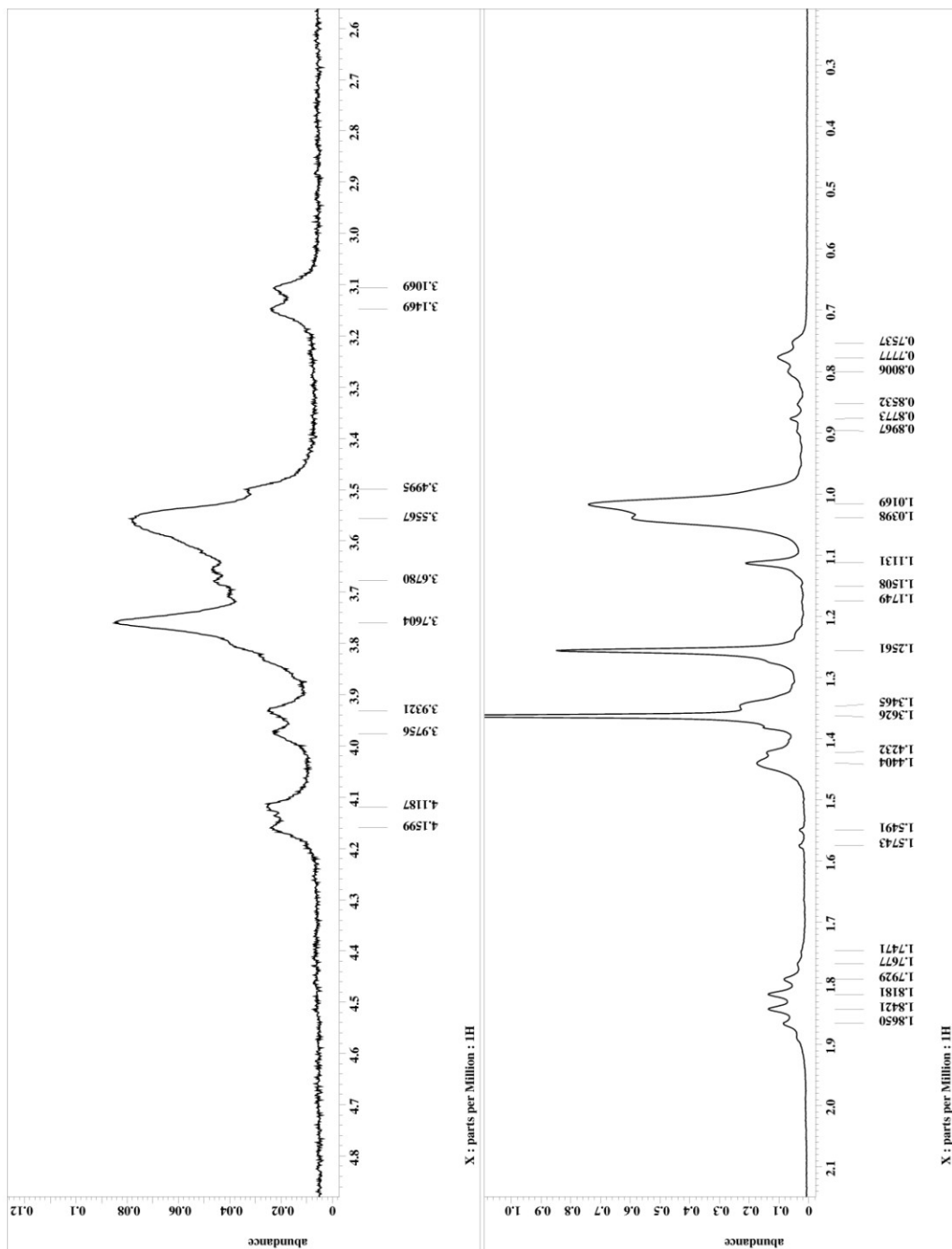
^{13}C NMR was recorded on Bruker Avance-400 MHz spectrometer.

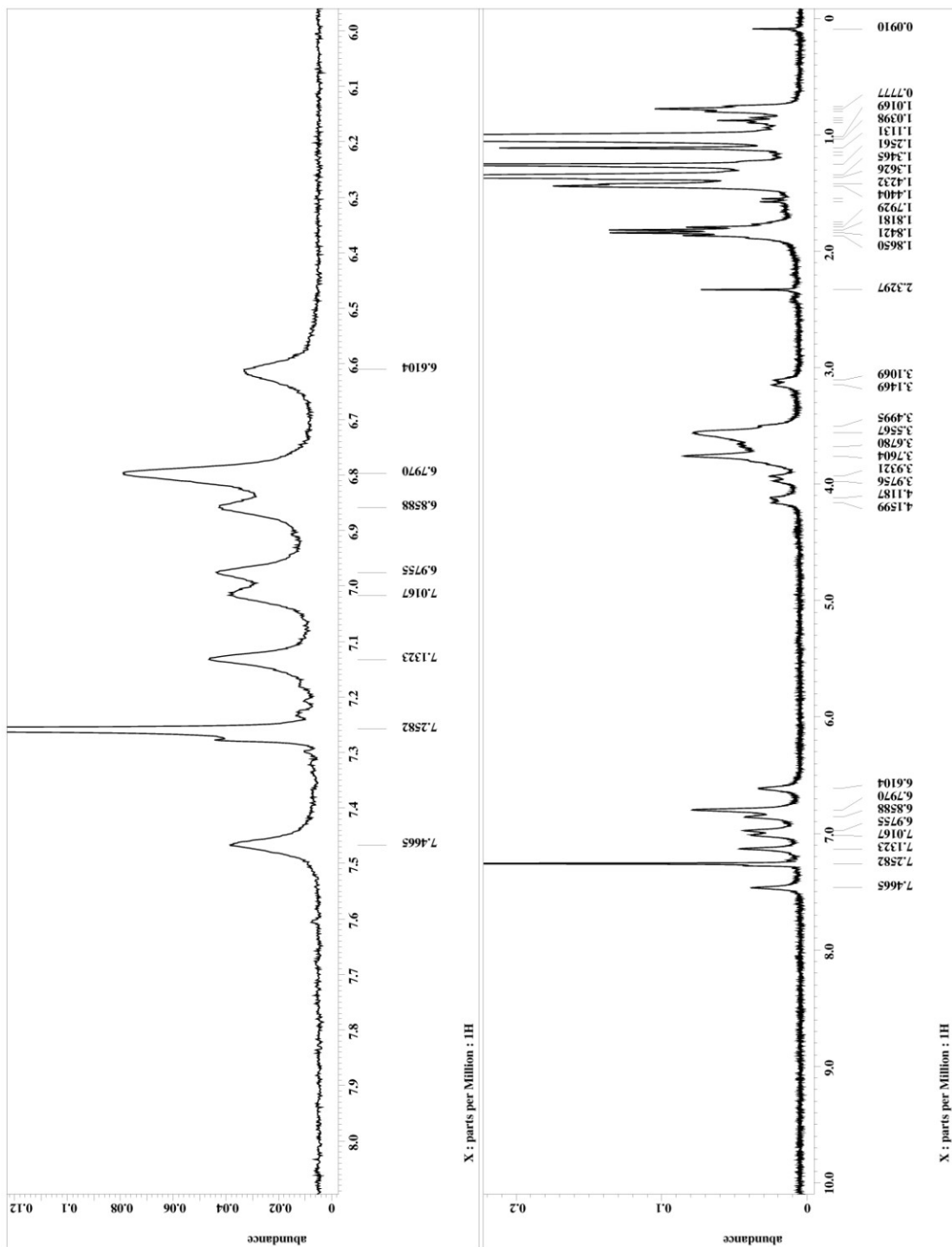
APPENDIX 30

¹H NMR SPECTRA OF

P-TERT-BUTYLCALIX[4]MONOHYDROQUINONE-NITROSONIUM COMPLEX (21)



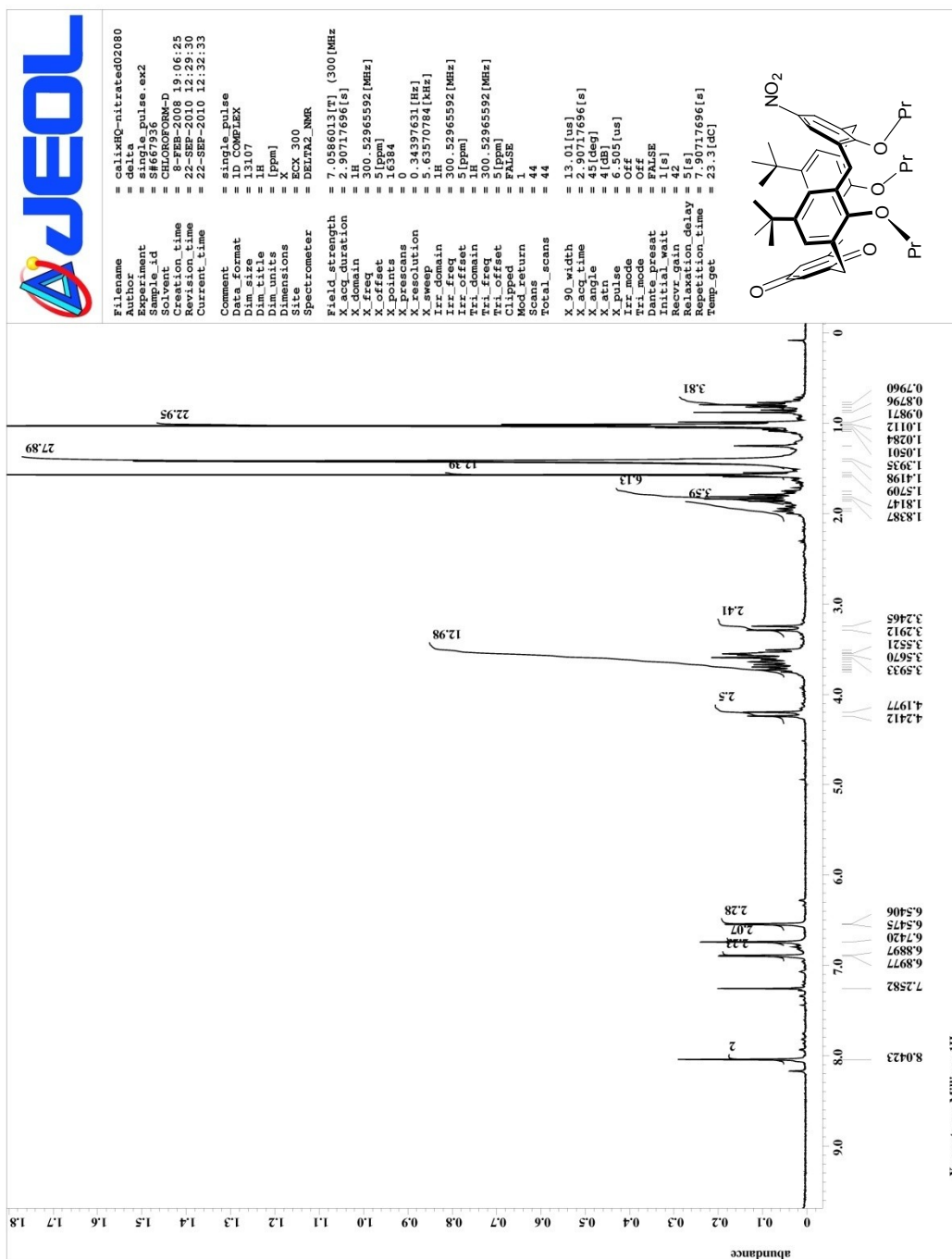


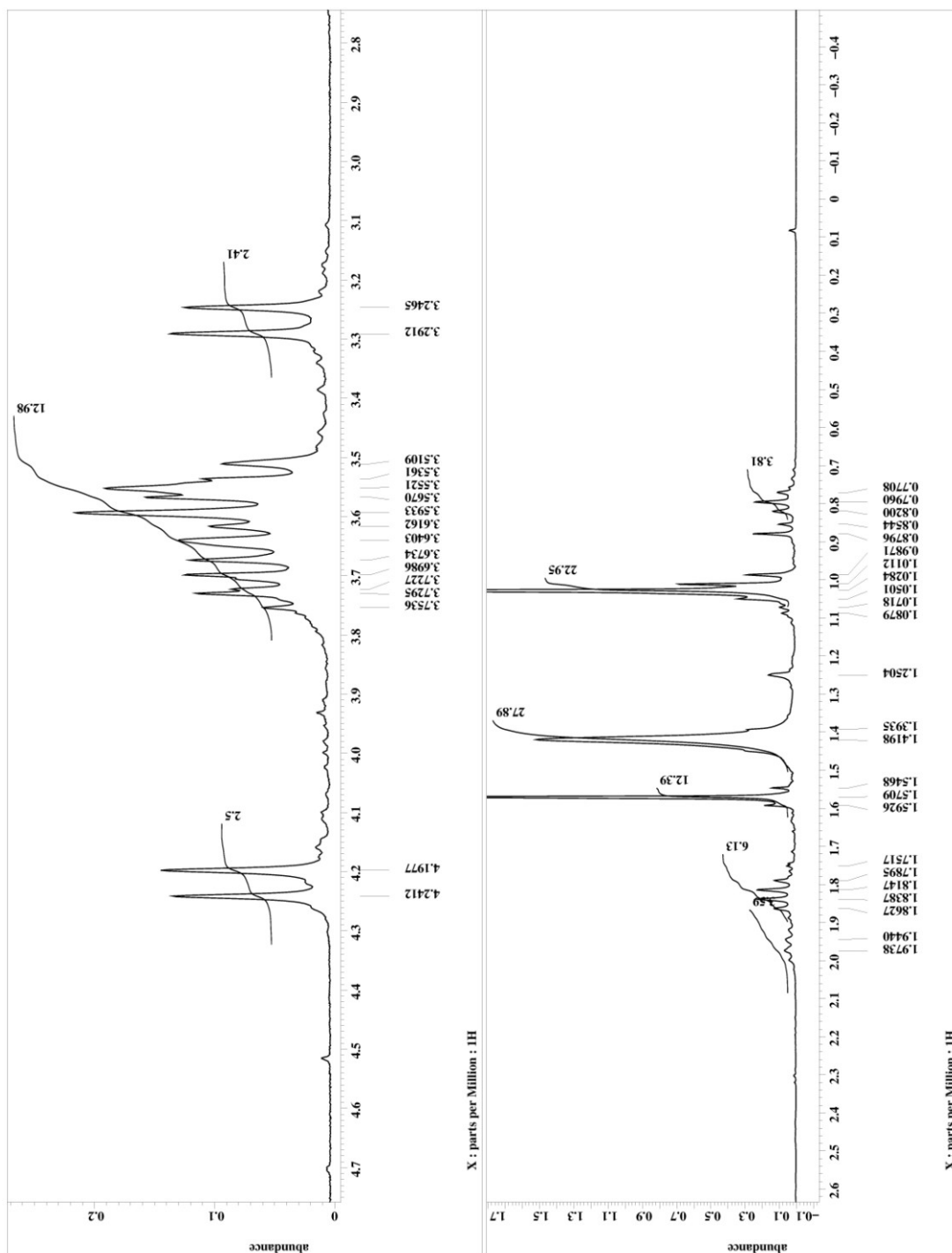


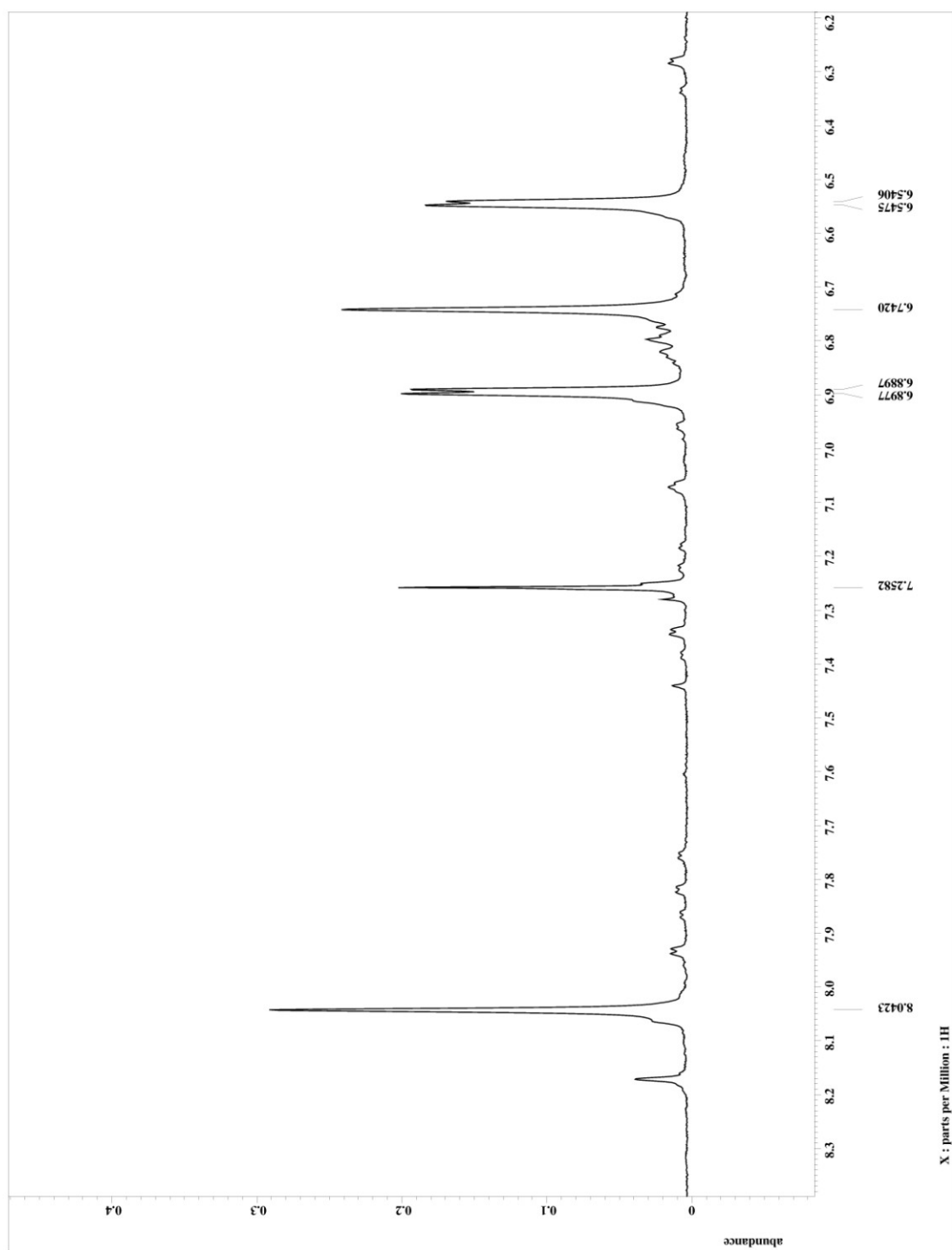
APPENDIX 31

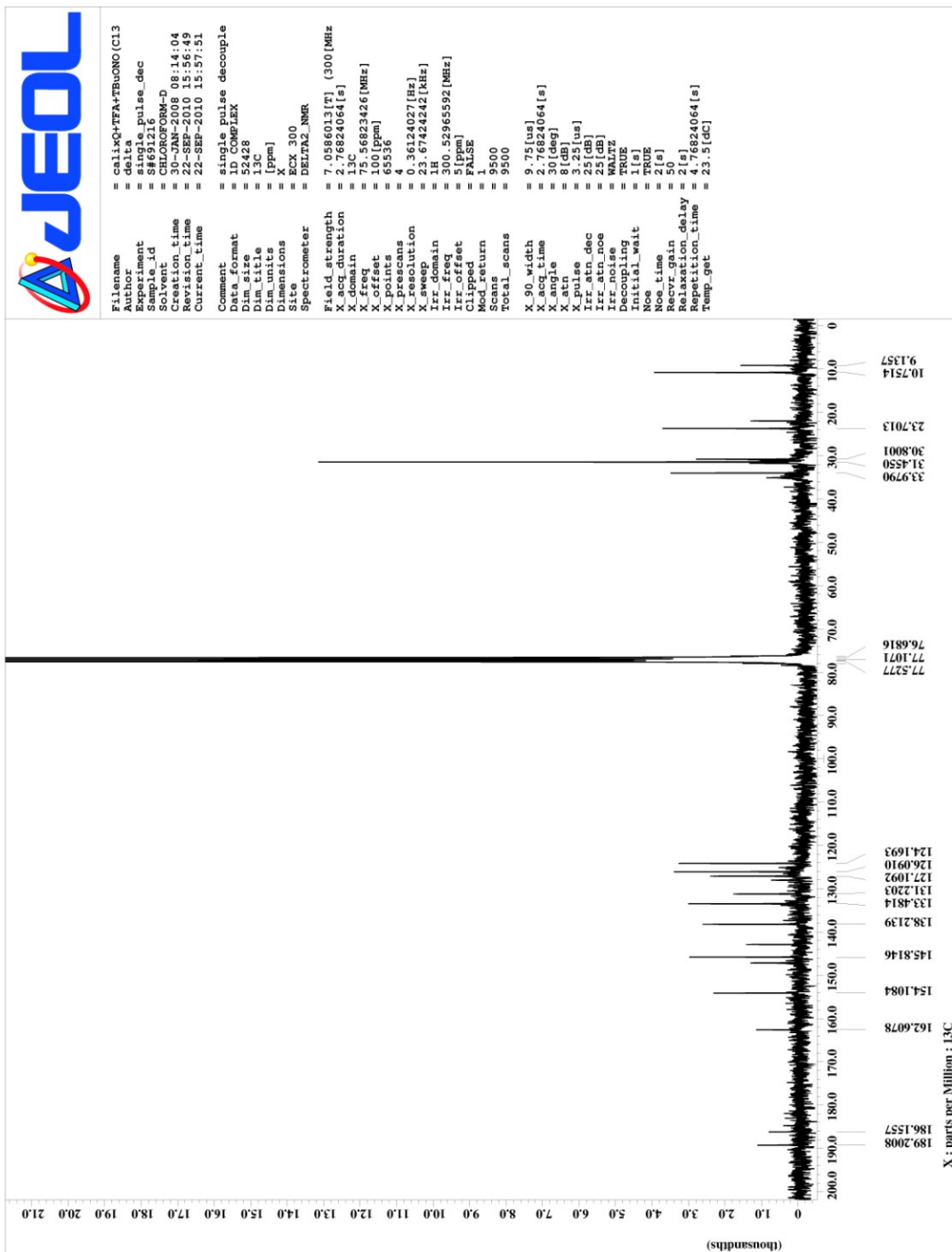
¹H AND ¹³C NMR SPECTRA OF

26,28-BIS(*N*-PROPYLOXY)-23-NITRO-*P*-*TERT*-BUTYLCALIX[4]MONOQUINONE (22)









APPENDIX 32
FULL CITATIONS OF CHAPTERS 2-8

Chapter 2: Payagala, Tharanga; Zhang, Ying; Wanigasekara, Eranda; Huang, Ke; Breitbach, Zachary S.; Sharma, Pritesh S.; Sidisky, Leonard M.; Armstrong, Daniel W.

Trigonal tricationic ionic liquids: A generation of gas chromatographic stationary phases, *Analytical Chemistry* **2009**, 81(1), 160-173.

Chapter 3: Wanigasekara, Eranda; Zhang, Xiaotong; Nanayakkara, Yasith; Payagala, Tharanga; Moon, Hyejin; Armstrong, Daniel W. **Linear Tricationic Room-Temperature Ionic Liquids: Synthesis, Physiochemical Properties, and Electrowetting Properties**. *ACS Applied Materials & Interfaces* **2009**, 1(10), 2126-2133.

Chapter 4: Breitbach, Zachary S.; Wanigasekara, Eranda; Warnke, Molly M.; Zhang, Xiaotong; Armstrong, Daniel W. **Evaluation of Flexible Linear Tricationic Salts as Gas-Phase Ion-Pairing Reagents for the Detection of Divalent Anions in Positive Mode ESI-MS**. *Analytical Chemistry* **2008**, 80(22), 8828-8834.

Chapter 5: Wanigasekara, Eranda; Perera, Sirantha; Crank, Jeffrey A.; Sidisky, Leonard; Shirey, Robert; Berthod, Alain; Armstrong, Daniel W. **Bonded ionic liquid polymeric material for solid-phase microextraction GC analysis** *Analytical and Bioanalytical Chemistry* **2010**, 396(1), 511-524.

Chapter 7: Wanigasekara, Eranda; Leontiev, Alexander V.; Organo, Voltaire G.; Rudkevich, Dmitry M. **Supramolecular, calixarene-based complexes that release NO gas**. *European Journal of Organic Chemistry* **2007**, (14), 2254-2256.

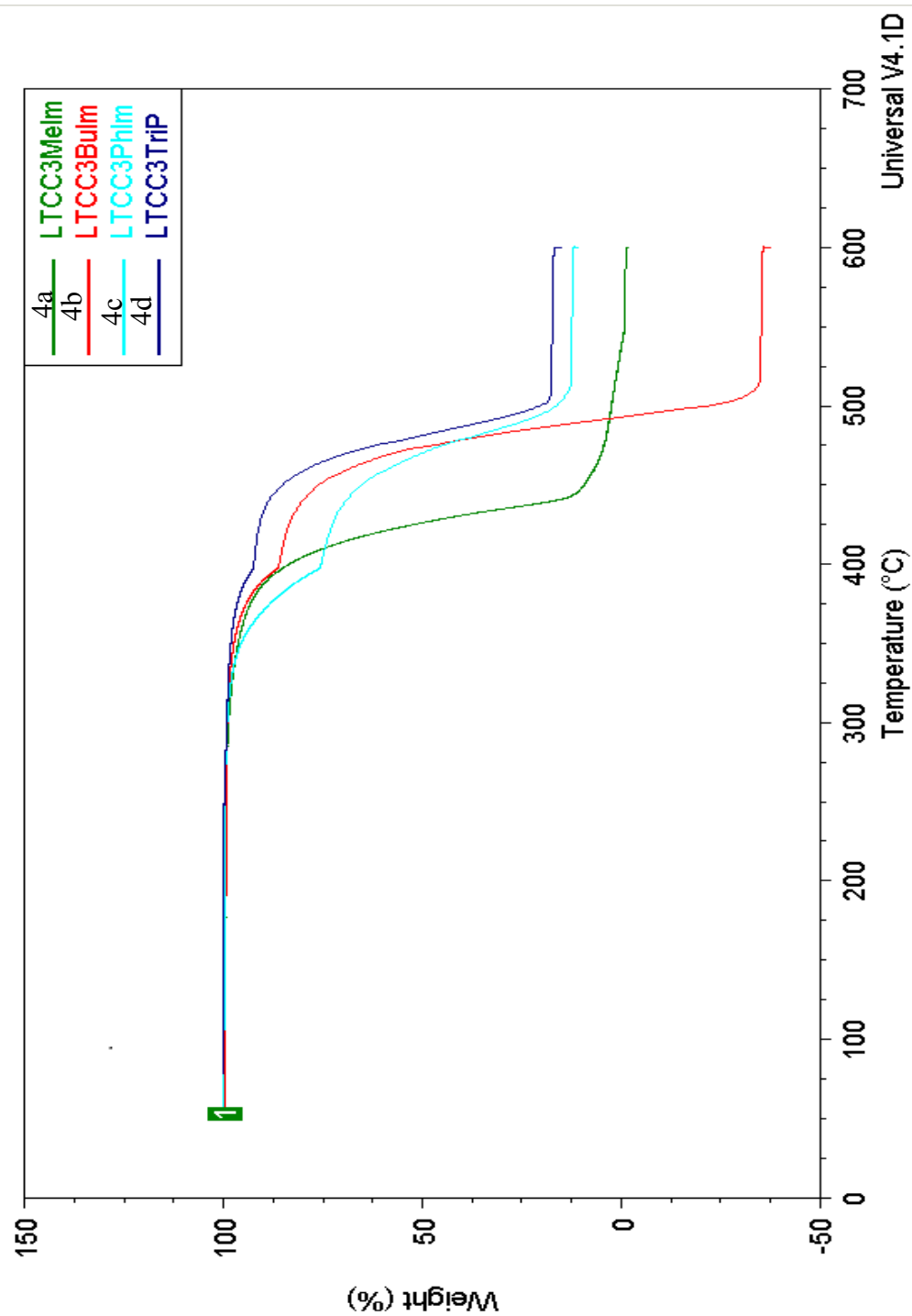
Chapter 8: Wanigasekara, Eranda; Gaeta, Carmine; Neri, Placido; Rudkevich, Dmitry M. **Nitric Oxide Release Mediated by Calix[4]hydroquinones**. *Organic Letters* **2008**, 10(6), 1263-1266

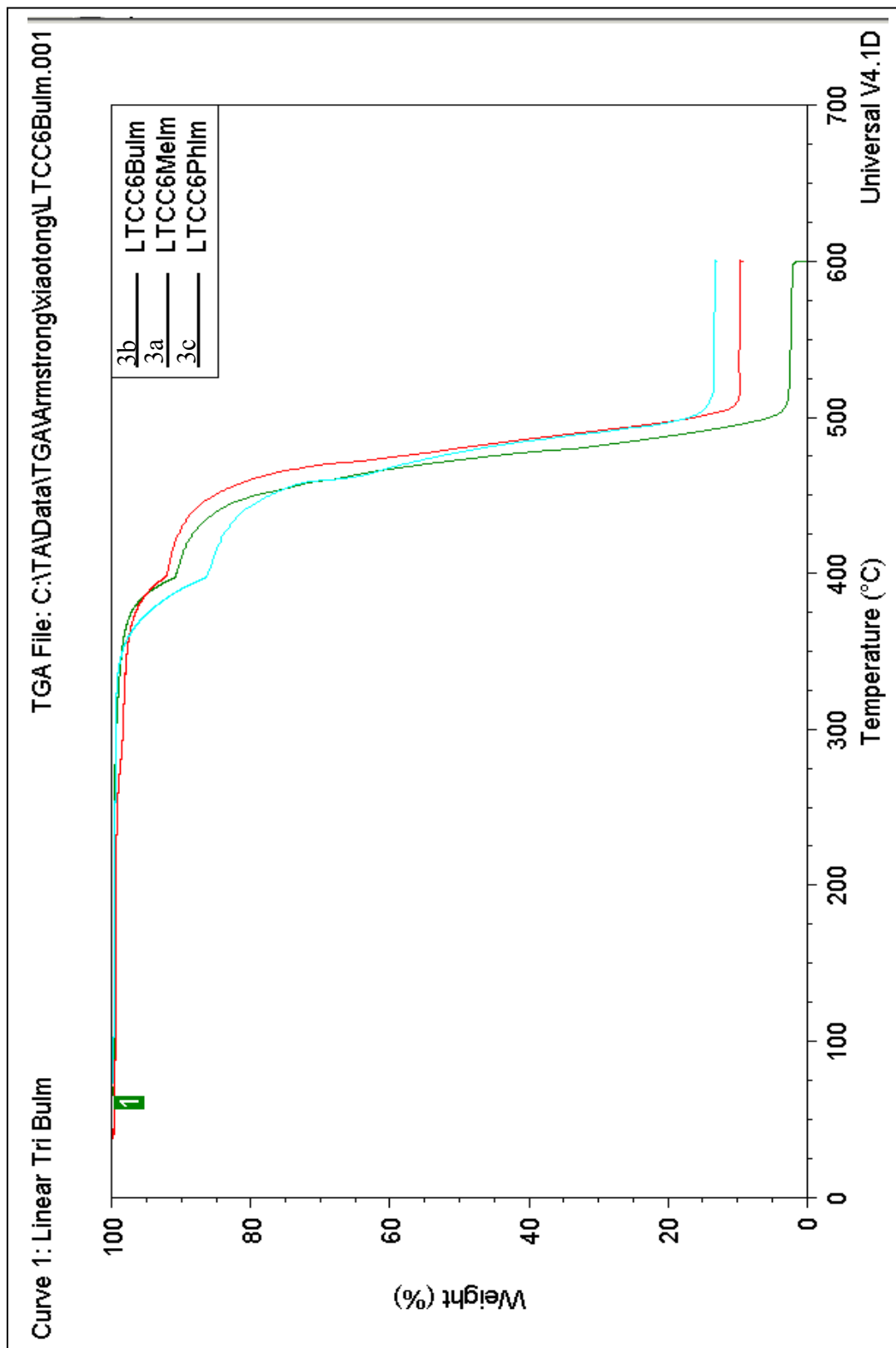
APPENDIX 33

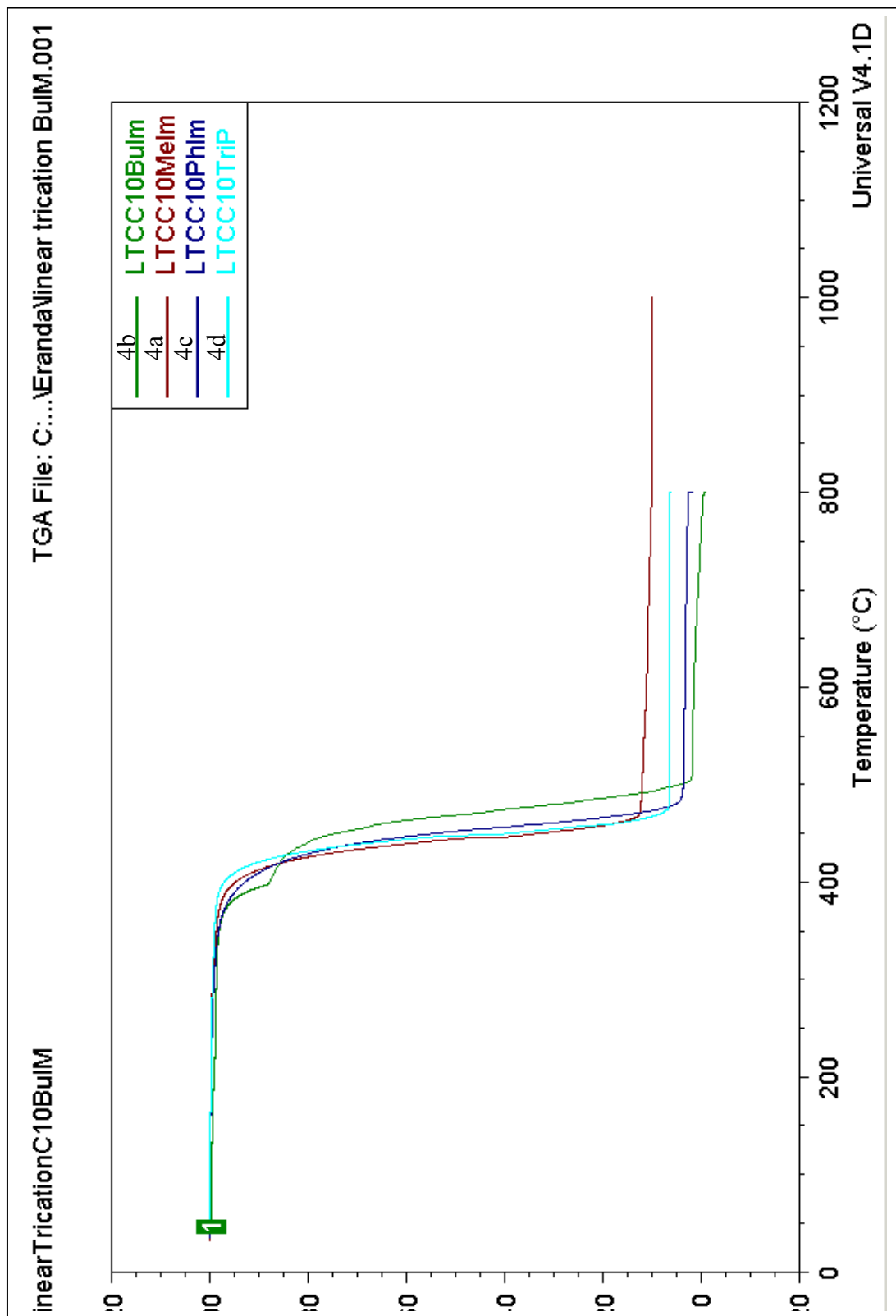
TGA CUREVES FOR LINEAR TRICATIONIC IONIC LIQUIDS

Curve 1: lineartricationC3Melm

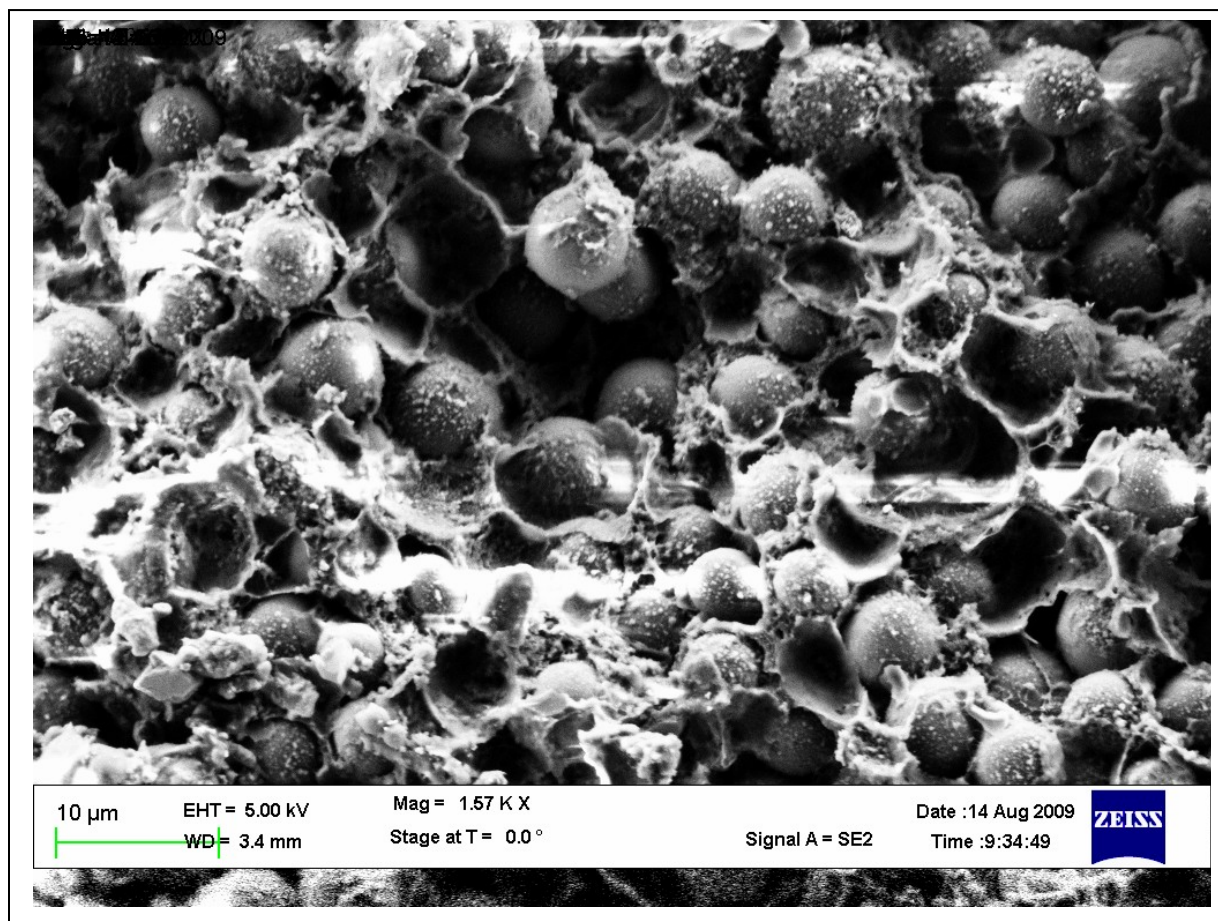
TGA File: C:\TA\Data\TGA\Armstrong\Eranda\LTCC3Melm.004



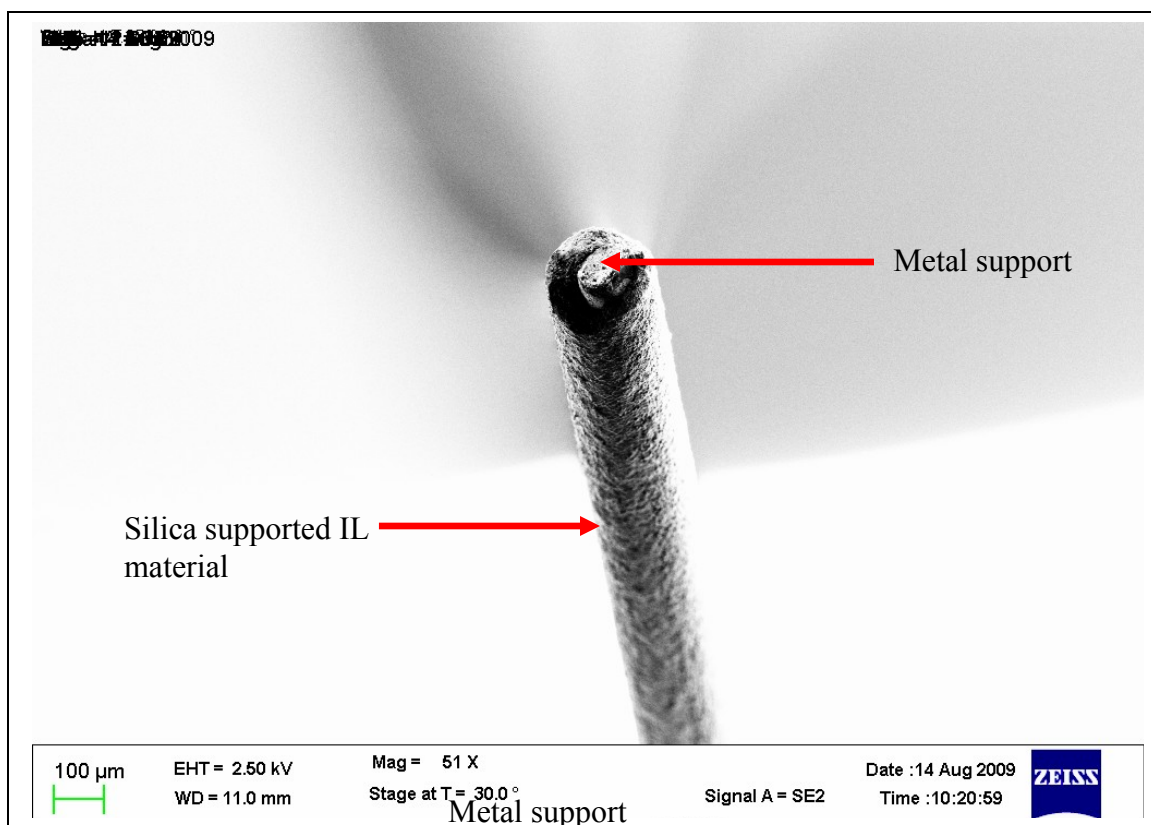




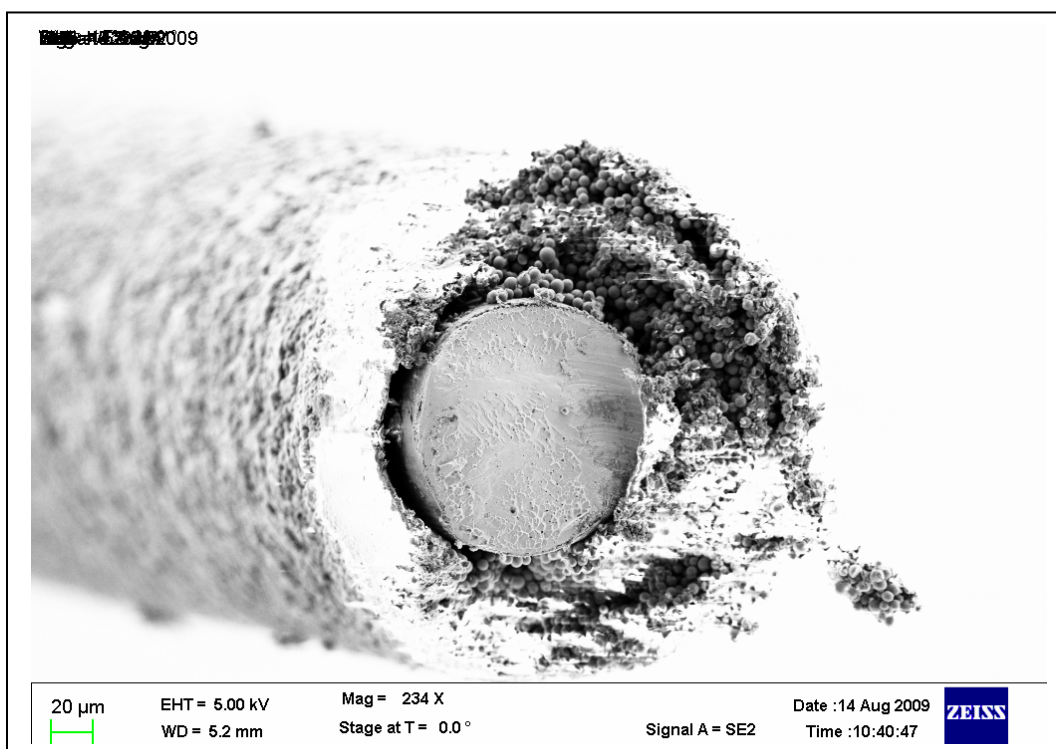
APPENDIX 34
SEM IMAGES OF SILICA BONDED
SPME COATINGS



SEM Image of IL3-NTf₂ silica bonded coating material



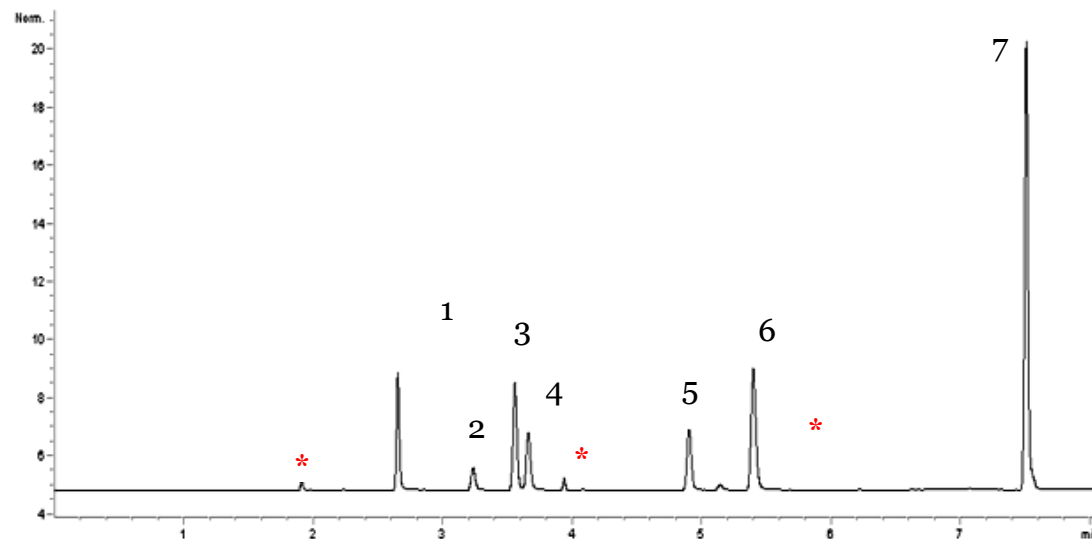
SEM Image of a IL3-NTf₂ fiber



Cross sectional area of a IL-based silica supported SPME fiber

APPENDIX 35
REPRESENTATIVE CHROMATOGRAMS OF SPME HEADSPACE
AND DIRECT IMMERSION ANALYSIS

HEADSPACE SPME

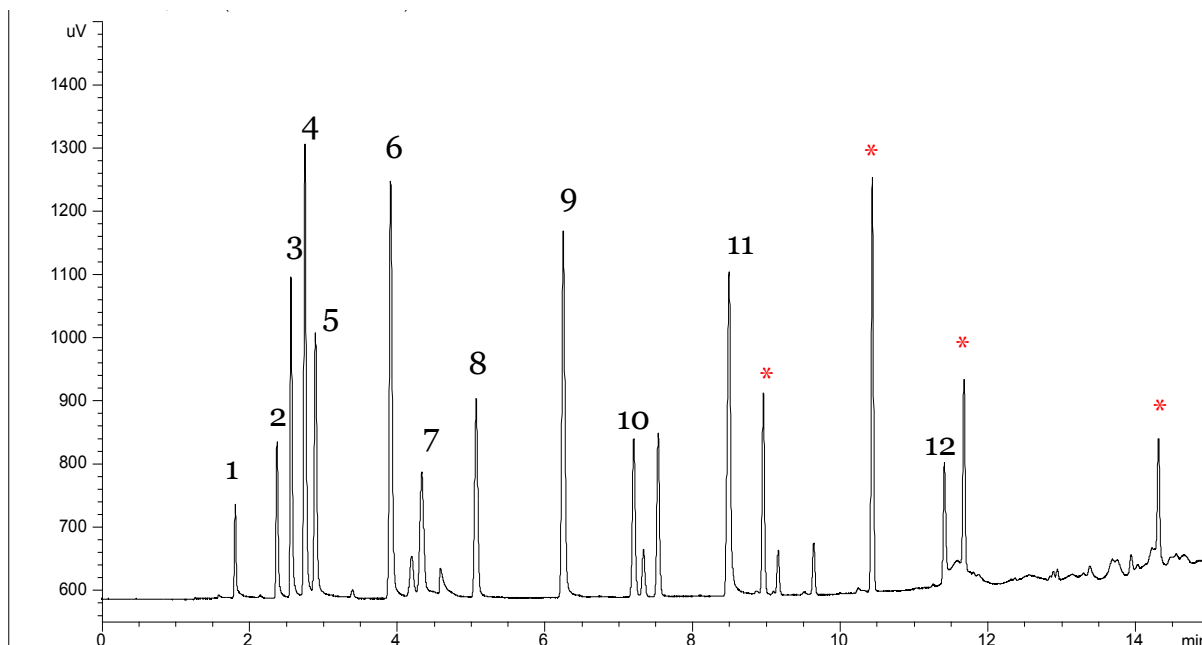


Chromatogram A1: Desorbed compounds from Polymeric Fiber #3 after headspace adsorption on a 5 ppm alcohol mixture. Chromatogram obtained on a Supelcowax 10, 30 m, 250 μ m, 0.25 μ m film thickness column; carrier gas helium, 1 mL/min, 35 cm/s giving t_0 = 1.43 min. Temperature program: 50°C for 4 min followed by a gradient 15°C/min for 6.7 min to 150°C.

ID#	Compound name (5 ppm each)	Retention time (min)
1	Acetone	2.65
2	Methanol	3.23
3	Isopropyl alcohol	3.55
4	Ethanol	3.65
5	Acetonitrile	4.90
6	n-Propanol	5.39
7	n-Butanol	7.51
*	Unknown	1.94; 3.92; 5.16

Table A1: Retention time for Polymeric Fiber #3 for 5 ppm alcohol mixture Chromatogram 1.

DIRECT IMMERSION SPME



Chromatogram A2: Desorbed compounds coming from Polymeric Fiber #3 after direct immersion adsorption on a polar mixture listed in Table 2. Chromatogram obtained on a SPB-1 Sulfur PDMS, 30 m, 320 μ m, 4 μ m film thickness column; carrier gas helium, 1.5 mL/min, 30 cm/s giving t_0 = 1.67 min. Temperature program: 45°C for 1.5 min followed by a gradient 8°C/min for 4.4 min next 20°C/min for 8.5 min to 250°C.

ID#	Compound name	Concentration (μ g/mL or ppm)	Retention time (min)
1	Methanol	20	1.74
2	Ethanol	20	2.42
3	Acetonitrile	20	2.60
4	Acetone	20	2.73
5	Isopropyl alcohol	20	2.91
6	n-Propanol	10	3.89
7	Methyl- <i>t</i> -butyl ether	0.5	4.28
8	Ethyl acetate	0.5	4.56
9	n-Butanol	10	6.11
10	Dioxane	20	7.18
11	Butyric acid	10	8.26
12	Phenol	0.2	10.70

Table A2: Retention time for Polymeric Fiber #3 for the polar mixture of Chromatogram 2.

APPENDIX 35
RIGHTS AND PERMISSIONS

AMERICAN CHEMICAL SOCIETY LICENSE
TERMS AND CONDITIONS

This is a License Agreement between Eranda P Wanigasekara ("You") and American Chemical Society ("American Chemical Society"). The license consists of your order details, the terms and conditions provided by American Chemical Society, and payment terms and conditions.

License Number	2514470747444
License date	Sep 22, 2010
Licensed content publisher	American Chemical Society
Licensed content publication	Analytical Chemistry
Licensed content title	Examination of Ionic Liquids and Their Interaction with Molecules, When Used as Stationary Phases in Gas Chromatography
Licensed content author	Daniel W. Armstrong et al.
Licensed content date	Sep 1, 1999
Volume number	71
Issue number	17
Type of Use	Thesis/Dissertation
Are you the Author of original article?	No
Format	Print and Electronic
Portion	Table/Figure/Micrograph
Number of Tables/Figures/Micrographs	1
Order reference number	
Title of the thesis / dissertation	IONIC LIQUIDS IN ANALYTICAL CHEMISTRY AND SUPRAMOLECULAR CHEMISTRY OF NOX GASES
Expected completion date	Dec 2010
Estimated size(pages)	200
Billing type	Invoice
Billing address	700 Planetarium place RM 130 Arlington, TX 76019 United States
Customer reference info	
Permissions price	0.00 USD

AMERICAN CHEMICAL SOCIETY LICENSE
TERMS AND CONDITIONS

This is a License Agreement between Eranda P Wanigasekara ("You") and American Chemical Society ("American Chemical Society"). The license consists of your order details, the terms and conditions provided by American Chemical Society, and the payment terms and conditions.

License Number	2467830447433
License date	Jul 14, 2010
Licensed content publisher	American Chemical Society
Licensed content publication	Journal of the American Chemical Society
Licensed content title	Structure and Properties of High Stability Geminal Dicationic Ionic Liquids
Licensed content author	Jared L. Anderson et al.
Licensed content date	Jan 1, 2005
Volume number	127
Issue number	2
Type of Use	Thesis/Dissertation
Are you the Author of original article?	No
Format	Print and Electronic
Portion	Table/Figure/Micrograph
Number of Tables/Figures/Micrographs	1
Order reference number	
Title of the thesis / dissertation	IONIC LIQUIDS IN ANALYTICAL CHEMISTRY AND SUPRAMOLECULAR CHEMISTRY OF NOX GASES
Expected completion date	Dec 2010
Estimated size(pages)	200
Billing type	Invoice
Billing address	700 Planetarium place RM 130 Arlington, TX 76019 United States
Customer reference info	
Permissions price	0.00 USD

JOHN WILEY AND SONS LICENSE
TERMS AND CONDITIONS

This is a License Agreement between Eranda P Wanigasekara ("You") and John Wiley and Sons ("John Wiley and Sons"). The license consists of your order details, the terms and conditions provided by John Wiley and Sons, and the payment terms and conditions.

License Number	2473101009689
License date	Jul 20, 2010
Licensed content publisher	John Wiley and Sons
Licensed content publication	Mass Spectrometry Reviews
Licensed content title	Practical implications of some recent studies in electrospray ionization fundamentals
Licensed content author	Cech Nadja B., Enke Christie G.
Licensed content date	May 1, 2002a
Start page	362
End page	387
Type of use	Dissertation/Thesis
Requestor type	University/Academic
Format	Print and electronic
Portion	Figure/table
Number of figures/tables	1
Original Wiley figure/table number(s)	Figure 1
Will you be translating?	No
Order reference number	
Total	0.00 USD

AMERICAN CHEMICAL SOCIETY LICENSE
TERMS AND CONDITIONS

This is a License Agreement between Eranda P Wanigasekara ("You") and American Chemical Society ("American Chemical Society"). The license consists of your order details, the terms and conditions provided by American Chemical Society, and the payment terms and conditions.

License Number	2474400373517
License date	Jul 22, 2010
Licensed content publisher	American Chemical Society
Licensed content publication	Analytical Chemistry
Licensed content title	A General, Positive Ion Mode ESI-MS Approach for the Analysis of Singly Charged Inorganic and Organic Anions Using a Dicationic Reagent
Licensed content author	Renee J. Soukup-Hein et al.
Licensed content date	Oct 1, 2007
Volume number	79
Issue number	19
Type of Use	Thesis/Dissertation
Are you the Author of original article?	No
Format	Print and Electronic
Portion	Table/Figure/Micrograph
Number of Tables/Figures/Micrographs	1
Order reference number	
Title of the thesis / dissertation	IONIC LIQUIDS IN ANALYTICAL CHEMISTRY AND SUPRAMOLECULAR CHEMISTRY OF NOX GASES
Expected completion date	Dec 2010
Estimated size(pages)	200
Billing type	Invoice
Billing address	700 Planetarium place RM 130 Arlington, TX 76019 United States
Customer reference info	
Permissions price	0.00 USD

AMERICAN CHEMICAL SOCIETY LICENSE
TERMS AND CONDITIONS

This is a License Agreement between Eranda P Wanigasekara ("You") and Elsevier ("Elsevier"). The license consists of your order details, the terms and conditions provided by Elsevier, and the payment terms and conditions.

License Number	2463880786025
License date	Jul 07, 2010
Licensed content publisher	Elsevier
Licensed content publication	Journal of the American Society for Mass Spectrometry
Licensed content title	The Evaluation and Comparison of Trigonal and Linear Tricationic Ion-Pairing Reagents for the Detection of Anions in Positive Mode ESI-MS
Licensed content author	Molly M. Warnke, Zachary S. Breitbach, Edra Dodbiba, Eranda Wanigasekara, Xiaotong Zhang, Pritesh Sharma, Daniel W. Armstrong
Licensed content date	March 2009
Licensed content volume number	20
Licensed content issue number	3
Number of pages	10
Type of Use	reuse in a thesis/dissertation
Requestor type	Not specified
Portion	full article
Format	both print and electronic
Are you the author of this Elsevier article?	Yes
Will you be translating?	No
Order reference number	
Title of your thesis/dissertation	IONIC LIQUIDS IN ANALYTICAL CHEMISTRY AND SUPRAMOLECULAR CHEMISTRY OF NOX GASES
Expected completion date	Dec 2010
Estimated size (number of pages)	200
Elsevier VAT number	GB 494 6272 12
Permissions price	0.00 USD
Value added tax 0.0%	0.00 USD
Total	0.00 USD

ELSEVIER LICENSE

TERMS AND CONDITIONS

This is a License Agreement between Eranda P Wanigasekara ("You") and Elsevier ("Elsevier"). The license consists of your order details, the terms and conditions provided by Elsevier, and the payment terms and conditions.

Get the printable license.

License Number	2483120793123
License date	Aug 06, 2010
Licensed content publisher	Elsevier
Licensed content publication	TrAC Trends in Analytical Chemistry
Licensed content title	New directions in sample preparation for analysis of organic compounds
Licensed content author	Janusz Pawliszyn
Licensed content date	March 1995
Licensed content volume number	14
Licensed content issue number	3
Number of pages	10
Type of Use	reuse in a thesis/dissertation
Requestor type	Not specified
Intended publisher of new work	other
Portion	figures/tables/illustrations
Number of figures/tables/illustrations	1
Format	both print and electronic
Are you the author of this Elsevier article?	No
Will you be translating?	No
Order reference number	
Title of your thesis/dissertation	IONIC LIQUIDS IN ANALYTICAL CHEMISTRY AND SUPRAMOLECULAR CHEMISTRY OF NOX GASES
Expected completion date	Dec 2010
Estimated size (number of pages)	200
Elsevier VAT number	GB 494 6272 12
Permissions price	0.00 USD
Value added tax 0.0%	0.0 USD / 0.0 GBP
Total	0.00 USD

ELSEVIER LICENSE

TERMS AND CONDITIONS

This is a License Agreement between Eranda P Wanigasekara ("You") and Elsevier ("Elsevier"). The license consists of your order details, the terms and conditions provided by Elsevier, and the payment terms and conditions.

Get the printable license.

License Number	2486671322413
License date	Aug 12, 2010
Licensed content publisher	Elsevier
Licensed content publication	Journal of Chromatography A
Licensed content title	Polymeric ionic liquids as selective coatings for the extraction of esters using solid-phase microextraction
Licensed content author	Fei Zhao, Yunjing Meng, Jared L. Anderson
Licensed content date	24 October 2008
Licensed content volume number	1208
Licensed content issue number	1-2
Number of pages	9
Type of Use	reuse in a thesis/dissertation
Requestor type	Not specified
Intended publisher of new work	other
Portion	figures/tables/illustrations
Number of figures/tables/illustrations	2
Format	both print and electronic
Are you the author of this Elsevier article?	No
Will you be translating?	No
Order reference number	
Title of your thesis/dissertation	IONIC LIQUIDS IN ANALYTICAL CHEMISTRY AND SUPRAMOLECULAR CHEMISTRY OF NOX GASES
Expected completion date	Dec 2010
Estimated size (number of pages)	200
Elsevier VAT number	GB 494 6272 12
Permissions price	0.00 USD
Value added tax 0.0%	0.0 USD / 0.0 GBP
Total	0.00 USD

AMERICAN CHEMICAL SOCIETY LICENSE
TERMS AND CONDITIONS

This is a License Agreement between Eranda P Wanigasekara ("You") and American Chemical Society ("American Chemical Society"). The license consists of your order details, the terms and conditions provided by American Chemical Society, and the payment terms and conditions.

License Number	2514500113256
License date	Sep 22, 2010
Licensed content publisher	American Chemical Society
Licensed content publication	Analytical Chemistry
Licensed content title	Evaluation of Flexible Linear Tricationic Salts as Gas-Phase Ion-Pairing Reagents for the Detection of Divalent Anions in Positive Mode ESI-MS
Licensed content author	Zachary S. Breitbach et al.
Licensed content date	Nov 1, 2008
Volume number	80
Issue number	22
Type of Use	Thesis/Dissertation
Are you the Author of original article?	Yes
Format	Print
Portion	Full article
Order reference number	
Title of the thesis / dissertation	IONIC LIQUIDS IN ANALYTICAL CHEMISTRY AND SUPRAMOLECULAR CHEMISTRY OF NOX GASES
Expected completion date	Dec 2010
Estimated size(pages)	200
Billing type	Invoice
Billing address	700 Planetarium place RM 130 Arlington, TX 76019 United States
Customer reference info	
Permissions price	0.00 USD

AMERICAN CHEMICAL SOCIETY LICENSE
TERMS AND CONDITIONS

This is a License Agreement between Eranda P Wanigasekara ("You") and American Chemical Society ("American Chemical Society"). The license consists of your order details, the terms and conditions provided by American Chemical Society, and the payment terms and conditions.

Get the printable license.

License Number	2514501076946
License date	Sep 22, 2010
Licensed content publisher	American Chemical Society
Licensed content publication	Analytical Chemistry
Licensed content title	Trigonal Tricationic Ionic Liquids: A Generation of Gas Chromatographic Stationary Phases
Licensed content author	Tharanga Payagala et al.
Licensed content date	Jan 1, 2009
Volume number	81
Issue number	1
Type of Use	Thesis/Dissertation
Are you the Author of original article?	Yes
Format	Print
Portion	Full article
Order reference number	
Title of the thesis / dissertation	IONIC LIQUIDS IN ANALYTICAL CHEMISTRY AND SUPRAMOLECULAR CHEMISTRY OF NOX GASES
Expected completion date	Dec 2010
Estimated size(pages)	200
Billing type	Invoice
Billing address	700 Planetarium place RM 130 Arlington, TX 76019 United States
Customer reference info	
Permissions price	0.00 USD

AMERICAN CHEMICAL SOCIETY LICENSE
TERMS AND CONDITIONS

This is a License Agreement between Eranda P Wanigasekara ("You") and American Chemical Society ("American Chemical Society"). The license consists of your order details, the terms and conditions provided by American Chemical Society, and the payment terms and conditions.

License Number	2463890263282
License date	Jul 07, 2010
Licensed content publisher	American Chemical Society
Licensed content publication	Applied Materials
Licensed content title	Linear Tricationic Room-Temperature Ionic Liquids: Synthesis, Physiochemical Properties, and Electrowetting Properties
Licensed content author	Eranda Wanigasekara et al.
Licensed content date	Oct 1, 2009
Volume number	1
Issue number	10
Type of Use	Thesis/Dissertation
Are you the Author of original article?	Yes
Format	Print
Portion	Full article
Order reference number	
Title of the thesis / dissertation	IONIC LIQUIDS IN ANALYTICAL CHEMISTRY AND SUPRAMOLECULAR CHEMISTRY OF NOX GASES
Expected completion date	Dec 2010
Estimated size(pages)	200
Billing type	Invoice
Billing address	700 Planetarium place RM 130 Arlington, TX 76019 United States
Customer reference info	
Permissions price	0.00 USD

JOHN WILEY AND SONS LICENSE
TERMS AND CONDITIONS

Dear Eranda Wanigasekara,

Thank you for your email.

- We hereby grant permission for the requested use expected that due credit is given to the original source.

- For material published before 2007 additionally: Please note that the (co-)author's permission is also required.

If material appears within our work with credit to another source, authorisation from that source must be obtained.

Credit must include the following components:

- Books: Author(s)/ Editor(s) Name(s): Title of the Book. Page(s). Publication year. Copyright Wiley-VCH Verlag GmbH & Co. KGaA. Reproduced with permission.

- Journals: Author(s) Name(s): Title of the Article. Name of the Journal. Publication year. Volume. Page(s). Copyright Wiley-VCH Verlag GmbH & Co. KGaA. Reproduced with permission.

With kind regards

Bettina Loycke

Bettina Loycke

Senior Rights Manager

Wiley-VCH Verlag GmbH & Co. KGaA

Boschstr. 12

69469 Weinheim

Germany

Phone: +49 (0) 62 01- 606 - 280

Fax: +49 (0) 62 01 - 606 - 332

Email: rights@wiley-vch.de

Wiley-VCH Verlag GmbH & Co. KGaA

Location of the Company: Weinheim

Chairman of the Supervisory Board: Stephen Michael Smith

Trade Register: Mannheim, HRB 432833

General Partner: John Wiley & Sons GmbH, Location: Weinheim

Trade Register Mannheim, HRB 432296

Managing Directors : Christopher J. Dicks, Bijan Ghawami, William Pesce

From: Eranda Wanigasekara [mailto:eranda.wanigasekara@mavs.uta.edu]
Sent: 19 August 2010 23:01
To: com
Cc: Permission Requests - UK
Subject: Request copyright permission

Dear Officer,

My name is Eranda Wanigasekara from University of Texas at Arlington, chemistry department. I would like to request you to grant permission to be included in my thesis which was authored by my supervisor. I already used Rightslink online and it gave the message that I need to contact you directly for this purpose.

Below is the reference that I need permission for using 3 figures for my thesis.

Emerging Supramolecular Chemistry of Gases
Angew. Chem. Int. Ed. 2004, 43, 558 – 571 by Prof.Dmitry M. Rudkevich

Sincerely

Eranda Wanigasekara.

JOHN WILEY AND SONS LICENSE
TERMS AND CONDITIONS

Dear Eranda Wanigasekara,

Thank you for your email.

We hereby grant permission for the requested use expected that due credit is given to the original source.

Please note that the author's permission is also required.

Please note that we only grant rights for a printed version, but not the rights for an electronic/ online/ web/ microfiche publication, but you are free to create a link to the article in question which is posted on our website (<http://www3.interscience.wiley.com>)

You may use the version of the contribution as originally submitted for publication for an electronic presentation of the thesis. The contribution may not be updated or replaced with the published version. The version posted must contain a legend as follows: This is the pre-peer reviewed version of the following article: FULL CITE.

With kind regards

Bettina Loycke

Bettina Loycke

Senior Rights Manager

Wiley-VCH Verlag GmbH & Co. KGaA

Boschstr. 12

69469 Weinheim

Germany

Phone: +49 (0) 62 01- 606 - 280

Fax: +49 (0) 62 01 - 606 - 332

Email: rights@wiley-vch.de

Wiley-VCH Verlag GmbH & Co. KGaA

Location of the Company: Weinheim

Chairman of the Supervisory Board: Stephen Michael Smith

Trade Register: Mannheim, HRB 432833

General Partner: John Wiley & Sons GmbH, Location: Weinheim

Trade Register Mannheim, HRB 432296

Managing Directors : Christopher J. Dicks, Bijan Ghawami, William Pesce

From: Eranda [<mailto:eranda8888@yahoo.com>]

Sent: 08 July 2010 00:04

To: Permission Requests - UK

Cc: Permissions - US

Subject: Permission to reuse in dissertation/thesis

Dear Officer,

My name is Eranda Wanigasekara from University of Texas at Arlington, chemistry department. I would like to request you to grant permission to be included in my thesis which was authored by me. I already used Rightslink online and following message was received:

Content Excluded

Permission to reproduce this content cannot be granted via the Rightslink® service. Please go to the Wiley Permission's web site <http://www.wiley.com/WileyCDA/Section/id-301703.html> or email your request details to permissionsUK@wiley.com or permissionsUS@wiley.com.

Reference:

Supramolecular, Calixarene-Based Complexes That Release NO Gas

Eranda Wanigasekara, Alexander V. Leontiev, Voltaire G. Organo, Dmitry M. Rudkevich*

Department of Chemistry and Biochemistry, The University of Texas at Arlington, Arlington, TX 76019-0065, USA, Fax: +1-817-272-3808

email: Dmitry M. Rudkevich (rudkevich@uta.edu)

Digital Object Identifier (DOI)

10.1002/ejoc.200700173

Thank you.

Sincerely,
Eranda Wanigasekara.

AMERICAN CHEMICAL SOCIETY LICENSE
TERMS AND CONDITIONS

This is a License Agreement between Eranda P Wanigasekara ("You") and American Chemical Society ("American Chemical Society"). The license consists of your order details, the terms and conditions provided by American Chemical Society, and the payment terms and conditions.

License Number	2494340888026
License date	Aug 22, 2010
Licensed content publisher	American Chemical Society
Licensed content publication	The Journal of Organic Chemistry
Licensed content title	Cofacial Phenylene Donors as Novel Organic Sensors for the Reversible Binding of Nitric Oxide
Licensed content author	Rajendra Rathore et al.
Licensed content date	Nov 1, 1998
Volume number	63
Issue number	24
Type of Use	Thesis/Dissertation
Are you the Author of original article?	No
Format	Print and Electronic
Portion	Table/Figure/Micrograph
Number of Tables/Figures/Micrographs	1
Order reference number	
Title of the thesis / dissertation	IONIC LIQUIDS IN ANALYTICAL CHEMISTRY AND SUPRAMOLECULAR CHEMISTRY OF NOX GASES
Expected completion date	Dec 2010
Estimated size(pages)	200
Billing type	Invoice
Billing address	700 Planetarium place RM 130 Arlington, TX 76019 United States
Customer reference info	
Permissions price	0.00 USD

AMERICAN CHEMICAL SOCIETY LICENSE
TERMS AND CONDITIONS

This is a License Agreement between Eranda P Wanigasekara ("You") and American Chemical Society ("American Chemical Society"). The license consists of your order details, the terms and conditions provided by American Chemical Society, and the payment terms and conditions.

License Number	2496201357971
License date	Aug 25, 2010
Licensed content publisher	American Chemical Society
Licensed content publication	Journal of Chemical Education
Licensed content title	Nitrogen-Based Diazeniumdiolates: Versatile Nitric Oxide-Releasing Compounds for Biomedical Research and Potential Clinical Applications
Licensed content author	Larry K. Keefer et al.
Licensed content date	Dec 1, 2002
Volume number	79
Issue number	12
Type of Use	Thesis/Dissertation
Are you the Author of original article?	No
Format	Print and Electronic
Portion	Table/Figure/Micrograph
Number of Tables/Figures/Micrographs	1
Order reference number	
Title of the thesis / dissertation	IONIC LIQUIDS IN ANALYTICAL CHEMISTRY AND SUPRAMOLECULAR CHEMISTRY OF NOX GASES
Expected completion date	Dec 2010
Estimated size(pages)	200
Billing type	Invoice
Billing address	700 Planetarium place RM 130 Arlington, TX 76019 United States
Customer reference info	
Permissions price	0.00 USD

JOHN WILEY AND SONS LICENSE
TERMS AND CONDITIONS

Dear Eranda Wanigasekara,

Thank you for your email.

We hereby grant permission for the requested use expected that due credit is given to the original source.

Please note that the author's permission is also required.

Please note that we only grant rights for a printed version, but not the rights for an electronic/ online/ web/ microfiche publication, but you are free to create a link to the article in question which is posted on our website (<http://www3.interscience.wiley.com>)

☐ ***You may use the version of the contribution as originally submitted for publication for an electronic presentation of the thesis. The contribution may not be updated or replaced with the published version. The version posted must contain a legend as follows: This is the pre-peer reviewed version of the following article: FULL CITE.***

With kind regards

Bettina Loycke

Bettina Loycke

Senior Rights Manager

Wiley-VCH Verlag GmbH & Co. KGaA

Boschstr. 12

69469 Weinheim

Germany

Phone: +49 (0) 62 01- 606 - 280

Fax: +49 (0) 62 01 - 606 - 332

Email: rights@wiley-vch.de

Wiley-VCH Verlag GmbH & Co. KGaA

Location of the Company: Weinheim

Chairman of the Supervisory Board: Stephen Michael Smith

Trade Register: Mannheim, HRB 432833

General Partner: John Wiley & Sons GmbH, Location: Weinheim

Trade Register Mannheim, HRB 432296

Managing Directors : Christopher J. Dicks, Bijan Ghawami, William Pesce

Von: Eranda Wanigasekara [<mailto:eranda.wanigasekara@mavs.uta.edu>]

Gesendet: Sonntag, 22. August 2010 22:35

An: Rights DE

Betreff: RE: Request copyright permission

Thank you very much. I need copyright permission for the following article for the same purpose (Dissertation use).

Title: Supramolecular Features of
Calixarene- Based Synthetic
Nanotubes
Author: Voltaire G. Organo,Alexander
V. Leontiev,Valentina
Sgarlata,H. V. Rasika
Dias,Dmitry M. Rudkevich
Publication: Angewandte Chemie
International Edition
Publisher: John Wiley and Sons
Date: May 13, 2005

Volume 44, Issue 20, pages 3043–3047, May 13, 2005

AMERICAN CHEMICAL SOCIETY LICENSE
TERMS AND CONDITIONS

This is a License Agreement between Eranda P Wanigasekara ("You") and American Chemical Society ("American Chemical Society"). The license consists of your order details, the terms and conditions provided by American Chemical Society, and the payment terms and conditions.

License Number	2503161264243
License date	Sep 06, 2010
Licensed content publisher	American Chemical Society
Licensed content publication	Organic Letters
Licensed content title	Nitric Oxide Release Mediated by Calix[4]hydroquinones
Licensed content author	Eranda Wanigasekara et al.
Licensed content date	Mar 1, 2008
Volume number	10
Issue number	6
Type of Use	Thesis/Dissertation
Are you the Author of original article?	Yes
Format	Print
Portion	Full article
Order reference number	
Title of the thesis / dissertation	IONIC LIQUIDS IN ANALYTICAL CHEMISTRY AND SUPRAMOLECULAR CHEMISTRY OF NOX GASES
Expected completion date	Dec 2010
Estimated size(pages)	200
Billing type	Invoice
Billing address	700 Planetarium place RM 130 Arlington, TX 76019 United States
Customer reference info	
Permissions price	0.00 USD

SPRINGER LICENSE
TERMS AND CONDITIONS

Nov 11, 2010

This is a License Agreement between Eranda P Wanigasekara ("You") and Springer ("Springer") provided by Copyright Clearance Center ("CCC"). The license consists of your order details, the terms and conditions provided by Springer, and the payment terms and conditions.

All payments must be made in full to CCC. For payment instructions, please see information listed at the bottom of this form.

License Number	2545981405174
License date	Nov 11, 2010
Licensed content publisher	Springer
Licensed content publication	Analytical and Bioanalytical Chemistry
Licensed content title	Bonded ionic liquid polymeric material for solid-phase microextraction GC analysis
Licensed content author	Eranda Wanigasekara
Licensed content date	Jan 1, 2009
Volume number	396
Issue number	1
Type of Use	Thesis/Dissertation
Portion	Full text
Number of copies	1
Author of this Springer article	Yes and you are a contributor of the new work
Order reference number	
Title of your thesis / dissertation	IONIC LIQUIDS IN ANALYTICAL CHEMISTRY AND SUPRAMOLECULAR CHEMISTRY OF NOX GASES
Expected completion date	Dec 2010
Estimated size(pages)	200
Total	0.00 USD

REFERENCES

- (1) Welton, T. *Chem. Rev. (Washington, D. C.)* **1999**, 99, 2071-2083.
- (2) Seddon, K. R. *Nat. Mater.* **2003**, 2, 363-365.
- (3) Seddon, K. R. *Kinet. Catal. (Transl. of Kinet. Katal.)* **1996**, 37, 693-697.
- (4) Walden, P. *Izv. Imp. Akad. Nauk* **1913**, 907-36,987-96.
- (5) Gabriel, S.; Weiner, J. *Berichte der deutschen chemischen Gesellschaft* **1888**, 21, 2669-2679.
- (6) Holbrey, J. D. *Chim. Oggi* **2004**, 22, 35-37.
- (7) Cornils, B. *Angew. Chem. , Int. Ed.* **2004**, 43, 274.
- (8) Carpov, A. *Cellul. Chem. Technol.* **2005**, 39, 158-159.
- (9) Maase, M. In *In Industrial applications of ionic liquids*. Section Title: History, Education, and Documentation; 2008; Vol. 2, pp 663-687.
- (10) Plechkova, N. V.; Seddon, K. R. *Chem. Soc. Rev.* **2008**, 37, 123-150.
- (11) Plechkova, N. V.; Seddon, K. R. In *In Ionic liquids: "designer" solvents for green chemistry*. Section Title: Physical Organic Chemistry; 2007; , pp 105-130.
- (12) Ahrens, S.; Peritz, A.; Strassner, T. *Angew. Chem. , Int. Ed.* **2009**, 48, 7908-7910, S7908/1-S7908/45.
- (13) Chen, Y.; Wang, Y.; Cheng, Q.; Liu, X.; Zhang, S. *J. Chem. Thermodyn.* **2010**, 42, 436.
- (14) Fox, D. M.; Awad, W. H.; Gilman, J. W.; Maupin, P. H.; De Long, H. C.; Trulove, P. C. *Green Chem.* **2003**, 5, 724-727.
- (15) Guo, Z.; Kahveci, D.; Oezcelik, B.; Xu, X. *New Biotechnol.* **2009**, 26, 37-43.
- (16) Handy, S. T.; Okello, M.; Dickenson, G. *Org. Lett.* **2003**, 5, 2513-2515.

- (17) He, X.; Yang, W.; Pei, X. *Macromolecules (Washington, DC, U. S.)* **2008**, *41*, 4615-4621.
- (18) Liu, H.; Liu, Y.; Li, J. *Phys. Chem. Chem. Phys.* **2010**, *12*, 1685-1697.
- (19) Liu, Y.; Zou, X.; Dong, S. *Electrochem. Commun.* **2006**, *8*, 1429-1434.
- (20) Yang, Z.; Pan, W. *Enzyme Microb. Technol.* **2005**, *37*, 19-28.
- (21) Zhao, Y.; Li, M.; Lu, Q. *Langmuir* **2008**, *24*, 3937-3943.
- (22) Chiappe, C. In *In Organic synthesis: ionic liquids in organic synthesis: effects on rate and selectivity*. Section Title: Physical Organic Chemistry; 2008; Vol. 1, pp 265-292.
- (23) Earle, M. J.; Seddon, K. R. *Proc. - Electrochem. Soc.* **2002**, 2002-19, 177-189.
- (24) Pavlinac, J.; Zupan, M.; Laali, K. K.; Stavber, S. *Tetrahedron* **2009**, *65*, 5625-5662.
- (25) Zhao, H.; Malhotra, S. V. *Aldrichimica Acta* **2002**, *35*, 75-83.
- (26) Buzzeo, M. C.; Evans, R. G.; Compton, R. G. *ChemPhysChem* **2004**, *5*, 1106-1120.
- (27) Sun, Q.; Liu, Y.; Lu, J. *Huaxue Tongbao* **2003**, *66*, 112-114, 124.
- (28) Wilkes, J. S.; Levisky, J. A.; Wilson, R. A.; Hussey, C. L. *Inorg. Chem.* **1982**, *21*, 1263-1264.
- (29) Anjan, S. T. *Chem. Eng. Prog.* **2006**, *102*, 30-39.
- (30) Billard, I.; Gaillard, C. *Radiochim. Acta* **2009**, *97*, 355-359.
- (31) Dupont, J. In *In Ionic liquids: structure, properties and major applications in extraction/reaction technology*. Section Title: Phase Equilibriums, Chemical Equilibriums, and Solutions; 2005; , pp 229-249.
- (32) Li, Z.; Chang, J.; Shan, H.; Pan, J. *Rev. Anal. Chem.* **2007**, *26*, 109-153.
- (33) Luczak, J.; Joskowska, M.; Hupka, J. *Physicochem. Probl. Miner. Process.* **2008**, *42*, 223-236.
- (34) Zhao, H.; Xia, S.; Ma, P. *J. Chem. Technol. Biotechnol.* **2005**, *80*, 1089-1096.
- (35) Zhang, M.; Kamavaram, V.; Reddy, R. G. *Miner. Metall. Process.* **2006**, *23*, 177-186.

- (36) Poole, C. F.; Poole, S. K. *J. Chromatogr. , A* **2010**, 1217, 2268-2286.
- (37) Hong, K.; Zhang, H.; Mays, J. W.; Visser, A. E.; Brazel, C. S.; Holbrey, J. D.; Reichert, W. M.; Rogers, R. D. *Chem. Commun. (Cambridge, U. K.)* **2002**, 1368-1369.
- (38) Watanabe, M. *Polym. Prepr. (Am. Chem. Soc. , Div. Polym. Chem.)* **2010**, 51, 6.
- (39) Winterton, N. *J. Mater. Chem.* **2006**, 16, 4281-4293.
- (40) Lu, W.; Fadeev, A. G.; Qi, B.; Mattes, B. R. *Proc. - Electrochem. Soc.* **2003**, 2003-17, 142-156.
- (41) Lu, W.; Fadeev, A. G.; Qi, B.; Mattes, B. R. *J. Electrochem. Soc.* **2004**, 151, H33-H39.
- (42) Kilpelainen, I.; Xie, H.; King, A.; Granstrom, M.; Heikkinen, S.; Argyropoulos, D. *S. J. Agric. Food Chem.* **2007**, 55, 9142-9148.
- (43) Anderson, J. L.; Ding, J.; Welton, T.; Armstrong, D. W. *J. Am. Chem. Soc.* **2002**, 124, 14247-14254.
- (44) Anderson, J. L.; Armstrong, D. W. *Anal. Chem.* **2003**, 75, 4851-4858.
- (45) Anderson, J. L.; Armstrong, D. W. *Anal. Chem.* **2005**, 77, 6453-6462.
- (46) Armstrong, D. W.; He, L.; Liu, Y. S. *Anal Chem* **1999**, 71, 3873-3876.
- (47) Ding, J.; Welton, T.; Armstrong, D. W. *Anal. Chem.* **2004**, 76, 6819-6822.
- (48) Payagala, T.; Huang, J.; Breitbach, Z. S.; Sharma, P. S.; Armstrong, D. W. *Chem. Mater.* **2007**, 19, 5848-5850.
- (49) Payagala, T.; Zhang, Y.; Wanigasekara, E.; Huang, K.; Breitbach, Z. S.; Sharma, P. S.; Sidisky, L. M.; Armstrong, D. W. *Anal. Chem. (Washington, DC, U. S.)* **2009**, 81, 160-173.
- (50) Anderson, J. L.; Armstrong, D. W.; Wei, G. -. *Anal. Chem. (Washington, DC, U. S.)* **2007**, 79, 4247.
- (51) Barber, D. W.; Phillips, C. S. G.; Tusa, G. F.; Verdin, A. J. *Chem. Soc.* **1959**, 18-24.
- (52) Pacholec, F.; Poole, C. F. *Chromatographia* **1983**, 17, 370-374.
- (53) Pacholec, F.; Butler, H. T.; Poole, C. F. *Anal. Chem.* **1982**, 54, 1938-1941.

- (54) Abraham, M. H. *Chem. Soc. Rev.* **1993**, 22, 73-83.
- (55) Kiridena, W.; Koziol, W. W.; Poole, C. F. *J. Chromatogr. , A* **2001**, 932, 171-177.
- (56) Anderson, J. L.; Ding, R.; Ellern, A.; Armstrong, D. W. *J. Am. Chem. Soc.* **2005**, 127, 593-604.
- (57) Reichardt, C. *Solvents and Solvent Effects in Organic Chemistry* (2nd ed.) **1988** p. 534.
- (58) Sekiguchi, Y.; Takayama, S.; Gotanda, T.; Sano, K. *Chem. Lett.* **2006**, 35, 458-459.
- (59) Touati, A.; Creuzenet, C.; Chobert, J. M.; Dufour, E.; Haertle, T. *J. Protein Chem.* **1992**, 11, 613-621.
- (60) Galceran, M. T.; Moyano, E. *J. Chromatogr.* **1992**, 607, 287-294.
- (61) Biedrzycka, Z.; Kamienska-Trela, K.; Witanowski, M. *J. Phys. Org. Chem.* **2010**, 23, 483-487.
- (62) Reichardt, C. *Angewandte Chemie International Edition in English* **1965**, 4, 29-40.
- (63) Berthod, A.; Zhou, E. Y.; Le, K.; Armstrong, D. W. *Anal. Chem.* **1995**, 67, 849-857.
- (64) Muldoon, M. J.; Gordon, C. M.; Dunkin, I. R. *J. Chem. Soc. , Perkin Trans. 2* **2001**, 433-435.
- (65) Carmichael, A. J.; Seddon, K. R. *J. Phys. Org. Chem.* **2000**, 13, 591-595.
- (66) Bonhote, P.; Dias, A.; Papageorgiou, N.; Kalyanasundaram, K.; Graetzel, M. *Inorg. Chem.* **1996**, 35, 1168-1178.
- (67) Aki, S. N. V. K.; Brennecke, J. F.; Samanta, A. *Chem. Commun. (Cambridge, U. K.)* **2001**, 413-414.
- (68) Abraham, M. H.; Whiting, G. S.; Doherty, R. M.; Shuely, W. J. *J. Chromatogr.* **1991**, 587, 213-228.
- (69) Abraham, M. H.; Whiting, G. S.; Andonian-Haftvan, J.; Steed, J. W.; Grate, J. W. *J. Chromatogr.* **1991**, 588, 361-364.
- (70) Abraham, M. H.; Whiting, G. S.; Doherty, R. M.; Shuely, W. J. *J. Chromatogr.* **1990**, 518, 329-348.
- (71) Chapman, S. *Phys. Rev.* **1937**, 52, 184-190.

- (72) Dole, M.; Mack, L. L.; Hines, R. L.; Mobley, R. C.; Ferguson, L. D.; Alice, M. B. *J. Chem. Phys.* **1968**, *49*, 2240-2249.
- (73) Fenn, J. B.; Mann, M.; Meng, C. K.; Wong, S. F.; Whitehouse, C. M. *Science (Washington, D. C. , 1883-)* **1989**, *246*, 64-71.
- (74) Andersen, J. S.; Svensson, B.; Roepstorff, P. *Nat Biotechnol* **1996**, *14*, 449-457.
- (75) Plattner, D. A. *Int. J. Mass Spectrom.* **2001**, *207*, 125-144.
- (76) Doerge, D. R.; Churchwell, M. I.; Beland, F. A. *J. Environ. Sci. Health, Part C: Environ. Carcinog. Ecotoxicol. Rev.* **2002**, *C20*, 1-20.
- (77) Lobinski, R.; Schaumloffel, D.; Szpunar, J. *Mass Spectrom. Rev.* **2006**, *25*, 255-289.
- (78) Sleighter, R. L.; Hatcher, P. G. *J. Mass Spectrom.* **2007**, *42*, 559-574.
- (79) Hansen, H. R.; Pergantis, S. A. In *In Electrospray ionization mass spectrometry: a complementary source for trace element speciation analysis*. Section Title: Inorganic Analytical Chemistry; 2007; , pp 251-276.
- (80) Cech, N. B.; Enke, C. G. *Mass Spectrom. Rev.* **2002**, *20*, 362-387.
- (81) Iribarne, J. V.; Thomson, B. A. *J. Chem. Phys.* **1976**, *64*, 2287-2294.
- (82) Thomson, B. A.; Iribarne, J. V. *J. Chem. Phys.* **1979**, *71*, 4451-4463.
- (83) Bruins, A. P.; Covey, T. R.; Henion, J. D. *Anal. Chem.* **1987**, *59*, 2642-2646.
- (84) Elkins, E. R.; Heuser, J. R. *J. AOAC Int.* **1994**, *77*, 411-415.
- (85) Dugo, G.; La Pera, L.; Pellicano, T. M.; Di Bella, G.; D'Imperio, M. *Food Chem.* **2005**, *91*, 355-363.
- (86) El Aribi, H.; Le Blanc, Y. J. C.; Antonsen, S.; Sakuma, T. *Anal. Chim. Acta* **2006**, *567*, 39-47.
- (87) Bruce, J. J. *Autom. Methods Manage. Chem.* **2002**, *24*, 127-130.
- (88) Arce, L.; Rios, A.; Valcarcel, M. *Fresenius' J. Anal. Chem.* **1998**, *360*, 697-701.
- (89) Brabcova, M.; Rychlovsky, P.; Nemcova, I. *Anal. Lett.* **2003**, *36*, 2303-2316.
- (90) Chen, Z.; Tang, C.; Yu, J. C. *J. High Resolut. Chromatogr.* **1999**, *22*, 379-385.
- (91) Smith, R.; Roth, D.; Krol, J.; Romano, J. *Am. Environ. Lab.* **1997**, *9*, 19-20, 22.

- (92) Wujcik, C. E.; Cahill, T. M.; Seiber, J. N. *Anal. Chem.* **1998**, *70*, 4074-4080.
- (93) Cahill, T. M.; Benesch, J. A.; Gustin, M. S.; Zimmerman, E. J.; Seiber, J. N. *Anal. Chem.* **1999**, *71*, 4465-4471.
- (94) Magnuson, M. L.; Urbansky, E. T.; Kelty, C. A. *Talanta* **2000**, *52*, 285-291.
- (95) Urbansky, E. T.; Magnuson, M. L.; Freeman, D.; Jelks, C. J. *Anal. At. Spectrom.* **1999**, *14*, 1861-1866.
- (96) Dudoit, A.; Pergantis, S. A. *J. Anal. At. Spectrom.* **2001**, *16*, 575-580.
- (97) van Staden, J. F.; Tlowana, S. I. *Fresenius' J. Anal. Chem.* **2001**, *371*, 396-399.
- (98) Hansen, K. J.; Johnson, H. O.; Eldridge, J. S.; Butenhoff, J. L.; Dick, L. A. *Environ. Sci. Technol.* **2002**, *36*, 1681-1685.
- (99) Guo, Z.; Cai, Q.; Yu, C.; Yang, Z. *J. Anal. At. Spectrom.* **2003**, *18*, 1396-1399.
- (100) Yamashita, N.; Kannan, K.; Taniyasu, S.; Horii, Y.; Okazawa, T.; Petrick, G.; Gamo, T. *Environ. Sci. Technol.* **2004**, *38*, 5522-5528.
- (101) Barron, L.; Paull, B. *Talanta* **2006**, *69*, 621-630.
- (102) Takiguchi, H.; Tsubata, A.; Miyata, M.; Odake, T.; Hotta, H.; Umemura, T.; Tsunoda, K. *Anal. Sci.* **2006**, *22*, 1017-1019.
- (103) Butler, R.; Lytton, L.; Godley, A. R.; Tothill, I. E.; Cartmell, E. *J. Environ. Monit.* **2005**, *7*, 999-1006.
- (104) Arienzo, M.; Capasso, R. *J. Agric. Food Chem.* **2000**, *48*, 1405-1410.
- (105) Benz, R. W.; Gonzalez, C. F.; Capraro, D. T.; Andrew, G. J.; Beyersdorf, A. J.; Wellman, D. E.; Williams, J. M.; Pilling, R. L. *Prepr. Ext. Abstr. ACS Natl. Meet. , Am. Chem. Soc. , Div. Environ. Chem.* **2001**, *41*, 156-158.
- (106) Blount, B. C.; Valentin-Blasini, L. *Anal. Chim. Acta* **2006**, *567*, 87-93.
- (107) Ahrer, W.; Buchberger, W. *J. Chromatogr. , A* **1999**, *854*, 275-287.
- (108) Martinelango, P. K.; Guemues, G.; Dasgupta, P. K. *Anal. Chim. Acta* **2006**, *567*, 79-86.
- (109) Chakraborty, D.; Das, A. K. *Talanta* **1989**, *36*, 669-671.
- (110) Doble, P.; Haddad, P. R. *J. Chromatogr. , A* **1999**, *834*, 189-212.

- (111) Munoz Leyva, J. A.; Hernandez Artiga, M. P.; Lozano Chaves, M. E. *Rev. Anal. Chem.* **1994**, *13*, 99-126.
- (112) Kaniansky, D.; Masar, M.; Marak, J.; Bodor, R. *J. Chromatogr. , A* **1999**, *834*, 133-178.
- (113) Klampfl, C. W. *Food Sci. Technol. (N. Y. , NY, U. S.)* **2004**, *138*, 1891-1918.
- (114) Padarauskas, A. *Rev. Anal. Chem.* **2001**, *20*, 271-301.
- (115) Isaac, A.; Davis, J.; Livingstone, C.; Wain, A. J.; Compton, R. G. *TrAC, Trends Anal. Chem.* **2006**, *25*, 589-598.
- (116) Sanchez, J.; del Valle, M. *Crit. Rev. Anal. Chem.* **2005**, *35*, 15-29.
- (117) Selig, W. S. *Microchem. J.* **1987**, *36*, 42-53.
- (118) Thomas, J. D. R. *Anal. Proc. (London)* **1990**, *27*, 117-118.
- (119) Atienza, J.; Herrero, M. A.; Maquieira, A.; Puchades, R. *Crit. Rev. Anal. Chem.* **1991**, *22*, 331-344.
- (120) Martinelango, P. K.; Anderson, J. L.; Dasgupta, P. K.; Armstrong, D. W.; Al-Horr, R. S.; Slingsby, R. W. *Anal. Chem.* **2005**, *77*, 4829-4835.
- (121) Wuilloud, R. G.; Altamirano, J. C.; Smichowski, P. N.; Heitkemper, D. T. *J. Anal. At. Spectrom.* **2006**, *21*, 1214-1223.
- (122) Olsen, G. W.; Hansen, K. J.; Stevenson, L. A.; Burris, J. M.; Mandel, J. H. *Environ. Sci. Technol.* **2003**, *37*, 888-891.
- (123) Salov, V. V.; Yoshinaga, J.; Shibata, Y.; Morita, M. *Anal. Chem.* **1992**, *64*, 2425-2428.
- (124) Nischwitz, V.; Pergantis, S. A. *J. Anal. At. Spectrom.* **2006**, *21*, 1277-1286.
- (125) Schmidt, T. C.; Buetehorn, U.; Steinbach, K. *Anal. Bioanal. Chem.* **2004**, *378*, 926-931.
- (126) Ells, B.; Barnett, D. A.; Purves, R. W.; Guevremont, R. *Anal. Chem.* **2000**, *72*, 4555-4559.
- (127) Soukup-Hein, R. J.; Remsburg, J. W.; Dasgupta, P. K.; Armstrong, D. W. *Anal. Chem.* **2007**, *79*, 7346-7352.

- (128) Soukup-Hein, R. J.; Remsburg, J. W.; Breitbach, Z. S.; Sharma, P. S.; Payagala, T.; Wanigasekara, E.; Huang, J.; Armstrong, D. W. *Anal. Chem. (Washington, DC, U. S.)* **2008**, *80*, 2612-2616.
- (129) Remsburg, J. W.; Soukup-Hein, R. J.; Crank, J. A.; Breitbach, Z. S.; Payagala, T.; Armstrong, D. W. *J. Am. Soc. Mass Spectrom.* **2008**, *19*, 261-269.
- (130) Straub, R. F.; Voyksner, R. D. *J. Am. Soc. Mass Spectrom.* **1993**, *4*, 578-587.
- (131) Jeannot, R. *Int. J. Environ. Anal. Chem.* **1994**, *57*, 231-236.
- (132) Jones, R. L. *Chem. Plant Prot.* **1995**, *11*, 3-18.
- (133) Sliwka-Kaszynska, M.; Kot-Wasik, A.; Namiesnik, J. *Crit. Rev. Environ. Sci. Technol.* **2003**, *33*, 31-44.
- (134) Dahotre, N. *Mater. Manuf. Processes* **2004**, *19*, 568-569.
- (135) Pawliszyn, J. *TrAC, Trends Anal. Chem.* **1995**, *14*, 113-122.
- (136) Zhang, Z.; Yang, M. J.; Pawliszyn, J. *Anal. Chem.* **1994**, *66*, 844A-853A.
- (137) Pawliszyn, J. In *In Solid phase microextraction*. Section Title: Organic Analytical Chemistry; 2002; Vol. 37, pp 389-477.
- (138) Pawliszyn, J. *Adv. Exp. Med. Biol.* **2001**, *488*, 73-87.
- (139) Risticvic, S.; Lord, H.; Gorecki, T.; Arthur, C. L.; Pawliszyn, J. *Nat. Protocols* **2010**, *5*, 122-139.
- (140) Louch, D.; Motlagh, S.; Pawliszyn, J. *Anal. Chem.* **1992**, *64*, 1187-1199.
- (141) Hook, G. L.; Kimm, G. L.; Hall, T.; Smith, P. A. *TrAC, Trends Anal. Chem.* **2002**, *21*, 534-543.
- (142) Gaurav; Kaur, V.; Kumar, A.; Malik, A. K.; Rai, P. K. *J Hazard Mater* **2007**, *147*, 691-697.
- (143) Koziel, J. A.; Pawliszyn, J. *J. Air Waste Manage. Assoc.* **2001**, *51*, 173-184.
- (144) Nerin, C.; Salafranca, J.; Aznar, M.; Batlle, R. *Anal Bioanal Chem* **2009**, *393*, 809-833.
- (145) Dietz, C.; Sanz, J.; Camara, C. *J. Chromatogr. , A* **2006**, *1103*, 183-192.
- (146) Jiang, G.; Huang, M.; Cai, Y.; Lv, J.; Zhao, Z. *J. Chromatogr. Sci.* **2006**, *44*, 324-332.

- (147) Kumar, A.; Gaurav; Malik, A. K.; Tewary, D. K.; Singh, B. *Anal. Chim. Acta* **2008**, *610*, 1-14.
- (148) Prosen, H.; Zupancic-Kralj, L. *TrAC, Trends Anal. Chem.* **1999**, *18*, 272-282.
- (149) Zhang, Z.; Yang, M. J.; Pawliszyn, J. *Anal. Chem.* **1994**, *66*, 844A-854A.
- (150) Risticovic, S.; Lord, H.; Gorecki, T.; Arthur, C. L.; Pawliszyn, J. *Nat. Protoc.* **2010**, *5*, 122-139.
- (151) Liu, J.; Li, N.; Jiang, G.; Liu, J.; Joensson, J. A.; Wen, M. *J. Chromatogr. , A* **2005**, *1066*, 27-32.
- (152) Scheppers Wercinski, S. A.; Editor **1999**, 257.
- (153) Tiwari, A.; Nema, A. K.; Das, C. K.; Nema, S. K. *Thermochimica Acta* **2004**, *417*, 133-142.
- (154) Zhao, F.; Meng, Y.; Anderson, J. L. *J. Chromatogr. , A* **2008**, *1208*, 1-9.
- (155) Seddon, K. R. *J. Chem. Technol. Biotechnol.* **1997**, *68*, 351-356.
- (156) Earle, M. J.; McCormac, P. B.; Seddon, K. R. *Green Chem.* **1999**, *1*, 23-25.
- (157) Dyson, P. J.; Ellis, D. J.; Welton, T.; Parker, D. G. *Chem. Commun. (Cambridge)* **1999**, 25-26.
- (158) Cole, A. C.; Jensen, J. L.; Ntai, I.; Tran, K. L. T.; Weaver, K. J.; Forbes, D. C.; Davis, J. H., Jr *J. Am. Chem. Soc.* **2002**, *124*, 5962-5963.
- (159) Sheldon, R. A.; Lau, R. M.; Sorgedragar, M. J.; van Rantwijk, F.; Seddon, K. R. *Green Chem.* **2002**, *4*, 147-151.
- (160) Ding, J.; Desikan, V.; Han, X.; Xiao, T. L.; Ding, R.; Jenks, W. S.; Armstrong, D. W. *Org. Lett.* **2005**, *7*, 335-337.
- (161) Handy, S. T.; Okello, M. *J. Org. Chem.* **2005**, *70*, 2874-2877.
- (162) Khosropour, A. R.; Khodaei, M. M.; Beygzadeh, M.; Jokar, M. *Heterocycles* **2005**, *65*, 767-773.
- (163) Han, X.; Armstrong, D. W. *Org. Lett.* **2005**, *7*, 4205-4208.
- (164) Xia, Y.; Wu, H.; Zhang, Y.; Fang, Y.; Sun, S.; Shi, Y. *Huaxue Jinzhan* **2006**, *18*, 1660-1667.

- (165) Rumbau, V.; Marcilla, R.; Ochoteco, E.; Pomposo, J. A.; Mecerreyes, D. *Macromolecules* **2006**, *39*, 8547-8549.
- (166) Paljevac, M.; Habulin, M.; Knez, Z. *Chem. Ind. Chem. Eng. Q.* **2006**, *12*, 181-186.
- (167) Naik, P. U.; Nara, S. J.; Harjani, J. R.; Salunkhe, M. M. *J. Mol. Catal. B: Enzym.* **2007**, *44*, 93-98.
- (168) Dickinson, E. V.; Williams, M. E.; Hendrickson, S. M.; Masui, H.; Murray, R. W. *J. Am. Chem. Soc.* **1999**, *121*, 613-616.
- (169) Ue, M.; Takeda, M. *J. Korean Electrochem. Soc.* **2002**, *5*, 192-196.
- (170) Lagrost, C.; Carrie, D.; Vaultier, M.; Hapiot, P. *J. Phys. Chem. A* **2003**, *107*, 745-752.
- (171) Doyle, K. P.; Lang, C. M.; Kim, K.; Kohl, P. A. *J. Electrochem. Soc.* **2006**, *153*, A1353-A1357.
- (172) Wang, C. Y.; Mottaghitalab, V.; Too, C. O.; Spinks, G. M.; Wallace, G. G. *J. Power Sources* **2007**, *163*, 1105-1109.
- (173) Jimenez, A.; Bermudez, M. *Tribol. Lett.* **2007**, *26*, 53-60.
- (174) Xia, Y.; Sasaki, S.; Murakami, T.; Nakano, M.; Shi, L.; Wang, H. *Wear* **2007**, *262*, 765-771.
- (175) Dai, S.; Ju, Y. H.; Barnes, C. E. *J. Chem. Soc., Dalton Trans.* **1999**, 1201-1202.
- (176) Chun, S.; Dzyuba, S. V.; Bartsch, R. A. *Anal. Chem.* **2001**, *73*, 3737-3741.
- (177) Carda-Broch, S.; Berthod, A.; Armstrong, D. W. *Anal. Bioanal. Chem.* **2003**, *375*, 191-199.
- (178) Li, C.; Xin, B.; Xu, W.; Zhang, Q. *J. Chem. Technol. Biotechnol.* **2007**, *82*, 196-204.
- (179) Germani, R.; Mancini, M. V.; Savelli, G.; Spreti, N. *Tetrahedron Lett.* **2007**, *48*, 1767-1769.
- (180) Armstrong, D. W.; Zhang, L.; He, L.; Gross, M. L. *Anal. Chem.* **2001**, *73*, 3679-3686.
- (181) Tholey, A.; Heinzle, E. *Anal. Bioanal. Chem.* **2006**, *386*, 24-37.
- (182) Laremore, T. N.; Zhang, F.; Linhardt, R. J. *Anal. Chem.* **2007**, *79*, 1604-1610.

- (183) Gordon, J. E.; Selwyn, J. E.; Thorne, R. L. *J. Org. Chem.* **1966**, *31*, 1925-1930.
- (184) Pacholec, F.; Poole, C. F. *Chromatographia* **1983**, *17*, 370-374.
- (185) Berthod, A.; He, L.; Armstrong, D. W. *Chromatographia* **2001**, *53*, 63-68.
- (186) Sumartschenkowa, I. A.; Verevkin, S. P.; Vasiltsova, T. V.; Bich, E.; Heintz, A.; Shevelyova, M. P.; Kabo, G. J. *J. Chem. Eng. Data* **2006**, *51*, 2138-2144.
- (187) Anderson, J. L.; Armstrong, D. W.; Wei, G. *Anal. Chem.* **2006**, *78*, 2893-2902.
- (188) Heintz, A.; Verevkin, S. P. *J. Chem. Eng. Data* **2005**, *50*, 1515-1519.
- (189) Pernak, J.; Skrzypczak, A.; Lota, G.; Frackowiak, E. *Chem. --Eur. J.* **2007**, *13*, 3106-3112.
- (190) Huang, K.; Han, X.; Zhang, X.; Armstrong, D. W. *Anal. Bioanal. Chem.* **2007**, *389*, 2265-2275.
- (191) Sharma, P. S.; Payagala, T.; Wanigasekara, E.; Wijeratne, A. B.; Huang, J.; Armstrong, D. W. *Chem. Mater.* **2008**, *20*, 4182-4184.
- (192) Hagiwara, R.; Ito, Y. *J. Fluorine Chem.* **2000**, *105*, 221-227.
- (193) Grob, K.; Grob, G.; Grob, K., Jr. *J. Chromatogr.* **1981**, *219*, 13-20.
- (194) McReynolds, W. O. *J. Chromatogr. Sci.* **1970**, *8*, 685-691.
- (195) Reichardt, C. *Angewandte Chemie International Edition in English* **1965**, *4*, 29-40.
- (196) Carmichael, A. J.; Seddon, K. R. *J. Phys. Org. Chem.* **2000**, *13*, 591-595.
- (197) Muldoon, M. J.; Gordon, C. M.; Dunkin, I. R. *J. Chem. Soc. , Perkin Trans. 2* **2001**, 433-435.
- (198) Bonhote, P.; Dias, A.; Papageorgiou, N.; Kalyanasundaram, K.; Graetzel, M. *Inorg. Chem.* **1996**, *35*, 1168-1178.
- (199) Aki, S. N. V. K.; Brennecke, J. F.; Samanta, A. *Chem. Commun. (Cambridge, U. K.)* **2001**, 413-414.
- (200) Reynolds, J. L.; Erdner, K. R.; Jones, P. B. *Org. Lett.* **2002**, *4*, 917-919.
- (201) Rohrschneider, L. *J. Chromatogr.* **1966**, *22*, 6-22.
- (202) Abraham, M. H.; Poole, C. F.; Poole, S. K. *J. Chromatogr. , A* **1999**, *842*, 79-114.

- (203) Vitha, M.; Carr, P. W. *J. Chromatogr. , A* **2006**, 1126, 143-194.
- (204) Grob, K., Jr.; Grob, G.; Grob, K. *J. Chromatogr.* **1978**, 156, 1-20.
- (205) Breitbach, Z. S.; Armstrong, D. W. *Anal. Bioanal. Chem.* **2008**, 390, 1605-1617.
- (206) Anonymous *Pure Appl. Chem.* **1979**, 51, 2503-2525.
- (207) Celik, M.; Tureli, C.; Celik, M.; Yanar, Y.; Erdem, U.; Kucukgulmez, A. *Food Chem.* **2004**, 88, 271-273.
- (208) Brodnjak-Voncina, D.; Kodba, Z. C.; Novic, M. *Chemom. Intell. Lab. Syst.* **2005**, 75, 31-43.
- (209) Rogers, R. D.; Seddon, K. R.; ACS Symp. Ser. **2003**, 856, 599.
- (210) Plechkova, N. V.; Seddon, K. R. *Chem. Soc. Rev.* **2008**, 37, 123-150.
- (211) Rogers, R. D.; Seddon, K. R. *Science* **2003**, 302, 792-793.
- (212) Ding, J.; Armstrong, D. W. *Chirality* **2005**, 17, 281-292.
- (213) Vaher, M.; Koel, M.; Kaljurand, M. *J. Chromatogr. , A* **2002**, 979, 27-32.
- (214) Law, G.; Watson, P. R. *Langmuir* **2001**, 17, 6138-6141.
- (215) Millefiorini, S.; Tkaczyk, A. H.; Sedev, R.; Efthimiadis, J.; Ralston, J. *J. Am. Chem. Soc.* **2006**, 128, 3098-3101.
- (216) Nanayakkara, Y. S.; Moon, H.; Payagala, T.; Wijeratne, A. B.; Crank, J. A.; Sharma, P. S.; Armstrong, D. W. *Anal. Chem. (Washington, DC, U. S.)* **2008**, 80, 7690-7698.
- (217) Moon, H.; Wheeler, A. R.; Garrell, R. L.; Loo, J. A.; Kim, C. *Lab Chip* **2006**, 6, 1213-1219.
- (218) Pollack, M. G.; Fair, R. B.; Shenderov, A. D. *Appl. Phys. Lett.* **2000**, 77, 1725-1726.
- (219) Wheeler, A. R.; Moon, H.; Kim, C.; Loo, J. A.; Garrell, R. L. *Anal. Chem.* **2004**, 76, 4833-4838.
- (220) Berge, B.; Peseux, J. *Eur. Phys. J. E* **2000**, 3, 159-163.
- (221) Hayes, R. A.; Feenstra, B. J. *Nature (London, U. K.)* **2003**, 425, 383-385.

- (222) Dubois, P.; Marchand, G.; Fouillet, Y.; Berthier, J.; Douki, T.; Hassine, F.; Gmouh, S.; Vaultier, M. *Anal. Chem.* **2006**, *78*, 4909-4917.
- (223) Chatterjee, D.; Hetayothin, B.; Wheeler, A. R.; King, D. J.; Garrell, R. L. *Lab Chip* **2006**, *6*, 199-206.
- (224) Catalan, J.; Claramunt, R. M.; Elguero, J.; Laynez, J.; Menendez, M.; Anvia, F.; Quian, J. H.; Taagepera, M.; Taft, R. W. *J. Am. Chem. Soc.* **1988**, *110*, 4105-4111.
- (225) Rao, S. P.; Sunkada, S. *Resonance* **2007**, *12*, 43-57.
- (226) Zhou, Z.; Matsumoto, H.; Tatsumi, K. *ChemPhysChem* **2005**, *6*, 1324-1332.
- (227) Sheldon, R. *Chem. Commun. (Cambridge, U. K.)* **2001**, 2399-2407.
- (228) Wasserscheid, P.; Keim, W. *Angewandte Chemie International Edition* **2000**, *39*, 3772-3789.
- (229) Bonhote, P.; Dias, A.; Papageorgiou, N.; Kalyanasundaram, K.; Graetzel, M. *Inorg. Chem.* **1996**, *35*, 1168-1178.
- (230) Bradaric, C. J.; Downard, A.; Kennedy, C.; Robertson, A. J.; Zhou, Y. *Green Chem.* **2003**, *5*, 143-152.
- (231) Han, X.; Armstrong, D. W. *Org. Lett.* **2005**, *7*, 4205-4208.
- (232) Gordon, C. M. *Appl. Catal. , A* **2001**, *222*, 101-117.
- (233) Zhu, Y.; Rosen, M. J.; Morrall, S. W. *J. Surfactants Deterg.* **1998**, *1*, 1-9.
- (234) Hebert, G. N.; Odom, M. A.; Craig, P. S.; Dick, D. L.; Strauss, S. H. *J. Environ. Monit.* **2002**, *4*, 90-95.
- (235) Magnuson, M. L.; Urbansky, E. T.; Kelty, C. A. *Talanta* **2000**, *52*, 285-291.
- (236) Hansen, K. J.; Johnson, H. O.; Eldridge, J. S.; Butenhoff, J. L.; Dick, L. A. *Environ. Sci. Technol.* **2002**, *36*, 1681-1685.
- (237) Cahill, T. M.; Benesch, J. A.; Gustin, M. S.; Zimmerman, E. J.; Seiber, J. N. *Anal. Chem.* **1999**, *71*, 4465-4471.
- (238) Ghanem, A.; Bados, P.; Kerhoas, L.; Dubroca, J.; Einhorn, J. *Anal. Chem. (Washington, DC, U. S.)* **2007**, *79*, 3794-3801.
- (239) Wujcik, C. E.; Cahill, T. M.; Seiber, J. N. *Anal. Chem.* **1998**, *70*, 4074-4080.

- (240) Martinelango, P. K.; Anderson, J. L.; Dasgupta, P. K.; Armstrong, D. W.; Al-Horr, R. S.; Slingsby, R. W. *Anal. Chem.* **2005**, *77*, 4829-4835.
- (241) Martinelango, P. K.; Guemues, G.; Dasgupta, P. K. *Anal. Chim. Acta* **2006**, *567*, 79-86.
- (242) Martinelango, P. K.; Tian, K.; Dasgupta, P. K. *Anal. Chim. Acta* **2006**, *567*, 100-107.
- (243) Barron, L.; Paull, B. *Talanta* **2006**, *69*, 621-630.
- (244) Yamashita, N.; Kannan, K.; Taniyasu, S.; Horii, Y.; Okazawa, T.; Petrick, G.; Gamo, T. *Environ. Sci. Technol.* **2004**, *38*, 5522-5528.
- (245) Wuilloud, R. G.; Altamirano, J. C.; Smichowski, P. N.; Heitkemper, D. T. *J. Anal. At. Spectrom.* **2006**, *21*, 1214-1223.
- (246) Mandal, B. K.; Ogra, Y.; Suzuki, K. T. *Chem. Res. Toxicol.* **2001**, *14*, 371-378.
- (247) Tsikas, D. *Clin. Chem. (Washington, DC, U. S.)* **2004**, *50*, 1259-1261.
- (248) Blount, B. C.; Valentin-Blasini, L. *Anal. Chim. Acta* **2006**, *567*, 87-93.
- (249) Olsen, G. W.; Hansen, K. J.; Stevenson, L. A.; Burris, J. M.; Mandel, J. H. *Environ. Sci. Technol.* **2003**, *37*, 888-891.
- (250) Dyke, J. V.; Kirk, A. B.; Kalyani Martinelango, P.; Dasgupta, P. K. *Anal. Chim. Acta* **2006**, *567*, 73-78.
- (251) Elkins, E. R.; Heuser, J. R. *J. AOAC Int.* **1994**, *77*, 411-415.
- (252) El Aribi, H.; Le Blanc, Y. J. C.; Antonsen, S.; Sakuma, T. *Anal. Chim. Acta* **2006**, *567*, 39-47.
- (253) Guo, Z.; Cai, Q.; Yu, C.; Yang, Z. *J. Anal. At. Spectrom.* **2003**, *18*, 1396-1399.
- (254) Dudoit, A.; Pergantis, S. A. *J. Anal. At. Spectrom.* **2001**, *16*, 575-580.
- (255) van Staden, J. F.; Tlowana, S. I. *Fresenius' J. Anal. Chem.* **2001**, *371*, 396-399.
- (256) Salov, V. V.; Yoshinaga, J.; Shibata, Y.; Morita, M. *Anal. Chem.* **1992**, *64*, 2425-2428.
- (257) Ahrer, W.; Buchberger, W. *J. Chromatogr. , A* **1999**, *854*, 275-287.
- (258) Nischwitz, V.; Pergantis, S. A. *J. Anal. At. Spectrom.* **2006**, *21*, 1277-1286.

- (259) Kappes, T.; Schnierle, P.; C. Hauser, P. *Anal. Chim. Acta* **1997**, 350, 141-147.
- (260) Isildak, I. *Chromatographia* **1999**, 49, 338-342.
- (261) Isildak, I.; Asan, A. *Talanta* **1999**, 48, 967-978.
- (262) Chakraborty, D.; Das, A. K. *Talanta* **1989**, 36, 669-671.
- (263) Buchberger, W. W. *J. Chromatogr. , A* **2000**, 884, 3-22.
- (264) Cech, N. B.; Enke, C. G. *Mass Spectrom Rev* **2001**, 20, 362-387.
- (265) Henriksen, T.; Juhler, R. K.; Svensmark, B.; Cech, N. B. *J. Am. Soc. Mass Spectrom.* **2005**, 16, 446-455.
- (266) Straub, R. F.; Voyksner, R. D. *J. Am. Soc. Mass Spectrom.* **1993**, 4, 578-587.
- (267) Cole, R. B.; Zhu, J. *Rapid Commun. Mass Spectrom.* **1999**, 13, 607-611.
- (268) Arthur, C. L.; Pawliszyn, J. *Anal. Chem.* **1990**, 62, 2145-2148.
- (269) Pawliszyn, J.; Pawliszyn, B.; Pawliszyn, M. *Chem. Educ.* **1997**.
- (270) Scheppers Wercinski, S. A. Solid phase microextraction. A practical guide. CRC Press, Boca Raton, FL, USA **1999**, 257.
- (271) Hinshaw, J. V. *LC-GC Eur.* **2003**, 16, 803-804,807.
- (272) Majors, R. E. *LCGC North Am.* **2008**, 26, 1074,1076,1078,1080,1082,1084,1086,1088,1090.
- (273) Pawliszyn, J.; Editor, Solid phase microextraction theory and practice. Wiley, New York, NY, USA. **1997**.
- (274) Earle, M. J.; Seddon, K. R. *Pure Appl. Chem.* **2000**, 72, 1391-1398.
- (275) Olivier-Bourbigou, H.; Magna, L. *J. Mol. Catal. A: Chem.* **2002**, 182-183, 419-437.
- (276) Berthod, A.; Ruiz-Angel, M. J.; Carda-Broch, S. *J. Chromatogr. , A* **2008**, 1184, 6-18.
- (277) Poole, C. F.; Kollie, T. O. *Anal. Chim. Acta* **1993**, 282, 1-17.
- (278) Vidal, L.; Psillakis, E.; Domini, C. E.; Grané, N.; Marken, F.; Canals, A. *Anal. Chim. Acta* **2007**, 584, 189-195.

- (279) Aguilera-Herrador, E.; Lucena, R.; Cardenas, S.; Valcarcel, M. *Anal. Chem. (Washington, DC, U. S.)* **2008**, *80*, 793-800.
- (280) Hsieh, Y.; Huang, P.; Sun, I.; Whang, T.; Hsu, C.; Huang, H.; Kuei, C. *Anal. Chim. Acta* **2006**, *557*, 321-328.
- (281) He, Y.; Pohl, J.; Engel, R.; Rothman, L.; Thomas, M. *J. Chromatogr. , A* **2009**, *1216*, 4824-4830.
- (282) Bara, J. E.; Hatakeyama, E. S.; Gabriel, C. J.; Zeng, X.; Lessmann, S.; Gin, D. L.; Noble, R. D. *J. Membr. Sci.* **2008**, *316*, 186-191.
- (283) Wu, C.; Chen, C.; Huang, C.; Lee, M.; Huang, C. *Anal. Lett.* **2004**, *37*, 1373-1384.
- (284) Sprunger, L. M.; Gibbs, J.; Proctor, A.; Acree, W. E., Jr.; Abraham, M. H.; Meng, Y.; Yao, C.; Anderson, J. L. *Ind. Eng. Chem. Res.* **2009**, *48*, 4145-4154.
- (285) Zhao, F.; Meng, Y.; Anderson, J. L. *J. Chromatogr. , A* **2008**, *1208*, 1-9.
- (286) Hinshaw, J. V. *LCGC North Am.* **2003**, *21*, 1056,1058-1061.
- (287) Kappe, T. *J. Inclusion Phenom. Mol. Recognit. Chem.* **1994**, *19*, 3-15.
- (288) Cadogan, F.; Nolan, K.; Diamond, D. In *In Sensor applications [of calixarenes]*. Section Title: Inorganic Analytical Chemistry; 2001; , pp 627-641.
- (289) Agrawal, Y. K.; Bhatt, H. *Bioinorg. Chem. Appl.* **2004**, *2*, 237-274.
- (290) El Nashar, R. M.; Wagdy, H. A. A.; Aboul-Enein, H. Y. *Curr. Anal. Chem.* **2009**, *5*, 249-270.
- (291) Kim, J. S.; Lee, S. Y.; Yoon, J.; Vicens, J. *Chem. Commun. (Cambridge, U. K.)* **2009**, 4791-4802.
- (292) Shinkai, S. *Top. Inclusion Sci.* **1991**, *3*, 173-198.
- (293) Chung, T. D.; Kim, H. *J. Inclusion Phenom. Mol. Recognit. Chem.* **1998**, *32*, 179-193.
- (294) Sliwka-Kaszynska, M. *Crit. Rev. Anal. Chem.* **2007**, *37*, 211-224.
- (295) Meyer, R.; Jira, T. *Curr. Anal. Chem.* **2007**, *3*, 161-170.
- (296) Baklouti, L.; Harrowfield, J.; Pulpoka, B.; Vicens, J. *Mini-Rev. Org. Chem.* **2006**, *3*, 355-384.

- (297) Gutsche, C. D. *Acc. Chem. Res.* **1983**, *16*, 161-170.
- (298) Gutsche, C. D.; Alam, I.; Iqbal, M.; Mangiafico, T.; Nam, K. C.; Rogers, J.; See, K. A. *J. Inclusion Phenom. Mol. Recognit. Chem.* **1989**, *7*, 61-72.
- (299) Iwamoto, K.; Araki, K.; Shinkai, S. *J. Org. Chem.* **1991**, *56*, 4955-4962.
- (300) Bernardino, R. J.; Cabral, B. J. C. *Supramol. Chem.* **2002**, *14*, 57-66.
- (301) Ouchi, M.; Oima, M.; Fujio, E.; Yamashita, T.; Shibata, H. *Kenkyu Hokoku - Hyogo-kenritsu Daigaku Daigakuin Kogaku Kenkyuka* **2009**, *61*, 20-24.
- (302) Pozar, J.; Preocanin, T.; Frkanec, L.; Tomisic, V. *J. Solution Chem.* **2010**, *39*, 835-848.
- (303) Curinova, P.; Stibor, I.; Budka, J.; Sykora, J.; Lang, K.; Lhotak, P. *New J. Chem.* **2009**, *33*, 612-619.
- (304) Dinares, I.; Garcia de Miguel, C.; Mesquida, N.; Alcalde, E. *J. Org. Chem.* **2009**, *74*, 482-485.
- (305) Hamdi, A.; Abidi, R.; Vicens, J. *J. Inclusion Phenom. Macrocyclic Chem.* **2008**, *60*, 193-196.
- (306) Kroupa, J.; Stibor, I.; Pojarova, M.; Tkadlecova, M.; Lhotak, P. *Tetrahedron* **2008**, *64*, 10075-10079.
- (307) Tuntulani, T.; Tumcharern, G.; Ruangpornvisuti, V. *J. Inclusion Phenom. Macrocyclic Chem.* **2001**, *39*, 47-53.
- (308) Arduini, A.; McGregor, W. M.; Paganuzzi, D.; Pochini, A.; Secchi, A.; Ugozzoli, F.; Ungaro, R. *J. Chem. Soc., Perkin Trans. 2* **1996**, 839-846.
- (309) Gustafsson, L. E. *Scand. J. Work, Environ. Health* **1993**, *19*, 44-49.
- (310) Schlesinger, R. B. *In Nitrogen oxides*. Section Title: Toxicology; 2009; , pp 823-868.
- (311) Rudkevich, D. M. *Angew. Chem., Int. Ed.* **2004**, *43*, 558-571.
- (312) J. L.; Steed, J. W.; Eds. *Organic Nanostructures*; Wiley-VCH, **2008**, 352.
- (313) Steed, J. W.; Atwood, J. L. *Supramolecular Chemistry: A Concise Introduction*, 2nd Ed.; Jhon Wiley & Sons: Wiltshire, UK, **2000**.
- (314) Cram, D. J.; Tanner, M. E.; Knobler, C. B. *J. Am. Chem. Soc.* **1991**, *113*, 7717-7727.

- (315) Springer, B. A.; Sligar, S. G.; Olson, J. S.; Phillips, G. N. *J. Chem. Rev.* **1994**, *94*, 699-714.
- (316) Goldberg, D. E. *Chem. Rev.* **1999**, *99*, 3371-3378.
- (317) Brucker, E. A.; Olson, J. S.; Ikeda-Saito, M.; Phillips, G. N. *Proteins: Structure, Function, and Bioinformatics* **1998**, *30*, 352-356.
- (318) Sessa, W. C. *J. Thromb. Haemostasis* **2009**, *7*, 35-37.
- (319) Butler, A. R.; Rhodes, P. *Nitric oxide in physiology and medicine*. Section Title: Mammalian Biochemistry; 1999; , pp 58-76.
- (320) Rathore, R.; Lindeman, S. V.; Rao, K. S. S. P.; Sun, D.; Kochi, J. R. *Angew. Chem., Int. Ed.* **2000**, *39*, 2123-2127.
- (321) Rathore, R.; Kochi, J. K. *J. Org. Chem.* **1998**, *63*, 8630-8631.
- (322) Zyryanov, G. V.; Kang, Y.; Stamp, S. P.; Rudkevich, D. M. *Chem. Commun. (Cambridge, U. K.)* **2002**, 2792-2793.
- (323) Bosch, E.; Rathore, R.; Kochi, J. K. *J. Org. Chem.* **1994**, *59*, 2529-2536.
- (324) Rathore, R.; Lindeman, S. V.; Rao, K. S. S. P.; Sun, D.; Kochi, J. R. *Angew. Chem., Int. Ed.* **2000**, *39*, 2123-2127.
- (325) Zyryanov, G. V.; Rudkevich, D. M. *J. Am. Chem. Soc.* **2004**, *126*, 4264-4270.
- (326) Organo, V. G.; Leontiev, A. V.; Sgarlata, V.; Dias, H. V. R.; Rudkevich, D. M. *Angew. Chem., Int. Ed.* **2005**, *44*, 3043-3047.
- (327) Sgarlata, V.; Organo, V. G.; Rudkevich, D. M. *Chem. Commun. (Cambridge, U. K.)* **2005**, 5630-5632.
- (328) Baklouti, L.; Harrowfield, J.; Pulpoka, B.; Vicens, J. *Mini-Rev. Org. Chem.* **2006**, *3*, 355-384.
- (329) Wang, P. G.; Xian, M.; Tang, X.; Wu, X.; Wen, Z.; Cai, T.; Janczuk, A. J. *Chem. Rev.* **2002**, *102*, 1091-1134.
- (330) Hrabie, J. A.; Keefer, L. K. *Chem. Rev. (Washington, D. C.)* **2002**, *102*, 1135-1154.
- (331) Culotta, E.; Koshland, D. E., Jr *Science* **1992**, *258*, 1862-1865.
- (332) Furchgott, R. F.; Zawadzki, J. V. *Nature (London)* **1980**, *288*, 373-376.

- (333) Furchgott, R. F. *Circ. Res.* **1983**, 53, 557-573.
- (334) Furchgott, R. F. *Annu. Rev. Pharmacol. Toxicol.* **1984**, 24, 175-197.
- (335) Furchgott, R. F.; Vanhoutte, P. M. *Faseb J.* **1989**, 3, 2007-2018.
- (336) Furchgott, R. F. *Acta Physiol. Scand.* **1990**, 139, 257-270.
- (337) Furchgott, R. F. *Semin Perinatol* **1991**, 15, 11-15.
- (338) Ignarro, L. J.; Buga, G. M.; Wood, K. S.; Byrns, R. E.; Chaudhuri, G. *Proc. Natl. Acad. Sci. U. S. A.* **1987**, 84, 9265-9269.
- (339) Ignarro, L. J. *Faseb J.* **1989**, 3, 31-36.
- (340) Ignarro, L. J. *Semin. Hematol.* **1989**, 26, 63-76.
- (341) Ignarro, L. J. *Circ. Res.* **1989**, 65, 1-21.
- (342) Ignarro, L. J. *Pharm. Res.* **1989**, 6, 651-659.
- (343) Ignarro, L. J. *Pharmacol. Toxicol. (Copenhagen)* **1990**, 67, 1-7.
- (344) Ignarro, L. J. *Hypertension (Dallas)* **1990**, 16, 477-483.
- (345) Ignarro, L. J. *Biochem. Pharmacol.* **1991**, 41, 485-490.
- (346) Murad, F.; Leitman, D.; Waldman, S.; Chang, C. H.; Hirata, M.; Kohse, K. *Cold Spring Harbor Symp. Quant. Biol.* **1988**, 53, 1005-1009.
- (347) Murad, F.; Forstermann, U.; Nakane, M.; Schmidt, H.; Pollock, J.; Sheng, H.; Matsumoto, T.; Warner, T.; Mitchell, J.; et al *Jpn. J. Pharmacol.* **1992**, 58, 150P-157P.
- (348) Murad, F.; Forstermann, U.; Nakane, M.; Pollock, J.; Tracey, R.; Matsumoto, T.; Buechler, W. *Adv. Second Messenger Phosphoprotein Res.* **1993**, 28, 101-109.
- (349) Murad, F. *Biochem. Soc. Trans.* **1988**, 16, 490-492.
- (350) Chen, H. I.; Hu, C. T.; Wu, C. Y.; Wang, D. J. *Biomed. Sci. (Basel)* **1997**, 4, 244-248.
- (351) Chen, H. I.; Huang, H. S.; Yang, J. G.; Wang, D. *Chin. J. Physiol. (Taipei)* **1992**, 35, 123-131.
- (352) Arnal, J. F.; El Amrani, A. I.; Chatellier, G.; Menard, J.; Michel, J. B. *Hypertension (Dallas)* **1993**, 22, 380-387.

- (353) Hanson, S. R.; Hutsell, T. C.; Keefer, L. K.; Mooradian, D. L.; Smith, D. J. *Adv. Pharmacol. (San Diego)* **1995**, *34*, 383-398.
- (354) de Belder, A. J.; Radomski, M. W.; Martin, J. F.; Moncada, S. *Eur. J. Clin. Invest.* **1995**, *25*, 1-8.
- (355) Kerwin, J. F., Jr.; Lancaster, J. R.; Feldman, P. L. *J. Med. Chem.* **1995**, *38*, 4343-4362.
- (356) Beckman, J. S.; Koppenol, W. H. *Am. J. Physiol.* **1996**, *271*, C1424-C1437.
- (357) Pfeiffer, S.; Mayer, B.; Hemmens, B. *Angewandte Chemie International Edition* **1999**, *38*, 1714-1731.
- (358) Napoli, C.; Ignarro, L. J. *Annu. Rev. Pharmacol. Toxicol.* **2003**, *43*, 97-123.
- (359) Wang, P. G.; Xian, M.; Tang, X.; Wu, X.; Wen, Z.; Cai, T.; Janczuk, A. J. *Chem. Rev.* **2002**, *102*, 1091-1134.
- (360) Granik, V. G.; Grigor'ev, N. B. *Russ. Chem. Bull.* **2002**, *51*, 1375-1422.
- (361) Mitchell-Koch, J. T.; Reed, T. M.; Borovik, A. S. *Angewandte Chemie International Edition* **2004**, *43*, 2806-2809.
- (362) Padden, K. M.; Krebs, J. F.; MacBeth, C. E.; Scarrow, R. C.; Borovik, A. S. *J. Am. Chem. Soc.* **2001**, *123*, 1072-1079.
- (363) Ding, X. D.; Weichsel, A.; Andersen, J. F.; Shokhireva, T. K.; Balfour, C.; Pierik, A. J.; Averill, B. A.; Montfort, W. R.; Walker, F. A. *J. Am. Chem. Soc.* **1999**, *121*, 128-138.
- (364) Kang, Y.; Zyryanov, G. V.; Rudkevich, D. M. *Chem. --Eur. J.* **2005**, *11*, 1924-1932.
- (365) Bosch, E.; Rathore, R.; Kochi, J. K. *J. Org. Chem.* **1994**, *59*, 2529-2536.
- (366) Borodkin, G. I.; Shubin, V. G. *Russ. Chem. Rev.* **2001**, *70*, 211-230.
- (367) Connelly, N. G.; Geiger, W. E. *Chem. Rev.* **1996**, *96*, 877-910.
- (368) Rathore, R.; Lindeman, S.; Rao, K. S. P.; Sun, D.; Kochi, J. *Angewandte Chemie* **2000**, *112*, 2207-2211.
- (369) Marmo, F. F. *J. Opt. Soc. Am.* **1953**, *43*, 1186-1190.
- (370) Zyryanov, G. V.; Kang, Y.; Rudkevich, D. M. *J. Am. Chem. Soc.* **2003**, *125*, 2997-3007.

- (371) Marletta, M. A.; Tayeh, M. A.; Hevel, J. M. *Biofactors* **1990**, 2, 219-225.
- (372) Fleming, I.; Busse, R. *J. Mol. Cell. Cardiol.* **1999**, 31, 5-14.
- (373) Parker, J. O. *N Engl J Med* **1987**, 316, 1635-1642.
- (374) Cirino, G. *Dig. Liver Dis.* **2003**, 35, S2-S8.
- (375) Nablo, B. J.; Chen, T.; Schoenfisch, M. H. *J. Am. Chem. Soc.* **2001**, 123, 9712-9713.
- (376) Cobbs, C. S.; Brenman, J. E.; Aldape, K. D.; Bredt, D. S.; Israel, M. A. *Cancer Res* **1995**, 55, 727-730.
- (377) Jenkins, D. C.; Charles, I. G.; Thomsen, L. L.; Moss, D. W.; Holmes, L. S.; Baylis, S. A.; Rhodes, P.; Westmore, K.; Emson, P. C.; Moncada, S. *Proc Natl Acad Sci U S A* **1995**, 92, 4392-4396.
- (378) Thomsen, L. L.; Miles, D. W.; Happerfield, L.; Bobrow, L. G.; Knowles, R. G.; Moncada, S. *Br J Cancer* **1995**, 72, 41-44.
- (379) Wang, P. G.; Xian, M.; Tang, X.; Wu, X.; Wen, Z.; Cai, T.; Janczuk, A. J. *Chem. Rev. (Washington, D. C.)* **2002**, 102, 1091-1134.
- (380) Burgaud, J.; Ongini, E.; Del Soldato, P. *Ann. N. Y. Acad. Sci.* **2002**, 962, 360-371.
- (381) Low, S. Y. *Mol. Aspects Med.* **2005**, 26, 97-138.
- (382) Hrabie, J. A.; Keefer, L. K. *Chem. Rev. (Washington, D. C.)* **2002**, 102, 1135-1154.
- (383) Stasko, N. A.; Schoenfisch, M. H. *J. Am. Chem. Soc.* **2006**, 128, 8265-8271.
- (384) Shin, J. H.; Metzger, S. K.; Schoenfisch, M. H. *J. Am. Chem. Soc.* **2007**, 129, 4612-4619.
- (385) Ding, X. D.; Weichsel, A.; Andersen, J. F.; Shokhireva, T. K.; Balfour, C.; Pierik, A. J.; Averill, B. A.; Montfort, W. R.; Walker, F. A. *J. Am. Chem. Soc.* **1999**, 121, 128-138.
- (386) Padden, K. M.; Krebs, J. F.; MacBeth, C. E.; Scarrow, R. C.; Borovik, A. S. *J. Am. Chem. Soc.* **2001**, 123, 1072-1079.
- (387) Mitchell-Koch, J. T.; Reed, T. M.; Borovik, A. S. *Angew. Chem., Int. Ed.* **2004**, 43, 2806-2809.

- (388) Rudkevich, D. M. *Angew. Chem. , Int. Ed.* **2004**, *43*, 558-571.
- (389) Rathore, R.; Lindeman, S. V.; Rao, K. S. S. P.; Sun, D.; Kochi, J. R. *Angew. Chem. , Int. Ed.* **2000**, *39*, 2123-2127.
- (390) Botta, B.; D'Acquarica, I.; Delle Monache, G.; Nevola, L.; Tullo, D.; Ugozzoli, F.; Pierini, M. *J. Am. Chem. Soc.* **2007**, *129*, 11202-11212.
- (391) Organo, V. G.; Rudkevich, D. M. *Chem. Commun. (Cambridge, U. K.)* **2007**, 3891-3899.
- (392) Wanigasekara, E.; Leontiev, A. V.; Organo, V. G.; Rudkevich, D. M. *Eur. J. Org. Chem.* **2007**, 2254-2256.
- (393) Lu, L.; Li, G.; Peng, X.; Chen, C.; Huang, Z. *Tetrahedron Lett.* **2006**, *47*, 6021-6025.
- (394) Reddy, P. A.; Kashyap, R. P.; Watson, W. H.; Gutsche, C. D. *Isr. J. Chem.* **1992**, *32*, 89-96.
- (395) Iwamoto, K.; Araki, K.; Shinkai, S. *J. Org. Chem.* **1991**, *56*, 4955-4962.
- (396) Kanamathareddy, S.; Gutsche, C. D. *J. Org. Chem.* **1992**, *57*, 3160-3166.
- (397) Bifulco, G.; Riccio, R.; Gaeta, C.; Neri, P. *Chem. --Eur. J.* **2007**, *13*, 7185-7194.
- (398) Bifulco, G.; Gomez-Paloma, L.; Riccio, R.; Gaeta, C.; Troisi, F.; Neri, P. *Org. Lett.* **2005**, *7*, 5757-5760.
- (399) Jaime, C.; De Mendoza, J.; Prados, P.; Nieto, P. M.; Sanchez, C. *J. Org. Chem.* **1991**, *56*, 3372-3376.
- (400) Borodkin, G. I.; Shubin, V. G. *Russ. Chem. Rev.* **2001**, *70*, 211-230.
- (401) Marmo, F. F. *J. Opt. Soc. Am.* **1953**, *43*, 1186-1190.
- (402) Oliviero, L.; Barbier, J.; Duprez, D. *Applied Catalysis B: Environmental* **2003**, *40*, 163-184.
- (403) Chen, J.; Rebek, J., Jr *Org. Lett.* **2002**, *4*, 327-329.
- (404) Iwasawa, T.; Mann, E.; Rebek, J., Jr *J. Am. Chem. Soc.* **2006**, *128*, 9308-9309.
- (405) Iwamoto, K.; Araki, K.; Shinkai, S. *J. Org. Chem.* **1991**, *56*, 4955-4962.

BIOGRAPHICAL INFORMATION

Eranda Wanigasekara is an alumnus of Trinity College-Kandy, Sri Lanka. He entered Trinity College in 1986 and continued school until the completion of advanced level studies in 1996. Then he earned B.Sc. honors degree in chemistry from the University of Peradeniya, Sri Lanka in 2004. He joined Institute of Fundamental Studies (IFS) at Hanthana, Kandy as a research assistant. At IFS, he studied the synthesis and anti HIV activities on β -mangostine derivatives. In fall 2005, Eranda started his Ph.D. studies in chemistry at the University of Texas at Arlington. His research areas mainly focus on synthesis of multiply charged ionic liquids and their applications in analytical chemistry such as development of gas chromatographic stationary phases and solid phase microextraction coating materials based on ionic liquids. He also has developed stationary phases for chiral and achiral liquid and supercritical fluid chromatography. He has authored and coauthored 20 publications and one patent during his graduate career. He obtained his PhD degree in Chemistry in November 2010.